DOTTORATO DI RICERCA IN CHIMICA

Convenzione tra
UNIVERSITÀ DEGLI STUDI DI TRIESTE
e
UNIVERSITÀ CA' FOSCARI DI VENEZIA

CICLO XXXIII

Intensifying organic processes: a "green" toolbox for the synthesis of benign-by-design chemicals from waste feedstocks

Settore scientifico-disciplinare: **Chim/06**

DOTTORANDO / A
Roberto Calmanti

COORDINATORE
PROF. ENZO ALESSIO

SUPERVISORE DI TESI
PROF. ALVISE PEROSA

ANNO ACCADEMICO 2019/2020

ABSTRACT

This Ph.D. thesis is centered on developing greener methodologies for the synthesis of bio-based compounds starting from waste or low-value feedstock. The work is divided in two main chapters based on output, one dealing with the synthesis of cyclic organic carbonates (Chapter 2), the other with the synthesis of glycerol derivatives (Chapter 3).

In Chapter 2 a novel class of tungstate ionic liquids (TILs) was studied. Different synthetic routes were followed, some already published, others that exploit a green halide-free protocol developed in this thesis. The TILs were initially investigated for the CO_2 fixation reaction into epoxides. Once established their potential use in this field, the TILs were investigated for the tandem direct oxidative carboxylation (DOC) of olefins to give cyclic organic carbonates (COCs). Tandem catalysis is a way to achieve process intensification by using the same catalyst for two or more sequential reaction steps having different mechanisms. TILs are demonstrated as effective tandem catalysts for the direct synthesis of COCs from olefins. In the first step, the TILs promote epoxidation of the olefin, while in the second step they catalyse insertion of CO_2 into the epoxide, without any intermediate work-up. The procedure is greener than current protocols from several standpoints: H_2O_2 is used as oxidant, atmospheric pressure of CO_2 is sufficient to achieve yields >90% in COCs and product recovery occurs by simple phase separation. Additionally, simple alkali metal halide salts (e.g., NaBr, NaI, KBr, KI) are sufficient to promote CO_2 insertion into epoxides in place of traditional costlier (for their environmental burden and resource use) ammonium halides.

The simple alkali metal halide salt NaBr is also used as catalysts in a new CO_2 insertion process run in continuous flow. In this case, NaBr is activated by diethylene glycol (DEG) that acts as an inexpensive and largely available complexing agent for Na^+ as well as a hydrogen-bond donor that promotes the ring-opening of the epoxides. An in-depth study of the continuous-flow conditions allowed to obtain COCs with high yields from terminal epoxides, and with a higher overall productivity compared to the batch process. A simple method for the recycling of the catalytic system was also developed.

In Chapter 3, focus is on the synthesis of high value-added glycerol derivatives, i.e., esters, acetals and orthoesters of glycerol. Initially, the acetylation of glycerol and glycerol acetals with esters (in lieu of the commonly used acetic acid and acetic anhydride) in continuous flow was developed. A thermal, catalyst-free, continuous flow protocol allowed to reach high conversions of the substrates. Among the different esters that were tested, isopropenyl acetate (iPAc) showed the highest performance, affording quantitative yields in marketable products such as Solketal acetate and triacetin. The better performance of iPAc is due to the fact that it promotes an irreversible esterification process caused by the release of acetone. Next, tandem acetalization of glycerol with the acetone released in situ was studied. This reaction did not proceed satisfactorily under catalyst-free conditions. The direct synthesis of Solketal acetate by tandem acetalization-acetylation reactions of glycerol with isopropenyl acetate was therefore explored using Amberlyst-15 as acid catalyst. By addition of acetic acid and/or acetone as co-reactant, the selective synthesis of Solketal acetate or of a 1:1 mixture of Solketal acetate and triacetin was attained.

Finally, new bio-based glycerol derivatives by reaction with orthoesters were investigated. The reactions of glycerol with this class of compounds – only scarcely explored in the 60s – yielded the first regioselective

synthesis of 5-membered ring diastereoisomeric derivatives of glycerols through a catalyst-free procedure.

In summary, more environmentally friendly and more sustainable chemical processes should encompass as many as possible of the principles of green chemistry. In our case the use of renewable reagents deriving from low-value feedstocks, the use of greener catalytic systems (or catalyst-free condition when appropriate), of greener solvents (or no solvents when appropriate), easier product recovery, more intensified processes such as continuous-flow syntheses and higher reaction efficiency were all combined in the present thesis toward this goal.

INDEX

List of abbreviations

AcOH	Acetic Acid
Ac_2O	Acetic Anhydride
AE	Atom Economy
APIs	Active Pharmaceuticals Ingredients
AsTC	Assisted tandem catalysis
AuTC	Auto tandem catalysis
BD	BioDiesel
BGE	Butyl Glycidyl Ether
BMIm	Butyl Methyl Imidazolium
BPR	Back-Pressure Regulator
BTX	Benzene-Toluene-Xylene
CCS	Carbon Capture and Storage
CCU	Carbon Capture and Utilization
CE	Carbon Efficiency
COCs	Cyclic Organic Carbonates
DMC	Dimethyl Carbonate
DMS	Dimethyl Sulfate
DOC	Direct Oxidative Carboxylation
EC	Ethylene Carbonate
E-Factor	Environmental Factor
EO	Ethylene Oxide
EMA	EMergetic Analysis
EMY	Effective Mass Yield
EPA	Environmental Protection Agency
ESO	Epoxidized Soybean Oil
FAMEs	Fatty Acid Methyl Esters
F	Flow
GAs	Glycerol Acetals
GDC	Glycerol Dicarbonate

GHG	GreenHouse Gases
Glyc	Glycerol
GOST	Green Organic Synthesis Team
HBD	Hydrogen Bond Donor
HT	High-Temperature
iPAc	IsoPropenyl Acetate
IUPAC	International Union of Pure and Applied Chemistry
LCA	Life Cycle Assessment
MTO	Methanol To Olefins
$[N_{4,4,4,4}]$	Tetrabutyl ammonium
$[N_{8,8,8,1}]$	Trioctyl Methyl Ammonium
OB	OxyBromination
OTC	Orthogonal tandem catalysis
$[P_{4,4,4,4}]$	Tetrabutyl Phosphonium
PC	Propylene Carbonate
PEG400	Polyethylene Glycol 400
PEG DME 500	Poly(Ethyleneglycol) Dimethyl Ether
PI	Process Intensification
PMI	Process Mass Intensity
PO	Propylene Oxide
RME	Reaction Mass Efficiency
SCF	Supercritical Fluid-Based
SolkAc	Solketal Acetate
SO	styrene oxide
Sty	Styrene
TBHP	Tert-Butyl Hydroperoxide
TIL	Tungstate Ionic Liquids
TILC	Tungstate Ionic Liquid Catalyst

Io faccio il mio e non lo faccio né per loro e né per l'oro,

lo faccio solamente perché sinno me moro

- Danno, Colle Der Fomento -

1 Introduction

1.1 Green chemistry: the current state

"Green chemistry efficiently utilizes (preferably renewable) raw materials, eliminates waste and avoids the use of toxic and/or hazardous reagents and solvents in the manufacture and application of [designed] chemical products"[1]

This quote from Sheldon may encompass the concepts underpinning a profound overhaul begun in the world of chemistry around thirty years ago and formalized by Anastas and Warner of the US Environmental Protection Agency (EPA) with the twelve principles of green chemistry, in 1998.[2]
These principles can be summarized and listed in few keywords (Table 1.1):

Table 1.1: The 12 principles of Green chemistry

	Green Chemistry Principle
1	Prevent waste formation
2	Atom Economy
3	Less hazardous chemical synthesis
4	Designing safer chemicals
5	Safer solvents and auxiliaries
6	Design for energy efficiency
7	Use of renewable feedstocks
8	Reduce derivatives
9	Use of catalysis
10	Design for degradation
11	Real-time analysis for pollution prevention
12	Inherently safer chemistry for accident prevention

The birth of green chemistry at the end of the twentieth century does not mean that the research on environmentally friendly chemistry did not exist before, merely that it did not have a name. Green

chemistry has been the politic and scientific answer to a genuine problem and to an ever-increasing mistrust of common people towards science, particularly chemistry.[3] The wellbeing of our society is strongly based on chemical industry and we all stand to benefit: suffice to say that more than 100000 chemical products are actually obtained from raw materials while the production capacity of the global chemical industry reaches some 2.3 billion tons in 2017, equivalent to 300 kilograms of chemicals per year for every person in the planet.[4] At the same time, mistrust towards chemistry had (and partly still has) its justified reasons as supported by many examples: the chemical disaster for methyl isocyanate release in Bhopal in 1984, where 4000 people were killed and more than 40000 injured; the *Exxon Valdez* and *Deepwater Horizon* oil spill, in 1989 and 2010 respectively, which still affect the marine ecosystem nowadays; the dioxin spills from chemical manufacturing plant in Seveso (Italy) and Times beach (Missouri) in 1976 and 1982, respectively; the release of cyanide and heavy metals into Danube river from a gold processing plant in Baia Mare (Romania) in 2000; the tragic birth defects from thalidomide; the leakage of toxic chemicals from a dumping ground of chemical waste produced by the Hooker chemicals and Plastics Corporation in the 1940 and '50s in Love Canal, New York; the repeated scandals related to the illegal waste dump in developed countries and the illegal exports of wastes in developing countries.[5] Not to mention the opacity of science to the general public due to the uncountable cases of funding publication bias, i.e. the tendency of scientific studies to support the interests of the financial sponsor.[6]

Chemists must contend with the past mistakes and tend not to repeat them. Green chemistry must represent an answer to well-known practical issues that will be faced in the short term:

- **Fossil resources are not endless**

Non-renewable sources are limited by definition, as first underlined by Meadows et al. [7]: fossil fuels account nowadays for about 80% of the world's energy supply while the chemical sector is the largest single industrial consumer of oil and natural gas accounting for 15% of total primary energy demand.[8] Estimates indicate that the existing supplies of petroleum, natural gas and coal will last for the next 45, 60 and 120 years respectively at the current consumption rates.[9]

Beyond the long-standing question on depleting fossil fuels, an increased awareness of the issue of chemical elements scarcity (Figure 1.1) – related also to the pollution caused by elements mining, to the recycling rates of each element and to their overuse in smart technologies – has grown tremendously in the past decades.[10] The recover, reuse and recycle of not-renewable raw materials and the shift to renewable feedstock are compulsory in the near future.

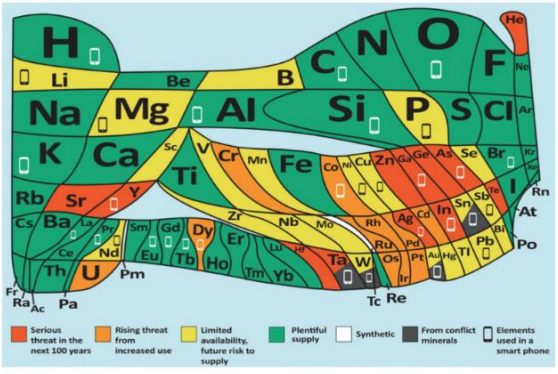

Figure 1.1: 90 elements that make up "everything" and their relative abundance on earth.[11]

- **Our planet will not bear an endless increase of waste burden**

In the past century waste production has risen ten-fold while the world's population has quadrupled. Waste generation will drastically outpace population growth and it is likely to grow by 70% by 2050 unless action is taken.[12] Plastic wastes choke the world's oceans and rivers, while rubbish is generated faster than other environmental pollutants, including greenhouse gases (GHG). The majority of waste goes to landfill or is merely incinerated instead of being recycled or reused. Another tremendous problem is related to the dizzying increase of electronic waste (e-waste) which often contains precious and/or low-availability metals that are quite challenging to be recovered and recycled.[13] E-waste may represents only 2% of solid waste streams yet it can represent up to 70% of the hazardous waste that ends up in landfill.[14]

Figure 1.2: "First world" countries are using Africa as a dump for old electronics

More than 50 Mtonnes of e-waste are produced every year in developed countries which legally or illegally send their e-waste in the developing countries taking to issues related to social injustice, environmental pollution and hazardous methods used by people that work by necessity on the recovery of metals from e-waste (Figure 1.2).[15] The concept of waste does not exist in nature, it is a human-based concept and we need to mimicking the natural systems by using waste as resources.

- **Environmental pollution is at the highest levels**

At an average growth rate of 2.6%/y (2000-2014) and with a yearly production of ca 35 gigatons,[16] anthropogenic CO_2 is among the major causes of global warming with average temperatures predicted to increase up to 2-4°C by 2100 (relatively to the pre-industrial level).[17] This will lead to a rise of the mean sea level and the probable disappearance of species that will not be able to adapt.

Green chemistry can be applied to decrease carbon dioxide emissions from chemical productions and processes and eventually reuse the CO_2 emitted and put it back in a closed carbon loop. The anthropogenic pollution of our atmosphere must be stopped since this increasing growth is NOT SUSTAINABLE. Sustainability is a concept that emerged before the conceiving of green chemistry and it will be deepened in the next paragraph.

1.2 Sustainability and sustainable development

The adjective "sustainable" derives from ancient Latin and implies the capability of something being maintained in existence without interruption or diminution. The environmental conceptualization of sustainability has a longtime history: a proverb attributed to native American indigenous cultures states that "We have not inherited the earth from our fathers, we are borrowing it from our children" while yet in 1901, Theodore Roosevelt declared "What we do will affect not only the present but future generations," speaking about the conservation of the Nation's natural resources in his first message at the congress of the United States of America. The official birth of sustainable development dates back to 1987 with the release of the "Brundtland Report – Our Common Future" written by the World Commission on Environment and Development in which it is declared that sustainable development "meets the needs of the present without compromising the ability of future generations to meet their own needs."[18]
Since its appearance, this definition was discussed, analyzed and adapted to the advantage of a wide series of individual and organization actors.[19] Sustainability is on everyone's lips (Figure 1.3).

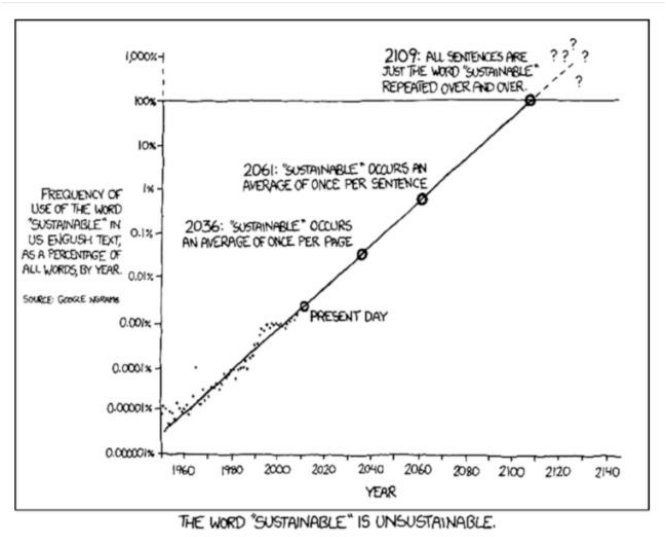

Figure 1.3: The unsustainability of sustainability. [20]

The beneficial effect of the widespread use of this term is evident: a key environmental concept is widely more comprehended and accepted than ever before. Meanwhile, there is an increasing tendency to talk about "sustainababble" in place of sustainability, a pun used for the first time by Engelman to indicate that the term sustainability is losing its meaning and impact through its overuse.[21] The term sustainability goes hand in hand with the practice called *green washing,* indicating the unjustified claim of environmental virtue by companies, industries, political entities or organizations to gain a positive image for themselves, their products and their businesses.[22] This has resulted in strong disputes on the definition of sustainable development, reduced to a quasi-rhetorical term or a "catch-phrase", to the point that the terms sustainability and sustainable development are practically counterposed.[23] For sure, environmental sustainability and economic development are different objectives that need to be understood separately before they are related: as G.H. Brundtland advocated in *Our Common Future* sustainable development

should lead to an enhanced cooperation respect to that imagined in a world currently driven by competition and individual accumulation of wealth.[24] Human activity should recognize its limits: the impossibility of indefinite growth in a finite world[7,25] and the assured depletion of limited resources if the constant increase of world population will be intrinsically related to growing consumption of these resources.[26] In this case demographic and economic growth will undoubtedly drive an increase in pollution and GHG emissions. The validity of the endless sustainable economic growth relies on the assumption that green growth could be decoupled from energy use and natural resources exploitation through technological development and increased efficiency, but this aspiration is to say the least, optimistic: a recent report on decoupling technologies from the European Environmental Bureau concluded that they are "a haystack without a needle".[27] In this sense, sustainability calls for a change in paradigm that breaks with the linear model of growth: we must appreciate that development is wider than growth and that in a limited world we can develop but we cannot grow limitless (at least until we will have only one planet!).

Despite the clear advancements achieved from the introduction of the debate on sustainable development are undeniable,[28] the basic global trends remain clearly and measurably unsustainable.[29] We are aware to live in Anthropocene, an era in which humankind is the main force shaping the future of life and where nature cannot be walled-off from human influence.[30] Precisely this awareness should encourage us to meet overall needs instead of a reductionist anthropocentric focus based solely on human needs. [31] We should pursue a tangible and truthful sustainability, although it may seem don quixotic. Lower GHG emissions is fundamental as well as strive for a "zero-emissions scenario" respect to an unconceivable "Business-as-Usual" scenario that foresees a mean temperature increase of 4 °C by 2100.[32] If this should occur, Business-as-Usual will have run its course much earlier (Figure 1.4).[21]

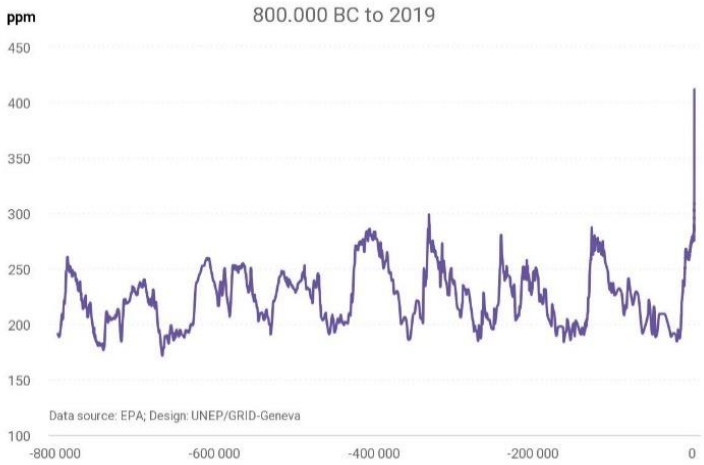

Figure 1.4: CO_2 emissions from 800000 BC to 2019 [32]

This discourse and these concepts on sustainable development could be applied to various subcategories such as sustainable cities, sustainable agriculture, sustainable architecture, sustainable engineering… and sustainable chemistry. Sustainable chemistry is a term that someone wants to match with green chemistry, while others are inclined to see substantial differences.[33] If sustainable chemistry is defined as

a chemistry that "meets the needs of the present without compromising the ability of future generations to meet their own needs", any chemist could say that industrial chemical production is presently un-sustainable .

The conceptual basis on which chemistry should be grounded to be green and sustainable will be detailed in the next paragraphs.

1.3 Designing a Green Sustainable chemistry future: green metrics and system thinking

"You cannot manage what you do not measure" is an old business adage. While, sometimes we have to manage things that are non-measurable and that we cannot quantify, the fact remains that metrics matter.
Green chemistry includes this concept since its birth and has established a series of metrics that allow a tangible measurement of the greenness of a process. From an historical viewpoint the original chemical metric has always been percentage yield: a process is good if the product yield is high. As a traditional metrics it looks at only one aspect instead of the overall system. Similarly, green chemists exploited a series of parameters to assess greenness of a process and to compare it with others in a simple but quantitative approach. The Clark group summarized green metrics in a comprehensive list of 60 different metrics.Here some of the most relevant green metrics are reported (table 1.2).[34]

Table 1.2: Examples of Green Metrics

Metric	Acronym	Formula
Atom Economy	AE	$\frac{Molecular\ Weight\ (MW)\ product}{\sum MW\ reagents} \times 100$
Carbon Efficiency	CE	$\frac{Carbon\ Mass\ in\ product\ [Kg]}{\sum Carbon\ Mass\ in\ reagents\ [Kg]} \times 100$
Reaction Mass Efficiency	RME	$\frac{Mass\ Product\ [Kg]}{\sum Mass\ Reagents\ [Kg]} \times 100$
Process Mass Intensification	PMI	$\frac{Total\ Mass\ in\ a\ Process\ or Process\ Step\ [Kg]}{Mass\ of\ Isolated\ Product\ [Kg]}$
Environmental Factor	E	$\frac{Total\ Waste\ [Kg]}{Product\ [Kg]}$
Effective Mass Yield	EMY	$\frac{Mass\ Product\ [Kg]}{\sum Mass\ Non\ Benign\ Reagents\ [Kg]} \times 100$

Atom Economy (AE) measures the degree of incorporation of reactants in the desired products but does not consider the yield or the nature of the waste. Carbon Efficiency (CE) and Reaction Mass Efficiency

(RME) combine the concepts of AE and Yield, while Process Mass Intensity (PMI) takes into account the mass of all the materials used in a synthetic route (including solvents and catalysts), yet still none of them contemplate the waste. The historical route to calculate the waste is the Environmental Factor (E-Factor) that measures the amount of waste generated for each kg of desired product. Different amounts of waste and E-factor depend on the industrial sector that is considered (Table 1.3)

Table 1.3: Waste produced in various Industry sector [35]

Industry Sector	Annual production (tonn)	E-factor	Waste produced (tonn)
Oil Refining	10^6 - 10^8	≈ 0.1	10^5 - 10^7
Bulk chemicals	10^4 - 10^6	< 1 – 5	10^4 – 5 x 10^6
Fine Chemicals	10^2 - 10^4	5 - 50	5 x 10^2 – 5 x 10^5
Pharmaceuticals	10 - 10^3	25 -200	2.5 x 10^2 – 10^5

The E-factor is essential and should be minimized in every industry sector, despite it does not take into account the nature of the waste. Sheldon attempted to use the environmental quotient to consider the E-factor and its intrinsic hazard[36], while Hudlicky et al. makes a distinction between benign and non-benign reagents for a mass metric, i.e. effective mass yield (EMY).[37] However, the design of a scale of benignity with shared and well-defined values for every single reagent and/or waste remains hard. No metrics should be assessed by itself, but rather a holistic approach should be used to evaluate the overall green credentials of a process. This was attempted at the University of York by developing a metric toolkit that indicated the prominence of quantitative metrics, while bearing in mind that qualitative factors should also be included with a view on sustainability.[38] The renewability of feedstock, the toxicity of a molecule, the market and social acceptance of an energetic technology, the environmental justice implications of a factory siting are all qualitative aspects that must be take into account.[39] Irrespective of the use of quantitative or qualitative analysis, chemists should abandon a typical reductionistic approach and pursue an improved holistic design in such a complex and dynamic system.[40] As early as 1972, the future Nobel physics prizewinner P.W. Anderson warned against the reductionistic and compartmentalized approaches that have resulted in impressive advantages but also unwanted and harmful consequences, lacking mental resilience:

> *"The arrogance of the particle physicists and their intensive research may be behind us (the discoverer of the positron said "the rest is chemistry"), but we have yet to recover from that of some molecular biologists, who seem determined to try to reduce everything about the human organism to 'only" chemistry, from the common cold and all mental disease to the religious instinct. Surely there are more levels of organization between human ethology and DNA than there are between DNA and quantum electrodynamics, and each level can require a whole new conceptual structure."*[41]

Currently, we are more aware of this: systems must be considered in their entireness to avoid solutions that simply shift the impacts or lead to undesired effects. The integration of system thinking in green chemistry is mandatory to address the complexity of the interconnections between the traditional and

innovative aspects of chemistry and sustainability.[42] An integrated holistic approach can bring to the comprehension of the various components and connections of human and natural systems, eventually mitigating the adverse consequences that result from the way that we, as chemists, have pursued our craft.[43] This concept and the related mistakes are well highlighted by Paul Anastas who refers to "doing the right thing wrong" and who described some simple examples[40]:

- Disinfection of water supply from pathogens, that ended up killing thousands of people every year with disinfectant substances that release by-products that are persistent, toxic, carcinogenic [44]
- Increased agricultural production by exploiting fertilizers and pesticides which contaminated aquifers, led to eutrophication, harmed biodiversity and ecosystem functions[45]
- Replacement of toxic bisphenol-A with bisphenol-S: recent studies proved the same toxicological concerns[46]
- Development of life-saving drugs that whilst increasing the quality of life and expectancy, contaminated wastewater at biologically active levels[47]
- Development of photovoltaics and wind turbines that capture the power of sun and wind relying on toxic, depleting materials and/or rare metals
- Pursuing biofuels that reduce fossil fuels dependency with 1st generation biofuels that compete with food and land use

The performance of a product should be assessed through a holistically extended approach to "Do the right thing well". Since the introduction of the first industrial chemical products, their performances were defined as the ability to efficiently accomplish a function. An extended meaning of performance should contain the inherent nature of chemicals embodied in the absolved function, including that products are non-depleting, nontoxic and non-persistent in the environment.[48] In this sense, the F-factor has been recently introduced, a metric that seeks to quantify the wish to have a desired function with the lower amount of a (preferably benign) chemical used.[49]

In conclusion, the conceptual basis of green chemistry are metrics: the ones introduced above are simple and single-sided metrics. More sophisticated and wide-spanning conceptual tools that chemists can use to understand the complexity and validity of a process are Life Cycle Assessment (LCA) and EMergetic Accounting (EMA).

LCA is a methodology for assessing impacts associated with all the stages of the life cycle of a commercial product, process or service. It stems from the awareness that processes generate impacts in all steps of their lifetime and it is considered a "cradle-to-grave" or "cradle-to-cradle" methodology if it includes also the recycling and reclamation of degraded environmental resources.[50] LCA can be coupled to EMA which provides complementary results. EMA is based on the concept of Emergy, a term derived from EMbodied enERGY and conceptualized for the first time by Odum, one of the most brilliant scientists in systemic analysis. Emergy is defined as the available energy of a kind directly or indirectly used in the transformations that generate a product or a service. [51] From a conceptual viewpoint, EMA shifts the attention from the value attributed to a product by the end-user (receiver-side value) to the real value invested upstream to create the product (donor-side value).[52] Recently, emergetic analysis has been used in large-scale chemical production systems such as production of bio-ethanol[53], a bio-gas-plant[52] and the comparison of various Carbon Capture and Utilization (CCU) processes.[54] Such holistic perspectives and approaches are needed to address complex global problems: LCA, emergy and system thinking represent

unique conceptual means to encompass all the aspects required by an integrated analysis of the sustainability of any system.[55]
In this context, another compulsory conceptual paradigm shift is the transition from a process linearity to a circular perspective in the chemical sector, as elegantly illustrated by Zimmermann et al. recently (Figure 1.5).[56]

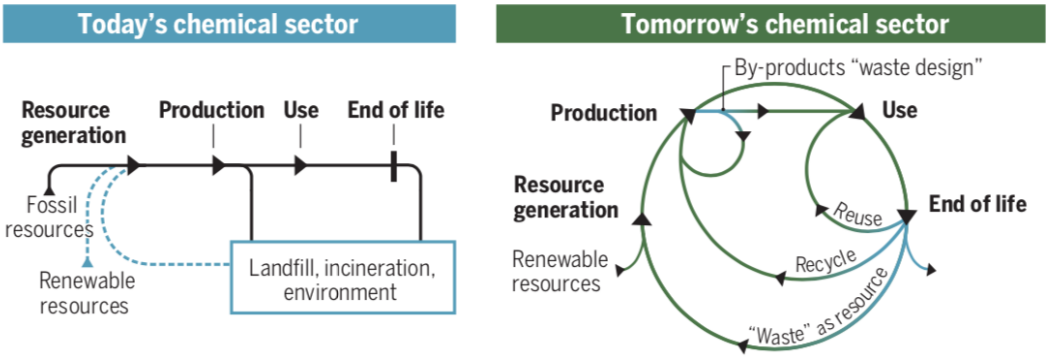

Figure 1.5: Characteristics of today's and tomorrow's chemical sector

Resources (fossil or renewable) should not be considered input for the synthesis of chemical products which go to landfill or incineration and only partly recycled at their end life. In a circular perspective, target molecules are synthesized in a benign way decreasing as much as possible the formation of by-products upstream (and thinking simultaneously to their reuse in other segments) while the long-life products are conceived to be reused, recycled and rescued as resources at the end of life. While the history of chemical production is essentially linear (take-make-waste), it is fundamental that it turns into a circular system in which materials and energy flows remains internal to the cycle.

1.4 Designing a Green Sustainable chemistry future: the practical basis

To achieve the conceptual objectives of green chemistry, four main application fields can be imagined by paraphrasing the initial citation by Sheldon[1]:

1.4.1 Use of renewable feedstock

Renewable feedstocks derive from sources that are naturally replenished at a higher rate than they are consumed. A principal raw material for chemistry is biomass. This is defined as any organic decomposable matter derived from plants or animals available on renewable basis. Biomass feeds for biofuels and biochemicals production mainly consists of three major categories: [57]

- Lignocellulose and -starch based plants
- Triglyceride sources and microalgae
- Terpenes and rubber-producing plants

Biomass in aggregate is composed of ca 75% carbohydrates or carbohydrate polymers (e.g. starch, cellulose, hemicellulose, including animal-based chitin), 20% lignin and around 5% of fats, terpenes, waxes and proteins.[58]
The direct exploitation of such renewable feedstocks for the production of biofuels and biochemicals poses concerns about the competition with food, land use and water use, and it is actually discouraged if not excluded at all.[59] For this reason the use of waste (agricultural, industrial, municipal or animal, Figure 1.6) becomes critical as a renewable feedstock, especially arguing that waste represent a costs instead of a resource nowadays.

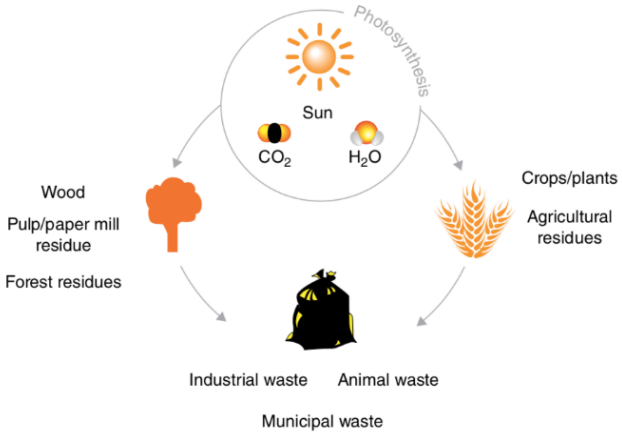

Figure 1.6: Use of waste as renewable feedstock

As already stated, waste is a human-centered concept. It is instead crucial to mimic the nature where the "waste" of a process nourishes, sustains and strengthens another one. There is hence a renewed interest into resources that are currently viewed as waste (especially agricultural and industrial residues) but also towards dedicated crops that do not compete with food and land use, such as algae which yield high amounts of lipids (i.e. triglycerides) with an increased productivity for land and water unit respect to other plants, even if processing and logistical challenges could lead to significant lifecycle impacts.[60] Figure 1.7 reports examples of renewable building block chemicals. The main classes are:

- Biobased Syngas, produced by subjecting biomass to extreme heat, typically 800-1500°C.[61]
- C_2-C_6 oxygen-rich small molecules (ethanol, glycerol, Propionic acid, 1,3-propanediol, butanol, 5-(hydroxymethyl)furfural, succinic acid, lactic acid, itaconic acid, levulinic acid, 2,5-Furan dicarboxylic acid, etc.)[61]
- Low molecular weights aromatic molecules from lignin (in particular phenol, phenol derivatives and benzene-toluene-xylene (BTX))[62]

- CO_2 (not shown in the figure) that can be exploited to synthesize urea, cyclic organic carbonates (COCs), C_1 small molecules (methanol, formic acid, formaldehyde) and C_2-C_4 olefins.

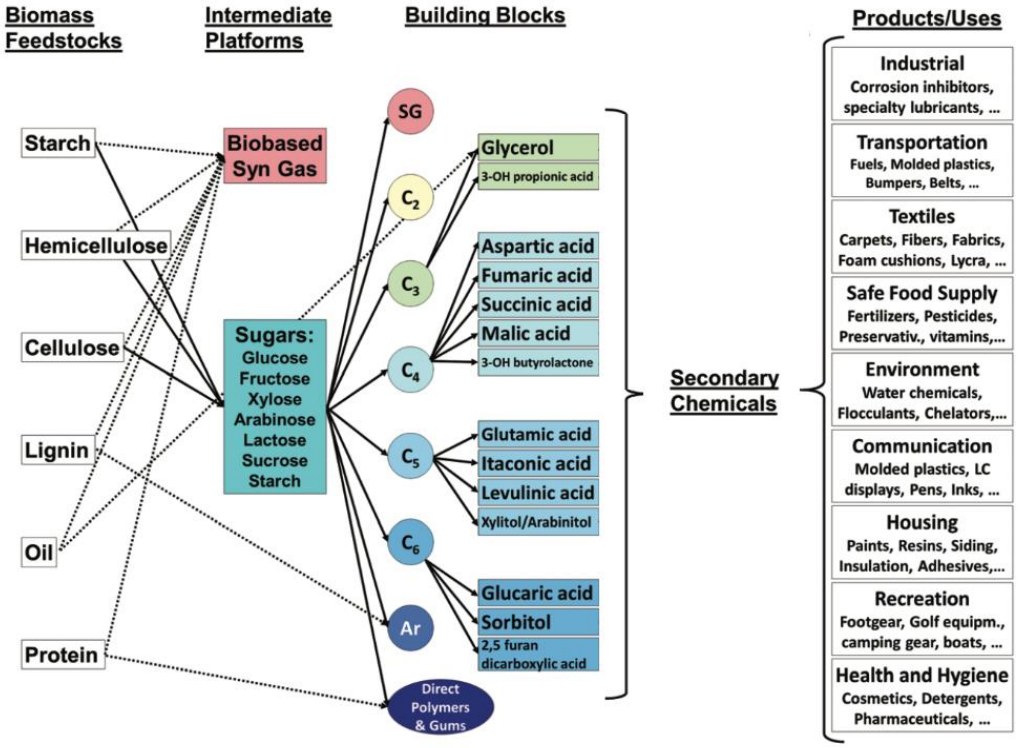

Figure 1.7: Examples of building blocks from renewable feedstocks[48]

Two waste feedstocks represent the fundamental starting material for this thesis work: carbon dioxide and glycerol. For this reason, their history and current status is described more in-depth in the following sections.

1.4.1.1 Carbon dioxide

Despite its existence has been known for over thousands of years, carbon dioxide was first recognized as a distinct gas by Van Helmont in the XVII century.[63] The French chemist Lavoisier first named it carbonic acid, discovered that it is produced by the combustion of carbon in presence of oxygen and that it contains 23.5-28.9 parts by mass carbon and 71.1-76.5 parts by mass oxygen.[64] Only a hundred years later the vital importance of carbon dioxide began to outline with the study of Julius Sachs on the photosynthesis reaction that converts CO_2 into glucose.[65] Despite the natural occurrence of carbon dioxide in the earth's lithosphere, hydrosphere and atmosphere, carbon dioxide is mainly seen as an enormous issue nowadays due to its massive anthropogenic production for electricity and heat generation, transport, and industrial uses. More than half of the CO_2 emitted form chemical industry comes from ammonia and hydrogen production.[8,63]

Thus, CO_2 use and its sequestration seem like a must to comply with the goal to reduce GHG emissions and keep the global average temperature increase below 1.5°C.[66] In the last years, the scientific world and

governments have proposed two principal CO_2-based technologies aiming at mitigate climate change: Carbon Capture and Storage (CCS) and Carbon Capture and Utilization (CCU).[67] In CCS, CO_2 typically emitted from large scale sources is captured, transported and permanently stored underground such as in depleted oil and gas fields.[68] CCU provides for the exploitation of a different set of technologies in which CO_2 is captured and used as feedstock for the production of chemicals, fuels or construction materials.[69]

CCU is a chemically fascinating field, since 2014 only 0.36% of global CO_2 emission has been used as feedstock for chemical production, hence there are limitless opportunities to improve CO_2 utilization.[70] Notwithstanding, recent studies showed the complexity of CCU and demonstrated that the chemical conversion of captured CO_2 will hardly account for more than 1% of the mitigation challenge.[71] Although CCU will not resolve issues related to the excessive anthropogenic emissions of CO_2, it is undeniable that CO_2 is a chemically attractive, abundant, renewable and non-poisonous C1 feedstock useful for the synthesis of various classes of compounds, such as carboxylic acids and derivatives, alcohols and organic carbonates.[72] The main CO_2 fixation products are reported in Figure 1.8.

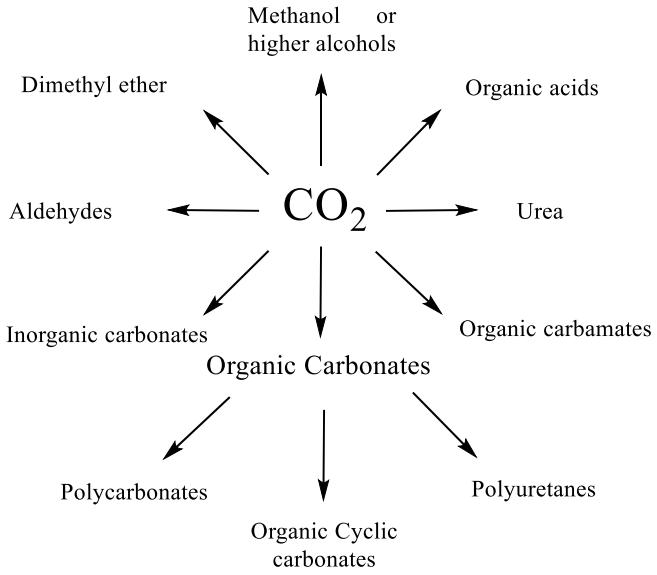

Figure 1.8: Main products of CO_2 fixation

The use of carbon dioxide as a C_1 synthon poses however challenges due to its thermodynamic stability and kinetic inertia. The former implies a large energy input that could generate more carbon dioxide than is consumed, while the latter requires the presence of catalysts able to activate CO_2 (e.g. Lewis base such as superbases [73], -hydroxyl or -amines containing species [74], n-heterocyclic carbenes [75], or transition metal for the formation of complex with CO_2[76]) and the use of highly-reactive substrates such as alkenes or alkynes [77], three membered rings (e.g. epoxides and aziridines [78]) or organometallics [79] to yield more thermodynamically-stable oxygenated products. In this context, a continuous effort has been done in the last years to identify bifunctional catalysts capable of contemporarily activating CO_2 and the substrate. Such robust single- or two-component systems are becoming the mainstay in the field of CO_2 chemistry.[80]

1.4.1.2 Glycerol

Glycerol is a clear, colourless, odourless and sweet-tasting viscous liquid, first identified in 1779 by the Swedish chemist Carl W. Scheele who obtained it by heating olive oil with litharge (PbO). [81]

It was originally obtained as a by-product of the soap industry. Thereafter, during the First World War, it was prepared also through microbial sugars fermentation until the early '40 when petroleum-based glycerol gained the upper hand, especially through the epichlorohydrin process from propylene.[82]

Today, such synthetic processes are outdated due to glycerol being obtained as a co-product of biodiesel manufacturing. Biodiesel (BD) is composed by fatty acid methyl esters (FAMEs) produced through the transesterification of triglycerides with light alcohols, such as methanol, conventionally catalysed by homogenous base catalysts.[83] This reaction takes to the co-formation of glycerol (Scheme 1.1): whatever the technology and the feedstock used, it is observed that approximately 10 wt% of the products consist of glycerol and around 3 million tonnes resulted in 2016 as by-product of biodiesel manufacture.[82] This fact implied an overproduction of glycerol respect its actual uses that encouraged academic world and chemical producers to look for its conversion in useful chemicals.

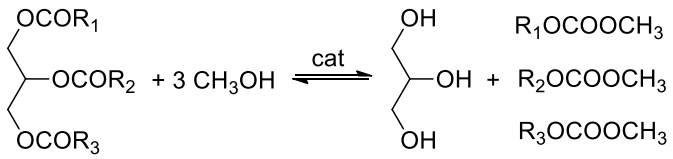

Scheme 1.1: Synthesis of Biodiesel

A remarkable issue for the exploitation of glycerol obtained from biodiesel is the low grade of the product. After the transesterification of natural TGs, the streams of (crude) have variable compositions, usually containing <65 wt% glycerol, 15-50 wt% MeOH, 10-30 wt% water, 2-7 wt% salts (primarily NaCl and KCl derived from the catalyst neutralization).[84] Therefore, crude glycerol must be usually purified before further processing. This implies rather energy-intensive operations like evaporation, desalting, ion exchange and distillation steps to achieve a technical (>90%) and pharmaceutical grade (>99.7%) product,[85] meaning that it is generally not worth refining glycerol unless it is employed as a platform chemical for the synthesis of high-added value products. An alternative route is the implementation of reactions for the direct transformation of raw glycerol followed by the isolation of the obtained products. This sequence, though more difficult to accomplish, is often cheaper and simpler than refining the crude reagent and then proceeding with its upgrading.

Glycerol is nontoxic to both humans and the environment and it has unique physical and chemical properties due to its three hydroxyl groups that are responsible for its solubility in water and alcohols, its hygroscopic properties, low volatility, low vapor pressure and its chemical reactivity mostly as an O-nucleophile. The most promising routes for glycerol conversion and the traditional applications for industrial glycerol are summarized in Figure 1.9. [81,86]

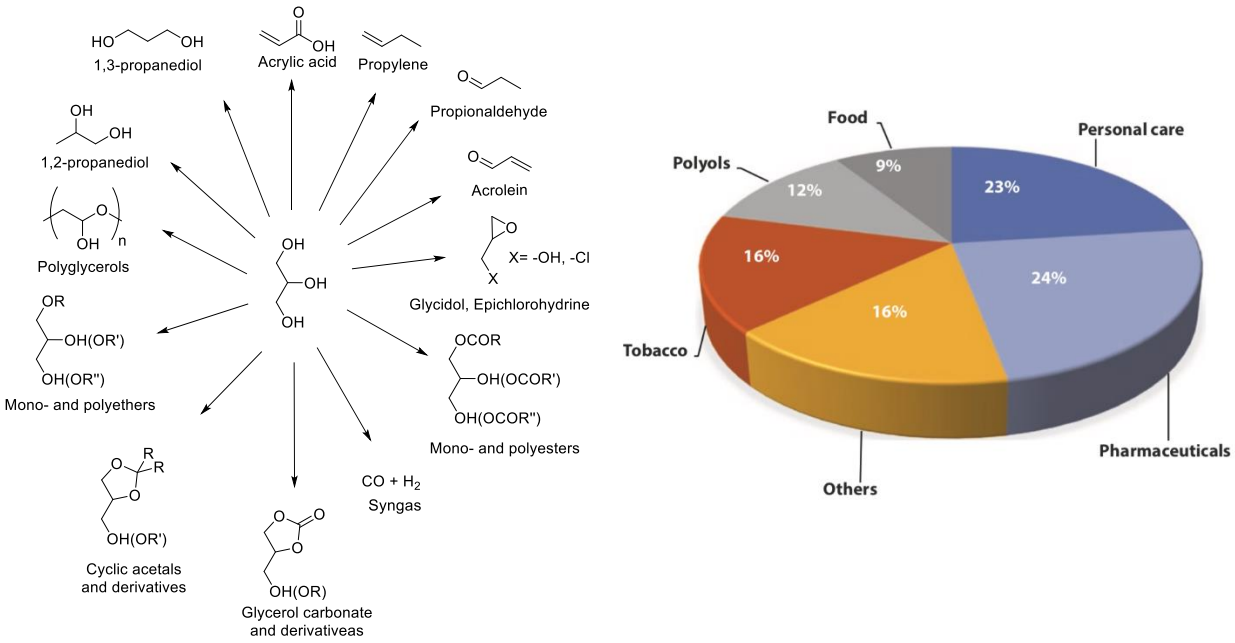

Figure 1.9: Most promising glycerol derivatives and traditional applications of industrial glycerol

1.4.2 Eliminate waste (better prevent than treat)

As mentioned before, it is mandatory to change our paradigms and transform waste into resources. We have however to avoid a pitfall: this does not mean that it should be possible to produce waste as usual (or more) since it is a resource. It is fundamental to rethink chemical syntheses and production routes that generate too much waste or by-products. To give an example, the E-factor of pharmaceutical industry is between 25 and 200, that is 25-200 kg of waste are generated for each kilo of active pharmaceutical ingredient (API) produced. A continuous effort to decrease these values is essential for chemists today and recent examples such as the synthesis of sertraline, diazepam and atropine, demonstrate that it is possible.[48,87] E-factor in the oil refining industry is in the range of 0.1 , meaning that almost all the oil finds a marketable application. We argue that renewable feedstocks must tend to the same goal since waste (irrespective of its nature) consumes resources, time, energy and money whenever it is created , handled and managed, particularly when it is hazardous and requires larger investments.

Various approaches can lead to this goal: one-pot processes which avoid isolation and purification of chemical intermediates, thereby reducing the amounts of solvents and separation steps[88]; process intensification to improve yields, quality of the products and process efficiency redesigning plant complexity, size and equipment units[89]; reactions conducted in the absence of solvents or auxiliary substances whenever possible[90]; green extractions based on the design of processes which reduce the quantity of solvents, energy consumption and that use alternative green/renewable solvents[91]; molecular self-assembly and self-separation to induce spontaneous reactions with lower utilization of resources to drive the system; integration of technologies and processes for heat, energy and waste recovery as starting point for other reactions. Some of these tools will be described in the next section.

1.4.3 Avoid the use of toxic and hazardous reagents

This aspect represents a basic precept of green chemistry. The International Union of Pure and Applied Chemistry (IUPAC) defines green chemistry as "the invention, design and application of chemical products and processes to reduce or to eliminate the use and generation of hazardous substances".[2] Green chemistry is thereby a hazard-based approach that focuses on minimizing hazard instead of circumstances and boundary conditions. To better explain this concept is important to introduce the concept of **risk**:

Risk = Hazard x Exposure

The traditional approach to risk reduction provides for the reduction of the exposition to hazard substances. This approach is often unsuccessful since accidents happen (e.g. equipment break down, human error, etc.) and in this case the risk is maximized. Green chemistry provides for the reduction of the risk by decreasing the hazard associated to the chemical product and transformations. In this way, the uncontrolled expositions to risks remains tolerable also in case of accident.
This concept can be included in the benign-by-design one: if chemicals (used and produced) are designed to be benign for humans, animals and the environment, the risk will always be low. Inherent safety must be included along with the desired function: as an example, it is important to design end-of-life biodegradability into a chemical product and its absence of toxicity, ecotoxicity or other adverse effects from the drawing-board of the process.

1.4.4 Synthesis of alternative green target molecules

As shown in Figure 1.7, bio-based building blocks obtained from renewable sources have a distinctive difference respect to fossil-based building blocks: they already contain O-based functional groups. Renewable feedstocks are essentially oxygen-rich molecules (50-75% C, 6-13% H, 11-44% O) if compared with fossil based-feedstock (85-89% C, 10-14% H, <1% O).[48] . Petroleum-based feedstock are represented primarily by syngas (CO/H_2) and hydrocarbons such as, ethylene, propylene and BTX aromatics. These compounds are furtherly transformed in high-added value compounds by the addition of various functional groups. It is conceivable to transform renewable feedstock into the same building blocks and chemicals attainable by fossil sources. However, considering the structural differences of the feedstocks it would be clearly smarter to exploit renewable platforms to obtain different target molecules, albeit with the same (or similar) function to the fossil-derived ones. This attitude would be also a route to displace the use of chemicals considered hazardous and/or with environmental concerns in favor of new target molecules with the same functions but different molecular structures leading to a minor intrinsic harmfulness and an increased processing facility. The difficulty in achieving this objective is strongly related to the hurdles posed by displacement of well-implemented and profitable processes and business. In this context, the biorefinery concept is fundamental.

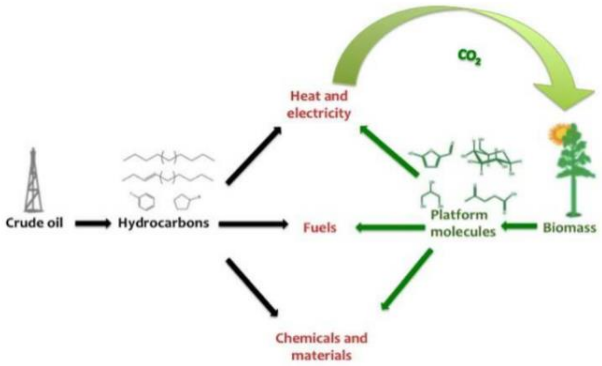

Figure 1.10: Pictorial comparison of petroleum and bio refineries

As shown in Figure 1.10, the aim of conventional or unconventional refineries is to obtain fuels, electricity, heat, chemicals and materials: the origin of platform molecules is less relevant compared to the function they fulfil. Moreover, the CO_2 co-produced by bio-factories should be recovered either by photosynthesis or by CCU within a "closed carbon loop" to limit GHG emissions.[92] The implementation of biorefineries that exploit biomass for the production of energy, fuels and renewable chemicals allows a potentially sustainable approach to the green transition problem, but they are still economically not-competitive compared to conventional refineries and can only merge onto the global market if they are forced to or if significant financial support is provided (e.g. governmental regulation, taxes reductions). Whatever the feedstock, technology and treatment used, energy, heat and biofuels are low-value products and, consequently, biorefineries will not be part of the global industrial sector unless they boost their profits by integrating the production of biofuels to that of high-added value biobased products.[93] In this perspective, biofactories will be designed to process biomass by first extracting relatively low volumes of surface chemicals and platform chemicals (high-value low-volume derivatives including nutraceuticals, insect repellents, cosmetics, etc.), and then by obtaining biofuels (low-value high–volume compounds) from residual organics.[94]

This Ph.D. thesis addressed the synthesis of two target chemicals: COCs and glycerol derivatives, i.e. glycerol acetals and esters.

1.4.4.1 Cyclic organic carbonates (COCs)

COCs find a plethora of applications as polar aprotic solvents, lithium ion-battery electrolytes, cosmetics, plasticizers, detergents and intermediates for polymers.[95] Owing to their biodegradability, lack of toxicity, and high boiling points bio-based COCs are considered greener alternatives to common fossil-based chemicals. Scheme 1.2 summarizes the main established routes to obtain cyclic carbonates from bimolecular reactions involving diols (a', a''), propargylic alcohols (b) and epoxides (c).

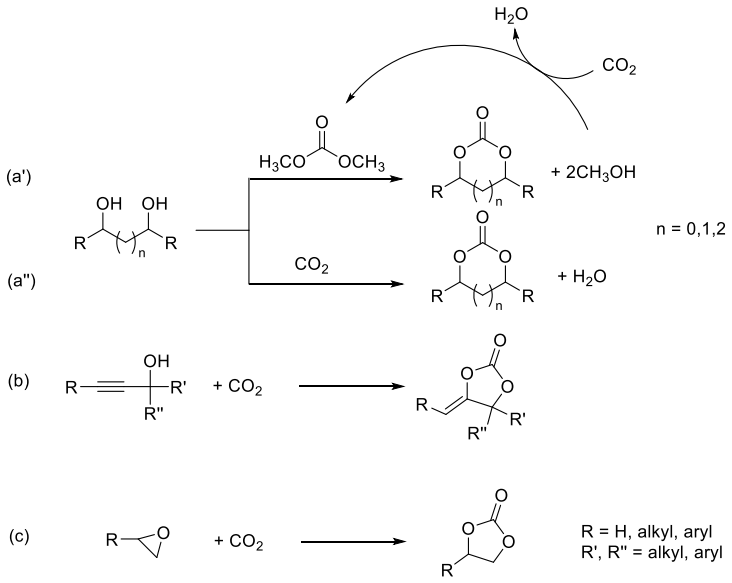

Scheme 1.2: Green synthesis of COCs through bimolecular reactions

The synthesis of COCs from diols and CO_2 can take place either indirectly by transesterification with dimethyl carbonate (DMC) accompanied by formation of methanol that can be converted back to DMC with CO_2 (Scheme 1.1a') [96, 97] or directly by incorporation of CO_2 with loss of water (Scheme 1.2a''). DMC can be seen as an environmentally friendly vector of CO_2 [98] which can be incorporated into diols and polyols from renewable resources. A number of homogeneous and heterogeneous catalysts were reported for the reaction of DMC with diols.[99] However, also clean catalyst-free protocols have been described to obtain cyclic carbonates selectively from the transesterification of DMC. We recently reported that operating under batch and continuous-flow modes, non-catalytic (thermal) procedures mediated by DMC were successful for the conversion of several diols and glycerol into the corresponding COCs and glycerol carbonate, respectively.[100] Diols and CO_2 can be coupled directly to obtain COCs (Scheme 1.2a'') by using metal- or organic-based catalysts but harsh conditions are needed and usually this route is strongly limited by the equilibrium that curbs conversion. Progress in this field is reviewed elsewhere.[101]

The direct, 100% atom economic synthesis of COCs with CO_2 is shown in Scheme 1.2b and 1.2c. The carboxylation of propargylic alcohols (Scheme 1.2b) with carbon dioxide – generally in the presence of Lewis acidic silver catalysts – yields COCs functionalized with exocyclic double bonds.[102] Most published reports are limited to easily cyclizable secondary and tertiary propargylic alcohols, with the exception of one recent work that describes the conversion of primary propargylic alcohols to exovinylene carbonates with high yields.[103] This procedure, however, can be hardly considered sustainable since propargylic alcohol is usually synthesized from formaldehyde (industrially obtained from methanol) and acetylene comes from the cracking of methane.[104]

The fixation of CO_2 into epoxides (Scheme 1.2c) is the most widely explored route for the synthesis of COCs. A large number of different catalysts (homogeneous, heterogeneous, metal- and organic-based)

are reported in the literature and summarized in recent review articles.[105] Notwithstanding the promise of this approach as indicated by the deployment on commercial scale of this route, the use of epoxides as chemical building-blocks can be considered neither safe nor green.[106] The industrially most relevant epoxides are ethylene and propylene oxides (EO and PO) which are produced respectively on a scale of 15 and 8 million tons/year from fossil-derived ethylene and propylene. The same non-renewable origin holds true for many other epoxides such as C_4-C_{10} linear aliphatic epoxides, isoamilene oxide, cyclohexene oxide, styrene oxide and norbornene oxide,) albeit these compounds are produced on smaller scale than EO and PO. [107] With the exception of ethylene oxide which is obtained by the direct reaction of ethylene with molecular oxygen as an economic and plentiful oxidant, the epoxidation of higher olefins requires burdensome conditions including hydrogen peroxide or organic peroxides in the presence of metal catalysts. This fact leads not only to a lower atom economy respect to the reaction with oxygen, but also poses issues related with the disposal or recycle of the waste when organic peroxides are used.[108] Additionally, one should consider additional costs and the environmental impact connected with the purification and isolation of the final products along with their toxicity: epoxides can bind to DNA, proteins and are potentially mutagenic.[109] With a view at sustainability, health and safety, it would be therefore highly recommended to avoid the use of these reactants.

A greener route for the synthesis of COCs that bypasses the isolation of the epoxides is the direct oxidative carboxylation of olefins (DOC, Scheme 1.3). Its industrial interest is confirmed by a number of patents registered between 1962 and 1989.[110] This reaction involves a tandem catalytic process which takes place through an in-situ epoxidation followed by CO_2 insertion.

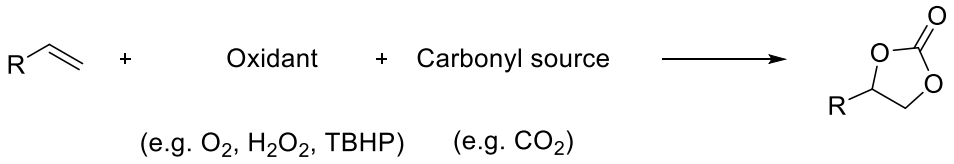

Scheme 1.3: Direct oxidative carboxylation of olefins

Direct oxidative carboxylation involves olefinic substrates that are widely available on the chemical market and are generally less toxic respect to the corresponding epoxides. Olefins can be of natural origin (e.g. terpenes and fatty acids) or can be obtained directly by processing renewable feedstocks including for example, ethylene from bioethanol, C_3-C_6 olefins from alcohol or methanol to olefins (MTO) processes, lignin-derived molecules.[111,112] From both economic and environmental standpoints, the best oxidants are either molecular oxygen or hydrogen peroxide. The latter, however, produce only water as waste and has been more widely legitimized and thoroughly explored,[113] while molecular oxygen has proven quite unreactive towards many olefins with a mechanism often leading to lower conversions and selectivity. Another group of epoxidation reagents is constituted by organic peroxides such as tert-butyl hydroperoxide (TBHP), cumene hydroperoxide, urea hydroperoxide, iodosyl benzene and meta chloroperbenzoic acid. These compounds show a generally high activity and epoxide selectivity, but they are also costly and pose issues related to the formation of by-products and disposal of wastes as reported above.

1.4.4.2 Glycerol derivatives: acetals and esters

As reported in Figure 1.9, glycerol is a relevant renewable feedstock that can give rise to a large amount of high-added value compounds in many fields. It may be used to obtain C_3 building blocks (otherwise derived from fossil resources) by low atom-economic reactions, such as propylene, acrylic acid, acrolein, propionaldehyde, 1,2-propanediol and 1,3-propanediol. Obtaining the same building blocks attainable by fossil-based feedstock through bio-based ones is important but it is even more important to obtain new bio-based compounds that can directly displace fossil-based end products in their functions. Glycerol acetals and glycerol esters fall within this category.

Glycerol acetals

Linear and cyclic acetals are usually prepared by the condensation of an aldehyde or a ketone with an alcohol (or a diol/polyol) in the presence of an acid catalyst. Acetal formation is a reversible reaction via a two-step mechanism (Figure 1.11).

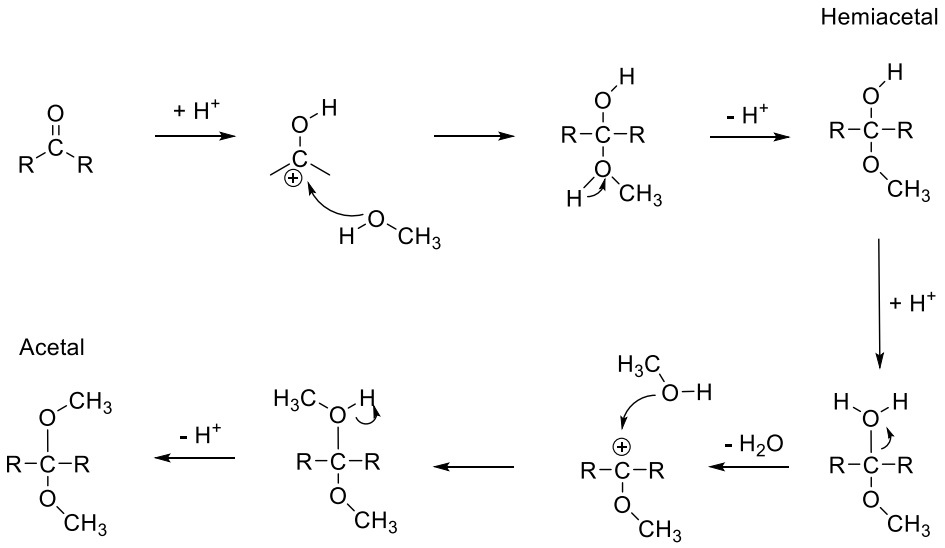

Figure 1.11: Mechanism of formation of hemiacetals and acetals

The first step is the formation of a hemiacetal and subsequent removal of water. Next another hydroxyl group rapidly forms the corresponding acetal by nucleophilic attack. Owing to their stability to aqueous and non-aqueous bases, to nucleophiles including organometallic reagents, and to hydride-mediated reductions, acetals are among the best-known protecting groups for carbonyl compounds.[114] Acetals, however, may be of interests also for their use as such. This happens for the case of cyclic glycerol acetals (GAs) formed with aldehydes or ketones (usually the reactions of Scheme 1.4 are shifted towards the formation of products up to C_4 aldehydes/ketones). The formation of the 1,3-dioxane ring (5-membered or 6-membered) strongly depends on the experimental conditions and the chosen catalyst, but the main factor is the starting aldehyde or ketone.

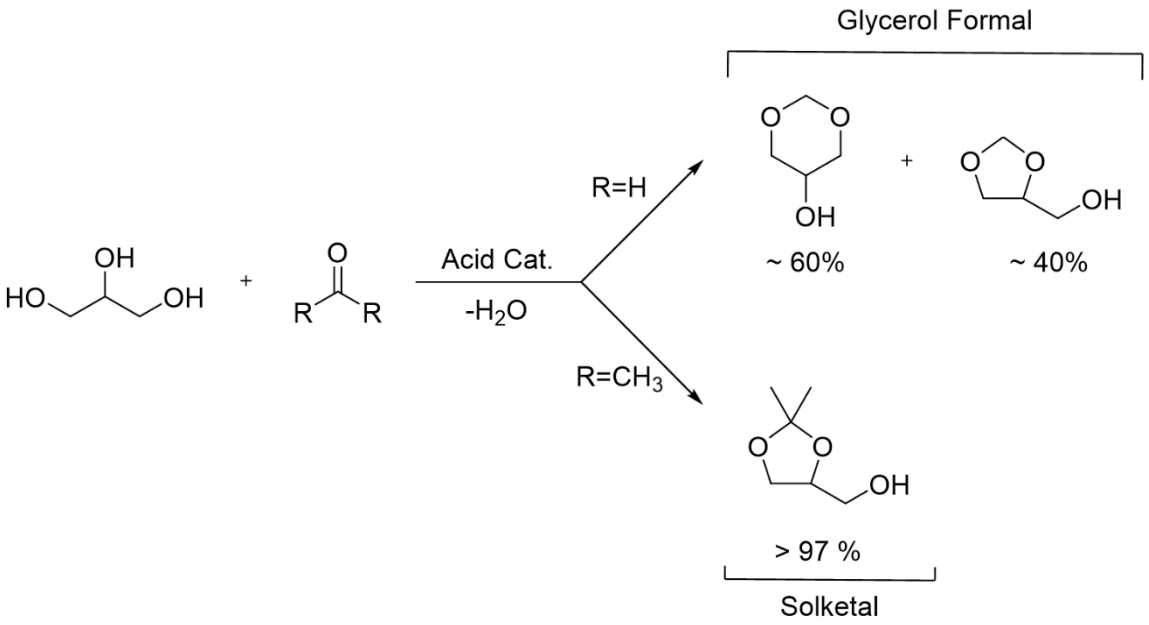

Scheme 1.4: Most common cyclic acetals from glycerol: glycerol formal (a 60:40 mixture of six-membered and 5-membered rings) and solketal

In the simplest case, i.e. formaldehyde and acetone, glycerol formal will be formed as a 3:2 mixture of C_6:C_5 ring isomers (5-hydroxy-1,3-dioxane and 1,3-dioxolan-4-yl)methanol respectively) while solketal (2,2-dimethyl-(1,3-dioxolan-4-yl)methanol]) is obtained as a single five-membered ring isomer (purity>97%). The formation of GAs is traditionally carried out over mineral Bronsted acids like H_2SO_4, HCl, p-toluenesulphonic acid or homogeneous Lewis acid catalysts but recent works on the use of heterogeneous catalysts, even under continuous-flow conditions is reviewed elsewhere.[115]
GAs are viscous, dense, non-toxic and thermally stable liquids with boiling points over 200 °C.[116] However, due to their structure, they possess polarity, hydrophobicity and hydrogen bond ability that make them more similar to simple aliphatic alcohols than to glycerol.[117] These aspects account for major applications of GAs in the synthesis of active pharmaceuticals ingredients (APIs), safe solvents or detergents, additives in the formulation of injectable preparations, paints, plastifying agents, insecticide delivery systems and flavors.[82] More recently, the use of GAs in the fuel sector has been investigated and demonstrated as potential improvers of some fuels properties such as cold filter plugging point, pour point and cloud point, increased octane number, decreased gum formation and pollutant emissions. [86]

Glycerol esters
The most famous ester of glycerol is glyceryl trinitrate, obtained from the reaction of glycerol with a mixture of nitric acid and sulfuric acid (Scheme 1.5). This was the famed unstable explosive nitroglycerin discovered by the Italian chemist Ascanio Sobrero in 1846 and developed by Alfred Nobel as a mixture of nitroglycerin with diatomaceous earth to form a deformable safe-to-handle paste known as dynamite, one of the most used explosives in the 20th century currently displaced by other safer explosives.

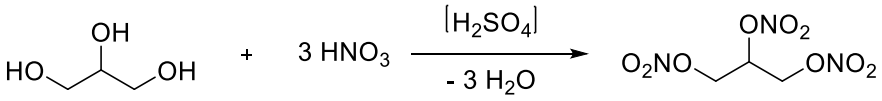

Scheme 1.5: Synthesis of nitroglycerin

The esters of organic acids are much more important glycerol derivatives. The three acetins, monoacetylglycerols (MAGs), Diacetinglycerols (DAGs) and triacetinglycerols (TAGs) are shown in Scheme 1.6.

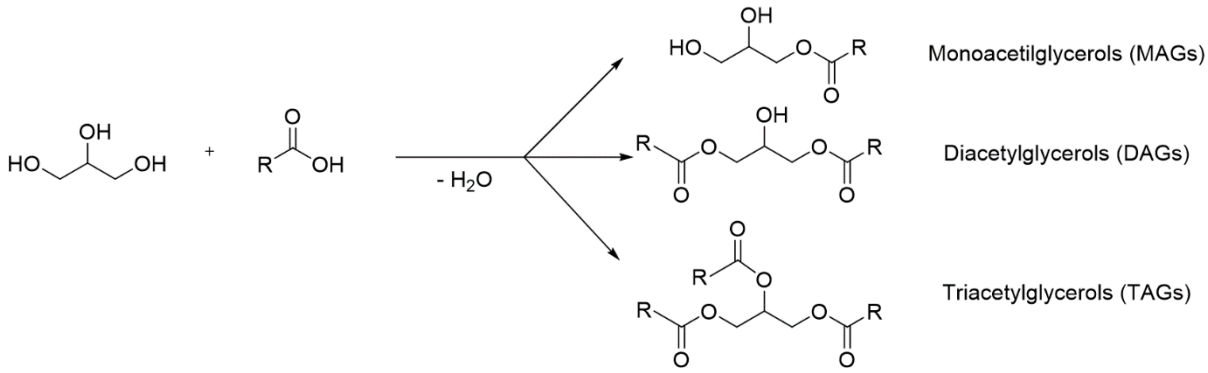

Scheme 1.6: Mono-, di- and tri- acetilglycerols obtained from the reaction of glycerol with organic acids

One of the most used TAG is triacetin (TA, R=CH_3) whose industrial production involves a first reaction of Glycerol with acetic acid (AcOH) to form the corresponding MAG that is further esterified using acetic anhydride (Ac_2O) after azeotropic distillation and removal of the exceeding acetic acid and water. However, issues related to the corrosivity of the reactants, the legal restrictions to the use of Ac_2O[118] and the co-production of water, high-energy demanding azeotropic distillation and poor selectivity when AcOH alone is used as acetylating agent boosted the academic attention towards more sustainable pathways. [119] TA is a commonly used food additive, solvent in cosmetics and pharmaceuticals, humectant and plasticizer. Moreover, it is used like GAs as an antiknock agent in gasoline and cold/viscosity improver in biodiesel.

MAGs and DAGs are of particular importance because they contain both a hydrophilic and a hydrophobic character and can therefore be used as emulsifiers in food and cosmetic industry. Monoesters can be synthesized by previous protection of two hydroxyl groups through the formation of a GAs (or glycerol orthoesters, GOEs) and subsequent reaction with a carboxylic group or a fatty acid.[120] Alternitavely, MAGs can be synthesized directly from Glycerol by esterification with one mole of carboxylic acid or fatty acid, but the synthesis is trivial due to the low selectivity and formation of DAGs and TAGs as by-products.[121]

1.5 Designing a green sustainable chemistry future: the tools

Various methodologies can be used to achieve the green objectives described in the preceding section: from the use of innovative catalysts (carbon dots, metal organic frameworks, frustrated Lewis pairs)[122] to

the synthesis of nanomaterials to obtain materials with exciting optical, physical and chemical properties,[123] the development of organic photocatalytic reactions[124], the use of ionic liquids or deep eutectic solvents as new alternative media[125] and the use of alternative engineering solutions to conduct organic reactions (e.g. ball milling)[126] or the synthesis of new plastics (i.e. polyhydroxyalkanoates) through the aerobic treatment of carbon-rich waste water[127]. And so on.
Here I will limit discussion to the green tools exploited in this thesis.

1.5.1 Tandem catalysis

Catalysis is a "kinetic phenomenon" that does not deal with thermodynamics. In a very general definition, we can say that a catalyst is something that makes a reaction go faster without being consumed in the process. Catalysis is one of the basic principles of green chemistry that allows to minimize waste and prevent the use of stochiometric reagents whenever possible. An enormous effort on catalysis research is occurring nowadays. Historically, chemical transformations require many steps, especially in industrial sectors such as the synthesis of fine chemicals and pharmaceuticals. In a multi-step process, there is the need for separation, extraction, isolation and purification of intermediates that results in loss of material and time, increased energy and use of auxiliaries such as solvents. The idea of combining multi-step synthetic sequences in one-pot processes has been the focus of both academic and industrial research in the last years. One-pot reactions are transformations carried out in the same reaction vessel without isolation of intermediate products, resulting in a process with significant improved efficiency and waste reduction. One-pot syntheses are tightly linked with *tandem catalysis:* the use of a catalyst is noteworthy to avoid the use of stochiometric reagent that can furthermore have a negative impact on subsequent steps if the reaction is carried out in the same vessel. The use of the same catalyst to get directly from A to C (Figure 1.12) without isolating B is even more advantageous from a process and economic standpoint. From a chemical point of view, coupling two or more different reactions is a process intensification that leads to maximize the output and to the reduction of isolation steps, purification of intermediates, cost, energy consumption and wastes. Additionally the use of catalytic systems fits perfectly into the concepts of green chemistry.[128] The coupling of different reactions in one reactor can be defined as a one-pot process that can involve multiple catalytic steps followed by a single work-up stage. One-pot reactions can be further divided in different subsets depending on the conditions and procedures used, as firstly reported by Fogg et Al. and summarized in Figure 1.12. [129]

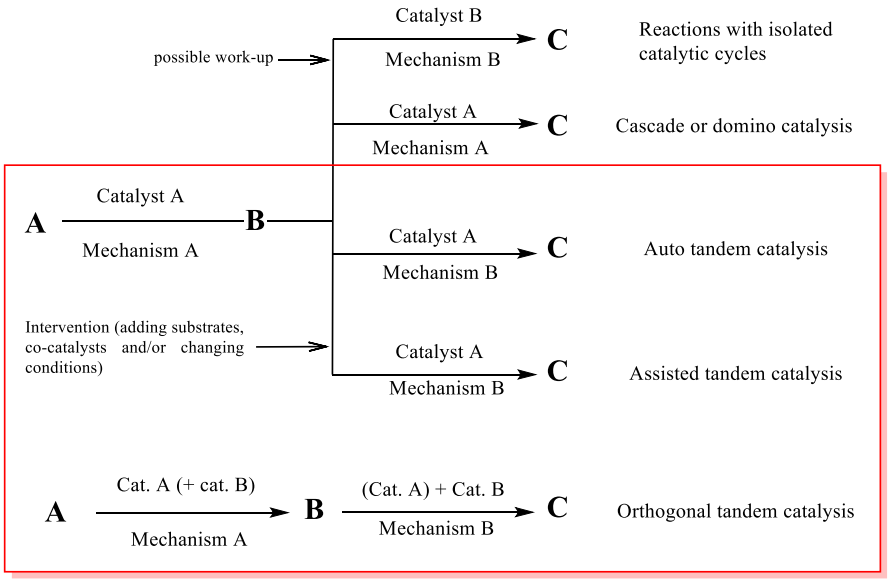

Figure 1.12: General description of one-pot processes

One-pot processes can be classified based on the nature of catalysts and on the mechanisms:

- Simple one-pot reactions with isolated catalytic cycles in which a second catalyst is added once the first catalytic transformation is complete and possibly an intermediate work-up is done (two catalysts for two consecutive mechanism).
- Domino (or cascade) reactions are two (or more) reactions that take place in one-pot conditions with the same catalytic system and by the same mechanism.
- Tandem reactions are one-pot transformation characterized by the occurrence of distinct sequential two (or more) mechanisms further subdivided in categories:
  - Auto tandem catalysis (AuTC) occurs when a single catalyst promotes two consecutive distinct mechanism cycles without any other input (red box, top).
  - Assisted tandem catalysis (AsTC) occurs when a single catalyst is present but some sort of input (such as adding a reagent, solvent, co-catalyst or changing pressure or temperature) is provided after that the first cycle is finished (red box, mid).
  - Orthogonal tandem catalysis (OTC) occurs when two different catalysts (or catalytic moieties) operate side-by-side to perform two sequential catalytic cycles.[130] This last categories can be further divided in orthogonal auto tandem catalysis and orthogonal assisted tandem catalysis depending on whether an input is provided after that the first cycle is finished. (red box, bottom).

AuTC and OTC reactions promote a higher process efficiency since both the steps occur under the same reaction conditions. This represents also their main drawback: it is hard to optimize the reaction conditions for each transformation within the process. AsTC reactions present a lower process efficiency but they are advantageous thanks to the chance to optimize reaction conditions for each intermediate generated within the process.[131]

In this Ph. D. thesis, we focused on two tandem reactions:

- A Tandem process concerning the bimolecular reaction between glycerol and isopropenyl acetate (iPAc, scheme 1.7):

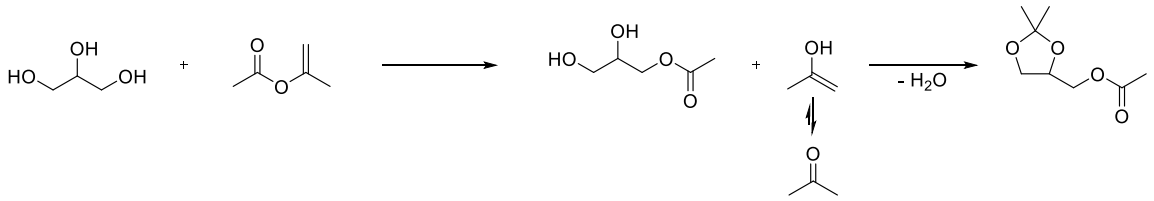

Scheme 1.7: The acetylation/acetalization tandem process between glycerol and isopropenyl acetate

The initial acetylation of glycerol induces the release of the enol form of acetone that can further react with the two residual hydroxyl group of glycerol by forming Solketal Acetate (SolkAc) through a tandem acetylation/acetalization process. Both the reaction mechanisms can be promoted by (Lewis or Bronsted) acid catalysis as mentioned above but also catalyst-free procedures were reported.[86,115] According to our knowledge, we were the first to promote this double role of IPAc on the reaction with glycerol and seek to optimize the reaction conditions for the tandem process.

- The main project of this Ph.D. thesis regards the direct oxidative carboxylation of olefins to obtain cyclic organic carbonates (COCs) by tandem oxidation followed by CO_2 insertion as renewable carbonyl source (Scheme 1.3). COCs are considered a renewable chemical that could replace various fossil-based chemicals and their properties and uses were mentioned in the paragraph 1.3.4.1.

To set up a project regarding the process-development of a catalytic tandem protocol, an in-depth analysis of the mechanisms involved in the separate steps is compulsory in order to take into account all the variables, including catalysts compatibility. In the following paragraph, existing literature on each step of the direct oxidative carboxylation reaction (*i.e.* olefin epoxidation and CO_2 insertion) will be collected and described separately so as to introduce the opportunities to implement a process of direct oxidative carboxylation of olefins.

1.5.1.1 Direct oxidative carboxylation: epoxidation and CO_2 insertion mechanisms

Epoxidation Three main categories of metal catalysts are reported in the literature for the epoxidation step: heterogeneous silver, gold or titanium catalysts, homogeneous early transition metal catalysts, and biomimetic late transition metal catalysts. [132]

Heterogeneous silver catalysts are based mainly on silver metal and used with molecular oxygen as oxidant. These catalysts are suitable for the epoxidation of ethylene and partly propylene, while they are ineffective for higher olefins due to both the low reactivity of oxygen and the presence of allylic hydrogen atoms which lead to a poor selectivity.[133] Other systems have been obtained by immobilizing gold particles on a variety of supports (silica, alumina, titania, metal oxides or carbon);[134] these have been used mainly for the gas-phase epoxidation of propene in the presence of O_2 or air.[135] The epoxidation of higher olefins

with O_2 has been achieved in the presence of TBHP as initiator, or with TBHP alone. [136] The catalytic activity of the gold particles is related to their size, dispersion on the support, oxidation state and on the nature of the support material, but the mechanism is not clearly understood.

Ti-based heterogeneous catalysts are well known for the direct oxidative carboxylation of olefins. Titanium(IV)-SiO_2 systems were initially reported for the epoxidation of propylene, later other catalysts based on titanium silicalite (TS-1), Ti-beta, Ti-MCM41 etc. were described for the epoxidation of bulkier olefins.[137] These materials are effective in the presence of dilute H_2O_2 (10-30% v/v) and polar protic (preferably alcohols) or aprotic solvents. The active sites are suggested to be tetrahedrally coordinated titanium atoms with Lewis-acidic character (Figure 1.13) able to form a Ti-OOH species stabilized by an alcohol (or water) through the formation of a five-membered ring. The peroxo oxygen vicinal to Ti of this intermediate reacts with the olefin to produce selectively the epoxide.

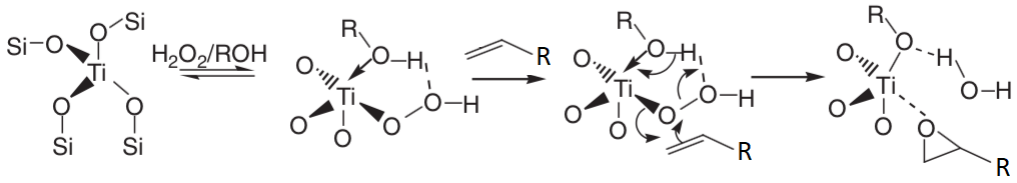

Figure 1.13: Ti active sites and proposed mechanism for the epoxidation of olefins

Homogeneous early transition metal complexes [in particular Ti(IV), V(V), W(VI) or Mo(VI)] behave like Lewis aids in coordinating peroxides.[107c] These metals are in their higher oxidation state and essentially do not have accessible lower oxidation states: this is fundamental in inhibiting metal-catalyzed decomposition of peroxides that may cause radical initiation, over-oxidation and consequent lower selectivity towards epoxides.[138] Figure 1.14 reports the mechanisms with aqueous and organic peroxides. M-OOH or M-OOR are the key active intermediates that promote electrophilic oxidation of the olefins through a concerted mechanism and direct oxygen transfer as proposed by Sharpless et al. and validated by quantum-chemical and DFT calculations.[139] The metal centers do not undergo redox reactions and the best catalysts are strong and mildly oxidizing Lewis acids .

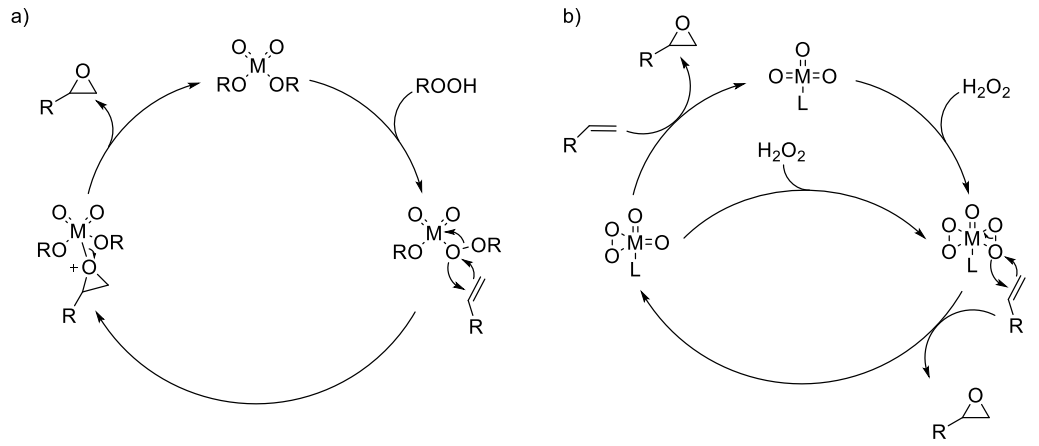

Figure 1.14: General mechanism for the epoxidation of olefins in the presence of early transition metals (a) with organic peroxides and (b) with hydrogen peroxide

Biomimetic transition metals (in particular Fe, Mn, Cr) follow instead a redox mechanism. The metal center is first oxidized forming the oxo species, which then oxidizes the olefin. The mechanism is shown in Figure 1.15: it can involve either a short route with single atom oxygen donor (peroxides, PhIO, NaClO, MCPBAetc.) or a long route with molecular oxygen that needs a source of protons for the reaction to occur. [107c]

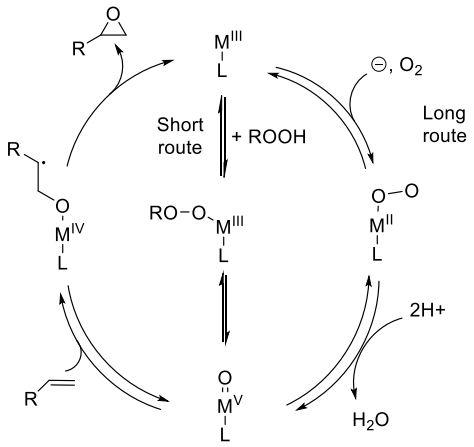

Figure 1.15: General mechanism for the epoxidation of olefins with peroxides or dioxygen in the presence of late transition metals

Either way, the metal forms an oxo-species that then transfers the oxygen to the olefin concurrently regenerating the reduced metal by an oxygen-rebound mechanism. A possible side reaction is homolytic O-O bond cleavage of the oxidant leading to the formation of RO· and prevailing allylic oxidation, lowering selectivity towards epoxide.[140] The best ligands for these metals are porphyrins, salen and nonheme

complexes that properly chelate metals. In some cases, it was demonstrated how this redox mechanism is paired with a Lewis acid mechanism due to the LA character of the metals involved.[141]

CO_2 insertion. The pathway for the catalytic formation of cyclic organic carbonates by CO_2 cycloaddition to epoxides is clearly established by several mechanistic studies based on experimental data and computational calculations and is fully and accurately described elsewhere.[105,142] The widely accepted mechanism (Figure 1.16) requires a Lewis or Brønsted acid (A^+) to electrophilically activate the epoxide and a nucleophile (Nu^-) to ring-open the epoxide. A Lewis base (LB: usually a carbonate or carbamate species) is beneficial to form an LB-COO^- species that activates CO_2 towards ring insertion.[143] The nucleophile must also be a good leaving group as it needs to be displaced in the ring-closure step to form the cyclic organic carbonate. Usually A^+ is a metal-based Lewis acid or a species with H-bonding ability, Nu^- is a halide (especially bromide or iodide), while the LB contains oxygen or nitrogen. In this context, the use of multifunctional single- or two- component catalytic system able to synergistically activate the olefinic substrate and CO_2 is becoming the mainstay.[144]

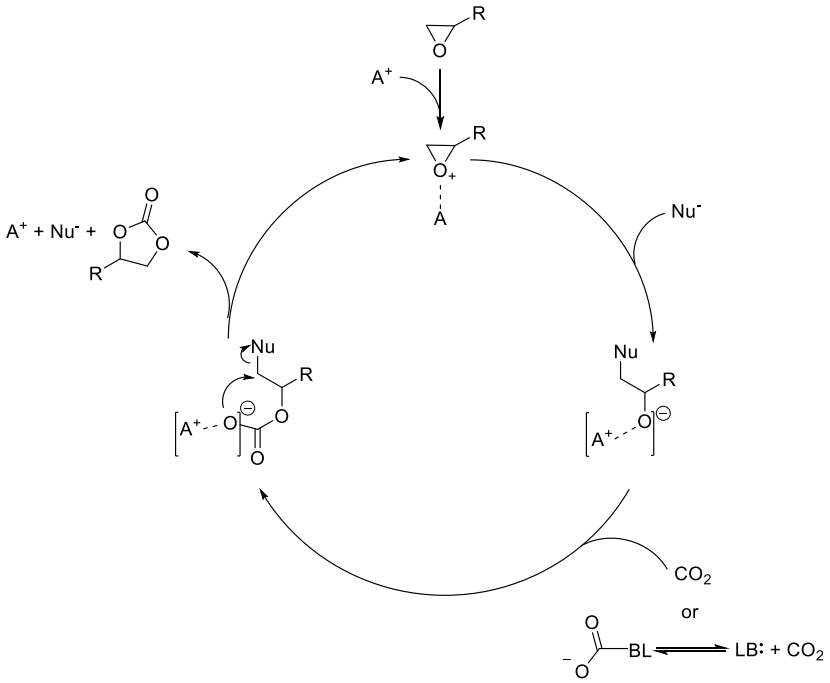

Figure 1.16: General mechanism for the CO_2 insertion into epoxides

In order to be able to integrate the two consecutive catalytic cycles described above in a one-pot tandem process, definition of the boundary conditions and the application of parameters suitable for both steps is essential. At the same time the potential thermodynamic and kinetic incompatibility of the individual reactions must be addressed and the reaction conditions carefully optimized.

To illustrate in a comprehensive way AuTC, AsTC and OTC processes, three examples of DOC of olefins are hereunder proposed:

1.5.1.2 Auto-tandem catalysis

In 2015 Ramidi et al. reported a AuTC process for the direct oxidative carboxylation of styrene by using a Mn(III) complex with an amido-amine ligand, tetrabutyl ammonium bromide (TBABr) as co-catalyst and anhydrous TBHP as oxidant. At 100 and 18 bar (CO_2 pressure), styrene carbonate reached a 43% yield after 6h.[145] Studies on the substrate scope showed that styrene and C_5-C_8 olefins afforded moderate yields (31-48%) while highly strained cyclic olefins such as cyclohexene and cyclooctene yielded lower amount of COCs (≈10%). Mn catalyst was demonstrated active in both the steps, resulting a truly catalyst for AuTC process. The Mn(III) complex was initially oxidized to a Mn(V)-oxo intermediate which was responsible for the conversion of the olefin to the epoxide (Figure 1.17, path a): evidence of formation of the Mn(V)-oxo species came from isotope labelling studies of the oxo group with ^{18}O. The Mn(III) complex was also crucial in the CO_2 insertion step as a Lewis acid for epoxide activation towards nucleophilic attack by TBABr (Figure 1.17, path b).

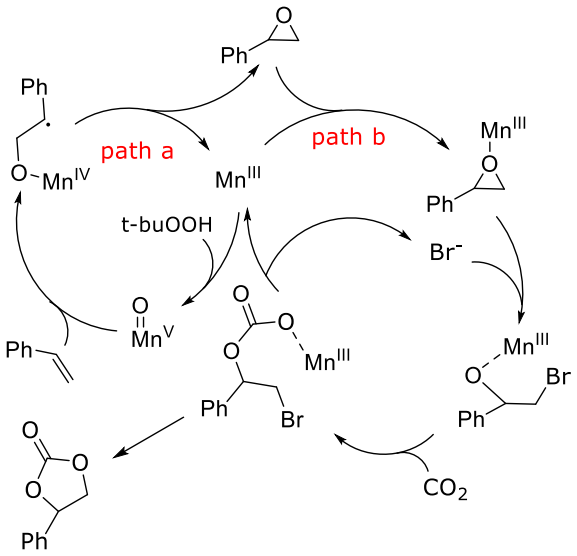

Figure 1.17: Mechanism hypothesized for the formation of SC from styrene in presence of Mn^{III} catalyst and bromide source

1.5.1.3 Assisted tandem catalysis

In 2018 Shi et al. described the synthesis of a CuMo-BPY MOF based on MoO_4^{2-} anion, μ_3-OH tricopper (II) cores and bipyridine as organic linker.[146] The crystalline solid possessed 2 different size cavities arranged alternately. The first cavity was purely inorganic with alkaline μ_3-OH and hydrophilicity conferred by Cu-Mo; while the second cavity was constituted by μ_3-OH Cu-Mo cores, hydrophobic organic BPY ligands and d^0 Mo(VI) catalytic sites which favored the oxidation of olefins (Figure 1.18).

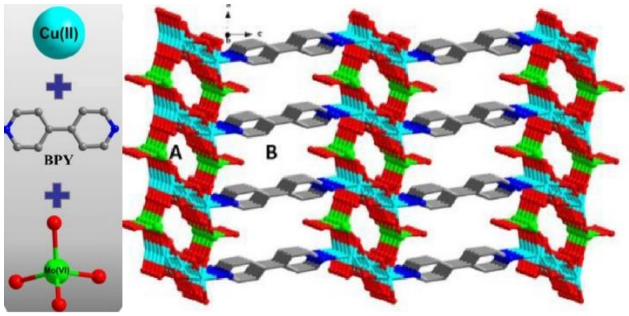

Figure 1.18: Schematic representation of CuMo-BPY: reprinted from ref. 146 with permission from Elsevier

Under AuTC conditions, CuMo-BPY reached only a moderate 55% yield in styrene carbonate with TBHP (2 eq), 5 bar of CO_2, 1% of catalyst and 10% mol of TBABr as co-catalyst at 50 °C for 120 h. Degradation of TBHP to t-BuOH in the presence of Mo and TBABr was deemed as the limiting cause as reported also in other papers.[147] The yield of styrene carbonate could be improved up to 90% by adopting an AsTC approach in which TBABr and CO_2 were added in a second step. Similar catalytic activity was obtained with other styrene derivatives (85-91% yields) while the catalyst was not active with C_6-C_8 cyclic olefins and with a bulky styrene-derived olefin such as 3,5-di-tert-butyl-4'-vinylbiphenyl. The authors suggested that the latter substrate was too large indicating that the reaction occurred inside the channel of the MOF and not on the surface. From a mechanistic perspective the authors proved that the MOF was active in both the step: they postulated the formation of a peroxomolybdate intermediate that favored the interaction with styrene and the epoxidation reaction; in the CO_2 insertion indeed they assumed that μ_3-OH Cu(II) activated carbon dioxide and increased its concentration around the reactive centers, the Lewis acidic character of Cu and Mo could favor the reaction while the bromide of TBABr provided the nucleophilic ring-opening of the epoxide.

1.5.1.4 Orthogonal tandem catalysis

Most OTC publications on DOC of olefins exploit gold as oxidation catalyst, but since this metal is not active for CO_2 fixation an additional catalyst or catalytic site must be present.

In 2005 Sun et al. reported a catalytic system consisting of silica-supported gold (Au/SiO_2), $ZnBr_2$ and TBABr as co-catalyst for the direct oxidative carboxylation of styrene with anhydrous TBHP (or cumene hydroperoxide), 10 bar of CO_2 at 80 °C for 4h.[148] The Au/SiO_2 catalyst possessed either metallic Au(0) or cationic Au(I) particles. The study of the epoxidation step showed that Au/SiO_2 was active while $ZnBr_2$ and TBABr had no effect. The epoxidation was rate determining for the whole process and metallic gold was more active than the cationic species. In the second step $ZnBr_2$ (as Lewis acid) and TBABr operated together to open the epoxide ring and allow CO_2 fixation while the Au/SiO_2 did not affect this reaction. Tetrabutyl ammonium chloride and tetrabutyl ammonium iodide were less active than TBABr since chloride was less nucleophilic than bromide and iodide was easily oxidized to I_2 by TBHP. Interestingly, the presence of CO_2 favored the epoxidation step in the interval 10 - 80 bar but decreased at higher pressures due to a lower solubility of the substrate. The authors reached a maximum 89% conversion and 35% yield in styrene carbonate. The main by-products were benzaldehyde (19%) and oligomers. The use of cumene hydroperoxide led to lower conversion of styrene (72%) but 42% selectivity towards styrene carbonate.

Later, the same research group described an improvement of these results by using an iron hydroxide supported gold catalyst ($Au/Fe(OH)_3$) with $ZnBr_2$ and TBABr as co-catalyst: the styrene conversion and the yield of styrene carbonate were 88% and 53%, respectively.[149] Differently from the previous case, the authors identified Au^{3+} as the active species. Comparison with similar supports (such as Fe_2O_3) indicated a synergistic effect between Au^{3+} and $Fe(OH)_3$ that led to better performance during the epoxidation step. Optimal catalytic activity was achieved with 5% Au $w/w_{support}$.

1.5.2 Continuous-flow chemistry

In 2000 Stankiewicz and Mouljin defined process intensification (PI) as "the development of novel apparatuses and techniques that, compared to those commonly used today, are expected to bring dramatic improvements in manufacturing and processing, substantially decreasing equipment size/production capacity ratio, energy consumption, or waste production, and ultimately resulting in cheaper, sustainable technologies".[150] Hence, PI represents any paradigm shift that led to enhancement in terms of efficiency (energetic, environmental, chemical, economic, etc.) of an existing process. Continuous Flow (CF) chemistry, that is the chemical synthesis in flow reactors in the place of batch reactors deserve to be included within the technologies that promote process intensification.

1.5.2.1 The apparatus

CF synthesis is achieved by pumping solutions of reactants through reactors in a continuous manner. A schematic representation of the typical CF equipment and reactions is reported in Figure 1.19.

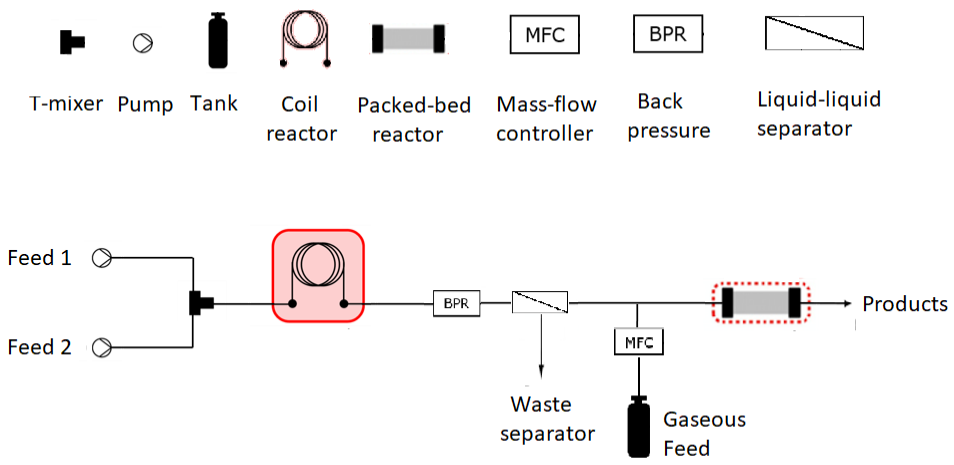

Figure 1.19: Equipment and schematic representation of a CF process

A CF apparatus is generally made up of the following components[151]:

- Pumps that delivers the solutions of the reactants (or the gaseous feeds) towards the reactors with the desired flows; a mass-flow controller can be used to regulate the gaseous streams.
- Reactors in which the reaction occurs under a precise control of temperature and pressure. The residence time of the reactants inside the reactor is determined by the total flow rate and reactor volume. Reactors can be subdivided into four main categories[152]:
    - Continuous Flow Stirred Tank Reactors that are historically the most commonly used for liquid-phase industrial reactions.
    - Packed-bed reactors that are tubular reactors which are filled with a packing material. The packing may consist of an inert material (e.g. Raschig rings or sand which serve to improve the contact between reactants) or a heterogeneous catalyst. In this case the advantages respect to batch processes are the higher effective molarity of the catalyst/reagent ratio decreasing the reaction time and the possibility to avoid the catalyst/reaction mixture separation step at the end of the reaction (even if there are issues related to the potential leaching, in particular for immobilized transition metal catalysts).[153]
    - Coil reactors that are widely used flow reactors made out of stainless steel or inert fluoropolymers tubing with outer diameters of 1/8" – 1/16" and various inner diameters. They are exploited mainly for high temperature and pressure applications but also for photochemical reactions. Moreover, the use of metal reactor tubing can provide a direct source of catalyst in flow reaction: the case reported by Bogdan and Sach on the use of a copper flow reactor for the synthesis of a library of triazoles through click reactions is noteworthy.[154]
    - Chip reactors that offers extremely high surface-to-volume ratios leading to a high accuracy in heat transfer and optimization of thermal reactions, despite their low throughput, tendency to clog and high cost
- Back-pressure regulator (BPR) are valves installed to operate at a constant upstream system pressure
- Separators that enable to perform aqueous work-up, drying, extraction and other purification procedures: their presence has noticeably advanced continuous-flow processes.

Since 2000, CF processes have had growing attention both from the academic world as well in the industrial sector. If IUPAC advocated that "flow chemistry has the potential to make our planet more sustainable"[155], at the same time industrial interests mainly concerned the cost savings: since the energy cost is a key element for industry [156]and CF reactions could remarkably reduce the energy input, it is logic that CF is attractive for both industries and academy, in particular in the synthesis of APIs[157], multistep synthesis[158], but also in the conversion of bio-based chemicals.[159]
It is noteworthy that while the top 30 petrochemicals and most of the top 300 chemicals are produced continuously, more than 90% of those ranked 301-30000 are made batch-wise.[160] This trend is surely related to the presence of conventional batch plants available with high production capacity, regulatory systems that do not encourage to move from traditional manufacturing, the uncertainty regarding the real benefit of CF reactors related also to the fact that multipurpose batch plants are capable of producing a large variety of products, providing for flexibility of batch manufacturing with a simple, robust and versatile design.[161]

However, CF chemistry is an excellent ally for green chemistry that can help to reach its objectives and respect its principle in a faster and more intensified way.[162,163] The green advantages brought about by CF processes can be categorized in three main keywords: Waste, Safety, Efficiency. We will briefly explore the greenness of CF processes through these three categories

1.5.2.2 Waste

The use of solvents is one of the most relevant factors when assessing the environmental, economic and safety impact of a process.[164] Thus, one strategy to reduce these impacts is to minimize the use of solvents (and consequently waste if we think that around 50% of the solvents used in industry are not recycled[165]) by performing syntheses under highly concentrated or even neat conditions. The optimal heat transfer of CF process due to high surface area to volume ratio that result from using small diameter tubing allows to perform neat or highly concentrated reactions: in particular reactants can be used in equimolar amounts with the minimal quantity of additional solvent, often with the use of heterogeneous catalysts immobilized in packed-bed reactor bringing about an enormous decrease of the E-factor respect to batch conditions as widely reported in literature, including in photochemical reactions.[164,166] Moreover, such as in tandem catalysis or one-pot processes, the implementation of multistep protocols allows to avoid intermediate isolation and purification thereby reducing the E-factor of the whole reactions.[167]

1.5.2.3 Safety

Increased safety is one of the main reasons why CF is so appealing.[168] First of all, the smaller reactor volumes intrinsically minimize the risk in case of an accident respect to batch reactors with the same productivity and for the same reason reactions conducted at high temperature and pressure presents low risk because of the low volume involved. Also exothermic reactions with fast kinetics are fully tailored to CF process with high mass- and heat- transfer rates that enhance the ability to continuously quench small volumes of product streams or rapidly cooling reactors.[169] Another intersection with tandem process is the possibility of in-situ generation of unstable or hazardous intermediates from benign precursors that are converted directly to products. Finally another well-known benefit of CF process is the chance to use safely solvents at temperature and pressure far beyond the solvents' boiling point: this could be useful with green solvents such as ethanol, acetone or ethyl acetate in the place of other polar protic and aprotic solvents with higher boiling points.

1.5.2.4 Efficiency

CF processes resulted in an overstepped efficiency respect to batch process where the amount of product formed is determined by the amount of starting material: the nature of continuous flow reactor prompt small volume reactors to produce large quantities of products. Moreover the high surface area to volume ratio, the heat transfer that benefit exothermic reactions carrying to an improvement in yield quality respect to batch reactors, the minimization of impurities formation, side-reactions and enhancement of selectivity towards the desired products improve the efficiency of CF processes. This is due also to the speed of reactions: in many reviews on the argument is highlighted how it is possible to reduce reaction times by an order of magnitude (typically from hours to minute and from minute to seconds) as a consequence of reduction of mass transfer hindrance in conjunction with more harsh process conditions.[170] When biphasic reactions are performed in flow reactors, the high interfacial surface area of the tubing can lead to an exciting increase in reaction rate compared to flask based reactions, either in

liquid-liquid that gas-liquid reactions.[171] Finally, an investment resource saving is undeniable. Flow reactions use smaller equipment than a comparable batch reaction, hence an increased throughput could be attained with a reduced equipment footprint and a lower capital cost: recent examples are the case of the manufacturing synthesis of the APIs evacetrapib end Galantimine HBr.[172,173]

1.5.2.5 Examples

A relevant example that encompasses all these aspects is the comparison of methylation protocols carried out with conventional hazardous reagents such as methyl iodide (MeI) or dimethyl sulfate(DMS), and the non-toxic dimethyl carbonate (DMC) as a green alternative. The use of naphthol with methyl iodide or dimethyl sulfate led to high yields, low temperature and fast reactions but required using toxic methyl sources producing a large amount of toxic wastes.[174] The use of a green methylation agent such as DMC promised environmental advantages with the drawback that long reaction times were needed due to the lower reactivity of the carbonate in batch conditions at 90 °C. [175] A pressure reactor could be used to work at higher temperatures and faster rates, but this implies higher costs and scale-up issues. On the other hand, the same reaction (DMC + naphthol) may be run in a simple CF-setup at higher temperature and at reaction times as short as twenty minutes in the presence of a catalytic amount of the base promoting the quantitative formation of the methylated product.[176]

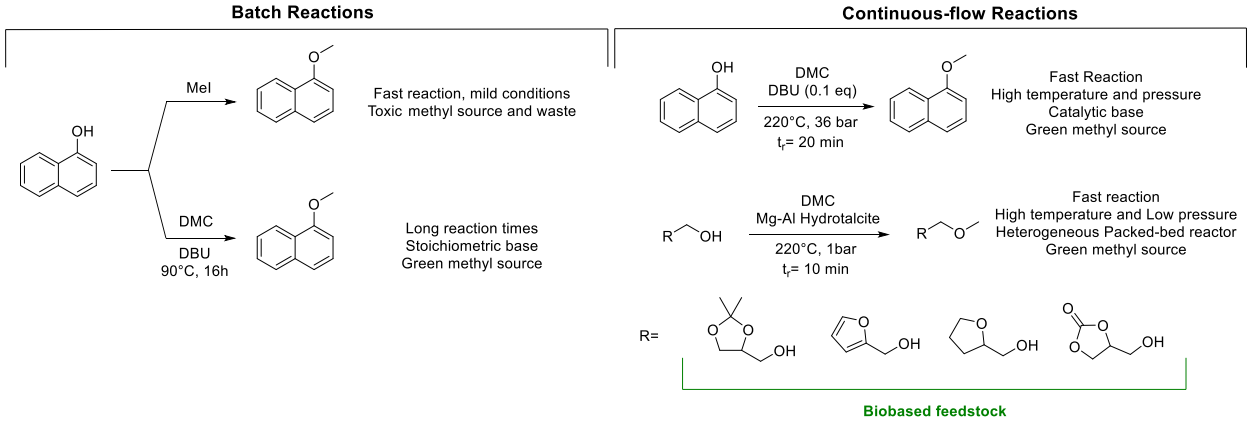

Figure 1.20: Comparison of methylation processes in batch and continuous-flow conditions

With a view of applying greener CF protocols to upgrade renewable-based molecules, recently our group described a CF procedures for the alkylation of OH-bearing biobased derivatives such as GAs, glycerol carbonate and furfuryl alcohols with dimethyl carbonate in presence of Mg-Al hydrotalcites as heterogeneous catalyst loaded in a packed bed reactor. This reaction provides for the quantitative methylation of the hydroxyl group avoiding the use of the catalytic base and subsequent isolation/purification of the product: it was possible to obtain an O-alkylation selectivity as high as 99% at complete conversion at 220 °C and atmospheric pressure with residence time of 20 minutes.[177]

In a recent example, Kralisch and co-workers looked at the environmental impact of performing the epoxidation of soybean oil in batch and flow conditions (Scheme 1.8).[178] Epoxidized soybean oil (ESO) is produced commercially at a rate of approximately 240 Mtonnes per year, usually using hydrogen peroxide as the oxidant in the presence of a carboxylic acid (e.g. formic acid) and a mineral acid catalyst (e.g. sulfuric

acid).This biphasic transformation takes place in two steps: conversion of the carboxylic acid to a peracid in the aqueous phase, followed by epoxidation in the organic phase. Ring opening of the epoxide and decomposition of hydrogen peroxide are undesired side reactions.

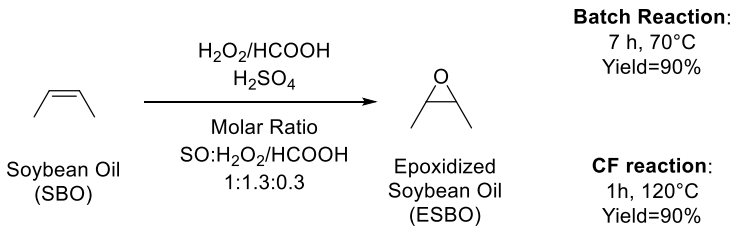

Scheme 1.8: Comparison of batch and CF process for the industrial epoxidation of soybean oil

In the industrial batch process, the oxidant is gradually added to the oil to control the exothermicity. Performing such a process in flow, improves mass transfer between the two phases, improves temperature control and provides higher selectivity. To determine if performing the epoxidation in flow was of any environmental benefit, a systematic evaluation of the input and output of material and energy was carried out. The energy demand per mole of product was found to be lowest when performed at high temperatures in a flow reactor (T= 120 °C) due to decreased reaction times, and the authors note that switching the existing process to a high temperature flow reaction can give approximately 12% reduction in global warming and human toxicity potential. Considering that the largest factors in environmental impact of the process are from the starting material supply which cannot be reduced beyond stoichiometric quantities, this is a significant improvement.[163]

Finally, it is interesting to report the description of the only two CF processes published to date on the DOC of olefins explored in the previous paragraph: they are good examples of CO_2 exploitation as C_1 source in CF reactions.

The first was published by Jamison et al. and involved an oxybromination (OB) first step.[179] OB is a stochiometric process in which the intermediate halohydrin is obtained by halonium or halide and an oxygen source (either X^+/water or X^-/peroxide) in stochiometric amounts.[180] As reported in the general mechanism of Figure 1.21, in the second step the halohydrin was deprotonated by a stochiometric nucleophile and reacted with CO_2 (path a) forming the intermediate that ring-closed by eliminating the halide to yield the cyclic carbonate. This pathway did not exclude formation of the epoxide, that would however exist in equilibrium with the bromohydrin.

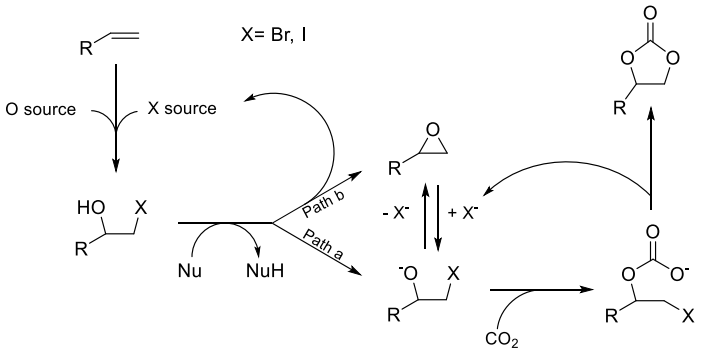

Figure 1.21: General mechanism for the DOC of olefins through oxybromination process

After an initial screening under batch conditions, the first continuous flow experiments with styrene demonstrated limits due to solubility and low selectivity towards COC. The authors showed the different pathways that can lead to the formation of the carbonate and hypothesized the occurrence of the NBS-DBU adduct D that competes with oxybromination and inhibits CO_2 insertion (Figure 1.22a). These issues were solved by the design of a multi-stream "assisted" CF system in which CO_2 and DBU were added in the second step. As shown in Figure 1.22b, an acetone solution of the olefin and NBS and an acqueous solution of ammonium acetate (0.1 eq.) were pumped separately, mixed on-stream, and reacted for a residence time of 30 min at 40 °C. The stream containing the bromohydrin was intercepted with a flow of CO_2 (9 bar) followed by a separate stream of aqueous DBU, and the resulting reaction mixture was heated at 100 °C for a residence time of 10 minutes. Styrene carbonate was obtained in 80% yield and a variety of terminal, internal and cyclic olefins could also be converted into their corresponding cyclic carbonates in 43–89% yields (22 examples).

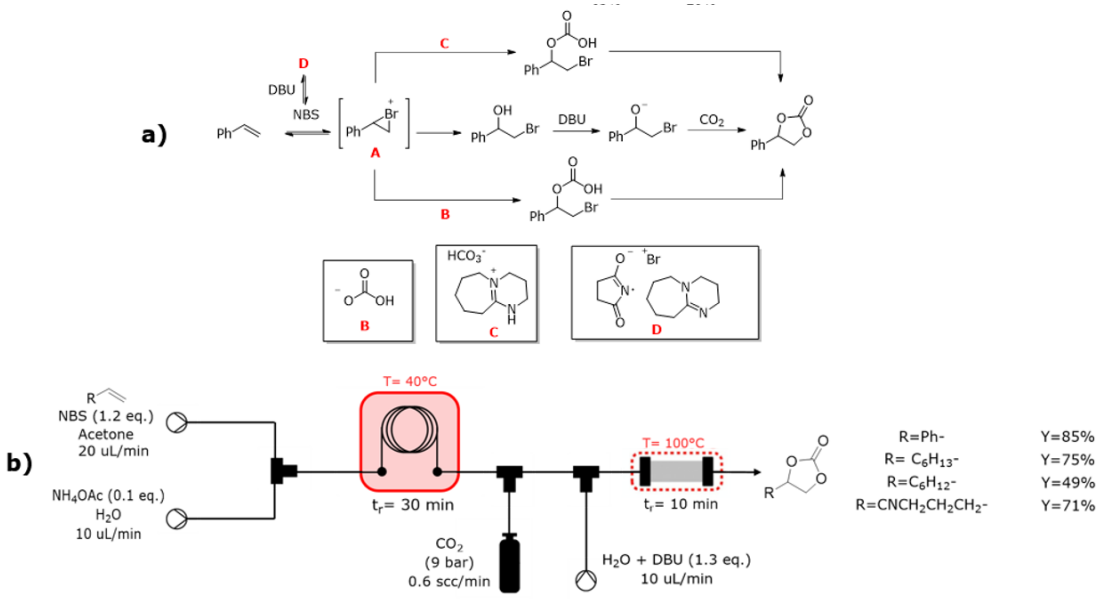

Figure 1.22: (a) Possible reaction mechanisms and (b) description of the multi stream assisted CF apparatus for the DOC of olefins from ref. 179

In 2017 Sathe et al. developed an elegant CF system for the direct oxidative carboxylation of olefins with hydrogen peroxide and CO_2.[181] The use of H_2O_2 represented an improvement in terms of sustainability as it avoided using excess halogen and base. Their strategy provided for a truly catalytic two-step (not-tandem) procedure in which a Re-based catalyst was used for epoxidation and an amino trisphenolate aluminum complex with tetrabutylammonium iodide (TBAI) for the second CO_2 cycloaddition step. A schematic representation of the CF system is depicted in Figure 1.23.Two sequential packed-bed reactors were built in PTFE to avoid the use of stainless steel and consequent degradation of the peroxide and filled with sand to increase reagent contact. The study of the two separate steps led to optimized reaction conditions [step 1. Solution of: methyltrioxorhenium (MTO, 1% mol), 3-methylpyrazole (Lewis base for the epoxidation, 24%mol), H_2O_2 (5 equiv), CH_2Cl_2 flowed at 11 µL/min; olefin (5 µL/min), 40° C, residence time = 1h. Step 2. Solution of: Al catalyst (2% mol) TBAI (10% mol), CH_2Cl_2, THF (5 µL/min); CO_2 (7.5 bar, 1 scc/min), 100°C, residence time: 40 minutes]. The key to success was the use of a membrane phase separator between the two reactors which enabled the separation of the mutually incompatible aqueous oxidant and Lewis basic carbonation catalyst. In this way styrene, styrene derivatives and terminal olefins (9 examples) could be efficiently transformed to the corresponding cyclic carbonates in 48– 98% yields, while no conversion was achieved with internal or cyclic olefins. The main issues encountered were the conversion of low molecular weight and water-soluble olefins that were not efficiently separated by the membrane separator and MTO partitioning between the two phases that was almost identical, making straightforward recycling difficult.

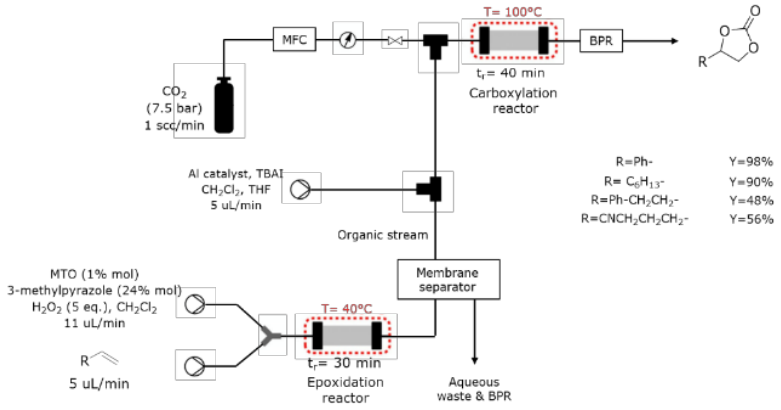

Figure 1.23: Schematic representation of the CF system described in ref. 181

1.5.3 Green Reaction Conditions

Another tool extensively used throughout the research work of this Ph.D. thesis is a continuous focus on using green reaction conditions. This is a larger conceptual tool respect to the use of the others, i.e. tandem catalysis and continuous flow processes, nonetheless it is still relevant since it represents an ever-present footprint left over the course of the 3-year project. Irrespective of the fact that in some instances (that will be pointed put during the course of the thesis) greener or more sustainable choice could be used, a continuous effort was done to “think green”, e.g. by avoiding the use of halogenated solvents;

synthesizing substrate, products and materials by green procedures; extract, isolate and purify compounds through low energy intensity and high environmentally friendly procedure.
As an illustration, here we reported two fields on which our attention was focused during the research work.

1.5.3.1 Use of solvents and solvent-free conditions

The fifth principle of Green Chemistry regards the use of auxiliary substances, which can be defined as all substances involved in the manipulation of a chemical. As already reported, the use of solvents is one of the more relevant factors when a process is evaluated, and solvents are by far the most used auxiliary substances. In Figure 1.24 is shown the composition by mass of the different types of materials used in pharmaceutical industry: solvents account for 80-90% of the non-aqueous mass used to manufacture APIs, while it is estimated that they are responsible of around 50% of GHG emissions in the same industrial sector.[182]

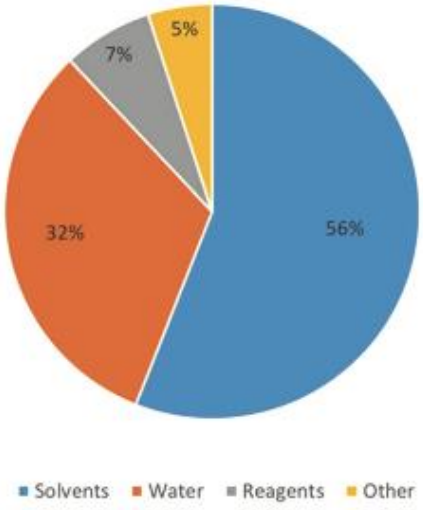

Figure 1.24: Contributions in mass of various classes of compounds in the synthesis of APIs[183]

On a global level, public perception, legislation, and research are contributing to move away from the traditional polluting and dangerous processes: halogenated solvents are becoming taboo at the point that a pharmaceutical company such as Pfizer has not implemented new processes that involve their use in the last years.[183] Many efforts to replace polar aprotic solvents (DMSO, DMF, NMP, etc) considered detrimental to humans and environment are still going on by the use of green and renewable based solvents such as γ-valerolactone, cyrene or the use of hydrogen bond donor – hydrogen bond acceptor solvent pairs.[184] Not to mention the advancements in biomass-derived solvents such as 2-methyltetrahydrofuran, glycerol derivatives, the use of switchable solvents, subcritical and supercritical fluids, deep eutectic solvents, ionic liquids and reaction in water and on-water. [185,186] A further possible "trick" is to use the same green compound as reactant and solvent. In this way the reactant-solvent could be recovered and recycled easily, especially when a complete conversion and selectivity towards the

desired product is reached. Examples from our research group regard the use of DMC and iPAc as transesterification agents.[99a,100,187]

While the use of greener solvents can be viewed as a step in the right direction, nonetheless the most desirable approach is to perform reactions in the absence of solvents. Solvent-free conditions allow to minimize E-factors and enhance productivity. It is important indeed to have a comprehensive insight of a process and to reduce all the auxiliary substances in neat reactions in all the steps. Suffice it to say that solvents are still extensively utilized for the isolation of the product, to such an extent that a 10 mmol reaction typically uses 10-20 ml of solvent for the reaction and 300-2000 ml for product isolation and purification.[90] Obviously, not all the reactions can be performed without solvents: a typical case is that of dangerous exothermic reactions that may require the presence of a solvent to dissipate heat. As mentioned above, this issue may be smartly solved by CF processes with high mass- and heat- transfer capability.

1.5.3.2 Use of catalyst and catalyst-free conditions

The use of catalysts is the cornerstone of the 9th principle of green chemistry. Both academic as well as industrial organic processes research are strongly grounded in the development of new catalysts. During this Ph.D. project we investigated and exploited tandem catalysis, that is the use of the same catalyst in consecutive steps to perform green one-pot procedures. Nonetheless, the use of a catalyst is convenient and smart when it allows to carry out processes faster, more selectively and under milder conditions. Nonetheless, the best catalyst is no catalyst.[188] The ideal reaction is one that proceeds thermally, under relatively mild conditions without the need for any additional reagents including catalyst to afford the desired product, preferably with 100% atom economy. Another potential issue is loss (e.g. leaching) of the catalyst during a reaction or during work-up, not to mention the phantom catalytic activity due to contamination, as recently demonstrated for magnetic stir bars.[189] Hence design and optimization of catalyst-free procedures is a benign-by-design approach to make chemistry more sustainable. Examples include various classes of reactions such as our batch and CF procedures for the catalyst-free synthesis of COCs and esters,[100,187] cycloaddition reactions[190], epoxide ring-opening[191].

1.6 Aim and summary of the Thesis

This work has been carried out in the Green Organic Synthesis Team (GOST) at the Dipartimento di Scienze Molecolari e Nanosistemi – Università Ca' Foscari di Venezia under the supervision of professor Alvise Perosa. The GOST research group has a longstanding interest in the green chemistry area: a particular focus is related to the use of bio-based building blocks for the synthesis of green molecules through environmentally-friendly procedures, the use of safe chemicals such as dialkylcarbonates as methylation agents, transesterification agents or for the synthesis of organic ionic liquids, the use of CO_2 as C_1 source or supercritical solvent, the employment of heterogeneous catalysis for photocatalytic applications.

The general aim of this Ph.D. work was the development of eco-friendly procedures for the synthesis of benign-by-design compounds that could displace the use of fossil-based compounds in various application fields (e.g. solvents, synthesis of polymers, intermediate in APIs manufacture, fuel additives, etc.).

The development of a sustainable chemistry for humans and the environment depends more and more upon the exploitation of renewable resources, in particular upon waste feedstocks particularly considering that man-made waste keeps increasing (e.g. solid waste production was 2 billion of tonnes in 2016 projected to increase to 4.4 bilions by 2050).[12] For this reasons two peculiar "waste" were used as renewable feedstock in this thesis: carbon dioxide and glycerol.

CO_2 is considered a waste feedstock since its emission to the atmosphere due to combustion has enormously increased over the last century (from 5 to 35 Gtonnes in the last century) and does not cease to increase, allowing to foresee serious consequences for climate. The use of carbon dioxide for the synthesis of chemical compounds has attracted the attention of chemists to reduce the emissions through its use. This does not mean that making chemicals from carbon dioxide can mitigate anthropogenic emissions of CO_2 since the two scales are totally decoupled (around 1% of the emitted CO_2 could be reused in the best scenario).[192] Nonetheless carbon dioxide utilization can provide value to emitted and/or captured CO_2 that otherwise would be only a worthless waste which fosters environmental concern.

Glycerol has been a valuable feedstock for one hundred and fifty years, but a glut of its production has occurred in the last twenty years as an industrial by-product in biodiesel manufacture. This has led the glycerol price to drop while its overabundance lured the attention of industrial and scientific actors. Despite 1st generation biodiesel manufacture will be probably overcome because of competition with food, water and land use, various promising 2nd and 3rd generation triglycerides feedstock such as microalgae suggests that a large amount of glycerol as biodiesel by-product will be generated until the transport sectors will be mainly based on liquid fuels.

In this thesis the use of these waste feedstocks is coupled with green intensified methodologies, such as increase of process efficiency and decrease of auxiliaries, hazardous reactants and wastes. The use of a green toolbox that contains continuous-flow reactors, tandem catalysis and the use of environmental-friendly reaction conditions, procedures and syntheses is the objective of the thesis.

The work has been articulated in two main sections through a target-oriented approach since two main classes of compounds are synthesized: cyclic organic carbonates and high-added value glycerol derivatives, i.e. glycerol acetals, glycerol esters and glycerol orthoesters. A brief summary of the results follows.

1.6.1 Synthesis of cyclic organic carbonates

1.6.1.1 Tungstate ionic liquids as catalysts for CO_2 fixation into epoxides

In this first part of the thesis we were interested in the synthesis of tungstate ionic liquids (TILs) and their use in the synthesis of COCs starting from epoxides and CO_2 (Figure 1.25). According to our knowledge, simple monotungstate-based catalysts were not known for this reaction. Initially different synthetic routes were explored for a series of ammonium, phosphonium, imidazolium and diazabycicloundecenium tungstate and peroxotungstate ionic liquids; their full spectroscopic characterisation (FT-IR, ^{1}H-, ^{13}C-and ^{183}W-NMR) was performed and a rational comparison of their properties and possible applications in catalysis was discussed. The synthetic procedures to obtain the ionic liquids rely on anion exchange and acid-base reactions – including an innovative route for the synthesis of tungstate and peroxotungstate ionic liquid using, for the first time, a completely organic halide-free ionic liquid (i.e. trioctylmethyl ammonium methylcarbonate) as precursor. The tungstate ionic liquids are then demonstrated as catalysts for CO_2 fixation in the model reaction of styrene oxide to styrene carbonate, after that also the substrate versatility was explored. Under optimized conditions, styrene carbonate is obtained in up to 67% yield at 90 °C with just butylmethylimidazolium tungstate and in yield >90% with tetrabutylammonium tungstate (or trioctyl methyl ammonium tungstate) coupled with tetrabutylammonium bromide. A cooperative effect with halide co-catalyst was demonstrated as reported for many others metal-based catalysts.[144b]

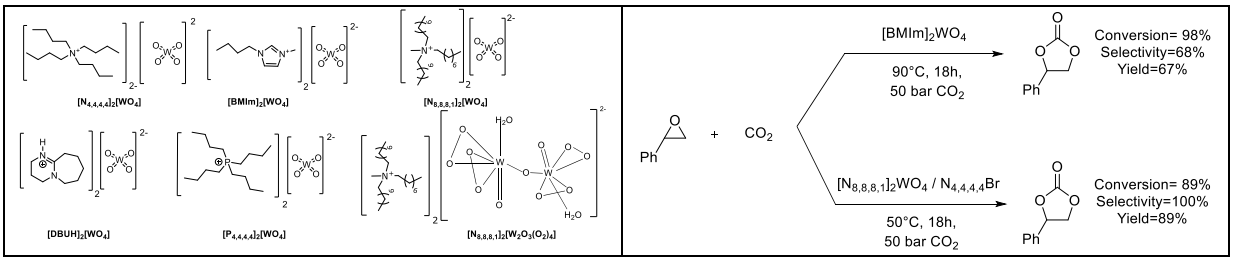

Figure 1.25: TILs synthesized and optimized conditions for the synthesis of styrene carbonate from styrene oxide and CO_2

1.6.1.2 Assisted tandem catalysis for the direct oxidative carboxylation of olefins into cyclic carbonates with tungsten-based catalysts

The results obtained in the first part of the work were used as the basis for a direct oxidative carboxylation path from olefins to cyclic organic carbonates. The activity of tungsten-based catalysts for epoxidation reactions has long been known and their use has been extensively studied.[193] The finding of their catalytic activity for the CO_2 fixation is novel and widens the interest towards a catalytic tandem process from olefin to COCs . The selected catalyst was $[N_{8,8,8,1}]_2[WO_4]$, ionic liquid obtained through a benign procedure that use methylcarbonate-onium ionic liquids as precursor: this synthetic route was by far greener than the other reported in the previous publications.

Preliminary tests showed that styrene could not be used as model substrate in the presence of peroxides (H_2O_2, TBHP) as oxidants and TILs as catalysts since styrene is strongly activated and undergoes rearrangement and over-oxidation reactions leading to the formation of several by-products. The less-activated class of olefins towards epoxidation is that of primary aliphatic ones: 1-decene was thus chosen

as model substrate, while H_2O_2 was selected as benign oxidant which allowed to work in a simple biphasic mixture that makes the separation of organic products easier and generates only water as by-product.
The reaction conducted in the presence of $[N_{8,8,8,1}]_2[WO_4]$ as catalyst and phosphoric acid as promoter give excellent performance: an almost quantitative conversion of 1-decene with a 92% selectivity towards decene oxide was achieved. However, the addition of CO_2 in the perspective of auto tandem catalysis gave low yields of the corresponding carbonate (<10%). The use of an assisted approach resulted successful in this case: the addition of 1 atm CO_2 and tetrabutyl ammonium iodide in the second step after the epoxidation without any intermediate work-up of the reaction mixture allowed to reach a gratifying 94% isolated yield in decene carbonate. The protocol was also easily reproduced on a 10-gram scale, demonstrating the scalability of the process. Similar performances were achieved starting from primary aliphatic olefins with different alkyl chain length (C_4-C_{16}), while low selectivity in the first epoxidation step heavily affect the DOC of substrates such as cyclohexene and styrene. Lastly, the procedure was attempted also on a renewable feedstock such as fatty esters: the optimized conditions for methyl oleate as model substrate allowed to reach a 70% yield in the corresponding COC by using potassium bromide as simple halide source. According to our knowledge, it is the first time that fatty esters are directly converted into COCs without the intermediate isolation and purification of the epoxide.

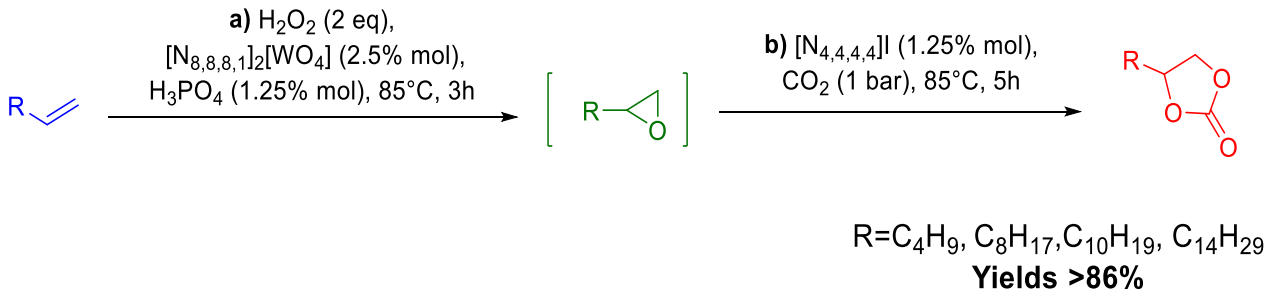

Figure 1.26: Direct oxidative carboxylation of primary olefins through an assisted tandem catalysis approach based on tungsten-based ionic liquids

1.6.1.3 DEG/NaBr catalyzed CO2 insertion into terminal epoxides: from batch to continuous flow

Along with the synthesis of novel metal-based ionic liquids, the exploration of catalytic systems based on inexpensive, sustainable, and commercially available compounds for CO_2 fixation in CF is a tool that could promote process intensification with the aim of making CO_2 incorporation ever more appealing also for the industrial sector.
In this third part of the work, CO_2 insertion reactions on terminal epoxides (8 examples) were performed in a binary homogeneous mixture comprising NaBr as halide source and diethylene glycol as complexing agent. Some authors had already exploited alkali halide (e.g. KI, CaI_2) with cation coordinating agents (*e. g.* glycols, crown ethers and polyethers)[194] but this pair was an innovative one and this is the first example of their use in a CF process. The reaction protocol was initially studied under batch conditions where a quantitative formation of the COCs were achieved at T = 100 °C and $p^0(CO_2)$ = 1 - 40 bar. These experimental tests allowed us also to prove the double role of diethylene glycol which acts as chelating agent for Na^+ but also as hydrogen-bond donor that activate the epoxide towards the ring-opening. The process was then transferred to continuous-flow and the effects of the reaction parameters (T, $p(CO_2)$, catalyst loading, and flow rates) were studied using microfluidic reactors. Albeit requiring harsh conditions (T = 220 °C and 120 bar) the CF conditions improved the productivity and allowed the recycle of the

catalytic system through a semi-continuous extraction procedure. For the model case of hexene oxide, the rate of formation of the corresponding carbonate, 4-butyl-1,3-dioxolan-2-one, was increased up to 27.6 mmol h^{-1} $equiv^{-1}$, a value 2.5 higher than in the batch mode(Figure 1.27). Moreover, the NaBr/DEG mixture was reusable without loss of performance for at least 4 subsequent CF-tests.[195]

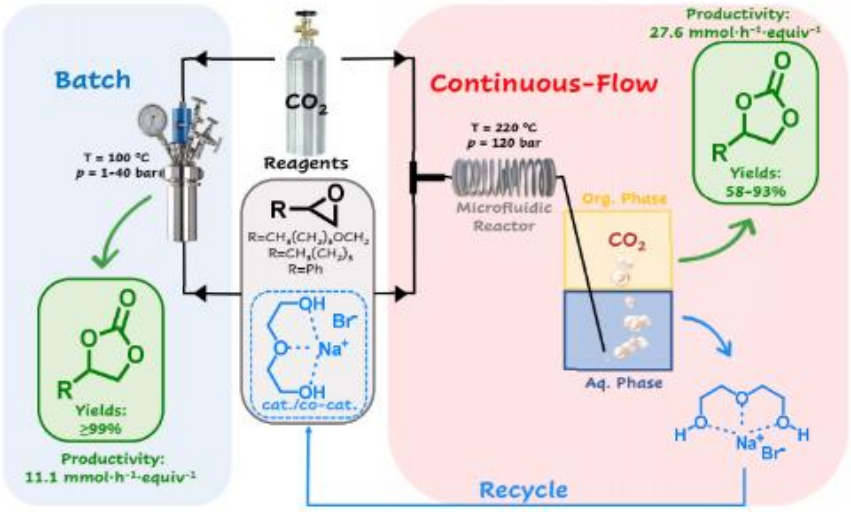

Figure 1.27: CO_2 insertion into terminal epoxides through the use of economic and commercially-available compounds as NaBr and Diethylene glycol as catalytic system through Batch and Continuous-flow processes.

1.6.2 Synthesis of high-added value glycerol derivatives

1.6.2.1 High-Temperature Batch and Continuous-Flow Transesterification of Alkyl and Enol Esters with Glycerol and Its Acetal Derivatives

The use of glycerol as renewable feedstock is a long-standing interest of the GOST research group in which this Ph. D. Thesis was carried out. In this perspective, the implementation of catalyst-free CF processes for the obtainment of glycerol derivatives having a plethora of applications is very attractive.

The transesterification of alkyl acetates and formates with model GAs (solketal and glycerol formal) was explored in the absence of any catalysts at high temperature (180−275°C). Highly selective transformations occurred in both batch and CF modes; particularly, the enol derivative isopropenyl acetate (iPAc) was the best performing reactant by which quantitative acetylation reactions were achieved with yields >95% on SolkAc and glycerol formal acetate. An excess acylating agent was necessary but the unconverted ester was fully recovered and could be reused. iPAc confirmed a superior performance than other esters also for the high-temperature conversion of glycerol: in this case the conditions were optimized to achieve the exhaustive transesterification of glycerol to triacetin, in both batch and CF modes. Triacetin, a chemical product with settled applications but also other ones in development, was isolated in 99% yield. Finally, we noted that the impressive performance and reactivity of IPAc compared to the other esters is due to the release of acetone in the reaction of iPAC that made the overall acetylation irreversible. We hypothesized that it was possible to achieve a tandem

acetylation/acetalization of glycerol through the released acetone. Unfortunately, the challenge of getting a good selectivity towards this product triggered by the high temperature and the plethora of equilibria and direct reactions involved, took to a maximum yield in SolkAc of 30% and 12%, in batch and CF mode respectively.[187a]

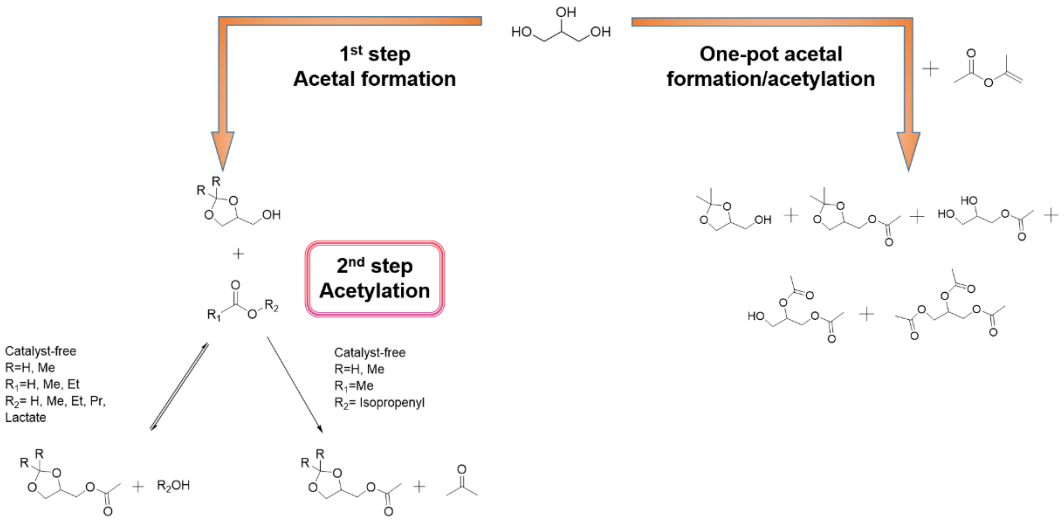

Figure 1.28: Application of isopropenyl acetate as transesterification agent for glycerol and glycerol acetals such as solketal and glycerol formal.

1.6.2.2 Development of a tandem process for the simultaneous acetylation/acetalization of glycerol

The hypothesis underlying the previous work was implemented through the use of an auto tandem catalytic approach. Isopropenyl acetate demonstrated a unique activity since it is capable to irreversibly acetylate glycerol by releasing acetone as a by-product. Here our scope was to find a route through which this by-product is transformed in an effective reactant able to couple with the residual vicinal hydroxyl present in glycerol to form an acetal.

In this research the use of Amberlyst-15 as catalyst promoted an auto tandem sequence to upgrade glycerol through selective acetylation and acetalization processes in the presence of a pool of innocuous reactants (isopropenyl acetate, acetic acid and acetone). The study provided evidence for the occurrence of multiple concomitant reactions: iPAc acted as a transesterification agent to provide glyceryl esters, and it was concurrently subjected to an acidolysis reaction promoted by acetic acid. Both these transformations co-generated acetone which converted glycerol into the corresponding acetals, while acidolysis sourced also acetic anhydride that acted as an acetylation reactant. By tuning the conditions, mostly by changing the reactant molar ratio and optimizing the reaction time, it was possible to steer the set of all reactions towards the synthesis of either a selective 1 : 1 mixture of solketal acetate and triacetin, or the solely formation of SolkAc in up to 91% yield, at complete conversion of glycerol. This represents a one-pot protocol with a high degree of control on the functionalization of glycerol via transesterification and acetalization reactions that exploit an auto tandem process catalyzed by a simple Brønsted acid catalyst such as Amberlyst-15. The procedure was also easily reproduced on a gram scale, thereby proving its efficiency for preparative purposes.[196]

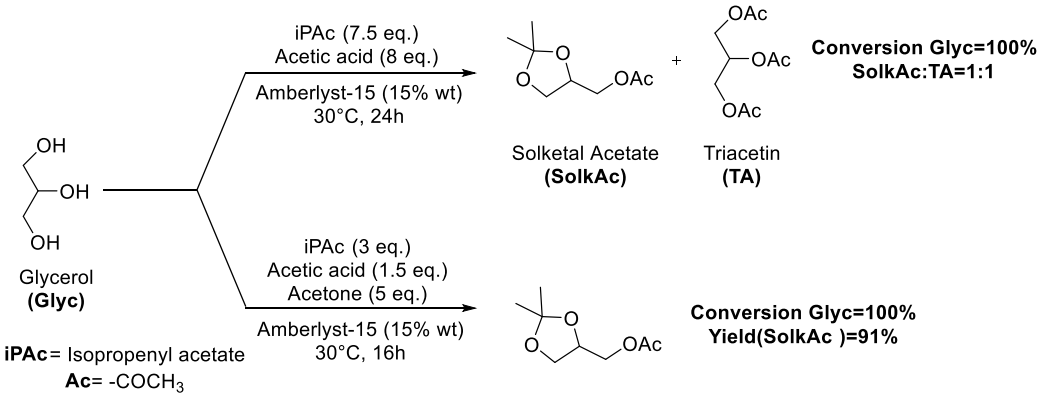

Figure 1.29: Optimized tandem reaction for the concurrent acetylation/acetalization of glycerol.

1.6.2.3 Reaction of Glycerol with Trimethyl Orthoformate: Towards the Synthesis of New Glycerol Derivatives

A continuous effort to identify new target molecules from waste resources prompted us to explore also the reactivity between glycerol and orthoesters. This class of compounds is massively exploited in organic chemistry as protecting group and their reactivity could be compared to that of acetals mentioned above (paragraph 1.4.4.2). The reactivity of glycerol with orthoesters was explored limitedly around 60 years ago but few studies have been carried out since then.[197] In this thesis, the reactions between glycerol and trimethyl orthoformate (TMOF) are explored with various molar ratio glycerol:TMOF, temperature, time of reaction, with or without the presence of simple acid and basic catalysts. The glycerol based orthoester 4-(dimethoxymethoxy)methyl)-2-methoxy-1,3-dioxolane was synthesized, under catalytic as well as catalyst-free conditions, by taking advantage of the thermodynamically controlled equilibrium between intermediates. Both Brønsted and Lewis acid catalysts accelerated the attainment of such an equilibrium, particularly Brønsted acidic ionic liquids $BSMImHSO_4$ was the most effective for this reaction. The kinetic profiles allowed to propose a mechanism that accounts for the selectivity of the reaction while an accurate study of the bidimensional NMR analysis of the products allowed to confirm the almost exclusive formation of the diastereoisomers relative to the 5-membered ring orthoester (red molecule) while the corresponding 6-membered isomer was find only in trace, similarly to what happen in the formation of solketal starting from glycerol and acetone. The product can be recovered with a high purity >97% via a green procedure that provides for the simple filtration of the catalyst (if any) and the evaporation of the TMOF in excess (that can be recovered and reused).[198]

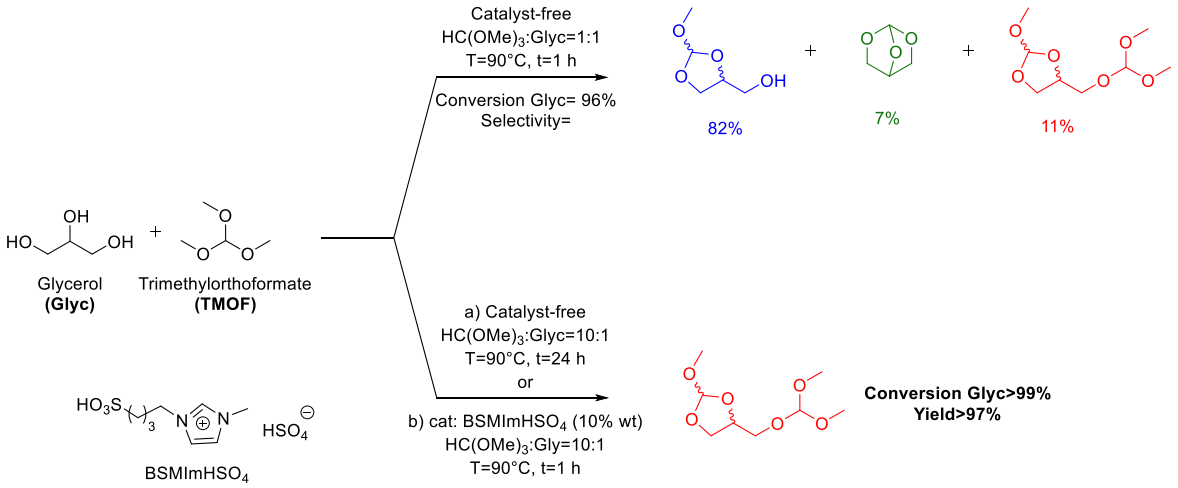

Figure 1.30: Examples taken from the study of the reactivity of glycerol with trimethyl orthoformate with various molar ratio between reactants and (eventually) the presence of an acid catalyst.

1.7 References

[1] R. A. Sheldon, Comptes Rendus de l'Académie des Sciences-Series IIC-Chemistry, 2000, **3**, 541-551.

[2] P. T. Anastas and J. C. Warner,*Green chemistry: Theory and practice*, Oxford University Press Inc, 1998, pp. 29-56.

[3] (a) B. Barber, Minerva, 1987, **25**, 123-134; (b) F. Hendriks, D. Kienhues and R. Bromme, *Trust and communication in a digitized world*, Springer, 2016, pp. 143-159.

[4] The evolving chemicals economy: Status and Trends relevant for sustainability - Global chemicals outlook II part I, UN Economic and Social commission, 2019.

[5] (a) WCO Secretariat, Illegal waste trafficking: more data is key to getting a better grip on this trade, WCO News, https://mag.wcoomd.org/magazine/wco-news-88/illegal-waste-trafficking-more-data-is-key-to-getting-a-better-grip-on-this-trade (accessed 05/01/2020); (b) Basel Action Network, Holes in the Circular Economy: WEEE Leakage from Europe, http://wiki.ban.org/images/f/f4/Holes_in_the_Circular_Economy_WEEE_Leakage_from_Europe (accessed 23/12/2020); (c) L. Cembalo, D. Caso, V. Carfora, F. Caracciolo, A. Lombardi and G. Cicia, *International Journal of Environmental Research and Public Health*, 2019, **16**, 165.

[6] (a) D. Michaels, *The Triumph of doubt: dark money and the science of deception*, Oxford University Press, 2020; (b) F. Lawrence, Nature, 2020, **578**, 28; (c) A. Lundh, J. Lexchin, B. Mintzes, J. B. Schroll and L. Bero, Cochrane Database of Systematic Reviews, 2017, **16**, 2; (d) A. Huss, M. Egger, K. Hug, K. Huwiler-Müntener and M. Röösli, Environmental health perspectives, 2007, **115**, 1-4; (e) J. Lexchin, L. A. Bero, B. Djulbegovic and O. Clark, Bmj, 2003, **326**, 1167-1170;

[7] D. H. Meadows, D. L. Meadows, J. Randers and W. W. Behrens, *The limits to growth*, Universe books, 1972.

[8] Chemicals, IEA, 2020, https://www.iea.org/reports/chemicals (accessed 22/12/2020)

[9] Resources to Reserves 2013: Oil, Gas and Coal Technologies for the Energy Markets of the Future, IEA Bioenergy, OECD Publishing, 2013.

[10] A New Circular Vision for Electronics: Time for a Global Reboot, World Economic Forum – Platform for Accelerating the Circular Economy, 2019.

[11] Designed by European chemical society (EuChemS), downloaded from https://www.euchems.eu/euchems-periodic-table (accessed on 22/12/2020)

[12] Kaza, Silpa, L. Yao, P. Bhada-Tata and F. Van Woerden, What a Waste 2.0: A global snapshot of Solid Waste Management to 2050, Whasington, DC, 2018.

[13] S. Needhidasan, M. Samuel and R. Chidambaram, Journal of Environmental Health Science and Engineering, 2014, **12**, 36.

[14] Multiple actions taken to address electronic waste - Evaluation report, US Environment Protection Agency, 2004.

[15] C. P. Balde, V. Forti, V. Gray, R. Kuehr and P. Stegmann, The Global E-waste Monitor 2017: Quantities, Flows and Resources, United Nations University, 2017.

[16] O. Edenhofer, *Climate change 2014: mitigation of climate change, Vol. 3*, Cambridge University Press, **2015**.

[17] COP21 report, Paris 2015, UN Framework Convention on Climate Change, 2015

[18] Brundtland Report - Our Common Future, World Commission on Environment and Development (WCED), 1987.

[19] D. Springett and M. Redclift, in *Routledge international handbook of sustainable development*, Routledge, 2015, pp. 25-60.

[20] https://xkcd.com/1007/ (accessed on 23/12/2020)

[21] R. Engelman, in *State of the World 2013*, Springer, 2013, pp. 3-16.

[22] M. Noe, Greener syntheses & solvents for fine and pharmaceutical chemicals, Ph. D. Thesis, Università Ca' Foscari Venezia, 2012.

[23] (a) A. Dobson, *Justice and the environment: Conceptions of environmental sustainability and theories of distributive justice*, Clarendon Press, 1998; (b) S. M. Lélé, World development, 1991, **19**, 607-621.

[24] Gro Harlem Brundtland, "Chairman's Foreword," WCED, p. xi in reference 18.

[25] B. Commoner, Chemistry in Britain, 1972, **8**, 52-56.

[26] N. Georgescu-Roegen, The Entropy Law and the economic problem, 1993, 75-88.

[27] T. Parrique, J. Barth, F. Briens, A. Kuokkanen and J. Spangenberg, Decoupling Debunked - Evidence and arguments against green growth as a sole strategy for sustainability, European Environmental Bureau, 2019.

[28] Among which: the damage to the ozone layer was halted by avoiding the use of ozone depleting substances; the access to safe water was improved worldwide; the use of renewable energies is increasing

by percentage more than fossil fuels; a cultural awareness on climate change, rainforests loss and biodiversity decline is growing too.

[29] As examples: the shrinking of aquifers; the global decline on biodiversity; the global poverty related to inequality between richer and poorer that it is ever increasing since it has been calculated for the first time[29] (bearing in mind that the richest 1% of the global population account for more polluting emissions than the poorest 50%[29]); the relentless march of warmer temperatures, higher sea levels and GHG emissions.

[30] P. W. Keys, V. Galaz, M. Dyer, N. Matthews, C. Folke, M. Nyström and S. E. Cornell, Nature Sustainability, 2019, **2**, 667-673.

[31] C. D. Rupprecht, J. Vervoort, C. Berthelsen, A. Mangnus, N. Osborne, K. Thompson, A. Y. Urushima, M. Kóvskaya, M. Spiegelberg and S. Cristiano, Global Sustainability, 2020, **3,** 1-12.

[32] https://www.unep.org/interactive/emissions-gap-report/2020/ (accessed on 23/12/2020)

[33] R. A. Sheldon, Green chemistry, 2008, **10**, 359-360.

[34] L. Summerton and A. Constandinou, in *Green and Sustainable Medicinal Chemistry*, 2016, pp. 41-53.

[35] P. J. Dunn, Chemical Society Reviews, 2012, **41**, 1452-1461.

[36] A. Sheldon, CHEMTECH, 1994, **24**, 3.

[37] T. Hudlicky, D. Frey, C. Claeboe and L. Brammer Jr, *Green Chemistry*, 1999, **1**, 57-59.

[38] C. R. McElroy, A. Constantinou, L. C. Jones, L. Summerton and J. H. Clark, Green Chemistry, 2015, **17**, 3111-3121.

[39] P. T. Anastas and J. B. Zimmerman, Green Chemistry, 2019, **21**, 6545-6566.

[40] P. T. Anastas, Trends in Chemistry, 2019, **1**, 145-148.

[41] P. W. Anderson, Science, 1972, **177**, 393-396.

[42] (a) S. A. Matlin, G. Mehta, H. Hopf and A. Krief, Nature Chemistry, 2016, **8**, 393-398; (b) T. E. Graedel, Pure and Applied Chemistry, 2001, **73**, 1243-1246.

[43] J. Liu, H. Mooney, V. Hull, S. J. Davis, J. Gaskell, T. Hertel, J. Lubchenco, K. C. Seto, P. Gleick and C. Kremen, Science, 2015, **347**.

[44] M. L. Brusseau and J. Artiola, in *Environmental and pollution science*, Elsevier, 2019, pp. 175-190.

[45] J. Pretty, Philosophical Transactions of the Royal Society B: Biological Sciences, 2008, **363**, 447-465.

[46] R. Viñas and C. S. Watson, Environmental health perspectives, 2013, **121**, 352-358.

[47] J. A. Becker and A. I. Stefanakis in *Pharmaceutical Sciences: Breakthroughs in Research and Practice*, IGI Global, 2017, pp. 1457-1475.

[48] H. C. Erythropel, J. B. Zimmerman, T. M. de Winter, L. Petitjean, F. Melnikov, C. H. Lam, A. W. Lounsbury, K. E. Mellor, N. Z. Janković and Q. Tu, Green chemistry, 2018, **20**, 1929-1961.

[49] J. Clark, R. Sheldon, C. Raston, M. Poliakoff and W. Leitner, Green Chemistry, 2014, **16**, 18-23.

[50] A. A. Burgess and D. J. Brennan, Chemical Engineering Science, 2001, **56**, 2589-2604.

[51] H. T. Odum*, Environmental accounting: emergy and environmental decision making*, Wiley, 1996.

[52] S. Spagnolo, G. Chinellato, S. Cristiano, A. Zucaro and F. Gonella, Journal of Cleaner Production, 2020, **277**, 124038.

[53] F. Coppola, S. Bastianoni and H. Østergård, Biomass and Bioenergy, 2009, **33**, 1626-1642.

[54] P. Nimmanterdwong, B. Chalermsinsuwan and P. Piumsomboon, Energy, 2017, **128**, 101-108.

[55] A. Perosa, F. Gonella and S. Spagnolo, Journal of Chemical Education, 2019, **96**, 2784-2793.

[56] J. B. Zimmerman, P. T. Anastas, H. C. Erythropel and W. Leitner, Science, 2020, **367**, 397-400.

[57] J. H. Clark and F. Deswarte*, Introduction to chemicals from biomass*, John Wiley & Sons, 2014.

[58] A. Behr and L. Johnen*, Handbook of Green Chemistry: Vol. 7 Green Processes: Green Synthesis*, John Wiley & Sons, 2010.

[59] S. Ulgiati, Critical Reviews in Plant Sciences, 2001, **20**, 71-106.

[60] P. M. Foley, E. S. Beach and J. B. Zimmerman, Green Chemistry, 2011, **13**, 1399-1405.

[61] E. De Jong, H. Stichnothe, G. Bell and H. Jorgensen, Bio-based chemicals - a 2020 update, 2020.

[62] E. Paone, T. Tabanelli, F. Mauriello, Current Opinion in Green and Sustainable Chemistry, 2020, **24**, 1–6.

[63] S. Topham, A. Bazzanella, S. Schiebahn, S. Luhr, L. Zhao, A. Otto and D. Stolten, Carbon Dioxide in *Ullmann's encyclopedia of industrial chemistry*, 2000, pp. 1-43.

[64] A.-L. Lavoisier, English translation:“Essays Physical and Chemical,” translated with notes and appendix by Thomas Henry, 2nd ed., Frank Cass, London, 1780.

[65] D. Thoday, Proceedings of the Royal Society of London. Series B, Containing Papers of a Biological Character, 1909, **82**, 1-55.

[66] IPCC, Global Warming of 1.5° C. An IPCC Special Report on the Impacts of Global Warming of 1.5° C Above Pre-Industrial Levels and Related Global Greenhouse Gas Emission Pathways, in the Context of

Strengthening the Global Response to the Threat of Climate Change, Sustainable Development, and Efforts to Eradicate Poverty, IPCC-World Organ Geneva, 2018.

[67] P. Markewitz, W. Kuckshinrichs, W. Leitner, J. Linssen, P. Zapp, R. Bongartz, A. Schreiber, T. E. Müller, Energy & environmental science 2012, **5**, 7281-7305.

[68] Since this is not properly a chemical strategy, it is not deepened

[69] K. Arning, J. Offermann-van Heek, A. Linzenich, A. Kaetelhoen, A. Sternberg, A. Bardow, M. Ziefle, Energy Policy 2019, **125**, 235-249.

[70] A. Otto, T. Grube, S. Schiebahn, D. Stolten, Energy & environmental science 2015, **8**, 3283-3297.

[71] N. Mac Dowell, P. S. Fennell, N. Shah, G. C. Maitland, Nature Climate Change 2017, **7**, 243–249.

[72] J. Artz, T. E. Müller, K. Thenert, J. Kleinekorte, R. Meys, A. Sternberg, A. Bardow, W. Leitner, Chemical Reviews 2018, **118**, 434–504.

[73] E. R. Pérez, R. H. Santos, M. T. Gambardella, L. G. De Macedo, U. P. Rodrigues-Filho, J.-C. Launay, D. W. Franco, The Journal of organic chemistry 2004, **69**, 8005-8011.

[74] (a) K. T., T. Okuyama, S. Kadosaki, M. U., T. E., Organic Letters 2019, **43**, 1–5; (b) M. Taheri, M. Ghiaci, A. Shchukarev, New Journal of Chemistry 2018, **42**, 587–597; (c) P. Yingcharoen, C. Kongtes, S. Arayachukiat, K. Suvarnapunya, S. V. C. Vummaleti, S. Wannakao, L. Cavallo, A. Poater, V. D' Elia, Advanced Synthesis and Catalysis 2018, **361**, 366–373; (d) Z.-Z. Yang, L.-N. He, Y.-N. Zhao, B. Li, B. Yu, Energy & Environmental Science 2011, **4**, 3971-3975.

[75] Y. Kayaki, M. Yamamoto, T. Ikariya, Angewandte Chemie International Edition 2009, **48**, 4194-4197.

[76] (a) D. Yu, S. P. Teong, Y. Zhang, Coordination Chemistry Reviews 2015, **293**, 279-291; (b) T. Kimura, K. Kamata, N. Mizuno, Angewandte Chemie International Edition 2012, **51**, 6700-6703.

[77] Y. Zhang, S. N. Riduan, Angewandte Chemie International Edition 2011, **50**, 6210-6212.

[78] R. Chawla, A. K. Singh, L. D. S. Yadav, RSC Advances 2013, **3**, 11385-11403.

[79] C. S. Yeung, V. M. Dong, Journal of the American Chemical Society 2008, **130**, 7826-7827.

[80] Q.-W. Song, Z.-H. Zhou and L.-N. He, Green Chemistry, 2017, **19**, 3707-3728.

[81] M. Pagliaro, *Glycerol: The Renewable Platform Chemical*, Elsevier, 2017.

[82] A. Behr and T. Seidensticker, in Chemistry of Renewables, Springer, 2020, pp. 89-109.

[83] D.Y.C. Leung, X. Wu, M.K.H. Leung, Applied Energy, 2010, **87(4)**, 1083-1095.

[84] Y. Xiao, G. Xiao, A. Varma, Industrial Engineering Chemistry Research, 2013**, 52**, 14291-14296.

[85] S. Hu, X. Luo, X., C. Wan, Y. Li, Journal of Agricultural Food Chemistry, 2012, **60**, 5915 −5921

[86] A. Cornejo, I. Barrio, M. Campoy, J. Lázaro and B. Navarrete, Renewable and Sustainable Energy Reviews, 2017, **79**, 1400-1413.

[87] L. Vaccaro, D. Lanari, A. Marrocchi and G. Strappaveccia, Green Chemistry, 2014, **16**, 3680-3704.

[88] Y. Hayashi, Chemical science, 2016, **7**, 866-880.

[89] C. Ramshaw, Green Chemistry, 1999, **1**, G15-G17.

[90] M. B. Gawande, V. D. Bonifacio, R. Luque, P. S. Branco and R. S. Varma, ChemSusChem, 2014, **7**, 24-44.

[91] F. Chemat, M. A. Vian and G. Cravotto, International journal of molecular sciences, 2012, **13**, 8615-8627.

[92] F. Capizzi, A. Das, T. Dauwe, I. Moorkens, R. Juhana, Renewable energy in Europe - Recent growth and knock-on effects, European Topic Centre on Climate Change Mitigation and Energy, 2019.

[93] W. M. Budzianowski, Renewable and Sustainable Energy Reviews, 2017, **70**, 793-804.

[94] T. M. Attard, J. H. Clark and C. R. McElroy, Current Opinion in Green and Sustainable Chemistry, 2020, **21**, 64-74.

[95] (a) L. Maisonneuve, O.A. Lamarzelle, E. Rix, E. Grau, H. Cramail, Chemical reviews, 2015, **115**, 12407-12439. (b) B. Schaffner, F. Schaffner, S.P. Verevkin, A. Borner, Chemical reviews, 2010, **110**, 4554-4581; (c) R.-S. Kühnel, N. Böckenfeld, S. Passerini, M. Winter, A. Balducci, Electrochimica Acta, 2011, **56**, 4092-4099.

[96] B.A. Santos, V.M. Silva, J.M. Loureiro, A.E. Rodrigues, ChemBioEng Reviews, 2014, **1**, 214-229.

[97] A.H. Tamboli, A.A. Chaugule, H. Kim, Chemical Engineering Journal, 2017, **323**, 530-544.

[98] G. Fiorani, A. Perosa, M. Selva, Green chemistry, 2018, **20**, 288-322.

[99] (a) M. Selva, A. Perosa, S. Guidi, L. Cattelan, Beilstein journal of organic chemistry, 2016, **12**, 1911-1924.; (b) W.K. Teng, G.C. Ngoh, R. Yusoff, M.K. Aroua, Energy conversion and management, 2014, **88**, 484-497; (c) Y. Ji, Catalysts, 2019, **9**, 581.

[100] S. Guidi, R. Calmanti, M. Noè, A. Perosa, M. Selva, ACS Sustainable Chemistry & Engineering, 2016, **4**, 6144-6151.

[101] N. Kindermann, T. Jose, A.W. Kleij, *Synthesis of Carbonates from Alcohols and CO_2, in Chemical Transformations of Carbon Dioxide*, Springer, 2017, pp. 61-88.

[102] K. Sekine, T. Yamada, Chemical Society Reviews, 2016, **45**, 4524-4532.

[103] S. Dabral, B. Bayarmagnai, M. Hermsen, J. Schießl, V. Mormul, A.S.K. Hashmi, T. Schaub, Organic letters, 2019, **21**, 1422-1425.

[104] P. Pässler, W. Hefner, K. Buckl, H. Meinass, A. Meiswinkel, H.-J. Wernicke, G. Ebersberg, R. Müller, J. Bässler, H. Behringer, Acetylene Production in *Ullmann's encyclopedia of industrial chemistry*, Wiley Eds., 2012, **1**, pp. 277-326

[105] (a) J.W. Comerford, I.D. Ingram, M. North, X. Wu, Green Chemistry, 2015, **77**, 1966-1987; (b) M. Alves, B. Grignard, R. Méreau, C. Jerome, T. Tassaing, C. Detrembleur, Catalysis Science & Technology, 2017, **7**, 2651-2684; (c) M. Liu, X. Wang, Y. Jiang, J. Sun, M. Arai, Catalysis Reviews, 2019, **61**, 214-269; (d) M. Selva, A. Perosa, G. Fiorani, L. Cattelan, CO_2 and Organic Carbonates for the Sustainable Valorization of Renewable Compounds, in *Green Synthetic Processes and Procedures,* 2019, pp. 319-342; (e) T.K. Pal, D. De, P.K. Bharadwaj, Coordination Chemistry Reviews, 2020, **408**, 213173; (f) F. Della Monica and A. W. Kleij, *Catalysis Science & Technology*, 2020, **10**, 3483-3501

[106] L.H. Pottenger, D.R. Boverhof, J.M. Waechter Jr, *Patty's Toxicology*, Wiley Eds., 2001, pp. 425-490.

[107] (a) S. Rebsdat, D. Mayer, Ethylene Oxide in *Ullmann's Encyclopedia of Industrial Chemistry*, Wiley Eds., 2012, **13,** pp. 547-572; (b) T.A. Nijhuis, M. Makkee, J.A. Moulijn, B.M. Weckhuysen, Industrial & engineering Chemistry research, 2006, **45**, 3447-3459; (c) S.T. Oyama, Rates, kinetics, and mechanisms of epoxidation: homogeneous, heterogeneous, and biological routes, in: *Mechanisms in homogeneous and heterogeneous epoxidation catalysis*, Elsevier, 2008, pp. 3-99.

[108] S. Huber, M. Cokoja, F.E. Kuehn, Journal of Organometallic Chemistry, 2014, **751**, 25-32.

[109] (a) L. Ehrenberg, S. Hussain, Mutation Research/Reviews in *Genetic Toxicology*, 1981, **86**, 1-113; (b) M.M. Manson, Occupational and Environmental Medicine, 1980, **37**, 317-336.

[110] (a) R. G. Austin, R. C. Michaelson and R. S. Myers, US4824969A, 1989; (b) S. E. Jacobson, US4483994A, 1984; (c) S. E. Jacobson, US4325874A, 1982; (d) J.-L. Kao, G. A. Wheaton, H. Shalit and M. N. Sheng, US4247465A, 1981; (e) C. Fumagalli, G. Caprara and P. Roffia, CA6010327A, 1977; (f) J. A. Verdol, US3025305A, 1962.

[111] A. Chieregato, J.V. Ochoa, F. Cavani, *Chemicals and Fuels from Bio-Based Building Blocks*, Wiley, 2016.

[112] A. Bazzanella, F. Ausfelder, Low carbon energy and feedstock for the European chemical industry, DECHEMA, Gesellschaft für Chemische Technik und Biotechnologie eV, 2017.

[113] B.S. Lane, K. Burgess, Chemical reviews, 2003, **103**, 2457-2474.

[114] P.G.M. Wuts, T.W. Greene, Protection for the Carbonyl group in *Greene's Protective Groups in Organic Synthesis*, 2006, Wiley, pp. 431-532.

[115] (a) A. R. Trifoi, P. Ş. Agachi and T. Pap, *Renewable and Sustainable Energy Reviews*, 2016, **62**, 804-814; (b) S. Guidi, M. Noè, P. Riello, A. Perosa and M. Selva, Molecules, 2016, **21**, 657; (c) M. R. Nanda, Z. Yuan, W. Qin, H. S. Ghaziaskar, M.-A. Poirier and C. C. Xu, Fuel, 2014, **117**, 470-477. 1; (d) V. R. Ruiz, A. Velty, L. L. Santos, A. Leyva-Pérez, M. J. Sabater, S. Iborra and A. Corma, Journal of Catalysis, 2010, **271**, 351-357.

[116] B. Burczyk, A. Piasecki and L. Weclas, J.Phys. Chem., 1985, **89**, 1032-1035.

[117] L. Moity, A. Benazzouz, V. Molinier, V. Nardello-Rataj, M. K. Elmkaddem, P. De Caro, S. Thiébaud-Roux, V. Gerbaud, P. Marion and J.-M. Aubry, Green Chemistry, 2015, **17**, 1779-1792.

[118] L. R. Odell, J. Skopec and A. McCluskey, Forensic science international, 2006, **164**, 221-229.

[119] (a) B. A. Meireles and V. L. P. Pereira, Journal of the Brazilian Chemical Society, 2013, **24**, 17-57; (b) M. Khayoon and B. Hameed, Applied Catalysis A: general, 2013, **460**, 61-69; (c) G. Morales, M. Paniagua, J. A. Melero, G. Vicente and C. Ochoa, Industrial & engineering chemistry research, 2011, **50**, 5898-5906.

[120] A. Perosa, A. Moraschini, M. Selva and M. Noè, Molecules, 2016, **21**, 170.

[121] (a) H. Rastegari, H. S. Ghaziaskar and M. Yalpani, Industrial & Engineering Chemistry Research, 2015, **54**, 3279-3284; (b) L. N. Silva, V. L. Gonçalves and C. J. Mota, Catalysis Communications, 2010, **11**, 1036-1039.

[122] (a) C. Rosso, G. Filippini and M. Prato, ACS Catalysis, 2020, **10**, 8090-8105; (b) T. A. Goetjen, J. Liu, Y. Wu, J. Sui, X. Zhang, J. T. Hupp and O. K. Farha, Chemical Communications, 2020, **56**, 10409-10418; (c) D. W. Stephan, in *Frustrated Lewis Pairs*, 2013, Springer, pp. 1-28.

[123] T. A. Saleh, Environmental Technology & Innovation, 2020, **20**, 101067.

[124] L. Capaldo and D. Ravelli, European Journal of Organic Chemistry, 2020, **19**, 2783-2806.

[125] R. Malolan, K. P. Gopinath, D.-V. N. Vo, R. S. Jayaraman, S. Adithya, P. S. Ajay and J. Arun, Environmental Chemistry Letters, 2020, **18**, 2031-2054.

[126] (a) J. Andersen and J. Mack, Green Chemistry, 2018, **20**, 1435-1443; (b) E. Colacino, G. Dayaker, A. Morère and T. Friščić, Journal of Chemical Education, 2019, **96**, 766-771.

[127] (a) G. Mannina, D. Presti, G. Montiel-Jarillo, J. Carrera and M. E. Suárez-Ojeda, Bioresource Technology, 2020, **297**, 122478; (b) L. Vogli, S. Macrelli, D. Marazza, P. Galletti, C. Torri, C. Samorì and S. Righi, Energies, 2020, **13**, 2706.

[128] D. Jagadeesan, Applied Catalysis A:General, 2016, **511**, 59-77.

[129] D. E. Fogg and E. N. dos Santos, Coordination Chemistry Reviews, 2004, **248**, 2365-2379.

[130] T. L. Lohr and T. J. Marks, Nature chemistry, 2015, **7**, 477.

[131] S. Abou-Shehada and J. M. Williams, Nature chemistry, 2014, **6**, 12-13.

[132] Since we will usea metal-based approach during this Ph.D. thesis, we will only report the metal-based mechanisms that have overwhelming validation for the epoxidation step.

[133] Demonstrated by studies on the epoxidation of ethylene or other substrates without allylic hydrogens such as styrene, norbornene, butadiene, see for example: (a) F. J. Williams, D. P. Bird, A. Palermo, A. K. Santra and R. M. Lambert, Journal of American Chemical Society, 2004, **126**, 8509-8514.; (b) J. T. Roberts, A. J. Capote and R. J. Madix, Journal of American Chemical Society 1991, **113**, 9848-9851; (c) J. T. Roberts and R. J. Madix, Journal of American Chemical Society 1988, **110**, 8540-8541.

[134] G. C. Bond, C. Louis and D. T. Thompson, *Catalysis by gold*, World Scientific, 2006.

[135] a) A. Corma and H. Garcia, Chemical Society Reviews, 2008, **37**, 2096-2126, (b) M. D. Hughes, Y.-J. Xu, P. Jenkins, P. McMorn, P. Landon, D. I. Enache, A. F. Carley, G. A. Attard, G. J. Hutchings and F. King, Nature, 2005, **437**, 1132-1135; (c) A. K. Sinha, S. Seelan, S. Tsubota and M. Haruta, Angewandte Chemie International Edition, 2004, **43**, 1546-1548.

[136] N. Patil, B. Uphade, P. Jana, S. Bharagava and V. Choudhary, Journal of Catalysis, 2004, **223**, 236-239.

[137] (a) A. Corma, M. Navarro and J. P. Pariente, Journal of Chemical Society Chemistry Communication, 1994, 147-148; (b) M.G. Clerici, P. Ingallina, Journal of Catalysis, 1993, **140**, 71-83.

[138] I. Arends, R. Sheldon, Topics in Catalysis, 2002, **19**, 133-141.

[139] (a) K. Sharpless, J. Townsend, D. Williams, Journal of the American Chemical Society, 1972, **94**, 295-296; (b) D.V. Deubel, J. Sundermeyer, G. Frenking, Journal of the American Chemical Society, 2000, **122**, 10101-10108; (c) P. Gisdakis, I.V. Yudanov, N. Rösch, Inorganic chemistry, 2001, **40**, 3755-3765.

[140] W. Nam, H.J. Han, S.-Y. Oh, Y.J. Lee, M.-H. Choi, S.-Y. Han, C. Kim, S.K. Woo, W. Shin, Journal of the American Chemical Society, 2000, **122**, 8677-8684.

[141] (a) J.P. Collman, L. Zeng, J.I. Brauman, Inorganic chemistry, 2004, **43**, 2672-2679; (b) G. Yin, M. Buchalova, A.M. Danby, C.M. Perkins, D. Kitko, J.D. Carter, W.M. Scheper, D.H. Busch, Inorganic chemistry, 2006, **45**, 3467-3474.

[142] (a) H. Buettner, L. Longwitz, J. Steinbauer, C. Wulf, T. Werner, Recent developments in the synthesis of cyclic carbonates from epoxides and CO_2, in *Chemical Transformations of Carbon Dioxide*, Springer, 2017, pp. 89-144; (b) C. Martin, G. Fiorani, A.W. Kleij, ACS Catalysis, 2015, **5**, 1353-1370; (c) V. D'Elia, J.D. Pelletier, J.M. Basset, ChemCatChem, 2015, **7**, 1906-1917.

[143] (a) K. Yamaguchi, K. Ebitani, T. Yoshida, H. Yoshida, K. Kaneda, Journal of the American Chemical Society, 1999, **121**, 4526-4527; (b) Y.M. Shen, W.L. Duan, M. Shi, Advanced Synthesis & Catalysis, 2003, **345**, 337-340.

[144] (a) M. North, R. Pasquale, Angewandte Chemie International Edition, 2009, **48**, 2946-2948; (b) R. Calmanti, M. Selva, A. Perosa, Molecular Catalysis, 2020, **486,** 110854.

[145] P. Ramidi, C.M. Felton, B.P. Subedi, H. Zhou, Z.R. Tian, Y. Gartia, B.S. Pierce, A. Ghosh, Journal of CO2 Utilization, 2015, **9**, 48-57.

[146] Z. Shi, G. Niu, Q. Han, X. Shi, M. Li, Molecular Catalysis, 2018, 456, 10-18.

[147] F. Chen, T. Dong, T. Xu, X. Li and C. Hu, Green Chemistry, 2011, **13**, 2518-2524.

[148] J. Sun, S.-i. Fujita, F. Zhao, M. Hasegawa, M. Arai, Journal of Catalysis, 2005, **230**, 398-405.

[149] Y. Wang, J. Sun, D. Xiang, L. Wang, J. Sun, F.-S. Xiao, Catalysis letters, 2009, **129**, 437-443.

[150] A. I. Stankiewicz and J. A. Moulijn, Chemical engineering progress, 2000, **96**, 22-34.

[151] J. Britton and T. F. Jamison, Nature Protocols, 2017, **12**, 2423.

[152] M. B. Plutschack, B. u. Pieber, K. Gilmore and P. H. Seeberger, Chemical reviews, 2017, **117**, 11796-11893.

[153] D. Cantillo and C. O. Kappe, ChemCatChem, 2014, **6**, 3286-3305.

[154] A. R. Bogdan and N. W. Sach, Advanced Synthesis & Catalysis, 2009, **351**, 849-854.

[155] F. Gomollón-Bel, Chemistry International, 2019, **41**, 12-17.

[156] N. Asprion, S. Mollner, N. Poth and B. Rumpf, Energy Management in *Chemical Industry in Ullmann's Encyclopedia of Industrial Chemistry*, Wiley Eds., 2010, **12**, pp. 501-519.

[157] L. Rogers and K. F. Jensen, Green chemistry, 2019, **21**, 3481-3498.

[158] J. Britton and C. L. Raston, Chemical Society Reviews, 2017, **46**, 1250-1271.

[159] R. Gerardy, D. P. Debecker, J. Estager, P. Luis and J.-C. M. Monbaliu, Chemical Reviews, 2020, **120**, 7219-7347.

[160] S. Falß, N. Kloye, M. Holtkamp, A. Prokofyeva, T. Bieringer and N. Kockmann, *Handbook of Green Chemistry*, Wiley-VCH, 2018.

[161] G. Allison, Y. T. Cain, C. Cooney, T. Garcia, T. G. Bizjak, O. Holte, N. Jagota, B. Komas, E. Korakianiti and D. Kourti, Journal of pharmaceutical sciences, 2015, **104**, 803-812.

[162] P. Poechlauer, J. Colberg, E. Fisher, M. Jansen, M. D. Johnson, S. G. Koenig, M. Lawler, T. Laporte, J. Manley and B. Martin, Organic Process Research & Development, 2013, **17**, 1472-1478.

[163] J. A. Lummiss, P. D. Morse, R. L. Beingessner and T. F. Jamison, The Chemical Record, 2017, **17**, 667-680.

[164] (a) S. Bonollo, D. Lanari, J. M. Longo and L. Vaccaro, Green chemistry, 2012, **14**, 164-169; (b) A. Palmieri, S. Gabrielli and R. Ballini, Green chemistry, 2013, **15**, 2344-2348; (c) A. Zvagulis, S. Bonollo, D. Lanari, F. Pizzo and L. Vaccaro, Advanced Synthesis & Catalysis, 2010, **352**, 2489-2496.

[165] D. J. Constable, C. Jimenez-Gonzalez and R. K. Henderson, Organic process research & development, 2007, **11**, 133-137.

[166] J. W. Tucker, Y. Zhang, T. F. Jamison and C. R. J. Stephenson, Angewandte Chemie International Edition, 2012, **51**, 4144-4147.

[167] (a) A. Harsanyi, A. Conte, L. Pichon, A. Rabion, S. Grenier and G. Sandford, Organic Process Research & Development, 2017, **21**, 273-276; (b) D. R. Snead and T. F. Jamison, Angewandte Chemie International Edition, 2015, **54**, 983-987.

[168] D. Dallinger and C. O. Kappe, Current Opinion in Green and Sustainable Chemistry, 2017, **7**, 6-12.

[169] B. P. Mason, K. E. Price, J. L. Steinbacher, A. R. Bogdan and D. T. McQuade, Chemical reviews, 2007, **107**, 2300-2318.

[170] V. Hessel, Chemical Engineering & Technology, 2009, **32**, 1655-1681.

[171] (a) L. Shui, J. C. T. Eijkel and A. van den Berg, Advances in Colloid and Interface Science, 2007, **133**, 35-49; (b) C. N. Baroud and H. Willaime, Comptes Rendus Physique, 2004, **5**, 547-555; (c) C. Aellig, D. Scholz, P. Y. Dapsens, C. Mondelli and J. Pérez-Ramírez, Catalysis Science & Technology, 2015, **5**, 142-149; (d) J. A. Kozak, J. Wu, X. Su, F. Simeon, T. A. Hatton and T. F. Jamison, Journal of the American Chemical Society, 2013, **135**, 18497-18501.

[172] S. A. May, M. D. Johnson, J. Y. Buser, A. N. Campbell, S. A. Frank, B. D. Haeberle, P. C. Hoffman, G. R. Lambertus, A. D. McFarland, E. D. Moher, T. D. White, D. D. Hurley, A. P. Corrigan, O. Gowran, N. G. Kerrigan, M. G. Kissane, R. R. Lynch, P. Sheehan, R. D. Spencer, S. R. Pulley and J. R. Stout, Organic Process Research & Development, 2016, **20**, 1870-1898.

[173] G. Van der Vorst, W. Aelterman, B. De Witte, B. Heirman, H. Van Langenhove and J. Dewulf, Green Chemistry, 2013, **15**, 744-748.

[174] W.-C. Shieh, S. Dell and O. Repič, Organic Letters, 2001, **3**, 4279-4281.

[175] U. Tilstam, Organic Process Research & Development, 2012, **16**, 1974-1978.

[176] T. N. Glasnov, J. D. Holbrey, C. O. Kappe, K. R. Seddon and T. Yan, Green Chemistry, 2012, **14**, 3071-3076.

[177] L. Cattelan, A. Perosa, P. Riello, T. Maschmeyer and M. Selva, ChemSusChem, 2017, **10**, 1571-1583.

[178] D. Kralisch, I. Streckmann, D. Ott, U. Krtschil, E. Santacesaria, M. Di Serio, V. Russo, L. De Carlo, W. Linhart, E. Christian, B. Cortese, M. H. J. M. de Croon and V. Hessel, ChemSusChem, 2012, **5**, 300-311.

[179] J. Wu, J.A. Kozak, F. Simeon, T.A. Hatton, T.F. Jamison, Chemical Science, 2014, **5**, 1227-1231.

[180] (a) A. Podgoršek, M. Zupan, J. Iskra, Angewandte Chemie International Edition, 2009, **48**, 8424-8450; (b) G. Rothenberg, J.H. Clark, Green Chemistry, 2000, **2**, 248-251; (c) C.O. Guss, R. Rosenthal, Journal of the American Chemical Society, 1955, **77**, 2549-2549.

[181] A.A. Sathe, A.M. Nambiar, R.M. Rioux, Catalysis Science & Technology, 2017, **7**, 84-89.

[182] C. Jimenez-Gonzalez, A. D. Curzons, D. J. Constable and V. L. Cunningham, Clean Technologies and Environmental Policy, 2004, **7**, 42-50.

[183] R. A. Sheldon, Green Chemistry, 2017, **19**, 18-43.

[184] F. Gao, R. Bai, F. Ferlin, L. Vaccaro, M. Li and Y. Gu, Green Chemistry, 2020, **22**, 6240-6257.

[185] S. Santoro, F. Ferlin, L. Luciani, L. Ackermann and L. Vaccaro, Green Chemistry, 2017, **19**, 1601-1612.

[186] C. J. Clarke, W.-C. Tu, O. Levers, A. Brohl and J. P. Hallett, Chemical reviews, 2018, **118**, 747-800.

[187] (a) R. Calmanti, M. Galvan, E. Amadio, A. Perosa and M. Selva, ACS Sustainable Chemistry & Engineering, 2018, **6**, 3964-3973; (b) M. Selva, S. Guidi and M. Noè, Green Chemistry, 2015, **17**, 1008-1023.

[188] R. A. Sheldon, Chemical Communications, 2008, 29, 3352-3365.

[189] E. O. Pentsak, D. B. Eremin, E. G. Gordeev and V. P. Ananikov, ACS Catalysis, 2019, **9**, 3070-3081.

[190] H. M. Ibrahim, H. Behbehani and N. S. Mostafa, ACS Omega, 2019, **4**, 7182-7193.

[191] C. Zhang, Y. Xia, R. Chen, S. Huh, P. A. Johnston and M. R. Kessler, Green Chemistry, 2013, **15**, 1477-1484.

[192] M. Poliakoff, W. Leitner and E. S. Streng, Faraday discussions, 2015, **183**, 9-17.

[193] (a) C. Venturello and R. D'Aloisio, The Journal of Organic Chemistry, 1988, **53**, 1553-1557; (b) N. Mizuno, K. Yamaguchi and K. Kamata, Coordination chemistry reviews, 2005, **249**, 1944-1956; (c) J.-M. Brégeault, M. Vennat, L. Salles, J.-Y. Piquemal, Y. Mahha, E. Briot, P. C. Bakala, A. Atlamsani and R. Thouvenot, Journal of Molecular Catalysis A: Chemical, 2006, **250**, 177-189.

[194] (a) G. Rokicki, W. Kuran, B. Pogorzelska-Marciniak, Monatsher Chemie, 1984, **115**, 205–214; (b) S. Kaneko, S. Shirakawa, ACS Sustainable Chemistry & Engineering 2017, **5**, 2836–2840; (c) J. Steinbauer, T. Werner, ChemSusChem 2017, **10**, 3025–3029; (d) Y. Hu, J. Steinbauer, V. Stefanow, A. Spannenberg, T. Werner, ACS Sustainable Chemical Engineering, 2019, **7**, 13257–13269.

[195] D. Rigo, R. Calmanti, A. Perosa, G. Fiorani, M: Selva, Chemcatchem, 2021, in press.

[196] D. Rigo, R. Calmanti, A. Perosa and M. Selva, Green Chemistry, 2020, **22**, 5487-5496.

[197] (a) G. Crank and F. Eastwood, Australian Journal of Chemistry, 1964, **17**, 1392-1398; (b) G. Crank and F. Eastwod, Australian Journal of Chemistry, 1964, **17**, 1385-1391; (c) H. Hall Jr, F. DeBlauwe and T. Pyriadi, Journal of the American Chemical Society, 1975, **97**, 3854-3854; (d) N. N. Tshibalonza and J.-C. M. Monbaliu, Green Chemistry, 2017, **19**, 3006-3013.

[198] R. Calmanti, E. Amadio, A. Perosa and M. Selva, Catalysts, 2019, **9**, 534.

2 Synthesis of cyclic organic carbonates

2.1 Tungstate ionic liquids as catalysts for CO_2 fixation into epoxides

2.1.1 Introduction

In the previous section (paragraph 1.4) we introduced the reasons why CO_2 is a so fascinating (waste) feedstock for organic chemists and why cyclic organic carbonates (COCs) are considered potential bio-based chemicals with a plethora of applications. The synthetic routes through which COCs can be obtained were summarized by highlighting that the insertion of CO_2 into epoxides is the most widely explored route as indicated by several recent review articles especially focused on the mechanisms involved and the catalytic activity of homogeneous, heterogeneous, metal-based and organo-based catalysts .[1,2,3,4]

The general catalytic mechanism for the formation of COCs starting from epoxides was briefly illustrated in paragraph 1.5.1.1 and the same figure is reported here for ease of reading (Figure 2.1).

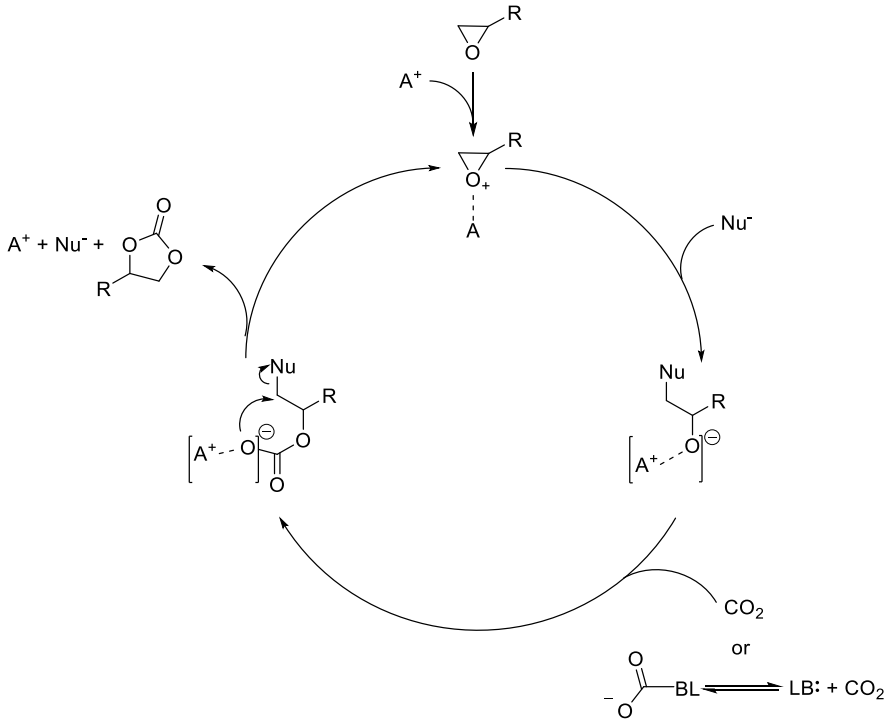

Figure 2.1: General mechanism for the CO_2 insertion into epoxides

The main features required for CO_2 fixation in epoxides are the following.

- A species (A+) with Lewis acidic character [usually a metal-based Lewis acid (e.g. Fe, Cr, Co, Al, Sn)][5] or H-bonding ability to activate the epoxide (e.g. -OH, -COOH, -NH group)[6]
- A nucleophile that ring-opens the epoxide and acts as a good leaving group in the last step in which COCs is formed; the classic nucleophiles used are halides, especially bromide and iodide.[7]
- In certain cases, a species with Lewis base character that activates CO_2 towards nucleophilic attack.[8]

The main competing reaction that can lower selectivity towards COCs is chain propagation of the ring-opened epoxide and consequent formation of polyethers or polycarbonates.[9] Alternatively, also hydrolysis or rearrangement of the epoxide catalyzed by Lewis acid.[1,10]

The catalytic mechanism involved explains why a continuous effort has been done in the last years to identify multifunctional catalysts capable of simultaneously activating CO_2 and the epoxide. The use of a halide nucleophile to promote the ring-opening seems unavoidable, even though a few recent articles have demonstrated the feasibility of halide-free processes.[11]

Among metal-based catalysts, Kimura et al. have recently shown that monomeric tungstate salts as tetrabutylammonium tungstate ($[N_{4,4,4,4}]_2[WO_4]$, were active systems for the chemical fixation of CO_2 into compounds such as aryldiamines, primary monoamines, propargylic alcohols or 2-aminobenzonitriles. The comparably higher basicity, nucleophilicity, and H-bonding character of $[WO_4]^{2-}$ compared to polyoxotungstates, accounted for the concurrent activation of CO_2 and reactant substrates.[12] Subsequently, Guo et al. also proved that silver tungstate acted as a bifunctional catalyst for the carboxylation of terminal alkynes with CO_2 under ambient conditions, in the presence of a stochiometric amount of a base and of butyl iodide.[13] Although interactions between the tungstate anion and CO_2 were known since 1985,[14] these were the first examples of catalytic exploitation of the tungstate-carbon dioxide adduct for CO_2 fixation.

In the field of CO_2 insertion into epoxides for the synthesis of cyclic organic carbonates, there is evidence in the literature for the use of complex catalytic systems based on W such as zinc-substituted sandwich type polyoxotungstates,[15] Keggin-type zinc polioxotungstate metal organic frameworks,[16] tetracarbonyl manganese selenotungstate derivatives.[17] Surprisingly however, simple monotungstate-based catalysts have not been reported so far.

2.1.2 Aim and summary of the work

The present study describes the synthesis of a series of different tungstate ionic liquids catalysts (TILCs) and their use for the insertion of CO_2 with epoxides. First, the routes reported in literature for the synthesis of TILCs were tested and compared with a novel halide-free synthesis implemented through the use of methylcarbonate -onium ionic liquids, an area that fashioned the interests of the research group in which this thesis was carried out over the years.[18,19] A full spectroscopic characterization (FT-IR, ^1H-, ^{13}C-and

^{183}W-NMR) of the synthesized TILCs allowed to explore their properties and their possible applications in catalysis. Subsequently, the CO_2 fixation into epoxides was investigated on a model substrate (i.e. styrene oxide) by varying reaction conditions such as temperature, time, amount of catalyst and CO_2 pressure. TILCs resulted suitable catalysts for the formation of COCs: the use of butilmethyl imidazolium tungstate ($BMIM_2WO_4$) allowed to reach up to 70% yield in styrene carbonate; a complete selectivity towards COCs was not achievable as a consequence of side reactions that promote the parallel formation of by-products when TILCs are used alone. The use of a simple halide co-catalyst enabled to improve the selective formation of styrene carbonate with isolated yields >85%.

2.1.3 Results and discussions

2.1.3.1 Tungstate ionic liquids catalysts (TILCs) synthesis

A series of onium (ammonium, phosphonium, imidazolium and diazabycicloundecenium) tungstate ionic liquids, $Q_2[WO_4]$, were initially prepared to start investigating the insertion of CO_2 into epoxides. Three different synthetic procedures were implemented.

The first protocol (Figure 2.2) was adapted from the literature[20] and involved metathesis between silver tungstate (Ag_2WO_4) and different onium bromide salts, Q^+Br^- in water, yielding the corresponding water-soluble tungstate ionic liquids and the insoluble silver halide.

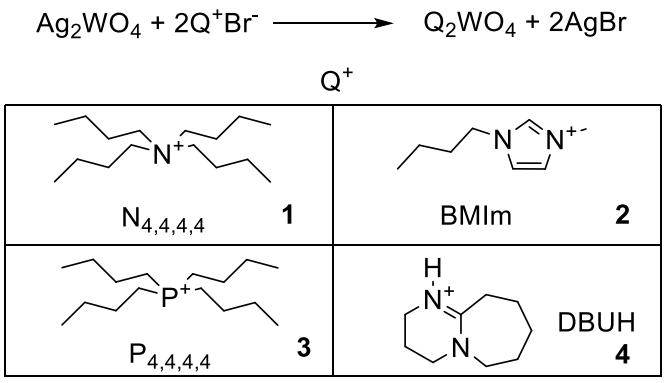

Figure 2.2: Tungstate ionic liquids by metathesis with Ag_2WO_4

After filtration and removal of water under vacuum, the desired tungstate salts: $[N_{4,4,4,4}]_2[WO_4]$ (**1**, $N_{4,4,4,4}$ = tetrabutylammonium, 80% yield), $[BMIm]_2[WO_4]$ (**2**, BMIm = n-butylmethylimidazolium, 86% yield), $[P_{4,4,4,4}]_2[WO_4]$ (**3**, $P_{4,4,4,4}$ = tetrabutylphosphonium, 92% yield), and $DBUH_2[WO_4]$ (**4**, DBUH = diazabycicloundecenium, 87% yield) were obtained as off-white hygroscopic solids.[21] The method proved to be a general synthetic benchmark, but it suffered from the use of silver salts with concurrent formation

of silver halides as by-products. Other procedures focused on more economic, sustainable, greener and halide-free routes, were then considered.

The second protocol (Figure 2.3) involved a direct acid-base reaction between diazabicycloundecene (DBU) as a strong organic base, and tungstic acid, H_2WO_4. DBU-based metal ionic liquids are proved to be efficient for the CO_2 fixation into epoxides.[13,22]

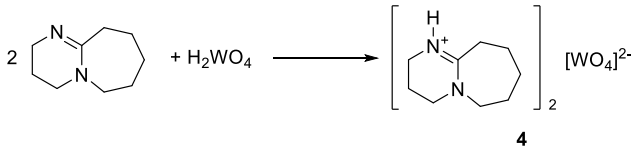

Figure 2.3: Acid-base method for the synthesis of TILCs

The dropwise addition of DBU to an aqueous suspension of tungstic acid[23] led in few minutes to the formation of a colorless clear solution with concurrent change of the pH from acid to neutral. Water was removed by evaporation under vacuum (50 °C, 0.1 mbar) yielding diazabicycloundecenium tungstate ($DBUH_2[WO_4]$, **4**) in >99% yield. Attempts to perform the same reaction with methylimidazole (MIm) and trioctylamine (N_{888}) were however unsuccessful. This was attributed to the relatively lower basicity of these substrates compared to DBU (MImH and $N_{8,8,8}H$ pK_a = 6.95 and 10.75 respectively, compared to pKa=13.5 of DBUH in water).[24]

With a view of establishing a general synthetic method that avoids silver precursors and halide salts, we investigated a third methodology based on an acid-base reaction between tungstic acid (H_2WO_4) and trioctylmethylammonium methylcarbonate {$N_{8,8,8,1}[CH_3OCOO]$; $N_{8,8,8,1}$= $(C_8H_{17})_3N^+CH_3$}. We have previously described the synthesis of $N_{8,8,8,1}[CH_3OCOO]$ from trioctylamine ($N_{8,8,8}$) and dimethylcarbonate ($CH_3OCOOCH_3$), followed by anion exchange with a Brønsted acid HA (Figure 2.4) to yield irreversibly a wide range of ammonium salts of general structure $N_{8,8,8,1}[A]$. This was a simple and clean protocol free of any work-up step, whose driving force was the formation of methylcarbonic acid (*i.e.* the half ester of carbonic acid) that spontaneously decomposed to methanol and CO_2 above -36°C.[19]

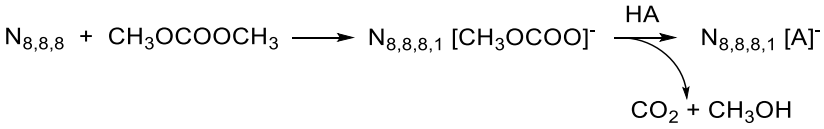

Figure 2.4: Synthesis of $N_{8,8,8,1}[CH_3OCOO]$ and subsequent anion exchange with a Brønsted acid

A similar procedure was here used to synthesize tungstate and peroxotungstate ionic liquids. As shown in Figure 2.5a, tungstic acid in slight stochiometric excess was slowly added to an aqueous solution of

$N_{8,8,8,1}[CH_3OCOO]$ at 70 °C, the solution was then stirred for 1.5 h during which time the pH went from 10 to 7. The product $[N_{8,8,8,1}]_2[WO_4]$ (**5**) was obtained as a yellowish ionic liquid in 86% yield after extraction with ethyl acetate.

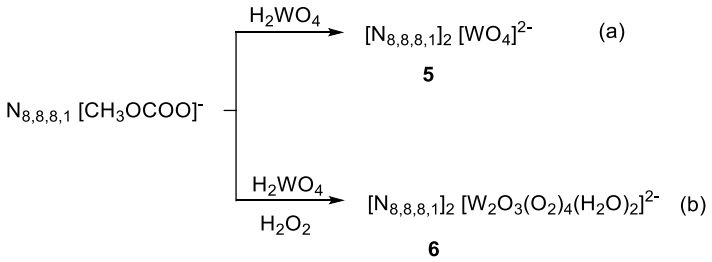

Figure 2.5: Trioctylmethylammonium methylcarbonate mediated synthesis of (a) tungstate ionic liquids; (b) peroxotungstate ionic liquids

The same methodology, with the addition of hydrogen peroxide (30% w/w), was used to synthesize the analogous peroxotungstate ionic liquid **6** (Figure 2.5b). The latter belongs to the class of peroxotungstates which are known as catalytic and stoichiometric oxidants,[25] but also proposed in one instance as catalytic intermediates formed during the insertion reaction of CO_2 to yield styrene carbonate from styrene via the bromohydrin.[26]

According to the literature, different peroxotungstate species exist in an aqueous solution depending on pH: at pH>9, three anions, $[W(O_2)_4]^{2-}$, $[WO_2(O_2)_2]^{2-}$and $[WO_3(O_2)]^{2-}$, form and their distribution depends on the H_2O_2/W ratio; at 1.3<pH<9, the dimer $[W_2O_3(O_2)_4(H_2O)_2]^{2-}$ (Figure 2.6) is the major species; and at pH < 1.3 in the presence of HCl, cis-$[WO(O_2)Cl_4]^{2-}$ is present.[25a,27]

In our case, the initial yellow acidic solution (pH ≈ 1.5-2) of H_2WO_4 and H_2O_2 slowly turned to colourless while the pH became neutral (pH ≈ 6-7). Upon complete dissolution of tungstic acid, the dimeric $[W_2O_3(O_2)_4(H_2O)_2]^{2-}$ peroxotungstate was likely the most abundant anion (Figure 2.6).[28]

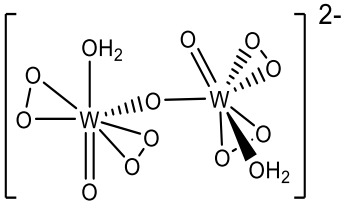

Figure 2.6: Main tungstate species present at 1.3< pH<9

To this dimer was slowly added an aqueous solution of $N_{8,8,8,1}[CH_3OCOO]$ causing immediate evolution of CO_2 and methanol and a pH increase to ≈ 9. The solution was stirred for additional 2 h and then extracted with ethyl acetate to afford, after solvent evaporation, a viscous oily compound whose characterization data were consistent with the ionic liquid $[N_{8,8,8,1}]_2[W_2O_3(O_2)_4(H_2O)_2]^{2-}$ (**6**) (spectroscopic data are discussed in the following section). To the best of our knowledge, this was the first successful halide-free route for the synthesis of a peroxotungstate ionic liquid using a completely organic ionic liquid as a precursor.[25,29]

2.1.3.2 Tungstate ionic liquid catalysts (TILCs) characterisation

The structures of the tungstate ionic liquids were confirmed by FT-IR, ^{1}H-, ^{13}C-and ^{183}W-NMR.[30]

The FT-IR spectra of silver tungstate and of the TILCs **1-6** are in the appendix (see appendix, Figures A.2.1-7). All the TILCs showed the characteristic bands associated to the cations while the presence of oxotungstate species was confirmed by the large adsorption associated to the W-O stretching vibration observed between 843 and 829 cm^{-1}, by the W-O-W adsorption at 751 cm^{-1} and by the W-O-O adsorption at 544 cm^{-1} for **6** (Figure A.2.7).[28,31]

Comparison of the ^{1}H-NMR spectra of $[BMIm]_2[WO_4]$ and of its precursor BMImBr highlighted differences in the chemical shifts of the three imidazolium protons H_2, H_4, H_5, indicative of different hydrogen-bonding ability (Figure A.2.8-9).[32]

As summarised in Table 2.1, $[BMIm]_2[WO_4]$ showed a 0.1 ppm upfield shift for H_4 and H_5 and a 0.2 ppm shift for H_2 with respect to the analogue BMImBr protons . Moreover, as can be seen in Figure A.2.9, H_2 resonance in $BMIm_2[WO_4]$ integrated less than unity, indicating that this proton was largely engaged in H-bonding with WO_4^{2-}, in line with the higher basicity of this anion compared to bromide anion.[33] The lower chemical shifts for the three $[BMIm]_2[WO_4]$ protons further corroborated stronger H-bonding between cation and anion for $[BMIm]_2[WO_4]$ with respect to BMImBr.[33,34,35]

Table 2.1: ^{1}H-NMR chemical shifts of the imidazolium protons in BMImBr and $[BMIM]_2[WO_4]$ relative to TMS

	Compound	H_2 (ppm)	H_4 (ppm)	H_5 (ppm)
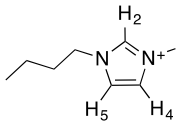	**BMIm[Br]**	8.84	7.51	7.48
	$[BMIm]_2[WO_4]$	8.65	7.43	7.38

A slight upfield shift was shown also in the spectra of $[DBUH]_2[WO_4]$ respect to DBU (see fig. A.2.10-11 in appendix) ascribed to the higher negative charge of $[WO_4]^{2-}$ respect to the bromide anion. As expected,

the ^{1}H-NMR spectra of $[P_{4,4,4,4}]_2[WO_4]$ and of $[N_{4,4,4,4}]_2[WO_4]$ were not significantly different from those of the precursors $[P_{4,4,4,4}]Br$ and $[N_{4,4,4,4}]Br$ (fig. A.2.12-15 in appendix), consistent with the weaker interactions between the ammonium and phosphonium cations with the tungstate anion. Likewise, no significant differences between the ^{1}H-NMR spectra of $[N_{8,8,8,1}]_2[WO_4]$ and $[N_{8,8,8,1}]_2[W_2O_3(O_2)_4]^{2-}$ and that of trioctylmethylammonium methylcarbonate were observed, although the peaks relative to the methylene and methyl groups close to the nitrogen atom showed slight upfield shifts. The ^{1}H- and ^{13}C-NMR spectra of $[N_{8,8,8,1}]_2[WO_4]$ and $[N_{8,8,8,1}]_2[W_2O_3(O_2)_4]^{2-}$ also confirmed the disappearance of the peaks relative to the methyl carbonate anion (see fig. A.2.18-21 in appendix).

Finally, the ^{183}W-NMR spectra of the TILCs **1**-**5** proved the presence of monomeric tungstate $[WO_4]^{2-}$ since one single resonance in the range +10 – -24 ppm (relative to the Na_2WO_4 reference) was observed excluding polyoxotungstate species.[36] Additionally, the interactions between the onium cations and tungstate anion lead to different chemical shifts respect to the sodium tungstate reference. (Figures A.2.22-S27 of the appendix).

A different behaviour was observed for the peroxotungstate ionic liquid **6** which showed a single signal at -612 ppm. This was assigned to the dimeric anion $[W_2O_3(O_2)_4(H_2O)_2]^{2-}$ consistent with the fact that this species was expected as the prevailing one at pH< 9 and H_2O_2/W>1 (see above). Indeed, given the presence of H_2O_2, a previous study reported that the tungsten resonance of $Na_2[W_2O_3(O_2)_4]^{2-}$ was at -699 ppm.[27] The same investigation also excluded peroxotungstate species $[W(O_2)_4]^{2-}$ expected to fall at ≈ -1250 ppm.

2.1.3.3 Catalytic fixation of CO_2 in epoxides catalyzed by the TILCs

Initially, $[N_{4,4,4,4}]_2[WO_4]$ was chosen as the model catalyst to study the CO_2 fixation reaction into styrene oxide **7** to yield styrene carbonate **8**. Table 2.2 reports the results obtained by screening a set of different temperatures (50, 90 and 130 °C), CO_2 pressures (1, 10 and 50 bar) and the use of three solvents (acetonitrile, diethylene glycol and toluene).

*Table 2.2: Fixation of CO_2 into styrene oxide **7** catalysed by $[N_{4,4,4,4}]_2[WO_4]$ [a]*

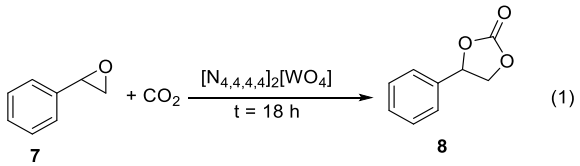

Entry [b]	T (°C)	CO_2 press. (bar)	Solvent	Conv. 7 (%)[c]	Sel. 8 (%)[c]	Yield 8 (%)[c]
1[d]	50	50		11	45	5
2	90	1		100	0	0
3	90	10		100	54	54

4	90	50		88	65	57
5	130	50		100	23	23
6[e]	90	50		0		
7	90	50	CH_3CN	92	73	67
8	90	50	$(CH_2CH_2OH)_2O$	90	73	66
9	90	50	C_7H_8	100	0	0

[(a)] Reaction conditions: **7** (4 mmol) with CO_2 (1-50 bar), T = 50-130 °C, t = 18 h in the presence of $[N_{4,4,4,4}]_2[WO_4]$ (0.12 mmol) and, where indicated, a solvent (1.2 mmol)**;** [(b)] in the selected conditions, CO_2 is always present in gas phase; [(c)] Conversion, selectivity and yield calculated by ^{1}H-NMR; [(d)] The reaction was conducted for 48 h; [(e)] in absence of catalyst.

Reactions run using styrene oxide **7** as solvent/reagent (entries 1-5), showed that the highest conversion (88%) and selectivity (65%) were reached at 90 °C and 50 bar of CO_2 (entry 4). If the temperature was decreased to 50 °C, conversion did not exceed 11% (entry 1), while at 130 °C (entry 5) the reaction was quantitative, but selectivity towards the desired product **8** dropped to 23%. Also, a remarkable effect of the pressure on the product distribution was observed. At 90 °C, increasing P from 1 to 10 and 50 bar progressively improved the selectivity towards **8** from 0 to 54% and to 65%, respectively (entries 2, 3, 4). It should be noted that the conversion of **7** was quantitative even under 1 bar of CO_2, yet the formation of different epoxide derivatives[37,38] instead of **8**, was observed under such conditions. A considerably higher pressure of CO_2 was required to steer the reaction towards the desired cyclic carbonate in the presence of the tungstate-based onium salt.

Finally, the effect of an added solvent was investigated by testing the reaction in acetonitrile, diethylene glycol and toluene as representative aprotic polar, protic polar and non-polar solvents, respectively. Acetonitrile and diethylene glycol slightly enhanced conversion (90 and 92%, respectively) and selectivity (73% in both cases) towards **8** (entries 7 and 8) while with toluene selectivity dropped to zero in favour of isomers, dimers or hydrolysed derivatives of **7** (entry 9).

Next, the catalytic activity of the other five different TILCs **2**, **3**, **4**, **5, 6**, was tested on the model CO_2 fixation reaction under the optimized operative conditions (90 °C, 50 bar CO_2, 18h). Results are summarized in Table 2.3.

The reaction conversion showed a fluctuating trend consistent with a strong influence of the cation: it was comparable for $[N_{4,4,4,4}]_2[WO_4]$, $[N_{8,8,8,1}]_2[WO_4]$ and $[N_{8,8,8,1}]_2[W_2O_3(O_2)_4]$ with $[N_{4,4,4,4}]_2[WO_4]$ slightly outperforming the others (82-88%: entries 1, 2, and 3). The conversion decreased with $[P_{4,4,4,4}]_2[WO_4]$ and $DBUH_2[WO_4]$ (57-60%: entries 4 and 5) and finally, it was significantly improved up to a substantially quantitative value (98%) in the presence of $[BMIm]_2[WO_4]$ (entry 6).

The selectivity towards carbonate **8** instead, remained relatively constant (60-68%) in all cases, suggesting that the tungstate anion favoured CO_2 fixation albeit still causing concurrent side-reactions, particularly the isomerization of **7** to acetophenone and phenylacetaldehyde (according to GC-MS analysis).

*Table 2.3: Fixation of CO_2 into styrene oxide **7** catalysed by different TILCs[a]*

Entry	Catalyst	Conversion 7 (%)[b]	Selectivity 8 (%)[b]	Yield 8 (%)[b]
1	$[N_{4,4,4,4}]_2[WO_4]$	88	65	57
2	$[N_{8,8,8,1}]_2[WO_4]$	84	61	51
3	$[N_{8,8,8,1}]_2[W_2O_3(O_2)_4]$	82	66	54
4	$[P_{4,4,4,4}]_2[WO_4]$	57	63	36
5	$DBUH_2[WO_4]$	60	60	36
6	$[BMIm]_2[WO_4]$	98	68	67
7[c]	$[N_{4,4,4,4}]Br$	88	82	72

[(a)] Conditions: **7** (4 mmol) $P[CO_2]$ = 50 bar, T = 90°C, t = 18h in the presence of the specified TILC (0.12 mmol). [(b)] Conversion, selectivity and yield calculated by ^{1}H-NMR; [(c)] The reaction was conducted for 5 h

For comparison, Table 2.3 also reports the results with $N_{4,4,4,4}Br$ as a catalyst (entry 7). Although the bromide salt apparently prompted the highest selectivity for CO_2 cycloaddition (82%), the yield of the carbonate **8** (72%) was comparable to that achieved with the tungstate-based imidazolium salt (67%, entry 6).

The established mechanism for CO_2 insertion in epoxides catalysed by ammonium halides (Figure 2.1) involves oxirane activation by the cation[39] while the halide acts first as a nucleophile that opens the epoxide (the rate-determining step) and then as a leaving group that drives CO_2 insertion. Recent investigations, however, have confirmed that the catalytic activity is affected by the strength of the interactions between the cation and anion of the catalyst, the presence of H-bonding between them, but also by the pK_a of any available hydrogen bond-donor in the cation.[6,40] For example, it is known that imidazolium ionic liquids activate the oxirane ring by H-bonding. This effect may explain the increased conversion achieved with $[BMIm]_2[WO_4]$ (Table 2.3, entry 6) respect to the other TILCs. Conversely, the pK_a and the steric hindrance of DBUH were critical factors that could negatively influence the catalytic efficiency of $DBUH_2[WO_4]$ (Table 2.3, entry 5).[4b]

Compared to tetrabutylammonium tungstate $[N_{4,4,4,4}]_2[WO_4]$, the phosphonium analogue ($[P_{4,4,4,4}]_2[WO_4]$ (entry 4) maintained selectivity in the same range, but conversion did not exceed 57% under the same

conditions. This observation is opposite to a recent study by Steinbauer et al. relative to the use of monofunctional and hydroxyl-functionalized ammonium and phosphonium halides for the CO_2 fixation into epoxides: under operative conditions similar to the ones used by us (solventless, 90° C, 6h, 10 bar CO_2, 2%mol catalyst) monofunctional tetrabutylphosphonium salts showed a higher activity compared to that of corresponding ammonium analogs.[41] The reversed trend of Table 2.3 was likely due to the different coulombic interactions between cation and tungstate that modulated the chemical, physical and catalytic properties of the TILCs.[42]

With the optimized conditions in hand and to broaden the scope of the coupling reaction, various linear and cyclic aliphatic compounds were examined for the formation of the corresponding cyclic carbonate by using the best catalyst, $[BMIm]_2WO_4$ (Figure 2.7).

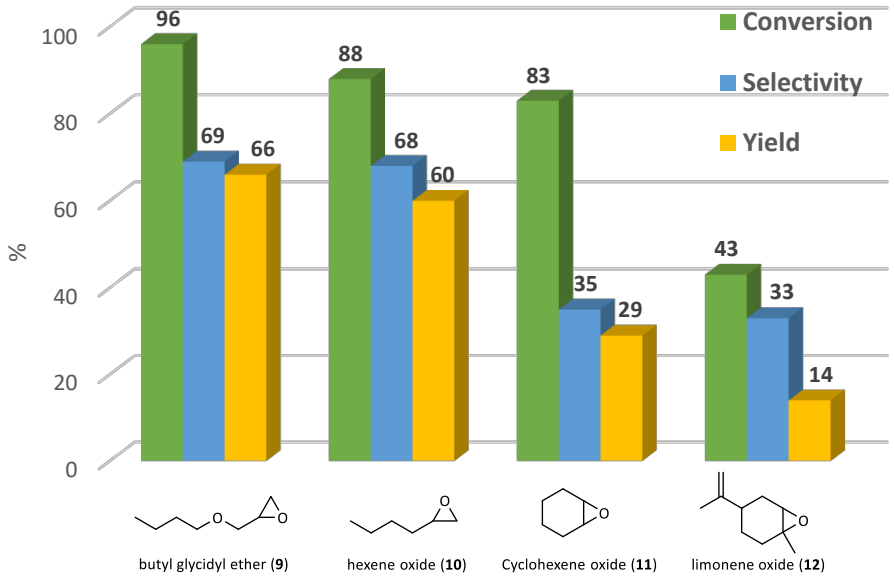

Figure 2.7: Fixation of CO_2 into various substrates (indicated) catalysed by $[BMIm]_2WO_4$. Reaction conditions: substrate (4 mmol), CO_2 (50 bar), T = 90 °C, t = 18 h, $[BMIm]_2WO_4$ (0.12 mmol)). Conversion, selectivity and yield calculated by ^{1}H-NMR.

The results show that terminal epoxides such as butyl glycidyl ether (**9**) and hexene oxide (**10**) were converted into the corresponding cyclic carbonate with conversion and selectivity similar to the one reported for styrene oxide. Evidently electron-rich substrates such as **7** and **9** are more easily activated towards CO_2 fixation respect to **10**. In the same conditions, even the less reactive cyclohexene oxide (**11**) is easily converted but the selectivity towards the carbonate declines presumably because of the steric hindrance caused by its ring structure. Finally, the challenging coupling of CO_2 with the bulky cyclic trisubstituted limonene oxide (**12**) presents lower conversion and selectivity but anyway uphold a 14% yield.

According to established reports, ^{183}W-NMR and single crystal X-Ray diffraction on tetrahedral $[WO_4]^{2-}$ and $[MoO_4]^{2-}$ show that CO_2 coordinates to one of the oxygen atoms and not to the metal, forming carbonate complexes of formula $[MO_3(CO_3)]^{2-}$. The latter species can react with diamines, aminonitriles, propargylic alcohols and terminal alkynes for CO_2 fixation, or with triethylsilane for CO_2 reduction.[12,13,43]

These observations led us to propose the mechanism described in Figure 2.8 for the CO_2 fixation into epoxides catalysed by TILCs.

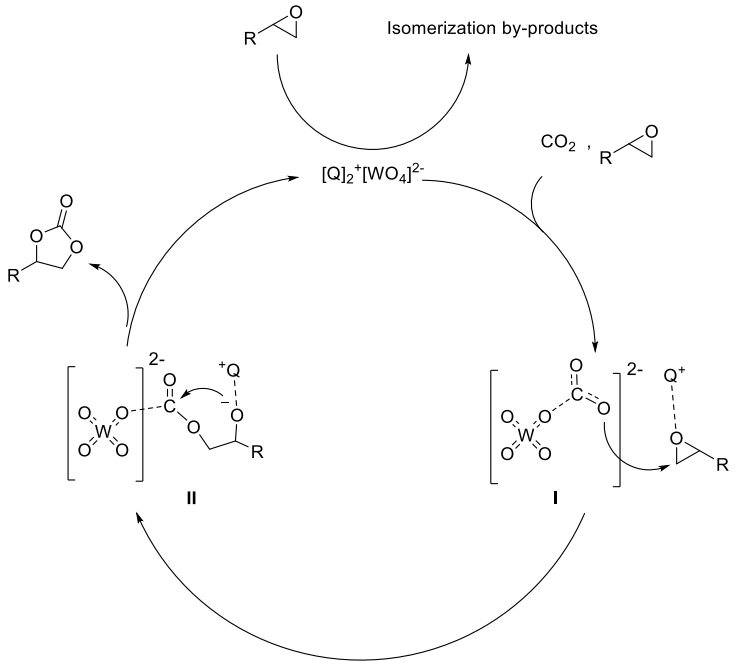

Figure 2.8: Mechanistic hypothesis for CO_2 fixation into epoxides catalysed by TILCs

The carbonate complex **I** formed *in situ* in the presence of CO_2 could act itself directly as the nucleophile and attack the cation-activated epoxide, yielding an intermediate **II** that was ready for ring-closure to give the organic carbonate and the starting tungstate. This mechanism was coherent with the fact that CO_2 insertion did not take place at 50 °C (entry 1, Table 2.2) while, above 70 °C, complex **I** was able to release activated CO_2, as already reported for $[MoO_3(CO_3)]^{2-}$.[43]

This mechanism is in accordance with the absence of an halide or an external nucleophile generally needed to promote the epoxide ring opening (Figure 2.1): nearly all the metal based catalytic systems explored in literature for the fixation of CO_2 into epoxides require the presence of a halide (Cl^-, Br^-, I^-) or nucleophile as co-catalyst to reach a not-negligible conversion of substrates,[2-5] while the experiments reported above clearly demonstrate that tungstate could promote itself the entire catalytic cycle in an halide-free fashion, even if it concurrently promote side isomerization reactions due to Meinwald rearrangement. The mechanism that lead to the formation of carbonate need to be different to the general accepted one reported in Figure 2.1 and our hypothesis find its justification in the evidence of the CO_2-tungstate complex formation mentioned above and the similarity of our mechanism to those

reported for the synthesis of polycarbonates mediated by metal complexes containing an alkoxide or an aryloxyde group (-OR) that are able to undergo CO_2 insertion into epoxides without the need of an external nucleophile.[44]

To verify whether a tungstate and halide anion could act in synergy, like for the other transition metals explored for CO_2 fixation,[4a] we then explored the combined use of a halide ammonium salt, *i.e.* $N_{4,4,4,4}Br$, along with our tungstate-based catalysts for the insertion reaction. Preliminary tests led us to lower the temperature and extend the reaction time (50 °C, 48 h) respect to the reaction conducted in presence of the sole TILCs (90 °C, 18 h). This choice was also in agreement with published protocols, in particular with a recent study where polyoxotungstate/zinc metal organic frameworks along with $N_{4,4,4,4}Br$ were utilized successfully at 50 °C.[2b,45]

As summarized in Table 2.4, at 50 °C the model reaction **7** → **8** in the presence of either $N_{4,4,4,4}Br$ or $[N_{4,4,4,4}]_2[WO_4]$ separately, proceeded with low conversion (entries 1 and 2: 53% and 11% conversion, respectively) and with low selectivity (87% and 45%, respectively). However, the combination of $N_{4,4,4,4}Br$ and $[N_{4,4,4,4}]_2[WO_4]$ (entry 3) led to an excellent conversion as high as 91% and complete selectivity towards the formation of **8**. The presence of bromide anions sourced by $N_{4,4,4,4}Br$ clearly had a dramatic effect to favour the CO_2 insertion with respect to competitive reaction pathways. A similar behaviour was noticed also for the $[N_{8,8,8,1}]_2[WO_4]/N_{4,4,4,4}Br$ mixture by which 100% selectivity was achieved at 89% conversion (entry 4). Other combinations such as $[N_{8,8,8,1}]_2[W_2O_3(O_2)_4]^{2-}/N_{4,4,4,4}Br$, $[P_{4,4,4,4}]_2[WO_4]/N_{4,4,4,4}Br$, and $DBUH_2[WO_4]/N_{4,4,4,4}Br$, offered poorer results since both the conversion and the selectivity dropped (entries 5, 6, and 7), the latter (selectivity) due to the formation of isomerization by-products.

*Table 2.4: Fixation of CO_2 into styrene oxide **7** catalysed by different TILCs: effect of $N_{4,4,4,4}Br$ [a]*

Entry	Catalyst system		Conversion 7 (%)[b]	Selectivity 8 (%)[b]	Yield 8 (%)[b,c]
1		$[N_{4,4,4,4}]Br$	53	87	46
2	$[N_{4,4,4,4}]_2[WO_4]$		11	45	5
3	$[N_{4,4,4,4}]_2[WO_4]$	$[N_{4,4,4,4}]Br$	91	100	91 (88)
4	$[N_{8,8,8,1}]_2[WO_4]$	$[N_{4,4,4,4}]Br$	89	100	89 (85)
5	$[N_{8,8,8,1}]_2$ $[W_2O_3(O_2)_4]^{2-}$	$[N_{4,4,4,4}]Br$	86	84	72
6	$[P_{4,4,4,4}]_2[WO_4]$	$[N_{4,4,4,4}]Br$	83	93	77
7	$DBUH_2[WO_4]$	$[N_{4,4,4,4}]Br$	73	77	56
8	$[BMIm]_2[WO_4]$	$[N_{4,4,4,4}]Br$	76	100	76

[(a)] Reaction conditions: **7** (4mmol), 50 bar of CO_2, T=50 °C, t=48h, tungstate-based catalyst (0.12 mmol) and $N_{4,4,4,4}Br$ (0.012 mmol) unless otherwise indicated. [(b)] Conversion, selectivity and yield calculated by ^{1}H-NMR. [c] Isolated yields are reported in brackets

Finally, $[BMIm]_2[WO_4]/[N_{4,4,4,4}]Br$ (entry 8) showed 100% selectivity albeit a lower conversion (76%) compared to $[N_{4,4,4,4}]_2[WO_4]/[N_{4,4,4,4}]Br$. In agreement with data of Table 2.3, this result confirmed that the imidazolium cation could play a beneficial role towards the formation of cyclic carbonate. Nonetheless, a feasible explanation of this lower conversion could be the concurrent interactions of the imidazolium moiety with bromide species that lead to a reduction of its nucleophilicity and ring-opening ability, as recently reported in the literature.[46]

Since the presence of halides is generally considered undesirable from a green chemistry standpoint, our final attempts were finalized at substituting $[N_{4,4,4,4}]Br$ with ionic liquids having a non-halide anion able to act as nucleophile-leaving group. The tested anions included two species already shown to act as catalysts for CO_2 fixation into epoxides by us: methylcarbonate (CH_3OCOO^-), acetate (CH_3COO^-);[11a] as well as levulinate (Lev: $CH_3(CO)CH_2CH_2CH_2COO^-$) and hydroxide that were recently reported as catalyst or co-catalyst for CO_2 fixation.[47,48] The results, however, were not as rewarding as expected (Table 2.5).

*Table 2.5: Fixation of CO_2 into styrene oxide **7** catalysed by $[N_{8,8,8,1}]_2WO_4$: influence of different organic co-catalysts[a]*

Entry	Co-Catalyst (0.03 eq.)	Conversion 7 (%)[b]	Selectivity 8 (%)[b]	Yield 8 (%)[b]
1	$N_{4,4,4,4}Br$	89	100	89
2	$BMImCH_3OCOO$	19	70	13
3	$[P_{8,8,8,1}]CH_3OCOO$	16	77	12
4	$[N_{8,8,8,1}]CH_3OCOO$	26	78	20
5	$[N_{8,8,8,1}]CH_3COO$	30	79	24
6	$[N_{8,8,8,1}]Lev$	35	80	28
7	$N_{4,4,4,4}OH$	47	51	24

[(a)] Reaction conditions: 7 (4mmol), 50 bar of CO_2, in presence of $[N_{8,8,8,1}]_2WO_4$ (0.12 mmol) and the indicated co-catalyst (0.012 mmol). [(b)] Conversion, selectivity and yield calculated by ^1H-NMR.

Conversions remained low (19-35%) since at this temperature the organic anions are not as good as nucleophiles. On the contrary, selectivity was generally good (70 – 80%) although it was not possible to prevent the formation of by-products. In the case of $N_{4,4,4,4}OH$, results were somewhat reversed: the conversion was slightly higher (47%), but the selectivity dropped to 51%.

2.1.4 Conclusions

A set of new tungstate ionic liquids (TILCs) were synthesized. A novel halide-free synthetic route was also developed, that provided access to both tungstate and peroxotungstate ionic liquids. These compounds proved viable catalysts for CO_2 fixation into epoxides: in particular, butylmethylimidazolium tungstate $BMIm_2[WO_4]$ promoted conversion of styrene oxide to the corresponding cyclic carbonate in 67% yield with 50 bar CO_2 at 90 °C. To account for these results, a reaction mechanism based on the formation of tungstate-carbonate as the active nucleophile was proposed. Although the investigated TILCs were less efficient than other metal-based catalysts coupled with nucleophile sources, TILCs exhibit a surprisingly higher catalytic activity respect to other metals when used alone. However, also in our case a cooperative effect was demonstrated by which using a binary mixture of a tungstate IL and a bromide IL, both conversion and selectivity towards the formation of the cyclic carbonate were boosted to substantially quantitative values. To the best of our knowledge, this paper describes the first example in which simple monotungstate catalysts are successfully used for the insertion of CO_2 to epoxides.

Considering the well-known oxidation activity of tungstate-based catalysts,[25b,49] some preliminary tests were carried out to evaluate the oxidation activity of our TILCs. Unfortunately, the epoxidation of styrene to **7** in presence of hydrogen peroxide (1-2 eq.) give unsatisfactory results, since the excessive oxidative activity of TILCs led to the prevailing formation of benzaldehyde. On the other hand, the same reaction conducted with a model substrate for epoxidation such as cyclooctene led to a quantitative conversion and an exciting 85% selectivity towards cyclooctene oxide. The possibility to refine the reaction operative conditions to get a tandem or one-pot olefin epoxidation – CO_2 fixation processes will be deepened in the next work.

2.1.5 Experimental Section

All chemicals were purchased from Aldrich and used as received. Trioctylmethyl ammonium methylcarbonate ($[N_{8,8,8,1}]CH_3OCOO$), Trioctylmethylammonium acetate ($[N_{8,8,8,1}]CH_3COO$) and trioctylmethylammonium levulinate ($[N_{8,8,8,1}]Lev$) were synthesized based on a procedure previously reported by us.[19]

2.1.5.1 Synthesis of TILCs

Synthesis of tungstate ionic liquids by metathesis

Tetrabutylammonium tungstate ($[N_{4,4,4,4}]_2[WO_4]$, **1**), butylmethylimidazolium tungstate ($BMIM_2[WO_4]$, **2**), tetrabutylphosphonium tungstate ($[P_{4,4,4,4}]_2[WO_4]$, **3**), diazabicycloundecenonium tungstate ($DBUH_2[WO_4]$, **4**) were synthesized by adapting reported procedures.[20] Representative procedure: an aqueous solution of 26 mmol $[N_{4,4,4,4}]Br$ was added to Ag_2WO_4 (13 mmol). The color of the mixture darkened immediately indicative of ion exchange and the reaction mixture was stirred for additional 10 minutes. AgBr was filtered under suction, washed three times with deionized water and the aqueous solution obtained was concentrated by rotary evaporation (60°C, 40 mbar) and dried under reduced

pressure (50 °C, 0.1 mbar) yielding off-white crystalline solids ($[N_{4,4,4,4}]_2WO_4$ =8.55 g, 10.4 mmol, yield=80%; $BMIm_2WO_4$= 6.88 g , 11.18 mmol, yield=86%; $[N_{4,4,4,4}]_2WO_4$= 9.10 g , 11.96 mol, yield=92%, $(DBUH)_2WO_4$= 6.27 g , 11.31 mol, yield= 87%). Contamination of the product by bromide ions was excluded by testing for halides. The TILCs were characterized by IR, ^{1}H-NMR, ^{13}C-NMR, ^{183}W-NMR and identified by comparison with spectral data from the literature when possible.

Synthesis of diazobycicloundecenium tungstate [$(DBUH)_2WO_4$] by acid-base reaction

$(DBUH)_2WO_4$ was synthesized also by a simple acid-base reaction by the following procedure: tungstic acid (0.51 g, 2.06 mmol) was suspended in 10 ml of milli-Q H_2O, stirring was started and then 0.63 g (4.12 mmol) of DBU were added dropwise, the solution turned from yellow to white in few minutes. The mixture was stirred for 1h, then it was concentrated by rotary evaporation (60 °C, 40 mbar) and dried under reduced pressure (50 °C, 0.1 mbar) yielding a white solid (1.14 g, yield >99%). $(DBUH)_2WO_4$ was characterized by IR, ^{1}H-NMR, ^{13}C-NMR and ^{183}W-NMR.

Synthesis of trioctylmethylammonium tungstate ($[N_{8,8,8,1}]_2[WO_4]$) via the methylcarbonate precursor.

H_2WO_4 (0.28g, 1.1 mmol) was slowly added to an aqueous solution of $[N_{8,8,8,1}][CH_3OCOO]$ (0.83g, 1.86 mmol) heated at 50 °C. The solution was stirred for 3h during which time the initial opalescent solution turned yellow. The solution was cooled, and ethyl acetate was added to extract $[N_{8,8,8,1}]_2[WO_4]$. The product ionic liquid (0.78 g, 0.79 mmol, yield=86%) was characterized by IR, ^{1}H-NMR, ^{13}C-NMR and ^{183}W-NMR.

Synthesis of trioctylmethylammonium peroxotungstate ($[N_{8,8,8,1}]_2[W_2O_3(O_2)_4]^{2-}$) via the methylcarbonate precursor.

H_2WO_4 (0.72 g, 2.89 mmol) was dissolved in hydrogen peroxide (30% v/v_{H2O}, 1.5 ml, 43.35 mmol) and the solution was heated at 50 °C and stirred until the solution turned from yellow to white opalescent. The mixture was filtered and then a 10 ml aqueous solution of $[N_{8,8,8,1}]_2CH_3OCOO$ (2.56 g, 5.78 mmol) was added. The solution turned immediately from white to yellow again, it was heated at 50 °C and an evident evolution of CO_2 suggested the formation of the desired product. The solution was stirred for 1h, then ethyl acetate was added to extract $[N_{8,8,8,1}]_2[W_2O_3(O_2)_4]^{2-}$**.** The ionic liquid obtained after rotary evaporation (2.49 g, 1.94 mmol, yield=67%) was characterized by IR, ^{1}H-NMR, ^{13}C-NMR and ^{183}W-NMR.

2.1.5.2 Catalytic tests

Typical procedure for CO_2 fixation reaction (CO_2 pressure = 10-50 bar)

The selected epoxide (4 mmol, 1 eq), tungstate catalyst (0.03 eq), mesitylene as internal standard (10% w/w substrate) and – where applicable – the co-catalyst (0.03 eq), were charged in a flat-bottomed glass reactor liner which was placed inside a 100-ml stainless steel autoclave. The autoclave was sealed, degassed via two vacuum-CO_2 cycles and pressurized with CO_2 (10 and 50 bar; the molar ratio CO_2:epoxide was ≈ 10:1 and ≈ 50:1 respectively). The autoclave was then electrically heated at the desired temperature (50-130°C) and the reaction was magnetically stirred for the desired time (5-48 h). At the end of each run, the autoclave was rapidly cooled in an ice bath and vented, and the final mixture was analysed by ^{1}H-NMR to calculate conversion, yield and selectivity.

Typical procedure for the CO_2 fixation reaction (CO_2 pressure=1 bar)

The selected epoxide (4 mmol, 1 eq), tungstate catalyst (0.03 eq) and mesitylene as internal standard (10% w/w substrate) were charged into a round-bottomed flask equipped with a magnetic stirrer. The flask was degassed via two vacuum-CO_2 cycles and a rubber reservoir containing about 1l of CO_2 was connected to the flask. The molar ratio CO_2: substrate was ≈ 10:1. The reaction vessel was sealed to prevent losses of substrates and/or CO_2 and stirred at 90 °C for 18h. After the chosen time, an aliquot of the reaction mixture was analysed by ^{1}H-NMR to determine substrate conversion, selectivity and yield. Additional tests with higher and lower molar ratio CO_2:substrate give the same result when CO_2 is used at atmospheric pressure, proving that CO_2:substrate molar ratio has no effect in the selected experimental conditions.

2.1.6 References

[1] (a) M. North and R. Pasquale, *Angewandte Chemie International Edition*, 2009, **48**, 2946-2948; (b) F. Della Monica and A. W. Kleij, *Catalysis Science & Technology*, 2020, **10**, 3483-3501.

[2] (a) C. Claver, M. B. Yeamin, M. Reguero and A. M. Masdeu-Bultó, *Green Chemistry*, 2020, **22**, 7665-7706; (b) C. Martin, G. Fiorani and A. W. Kleij, *ACS Catalysis*, 2015, **5**, 1353-1370.

[3] (a) A. A. Marciniak, K. J. Lamb, L. P. Ozorio, C. J. A. Mota and M. North, *Current Opinion in Green and Sustainable Chemistry*, 2020, **26**, 100365; (b) T. K. Pal, D. De and P. K. Bharadwaj, *Coordination Chemistry Reviews*, 2020, **408**, 213173; (c) J. W. Comerford, I. D. Ingram, M. North and X. Wu, *Green Chemistry*, 2015, **17**, 1966-1987.

[4] (a) V. D'Elia, J. D. Pelletier and J. M. Basset, *ChemCatChem*, 2015, **7**, 1906-1917; (b) M. Alves, B. Grignard, R. Méreau, C. Jerome, T. Tassaing and C. Detrembleur, *Catalysis Science & Technology*, 2017, **7**, 2651-2684.

[5] (a) A. Decortes, A. M. Castilla and A. W. Kleij, *Angewandte Chemie International Edition*, 2010, **49**, 9822-9837; (b) J. W. Comerford, I. D. Ingram, M. North and X. Wu, *Green Chemistry*, 2015, **17**, 1966-1987; (c) F. Della Monica, M. Leone, A. Buonerba, A. Grassi, S. Milione and C. Capacchione, *Molecular Catalysis*, 2018, **460**, 46-52.

[6] (a) P. Yingcharoen, C. Kongtes, S. Arayachukiat, K. Suvarnapunya, S. V. Vummaleti, S. Wannakao, L. Cavallo, A. Poater and V. D'Elia, *Advanced Synthesis & Catalysis*, 2019, **361**, 366-373; (b) M. Liu, X. Wang, Y. Jiang, J. Sun and M. Arai, *Catalysis Reviews*, 2019, **61**, 214-269.

[7] (a) A.-L. Girard, N. Simon, M. Zanatta, S. Marmitt, P. Gonçalves and J. Dupont, *Green Chemistry*, 2014, **16**, 2815-2825; (b) T. Werner and H. Büttner, *ChemSusChem*, 2014, **7**, 3268-3271; (c) C. J. Whiteoak, A. Nova, F. Maseras and A. W. Kleij, *ChemSusChem*, 2012, **5**, 2032-2038.

[8] (a) K. Yamaguchi, K. Ebitani, T. Yoshida, H. Yoshida, K. Kaneda, *Journal of the American Chemical Society*, 121 (1999) 4526-4527; (b) Y.M. Shen, W.L. Duan, M. Shi, *Advanced Synthesis & Catalysis*, 2003, **345**, 337-340; (c) T. Zhao, X. Hu, D. Wu, R. Li, G. Yang and Y. Wu, *ChemSusChem*, 2017, **10**, 2046-2052.

[9] (a) S. J. Poland and D. J. Darensbourg, *Green Chemistry*, 2017, **19**, 4990-5011; (b) Y. Wang and D. J. Darensbourg, *Coordination Chemistry Reviews*, 2018, **372**, 85-100.

[10] (a) G. Fiorani, M. Stuck, C. Martín, M. Martinez Belmonte, E. Martin, E. C. Escudero-Adan and A. W. Kleij, *ChemSusChem*, 2016, **9**, 1304-1311; (b) J. R. Lamb, Y. Jung and G. W. Coates, *Organic Chemistry Frontiers*, 2015, **2**, 346-349.

[11] (a) M. Galvan, M. Selva, A. Perosa and M. Noè, *Asian Journal of Organic Chemistry*, 2014, **3**, 504-513; (b) B. Zou and C. Hu, *Current Opinion in Green and Sustainable Chemistry*, 2017, **3**, 11-16; (c) A. Chen, C. Chen, Y. Xiu, X. Liu, J. Chen, L. Guo, R. Zhang and Z. Hou, *Green Chemistry*, 2015, **17**, 1842-1852; (d) X. Wu, C. Chen, Z. Guo, M. North and A. C. Whitwood, *ACS Catalysis*, 2019, **9**, 1895-1906;

[12] (a) T. Kimura, H. Sunaba, K. Kamata and N. Mizuno, *Inorganic chemistry*, 2012, **51**, 13001-13008; (b) T. Kimura, K. Kamata and N. Mizuno, *Angewandte Chemie International Edition*, 2012, **51**, 6700-6703.

[13] C.-X. Guo, B. Yu, J.-N. Xie and L.-N. He, *Green Chemistry*, 2015, **17**, 474-479.

[14] D. J. Darensbourg, R. K. Hanckel, C. G. Bauch, M. Pala, D. Simmons and J. N. White, *Journal of the American Chemical Society*, 1985, **107**, 7463-7473.

[15]M. Sankar, N. Tarte and P. Manikandan, *Applied Catalysis A: General*, 2004, **276**, 217-222.

[16] Q. Han, B. Qi, W. Ren, C. He, J. Niu and C. Duan, *Nature communications*, 2015, **6**, 10007.

[17] J. Lu, X. Ma, V. Singh, Y. Zhang, P. Wang, J. Feng, P. Ma, J. Niu and J. Wang, *Inorganic chemistry*, 2018, **57**, 14632-14643.

[18] (a) M. Selva, A. Perosa, S. Guidi and L. Cattelan, *Beilstein journal of organic chemistry*, 2016, **12**, 1911-1924; (b) M. Selva, A. Caretto, M. Noè and A. Perosa, *Organic & biomolecular chemistry*, 2014, **12**, 4143-4155; (c) M. Selva, M. Noè, A. Perosa and M. Gottardo, *Organic & biomolecular chemistry*, 2012, **10**, 6569-6578.

[19] M. Fabris, V. Lucchini, M. Noè, A. Perosa and M. Selva, *Chemistry–A European Journal*, 2009, **15**, 12273-12282.

[20] (a) Y. Qiao, J. Hu, H. Li, L. Hua, Y. Hu, B. Feng, Z. Hou, *Journal of Electrochemical Society*, 2010, **157**, F124-F129; (b) M. Vafaeezadeh, M. M. Hashemi, M. Shakourian-Fard, *Catalysis Communication*, 2012, **26**, 54.

[21] Unexpected for $BMIm_2[WO_4]$ that was previously reported as a colorless liquid (ref. 20b). However, all tungstate ionic liquids are very hygroscopic and must be stored under inert atmosphere to prevent deliquescence.

[22] (a) N. Fanjul-Mosteirín, C. Jehanno, F. Ruipérez, H. Sardon and A. P. Dove, *ACS Sustainable Chemistry & Engineering*, 2019, **7**, 10633-10640; (b) C. Yang, M. Liu, J. Zhang, X. Wang, Y. Jiang and J. Sun, *Molecular Catalysis*, 2018, **450**, 39-45.

[23] Tungstic acid was only partly soluble in the aqueous solution while $[DBUH]_2[WO_4]$ was completely soluble.

[24] See evans.rc.fas.harvard.edu/pdf/evans_pKa_table.pdf, accessed 10/12/2020.

[25] (a) M. Amini, M. M. Haghdoost, M. Bagherzadeh, *Coordination Chemistry Reviews*, 2014, **268**, 83-100; (b) Y. Qiao, Z. Hou, H. Li, Y. Hu, B. Feng, X. Wang, L. Hua, Q. Huang, *Green Chemistry*, 2009, **11**, 1955-1960.

[26] J.-L. Wang, J.-Q. Wang, L.-N. He, X.-Y. Dou, F. Wu, *Green Chemistry*, 2008, **10**, 1218–1223.

[27] V. Nardello, J. Marko, G. Vermeersch, J. Aubry, *Inorganic Chemistry*, 1998, **37**, 5418-5423.

[28] N. J. Campbell, A. C. Dengel, C. J. Edwards, W. P. Griffith, *Journal of Chemical Society*, Dalton, 1989, **6**, 1203-1208.

[29] N. Mizuno, K. Yamaguchi and K. Kamata, *Coordination chemistry reviews*, 2005, **249**, 1944-1956.

[30] The TILCs synthesized by halide metathesis were halide-free as determined by the Seddon test.

[31] G. Busca, *Journal of Raman Spectroscopy*, 2002, **33**, 348-358.

[32] F. Cesare Marincola, C. Piras, O. Russina, L. Gontrani, G. Saba and A. Lai, *ChemPhysChem*, 2012, **13**, 1339-1346.

[33] A. D. Headley and N. M. Jackson, *Journal of physical organic chemistry*, 2002, **15**, 52-55.

[34] H. S. Schrekker, D. O. Silva, M. A. Gelesky, M. P. Stracke, C. M. Schrekker, R. S. Gonçalves and J. Dupont, *Journal of the Brazilian Chemical Society*, 2008, **19**, 426-433.

[35] Qiao et al. (reference 20a) observe the same H-bonding for hexylmethylimidazolium tungstate $HMIm_2[WO_4]$.

[36] Y.-G. Chen, J. Gong and L.-Y. Qu, *Coordination chemistry reviews*, 2004, **248**, 245-260.

[37] GC-MS showed acetophenone, phenylacetaldehyde, styrene diol and dimerization products due to Lewis acid-promoted Meinhald rearrangement, in agreement also with reference 25b, 38.

[38] (a) V. Conte and O. Bortolini, *PATAI'S Chemistry of Functional Groups*, 2009, Wiley VCH; (b) V. Hulea and E. Dumitriu, *Applied Catalysis A: General*, 2004, **277**, 99-106.

[39] (a) J. Langanke, L. Greiner and W. Leitner, *Green chemistry*, 2013, **15**, 1173-1182; (b) H. Yasuda, L.-N. He, T. Sakakura and C. Hu, *Journal of Catalysis*, 2005, **233**, 119-122.

[40] (a) F. D. Bobbink and P. J. Dyson, *Journal of catalysis*, 2016, **343**, 52-61; (b) L. P. da Silva, *Molecular Catalysis*, 2019, **474**, 110425.

[41] J. Steinbauer, C. Kubis, R. Ludwig and T. Werner, *ACS Sustainable Chemistry & Engineering*, 2018, **6**, 10778-10788.

[42] P. J. Carvalho, S. P. Ventura, M. L. Batista, B. Schröder, F. Gonçalves, J. Esperança, F. Mutelet and J. A. Coutinho, *The Journal of chemical physics*, 2014, **140**, 064505.

[43] I. Knopf, T. Ono, M. Temprado, D. Tofan and C. C. Cummins, *Chemical Science*, 2014, **5**, 1772-1776.

[44] (a) P. P. Pescarmona and M. Taherimehr, *Catalysis Science & Technology*, 2012, **2**, 2169-2187; (b) G. W. Coates and D. R. Moore, *Angewandte Chemie International Edition*, 2004, **43**, 6618-6639.

[45] Q. Han, B. Qi, W. Ren, C. He, J. Niu and C. Duan, *Nature communications*, 2015, **6**, 10007.

[46] F. D. Bobbink, D. Vasilyev, M. Hulla, S. Chamam, F. Menoud, G. b. Laurenczy, S. Katsyuba and P. J. Dyson, *ACS Catalysis*, 2018, **8**, 2589-2594.

[47] Y. Hu, J. Song, C. Xie, H. Wu, T. Jiang, G. Yang and B. Han, *ACS Sustainable Chemistry & Engineering*, 2019, **7**, 5614-5619.

[48] T. Ema, K. Fukuhara, T. Sakai, M. Ohbo, F.-Q. Bai and J.-y. Hasegawa, *Catalysis Science & Technology*, 2015, **5**, 2314-2321.

[49] R. Noyori, M. Aoki and K. Sato, *Chemical Communications*, 2003, 1977-1986.

2.2 Assisted tandem tungsten-based catalysis for the direct oxidative carboxylation of olefins into cyclic carbonates

2.2.1 Introduction

The previous work paved the way for the study of the feasibility of a tandem process for the direct oxidative carboxylation (DOC) of olefins mediated by tungsten-based catalysts, in particular TILCs (Scheme 2.1). The use of tungstate and phosphotungstate species for the epoxidation of olefins is widely accepted and explored in literature,[1] while we demonstrated that simple monotungstate TILCs can be nimbly used also for the CO_2 fixation reactions.

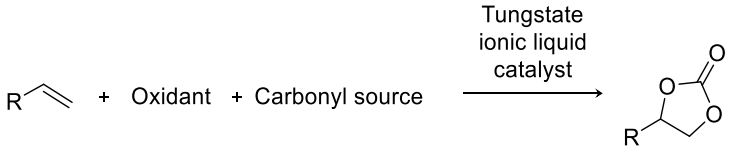

Scheme 2.1: Direct oxidative carboxylation of olefins

The DOC route can be an alternative for the synthesis of cyclic organic carbonates that enables bypassing isolation of the epoxides whose use as starting materials cannot be considered sustainable, safe or green:[2] tandem DOC approach provides for the direct utilization of olefins avoiding intermediate work-up, isolation and handling of highly toxic epoxides.

As defined in the introduction (paragraph 1.5.1), tandem catalytic transformations are "coupled catalyses in which sequential formation of the substrate occurs via two (or more) mechanistically distinct processes".[3] Tandem catalysis can be divided into subcategories:

1. Auto tandem catalysis (AuTC) in which the distinct reactions are promoted by a single catalyst.
2. Assisted tandem catalysis (AsTC) in which there is one single catalyst that however requires an intermediate change in reaction conditions (e.g. temperature, addition of a co-catalyst or co-reactant, etc.) to shift from one catalytic mechanism to another.
3. Orthogonal tandem catalysis (OTC) that requires the use of two or more catalytic moieties (or catalysts) that have distinct mechanisms operating concurrently.[4]

For what concerns the DOC of olefins, various AuTC, AsTC, OTC, continuous-flow and oxybromination processes (in which stochiometric amounts of halide source and O source were used to form halohydrins intermediate to the formation of COCs) were implemented. However, the challenge of integrating two steps in one-pot fashion leads to a limited amount of research on the topic (about 60 papers and patents since the first patent registered in 1962) when compared to countless scientific papers regarding the single steps (i.e. epoxidation of olefins and CO_2 insertion into epoxides). A comprehensive review of the advances in this field was recently published by us.[5]

The design of tandem processes should always pay attention to the sustainability and greenness of the entire process and a crucial issue is the selection of reactants. While the use of carbon dioxide is the most

environmental-friendly choice as carbon source, a greater emphasis should be given to the oxidant selection: most of the research regarding DOC of olefins published to date employed tert-butyl hydroperoxide (TBHP) or other organic peroxides as oxidants while only 10 papers exploit O_2 or H_2O_2 as oxidant. Organic peroxides should be definitely discarded from an economic and environmental standpoint according to green principles, while the use of molecular oxygen (with or without an aldehyde as sacrificial donor) has a strong green connotation but a low applicability so far due to its inertness towards high molecular weight or inactivated olefins and to its potential side reactions due to radical mechanisms.[6]

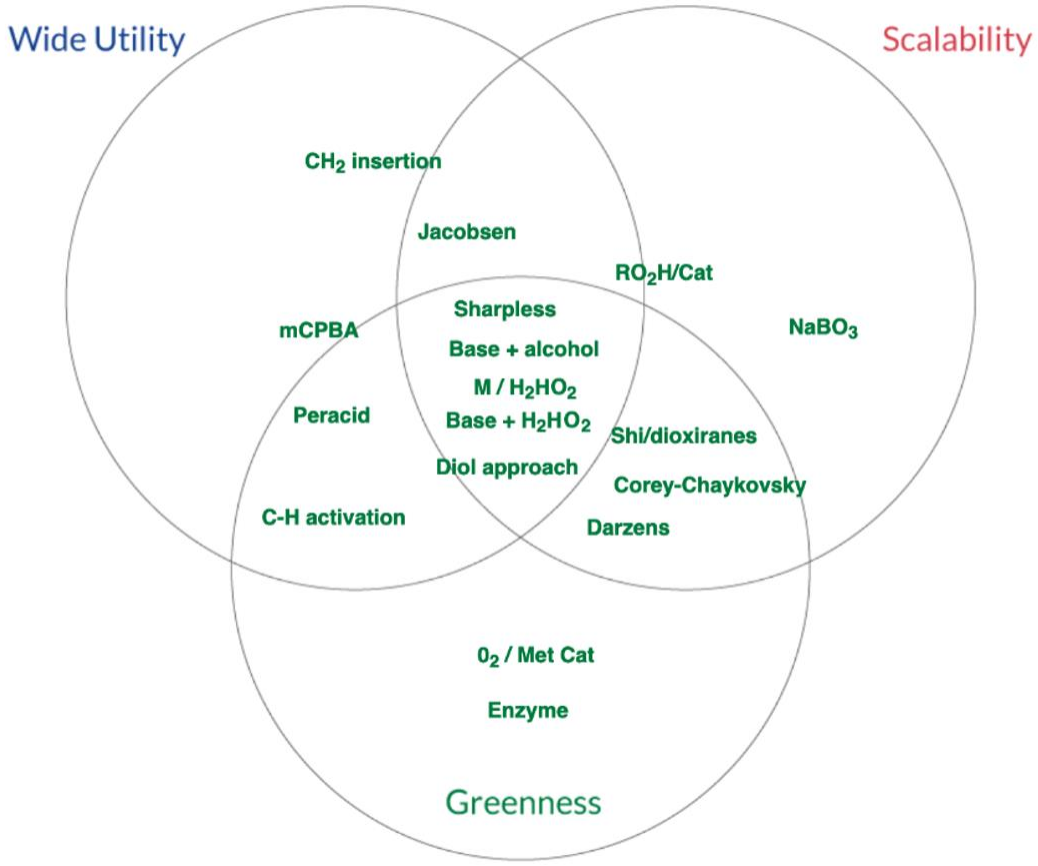

Figure 2.9: Venn diagram related to the use of different oxidants for epoxidation reactions. [7]

Hydrogen peroxide is one of the few oxidants that combines wide utility, potential scalability, and greenness as reactant. H_2O_2 present high atom efficiency (only water as by-product), low safety concerns if used at concentration <30%wt, negligible toxicity and environmental impact, low cost, high availability and overall sustainability.[8] In this frame, the Venn diagram represented in Figure 2.9 and published by the ACSGCIPR (American Chemical Society - Green Chemistry Institute - Pharmaceutical Roundtable) shows that the use of hydrogen peroxide with a metal catalyst (M/H_2O_2) is one of the best solutions for epoxidation reactions.

The coupling of the epoxidation of olefins with H_2O_2 in absence of added solvents with a subsequent CO_2 fixation in a tandem fashion is a very attractive route for the synthesis of COCs but issues such as miscibility of the reactant in a multiphasic mixture and potential over oxidation have to be addressed. Very few researches went in this direction. These publications will be briefly discussed here following.

In 2007 Eghbali et Li published a communication regarding a catalytic OB procedure (in which the intermediate is the bromohydrin in the place of the epoxide) for the DOC of olefins with H_2O_2 (6 equiv.), $[N_{4,4,4,4}]Br$ (0.15 eq), DBU (0.15 eq.) and 25 bar of CO_2 as C source: the authors claimed the in-situ formation of Br_2 that in presence of water led to the formation of bromohydrin, its deprotonation by DBU and further insertion of CO_2. They achieve good yields in COCs from activated aromatic olefins (>70%) and moderate yields (27-47%) from aliphatic ones.[9] A year later Wang et al. exploited a similar catalytic OB in water in the presence of H_2O_2 (6 eq.) $Na_2H_5P(W_2O_7)_6$ (10% mol.), TBABr (30% mol), an over-stoichiometric amount of $NaHCO_3$ and 25 bars of CO_2. The mechanistic hypothesis (Figure 2.10) involved the formation of a peroxotungstate species that reacted with TBABr to form BrO^-. The latter species formed the bromohydrin by reaction with the olefin. Subsequent deprotonation of the bromohydrin with a stochiometric base promoted CO_2 insertion. In this reaction large amounts of phenacyl benzoate were observed as by-product, due to the reaction between benzoic acid formed by over-oxidation and the bromohydrin. The DOC of styrene and styrene derivatives afforded 34-83% yield in the corresponding cyclic carbonates, while no selectivity towards COCs was determined for terminal and internal aliphatic olefins.[10]

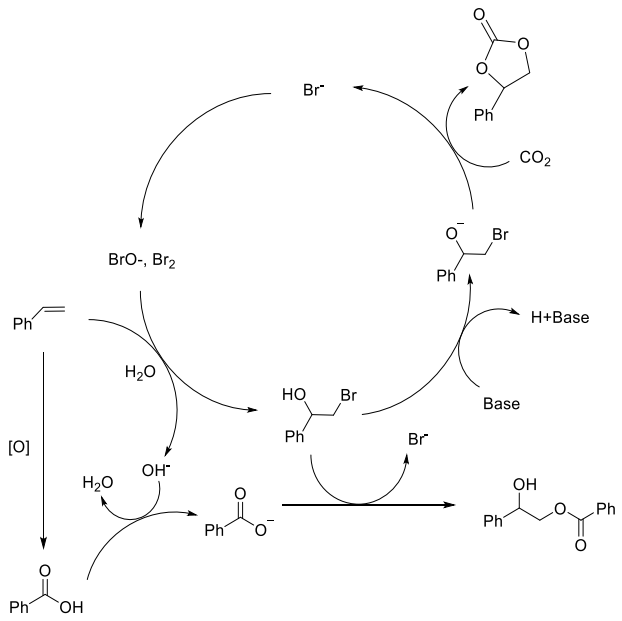

Figure 2.10: Possible pathways for the formation of styrene carbonate and phenacyl benzoate hypothesized by Wang et al. in ref. 10

In 2018 Dias et al. studied the oxidative carboxylation of olefins by using porphyrin metal complexes (Mn and Cr) anchored to ferromagnetic silica in presence of ammonium acetate as axial ligand, H_2O_2, 10 bar of

CO_2 and bis(triphenylphosphine)iminium chloride as co-catalyst for its insertion.[11] However, the authors did not attempt tandem catalysis since the two steps were incompatible and a cumbersome one-pot two-step procedure with intermediate work-up dehydration of the reaction mixture and addition of catalyst and co-catalyst for the second step was performed to obtain a 70% yield in styrene carbonate. These results are attractive, but this process cannot be considered at all an example of tandem catalysis.

Finally, Sathe et al explored an effective CF procedure for the DOC of olefins yet carefully reported in paragraph 1.5.2.5. [12] This is essentially a one-pot two-step system in which two packed-bed flow reactors were used in series. In the first epoxidation step the olefin was co-flowed with H_2O_2 as oxidant, CH_2Cl_2 as co-solvent, 3-methylpyrazole as Lewis base and MTO as Re-based catalyst. After the reaction in the first packed bed reaction, the use of an intermediate membrane phase separator was mandatory to divide the aqueous phase and H_2O_2 from the organic stream that was directed towards the second packed-bed reactor along with a co-flow of CO_2 as C1 source (7.5 bar, 1ml/min), an amino triphenolate aluminum complex as catalyst, tetrabutylammonium iodide (TBAI) as co-catalyst, CH_2Cl_2 and THF as co-solvent. Good 48-98% yields of COCs were afforded with aromatic and terminal aliphatic olefins while no selectivity was obtained with internal or cyclic olefins.

2.2.2 Aim and summary of this work.

In this work, we report the first truly AsTC procedure for the DOC of olefins – terminal and internal ones – in the presence of H_2O_2 as oxidant and CO_2 as carbon source. Our idea initiated from well-known and studied Venturello-Ishii catalysts, i.e. peroxotungstophosphate salts used under phase transfer catalysis (PTC) conditions that are widely used for the epoxidation of olefins with hydrogen peroxide in biphasic acqueous-organic (e.g. CH_2Cl_2, $CHCl_3$) mixtures.[1] More recently, Kamata et al. suggested that simple monomeric tungstate salts could be used for the insertion of CO_2 in various substrates such as aryldiamines, primary monoamines, propargylic alcohols or 2-aminobenzonitriles. We propose their use for CO_2 fixation into epoxides. [13,14]

On these bases, we synthesized a simple ionic liquid (trioctylmethyl ammonium tungstate ($[N_{8,8,8,1}]_2[WO]_4$)) through a green halide-free procedure starting from trioctylamine, dimethylcarbonate and tungstic acid as reported in our previous work.[14]

This TILC was tested for epoxidation and CO_2 fixation: the two steps were separately studied with 1-decene and 1-decene oxide as model substrates and a tandem protocol was optimized and extended to other terminal and internal substrates, including a renewable model unsaturated substrate such as methyl oleate. The use of catalytic amounts of H_3PO_4 as promoter led to high conversion and selectivity towards epoxides, while the use of a halide co-catalyst in the CO_2 fixation step was mandatory to obtain high yields of the corresponding COCs. Interestingly, the reaction must be performed with an assisted tandem approach since the presence of halide source during the epoxidation completely inhibited the reaction. The optimized process for 1-decene provides for the use of H_2O_2 (2 equiv.), $[N_{8,8,8,1}]_2[WO]_4$ (2.5% mol), H_3PO_4 (1.25% mol) at 85°C for 3h followed by the raw addition of $[N_{4,4,4,4}]I$ (1.25% mol) with atmospheric pressure of CO_2 (1 bar) at 85°C for 5h, leading to a 92% isolated yield in 1-decene carbonate.

2.2.3 Results and discussion

As reported in the previous work (paragraph 2.1.4), preliminary tests were performed on styrene to explore its use as model substrate for the direct synthesis of styrene carbonate in a tandem approach. Unfortunately, styrene resulted too activated and easily undewent overoxidation and rearrangement reactions in the presence of hydrogen peroxide as oxidant and TILCs as catalysts.

For this reason, 1-decene (**1**) was chosen as the model substrate to separately study the two steps for DOC of olefins, epoxidation of 1-decene (**1**) (Figure 2.11a) and CO_2 insertion into 1-decene oxide (**2a**) (Figure 2.11b). 1-decene as a terminal aliphatic olefin represents a less activated olefin towards epoxidation, since the more the olefins are substituted, the easier they are epoxidized.[15] Conversely, the insertion of carbon dioxide into the terminal epoxide of decene resulted easier than the conversion of internal and more sterically congested substrates.[16] For the sake of completeness, Figure 2.11a reports also the main by-products identified in the first step due to overoxidation of the epoxide **2a.**[17] The structures of derivatives **2a-2d** and **3** were assigned by GC/MS and NMR analyses and by comparison, when possible, with authentic commercial samples.

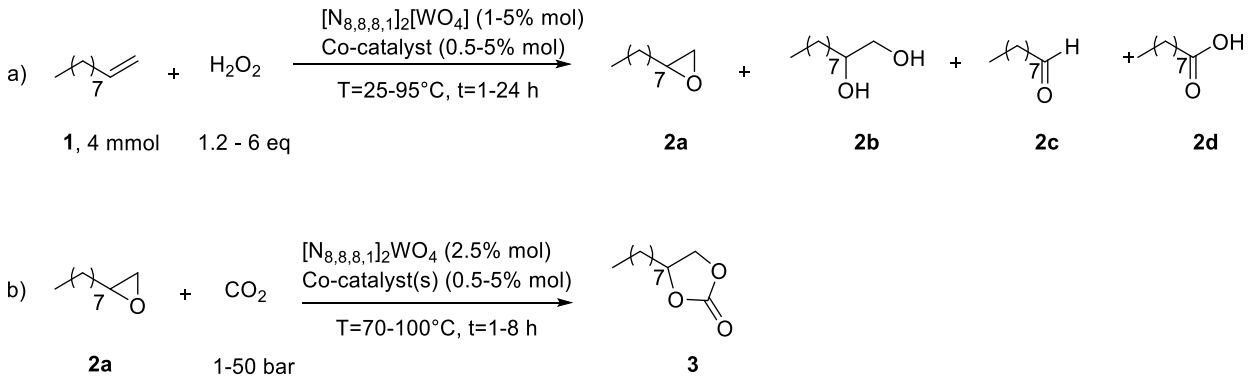

Figure 2.11: Model reactions to explore the tandem process in presence of $[N_{8,8,8,1}]_2[WO]_4$ as catalyst.

2.2.3.1 Epoxidation step

Table 2.6 reports the results obtained by screening the epoxidation of 1-decene (**1**, 4 mmol) in the presence of different amounts of the oxidant (H_2O_2, 30% wt, 2-6 equiv.), catalyst ($[N_{8,8,8,1}]_2[WO]_4$) and phosphoric acid as co-catalyst (if present) at 95°C for 2 hours. We decided to pursue a sustainable solvent-free procedure since our tungstate ionic liquid could act simultaneously as oxidation catalysts and phase transfer catalyst (PTC) allowing the successful outcome of the biphasic reaction.

Table 2.6: Effect of the amount of oxidant (H_2O_2), catalyst ($[N_{8,8,8,1}]_2[WO]_4$) and co-catalyst (H_3PO_4) on the epoxidation of 1-decene to 1-decene oxide.[a]

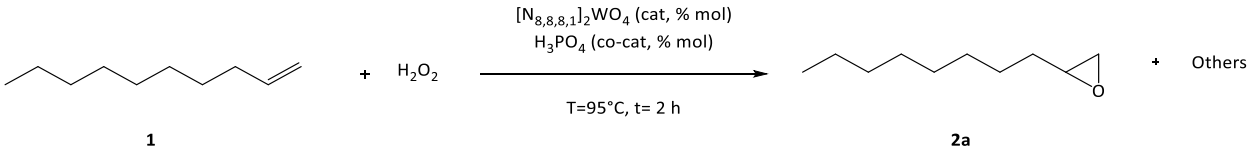

Entry	H_2O_2 (eq.)	$[N_{8,8,8,1}]_2[WO]_4$ (% mol)	H_3PO_4 (% mol)	1 (%)[b,c]	2a (%)[b,c]	Others (%)[b,c]
1	2			100	0	0
2	2	5		55	44	1
3	4	5		44	49	7
4	6	5		30	58	12
5	2	5	2.5	20	76	4
6	4	5	2.5	4	87	9
7	6	5	2.5	1	70	29[d]
8	2		2.5	100		
9	2	2.5	1.25	22	76	2
10	2	1.25	0.5	55	43	2
11	2	2.5	0.5	50	48	2
12	2	2.5	2.5	20	75	5
13	2	2.5	5	3	23	74[e]

[(a)] Reaction conditions: **1** (4 mmol), H_2O_2 (30% w/w, 2-6 equiv.), T = 95 °C, t = 2 h in the presence of $[N_{8,8,8,1}]_2[WO_4]$ (1-5% mol) and, where indicated, H_3PO_4 (0.5-5% mol)**;** [(b)] Product distribution calculated by GC analysis using mesitylene as internal standard;[c] tests were repeated three times to ensure reproducibility: afforded values of conversion and amounts of products differed by less than 3% from one experiment to another [d] **2b**: 3%, **2c**: 4%; **2d**: 16%; other unidentified by-products: 6%; [e] **2b**: 40%, **2c**: 17%, **2d**: 10%; other unidentified by-products: 7%

Reactions performed using only $[N_{8,8,8,1}]_2[WO]_4$ as catalyst with different amounts of oxidant (entry 2-4, 2-6 equivalents of H_2O_2 respect to the substrate) showed high selectivity towards **2a** (>90%) and discrete yet not satisfactory conversion respect to the blank test in catalyst-free conditions (entry 1). Longer 24h reactions in the same conditions of entry 2-4 (see appendix, figure A.2.31) showed that it was not possible

to achieve high conversions even for longer times: the reaction seems to stop after 2 hours of reaction. The selectivity towards **2a** remains very stable (>93%) over time when 2 equiv. of H_2O_2 was used while it decreased by increasing the excess of hydrogen peroxide.

Results were exciting when a phosphorous-based promoter (in our case H_3PO_4) was used to enhance the epoxidation as widely described in literature.[1,18] As reported in entry 5, it was possible to reach 80% conversion of **1** and 95% selectivity towards the corresponding epoxide using 2 equiv. of H_2O_2, 5% mol of $[N_{8,8,8,1}]_2[WO]_4$, 2.5% mol of H_3PO_4 by conducting the reaction at 95 °C for 2 hours. The increase in the amount of oxidant (entry 6-7) led to higher conversions but also to over-oxidation of **2a** and subsequent formation of by-products **2b-d**. The promoter effect of H_3PO_4 was proven by carrying out the reaction in the absence of $[N_{8,8,8,1}]_2[WO]_4$: no activation of hydrogen peroxide nor phase transfer capability was possible without TILC (entry 8). The following tests (entry 9-14) were designed to optimize the amount and relative molar ratio co-catalyst:catalyst, an important feature according to the literature. [18a,19] Entry 9 demonstrated that it was possible to halve both the amounts and keep comparable results with respect to conversion and selectivity, while conversion of **1** collapsed still halving their amounts (entry 10) or the ratio H_3PO_4:$[N_{8,8,8,1}]_2[WO]_4$ (entry 11). Finally, it was interesting to point out that increasing the ratio co-catalyst:catalyst led to slightly lower selectivity towards **2a**. In particular, the main reaction product result to be 1,2-decanediol (40%, entry 13) if the molar ratio was increased to 2.

Once the H_2O_2 equivalents, catalyst and co-catalyst amounts, were optimized, the effect of temperature was studied in order to maximize conversion of **1** and selectivity towards **2a**. Results reported in Figure 2.12 are quite unexpected: when the reaction was conducted at 95 °C, a maximum yield of 76% (conversion **1**=80%) was reached after 2h but no increase in conversion and a slight decrease of **2a** yield was revealed by prolonging the reaction time (blue line). This is due to the fast decomposition of hydrogen peroxide at this high temperature.[20] The reaction was slightly slower by lowering the temperature at 85°C (red line), but it was possible to obtain a quantitative conversion and 92% yield of **2a** after 3h: evidently the decomposition of peroxide in presence of $[N_{8,8,8,1}]_2[WO]_4$ is not as fast as at 95°C and allows to convert completely the substrate.[21] Conversely, the (useless) extension of time led to slight formation of by-products (85%). The kinetics of the reaction are strongly temperature-dependent: when the reaction was conducted at 75 and 50 °C (green and yellow line respectively), it was possible to obtain quantitative conversion and high yields of **2a** but in much longer times (21-24 h) in comparison with the reaction conducted at 85°C. Finally, the reaction at 25°C is very slow and the yield of **2a** was only 27% in 24 h, achieving 75% after 96 hours.

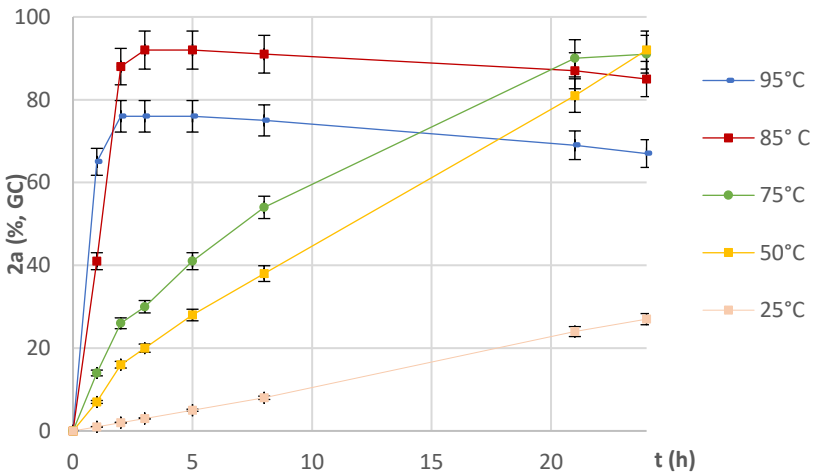

*Figure 2.12. Effect of temperature on the epoxidation of 1-decene (**1**) to decene oxide (**2a**). Reaction conditions: **1** (4 mmol), H_2O_2 (2 equiv.), $[N_{8,8,8,1}]_2[WO_4]$ (2.5% mol), H_3PO_4 (1.25% mol) T = 25-95°*

Once the optimal conditions for the epoxidation step were fixed [85°C, 3h, $[N_{8,8,8,1}]_2[WO]_4$ (2.5% mol), H_3PO_4 (1.25% mol)], it was intriguing to delve into the role of phosphoric acid in this system. Various other co-catalysts such as sodium salts of H_3PO_4, Bronsted acids and Lewis acids were tested to explore the effect of the acidity. Data are reported in Figure 2.13.

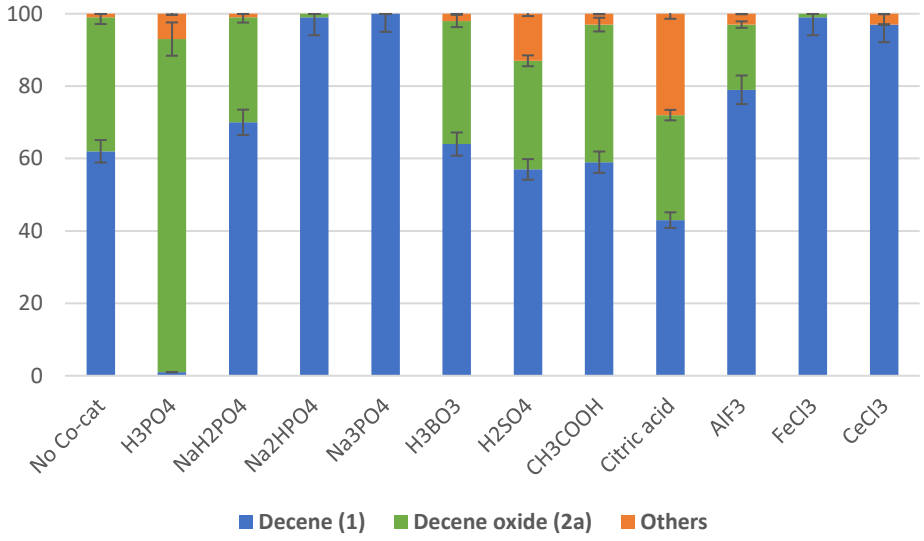

*Figure 2.13: Products distribution related to the effect of the use of different co-catalysts on the epoxidation of 1-decene (**1**). Reaction conditions: **1** (4 mmol), H_2O_2 (2 equiv.), $[N_{8,8,8,1}]_2[WO_4]$ (2.5% mol), selected co-catalyst (1.25% mol) T = 85° C, 3h.*

H_3PO_4 is the only co-catalyst that promotes high epoxidation reactivity. The use of NaH_2PO_4 led to slightly poorer performance respect to the reaction conducted without co-catalyst, while the use of disodium hydrogen phosphate and trisodium phosphate took to the complete inhibition of the reaction, i.e. no conversion of 1-decene. A measure of the pH of the hydrogen peroxide solutions with the addition of the

various co-catalysts is reported in fig. A.2.32. As we can clearly see, phosphoric acid increased the acidity of H_2O_2 solution, while the other derivatives led to pH more and more basic with the substitution of hydrogen with sodium. The high acidity of the hydrogen peroxide aqueous phase in presence of phosphoric acid is a key aspect in epoxidation reaction, as extensively reported in literature.[22] We decided hence to compare the activity of mineral and organic acids (H_2SO_4, H_3BO_3, CH_3COOH and citric acid) that could maintain the acidity of the aqueous phase and act as Brønsted acids. Results are much worse respect to the use of H_3PO_4: conversion of **1** resulted similar to that obtained in absence of co-catalyst, but a certain over-oxidation to **2d** is evidenced (6% and 22% with H_2SO_4 and citric acid respectively). It was hence demonstrated that the acidity effect is important but not the unique factor involved. Finally, the use of some Lewis acids was explored to determine the activity of Lewis acidity in this reaction: low or no conversion of the substrate was highlighted also in this case.[23]

Phosphoric acid plays a key role in the formation of active species with tungsten-based catalysts that could operate at the interphase of the biphasic mixture leading to selectivity towards the formation of the epoxide and better performance compared to the reactions conducted in the absence of H_3PO_4.[1,24] This aspect will be further discussed in the paragraph regarding the study of the mechanism.

2.2.3.2 CO_2 fixation test

The study of the CO_2 fixation into 1-decene oxide was only partially interesting to our scope, since the presence of residual H_2O_2 and H_2O will definitely affect the catalytic performance in our system. Moreover, a detailed investigation on the use of tungstate catalysts for the CO_2 insertion into various epoxides was already carried out in the previous work, hence few experiments were performed on the carbon dioxide fixation into our model substrate (**2a**, 1-decene oxide) that was not tested before.[14] This was also an opportunity to check the scalability of our catalytic system in the epoxidation of **1**: a twentyfold increase of the starting material (1-decene, 10 g, 71.4 mmol) showed that our system was fully scalable and a 88% isolated yield of 1-decene oxide (9.82 g, 62.8 mmol, >97% purity according to GC analysis and ^{1}H NMR) was obtained with the procedure reported in the experimental part.

Preliminary experiments for the CO_2 fixation were performed in an autoclave with **2a** and 50 bar of CO_2 for 8 h. Figure 2.14 shows that the use of $[N_{8,8,8,1}]_2[WO]_4$ or $[N_{4,4,4,4}]Br$ alone did not allow to obtain quantitative conversions and selectivity to **3 (**tests **a** and **b**) , while their simultaneous use led to a 94% selectivity towards **3** and quantitative conversion of the substrate (test **c**). As in our previous work, the mutual activity of $[N_{8,8,8,1}]_2[WO]_4$ and a model co-catalyst as $[N_{4,4,4,4}]Br$ was proved to be effective to obtain high yield in the corresponding carbonate in a solvent-less system. Experiments reported in columns **(d)** and **(e)** demonstrated an unexpected behavior of the system: the addition of H_3PO_4 (test **d**) to the mixture proved that its presence even slightly improve conversion of **2a** and selectivity to **3** in the CO_2 fixation step; the presence of added water (test **e**) results in a slightly lower conversion of **2a** (90%) but an excellent selectivity towards **3**: no formation of by-products such as 1,2-decanediol was seen with this amount of water that is similar to that contained in the reaction conditions optimized for the epoxidation step (Figure 2.12).

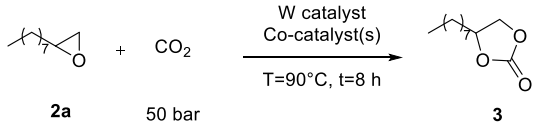

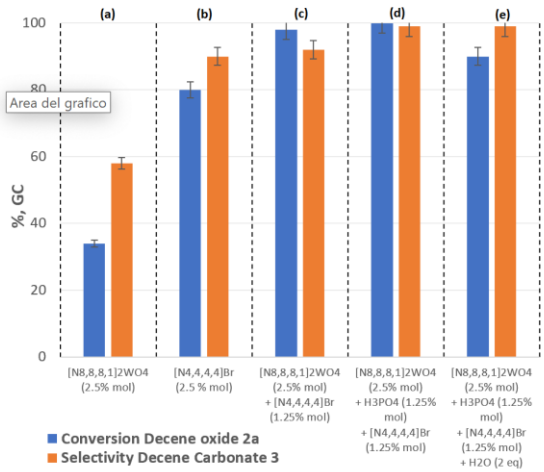

*Figure 2.14: CO_2 fixation into **2a**. Reaction conditions: **2a** (4 mmol), $[N_{8,8,8,1}]_2WO_4$ (0-2.5% mol), $[N_{4,4,4,4}]Br$ (0-2.5% mol), H_3PO_4 (0-1.25% mol), 50 bar of CO_2, 85°C, 8h. Test **(e)** was performed in presence of H_2O (2 equiv. respect to the substrate **2a**).*

2.2.3.3 One-pot process

The auto tandem catalytic procedure in which all the reactants are added at time zero was initially explored. Results are reported in Table 2.7. The presence of 50 bar of CO_2 (entry 2) from the start (entry 1) slowed the conversion of **1** (78 vs 99%) while the selectivity towards **2a** remains practically unchanged (95% vs 93%): only traces of carbonate **3** were detected in these conditions. Nonetheless the feasibility of the direct synthesis of **3** was demonstrated by prolonging the reaction time to 18h (entry 3): the AuTC approach can be exploited to obtain **3** but only in low yield (10%) along with minor formation of unidentified side-products. The further addition of $[N_{4,4,4,4}]Br$ at the beginning of the reaction (entry 4) strikingly stopped the reaction and only a 10% conversion of **1** was obtained while the formation of 1,2-dibromodecane was noticed: there were no chances to obtain **3** directly from **1** in these conditions. A further experiment was conducted without added carbon dioxide, and in the presence of the bromide source (entry 5) demonstrating a detrimental interaction between H_2O_2 activated from $[N_{8,8,8,1}]_2[WO]_4$ and bromide anions: no conversion of the substrate was detected. This result was due to the formation of BrO^- and Br_2 that lead to the consumption of H_2O_2 and no chance to convert **1**. The interaction of bromide anions with H_2O_2 is reported and exploited in previous works for the bromination of various classes of substrates, hence the epoxidation of the substrate is not achievable in the simultaneous presence of these reactants.[25] Therefore, we decided to shift to an assisted tandem catalysis (AsTC) protocol in which the halide co-catalyst (2.5% mol) and carbon dioxide (50 bar) were added only when the epoxidation step was complete: the second step was conducted at 85°C for 8h. Impressively, in these conditions we were able to obtain a 90% yield in cyclic carbonate **3**.

*Table 2.7: Auto tandem reaction for the direct synthesys of 1-decene carbonate (**3**) from 1-decene (**1**).[a]*

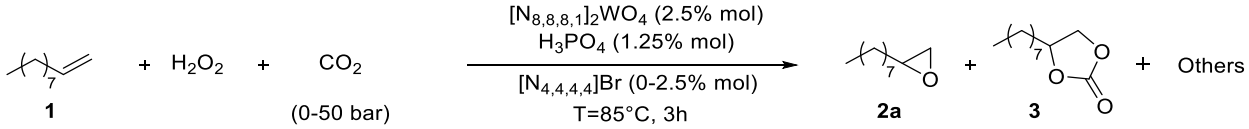

1 **2a** **3**

Entry	CO_2 (bar)	Br source (% mol)	1 (%)[b,c]	2a (%)[b,c]	3 (%)[b,c]	Others (%)[b,c]
1			1	92	0	7
2	50		22	74	1	3
3[d]	50		15	58	10	17
4	50	$[N_{4,4,4,4}]Br$ (2.5%)	90	0	6	4
5		$[N_{4,4,4,4}]Br$ (2.5%)	97	2	0	1
6[e]	50	$[N_{4,4,4,4}]Br$ (2.5%)	1	2	90	7

[a] Reaction conditions: **1** (4 mmol), H_2O_2 (2 eq.), CO_2 (0-50 bar), $[N_{8,8,8,1}]_2[WO_4]$ (2.5% mol), H_3PO_4 (1.25% mol), *$[N_{4,4,4,4}]Br$ (0-2.5% mol)* T =85°C, t=3h unless otherwise stated; [(b)] Product distribution calculated by GC analysis using mesitylene as internal standard;[c] tests were repeated three times to ensure reproducibility: afforded values of conversion and amounts of products differed by less than 3% from one experiment to another; [d] reaction conducted for 18 h; [e] AsTC approach: $[N_{4,4,4,4}]Br$ and carbon dioxide were added when the epoxidation step was over (after 3h at 85°C), and the reaction was conducted for additional 8h at 85°C.

Stimulated by this excellent result, we investigated the role of water and residual hydrogen peroxide in the reaction mixture in the one-pot process. Results are reported in Figure 2.15.

As expected from the peroxide efficiency tests, the use of 1.2 equiv. of hydrogen peroxide did not allow to obtain a complete conversion of **1** in the first step (83% conversion, 97% selectivity to **2a**)[26]. Moreover, the complete conversion of **2a** to **3** was not reached even after the addition of bromide source and CO_2: an overall 80% yield of 1-decene carbonate was obtained. The presence of 2 equivalents of H_2O_2 is optimal both for the first and second step and leads to the quantitative conversion of **1** and 90% yield in **3**. This behavior could be ascribed to the presence of the right amount of water as elegantly demonstrated with other catalytic systems,[27] but also to water interaction with added CO_2 that changes the pH of the solution and possibly improves the hydrogen bond donor (HBD) capability of water.[28]

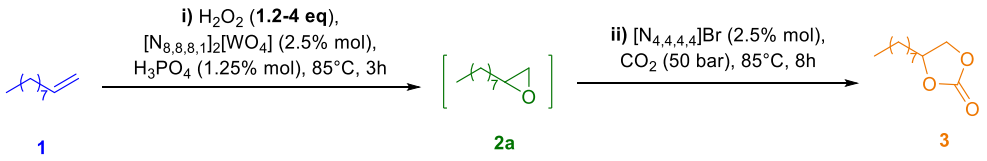

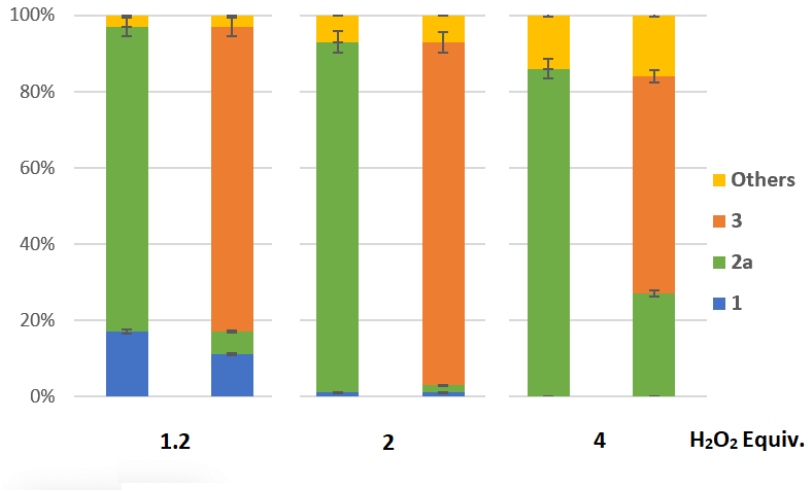

Figure 2.15: Effect of the hydrogen peroxide amount on the tandem direct synthesis of 1-decene carbonate from 1-decene. Reaction conditions: ***1*** *(4 mmol), H_2O_2 (1.2 - 4 eq.), $[N_{8,8,8,1}]_2[WO_4]$ (2.5% mol), H_3PO_4 (1.25% mol), performed at 85°C for 3 hours followed by the raw addition of CO_2 (50 bar) and $[N_{4,4,4,4}]Br$ (0-2.5% mol) without any intermediate work-up and the continuous of the reaction at the same temperature for further 8 hours.*

This was proved also in the single CO_2 fixation step: the experiment reported in Figure 2.14 on the formation of 1-decene carbonate starting from 1-decene oxide with the addition of the amount of water corresponding to that contained in 30% wt H_2O_2 (test **e**) had confirmed the beneficial role of water in this reaction conditions: conversion of **2a** was slightly lower with added H_2O but an astonishing 100% selectivity to **3** was highlighted, hence demonstrating (at least) that the presence of the selected amount of water is not detrimental to the CO_2 fixation. Finally, Figure 2.15 demonstrated that the increase to 4 equivalents of H_2O_2 had a marked negative contribution in the CO_2 fixation and led to a drastic decrease in converting **2a** to **3** in the second step.

Once established the right H_2O_2 amount for the one-pot process, the effect of various parameters such as temperature, CO_2 pressure and time were screened to optimize the reaction conditions of the second step. As we can see in Figure 2.16, 85°C is the optimum temperature of the 2nd step. It was noticed a drop in conversion when temperature was lowered to 70°C, while the increase to 100°C allowed a complete conversion but also the formation of high-molecular weight unidentified by-products increased up to ≈ 20%. Surprisingly, it was possible to lower the CO_2 pressure up to 10 bar without substantial diminution in yield of **3**. Conversely the cyclic carbonate formation was possible but not complete by operating at atmospheric pressure of CO_2 (yield **3**: 25%). Kinetic studies of the reaction allowed us also to shorten the overall reaction time to 5 hours (figure A.2.33).

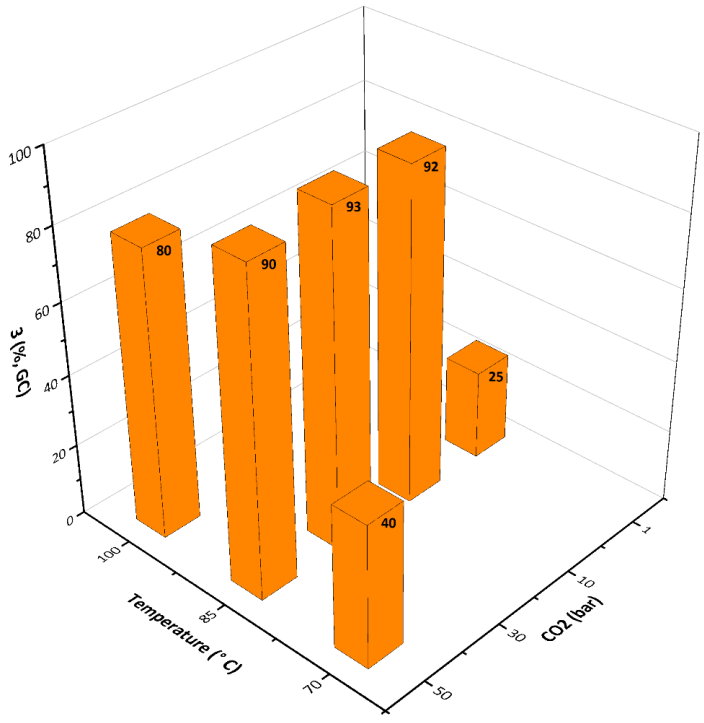

*Figure 2.16. Effect of temperature and CO_2 pressure in the tandem direct synthesis of 1-decene carbonate (**3**) from 1-decene (**1**). Reaction conditions: **1** (4 mmol), H_2O_2 (2 equiv), $[N_{8,8,8,1}]_2[WO_4]$ (2.5% mol), H_3PO_4 (1.25% mol), performed at 85°C for 3 hours followed by the raw addition of $[N_{4,4,4,4}]Br$ (2.5% mol), CO_2 (1-50 bar) without any intermediate work-up. The reaction was performed for further 8h at T=70-100°C. Yields were calculated by GC analysis using mesitylene as internal standard. Tests were repeated two times to ensure reproducibility: afforded yieds of **3** differed by less than 3% from one experiment to another.*

Finally, the amount and the role of co-catalyst was examined (

Table *2.8*). A low amount as 1.25% mol of $[N_{4,4,4,4}]Br$ respect to the substrate could be used to reach a quantitative conversion and high yield in **3**. If the amount was lowered to 0.5% mol, yield of **3** dropped to 33% (entry 1-3). Then, the use of different halides were tested: as already deepened in other researches, in presence of HBDs (or water) the typical catalytic activity scale of halides for CO_2 fixation is $Cl^- < Br^- < I^-$.[29,30] This behavior was confirmed: the use of chloride showed lower performance respect to Br^- (entry 4), while the superior reactivity of iodide allowed to achieve stunning results: the reaction take to 94% yield of **3** with 10 bar of CO_2 (entry 5) but also by working with an atmospheric pressure of CO_2 simply kept by a balloon reservoir.

*Table 2.8: Effect of co-catalyst on the AsTC reaction for the direct synthesys of 1-decene carbonate (**3**) from 1-decene (**1**).[a]*

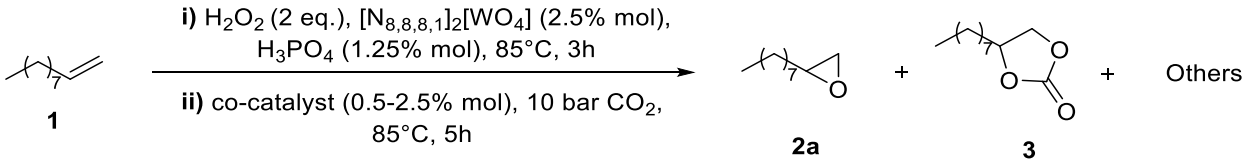

Entry[b]	Co-catalyst (%mol)	Products distribution [c,d]		
		2a (%)	3 (%)	Others (%)
1	$[N_{4,4,4,4}]Br$ (2.5)	2	90	7
2	$[N_{4,4,4,4}]Br$ (1.25)	1	93	5
3	$[N_{4,4,4,4}]Br$ (0.5)	60	33	5
4	$[N_{4,4,4,4}]Cl$ (1.25)	59	27	3
5	$[N_{4,4,4,4}]I$ (1.25)	1	94	4
6[e]	$[N_{4,4,4,4}]I$ (1.25)	1	94	4

[a] Reaction conditions: **1** (4 mmol), H_2O_2 (2 eq.), $[N_{8,8,8,1}]_2[WO_4]$ (2.5% mol), H_3PO_4 (1.25% mol), performed at 85°C for 3 hours followed by the raw addition of a co-catalyst (0.5-2.5% mol), CO_2 (10 bar) without any intermediate work-up. The reaction was further performed for 5 h at T=85°C; [b] Conversion of **1** is always >98%; [c] Products distribution according to GC analysis using mesitylene as internal standard [d] Tests were repeated two times to ensure reproducibility: afforded yields of **3** differed by less than 3% from one experiment to another; [e] reaction conducted with 1 bar of CO_2.

This outcome represents a breakthrough in a green perspective: only 4 very recent papers reported the direct oxidative carboxylation of olefins at atmospheric pressure of CO_2.[31] However, all these publications reported catalysts active in presence of anhydrous TBHP as oxidant that operate only for the DOC of highly active styrene to styrene-carbonate, while no other aliphatic terminal or internal olefins were suitable for these catalytic systems. Three of them use metal organic frameworks (MOFs) based on rare-earth metals (Zirconium[29a], Neodymium[29b] and Cobalt-neodymium[29c] respectively) and achieved yields in styrene carbonate >90%, while the fourth is based on the use of an organic phosphonate salt[29d] in the presence of $ZnBr_2$ and reached a quantitative conversion of styrene and a maximum 70% selectivity towards styrene carbonate.

Our reaction has 92% atom economy, a 100% carbon efficiency and produces only H_2O as by-product, although the recycle of the catalyst was not developed in the present work. Attempts to recover and reuse the tungstate ionic liquid were unsuccessful so far, but research work is ongoing in our lab. The scalability of the entire process was tested also in this case: a twentyfold increase of the starting material (1-decene, 10 g, 71.4 mmol) proved that our system was fully scalable and an 86% isolated yield of 1-decene carbonate (12.28 g, 61.4 mmol, >98% purity according to GC analysis and ^1H NMR) was obtained with the procedure reported in the experimental part.

2.2.3.4 Mechanistic hypothesis

A mechanistic hypothesis including for the formation of the active catalytic species is proposed based on the literature, experimental results, ^{31}P NMR and ^{183}W NMR.

Starting from pioneering studies by Venturello-Ishii, the use of a tungsten precursor, hydrogen peroxide, phosphoric acid and a halide quaternary ammonium salt to obtain peroxotungstophosphate species able to catalyse epoxidation reactions was studied further by several authors.[32] According to literature, ^{31}P-NMR studies can give information about structural changes and active species formed by the interaction between tungsten species, phosphoric acid and hydrogen peroxide.[1,18,19,24] Also in our case, ^{31}P analysis proved that such structural changes were occurring during the reaction in our conditions. Spectra reported in fig. A.2.34 in the appendix revealed an evident shift of the H_3PO_4 peak (fig. A.2.34a) by sequential addition of hydrogen peroxide and $[N_{8,8,8,1}]_2[WO]_4$ (fig. A.2.34b and A.2.34c respectively) indicative of the formation of peroxotungstophosphate species during the reaction. According to the literature and based on the presence of only one peak in ^{31}P NMR, our conditions took to the unambiguous formation of a single NMR species that is recognized as the dimeric peroxotungstophospate $[HPW_2O_{14}]^{2-}$ species (fig. A.2.34c).[24b] As reported in several papers and demonstrated also by experimental results in

Table 2.6 (entry 1-3) and figure A.2.36, this species is often not the only one present, but also a simple peroxotungstate species such as $[W_2O_3(O_2)_4{\cdot}2H_2O]^{2-}$ (Figure 2.6 and Figure 2.17a) is active in the epoxidation of olefins. Hence, the epoxidation step is expected to proceed through the action of these two catalytic species as depicted in Figure 2.17.

Once the epoxide was formed, two parallel pathways could be responsible for CO_2 fixation: the first was due to the activity of tungstate anion as Lewis base that activates carbon dioxide (depicted in Figure 2.17b). The formation of a new species was demonstrated by ^{183}W-NMR of $[N_{8,8,8,1}]_2WO_4$ exposed to CO_2 (see fig. A.2.33 for the ^{183}W NMR spectra), there is the rise of a peak at 43.9 ppm with the complete disappearance of the tungstate $[WO_4]^{2-}$ peak at 7.5 ppm. The formation of this new peak is already reported in the literature for tetrabutylammonium tungstate [13] and it is due to the formation of an adduct between tungstate and carbon dioxide ($WO_4{\cdot}CO_2$) that activates CO_2 towards further reactions in the presence of organic substrates. As shown in the experimental part (Table 2.7, entry 3), this species can promote the formation of COC by reacting with epoxides, but high conversions and selectivity were achievable only in the presence of halide anions as co-catalyst: tungstate catalysts alone promoted also side competitive reactions that mainly led to the formation of isomers of the epoxides. The presence of a halide source favoured the classical and widely accepted mechanism for the CO_2 fixation reported in Figure 2.17c.[33] As illustrated in the figure, also in this pathway a possible enhancement of the reaction related to the presence of carbon dioxide activated by tungstate anion could be hypothesized. Both the route (**b** and **c**) required the preliminary activation of the epoxide by a Lewis or Bronsted acid (A^+). A specific study of which species act as a A^+ trigger was not conducted in this research but we can speculate about the presence of several species that could assume this key role: i) W in tungstate anions present a pronounced Lewis acidic character; ii) H_3PO_4 is a well-known Bronsted acid catalyst and the test for CO_2 fixation into epoxide showed that its presence took to a better selectivity (Figure 2.14, test **d**); iii) The presence of an acidic aqueous solution in the biphasic mixture could give HBDs that activate the ring-

opening of the epoxide;[27] (iv) also tetraalkylammonium cation could enable the activation of the epoxide.[34]

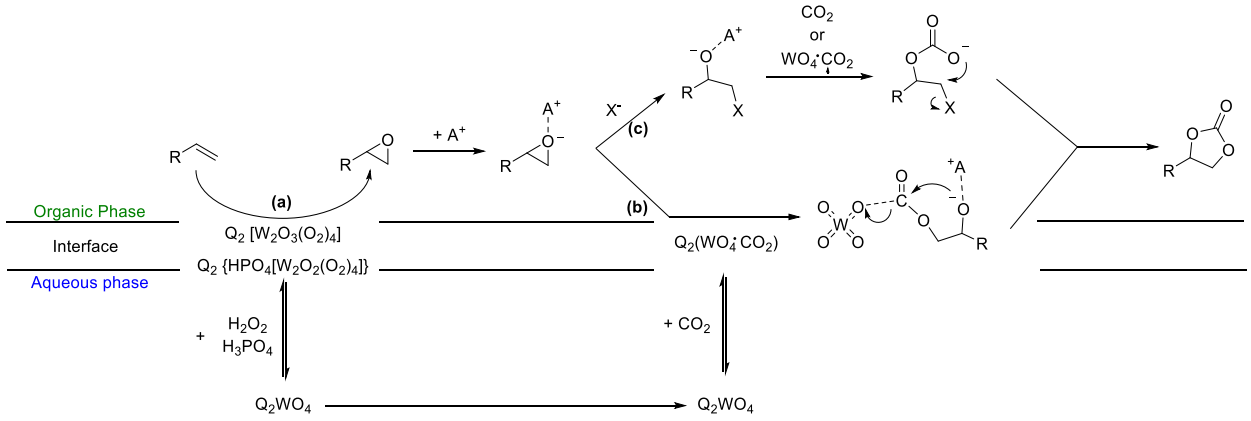

Figure 2.17: Schematic representation of the main pathways for the formation of cyclic carbonate in the assisted tandem process discussed above

2.2.3.5 Substrate scope

The substrate scope was investigated in the reaction conditions optimized in

Table *2.8*. A tubular glass reactor equipped with a magnetic stirrer and a condenser was charged with $[N_{8,8,8,1}]_2[WO]_4$ (2.5% mol), H_3PO_4 (1.25% mol), H_2O_2 (2 equiv.) and the selected olefin (4mmol, 1 equiv.). The mixture was heated at 85°C for 3h, after that $[N_{4,4,4,4}]I$ (1.25% mol) was added and the reaction was continued at 85°C for additional 5 hours under an atmospheric pressure of CO_2 attained through a rubber reservoir containing about 1 liters of CO_2. The COCs synthesized are reported in Figure 2.18.

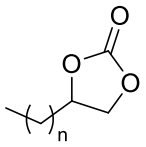

n=3 (**3a,** 87%)
n=5 (**3b**, 88%)
n=11 (**3c,** 93%)
n=13 (**3d,** 91%)

Figure 2.18: Terminal COCs obtained through the assisted tandem direct oxidative carboxylation protocol developed in this work (yields in parentheses).

Our protocol is suitable to the synthesis of a wide range of terminal COCs: all linear olefins (C_6-C_{16}) were obtained with yields >87%, demonstrating the suitability of our catalytic system in biphasic mixture.

Unfortunately, attempts to implement this protocol with other classical substrates such as styrene or cyclohexene afforded low selectivity towards the corresponding epoxide (<20%) in the first step. The formation of several over-oxidation and isomerization compounds is due to the higher attitude towards oxidation of cyclic olefins and electron-rich aromatic olefins such as styrene.[35,36] Changing parameters (temperature: 25 - 85°C , time: 0.5 – 3 h; amount of H_2O_2: 1 - 2 equiv. respect to the substrate) did not allow to improve selectivity towards the desired epoxides. No further investigations were carried out in this respect.

2.2.3.6 Assisted tandem direct oxidative carboxylation of methyl oleate

A separate discussion regards the DOC of renewable feedstocks such as fatty acid methyl esters (FAMEs) that contain a *cis* olefin in their structure. The synthesis of the corresponding COCs of FAMEs attracted increasing interest from academic research in recent years since their potential use in the sustainable formation of isocyanate-free polyhydroxyuretanes.[37] Since the higher reactivity of disubstituted internal olefins respect to terminal ones, the possibility to extend the protocol to fatty acid methyl esters with a simplified procedure for the epoxidation step was investigated. Methyl oleate (**1g**) was selected as model substrate.[38] A study of the epoxidation step in the presence of $[N_{8,8,8,1}]_2[WO_4]$ as catalyst with or without the addition of H_3PO_4 as co-catalyst was initially performed.[39] Data are reported in Figure 2.19.

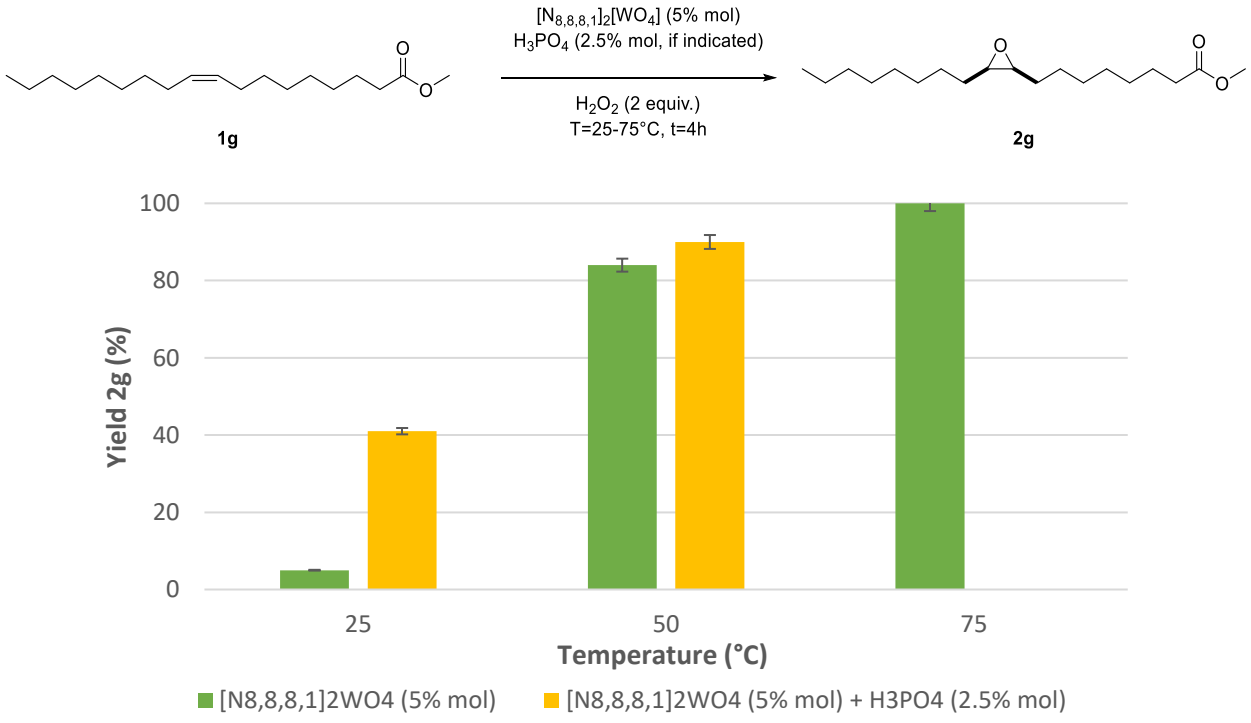

*Figure 2.19: Epoxidation of methyl oleate (1.67 mmol) in presence of H_2O_2 (2 equiv.) at T=25-75°C for 4h in presence of $[N_{8,8,8,1}]_2[WO_4]$ as catalyst and H_3PO_4 as co-catalyst (when indicated). Yields calculated according to ^{1}H NMR analysis by using mesitylene as internal standard. Selectivity towards **2g** is always quantitative.*

The epoxidation performed at 25°C showed a great difference of reactivity if the reaction is conducted in the presence of the TILC solely, or with the addition of H_3PO_4 as co-catalyst (5 – 41% yield in **2g** respectively). This difference was less evident when the reaction was operated at higher temperature (50 °C) and the **2g** yields were 84% and 90% respectively. This prompted us to increase the temperature to 75°C in the co-catalyst-free reaction; a quantitative conversion of **1g** with a complete selectivity to **2g** was afforded. Since the use of a simplified procedure that excludes the use of auxiliaries is beneficial from a green perspective, we pursued our investigation without the addition of H_3PO_4 as co-catalyst. In this case, the peroxotungstate species is accountable for the epoxidation of the substrate. A blank test conducted at 75°C for 4 h in absence of any catalyst confirmed a lack of conversion in these conditions.

In analogy to the experiments with terminal olefins, the effect of oxidant amount (H_2O_2=1-4 equiv. respect to the substrate **1g**) was subsequently studied with two different amounts of catalyst (2.5-5% mol) and is reported in Figure 2.20.

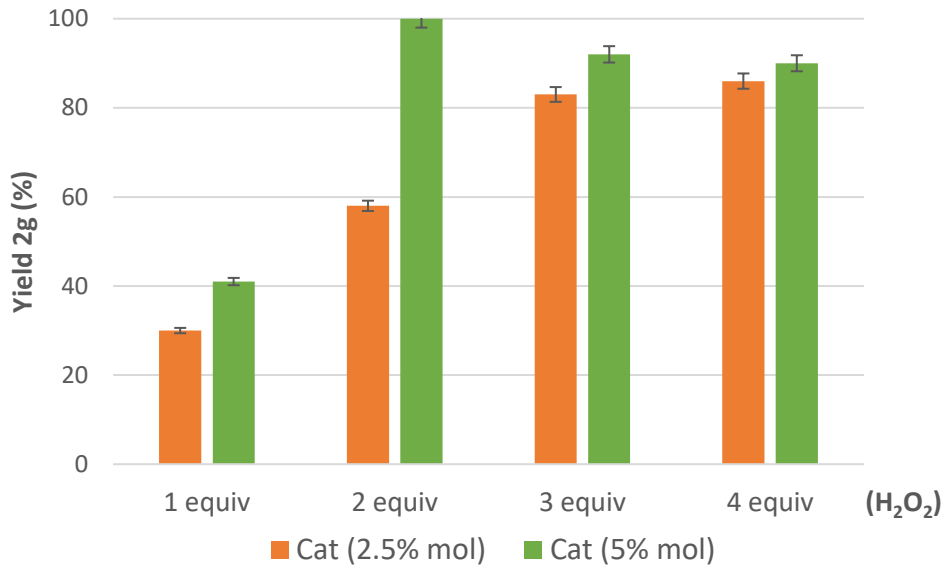

*Figure 2.20: Epoxidation of methyl oleate (1.67 mmol) in presence of different amount of H_2O_2 (1-4 equiv.) at T=75°C, t=4h in presence of $[N_{8,8,8,1}]_2[WO_4]$ (Cat=2.5-5% mol) as catalyst). Yields calculated according to ^{1}H NMR analysis by using mesitylene as internal standard. Selectivity towards **2g** is always quantitative.*

The use of a 2.5% mol amount of catalyst (orange columns) is not enough to achieve quantitative conversions: a linear growth of the yield is observed increasing the peroxide amount from 1 to 4 equivalents, reaching a maximum yield of 86%. On the other hand, the use of 5% mol of $[N_{8,8,8,1}]_2[WO_4]$ with an equimolar amount of H_2O_2 afforded a 41% yield, while the use of 2 equiv. H_2O_2 resulted the best choice: a quantitative conversion of **1g** and complete selectivity to **2g** was observed in these conditions.[40] Unexpectedly, a larger excess of hydrogen peroxide (3-4 equiv.) led to poorer performance compared to the use of 2 equivalents. This large amount of oxidant and low pH in the aqueous phase could affect the biphasic system and lead to low efficiency of hydrogen peroxide, formation of less active peroxo-species and larger dilution and solubility of the tungstate catalyst in the aqueous phase, as already reported in

similar papers on epoxidation reaction promoted by tungsten-based catalyst.[41,42] Moreover, large amounts of hydrogen peroxide can negatively affect one-pot tandem reaction as already showed in Figure 2.15 for the DOC of 1-decene: 2 equiv. of H_2O_2 with 5% mol of $[N_{8,8,8,1}]_2[WO_4]$ as catalyst represent the optimized amount also for the epoxidation of methyl oleate.

Then we briefly explored CO_2 fixation into **2g** in the presence of $[N_{8,8,8,1}]_2[WO_4]$ (5% mol), $[N_{4,4,4,4}]Br$ (2.5% mol) as model halide source or with a mixture of the two. Results are reported in Table 2.9. In this case, 100 °C and 50 bar of CO_2 were chosen as experimental conditions based on previous similar works reported in the literature for less reactive internal epoxides.[37e] $[N_{8,8,8,1}]_2[WO_4]$ proved to be an active catalyst for CO_2 fixation but only a 28% conversion and 64% selectivity towards the corresponding COC **3g** was observed (entry 1). This outcome was similar to that reported by us for the CO_2 insertion into styrene oxide and terminal olefins (Figure 2.7 and Figure 2.14).[14] The main by-products were isomerization by-products due to Meinwald rearrangement of the epoxide to the corresponding ketones, as already reported in the literature.[37d]

*Table 2.9: CO_2 fixation into epoxidized methyl oleate (**2g**)*

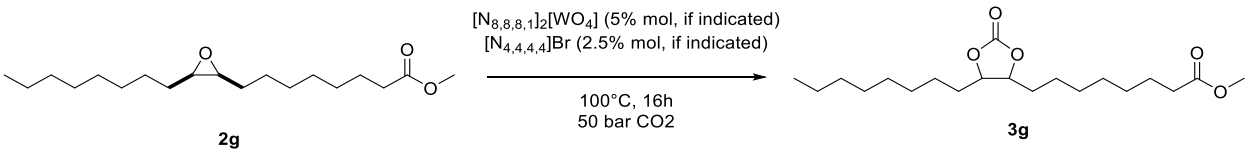

Entry	$(N_{8,8,8,1})_2$-WO_4 (% mol)	TBABr (% mol)	Conversion	Selectivity	Cis : Trans Ratio
1	5		28	64	99 : 1
2		2.5	80	91	56:44
3	5	2.5	87	95	99 : 1

Reaction conditions: **2g** (1.67 mmol), $[N_{8,8,8,1}]_2[WO_4]$ (5% mol, if indicated), $[N_{4,4,4,4}]Br$ (2.5% mol, if indicated), CO_2= 50 bar, 100°C, 16h. Conversion, selectivity and cis:trans ratio calculated according to ^1H NMR analysis by using mesitylene as internal standard.

Even the use of $[N_{4,4,4,4}Br]$ did not afford a complete conversion and selectivity towards **3g** (80% and 91% respectively, entry 2) but more importantly the reaction was not stereoselective: a 56:44 cis:trans ratio was detected by ^1H-NMR analysis of the organic phase. The stereoselectivity could be controlled in presence of both $[N_{8,8,8,1}]_2[WO_4]$ and $[N_{4,4,4,4}]Br$: in this case an 87% conversion of **2g**, 95% selectivity to **3g** and a 99:1 cis:trans ratio was detected. This trend (entry 1-3) was explained through the mechanisms of TILCs and halide salt in the CO_2 fixation of internal cis-epoxides such as epoxidized methyl oleate **3g**, depicted in Figure 2.21**.** The first step is the activation of the epoxide through a Lewis acid (A^+), in this case tungstate species, as reported for a plethora of early transition metals such as niobium,[43] molybdenum,[44] vanadium,[45] zirconium[46] and so on. The first CO_2 insertion route (path **a**, Figure 2.21) was already discussed in this thesis and it involves the formation of an active adduct $WO_4{\cdot}CO_2$ as indicated by ^{183}W NMR (figure A.2.37) and already reported in literature.[13] This pathway leads to the direct insertion of CO_2 in the epoxide

ring with consequent exclusive formation of the cis carbonate. Path **b** provides for the ring-opening of the epoxide prompted by halide (X^-) and formation of the alcoholate species. According to experimental test this route is faster and predominant respect to path **a** in the formation of COCs (entry 1-2, Table 2.9). Along with the Lewis acidity effect of tungsten species, it is noteworthy that tetraalkylammonium species (Q_1^+ and Q_2^+, i.e. $[N_{8,8,8,1}]$ and $[N_{4,4,4,4}]$) could affect the stabilization of this alcoholate intermediate formed. The formation of cis/trans isomers can be reasonably explained by considering both type of nucleophilic substitution, S_N2 and S_N1 in the ring-closure of the linear carbonate species (path **b.1** and **b.2** respectively).[37e] The combination of tungsten-based catalysts and halide salt takes to conversion of **2g** and selectivity to **3g** comparable to that observed when $[N_{4,4,4,4}]Br$ was used alone (entry 3 and 2 Table 2.9), while a great increase in cis:trans ratio was observed. We hypothesized that the main action of tungstate species must be the CO_2 activation that increases the rate of CO_2 insertion into alcoholate species and the subsequent higher rate of the ring-closure that promote the **b.1** pathway respect to the preliminary release of X^- with consequent **b.2** pathway and potential formation of cis/trans carbonate. This synergistic increased *cis*- selectivity was already observed by Leitner et al. in the synthesis of cyclic carbonates from oleochemical epoxides and CO_2 in presence of ammonium halide and transition metal substituted silicotungstate polioxometallates.[47]

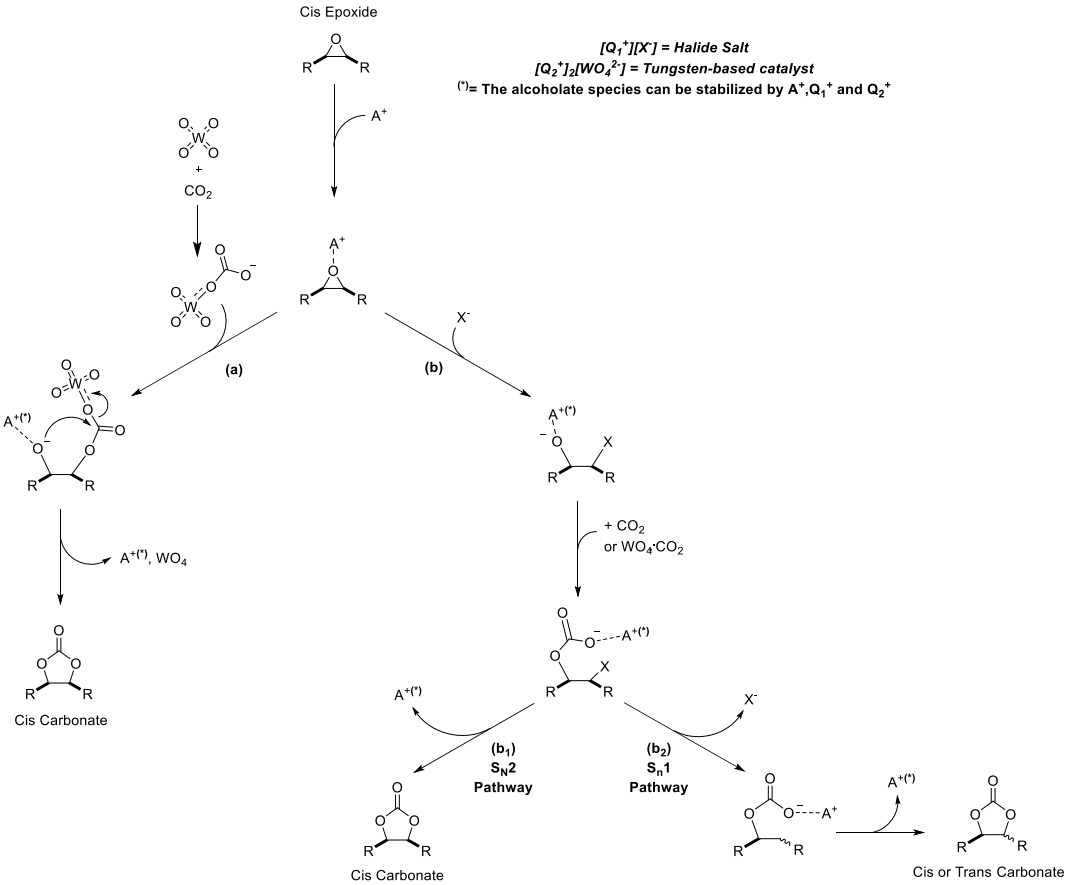

Figure 2.21: Potential reaction mechanisms involved in the CO_2 fixation into internal cis epoxide in presence of TILCs and halide salts.

Finally, experiments on the assisted DOC of methyl oleate are reported in Table 2.10. In this case, methyl oleate (1.67 mmol) and H_2O_2 (2 equiv.) were added in a glass reactor in presence of $[N_{8,8,8,1}]_2WO_4$ (5% mol) and stirred at 75 °C for 4 hours. Then, a selected co-catalyst (with chloride, bromide and iodine anions for comparison, 2.5% mol) was added to the reaction mixture, the reactor was placed in an autoclave with 50 bar of CO_2. This second step was conducted for 16 hours at 100°C.

The use of tetrabutylammonium halide (Cl^-, Br^-, I^-, entry 1-3 respectively) gave mild selectivity towards **3g** and retention of stereoselectivity with formation of the cis-carbonate (99:1 for chloride and bromide, 90:10 for iodine) confirming the beneficial role of tungsten in the epoxidation step (conversion of **1g** is quantitative in all the reactions, entry 1-9) but also in the control of stereoselectivity. The low selectivity towards **3g** is probably caused by the presence of the biphasic system that decreases the rate of the CO_2 fixation process respect of the CO_2 fixation tests reported above (see entry 2-3, Table 2.9 and entry 2, Table 2.10 for comparison). Given this low performance, we decided to test the effect of simple alkali halides (entry 4-9). This class of compounds is not active for the CO_2 insertion into epoxide in the absence of additional cryptands such as crown ethers or polyethylene glycols[48,49] but we speculated that the salt can solubilize in the aqueous phase while $[N_{8,8,8,1}]_2WO_4$ that act as H_2O_2 activator and phase transfer catalyst (PTC) in the first step could act as PTC also in this second step allowing the CO_2 fixation. Our hypothesis was confirmed by experimental results: the one-pot assisted tandem process with alkali halide salts as co-catalyst allowed similar or improved performances compared to that obtained through tetraalkylammonium halide salts (entry 4-9). The product distribution with different halides complied with the trend already detected in literature for the CO_2 insertion in presence of added water ($Cl^-<Br^-<I^-$).[30a,47] In particular, **3g** yields obtained with the sodium series of the halide salts (entry 4-6, 22, 46% and 67% respectively) are comparable to that obtained with tetraalkylammonium salts (entry 1-3: 20, 45% and 65% respectively). But while NaCl and NaBr allowed a complete selectivity to **3g** and stereospecific reactions with 99:1 cis:trans ratio (entry 4-5), the use of NaI (entry 6) led to the formation of by-products (in particular the corresponding ketones and diol due to hydrolysis of the formed epoxide) and an overall 87% selectivity towards **3g**. Moreover, in this case a 56:44 cis:trans ratio was detected as a consequence of the increasing rate of the **b.2** route reported in Figure 2.21. This S_N1 pathway is promoted by the presence of iodide, that is a better nucleophile but also a better leaving group compared to bromide and chloride, as already reported in literature in the synthesis of fatty acid carbonates.[37d-e] This effect was practically inhibited using potassium halide salts. In this case, KBr and KI gave similar conversions (entry 8-9, 70 and 65% conversion respectively) with a complete selectivity towards **3g** and a cis:trans ratio > 95:5, hence a substantial stereospecific reaction, occurred.

Finally, we highlight that the use of the assisted tandem process, despite a decreased reaction rate respect to the CO_2 fixation experiments reported in Table 2.9, allowed always a quantitative selectivity towards the carbonate **3g** (except for the case of NaI) while the tests performed on the simple CO_2 fixation showed a lower selectivity due to the formation of isomerization by-products (compare Table 2.9 and Table 2.10): the presence of the biphasic mixture hence promoted the chemoselectivity towards the COC synthesis despite lowering the reaction rate. According to our knowledge, this is the first example of direct oxidative carboxylation of an oleochemical compound such as methyl oleate.

Table 2.10: Assisted direct oxidative carboxylation of methyl oleate

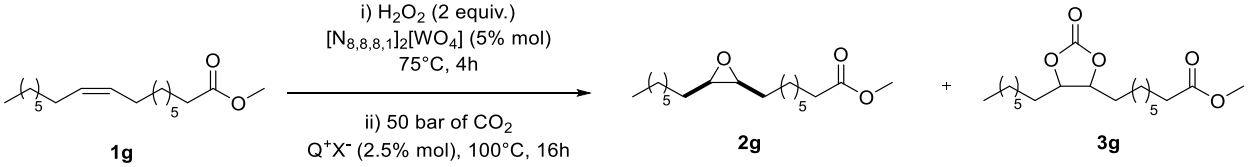

Entry	Co-Catalyst (2.5% mol)	Product distribution [a,b]		3g Cis:Trans Ratio
		2g (%)	3g (%)	
1	$[N_{4,4,4,4}]Cl$	80	20	99:1
2	$[N_{4,4,4,4}]Br$	55	45	99:1
3	$[N_{4,4,4,4}]I$	35	65	90:10
4	NaCl	78	22	99 : 1
5	NaBr	54	46	99 : 1
6[c]	NaI	23	67	56:44
7	KCl	77	23	99:1
8	KBr	30	70	95 : 5
9	KI	35	65	96 : 4

Reaction conditions: Methyl oleate (**1g**, 1.67 mmol), H_2O_2 (2 equiv.), $[N_{8,8,8,1}]_2WO_4$ (5% mol) performed at 75°C for 4 hours followed by the addition of a selected co-catalyst (Q^+X^- (2.5% mol), where Q^+= $[N_{4,4,4,4}]$, Na, K; X^-= Cl^-, Br^-, I^-) was added to the reaction mixture, the reactor was sealed and placed in an autoclave with 50 bar of CO_2. This second step was conducted for 16 hours at 100°C. [a] Conversion of **1g** is always quantitative; [b] Conversion, product distribution and cis:trans ratio calculated by NMR analysis using mesytilene as internal standard; [c] the other by-products formed are the dihydroxylated methyl oleate (4%) and the corresponding ketones due to Meinwald rearrangement (6%).

2.2.4 CONCLUSIONS

In the present part of the work, we demonstrated the feasibility of the direct synthesis of cyclic organic carbonates from terminal and internal olefins through an assisted tandem procedure based on the use of tungstate ionic liquid catalyst (i.e. trioctylmethyl ammonium tungstate). The concurrent use of hydrogen peroxide as oxygen source and the use of carbon dioxide at atmospheric pressure as C_1 source make the present procedure one of the greenest direct oxidative carboxylation published up to date. Terminal olefins, which are amongst the most unreactive olefins towards epoxidation, need the use of phosphoric acid as promoter to form *in situ* peroxophosphotungstate species known as very active species for the formation of epoxide in biphasic mixture along with simpler peroxotungstate species. Moreover, an auto tandem catalysis approach cannot be exploited since the halide source used to promote the ring-opening

of the epoxide has a detrimental interaction with the hydrogen peroxide activated by tungstate catalyst if added at the beginning of the reaction, leading to a low conversion of the substrates. For this reason, an assisted tandem protocol was implemented in which tetrabutyl ammonium iodide was added after the completion of the epoxidation step (without any intermediate work-up or purification of the reaction mixture) by carrying on the reaction under CO_2 atmosphere. C_6-C_{16} terminal cyclic organic carbonates were isolated with yields > 87% through this procedure. Unfortunately, this route was not applicable to the direct oxidative carboxylation of cyclic olefins (i.e. cyclohexene) or styrene due to over-oxidation side pathways favoured in the first step of reaction. However, we implemented also a simplified procedure for the direct oxidative carboxylation of renewable oleochemicals (i.e. methyl oleate) in the presence of H_2O_2, 50 bar of CO_2, tungstate ionic liquid as catalyst and alkali halide salts as co-catalyst that promote the CO_2 insertion. These salts confined in the aqueous phase can carry out their task because of the presence of the tungstate ionic liquid that act also as phase transfer catalyst in the biphasic mixture. In the presence of $[N_{8,8,8,1}]_2[WO_4]$ as catalyst and KBr as co-catalyst a maximum 70% yield in carbonated methyl oleate was obtained. Tungstate ionic liquid allowed also an almost complete retention of configuration with a 96:4 cis:trans ratio in the carbonated methyl oleate. This is the first example of direct oxidative carboxylation of unsaturated fatty acid methyl esters reported in literature.

2.2.5 Experimental section

2.2.5.1 General

All chemicals (1-decene, 1-hexene, 1-hexadecene, oleic acid, H_2O_2 (39% w/w), trioctylamine, dimethylcarbonate (DMC), ethyl acetate, diethyl ether, mesitylene, phosphoric acid (>99% purity), tetrabutylammonium bromide, tetrabutylammonium chloride, tetrabutylammonium iodine, sodium chloride, sodium bromide, sodium iodine, potassium chloride, potassium bromide, potassium iodide, deuterated chloroform were purchased from Aldrich and used as received. Styrene was purchased from Aldrich and distilled before use.

GC-MS (EI, 70 eV) analyses were run using a capillary column (L=30 m, Ø=0.32 mm, film thickness=1.8 µm). The following conditions were used. The following conditions were used. Carrier gas: He; flow rate: 1.2 mL min^{-1}; split ratio: 100:1; initial T: 100 °C (2 min), ramp rate: 20 °C min^{-1} to 240 °C; (10 min). ^1H, $^{13}C\{1H\}$, ^{31}P NMR and ^{183}W NMR spectra were recorded on a Bruker 400 MHz (^1H: 400 MHz; ^{13}C: 100 MHz) spectrometer.

Conversions, yields and selectivity were calculated by GC analysis by using mesitylene as internal standard. Tests were repeated at least two times to ensure reproducibility: conversion of substrate and products distribution differed by less than 3% from one experiment to another repeated. Peroxide titration tests were performed according to literature procedure.[50]

2.2.5.2 Synthesis of catalysts

Synthesis of trioctylmethylammonium methylcarbonate

Trioctylmethyl ammonium methylcarbonate ($[N_{8,8,8,1}]CH_3OCOO$), was synthesized based on a procedure previously reported by our research group.[51] Briefly trioctylamine (20 mL, 16.2 g, 45.7 mmol), DMC (30

mL, 32.1 g, 356 mmol) and methanol (20 mL) were combined (two phases) in a sealed 200 mL steel autoclave fitted with a pressure gauge and a thermocouple for temperature control. Three vacuum-nitrogen cycles were carried out to ensure complete removal of air. The empty volume was then filled with nitrogen. The autoclave was heated for 20 h at 140°C with magnetic stirring, after which time it was cooled and vented. Methanol and residual DMC were removed from the mixture by rotary evaporation to give $[N_{8,8,8,1}][CH3OCOO]$ (20.0 g, 99%) as a viscous clear pale yellow liquid. The ionic liquid was characterized through ^{1}H NMR and ^{13}C NMR (see appendix, Figure A.2.16-17)

Synthesis of trioctylmethylammonium tungstate ($[N_{8,8,8,1}]_2[WO_4]$) via the methylcarbonate precursor.

H_2WO_4 (0.28g, 1.1 mmol) was slowly added to an aqueous solution of $[N_{8,8,8,1}][CH_3OCOO]$ (0.83g, 1.86 mmol) heated at 50 °C. The solution was stirred for 3h during which time the initial opalescent solution turned yellow. The solution was cooled, and ethyl acetate was added to extract $[N_{8,8,8,1}]_2[WO_4]$. The product ionic liquid (0.78 g, 0.79 mmol, yield=86%) was characterized by FT-IR, ^{1}H-NMR, ^{13}C-NMR and ^{183}W-NMR and data are reported in the appendix (Figure A.2.6, A.2.18-19, A.2.35).

2.2.5.3 Catalytic experiments

Typical procedure for the epoxidation reaction

$(N_{8,8,8,1})_2(WO_4)$ (1.25-5% mol respect to the substrate **1**), hydrogen peroxide (30% w/w_{H2O}, 1-6 eq.), mesitylene as internal standard (10% $w/w_{substrate}$) and – where applicable – an acid co-catalyst (0-5% mol respect to the substrate) were charged into a tubular glass reactor equipped with a magnetic stirrer. The mixture was stirred for 1 minutes and 1-decene (**1**, 4 mmol, 1 eq) was added into the glass tube. The reactor was heated at the selected temperature (T=25-95°C) and the mixture stirred at 800 rpm. At chosen intervals, an aliquot of the reaction mixture was whitdrawn and eluted with Et_2O in a Pasteur tube in which it was placed a piece of cotton and 2-3 cm of silica in order to separate the catalyst and extract the organic compounds. Any aliquot was analyzed by GC-MS to calculate conversion, selectivity and yield.

Typical procedure for CO_2 fixation reaction

1-decene oxide (**2a**, 4 mmol, 1 eq), $(N_{8,8,8,1})_2(WO_4)$ (2.5% mol), mesitylene as internal standard (10% w/w substrate) and – where applicable – H_3PO_4 (0-1.25% mol) and $[N_{4,4,4,4}]Br$ (0-2.5% mol), were charged in a tubular glass reactor equipped with a magnetic stirrer and closed with a perforated cap that allows the gas entrance and block the leakage of liquids. The glass reactor was placed inside a 100-ml stainless steel autoclave that was sealed, degassed via two vacuum-CO_2 cycles and pressurized with 50 bar of CO_2. The autoclave was then electrically heated at 85°C and the reaction was magnetically stirred for 8 hours. At the end of each run, the autoclave was rapidly cooled in an ice bath and vented, and the final mixture was analyzed by GC-MS to calculate conversion, yield and selectivity. The organic phase was finally extracted with Et_2O and washed several times with water.

Typical procedure for the one-pot reaction conducted with an auto tandem catalysis approach

1-decene (**1**, 4 mmol) $(N_{8,8,8,1})_2(WO_4)$ (2.5 % mol), hydrogen peroxide (30% w/w, 2 equivalent respect to the substrate), , H_3PO_4 (1.25% mol) mesitylene as internal standard (10% w/w substrate) and – when applicable – $[N_{4,4,4,4}]Br$ (2.5% mol) were charged into a tubular glass reactor equipped with a magnetic stirrer and closed with a perforated cap. The reactor was placed inside a 100-ml stainless steel autoclave

that was sealed, degassed via two vacuum-CO_2 cycles and pressurized with 50 bar of CO_2. The autoclave was then electrically heated at 85°C and the reaction was magnetically stirred for 3-18 hours. At the end of each run, the autoclave was rapidly cooled in an ice bath and vented, and the final mixture was analyzed by GC-MS to calculate conversion, yield and selectivity.

Typical procedure for the one-pot reaction conducted with an assisted tandem catalysis approach (CO_2 pressure= 10-50 bar)

$(N_{8,8,8,1})_2(WO_4)$ (2.5% mol respect to the substrate **1**), hydrogen peroxide (30% w/w_{H2O}, 1.2-4 equivalent respect to the substrate **1**), H_3PO_4 (1.25% mol), mesitylene as internal standard (10% $w/w_{substrate}$) were charged into a tubular glass reactor equipped with a magnetic stirrer. The mixture was stirred for 1 minute and 1-decene (**1**, 4 mmol, 1 equivalent) was added into the glass tube. The reactor was heated at 85°C and the mixture stirred at 800 rpm. After 3 hours the reaction was stopped and the selected halide co-catalyst (0.5-2.5% mol) was added top the reaction mixture. The tubular glass reactor was then closed with a perforated cap and it was placed inside a 100-ml stainless steel autoclave that was sealed, degassed via two vacuum-CO_2 cycles and pressurized with 10-50 bar of CO_2. The autoclave was then electrically heated at the selected temperature (70-100°C) and the reaction was magnetically stirred for 3-18 hours. At the end of each run, the autoclave was rapidly cooled in an ice bath and vented, and the final mixture was analyzed by GC-MS to calculate conversion, yield and selectivity.

Typical procedure for the one-pot reaction conducted with an assisted tandem catalysis approach (CO_2 pressure = 1 bar)

$(N_{8,8,8,1})_2(WO_4)$ (2.5% mol respect to the selected olefin), hydrogen peroxide (30% w/w_{H2O}, 2 equivalent respect to the selected olefin), H_3PO_4 (1.25% mol), mesitylene as internal standard (10% $w/w_{substrate}$) were charged into a tubular glass reactor equipped with a magnetic stirrer. The mixture was stirred for 1 minute and the selected olefin (4 mmol, 1 equivalent) was added into the glass tube. The reactor was heated at 85°C and the mixture stirred at 800 rpm. After 3 hours the reaction was stopped and the selected halide co-catalyst (1.25% mol) was added to the reaction mixture. The reactor was degassed via three vacuum-CO_2 cycles and a rubber reservoir containing about 2l of CO_2 was connected to the reactor. The reaction vessel was sealed to prevent losses of substrates and/or CO_2 and stirred at 85 °C for 5h. At the end of the reactione an aliquot of the reaction mixture was analysed by GC to determine substrate conversion, selectivity and yield.

Typical procedure for the epoxidation of methyl oleate

In a typical procedure, a 50-mL round-bottomed flask equipped with a condenser was charged with methyl oleate (**1g**, 500mg, 1.67 mmol), H_2O_2 (30% w/w, 1-4 equiv.), mesitylene as internal standard (10% w/w of the substrate) and $[N_{8,8,8,1}]_2WO_4$ (2.5-5% mol). The reaction was then performed at 75°C for 4 hours, by heating the mixture under magnetic stirring (1000 rpm). At intervals of one hour, the mixture was sampled and analyzed by ^{1}H-NMR. The described procedure was also used to explore the addition of 2.5% mol of H_3PO_4. An additional test was also performed at 75 °C in the absence of any catalyst by using 2 equiv. of H_2O_2.

Typical procedure for the CO_2 fixation reaction into epoxidized methyl oleate (2g)

In a typical procedure, a stainless steel autoclave with an internal volume of 200 mL, equipped with a pressure gauge, a thermocouple and two valves, was charged with a mixture of epoxidized methyl oleate (**2g**, 1.67 mmol), $[N_{8,8,8,1}]_2WO_4$ (5% mol) and eventually $[N_{4,4,4,4}]Br$ (2.5% mol). The autoclave was purged at room temperature by three vacuum-CO_2 purge cycles and pressurized with CO_2 (50 bar). The autoclave was then heated at 100°C and the reaction was magnetically stirred (1000rpm) for the desired time (16h). The autogenous pressure was 70 bar. After 16 hours, the autoclave was cooled, slowly vented, and opened. The mixture was then sampled and analyzed by ^{1}H-NMR.

Typical procedure for the direct oxidative carboxylation of methyl oleate (1g)

In a typical procedure, a 50-mL round-bottomed flask equipped with a condenser was charged with methyl oleate (**1g**, 1.67 mmol), H_2O_2 (30% w/w, 2 equiv.), mesitylene as internal standard (10% w/w of the substrate) and the catalyst $[N_{8,8,8,1}]_2WO_4$ (5% mol). The reaction was then performed at 75°C, by heating the mixture under magnetic stirring (1000 rpm) for 4 hours. Once the reaction reached a complete conversion, the biphasic solution was allowed to cool at room temperature and 2.5% mol of an halide source (Q^+X^-, Q= $[N_{4,4,4,4}]$, Na, K; X^-= Cl^-, Br^-, I^-) was added as co-catalyst. The round-bottom glass flask was fitted inside a stainless steel autoclave (internal volume: 200 mL) equipped with a pressure gauge, a thermocouple and two valves. The autoclave was purged at room temperature by three vacuum-CO_2 purge cycles and pressurized with CO_2 (50 bar). The autoclave was then heated at 100°C and the reaction was magnetically stirred (1000rpm) for 16 hours. The autogenous pressure was 70 bar. After 16 hours, the autoclave was cooled, vented, and opened. The mixture was then sampled and analyzed by ^{1}H-NMR.

^{31}P NMR test

H_3PO_4 (4.9 mg, 0.05 mmol, the same amount used in the optimized catalytic tests) was added in an NMR tube with 0.3 ml of D_2O and a ^{31}P NMR spectra was recorded. Then, a large excess of H_2O_2 (30% w/w, ≈ 0.5 ml) was added inside the tube that was heated at 50°C for 30 minutes, after that another ^{31}P NMR spectra was recorded. Finally, $[N_{8,8,8,1}]_2[WO]_4$ (94.0 mg, the same amount used in the optimized catalytic test) was added, the tube was heated again at 50°C for 30 minutes and a last ^{31}P NMR spectra was recorded to reveal the formation of new peroxophosphotungstate species.

Test for the scalability of 1-decene epoxidation

$(N_{8,8,8,1})_2(WO_4)$ (2.5% mol respect to the substrate **1**), hydrogen peroxide (30% w/w_{H2O}, 2 equivalents), and H_3PO_4 as co-catalyst (1.25% mol respect to the substrate) were charged into a round-bottomed flask equipped with a magnetic stirrer and a condenser. The mixture was stirred for 1 minutes and 1-decene (**1**, 10 g, 71.4 mmol) was slowly added into the flask. The mixture was heated at 50°C and stirred at 800 rpm for 24 hours. At the end of the reaction, the organic phase was separated and passed through a short plug of silica with diethyl ether as solvent in order to separate any trace of the catalyst. The organic phase was then concentrated under reduced pressure (60°C, 10 mbar) and 1-decene oxide was obtained with a 88% yield (9.82 g, 62.8 mmol, >97% purity according to GC analysis and ^{1}H NMR).

Test for the scalability of the direct oxidative carboxylation of 1-decene

$(N_{8,8,8,1})_2(WO_4)$ (2.5% mol respect to the substrate **1**), hydrogen peroxide (30% w/w_{H2O}, 2 equivalents), and H_3PO_4 as co-catalyst (1.25% mol respect to the substrate) were charged into a two-neck round-bottomed flask equipped with a magnetic stirrer and a condenser. The mixture was stirred for 1 minutes and 1-decene (**1**, 10 g, 71.4 mmol) was slowly added into the flask. The mixture was heated at 85°C and stirred at 800 rpm. After 3 hours, the reaction was stopped, $[N_{4,4,4,4}]I$ (1.25% mol) was added, the flask was degassed via three vaccum-CO_2 cycles and a rubber reservoir containing about 2l of CO_2 was connected to the flask. The reaction was conducted at 85°C for additional 5 hours. At the end of the reaction, the organic phase was separated and a flash column chromatography with petroleum ether:ethyl acetate 9:1 was performed to obtain an 86% isolated yield of decylene carbonate (12.28 g, 61.4 mmol, >98% purity according to GC analysis and ^1H NMR).

2.2.6 References

[1] C. Venturello, E. Alneri, M. Ricci, *The Journal of Organic Chemistry*, 1983, **48**, 3831-3833; (b) C. Venturello, R. D'Aloisio, *The Journal of Organic Chemistry*, 1988, **53**, 1553-1557; (c) Y. Ishii, Y. Sakata, *The Journal of Organic Chemistry*, 1990, **55** 5545-5547, (d) S. Sakaguchi, Y. Nishiyama, Y. Ishii, *The Journal of Organic Chemistry*, 1996, **61**, 5307-5311

[2] L.H. Pottenger, D.R. Boverhof, J.M. Waechter Jr, *Patty's Toxicology*, **2001**, 425-490.

[3] D.E. Fogg, E.N. dos Santos, *Coordination chemistry reviews*, 2004, **248**, 2365-2379.

[4] S. Abou-Shehada, J.M. Williams, *Nature chemistry*, 2014, **6**, 12-13.

[5] R. Calmanti, M. Selva and A. Perosa, Green Chem., 2021, **23**, 1921-1941.

[6] (a) S.T. Oyama, Rates, kinetics, and mechanisms of epoxidation: homogeneous, heterogeneous, and biological routes, in: *Mechanisms in homogeneous and heterogeneous epoxidation catalysis*, Elsevier, 2008, pp. 3-99; (b) S.A. Hauser, M. Cokoja, F.E. Kühn, *Catalysis Science & Technology*, 2013, **3**, 552-561.

[7] https://reagents.acsgcipr.org/reagent-guides/epoxidation/venn-diagram last accessed on 12/12/2020

[8] M. Costas, Green Oxidation in Organic Synthesis, 2019, 123-157.

[9] N. Eghbali, C.-J. Li, *Green Chemistry*, 2007, **9**, 213-215.

[10] J.-L. Wang, J.-Q. Wang, L.-N. He, X.-Y. Dou, F. Wu, *Green Chemistry*, 2008, **10**, 1218-1223.

[11] L.D. Dias, R.M. Carrilho, C.A. Henriques, M.J. Calvete, A.M. Masdeu-Bultó, C. Claver, L.M. Rossi, M.M. Pereira, *ChemCatChem*, 2018, **10**, 2792-2803.

[12] A.A. Sathe, A.M. Nambiar, R.M. Rioux*, Catalysis Science & Technology*, 2017, **7**, 84-89.

[13] T. Kimura, K. Kamata, N. Mizuno, *Angewandte Chemie International Edition*, 2012, **51**, 6700-6703.

[14] R. Calmanti, M. Selva, A. Perosa, *Molecular Catalysis*, 2020, **48**, 110854.

[15] J. Clayden, N. Greeves, S. Warren and P. Wothers, *Organic chemistry*, Oxford university press Oxford, 2014.

[16] F. Castro-Gómez, G. Salassa, A. W. Kleij and C. Bo, *Chemistry–A European Journal*, 2013, **19**, 6289-6298.

[17] H. Adolfsson, Transition metal-catalyzed epoxidation of alkenes in *Modern Oxidation Methods*, Wiley-VCH, 2010.

[18] (a) K. Sato, M. Aoki, M. Ogawa, T. Hashimoto, R. Noyori, *The Journal of organic chemistry*, 1996, **61**, 8310-8311; (b) Mahha, L. Salles, J.-Y. Piquemal, E. Briot, A. Atlamsani, J.-M. Brégeault, *Journal of Catalysis*, 2007, **249**, 338-348.

[19] (a) Q. Wang, X. Zhang, L. Wang, Z. Mi*, Journal of Molecular Catalysis A: Chemical*, 2009, **309**, 89-94; (b) M.-L. Wang, T.-H. Huang, W.-T. Wu, *Chemical Engineering Communications*, 2004, **191**, 27-46.

[20] In this reaction conditions [**1** (4 mmol), H_2O_2 (2 eq.), $[N_{8,8,8,1}]_2[WO_4]$ (2.5% mol), H_3PO_4 (1.25% mol) T = 95°C], the test was repeated and stopped after 2 hours: peroxide titration tests on the aqueous phase with $KMnO_4$ proved the absence of residual H_2O_2 in these experimental conditions.

[21] In this case $KMnO_4$ titration test showed the presence of residual hydrogen peroxide in the aqueous phase after 3h. The peroxide efficiency resulted to be 73% according to titration tests performed on three repeated reactions in the same experimental conditions [**1** (4 mmol), H_2O_2 (2 eq.), $[N_{8,8,8,1}]_2[WO_4]$ (5% mol), H_3PO_4 (2.5% mol) T = 85°C, 3h). This result suggested that after 3h (when the conversion of **1** was quantitative) ≈0.5 equivalents of H_2O_2 were still present. The reaction could be conducted with only 1.5 equiv. of H_2O_2 if this peroxide efficiency is confirmed. However, we decided to continue our investigation with 2 equiv. of H_2O_2 in order to work in a slight excess of the required oxidant to achieve complete conversion of the olefin in these reaction conditions.

[22] (a) W.B. Cunningham, J.D. Tibbetts, M. Hutchby, K.A. Maltby, M.G. Davidson, U. Hintermair, P. Plucinski, S.D. Bull, *Green Chemistry*, 2020, **12**, 513-524; (b) B.-J.K. Ahn, S. Kraft, X.S. Sun, *Journal of Materials Chemistry*, 2011, **21**, 9498-9505; (c) E. Santacesaria, R. Tesser, M. Di Serio, R. Turco, V. Russo, D. Verde, *Chemical Engineering Journal*, 2011, **173**, 198-209; (d) E. Poli, J.-M. Clacens, J. Barrault, Y. Pouilloux, *Catalysis Today*, 2009, **140**, 19-22; (e) Y. Ogata, Y. Sawaki, T*etrahedron*, 1964, **20**, 2065-2068.

[23] In particular the use of $FeCl_3$ or $CeCl_3$ took to a rapid exothermic Phenton-like reaction that forms oxygen radicals and degrades hydrogen peroxide that could not be active for the epoxidation of **1**. See for example: (a) J. De Laat, T.G. Le, *Applied Catalysis B: Environmental*, 2006, **66**, 137-146; (b) E.G. Heckert, S. Seal, W.T. Self, *Environmental science & technology*, 2008, **42**, 5014-5019.

[24] (a) C. Aubry, G. Chottard, N. Platzer, J.M. Bregeault, R. Thouvenot, F. Chauveau, C. Huet, H. Ledon, *Inorganic Chemistry*, 1991, **30** 4409-4415; (b) L. Salles, C. Aubry, R. Thouvenot, F. Robert, C. Doremieux-Morin, G. Chottard, H. Ledon, Y. Jeannin, J.M. Bregeault, Inorganic Chemistry, 1994, **33**, 871-878; (c) D.C. Duncan, R.C. Chambers, E. Hecht, C.L. Hill, *Journal of the American Chemical Society*, 1995, **117** 681-691.

[25] (a) B. Sels, D. De Vos, M. Buntinx, F. Pierard, A. Kirsch-De Mesmaeker, P. Jacobs, *Nature*, 1999, **400**, 855-857; (b) U. Bora, G. Bose, M.K. Chaudhuri, S.S. Dhar, R. Gopinath, A.T. Khan, B.K. Patel, *Organic Letters*, 2000, **2**, 247-249; (c) B. Ganchegui, W. Leitner, *Green Chemistry*, 2007, **9**, 26-29; (d) A. Podgoršek, M. Zupan, J. Iskra, *Angewandte Chemie International Edition*, 2009, **48**, 8424-8450; (e) F. Mendoza, R. Ruíz-Guerrero, C. Hernández-Fuentes, P. Molina, M. Norzagaray-Campos, E. Reguera, *Tetrahedron Letters*, 2016, **57**, 5644-5648.

[26] Not a complete conversion was achievable also by prolonging the time, due to absence of residual H_2O_2 proved by peroxide titration test

[27] (a) J. Wang, Y. Zhang, *ACS Catalysis,* 2016, **6**, 4871-4876; (b) Y.A. Alassmy, P.P. Pescarmona, *ChemSusChe*m, 2019, **12**, 3856-3863.; (c) Y. Alassmy, Z. Asgar Pour, P.P. Pescarmona, *ACS Sustainable Chemistry & Engineering*, 2020, **21**, 7993-8003.

[28] (a) D. Hâncu, J. Green, E.J. Beckman, *Industrial & engineering chemistry research*, 2002, **41**, 4466-4474; (b) Nolen, J. Lu, J.S. Brown, P. Pollet, B.C. Eason, K.N. Griffith, R. Gläser, D. Bush, D.R. Lamb, C.L. Liotta, *Industrial & engineering chemistry research*, 2002, **41**, 316-323.

[29] F. Chen, T. Dong, T. Xu, X. Li, C. Hu, *Green Chemistry*, 2011, **13**, 2518-2524.

[30] (a) F.D. Bobbink, D. Vasilyev, M. Hulla, S. Chamam, F. Menoud, G.b. Laurenczy, S. Katsyuba, P.J. Dyson, *ACS Catalysis*, 2018, **8**, 2589-2594; (b) P. Yingcharoen, C. Kongtes, S. Arayachukiat, K. Suvarnapunya, S.V. Vummaleti, S. Wannakao, L. Cavallo, A. Poater, V. D'Elia, *Advanced Synthesis & Catalysis*, 2019, **361**, 366-373.

[31] (a) P.T. Nguyen, H.T. Nguyen, H.N. Nguyen, C.A. Trickett, Q.T. Ton, E. Gutiérrez-Puebla, M.A. Monge, K.E. Cordova, F. Gándara, *ACS applied materials & interfaces*, 2018, **10**, 733-744; (b) H.T. Nguyen, Y. Tran, H.N. Nguyen, T.C. Nguyen, F. Gándara, P.T. Nguyen*, Inorganic chemistry*, 2018, **57**, 13772-13782; (c) H.-G. Jin, F. Chen, H. Zhang, W. Xu, Y. Wang, J. Fan, Z.-S. Chao, *Journal of Materials Science*, 2020, **2**, 1-13; (d) J. Fang, K. Li, Z. Wang, D. Li, Y. Ma, X. Gong, Z. Hou*, Journal of CO2 Utilization*, 2020, **40**, 101204.

[32] We want to note here that our halide-free synthesis to obtain trioctyl methyl ammonium tungstate (with the use of only water as solvent and ethyl acetate for the extraction of the ionic liquid) is greener that the routes previously reported in literature for the synthesis of tungstate, polioxotungstate, peroxotungstate and phosphotungstate compounds; see for example references 1, 13, 18, 19, 24.

[33] (a) C. Martin, G. Fiorani, A.W. Kleij, *Acs Catalysis*, 2015, **5** 1353-1370; (b) J.W. Comerford, I.D. Ingram, M. North, X. Wu, *Green Chemistry*, 2015, **17**, 1966-1987.

[34] H. Yasuda, L.-N. He, T. Sakakura and C. Hu, *Journal of Catalysis*, 2005, **233**, 119-122.

[35] U. Schuchardt, D. Cardoso, R. Sercheli, R. Pereira, R. S. Da Cruz, M. C. Guerreiro, D. Mandelli, E. V. Spinacé and E. L. Pires, *Applied Catalysis A: General*, 2001, **211**, 1-17.

[36] M. R. Maurya, M. Kumar and S. Sikarwar, *Reactive and Functional Polymers*, 2006, **66**, 808-818.

[37] (a) W. Natongchai, S. Pornpraprom and V. D'Elia, *Asian Journal of Organic Chemistry*, 2020, **9**, 801-810; (b) T. Cai, J. Liu, H. Cao and C. Cui, *Industrial Crops and Products*, 2020, **145**, 112155; (c) F. Chen, Q.-C. Zhang, D. Wei, Q. Bu, B. Dai and N. Liu, *The Journal of organic chemistry*, 2019, **84**, 11407-11416; (d) L. P. Carrodeguas, À. Cristòfol, J. M. Fraile, J. A. Mayoral, V. Dorado, C. I. Herrerías and A. Kleij, *Green Chemistry*, 2017, **19**, 3535-3541; (e) N. Tenhumberg, H. Büttner, B. Schäffner, D. Kruse, M. Blumenstein and T. Werner, *Green Chemistry*, 2016, **18**, 3775-3788; (f) L. Longwitz, J. Steinbauer, A. Spannenberg and T. Werner, *ACS Catalysis*, 2018, **8**, 665-672.

[38] Methyl oleate is synthesized starting from oleic acid through a literature procedure reported in the experimental part.

[39] Epoxidation is stereospecific, hence the cis-olefin gives only the cis-epoxide

[40] H_2O_2 titration test showed the complete disappearance of hydrogen peroxide after the completion of the reaction (75°C, 4h). This suggested an overall 50% efficiency of hydrogen peroxide in these experimental conditions.

[41] (a) M. F. M. G. Resul, A. M. L. Fernández, A. Rehman and A. P. Harvey, *Reaction Chemistry & Engineering*, 2018, **3**, 747-756; (b) M.-L. Wang and T.-H. Huang, *Industrial & engineering chemistry research*, 2004, **43**, 675-681.

[42] N. Mizuno, K. Yamaguchi and K. Kamata, *Coordination chemistry reviews*, 2005, **249**, 1944-1956.

[43] A. Chen, C. Chen, Y. Xiu, X. Liu, J. Chen, L. Guo, R. Zhang and Z. Hou, *Green Chemistry*, 2015, **17**, 1842-1852.

[44] (a) J.-H. Chen, C.-H. Deng, S. Fang, J.-G. Ma and P. Cheng, *Green Chemistry*, 2018, **20**, 989-996; (b) Z. Shi, G. Niu, Q. Han, X. Shi and M. Li, *Molecular Catalysis*, 2018, **461**, 10-18.

[45] (a) A. Coletti, C. J. Whiteoak, V. Conte and A. W. Kleij, *ChemCatChem*, 2012, **4**, 1190-1196; (b) X. Jiang, M. Fu, F. Wu, H. Zhang and Q. He, *Science of Advanced Materials*, 2019, **11**, 1140-1145.

[46] J. Fernández-Baeza, L. F. Sánchez-Barba, A. Lara-Sánchez, S. Sobrino, J. Martínez-Ferrer, A. Garcés, M. Navarro and A. M. Rodríguez, *Inorganic Chemistry*, 2020, **59**, 12422-12430; (b)

[47] J. Langanke, L. Greiner and W. Leitner, *Green chemistry*, 2013, **15**, 1173-1182.

[48] G. Rokicki, W. Kuran, B. Pogorzelska-Marciniak, *Monatsh. Chem*. 1984, **115**, 205–214; (b) J. Tharun, G. Mathai, A. C. Kathalikkattil, R. Roshan, J.-Y. Kwak, D.-W. Park, *Green Chemistry,* 2013, **15**, 1673–1677; (c) S. Kaneko, S. Shirakawa, *ACS Sustainable Chemistry & Engineering*, 2017, **5**, 2836–2840.

[49] A test of the CO_2 fixation into **2g** in presence of NaI (5% mol) in the same conditions reported in table 2.9 confirmed no conversion of the substrate in these conditions.

[50] G.H. Jeffrey, J. Basset, J. Mendham and R. C. Denney, *Vogel's textbook of quantitative chemical analysis*, John Wiley & Sons, 1989.

[51] M. Fabris, V. Lucchini, M. Noè, A. Perosa and M. Selva, *Chemistry–A European Journal*, 2009, **15**, 12273-12282.

2.3 DEG/NaBr catalyzed CO_2 insertion into terminal epoxides: from batch to continuous flow

2.3.1 Introduction

The catalytic system based on TILCs reported in the previous two sections (paragraph 2.1 and 2.2) resulted an optimum protocol in batch conditions but its application in continuous-flow (CF) reactors is hard to implement: one potential route to reach this scope is the immobilization of ionic liquids onto silica supports as recently reported in literature for CO_2 fixation into epoxides.[1] However, issues related to the miscibility of a biphasic system in CF coupled with the concurrent reaction with gaseous carbon dioxide and the potential leaching of active species during continuous-flow reactions (in particular for immobilized ionic liquids and transition metal catalysts)[2] make this project very challenging. These reasons coupled with international mobility problems related to the COVID-19 outbreak forced us not to explore this fascinating route and focus our attention into other commercial catalytic system for the CO_2 fixation into epoxides in CF reactors.

The synthesis of COCs through CO_2 fixation in CF processes is not trivial, as reported in a recent review on the argument by Jamison et al. This statement can be confirmed from the scarcity of the published papers (≈ 20) on this topic, especially if compared to the large amount of papers published yearly on COCs through batch processes.[3] One of the first CF-examples described a Co^{II}-salen complex immobilized on MCM-41 silica gel: at T = 110 °C, $p(CO_2)$ = 125 bar and flow (F) = 10-20 mL·h^{-1}, in the presence of tetrabutylammonium bromide ([$N_{4,4,4,4}$Br]) as a co-catalyst, ethylene oxide (EO) was converted up to 86% into ethylene carbonate (EC) with > 99 % selectivity.[4] Another approach proposed a Zn-based imidazolium ionic liquid ([AeMIM][Zn_2Br_5]) supported on MCM-22 molecular sieves, to obtain propylene carbonate (PC) from propylene oxide (PO). A steady PC yield of 62% was reported after > 50 h of time-on-stream, at T = 130 °C, $p(CO_2)$ = 20 bar, LHSV = 0.75 h^{-1} employing a molar ratio CO_2/PO = 3.[5] An Al^{III}-salen complex modified with (diethylbenzyl)ammonium bromide immobilized on amorphous silica proved effective for the first continuous-flow synthesis of EC designed for using waste CO_2 originated for example, in the exhaust stream of a fossil fuel power station. At T = 150 °C, when a binary mixture of N_2 and CO_2 at a total flow rate of 4.7 mL min^{-1}, was allowed to pass through (pressurized) liquid EO, 57% of the carbon dioxide was converted into ethylene carbonate, with a TOF of 7.6 h^{-1}.[6] More recently, CF CO_2 insertion was performed in a tube-in-tube gas-liquid reactor comprised of a CO_2 permeable inner coil continuously fed by styrene oxide (SO) and a mixture of tetrabutylammonium bromide and zinc bromide ([$N_{4,4,4,4}$Br]/$ZnBr_2$ as a homogeneous catalyst), surrounded by an external jacket pressurized with CO_2: this configuration allowed a quantitative SO conversion under relatively mild conditions (T = 120 °C, $p(CO_2)$ = 6 bar).[7] Heterogeneous catalytic systems based on d-block metal catalysts were also employed for CO_2 insertion in CF conditions. For instance, $NbCl_5$ and the ionic liquid 1-hydroxypropyl-3-n-butylimidazolium chloride, supported on protonated carboxymethylcellulose (HBimCl-$NbCl_5$/HCMC), were tested as catalysts for CO_2 insertion in a library of epoxides at T = 130 °C and $p(CO_2)$ = 15 bar (6 examples, yields=68 - 99%).[8] In another recent work, a metal-organic framework modified with Sc [MOF MIL-101(Sc)] was active for the conversion of PO to PC in up to 57 % yield, using chlorobenzene as a solvent at T = 100 °C and $p(CO_2)$ = 5 bar.[9]

On the other hand, catalytic systems based on salts/complexes of alkali and alkaline earth metals have been scarcely investigated for the preparation of COCs. One of the few available studies reported a Cs-P-Si fixed bed reactor which, albeit active for the transformation of propylene oxide (PO) to propylene carbonate (T = 200 °C, $p(CO_2)$ = 140 bar, PO/CO_2 at flow = 0.2 mL·min^{-1}, conversions up to 81%), showed extensive catalyst leaching with complete deactivation after 5 h.[10] Other strategies to carry out CO_2 insertion into terminal epoxides over alkali/alkaline earth metal-based catalysts were limited only to batch conditions. Typically, reactions were

performed in homogenous conditions in the presence of co-catalysts acting as both hydrogen bond donor and cation coordinating agents,[11] *e. g.* glycols, crown ethers and polyethers,[12] which were also necessary to overcome the well-known solubility issues of metal salts in epoxides/organic solvents. For example, a system comprised of KBr embedded in polyethylene glycol 400 (PEG400) was reported for the conversion of a library of epoxides (13 examples) into the corresponding carbonates with yields > 90 % in all cases.[13] More recently, in a similar fashion, CaI_2 in combination with poly(ethyleneglycol) dimethyl ether (PEG DME 500) proved effective towards CO_2 insertion into both terminal and internal epoxides: at T = 25-90 °C and $p(CO_2)$ of 10-50 bar, the corresponding COCs (27 examples) were obtained in variable yields from 51 to 99%. The catalytic system was then further optimized using PEG400 dimethyl ether as a complexing agent, allowing a scaling up of the CO_2 insertion reaction starting from 10 g of reacting epoxides.[14,15]

2.3.2 Aim and summary of the work.

In light of the results above mentioned, we were prompted to investigate whether mixtures of organic ligands based on oligo- and poly-glycols and alkali/alkaline earth metal halides, could be used for the preparation of COCs in CF mode. This was a substantially unexplored area with major challenges associated to the control of the viscosity of the complexing agent and the design of a liquid/gas biphasic system able to ensure reactants/catalyst miscibility and suitable contact time for the process. We report here that CO_2 insertion in model epoxides succeeded by using a diethylene glycol (DEG)/NaBr catalytic system. DEG was chosen as a model hydrogen bond donor moiety due to its ability to coordinate Na^+ cations. An initial screening on the effects of reaction parameters in batch conditions allowed to confirm the suitability of the catalytic system towards CO_2 fixation with mild reaction conditions (100°C, 3h, 1-40 bar of CO_2). Then the reaction was implemented in the continuous mode by making a homogenous mixture of DEG, NaBr and the selected epoxide flow through a capillary steel column (the CF-reactor), under controlled flow/pressure of CO_2. At T= 140 - 220 °C and $p(CO_2)$ = 120 bar, conversions of the tested epoxides ranged from 75 to > 99 %, and the corresponding COCs were achieved with selectivity up to 93 %. The CF-setup proved robust and flexible since the products were separated by continuous extraction at the reactor outlet, while the (homogenous) catalyst as a DEG/NaBr mixture was recovered and reused**.**

2.3.3 Results and discussion

2.3.3.1 Batch conditions

Choice of cation complexing agent (co-catalyst). The insertion of CO_2 into styrene oxide (**1a**) was chosen as a model reaction, in the presence of NaBr as the catalyst and different glycols and alcohols as co-catalysts/complexing agents in batch conditions. Diethylene glycol (DEG), diethylene glycol dimethyl ether (DEGDME), 1-hexanol and 1,6-hexanediol were tested. With the aim to preliminarily explore the effects of reaction parameters, a 200 mL steel pressure vessel was charged with a homogenous solution of **1a** (0.4 g, 3.33 mmol), NaBr and the selected glycol in **1a**/NaBr/glycol 1:0.1:0.3 molar ratio. The mixture was heated at 50-100 °C, under 40 bar of CO_2 with magnetic stirring. Results are summarized in Table 2.11. that shows the conversion of **1a** and the yield of styrene carbonate (**2a**: 4-phenyl-1,3-dioxolan-2-one) after 5 h. Hexanol, 1,6-hexanediol and the methyl capped-glycol (DEGDME) offered poor conversions not exceeding 12, 14 and 3 % at T = 100 °C, respectively (Entries 1-3). By contrast, quantitative and exclusive formation of **2a** was achieved when DEG was used as a co-catalyst (entry 6). Diethylene glycol proved active even at temperatures between 50 and 70 °C, albeit with lower conversions (21 and 62%, respectively: entries 4-5). These experiments demonstrated the superior performance of DEG suggesting that its structure was particularly suited for the complexation of Na^+ and

consequent activation of bromide and of the reactant epoxide. To the best of our knowledge, the use of DEG/NaBr was an unprecedented combination to promote CO_2 insertion reactions.

Table 2.11: CO_2 insertion in SO catalyzed by NaBr/glycol: effects of the co-catalyst and the temperature under batch conditions

Entry	Co-catalyst	T (°C)	Yield [a],[b]
1	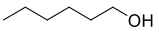 1-hexanol	100	12
2	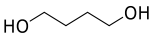 1,6-hexanediol	100	14
3	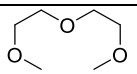 DEGDME	100	3
4	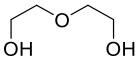 DEG	50	22
5		75	63
6		100	99

All reactions were carried out for t = 5 h in an autoclave charged with a mixture of SO (3.33 mmol), NaBr and the co-catalyst in a 1:0.1:0.3 molar ratio, respectively. [a] Yields were determined by GC using mesitylene (10 % mol) as an internal standard. [b] Selectivity were always > 99% according to GC and ^{1}H NMR analysis.

Effects of reaction time, reactant:catalyst molar ratio, and CO_2 pressure. A series of experiments was carried out at 100 °C by changing one at a time, the reaction parameters of Table 2.11, specifically by decreasing: i) the reaction time (t) from 5 to 3 and 2 h, respectively; ii) the **1a**:NaBr:DEG molar ratio (W) from 1:0.1:0.3 to 1:0.05-0.025:0.3 and then 1:0.1:0.2 and finally, in the absence of either DEG or NaBr; iii) the CO_2 pressure from 40 to 10, 2 and 1 bar. In the latter case (1 bar = atmospheric pressure), the reaction was carried out in a conventional glass flask (50 mL) equipped with a 2 L CO_2 reservoir. All reactions were run in duplicate for reproducibility ensuring <5% difference in conversion and selectivity between repeated tests. The results are reported in Table 2.12.

Compared to the 5 h tests of Table 2.11, 3 h were sufficient for quantitative reactions, while a slight decrease of the conversion (from 99 to 96%) was noticed after 2 h (Entries 1-3, Table 2.12). Further experiments were conducted on this basis (3 h). A pronounced effect, particularly on the extent of the **1a** conversion, was observed by varying the reactant/catalyst/DEG molar ratio. Indeed, when the catalyst (NaBr) was reduced from 10 to 5 mol% and then to 2.5 mol%, the conversion of the epoxide dropped from 99 to 62 and 20%, respectively (Entries 2, 4 and 5). This clearly indicated the role of the halide salt concentration in the process kinetics, pointing out how the bromide-mediated ring opening of the epoxide was the rate-determining step of the overall CO_2 insertion process. In line with this observation, decreasing the loading of the co-catalyst (DEG) from 30 to 20 mol % caused a reduction of the **1a** conversion, from 99 to 85%, (Entries 2 and 6) consistent with a lower bromide activation. In addition, DEG could assist the reaction through its hydrogen bond donor activity, making the epoxide ring cleavage easier (see later, Figure 2.22). The synergic action of the catalyst and the co-catalyst was unambiguously

proved by the tests in the absence of either NaBr or DEG where no reaction took place (Entries 7 and 8). Conditions investigated so far suggested that the best results were achieved using the mixture of **1a**, NaBr, and DEG in the W= 1:0.1:0.3 molar ratio, respectively. This W ratio was fixed to study the pressure effect. Experiments demonstrated that the reaction outcome was not affected neither by the pressure over the range 1-40 bar nor by the CO_2:epoxide molar ratio (see experimental part), wherein styrene oxide was quantitatively converted into styrene carbonate (Entries 9-11).

Table 2.12: CO_2 insertion into styrene oxide catalyzed by NaBr/DEG: effects of reaction time, reactant:catalyst molar ratio, and CO_2 pressure.

Entry	CO_2 (bar)	t (h)	1a:NaBr:DEG (mol/mol)	Yield [(a),(b)]
1	40	5	1:0.1:0.3	>99
2	40	3	1:0.1:0.3	>99
3	40	2	1:0.1:0.3	96
4	40	3	1:0.05:0.3	62
5	40	3	1:0.025:0.3	23
6	40	3	1:0.1:0.2	86
7	40	3	1:0:0.3	0
8	40	3	1:0.1:0	0
9	10	3	1:0.1:0.3	>99
10	2	3	1:0.1:0.3	>99
11	1	3	1:0.1:0.3	>99

All reactions were carried out at 100 °C, in an autoclave charged with a mixture of **1a** (3.33 mmol), NaBr and DEG in the reported molar ratio. [(a)] Yields were determined by GC using mesitylene (10 % mol) as an internal standard. [(a)] Selectivity were always > 99% according to GC and ^{1}H NMR analysis

A plausible mechanistic hypothesis for catalyst activation by DEG is shown in Figure 2.22: diethylene glycol plausibly played a double role acting as a chelating agent for Na^+ but also as a hydrogen bond donor (HBD) that assisted the ring-opening of the reactant epoxide. Both the complexing and HBD activity of polyethylene glycols are indeed widely reported. [13-15,16]

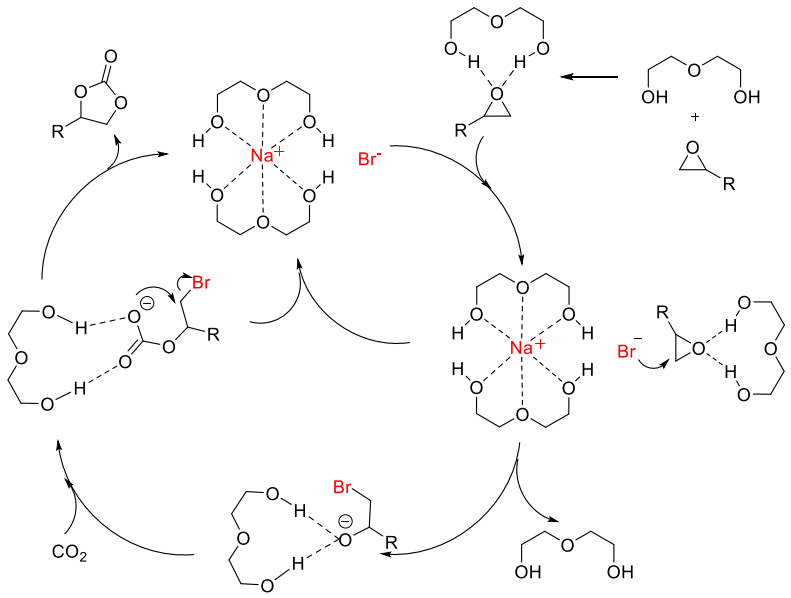

Figure 2.22: Proposed mechanism for the co-catalytic effect of DEG. Top, mid: the activation of NaBr; top-to-bottom, right: hydrogen bond donor assistance to the epoxide ring cleavage.

Substrate scope. Under the best conditions for the conversion of **1a** (Entries 2 and 11, Table 2.12), the activity of the NaBr/DEG binary mixture was tested for 6 other terminal epoxides including 1,2-epoxybutane (**1b**), 1,2-epoxyhexane (**1c**), 1,2-epoxydecane (**1d**), butyl glycidyl ether (**1e**), phenyl glycidyl ether (**1f**), and 1,4-butanediol diglycidyl ether (**1g**). Reactions were carried out at T = 100 °C for t = 3 h, using a solution of the epoxide, NaBr, and DEG in a 1:0.1:0.3 molar ratio, respectively. Experiments were performed at high and low CO_2 pressure (40 bar and atmospheric pressure). All the tested epoxides were quantitively and selectively converted into the corresponding COCs (**2b-g**), (Scheme 2.2), thereby confirming that: i) the batch protocol could be extended to a range of different terminal epoxides; ii) CO_2 insertion reactions were not substantially affected by the CO_2 pressure and the CO_2:epoxide molar ratio (see experimental part). In the case of the di-epoxide **1g**, the bis-cyclic carbonate **2g** was obtained.

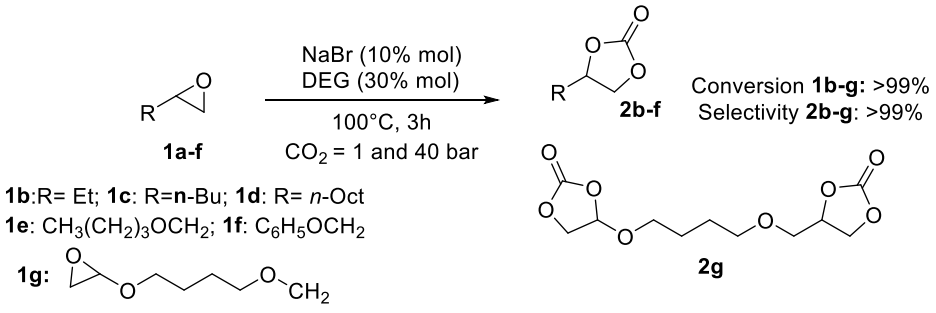

Scheme 2.2: NaBr/DEG catalyzed CO_2 insertion in terminal epoxides: substrate scope. Conversion and selectivity were determined by GC in the presence of mesitylene as internal standard.

The batch protocol was also examined using the internal epoxide of methyl oleate, *i.e.* methyl 8-(3-octyloxiran-2-yl) octanoate (**1h**) in its pure diastereomeric cis form.[17] Under the conditions of Scheme 2.3, the reaction

conversion was 66% and the selectivity to the carbonate derivative, methyl 8-(5-octyl-2-oxo-1,3-dioxolan-4-yl) octanoate (**2h**), was 50% (60:40 cis/trans). The only observed by-product (16%) was methyl 9-oxooctadecanoate coming from a Meinwald rearrangement of the starting epoxide. [18]

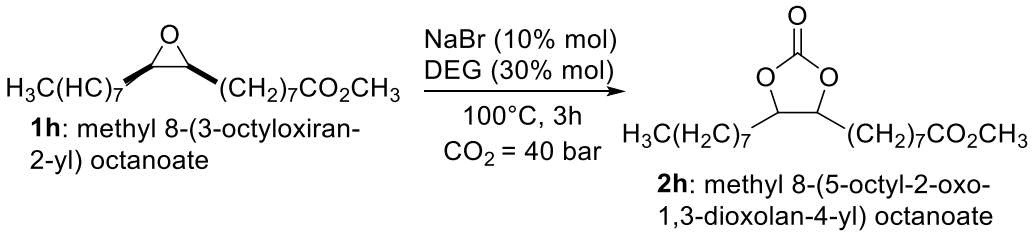

*Scheme 2.3: NaBr/DEG catalyzed CO_2 insertion in the internal epoxide **1h**. Conversion and selectivity were determined by ^1H NMR in the presence of mesitylene as internal standard.*

As widely reported in the literature, it is reasonable to assume that both S_N1 and S_N2 mechanisms can take place in the ring-closure to yield the cyclic carbonate species, accounting for the presence of the carbonate **2h** product in a 60:40 cis/trans mixture.[18,19]

CO_2 insertion under batch conditions: solvent choice. Finally, the identification of a liquid carrier (solvent) to achieve a homogeneous solution of epoxide, NaBr and DEG with low enough viscosity was studied in view of extending the protocol to CF. A comparative study of different solvents including toluene, THF, chloroform, 2-butanone, acetonitrile and DEG under batch conditions is summarized in Table 2.13 proving that the latter (DEG) was not only an excellent complexing agent, but was also the perfect solvent. In this case 1,2-epoxyhexane (**1c**) was used as model epoxide for the investigation of the CF processes due to its relatively low toxicity and reduced risks associated to its use in CF systems under pressure. To a mixture of **1c** (3.33 mmol), NaBr, and DEG in a 1:0.1:0.3 molar ratio, respectively, the chosen solvent was added to obtain a 5 M solution of the epoxide and the CO_2 insertion was performed under the optimized conditions (T = 100 °C, 40 bar of CO_2, t=3 h).

*Table 2.13: Insertion of CO_2 in 1,2-epoxyhexane (**1c**) catalyzed by NaBr/DEG, in the presence of a solvent.*

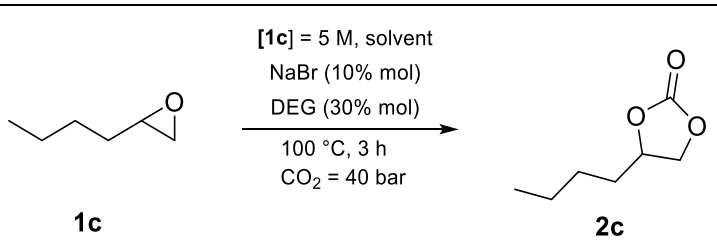

Entry	Solvent	ε[a]	1c, Conv. (%)	2c, Sel. (%)	By-products (%)
1	Toluene	2.38	41	54	19
2	Chloroform	4.81	49	70	15

3	THF	7.58	28	39	17
4	2-butanone	18.6	18	67	6
5	Acetonitrile	37.5	18	>99	-
6[b]	DEG	37.0	>99	>99	-

All reactions were run in batch conditions (autoclave). Conversion of **1c** and selectivity towards **2c** were determined by ^{1}H NMR and GC analysis in presence of an internal standard (mesitylene). [a] The polarity of the investigated solvents was compared through the corresponding dielectric constant. [b] The reaction afforded quantitative conversion of epoxide and selectivity towards the corresponding COC also when other starting epoxide were employed (styrene oxide (**1a**) and butyl glycidyl ether (**1d**).

The conversion decreased with increasing solvent polarity, from 40-50% in toluene and chloroform (Entries 1-2, Table 2.13), to 18% in 2-butanone and acetonitrile (Entries 4-5). However, the higher the conversion the lower the selectivity, due to the formation of by-products. In all cases, these by-products could not be identified unambiguously by ^{1}H NMR and GC-MS. Whichever the reasons for this behavior, the overall results were unsatisfactory with respect to those in the absence of solvents where 100% selectivity was achieved at complete conversion. Entry 6 proved that DEG was not only an excellent complexing agent, but it could also act as the best reaction medium. The reaction occurred smoothly, retaining high conversion and selectivity (both > 99%) reported in Scheme 2.2. This result seemed quite unexpected: considering the dielectric constant, the values of DEG and CH_3CN are similar while DEG is more polar than CH_3CN according to the Dimroth–Reichardt solvent scale.[20] Indeed, if we only consider solvent polarity, a polar aprotic solvent like CH_3CN should activate effectively the anionic nucleophile according to the well-known "naked anion" effect and destabilize the thus formed alkoxide intermediate (i.e. the rate-determining step), favouring the fast, subsequent CO_2 insertion process. However, catalytic CO_2 insertion into epoxides is strongly influenced by the nature of the solvent, and polar protic solvents as DEG can play a non-innocent role in the overall process, acting as HBD and favouring epoxide ring-opening upon coordination on the alkoxide intermediate (Figure 2.17). The participation of DEG in the catalytic process can explain its improved activity compared to the use of a polar aprotic solvent such as CH_3CN.

2.3.3.2 Continuous-flow process

CF-setup. The encouraging results obtained investigating the CO_2 insertion in batch mode prompted us to extend the protocol under continuous-flow conditions.[21] Flow chemistry is one of the top ten emerging technologies with high potential for sustainable syntheses, yet, from a chemical engineering standpoint, the transfer from a batch to a continuous process poses some issues especially when a setup comprised of a polar liquid mixture and nonpolar (gaseous or liquid/supercritical) CO_2 are present as in the case of this work.

Based on our expertise in flow chemistry,[22] the CF-apparatus was designed and in-house assembled, using a microfluidic reactor in the shape of 1/16" stainless-steel coil (Figure 2.23). CO_2 was supplied as a liquid from a commercial CO_2 cylinder equipped with a dip-tube and then compressed at the desired pressure and flow by a refrigerated dual head pump ($\mathbf{P_{CO2}}$). The solution of epoxide, NaBr and DEG was delivered by an HPLC pump ($\mathbf{P_L}$). The CO_2 and liquid streams were mixed in T junction (**T**) and conveyed to the CF-reactor (**coil C**) placed inside an oven for the temperature control. A back-pressure regulator (**BPR**) maintained a constant operating pressure

throughout the system and allowed the depressurization and recovery of the reaction mixture in the extractor (**E**) where the COC product was separated from the NaBr catalyst and DEG co-catalysts which were recycled.

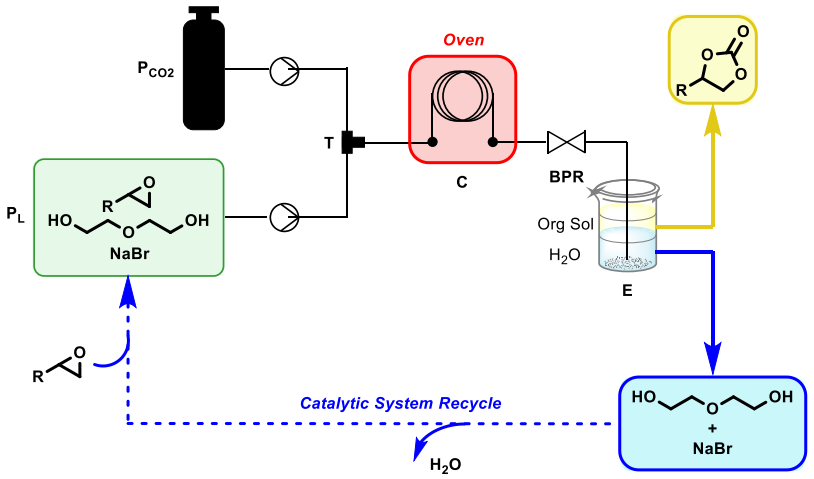

Figure 2.23: CF apparatus used for CF CO_2 insertion into epoxides

The CF insertion of CO_2 into 1,2-epoxyhexane (**1c**). Compound **1c** was chosen as a model terminal epoxide to begin the study of CF CO_2 insertions. Experiments were carried out using a 1 M solution of **1c** in DEG in the presence of NaBr (0.1-1 molar equiv. with respect to **1c**). This mixture was fed along with CO_2 to the CF-reactor of Figure 2.23: for screening tests, the dimensions of the steel coil were 2500 x 0.2 mm (length x internal diameter; $7.85 \cdot 10^{-2}$ cm^3 internal volume). Check valves were placed to avoid cross-contamination. All tests were run for t = 2 h by changing different pressure, temperature, and flow rates of the liquid solution (F_L) and CO_2 (F_{CO2}) stream in the range of 60-150 bar, 150-220 °C, 0.1-1.0 mL min^{-1}, and 1.0-4.0 mL min^{-1}, respectively. GC and GC-MS analyses of reaction mixtures samples confirmed the formation of 3 different products: hexene carbonate (**2c**), 1-bromohexan-2-ol (**3c**), and hexane-1,2-diol (**4c**) (Table 2.14). The bromohydrin (**3c**: BHO) is a reaction intermediate formed by the nucleophilic attack of the bromide anion to the primary carbon atom of the epoxide ring, as confirmed by GC-MS and NMR (see appendix for further details, Figure A.2.56-57). Formation of the diol **4c** (MS spectrum in Figure A.2.58) was due to hydrolysis of the starting epoxide plausibly promoted by traces of water in the highly hygroscopic DEG.[23] Results are reported in Table 2.14.

At the lowest investigated pressure, Q ratio and flow rates (60 bar, F_L = 0.1 and mL·min^{-1}, F_{CO2} = 1 mL min^{-1} and Q = 0.2), the epoxide conversion was very low at T = 150 °C (8 %) and it was limited even at T = 200 °C, not exceeding 15% (Entries 1 and 2). Formation of the desired COC product, 4-butyl-1,3-dioxolan-2-one (**2c**), was also unsatisfactory (up to 13 %), because of the predominant presence of the bromohydrin intermediate (BHO, 80 %). Doubling the system pressure up to *p* = 120 bar had a modest influence: the corresponding epoxide conversion and selectivity to **2c** were 18 and 19%, respectively (Entry 3). Further testing showed that significant improvements of the reaction outcome could be reached through the cooperative effects of T and the Q ratio variation. This was exemplified by the results of Entries 4 and 5: at *p* = 120 bar, when the temperature and the catalyst loading were progressively raised from 200 to 220 °C and from 0.1 to 0.3 and 1 molar equiv., respectively, the epoxide conversion also increased from 18 to 25 and 88% and the carbonate selectivity was enhanced to 81% (Entry 5). Under such conditions, an effect of the pressure was also noticed: albeit an increase to *p* = 140 bar did not produce appreciable changes, a decrease to *p* = 100 bar brought about a 8 % reduction of the conversion (from 90 to 82%, compare Entries 6 and 7). The CF system pressure, therefore, must be set at a sufficiently high threshold value ($p \geq 120$ bar) to ensure a constant CO_2 concentration in the reaction environment.

*Table 2.14: Synthesis of **2c** from **1c** and CO_2 in continuous flow. Effects of key reaction parameters*

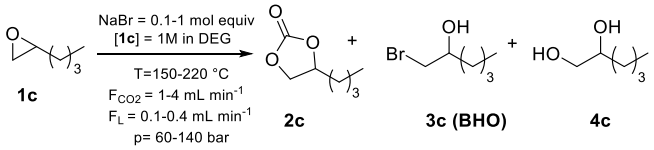

Entry	**1c**:NaBr (Q, mol:mol)	F_L/F_{CO2} (mL/min)	p (bar)	T (°C)	Conv. (%) [a]	Sel. (%) [a]		
						EHxC **2c**	BHO **3c**	EHxD **4c**
1	0.1	0.1/1	60	150	8	-	>99	-
2	0.1	0.1/1	60	200	15	13	80	7
3	0.1	0.1/1	120	200	18	19	74	7
4	0.3	0.1/1	120	200	25	26	67	7
5	1	0.1/1	120	220	88	81	15	4
6	1	0.1/1	140	220	90	82	15	3
7	1	0.1/1	100	220	82	79	18	4
8	1	0.2/1	120	220	88	78	17	5
9	1	0.4/1	120	220	84	79	16	4
10	1	1/1	120	220	73	63	30	7
11	1	0.1/4	120	220	69	77	19	4

All reactions were run for t = 2 h and tests were run in duplicate for reproducibility: in repeated reactions, conversion and selectivity differed <5% from one experiment to another. [a] Conversion and selectivity were determined by GC-MS analysis.

In light of these results, the study was continued choosing T, p, and Q (NaBr:**1c** molar ratio) of 220 °C, 120 bar, and 1, respectively. A partial thermal degradation of DEG was noticed above 220 °C resulting in clogging of the CF-reactor. Therefore, temperatures > 220 °C were not explored. The influence of changing the flow rate of both the reactant solution (F_L) and CO_2 (F_{CO2}) stream was then investigated. Experiments were first carried out by increasing F_L from 0.1 to 0.2 and 0.4 mL·min^{-1}, at a constant F_{CO2} (1 mL min^{-1}). No apparent effects on the reaction outcome were noticed (Entries 5 and 8-9, Table 2.14). The reaction productivity [defined as moles of carbonate product · (h · cat. equivs)$^{-1}$], however, was substantially enhanced: by quadrupling F_L, the rate of EHxC formation went up from 4.3 mmol h^{-1} equiv^{-1} to 15.9 mmol h^{-1} equiv^{-1} with an increase by a factor of 3.7. When F_L was further raised to 1 mL min^{-1}, a drop of both the conversion (73 %) and the carbonate selectivity (63 %) was observed (Entry 10); yet the productivity continued to increase up to 27.6 mmol h^{-1} equiv^{-1}. In this case the nominal molar ratio CO_2:epoxide is ≈ 18:1 with a decreased by a factor of 10 compared to the best conditions highlighted in the entry 6, hence also the molar ratio CO_2:epoxide could affect the performance of the reaction. No further investigations were carried out in this respect, but it should be noted here that under batch conditions, the maximum productivity for carbonate **2c** was 11.1 mmol h^{-1} equiv^{-1} (Scheme 2.3), about 2.5-fold lower than that

in the CF-mode. Increasing F_{CO2} from 1 to 4 mL min^{-1} (at constant F_L = 0.1 mL min^{-1}) was also detrimental for the epoxide conversion, which was reduced from 88 to 69 % (compare Entries 5 and 11, Table 2.14). These findings highlighted how the feed rates of the liquid solution (F_L) and of supercritical CO_2 (F_{CO2}) affected the CF reaction: higher flow rates resulted in lower contact times, lower epoxides conversion and lower COC selectivity, demonstrating that the increase of the molar ratio CO_2:substrate negatively affect the performance of the CF process. Overall, the concept was proved: the CO_2 insertion into **1c** could be engineered to proceed in CF mode in the presence of a homogenous catalyst/co-catalyst system (NaBr/DEG).

Two major challenges remained open: i) devising a purification protocol to allow an efficient separation of products, while effectively recycling the NaBr/DEG "catalytic" mixture; ii) improving the selectivity towards the carbonate product (EHxC). Changes of the reaction parameters investigated in Table 2.14 were not effective in this respect: the **2c** selectivity apparently levelled off, never exceeding 82%, mainly because of the formation of the bromohydrin intermediate which persisted in the final reaction mixtures.

Catalytic system recycling and mass balance. For the recovery of the products of Table 2.14, the adopted method was to convey the reaction mixture to a separatory flask containing a biphase system of water and an organic solvent (30 mL of each phase). Five different solvents including diethyl ether, diethyl carbonate, cyclopentyl methyl either (CPME), n-hexane and ethyl acetate were tested and compared to this purpose. Diethyl carbonate (DEC) was finally chosen for its suitability for carbonate products and its low toxicity and safety (details on the solvent choice are reported in the appendix, table A.2.1). The unconverted reactant and products were extracted in DEC, while the catalyst/co-catalyst (NaBr/DEG) were quantitatively dissolved in the aqueous solution (Figure 2.23). Experiments on the recycling of the NaBr/DEG system were carried out under the experimental conditions of Entry 5, Table 2.14 ([**1c**] = 1 M in DEG; NaBr (1.0 equiv.); F_L = 0.1 mL·min^{-1}, F_{CO2} = 1 mL·min^{-1}, *p* = 120 bar, T = 220 °C), as summarized in Scheme 2.4.

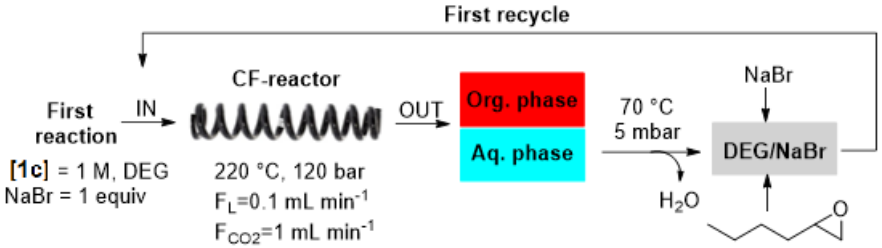

Scheme 2.4: Catalytic system recycling in CF-mode

The catalytic system (DEG and NaBr) present exclusively in the aqueous layer, was collected and evaporated under reduced pressure (T = 70 °C, *p* = 5 mbar) until complete removal of water. To the resulting liquid was added fresh epoxide (EHx: 12 mmol to obtain a 1 M solution in DEG) and an additional aliquot of NaBr (163 mg, 1.6 mmol). The latter was necessary to integrate the amount of catalyst consumed by the formation of the bromohydrin intermediate (BHO), and it was calculated to restore the initial quantity of NaBr (*i.e.* to achieve an epoxide:catalyst molar ratio of 1, based on 88% conversion and 15% selectivity towards BHO, see Entry 5, Table 2.14). The solution was then delivered to the CF-reactor for the first recycle run. The steps of Scheme 2.4 were repeated for 4 subsequent recycles. The amount of fresh NaBr was adjusted after each experiment according to the conversion and the selectivity achieved case-by-case. Results are reported in Figure 2.24.

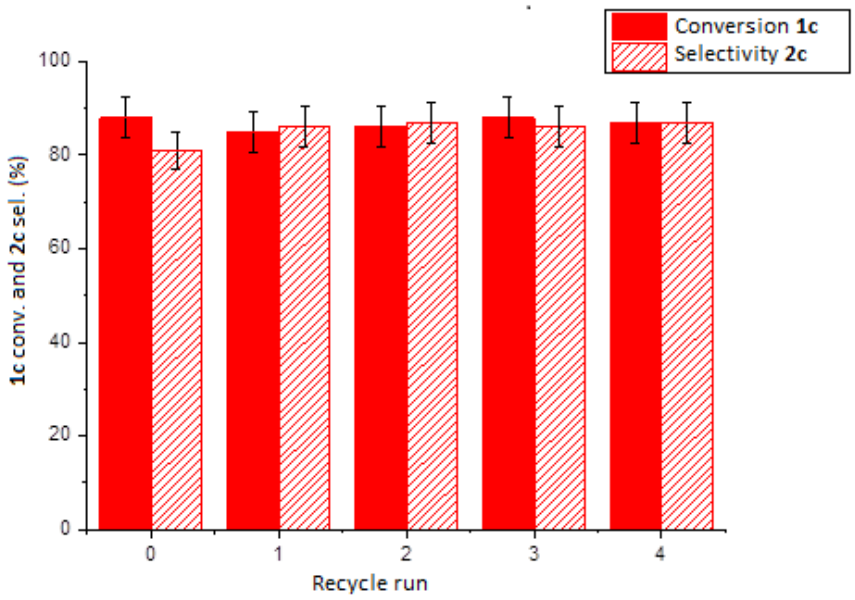

*Figure 2.24: DEG/NaBr system recycling upon CF synthesis of EHxC (**2c**). Conditions: [EHx, **1c**] = 1 M in DEG, NaBr:**1c** = 1.0 mol/mol; F_L = 0.1 mL·min^{-1}, F_{CO2} = 1 mL·min^{-1},* p *= 120 bar, T = 220 °C. Run 0 (first reaction) refers to the result of Entry 5, Table 2.14*

After each recycle, both the conversion and **2c** selectivity were substantially steady at ca 85-90% and 80-85%, respectively, thereby proving that the NaBr/DEG catalytic mixture was reusable without loss of performance. It should be noted however, that the formation of bromohydrin **3c** produced NaOH as by-product which accumulated in the DEG solution, making it denser and (slightly) more viscous after each cycle. Although this feature was not investigated in detail, nor its consequences were apparent from Figure 2.24, nevertheless it could plausibly bring about a limitation in view of an indefinite recycle of the DEG solution: the higher its viscosity/density, the more difficult the mass transport, especially in microfluidic reactors.[24] Moreover, part of NaBr was irreversibly consumed in each reaction run.

Recycle experiments allowed to confirm the reaction mass balance. To this aim, the organic phase (containing exclusively the products) was collected and concentrated *in vacuo* (T = 30 °C, *p* = 50 mbar) and dried. The desired product, **2c** was then isolated by FCC, with isolated yields ranging between 66 and 71 %, consistent with the conversion and selectivity reported in Figure 2.24 (see appendix for further details, Table A.2.2).

Improving the selectivity: effect of reactor length (contact time) and substrate scope. Previous experiments highlighted that the selectivity towards **2c** was mostly limited by formation of **3c**. Increasing the contact (residence) time could plausibly favor the conversion of the bromohydrin into the corresponding COC. However, the technical specs of the pumps of our CF system did not allow flow rates lower than the values specified in Table 2.14 (F_L = 0.1 mL·min^{-1} and F_{CO2} = 1 mL·min^{-1}). A redesign of the CF reactor was therefore required. The same 1/16" steel coil (internal diameter = 0.2 mm) was used, but the reactor length and internal volume were doubled from 250 to 500 cm, and from 7.85·10^{-2} to 0.157 cm^3, respectively. Experiments were performed under the optimized conditions ([**1c**] = 1 M in DEG; NaBr (1.0 equiv.); F_L = 0.1 mL·min^{-1}, F_{CO2} = 1 mL·min^{-1}, *p* = 120 bar, T = 220 °C). Results are reported in Table 2.15, which compares the conversion and the selectivity towards the desired COC product and the bromohydrin by-product (products 2 and 3, respectively) achieved by performing CO_2 insertion reactions in both the *available* reactors (l = 250 and 500 cm, respectively). When choosing **1c** as a model substrate, increasing the reactor length slightly improved the conversion (from 88 to 92%), but had a more pronounced

effect on the selectivity towards the desired **2c** product which increased from 81 to 91% (Entries 1 and 2). The corresponding diol **4c** was not detected, not even in trace levels. A similar effect was observed when performing CF CO_2 insertion reactions on butyl glycidyl ether (**1e**): increasing coil length resulted in a quantitative conversion with an excellent selectivity to the corresponding COC product (93%, entry 4). Overall, a positive effect on products distribution was observed, thereby proving that CF system could be flexibly engineered to overcome the kinetic issues associated to the two consecutive reactions (bromohydrin formation and CO_2 insertion). A more quantitative explanation of these results should consider the estimation and comparison of the contact time under the investigated conditions: a flowing system comprising a polar liquid (epoxide in DEG/NaBr) and a non-polar supercritical gas-like phase (CO_2 with a density as low as 0.14 g·mL^{-1} at 220 °C and 120 bar) made this study challenging, if at all possible.[25]

Additional experiments were performed using also styrene oxide (**1a**). In this case, at T = 220 °C, when the shorter reactor (250 cm) was used, the conversion of **1a** was 99% but a significant formation of products deriving for the Meinwald rearrangement of **1a** (phenylacetaldehyde and acetophenone) was noticed (entry 5).[26] The presence of an electron withdrawing substituent as the aryl ring [27] altered the reactivity of **1a** with respect to both hexene oxide (**1c**) and butyl glycidyl ether (**1e**). The isomerization side-reaction was almost suppressed by lowering the temperature at 140 °C. Under such conditions, however, the conversion was reduced to 64% and a significant amount of unreacted bromohydrin intermediate (**3a**, 2-bromo-1-phenylethan-1-ol: 26%) was detected in the final mixture (entry 6). Increasing the reactor length to 500 cm, improved the conversion to 75% with no appreciable effects on the products distribution. The best selectivity towards styrene carbonate (**2a**) and the bromohydrin intermediate (**3a**) were 73% and 23%, respectively (entry 7).

Table 2.15: CO_2 insertion reactions in terminal epoxides: influence of CF reactor length.

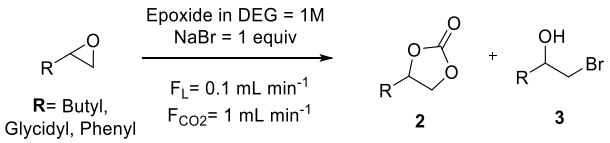

Entry	Epoxide	CF-reactor length (mm)	T (°C)	Conv (%)	Product Sel. (%)	
					2	**3**
1 [(a)]	**1c**	250	220	88	81	15
2		500		92	91	9
3	**1e**	250	220	95	85	15
4		500		99	93	7
5	**1a**	250	220	99	52	7
6		250	140	64	70	26
7		500	140	75	73	23

t = 2 h for all reactions. Conversion and selectivity were determined by GC-MS analysis. [(a)] Hexane-1,2-diol (4%) was also detected among reaction products; [(b)] The main byproducts were due to isomerization of the staring epoxide: phenylacetaldehyde (36%) and acetophenone (5%) was noticed according to GC-MS analysis.

2.3.4 Conclusions

This work reports the first application of a simple non-polymeric glycol such as diethylene glycol (DEG) for the catalytic activation of NaBr in the insertion of CO_2 to terminal epoxides. The binary system made of NaBr/DEG has proven efficient for the batch conversion of different substrates including styrene oxide, butyl glycidyl ether, phenyl glycidyl ether, 1,4-butanediol diglycidyl ether, and C_4-C_{10} linear terminal olefins but even more importantly, the characteristics of DEG (viscosity, density, diffusivity) made it suitable to act concurrently as a co-catalyst (cation coordinating agent) and a solvent/carrier for the implementation of the reaction in continuous-flow. Translating the reaction conditions from batch to continuous flow was challenging. The results gathered so far highlight that the batch reaction can be run under conditions far milder (T = 100 °C, CO_2 =1 bar) than those required in CF-mode (T = 220 °C, CO_2= 120 bar); nevertheless, the potential of CF in terms of process intensification can be appreciated. Notably, in the explored range of flow rates, a microfluidic reactor with a capacity of just $7.85 \cdot 10^{-2}$ cm^3 allows a productivity 2.5 higher compared to the corresponding batch process carried out on a gram scale.

Recycle experiments have also confirmed that the NaBr/DEG catalytic mixture is reusable without loss of performance, for at least four subsequent CF-runs. Moreover, a significant advance with respect to other reports in literature is the continuous recyclability of the homogeneous mixture that bypasses typical drawbacks associated to heterogeneous catalyst deactivation.[3]

Although further optimization is required in terms of process engineering to improve the CF system design and maximize delivery/contact between the polar liquid solution of reactant/catalyst/co-catalyst and gas-like apolar supercritical CO_2, the study provides a proof of concept which paves the way for future advances in the field.

2.3.5 Experimental section

2.3.5.1 General

Commercially available reagents and solvents were used as received unless otherwise stated. Styrene oxide (**1a**), 1,2-epoxybutane (**1b**), 1,2-epoxyhexane (**1c**), 1,2-epoxydecane (**1d**) butyl glycidyl ether (**1e**), phenyl glycidyl ether (**1f**), 1,4-butanediol diglycidyl ether (**1g**), ethanol, NaBr, diethylene glycol (DEG), diethylene glycol dimethyl ether (DEGME), 1-hexanol and 1,6-hexanediol, diethyl ether, diethyl carbonate, tetrahydrofuran, ethyl acetate, acetonitrile were sourced from Sigma-Aldrich (now Merck).

GC-MS (EI, 70 eV) analyses were performed with an Agilent 6890N GC, equipped with a HP5-MS capillary column (l = 30 m, Ø = 0.32 mm, film thickness = 0.25 mm), coupled with an Agilent 5975 EI detector. GC-FID analyses were performed with a HP 6890 GC mounting an Elite-624 capillary column (l = 30 m, Ø = 0.32 mm, film thickness = 1.8 mm). ^1H and ^{13}C NMR spectra were recorded with a Bruker Ascend 400 instrument operating at 400 and 100 MHz, respectively. The chemical shifts were reported downfield from tetramethylsilane (TMS). $CDCl_3$ and DMSO-d_6 were chosen as deuterated solvents. GC-MS, ^1H and ^{13}C spectra of the synthesized COCs are reported in the appendix (figure A.2.59-79).

2.3.5.2 Synthesis of methyl 8-(3-octyloxiran-2-yl) octanoate (1h, epoxidized methyl oleate)

1h was synthesized through a simple procedure reported in the section 2.2. Briefly, a mixture of methyl oleate (1.48 g, 5 mmol), H_2O_2 (30%w/w, 1.1 ml, 2 equiv.) and trioctylmethyl ammonium tungstate ($[N_{8,8,8,1}]_2WO_4$, 5% mmol) as catalyst was added in a round-bottomed flask equipped with a magnetic stirrer and a condenser. The flask was heated at 75°C for 4h under stirring. At the end of the reaction, the organic phase was separated and

dried on sodium sulfate. **1h** was obtained in 95% yield without further purification (purity>99% according to GC) and characterized by GC-MS, ^{1}H NMR and ^{13}C NMR (Figure A.2.50-52).

2.3.5.3 Experimental tests

General procedure for CO_2 insertion reactions with terminal epoxides in batch conditions, CO_2= 2-40 bar. The selected epoxide (3.33 mmol, 1 equiv.), NaBr (0.025 – 0.1 eq), the co-catalyst (DEG, DEGME, 1-hexanol or 1,6-hexanediol, 0.2 - 0.3 eq), and mesitylene (0.33 mmol, 0.1 equiv., as the internal standard) were charged in a round-bottomed flask shaped as a test tube and equipped with a pierced glass cap and a stirring bar. The flask was placed inside a 100-mL stainless steel autoclave which was sealed, degassed via three vacuum-CO_2 cycles, pressurized with CO_2 (2, 10 and 50 bar; the molar ratio CO_2:epoxide was ≈ 2.5:1, 12:1 and 60:1 respectively), and finally heated at T of 50-100°C for 2-5 h. Thereafter, the autoclave was cooled to rt and vented. A sample of the crude mixture was analysed by ^{1}H NMR and GC-FID to determine conversion, yield and selectivity.

General procedure for CO_2 insertion reactions with terminal epoxides in batch conditions, CO_2= 1 bar. The selected epoxide (3.33 mmol, 1 eq), NaBr (0.1 equiv.), DEG (0.3 equiv.) and mesitylene as internal standard (0.33 mmol, 0.1 equiv., as the internal standard) were charged into a round-bottomed flask equipped with a magnetic stirrer. The flask was degassed via two vacuum-CO_2 cycles and a rubber reservoir containing about 2l of CO_2 was connected to the flask (the molar ratio CO_2:epoxide was ≈ 24:1). The reaction vessel was sealed to prevent losses of substrates and/or CO_2 and stirred at 100 °C for 3h. After the chosen time, an aliquot of the reaction mixture was analysed by ^{1}H-NMR and GC-FID to determine substrate conversion, selectivity and yield.

General procedure for CO_2 insertion reactions in CF conditions. Reactions were performed using the apparatus of Figure 2.23. In a typical procedure, the CF apparatus was first conditioned with DEG (FL = 0.5 mL·min^{-1}), and CO_2 (F_{CO2} = 4 mL·min^{-1}) for t = 30 min. Then, a homogeneous 1 M solution of the selected epoxide and NaBr (0.1-1 equiv. with respect to the epoxide) in DEG was continuously delivered to the CF-reactor at the desired T and flow rates (T = 140−220 °C, F_L = 0.1−0.4 mL·min^{-1} and F_{CO2} = 1-4 mL·min^{-1}). Reactions were allowed to proceed for t = 2 h, though some prolonged tests were carried out for up to t = 6 h. The reaction mixture was fluxed into a separatory flask containing a biphase system of water and the selected organic solvent (30 mL of each phase). The unconverted reactant and products were extracted into the organic solvent, while the catalyst/co-catalyst (NaBr/DEG) were quantitatively dissolved in the aqueous solution. After each test, the CF system was washed with distilled water (10 mL) and ethanol (10 mL) and dried with a CO_2 flow (F_{CO2} = 4 mL·min^{-1}) for 10 minutes.

General procedure for the recycle of the catalytic system. The catalytic system (DEG and NaBr) present exclusively in the aqueous layer, was collected and evaporated under reduced pressure (T = 70 °C, *p* = 5 mbar) until complete removal of water. To the resulting liquid was added fresh epoxide (**1c**: 12 mmol to obtain a 1 M solution in DEG) and an additional aliquot of NaBr calculated to restore the initial quantity of NaBr and integrate the amount of catalyst consumed by the formation of the bromohydrin. The solution was then delivered to the CF-reactor for the recycle run operating at the reaction conditions selected.

2.3.6 References

[1] (a) A. Sainz Martinez, C. Hauzenberger, A. R. Sahoo, Z. Csendes, H. Hoffmann and K. Bica, *ACS Sustainable Chemistry & Engineering*, 2018, **6**, 13131-13139; (b) Y. Zhang, Z. Tan, B. Liu, D. Mao and C. Xiong, *Catalysis Communications*, 2015, **68**, 73-76.

[2] (a) E. García-Verdugo, B. Altava, M. I. Burguete, P. Lozano and S. Luis, *Green Chemistry*, 2015, **17**, 2693-2713; (b) D. Cantillo and C. O. Kappe, *ChemCatChem*, 2014, **6**, 3286-3305

[3] H. Seo, L. V. Nguyen and T. F. Jamison, *Advanced Synthesis & Catalysis*, 2019, **361**, 247-264.

[4] X. B. Lu, J. H. Xiu, R. He, K. Jin, L.-M. Luo, X.-J. Feng, *Applied Catalysis A: General,* 2004, **275**, 73–78.

[5] L. Guo, L. Deng, X. Jin, Y. Wang, H. Wang, *RSC Advances*, 2018, **8**, 26554–26562.

[6] M. North, P. Villuendas, C. Young, *Chemistry - A European Journal*, 2009, **15**, 11454–11457.

[7] A. Rehman, A. M. López Fernández, M. F. M. G. Resul, A. Harvey, *Journal of CO2 Utilization*, 2018, **24**, 341–349.

[8] X. Wu, M. Wang, Y. Xie, C. Chen, K. Li, M. Yuan, X. Zhao, Z. Hou, *Applied Catalysis A: General,* 2016, **519**, 146–154.

[9] B. R. James, J. A. Boissonnault, A. G. Wong-Foy, A. J. Matzger, M. S. Sanford, *RSC Advances,* 2018, **8,** 2132–2137.

[10] H. Yasuda, L. He, T. Takahashi, T. Sakakura, *Applied Catalysis A: General*, 2006, **298**, 177–180.

[11] V. H. Jadhav, S. H. Jang, H.-J. Jeong, S. T. Lim, M.-H. Sohn, J.-Y. Kim, S. Lee, J. W. Lee, C. E. Song, D. W. Kim, *Chemistry: A European Journal*, 2012, **18**, 3918–3924.

[12] (a) G. Rokicki, W. Kuran, B. Pogorzelska-Marciniak, *Monatsh. Chem*. 1984, **115**, 205–214; (b) J. Tharun, G. Mathai, A. C. Kathalikkattil, R. Roshan, J.-Y. Kwak, D.-W. Park, *Green Chemistry* 2013, **15**, 1673–1677; (c) S. Kaneko, S. Shirakawa, *ACS Sustainable Chemistry & Engineering*, 2017, **5**, 2836–2840.

[13] S. Kumar, S. L. Jain, *Industrial Engineering Chemistry Research*, 2014, **53**, 541–546.

[14] (a) J. Steinbauer, T. Werner*, ChemSusChem* 2017, **10**, 3025–3029; (b) J. Steinbauer, A. Spannenberg, T. Werner, *Green Chemistry*, 2017, **19**, 3769–3779; (c) Y. Hu, J. Steinbauer, V. Stefanow, A. Spannenberg, T. Werner, *ACS Sustainable Chemistry & Engineering,* 2019, **7**, 13257–13269.

[15] (a) V. Butera, H. Detz, *ACS Omega,* 2020, 5, 18064–18072; (b) C. C. Truong, D. K. Mishra*, Journal of CO2 Utilization*, 2020, **41**, 101252.

[16] M. Liu, X. Wang, Y. Jiang, J. Sun and M. Arai, *Catalysis Review*, 2018, **61**, 214-269

[17] The epoxidized methyl oleate (**1h**) was synthesized according to a procedure reported in the experimental section

[18] N. Tenhumberg, H. Büttner, B. Schäffner, D. Kruse, M. Blumenstein and T. Werner, *Green Chemistry*, 2016, **18**, 3775-3788.

[19] F. Chen, Q.-C. Zhang, D. Wei, Q. Bu, B. Dai and N. Liu, *The Journal of organic chemistry*, 2019, **84**, 11407-11416.

[20] C. Reichardt, *Solvents and Solvent Effects in Organic Chemistry*, Wiley-VCH Publishers, 3rd ed., 2003

[21] (a) M. B. Plutschack, B. Pieber, K. Gilmore, P. H. Seeberger, *Chemical Reviews* 2017, **117**, 11796–11893; (b) F. Gomollón-Bel, Chemistry International 2019, **41**, 12–17.

[22] (a) R. Calmanti, M. Galvan, E. Amadio, A. Perosa, M. Selva, ACS Sustainable Chemistry Engineering, 2018, **6**, 3964–3973; (b) L. Cattelan, G. Fiorani, A. Perosa, T. Maschmeyer, M. Selva, ACS Sustainable ACS Sustainable ChemistryEngineering, 2018, **6**, 9488–9497.

[23] S. Lohse, B. T. Kohnen, D. Janasek, P. S. Dittrich, J. Franzke, D. W. Agar, *Lab Chip*, 2008, **8**, 431.

[24] M. Brivio, W. Verboom, D. N. Reinhoudt, *Lab Chip* 2006, **6**, 329.

[25] (a) T. Andersson, P. Pucar, Journal of Process Control 1995, **5**, 9–17; (b) S. Lohse, B. T. Kohnen, D. Janasek, P. S. Dittrich, J. Franzke, D. W. Agar, *Lab Chip*, 2008, **8**, 431.

[26] V. V. Costa, K. A. da Silva Rocha, I. V. Kozhevnikov, E. V. Gusevskaya, *Applied catalysis A: General*, 2010, **383**, 217-220.

[27] G.-P. Wu, S.-H. Wei, W.-M. Ren, X.-B. Lu, B. Li, Y.-P. Zu, D. J. Darensbourg, *Energy Environmental Science*, 2011, **4**, 5084-5092.

3 Synthesis of high value-added glycerol derivatives

3.1 High-Temperature Batch and Continuous-Flow Transesterification of Alkyl and Enol Esters with Glycerol and its Acetal Derivatives

3.1.1 Introduction

As mentioned in the introduction (sections 1.4.1.2 and 1.4.4.2), bio-based glycerol and its acetal derivatives (glycerol acetals, GAs) fit in the current list of top biomass-derived platform chemicals which are used as building blocks for higher value-added chemical products and materials.[1]

We have also highlighted the importance of continuous-flow (CF, paragraph 1.5.2) protocols and catalyst-free reactions (par. 1.5.3.2) among the tools used in this thesis to reach the objective of greener processes. Both these tools were exploited during this thesis work by developing a procedure that also included the use of solvent-free conditions (par. 1.5.3.1): in this case, no extra-solvents were added while one of the reactants (i.e. the acetylation agent) was used contemporary as reactant and solvent: this benign arrangement allows an easy recover and reuse of the excess reactant at the end of the reaction.

The conversion of bio-based feedstock through catalyst-free, solvent-free, thermal protocols has attracted the attention of academic and industrial research in the last years: the study of high-temperature (HT) protocols was originally aimed at improving biodiesel production not only through the transesterification of natural oils, but also by the simultaneous conversion of the co-product glycerol (Glyc) into glycerol dicarbonate (GDC) or triacetin (TA), respectively.[2] To this end, supercritical fluid-based (SCF) reactions with non-toxic acyl acceptors such as dimethyl carbonate (DMC) or methyl acetate were described (Scheme 3.1).

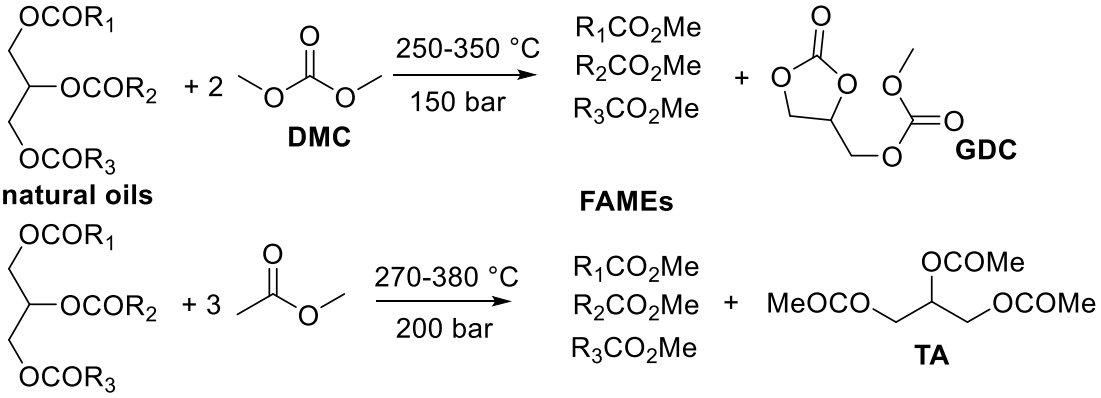

Scheme 3.1 Transesterification of natural triglycerides with DMC or methyl acetate.

At 250-380 °C and 150-200 bar, such SCF-technologies proved highly tolerant towards impurities (free fatty acids and water) commonly present in the reactant oils and allowed extremely fast kinetics and yields >90% with simplified downstream processing in which high-standard glycerol-free biodiesel as blends of fatty acid methyl esters (FAMEs) and GDC or TA were obtained without further purification.[3] Moreover, energy costs and capital investments of plants running on SCF-technologies (SCF-plants) could be efficiently mitigated by integrating the SCF-based reactions within biorefinery units able to recover or exchange waste or heat.[4] Comparative studies and simulations demonstrated that the total energy consumption and the potential environmental impact per mass of product obtained from SCF-plants for biodiesel production could be even lower than that of conventional base-catalyzed transesterification processes.[5,6]

HT-reactions were also successfully investigated by us for the upgrading of model glycerol acetals, specifically glycerol formal, Solketal and glycerol by using dialkyl carbonates.[7] For example, at 275-300 °C and 20-40 bar, the continuous-flow (CF) reaction of DMC with GAs yielded mono-transcarbonated products with a 98% selectivity at complete conversion; while the same CF-process with glycerol was optimized to obtain glycerol carbonate in a 83-92% yield. Other authors recently described also a batch reaction between supercritical DMC and glycerol to isolate glycerol carbonate in a 98% yield after only 15 min.[8]

This background prompted us to further investigate HT-reactions with the objective of implementing the conversion of glycerol and GAs into the corresponding ester derivatives.

As reported in paragraph 1.4.4.2, monoacetylglycerols (MAGs), diacetylglycerols (DAGs) and triacetylglycerols (TAGs) are already produced on an industrial scale and have a plethora of applications in food and cosmetic industry as surfactants and emulsifiers. In particular, MAGs are used as food additives, in manufacturing explosives and smokeless powder[9] but are also valuable in pharmacochemistry for the preparation of specific antidotes.[10] DAGs are used in the synthesis of structural lipids[11], plasticizer coating and foodstuffs.[12] Mixtures of MAGs, DAGs and TAGs have indeed specific applications in cryogenics and biodegradable polyesters.[13] A separate discussion can be done for triacetin (TA). This is a commercially valuable and stable compound with no toxicity used as food additive (humectant, leavening agent), solvent in flavorings and fragrances, plasticizer for cellulose and in pharmaceutical industry.[14] Moreover its use as fuel additive and anti-knock agent for gasoline or cold and viscosity improver for biodiesel is explored and various LCA analysis confirmed its beneficial aspects in a cradle-to-emission perspective.[15] TA alone accounts for ca. 10% of the worldwide glycerol market, with a global demand of 110 000 tonnes per year and an estimated CAGR (Compound Annual Growth Rate) of 4.4% for the next 8 years.[16]

TA is industrially obtained through a process reported in Figure 3.1. Glyc is first reacted with acetic acid (AcOH) by forming mostly MAG that is furtherly esterified with acetic anhydride (Ac_2O) in a second reactor. The water produced as by-product is removed by azeotropic distillation while triacetin is purified in an evaporator from higher boiling waste products.

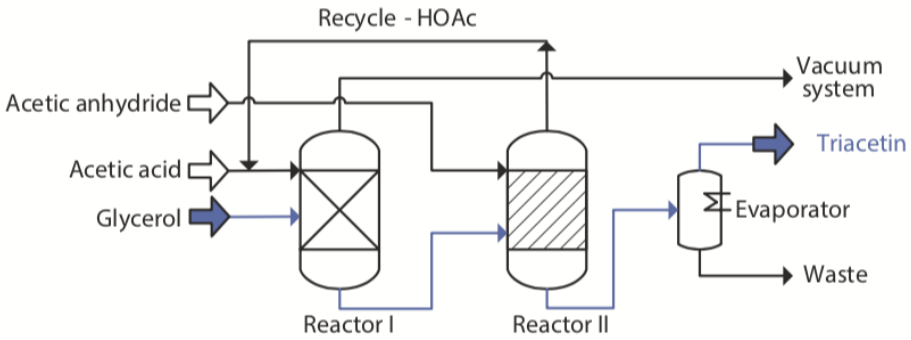

Figure 3.1: Diagram for the triacetin production

Issues related to the corrosivity of reactants, the legal restrictions to the use of Ac_2O, and the formation of co-product water [17] boosted an interest on alternative catalytic procedures that use carboxylic acid or anhydrides as acetylating agents: in this case issues related to the by-produced water concerns not only the alteration of the esterification equilibrium, but also the deactivation of catalysts.[18] Conversely, literature on catalyst-free esterification of glycerol is limited: poor conversions (35-49%) and moderate product yields (70%, triacetin) are reported by using AcOH and Ac_2O as acetylation agent.[19,20]

A literature survey indicated that the transesterification reactions of esters with both glycerol and GAs were more promising and safer processes. The acetylation of glycerol with alkyl (methyl, ethyl) acetates was reported over several homogeneous and heterogeneous acid and base catalysts,[21,22] while the transesterification of esters with GAs was almost exclusively finalized at the kinetic resolution of racemic GAs esters by lipase-based biocatalysts.[23] However, no attempts to conduct the acetylation of glycerol derivatives with organic esters in absence of catalyst through a flow reactor has been reported.

3.1.2 Aim and summary of the research

In the present work, a systematic inspection of acetylation of glycerol and its GAs derivatives has been carried out by using acetylating reagents such as formate, acetate, lactate esters and isopropenyl acetate. The reactions were explored in batch conditions and then optimized in flow reactors. Given the absence of any catalyst, we were interested also into understand the equilibria between the reactions involved and the mechanisms related to the formation of the products. At 200-240 °C and 10-50 bar, in the absence of any catalysts, the selective and high-yield synthesis of esters of GAs and triacetin were achieved with batch and continuous-flow protocols. We questioned if the procedure studied with GAs was exploitable also with the more challenging glycerol and the different reactivity of methyl acetate and iPAc was compared. Finally, the role of iPAc (i.e., the most active acetylating agent) [24] was explored: since its higher reactivity is due to the release of acetone as a by-product, some experiments were conducted to explore the chances to exploit the acetone formed as acetalization reactant for the synthesis of glycerol acetals in a tandem non-catalytic procedure.

3.1.3 RESULTS AND DISCUSSIONS

3.1.3.1 Batch HT-transesterification of different esters with glycerol acetals

Conditions to begin this study were chosen based on the results reported by our research group for the transcarbonation of dialkyl carbonates with glycerol acetals.[9a] As described in the experimental section, mixtures of **1a** and each of the esters **2a-2f** in a 1:20 molar ratio (Q), respectively, were set to react in an autoclave at different temperatures (150 to 220 °C) and times (1 to 10 h).

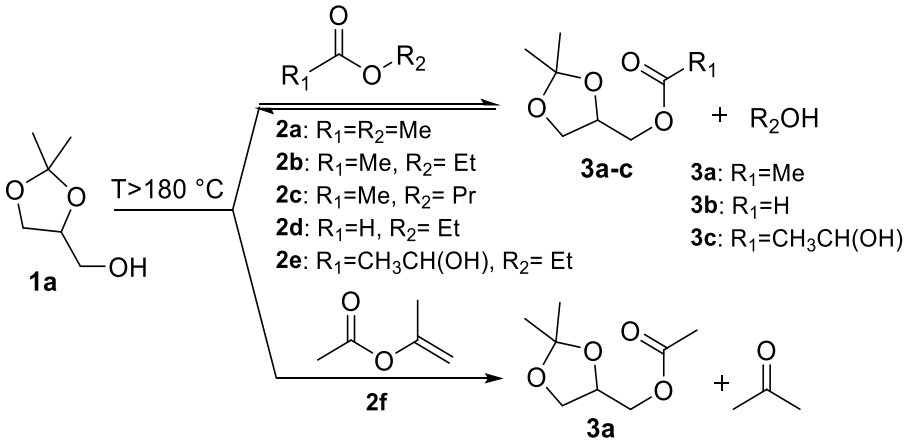

Scheme 3.2: Reactions of Solketal with different esters at high temperatures.

In the absence of catalyst, the transesterification process occurred at T ≥ 180 °C. The structure of the products, *i.e.* Solketal esters **3a**, **3b**, and **3c** (R1=Me, H, and $CH_3CH(OH)$, respectively; Scheme 3.2) was confirmed by GC/MS and $^{1}H/^{13}C$ MNR. Compounds **3a** and **3b** were also isolated in 96 and 60% yields from the reactions of **1a** with **2f** and **2d**, respectively.

Each reactant ester **2a-2f** gave remarkably different outcomes. Figure 3.2 compares the results achieved at 200 °C for 5 h, under an autogenous pressure of 8 bars. The conversion of Solketal did not exceed 10% with acetates **2a-c**, while it was substantially higher for ethyl formate, ethyl lactate (**2d-e**) and *iso*propenyl acetate (**2f**): 67%, 57% and 100% (blue bars), respectively. Except for ethyl lactate, the transesterification selectivity was always very high (≥98%, red bars). Only trace amounts of MAGs, DAGs and TAGs were observed (<2%, in total). These were plausibly originated by the hydrolytic ring-opening of Solketal followed by the acetylation of the product glycerol. The water responsible for the hydrolysis process was present in the starting acetal **1a** (see below).

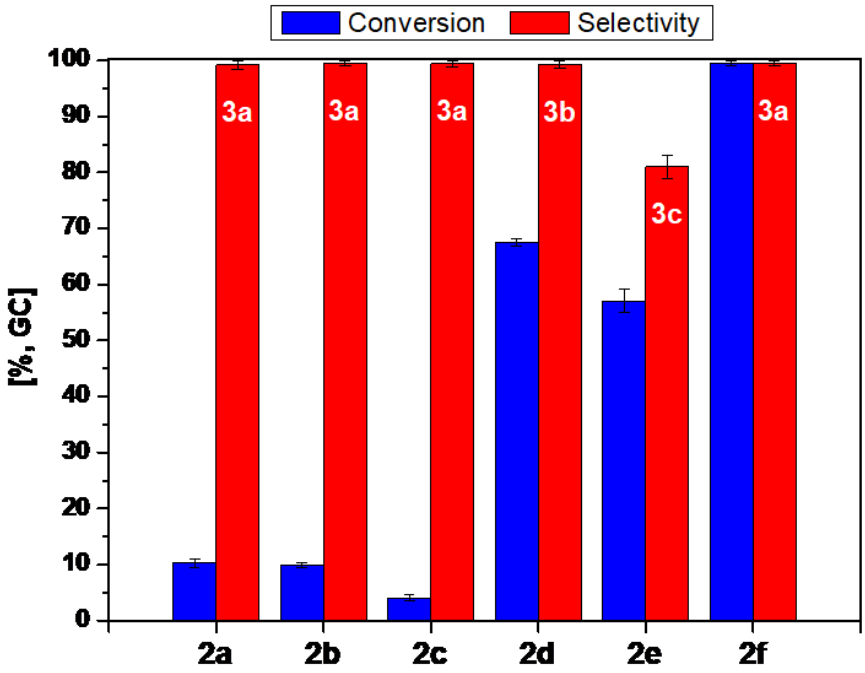

*Figure 3.2. Batch HT-reaction between Solketal and esters **2a-f**: conversion of Solketal and selectivity towards Solketal esters **3a**, **3b**, and **3c** are shown. Conditions: ester:Solketal molar ratio, Q=20, 200 °C, 5h.*

Different reasons could plausibly explain the observed behavior: i) irrespective of the mechanism considered, the formate ester **2d** was expected to serve as a more powerful electrophile than the acetate homologues **2a**-**c**;[25] ii) thermodynamic calculations indicated that small, but non-negligible variations in energy and stability were expected throughout the series of reactants **2** due to intermolecular H-bonds and interactions between alkyl chains of different lengths and ester groups.[26] The inconsistency observed for ethyl lactate (**2e**) was due to the occurrence of two by-products (11 % combined, by GC/MS) which plausibly derived from the self-transesterification of ethyl lactate followed by the reaction with Solketal (although the structure of these compounds was not resolved, details of MS analyses are reported in the appendix, figure A.3.14 and A.3.15).[27] iii) the co-product alcohols (R_2OH, Scheme 3.2, top) had limited, if any, leaving group effects since similar conversions were obtained regardless of the release of MeOH, EtOH, or PrOH in the series of acetates **2a-c**. By contrast, the release of acetone in the reaction of iPAc made the overall transformation irreversible (Scheme 3.2, bottom). This was further confirmed when the reverse process was attempted by heating a mixture of **3a** and acetone at 200°C for 5 h. Obviously, no reaction took place: isopropenyl acetate could not be formed because this would have required the intermediacy of an unstable enol derivative (see below, Scheme 3.3). Overall, due to this (non-reversible) behaviour, iPAc was by far the best performing reagent among the tested reactant esters, yielding the almost exclusive formation of compound **3a** at total conversion. It should be noted that under the conditions of Figure 3.2 (200 °C, Q=20), the reaction of Solketal with iPAc showed a conversion as high as 73% after only 3 hours.

The potential of iPAc was confirmed by a more in-depth investigation of its batch reaction with Solketal. Figure 3.3 describes the most representative results by reporting the reaction conversion as a function of T and Q (molar ratio of reactants), in the range 120-220 °C and 5-20, respectively. Selectivity towards ester **3a** was always > 96% by GC/MS and is therefore not shown.

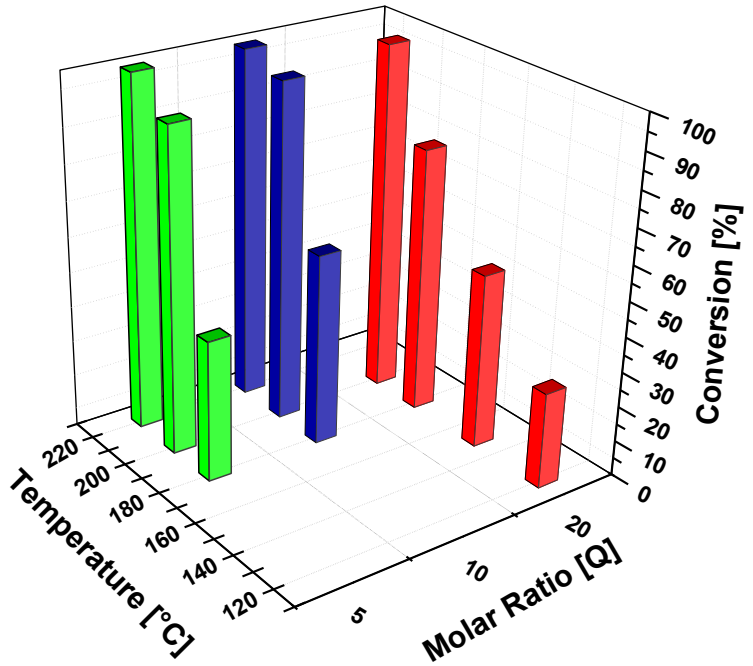

*Figure 3.3: Conversion of Solketal as a function of the temperature and the reactants molar ratio (Q) during the batch reaction of Solketal and iPAc. All tests were carried out for 5 hours. The selectivity towards product **3a** was always > 96%.*

The conversion was favoured both by higher temperature (bars of the same colour) as well as by higher Q ratio (left to right). Yet, a quantitative reaction took place also with a moderate excess of iPAc (Q = 5, 220 °C: green bar). This behaviour was further substantiated by a separate experiment, not reported in Figure 3.3, demonstrating that at the same T (220 °C), the transesterification could be completed even at Q=2, albeit over 10 hours. Whichever the conditions used, simple vacuum distillation of the final mixtures allowed an almost complete recovery of the unconverted excess reagent: more than 95 wt% of iPAc not reacted during the reaction could be reused as such for further transesterification reactions.

GC/MS analyses of the final mixtures also provided some insight to speculate on the reaction mechanism, particularly the detection of traces of acetic acid among the reaction products. The presence of AcOH was plausibly due to a hydrolysis side-reaction of iPAc occurring at high temperature.[28] In fact, both commercial Solketal and iPAc had water contents of ~1, and 0.1-0.15 mol%, respectively (see Karl-Fisher tests and table A.3.1 in the appendix for details), and attempts to dehydrate Solketal failed because of its highly hydrophilic nature. This suggested that the investigated transesterification could be an acid-catalysed process. To explore this hypothesis, further reactions of Solketal and iPAc in the presence of

added AcOH (1-20 mol% respect to Solketal) were run. Results are shown in Table 3.1 and in the appendix, figure A.3.2.

Table 3.1: The reaction of iPAc with Solketal in the presence of added AcOH.

Entry	Added AcOH (mol%)[a]	Q[b]	T/t[b]	Conv. (%)[c]
1	none[d]	20	180 °C 3 h	57
2	1			68
3	5			69
4	20			83

[a] mol % with respect to Solketal. [b] Q was the iPAc:Solketal molar ratio; Q, T and t (temperature and time, respectively) were kept constant throughout runs 1-4. [c] Conversion of Solketal by GC/MS. [d] Traces of AcOH (<1% respect to the product Solketal ester **3a**) were detected at the end of the reaction (See ref. 18a).

With respect to the blank test (entry 1), the conversion of Solketal only slightly increased by using 1 and 5 mol% of AcOH (entries 2-3), while the selectivity towards ester **3a** was not altered (>98%). The effect still appeared limited even by quadrupling the acid amount (20 mol%, entry 4). A similar poor catalytic performance of AcOH was reported also for the closely related esterification of fatty acids with supercritical methyl acetate.[29] This led to conclude that an acid-catalysed pathway was hardly the only active mechanism for reactions of Figure 3.3.

An autoprotolysis equilibrium of Solketal could also be invoked.[30] Analogous (autoprotolysis) processes have been described for OH groups of both aliphatic alcohols and phenols at elevated temperatures in the absence of any catalyst.[31] Figure 3.4 illustrates two mechanistic hypotheses.

In the right-hand side red pathway, a high temperature hydrolysis of iPAc forms acetic acid which catalyzes the subsequent transesterification reaction through electrophilic activation. In left-hand side blue pathway, HT-induced autoprotolysis of Solketal generates an ion pair [$(ROH_2^+)(RO^-)$] whose components act cooperatively: the cation as a proton donor and the anion as a nucleophile. In both cases, the coproducts enol or enolate rapidly tautomerize to acetone. Also, traces of water present in the reactants might play a role in the autoprotolysis equilibrium.[32]

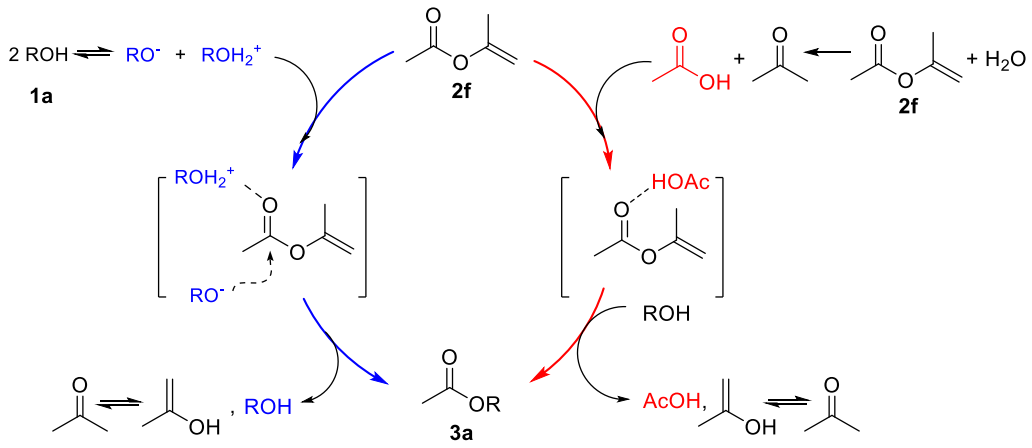

Figure 3.4: Transesterification of iPAc with Solketal. Right and left: electrophilic and cooperative activation of reactants, respectively.

Similar mechanisms were hypothesized also for esters **2a-e**; though, the corresponding acids (AcOH, HCO_2H, and $CH_3CH(OH)CO_2H$) were not observed. The concentration of these compounds (acids) could be below the detection limit because of the moderate hydrolysis of esters **2a-e** which were far less reactive than **2f** (see Figure 3.2).

Glycerol Formal (GLyF) was investigated as another model acetal of glycerol. GlyF was used as a 3:2 commercially available mixture of 5-hydroxy-1,3-dioxane (**4a**) and (1,3-dioxolan-4-yl)methanol (**4a'**) respectively. Isomers **4a**/**4a'** were set to react under conditions similar to those of Figure 3.3 (T=120-220 °C, 5 h) by using methyl acetate (**2a**), ethyl formate (**2d**), and iPAc (**2f**) in a 20-molar excess (Q=20).

The HT-reaction proved feasible for all the reactant esters, and as for Solketal, the best results were achieved with iPAc. At 220 °C and after 5 hours, the reaction of **2a**, **2d** and **2f** with GlyF showed a conversion of 13%, 54% and 96%, respectively, thereby confirming the same reactivity trend previously noticed, *i.e.* methyl acetate < ethyl formate < iPAc. The selectivity towards the expected formate and acetate derivatives of GlyF was always > 97%, and the structure of products (**5a-a**'and **5b-b'**) was confirmed by GC/MS and $^{1}H/^{13}C$ MNR analyses (Scheme 3.3). The mixtures of isomers **5a-a'** and **5b-b'** were isolated in 92% and 45% yields, respectively, in the same 3:2 isomeric ratio of the reagent (**4a** and **4a'**).

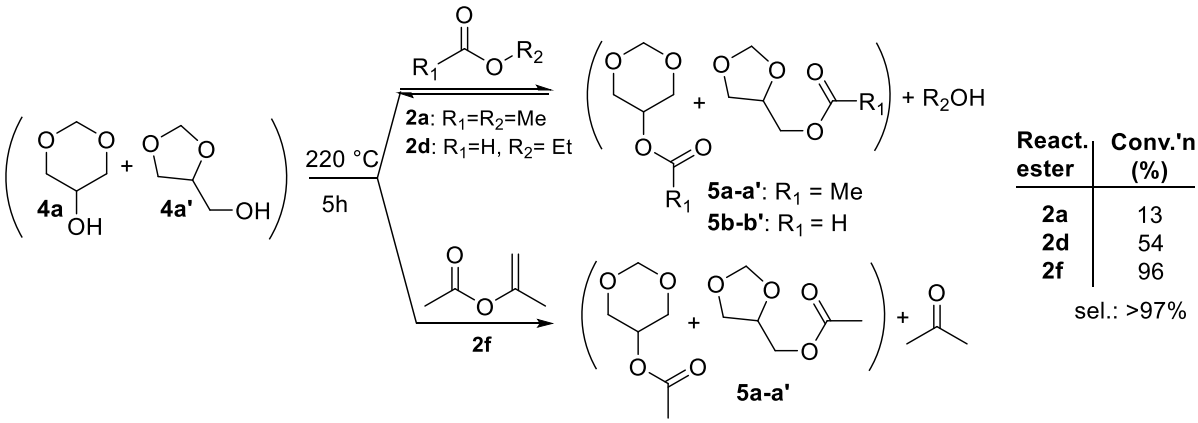

*Scheme 3.3: Batch HT-transesterification of esters **2a**, **2d** and **2f** with glycerol formal.*

Figure 3.5 shows some illustrative results of the effect of the temperature on conversion and selectivity of the HT-transesterification of iPAc with GlyF.

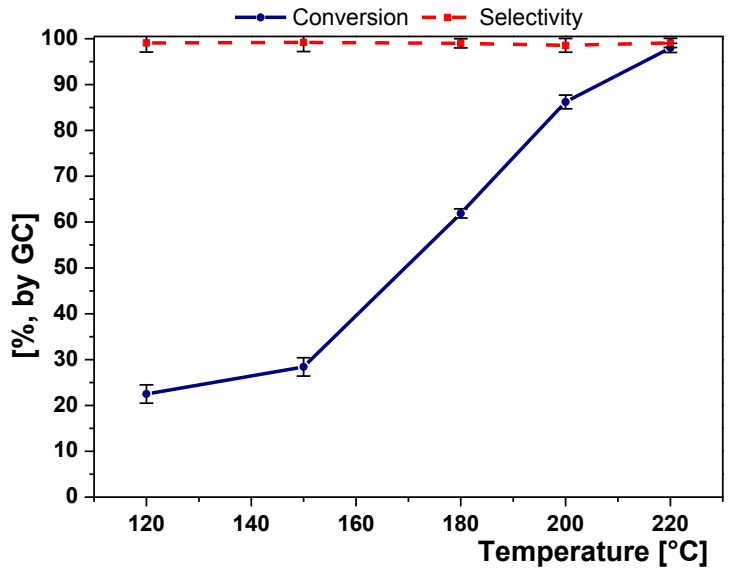

*Figure 3.5: Conversion and selectivity towards isomer esters **5a-a'** for the batch reaction between glycerol formal and iPAc in the range of 120-220 °C. Reaction conditions: molar ratio iPAc:GlyF (Q) = 20, t=5h.*

The conversion gradually improved from 24% up to a quantitative value as the temperature was increased from 120 to 220 °C. In this interval however, the comparison of Figures 3.3 and 3.5 showed that GlyF was systematically less reactive than Solketal. The same trend was noted before by our group in the reaction of GlyF and Solketal with light dialkyl carbonates,[7a] and similar findings were recently described also by others:[33] more in general, the application/implementation of the Hansen approach and the COSMO-RS model indicated that glycerol formal had not only a stronger structuration in the liquid state than Solketal, but formaldehyde-based acetals were less reactive than ketal acetone-based homologues, under acidic

(hydrolytic) conditions. Although this offers an interesting basis for discussion, the interpretation of experimental and modelling results is still far from explaining the different behaviour of GAs at a molecular level. Further investigations would be necessary to clarify such aspects.

Intriguingly, it is noteworthy a minor competitive process of transacetalization of GlyF with acetone (coproduced from iPAc) observed under the conditions of Figure 3.5. Traces of Solketal acetate (**3a**, <2%) were detected.

3.1.3.2 Continuous-flow HT-procedures for the acetylation of glycerol acetals with various esters

As already reported CF conditions generally allow a better control of reaction parameters (T, p, reactants ratio), an optimization of mass and heat transfer, recycling, recovery operations, and an overall process intensification compared to batch process.[34] This prompted us to explore the HT-transesterification of esters with both Solketal and glycerol formal also in the CF-mode. The CF-apparatus used in this work is composed by an empty tubular steel tube (¼"x 52 cm=diam. x length, inner void volume=2.1 mL) reactor filled with ground-glass Raschig rings. This inert filler (Raschig rings) could improve both mass/heat transfer and the contact between reagents and avoid preferential pathways of the reactants stream throughout the reactor (further details are in the experimental section).[35]

Initial tests were carried out to study the CF-reaction of Solketal with the same model esters used in batch, specifically methyl-, ethyl-, and propyl- acetates (**2a-c**), ethyl formate (**2d**), and iPAc (**2f**). Solutions of the selected compound **2** and Solketal in a 20:1 molar ratio, respectively, were delivered at 0.1 mL/min to the CF-reactor: at first, isobaric experiments were run at 50 bars, by progressively increasing the temperature from 225, to 250 and 275 °C. Then, in the same range of T, the effect of the pressure from ambient to 50 bars was investigated only for the case of iPAc.

Results are reported in Figure 3.6 which show the conversion of Solketal as a function of: i) T for different esters (Figure 3.6a); ii) p and T for the reaction of iPAc (Figure 3.6b). The selectivity towards the expected products, esters **3a** and **3b** was always above 97% and is not indicated.

Irrespective of the structure of the ester **2**, CF-runs required a higher temperature than batch experiments (Figures 3.2-3.3: 120-220 °C; Figure 3.6: 225-275 °C). This was consistent with the features of the CF-arrangement: given the volume of the reactor (2.1 mL) and the operating flow rate (0.1 mL/min), the residence time (τ) in the continuous mode was of only 20 min compared to 5 h of batch reactions. An extra energy input was therefore necessary to impart sufficiently fast kinetics to the CF-processes. Notwithstanding this, Figure 3.6a shows that esters **2** followed the same trend of reactivity of Figure 3.2. For example, when methyl acetate, ethyl formate and iPAc were used, the corresponding conversions of Solketal were 15, 51, and 93%, and 27, 67, and 100 % at 250 and 275 °C, respectively, thereby confirming iPAc as the best reagent also for the HT-transesterification reaction in the CF-mode. iPAc could afford a mild conversion (71%) even at 225 °C.

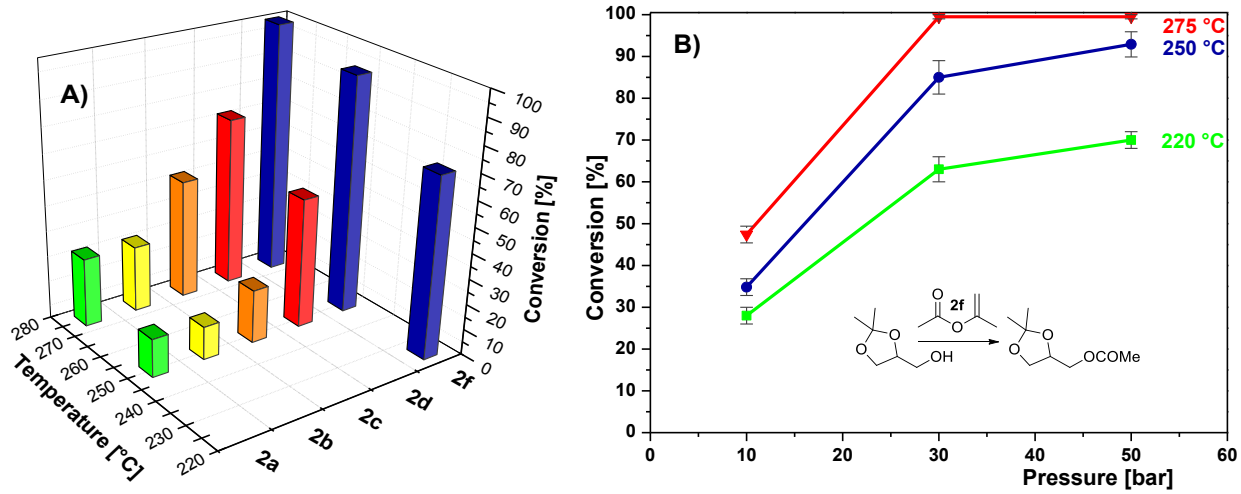

*Figure 3.6: The HT-transesterification of esters **2a**, **2d**, and **2f** with Solketal in the CF mode. A) Effect of the temperature on the reaction conversion at a constant p of 50 bar. B) only for the case of iPAc (**2f**): effect of the pressure on the reaction conversion at 225, 250, and 275 °C. Other conditions: molar ratio ester: Solketal (Q) =20, flow rate =0.1 mL/min. The selectivity is always >97%.*

The transesterification of iPAc with Solketal was clearly influenced by the pressure (Figure 3.6b). At each of the selected temperatures, the conversion was more than doubled when the pressure was increased from 10 to 30 bars: particularly, a quantitative reaction was achieved at 275 °C. Only minor improvements (≤ 8%) were noticed by further rising the pressure up to 50 bars at both 225 and 250 °C. By contrast, the conversion was lower than 15% for reactions run at the same temperatures, but at atmospheric pressure. These results highlighted the fundamental role of phase transitions in the investigated reactions. If the pressure was high enough, despite the high T, most of the reacting mixture was present as a condensed liquid phase in which the contact between iPAc and Solketal was effective for a productive reaction. On the contrary, an abrupt decrease of the conversion occurred below a threshold value of about 30 bars when reactants, especially the more volatile iPAc (bp = 97 °C), preferentially partitioned in the vapor phase inside the reactor. To get further insights into this aspect, the phase diagram of pure iPAc was also predicted by using an extended Antoine equation (for details, see Figure A.3.1 in appendix).[36] Under the assumption that the theoretic liquid-vapor pressure profile of pure iPAc could be an acceptable approximation for the binary mixtures of Figure 3.6b (that contained a large excess of the ester **2f**: Q=20), the change of conversion shown in the range of 10-30 bars well matched the predicted liquid-vapor transition of iPAc. Moreover, lowering the pressure could negatively affect the actual temperature of the reaction mixture due to the latent heat of vaporization.

Under the optimized conditions for T and p (275 °C and 30 bars), the iPAc:Solketal molar ratio (Q) was scaled down from 20 to 2 to examine the effect of the relative amounts of reactants. Experiments proved that the Q ratio could be substantially decreased: a quantitative process was still observed at Q=5, *i.e.* fourfold below the initial value. However, a further reduction impacted on the conversion of **1a** which did not exceed 82% at Q=2. In all cases, the selectivity towards ester **3a** was >98%. Considering the (limited) capacity of the CF-reactor, the results confirmed not only the reliable performance of the process, but

also the perspective for large-scale applications and further process intensification, in line with the principles of green engineering.[37] The CF-arrangement could operate virtually indefinitely once the high-temperature regime was reached. No catalyst had to be prepared, activated, recovered or disposed of, thereby simplifying both upstream and downstream operations for the delivery of reactants, the recovery of products and the recycle of the unconverted iPAc. Not to mention that iPAc was a cheap reactant available on a large scale, and that the integration of the process in a waste heat recovery system provided by a biorefinery, could efficiently relieve the energy demand of the reaction. In short, if the framework of energy existing within an industrial park could be used, high-temperature reactions could be driven at very competitive, if any, costs with a further valorization of "waste" energy.[4,37]

The CF-protocol proved efficient also for the reaction of iPAc with glycerol formal; though, in analogy to batch reactions, GlyF was less reactive than Solketal. At 30 bars, conversions of GlyF did not exceed 31% and 76% at 225 and 250 °C, respectively. Only at 275 °C, a substantially quantitative reaction was achieved (conv.: 97%): isomer esters **5a** and **5a'** were obtained in a ~3:2 ratio and with an overall transesterification selectivity > 96%.

3.1.3.3 Batch and continuous-flow reactions of glycerol with methyl and isopropenyl acetates.

The simplified system for the transesterification of Gas was then explored: batch and continuous-flow reactions were performed by using mixtures of glycerol and methyl or isopropenyl acetates (**2a** and **2f**) in a molar ratio (Q= **2:**Glyc) variable between 1 and 20. Batch (autoclave) tests were run at 120-220 °C. In the absence of any catalyst, the reactions proceeded with both esters. The whole spectrum of the observed products is shown in Scheme 3.4.

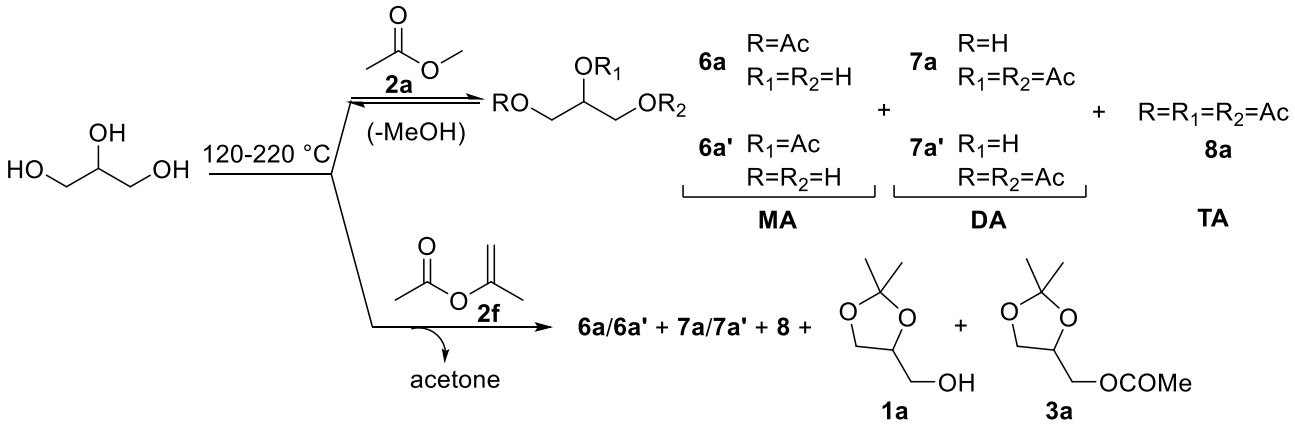

*Scheme 3.4: The batch reaction of Glyc with esters **2a** and **2f***

The structure of the acetals (**1a** and **3a**) and acetins (**6**, **7** and **8**) were assigned by GC/MS and by comparison to authentic samples when available (compounds **1a** and **8**).

The reaction conversion and the product distribution achieved under the best conditions, are described in Table 3.2. At 180°C, the batch transesterification of methyl acetate with glycerol yielded mono-, di-,

and tri-acetin products. As expected, increasing of the Q ratio and of the reaction time favoured the conversion, but it also resulted in the formation of derivatives of multiple transesterification (entries 1-3). The selectivity was elusive also for catalytic processes reported in literature[21c,22a]: although these were faster than our HT-reactions, not even triacetin **8** was obtained as a sole product despite the use of a large excess of ester **2a**.

Table 3.2: Batch and continuous-flow reactions of glycerol with methyl and isopropenyl acetate

Ent.	Cond. [a]	Ester	Q[b]	T/p/t (°C/bar/h)[c]	Conv. (%)[d]	Products distribution (%) [d]				
						6a-6a'	7a-7a'	8	1a	3a
1	Batch	**2a**	1	180/10/5	20	90	10			
2			5	180/10/24	44	80	29	1		
3			20	180/10/24	84	63	35	2		
4		**2f**	1	180/8/5	73	43	12	1	32	12
5			5	180/8/5	73	54	16	1	22	7
6			20	180/8/24	100			100		
7[e]	Cont.-flow	**2a**	20	300/50/5	78	65	33	2		
8[e]		**2f**	20	300/50/5	100			100		

[a] The catalyst (if present) and reactions conditions (batch or continuous-flow) used. [b] Q = Glycerol:ester molar ratio. [c] For batch reactions, p was the autogenous pressure in the autoclave reactor (entries 1-2, and 5-7). [d] Conversion of glycerol and products distribution determined by GC/MS. [e] Under continuous-flow conditions, a mixture of glycerol, ester and diglyme as a co-solvent in a 1:20:33 molar ratio, respectively, was used.

This behaviour is clearly due to the equilibria involved in the consecutive transesterification steps perturbed by the increasing amount of MeOH originated as a reaction co-product. In analogy to previously reported studies for catalytic processes,[38] the reversible nature of these reactions was confirmed when a solution of triacetin and methanol in a 1:10 molar ratio, respectively, was set to react at 180 °C for 5 hours. A mixture of diacetin, monoacetin, and glycerol in 17, 1, and 1 % amounts, respectively, was achieved.

As in the case of acetals, the HT-conversion of glycerol was higher with iPAc (**2f**) than with methyl acetate. At 180 °C and moderate Q ratios (1-5), batch reactions of **2f** yielded complex mixtures including not only acetins, but also Solketal (**1a**) and its methyl ester (**3a**) (entries 4-5). These results allowed to conduct a tandem non-catalytic process by exploiting the acetone released during the reaction that formed **1a** and **3a** through a competitive acetalization of glycerol induced by the acetone released during the transesterification with iPAc (Scheme 3.2). According to our knowledge this tandem behaviour was previously noted only once in literature for the reaction of iPAc with carbohydrates in presence of

molecular iodine as catalyst.[39] The feasibility of the acetalization reaction was confirmed also by an additional experiment in which a mixture of glycerol and acetone in a 1: 20 molar ratio, respectively, was set to react at 180 °C for 5 hours. A 75% conversion was achieved with full selectivity towards Solketal **1a**. This test proved also that in the same experimental conditions (Q=20, T=180°C, 5h) the acetylation of Glyc with iPAc is kinetically favoured compared to the acetalization of Glyc with acetone: in the first case a quantitative conversion of Glyc and full acetylation was obtained (TA Yield=99%, entry 6, table 3.2) while only a 70% conversion of Glyc was obtained with acetone in the same catalyst-free HT conditions.

These first achievements with an equimolar ratio glycerol:iPAc prompted us to explore several different reaction conditions to afford a non-catalytic tandem acetylation/acetalization reaction but the results were unsatisfactory: we managed roughly to enhance the selectivity towards the acetalized products, but it was hard to obtain exclusively **3a**. For instance, the lowering of the reaction temperature (T=150°C, figure A.3.3) took to the collapse of Glyc conversion (73 to 39%) not supported by a higher selectivity towards **1a-3a**, while the conversion was slightly improved (up to 88%) increasing the temperature to 200-220 °C but there was a shift towards the formation of acetylation products **6-8**. Far more attractive was the reaction conducted in the presence of CO_2 as inert gas that likely contributes to shift the liquid/gas equilibrium of the released acetone as reported in a previous work regarding the esterification of glycerol with dimethylcarbonate.[7c] As reported in appendix (fig. A.3.4), the reaction was definitively slower (15h to reach conversion of Glyc >80%) but experiments proved that the addition of CO_2 allowed to control the thermal reaction of iPAc and Glyc for a more selective synthesis of acetalization products: the overall selectivity towards **1a**-**3a** increased from 27% without the addition of CO_2 to 65% when 60 bar of CO_2 are present. Two main reasons could explain this trend, although they are far from being exhaustive: i) CO_2 presence affects the reactivity of liquid-vapor phases and their relative partitioning, especially acetone (bp=58°C, the most volatile compound in the autoclave) that is more concentrated in the liquid phase, hence increasing Glyc-acetone contact; ii) the slight acidic nature of CO_2 in supercritical phase favour the acetalization reaction compared to acetylation reaction.
However, it was not possible to shift completely the selectivity towards **3a** with a catalyst-free approach and the following section 3.2 will describe further studies on how to achieve a tandem catalytic procedure.

Finally, as shown in table 3.2, a larger iPAc excess substantially inhibited the acetalization reaction and, at the same time, the irreversible loss of acetone from **2f** promoted not only a quantitative process, but also the exhaustive acetylation of glycerol towards triacetin **8** (entry 6, Q=20). This derivative was isolated in 99% yield while the excess iPAc could be easily recovered and reused.

In continuous-flow, mixtures of mono-, di-, and tri-acetin products were still obtained with methyl acetate (entry 7, table 3.2), while the reaction of **2f** proved successful for the selective synthesis of triacetin (entry 8, table 3.2). Although preliminary, these data proved the concept that iPAc was not only effective for the conversion of GAs into the corresponding methyl esters, but also for the straightforward transesterification of glycerol into its fully acetylated derivative triacetin.

This outcome also raised two challenging perspectives. i) The CF- transesterification of crude glycerol as obtained from biodiesel production. The here presented HT-strategy would avoid costly techniques required for the purification of off-grade glycerol and common drawbacks due to the poisoning of

catalysts by the impurities of the crude reagent (salts, soaps, etc.).[40] ii) A selective one-pot preparation of Solketal ester (**3a**) by reacting glycerol with iPAc. The latter will be presented in the following section.

3.1.4 Conclusions

In conclusion, the here described HT-processes exemplify an archetype of clean reactions for the conversion of glycerol and its acetals to their ester derivatives, by using innocuous reagents and producing minimal, if any, wastes. The overall protocol discloses a new perspective for the upgrading of renewables, though for a genuine sustainable path, the procedure could in principle be conveniently integrated within a biorefinery plant where synthetic operations may take advantage of modern technologies for the recovery of waste/excess heat and the recycle of reactants/solvents. The complete acetylation of GAs (i.e., Solketal and glycerol formal acetate, yields>99%) and glycerol (Triacetin Yield>99%) was achieved in both batch and continuous-flow processes by using isopropenyl acetate as acetylating agent that stood out among the other organic acetate and formate tested. Its superior acetylating activity is clearly due to its reactivity since, in presence of a hydroxyl group, it results in the formation of an ester and an enol (i.e. 2-hydroxypropene) that quickly isomerises into acetone, making the overall transformation irreversible. Intriguingly, we noted that the acetone formed can react with the vicinal hydroxyl groups contained in glycerol and lead to the concurrent formation of acetal species (i.e. Solketal and Solketal acetate) through a tandem non-catalytic process. Unfortunately, under the explored catalyst-free HT conditions it was not possible to tune the experimental parameters in order to devise a 100% carbon efficient tandem process in which all the acetone released by the acetylation process is quantitively used in the following acetalization step. This finding, however, paves the way for the study of the tandem catalytic process that will be illustrated in the next section.

3.1.5 Experimental section

3.1.5.1 General

Solketal (**1a,** purity=97%, the 6-membered ring isomer is present in amount ≈3%), Methyl acetate (**2a**), ethyl acetate (**2b**), propyl acetate (**2c**), ethyl formate (**2d**), ethyl lactate (**2e**) and isopropenyl acetate (**2f**), glycerol formal [commercially available as a 3:2 mixture of 5-hydroxy-1,3-dioxane (**4a**) and (1,3-dioxolan-4-yl)methanol (**4a'**)], 1,2,3-trihydroxypropane (glycerol), acetone, 1-Methoxy-2-(2-methoxyethoxy)ethane (Diglyme) were ACS grade from Aldrich and were used as received.

Commercially available esters used in this study were safe and nontoxic compounds. Reactants **2a**-**2f** were flammable products with hazardous (H) phrases and precautionary statements (P) as H225, P210, and P403 + P235. However, they were low toxic compounds. For example, LD50 (oral, acute) for methyl-, ethyl, and propyl acetates are 5001 mg/kg, 5620 mg/kg, and 6640 mg/kg.[41] Ethyl lactate is even edible and present in many foods. Overall, such esters were safer than acids or anhydrides as esterification reagents.

All the reactions described in the experimental and the results and discussion sections, were repeated twice to ensure reproducibility. Under the same set of conditions (T, p, flow rates) duplicated tests afforded values of conversion and amount of products (determined by GC/MS) which differed by less than 5% from one experiment to another.

Analysis instruments. GC/FID analysis were run using a Perkin Elmer Elite-624 capillary column (L=30 m, Ø=0.32 mm, film thickness=1.8 μm). The following conditions were used. Carrier gas: N_2; flow rate: 3.5 mL min-1; split ratio: 1:1; initial T: 50 °C (2 min), ramp rate: 15 °C min-1; final T: 240 °C (1 min).

GC/MS (EI, 70 eV) analysis were run using a Grace AT-624 capillary column (L=30 m, Ø=0.32 mm, film thickness=1.8 μm). The following conditions were used. Carrier gas: He; flow rate: 1.2 mL min^{-1}; split ratio: 10:1; initial T: 60 °C (2 min), ramp rate: 20 °C min^{-1}; final T: 220 °C (2 min).

^1H NMR were recorded at 400 MHz, ^{13}C spectra at 100 MHz and chemical shift were reported in δ values downfield from TMS; $CDCl_3$ was used as solvent.

Products characterization. The product esters included: (2,2-dimethyl-1,3-dioxolan-4-yl)methyl acetate (**3a**: Solketal acetate, (2,2-dimethyl-1,3-dioxolan-4-yl)methyl formate (**3b**: Solketal formate), (2,2-dimethyl-1,3-dioxolan-4-yl)methyl 2-hydroxypropanoate (**3c**: Solketal lactate), a 3:2 isomer mixture of 1,3-dioxan-5-yl formate and (1,3-dioxolan-4-yl)methyl formate (**5a-a'**: isomers of glycerol formal formate), a 3:2 isomer mixture of 1,3-dioxan-5-yl acetate and (1,3-dioxolan-4-yl)methyl acetate (**5b-b'**: isomers of glycerol formal acetate), and triacetin (**8**) (see Schemes 3.2, 3.3 and 3.4 for detailed structures). These compounds were purified and characterized by MS, ^1H and ^{13}C NMR. All data including also isolated yields are reported in the appendix (figure A.3.5-26).

3.1.5.2 Batch tests

Batch apparatus. The autoclaves used in this work were in-house manufactured by the workshop of Ca' Foscari University. They were two 100-mL stainless-steel reactors each equipped with a thermocouple to monitor the temperature, a pressure gauge and two high pressure taps.

Batch reactions. Mixtures of acetal **1a** or **4a-a'** and each ester **2a-f** were prepared by varying the reactant molar ratio (Q= ester:acetal) from 1 to 20, the (excess) ester serving both as a reagent and a solvent. Each homogeneous solution was charged in a flat-bottomed glass reactor fitted with a magnetic stirrer and a glass stopper onto which a capillary tube was welded (for the compensation of the external pressure). The flask was placed inside the autoclave (this expedient avoided the contact of reagents with the autoclave walls, thereby ruling out metal catalysis). The autoclave was sealed, degassed via three vacuum-nitrogen cycles, and then electrically heated at the desired temperature (120-220 °C). The reaction was allowed to proceed from 1 to 24 h, during which the reacting mixture was kept under magnetic stirring. The observed autogenous pressure was in the range 2-20 bar. At the end of the experiment the reactor was rapidly cooled to rt and vented. The reaction mixtures were analysed by GC/FID or GC/MS.

The same procedure was used also to run experiments with: i) added AcOH in a 1-20 mol% amount with respect to the reacting acetal; ii) glycerol in place of acetals. In this case, irrespective of the reactants molar ratio (ester:glycerol, from 1 to 20), starting mixtures were biphasic, but turned to homogeneous solutions at the end of the experiments.

3.1.5.3 Continuous-flow tests

Continuous-flow apparatus. The apparatus used for the investigation was in-house assembled according to Figure 3.7. An HPLC Pump (Shimazdu LC-10AS) was used to send the reactants mixture (substrate, selected ester and a co-solvent where necessary) to a stainless-steel tubular reactor (L=0.52 m, Ø=1/4", inner volume ~2.1mL) filled with Raschig glass. The reactor was heated at the desired temperature by means of an oven (HP 5890 GC oven). At the outlet of the oven, the reacting mixture was allowed to cool to rt by flowing through an additional segment of an empty capillary stainless-steel tube (L=0.70 m, Ø=1/16") which was further cooled by a fan. The mixture was then conveyed to a Rheodyne valve (7725i) with a 100 µL loop by which samples were taken up for GC and GC/MS analyses. Finally, the liquid stream entered a manual Swagelok KPB1N0G412 back pressure regulator (BPR) equipped with an electronic pressure sensor.

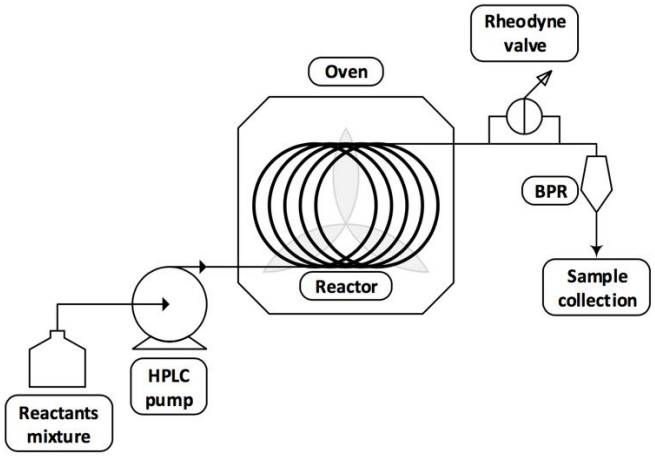

Figure 3.7: Schematic diagram for the in-house built continuous-flow apparatus

Continuous-flow (CF) reactions. Homogeneous solutions of acetal **1a** or **4a-4a'** and the selected ester (**2a-f**) were prepared by mixing the reactants in different molar ratios from 5 to 20. Before any reaction, the CF-reactor (a stainless-steel tubular reactor: 0.52 m x 1/4'' filled with ground-glass Raschig rings) was primed and conditioned by delivering the chosen solution of reactants (10 mL) at room temperature and atmospheric pressure, and at a flow rate of 0.1 mL/min. The reaction was then started by setting the temperature and the pressure at the desired values (200–275 °C and 1-50 bars, respectively). T and p were controlled by a thermostatic oven and a back-pressure regulator. Once an amount of the reacting mixture equalled 5 times the inner volume of the reactor (2.1 mL) was allowed to flow, samples at the outlet of the reactor were taken up at regular intervals of 30 minutes through a Rheodyne valve, and analysed by GC/FID and GC/MS. At the end of the experiment, the oven was set to 100 °C and the reactor was flushed with methanol (100 mL at 0.5 mL/min), cooled to room temperature and vented.

A similar procedure was used also for the CF-reactions of glycerol with both methyl and isopropenyl acetates. Diglyme was necessary as a co-solvent due to the poor mutual miscibility of the reactants.

Homogeneous solutions were achieved by mixing glycerol, the selected ester (**2a** or **2f**), and diglyme in a 1:1-20:33 molar ratio, respectively. This mixture was used to run experiments described in Table 3.2.

3.1.6 References

[1] a) J. J. Bozell and G. R. Petersen, *Green Chemistry*, 2010, **12**, 539-554; b) M. Pagliaro, *Glycerol: The Renewable Platform Chemical*, Elsevier, 2017; c) C. Len and R. Luque, *Sustainable Chemical Processes*, 2014, **2**, 1.

[2] a) D. Fabbri, V. Bevoni, M. Notari and F. Rivetti, *Fuel*, 2007, **86**, 690-697; b) S. Saka and Y. Isayama, *Fuel*, 2009, **88**, 1307-1313; c) Saka, S.; Isayama, Y. *Fuel* **2009**, *88* (7), 1307–1313. c) V. Rathore, S. Tyagi, B. Newalkar and R. Badoni, *Industrial & Engineering Chemistry Research*, 2014, **53**, 10525-10533.

[3] It should be noted that due to the presence of water and free fatty acid in natural oils, transesterification reactions with both DMC and methyl acetate (Scheme 3.1) also yielded minor amounts of glycerol carbonate and acetic acid, respectively. a) K. T. Tan and K. T. Lee, *Renewable and Sustainable Energy Reviews*, 2011, **15**, 2452-2456; b) S. Marx, *Fuel Processing Technology*, 2016, **151**, 139-147.

[4] R. T. Ng, D. H. Tay and D. K. Ng, *Energy & fuels*, 2012, **26**, 7316-7330.

[5] V. F. Marulanda, *Journal of Cleaner Production*, 2012, **33**, 109-116..

[6] a) S. Glisic and D. Skala, *The journal of supercritical fluids*, 2009, **49**, 293-301; b) J. Van Kasteren and A. Nisworo, *Resources, Conservation and Recycling*, 2007, **50**, 442-458.

[7] a) M. Selva, S. Guidi and M. Noè, *Green Chemistry*, 2015, **17**, 1008-1023.

c) S. Guidi, R. Calmanti, M. Noè, A. Perosa and M. Selva, *ACS Sustainable Chemistry & Engineering*, 2016, **4**, 6144-6151.

[8] Z. Ilham and S. Saka, *SpringerPlus*, 2016, **5**, 923.

[9] B. Nebel, M. Mittelbach and G. Uray, *Analytical chemistry*, 2008, **80**, 8712-8716.

[10] X. Liao, Y. Zhu, S.-G. Wang, H. Chen and Y. Li, *Applied Catalysis B: Environmental*, 2010, **94**, 64-70.

[11] T. Watanabe, M. Sugiura, M. Sato, N. Yamada and K. Nakanishi, *Process Biochemistry*, 2005, **40**, 637-643.

[12] S. Cabrera, J. Rojas and A. Moreno, *Journal of Food Nutritional Research*, 2020, **8**, 172-182.

[13] Y. Taguchi, A. Oishi, Y. Ikeda, K. Fujita and T. Masuda, JP Patent 298099, 2000.

[14] A. Behr and T. Seidensticker, in *Chemistry of Renewables*, Springer, 2020, pp. 89-109.

[15] (a) C. Odibi, M. Babaie, A. Zare, M. N. Nabi, T. A. Bodisco and R. J. Brown, *Energy Conversion and*

Management, 2019, **198**, 111912; (b) M. Tabatabaei, M. Aghbashlo, B. Najafi, H. Hosseinzadeh-Bandbafha, S. F. Ardabili, E. Akbarian, E. Khalife, P. Mohammadi, H. Rastegari and H. S. Ghaziaskar, *Journal of cleaner production*, 2019, **223**, 466-486.

[16] https://www.globenewswire.com/news-release/2019/07/15/1882588/0/en/Triacetin-Glyceral-Triacetate-Market-To-ReachUSD-255-6-Million-By-2026-Reports-And-Data.html (accessed on 15/10/2020)

[17] a) G. Yadav and A. Joshi, *Clean technologies and environmental policy*, 2002, **4**, 157-164; b) 1. L. R. Odell, J. Skopec and A. McCluskey, *Forensic science international*, 2006, **164**, 221-229.

[18] a) N. Venkatesha, Y. Bhat and B. J. Prakash, *RSC advances*, 2016, **6**, 45819-45828; b) M.-Y. Huang, X.-X. Han, C.-T. Hung, J.-C. Lin, P.-H. Wu, J.-C. Wu and S.-B. Liu, *Journal of catalysis*, 2014, **320**, 42-51; c) B. O. Dalla Costa, H. P. Decolatti, M. S. Legnoverde and C. A. Querini, *Catalysis Today*, 2017, **289**, 222-230; d) J. R. Dodson, T. d. C. Leite, N. S. Pontes, B. Peres Pinto and C. J. Mota, *ChemSusChem*, 2014, **7**, 2728-2734; e) A. Perosa, A. Moraschini, M. Selva and M. Noè, *Molecules*, 2016, **21**, 170; f) E. Garcia, M. Laca, E. Pérez, A. Garrido and J. Peinado, *Energy & fuels*, 2008, **22**, 4274-4280.

[19] a) J. Sun, X. Tong, L. Yu and J. Wan, *Catalysis Today*, 2016, **264**, 115-122; b) M. Rezayat and H. S. Ghaziaskar, *Green Chemistry*, 2009, **11**, 710-715.

[20] B. C. Ranu, S. S. Dey and A. Hajra, *Green Chemistry*, 2003, **5**, 44-46.

[21] a) G. Morales, M. Paniagua, J. A. Melero, G. Vicente and C. Ochoa, *Industrial & engineering chemistry research*, 2011, **50**, 5898-5906; b) B. A. Meireles and V. L. P. Pereira, *Journal of the Brazilian Chemical Society*, 2013, **24**, 17-57; c) M. Khayoon and B. Hameed, *Applied Catalysis A: general*, 2013, **460**, 61-69.

[22] a) S. Sandesh, P. K. R. Kristachar, P. Manjunathan, A. Halgeri and G. V. Shanbhag, *Applied Catalysis A: General*, 2016, **523**, 1-11; b) N. Mallesha, S. P. Rao, R. Suhas and D. C. Gowda, *Journal of Chemical Research*, 2011, **35**, 536-539.

[23] a) E. Vänttinen and L. T. Kanerva, *Journal of the Chemical Society, Perkin Transactions 1*, 1994, 3459-3463.

b) T. Sakai, T. Kishimoto, Y. Tanaka, T. Ema and M. Utaka, *Tetrahedron letters*, 1998, **39**, 7881-7884.

[24] a) T. Zeng, G. Song and C.-J. Li, *Chemical Communications*, 2009, 6249-6251; b) R. Pelagalli, I. Chiarotto, M. Feroci and S. Vecchio, *Green Chemistry*, 2012, **14**, 2251-2255; c) I. Chiarotto, *Synthetic Communications*, 2016, **46**, 1840-1847; d) G. Assaf, G. Checksfield, D. Critcher, P. J. Dunn, S. Field, L. J. Harris, R. M. Howard, G. Scotney, A. Scott and S. Mathew, *Green chemistry*, 2012, **14**, 123-129.

[25] M. B. Smith, *March's advanced organic chemistry: reactions, mechanisms, and structure*, John Wiley &

Sons, 2020.

[26] A. K. Baev, *Specific intermolecular interactions of organic compounds*, Springer Science & Business Media, 2012.

[27] a) T. H. T. Vu, H. T. Au, T. H. T. Nguyen, T. T. T. Nguyen, M. H. Do, N. Q. Bui and N. Essayem, *Catalysis letters*, 2013, **143**, 950-956.

[28] D. S. Noyce and R. M. Pollack, *Journal of the American Chemical Society*, 1969, **91**, 7158-7163.

[29] P. Campanelli, M. Banchero and L. Manna, *Fuel*, 2010, **89**, 3675-3682.

[30] D. L. Purich and R. D. Allison, *Handbook of biochemical kinetics: a guide to dynamic processes in the molecular life sciences*, Elsevier, 1999, pp. 75

[31] a) I. Vieitez, C. da Silva, I. Alckmin, G. R. Borges, F. C. Corazza, J. V. Oliveira, M. A. Grompone and I. Jachmanián, *Renewable Energy*, 2010, **35**, 1976-1981; b) Y. Horikawa, Y. Uchino and T. Sako, *Chemistry letters*, 2003, **32**, 232-233.

[32] (a) M. Roses, C. Rafols and E. Bosch, *Analytical Chemistry*, 1993, **65**, 2294-2299; (b) G. Fonrodona, C. Ràfols, E. Bosch and M. Rosés, *Analytica chimica acta*, 1996, **335**, 291-302.

[33] L. Moity, A. Benazzouz, V. Molinier, V. Nardello-Rataj, M. K. Elmkaddem, P. De Caro, S. Thiebaud-Roux, V. Gerbaud, P. Marion and J.-M. Aubry, *Green Chemistry*, 2015, **17**, 1779-1792.

[34] a) G. Jas and A. Kirschning, *Chemistry–A European Journal*, 2003, **9**, 5708-5723; b) C. Wiles and P. Watts, *Green Chemistry*, 2012, **14**, 38-54.

[35] a) P. Harriott, *Chemical reactor design*, CRC Press, 2002; b) E. E. Kwon, H. Yi and Y. J. Jeon, *Chemosphere*, 2014, **113**, 87-92.

[36] Z. Wang, B. Wu, J. Zhu, K. Chen and W. Wang, *Fluid phase equilibria*, 2012, **314**, 152-155.

[37] P. T. Anastas and J. B. Zimmerman, *Environmental Science and technology*, 2003, **37**, 94A-101A

[38] D. E. Lopez, J. G. Goodwin Jr, D. A. Bruce and E. Lotero, *Applied Catalysis A: General*, 2005, **295**, 97-105.

[39] D. Mukherjee, B. Ali Shah, P. Gupta and S. C. Taneja, *The Journal of organic chemistry*, 2007, **72**, 8965-8968.

[40] S. Guidi, M. Noè, P. Riello, A. Perosa and M. Selva, *Molecules*, 2016, **21**, 65.

[41] www.sigmaaldrich.com, (accessed on 20/10/2020; see, SDS).

3.2 Development of a catalytic tandem process for the concurrent acetylation/acetalization of glycerol

3.2.1 Introduction

In the previous work we demonstrated the outstanding performances of enol esters (i.e. isopropenyl acetate, iPAc) as acetylating agent and the chances to exploit the by-produced acetone to acetalize vicinal hydroxyl groups. iPAc is a wide commercial and unexpensive compound employed as a starting material for the production of acetyl acetone, which is an intermediate for the synthesis of a plethora of biologically active compounds, APIs and dyes. The industrial route for the production of iPAc is based on the reaction between ketene and acetone in presence of a strong acid catalyst.[1] Although the industrial use of ketene represent a cause of concern due to its high toxicity (prolonged exposure to ketene gave adverse effects similar to that revealed for the exposure to phosgene)[2], its production could be considered renewable since it is currently achieved through pyrolysis of acetic acid. Nonetheless iPAc is evaluated as a relatively harmless and safe-to-handle compound.[3] The valuable insight regarding the use of iPAc as a trigger for tandem acetylation/acetalization reactions is further deepened in the present section.

The previous thermal (catalyst-free) study on the reaction of iPAc with glycerol demonstrated the feasibility of the tandem process but did not allow the control of product distribution: at T>150°C and with a molar ratio glycerol:iPAC=Q=1, a mixture of the acetylated products was obtained along with a variable amount of cyclic acetals (Solketal and Solketal acetate) that were derived from a tandem acetalization reaction promoted by acetone release during the transesterification step (Scheme 3.4). The acetylation was clearly favoured respect to acetalization, and it was not possible to devise a 100% carbon efficiency tandem process in which the whole amount of acetone released during the reaction was used. This is probably due to the high temperature used that affect the liquid-vapor phases (hence the relative portioning of the low-boiling point acetone) and favoured kinetically acetylation products respect to acetalized ones, as already reported in previous works.[4,5]

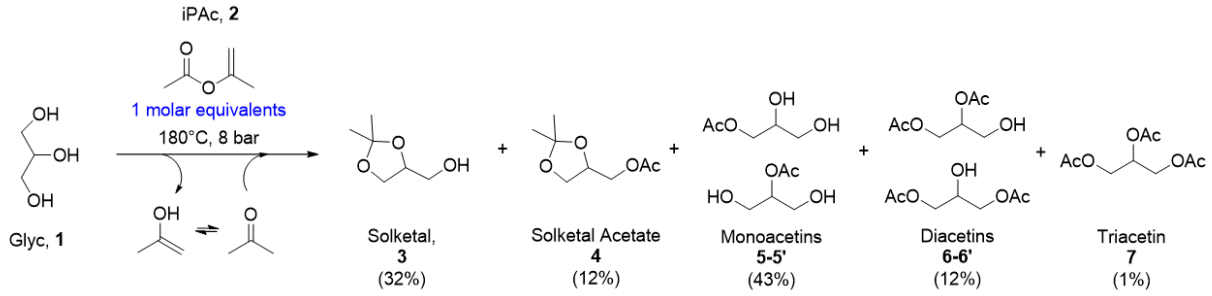

Scheme 3.5: The tandem reaction of glycerol promoted by isopropenyl acetate

Moreover, acetalization appears slower than acetylation reaction in catalyst-free reaction. A catalytic process conducted at lower temperature may be a strategy to reach the tandem scope but a closer focus on the implied mechanisms is mandatory. As already reported in the introduction (paragraph 1.3.2) acetalization of glycerol is widely studied and it is typically catalysed by Brønsted acids (H_2SO_4, HCl, formic acid, p-toluene sulfonic acid)[6,7] or Lewis acids (AlF_3, $ZnCl_2$tungstophosphoric acid etc.)[8,9] while acetylation is a classic equilibrium process that can be easily accelerated by acid or base catalysts.[10,11] According to our knowledge, Taneja et al. published the unique research work that provides for the tandem exploitation of iPAc through the concurrent acetalization/acetylation of carbohydrates. In this case, the authors developed a facile experimental protocol for a single-step, fast and solvent-free reaction for the synthesis of acetalized and acetylated sugars with moderate to high yields. The authors claimed a strict control on the outcome of the reaction through the variation of temperature: at -20 °C it was possible to obtain the acetal acetate as a single product from D-glucose while at higher temperature (T = 80 °C) the polyacetylated form was the major product.[4] However this protocol used molecular iodine as catalyst, requires a tedious work-up for the purification and the catalyst cannot obviously be reused hence it cannot be considered safe nor green. More recently our group reported another route for the use of iPAc in a tandem reaction with 1,2-diols to obtain simultaneously acetals and acetylated products (Scheme 3.6) in the presence of cyclopenthylmethylether (CPME) as solvent and amberlyst-15 (Amb15, an ionic exchange resins characterized by a strong Brønsted acidity due to sulfonic groups) at 50 and 30 °C in batch and continuous-flow mode respectively.

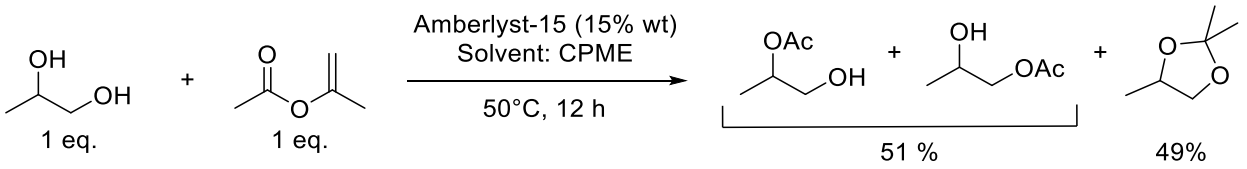

Scheme 3.6: Tandem reaction of iPAc with 1,2-propanediol

Based on this work and bearing in mind the stability and activity of Amb15 for both acetalization and acetylation reactions reported in literature respect to other heterogeneous acids such as K-10, montmorillonite, niobic acid and zeolites (HZSM-5 and HUSY), we decided to test this catalyst for the model study of the tandem reaction with glycerol.[4,12,13]

Another issue that we had to face was the immiscibility of Glycerol and iPAc in a molar ratio iPAc: Glyc =Q=1-20. As reported in previous work, polar aprotic solvents (such as CPME, THF, CH_3CN, DMF) could be useful to the scope of the reaction while other classic solvents like Et_2O, toluene or dichloromethane failed to promote conversion.[4,5] Polar protic solvents such as alcohols could not be obviously used for their intrinsic reactivity in this reaction. Nonetheless the solvency properties and the mild acetylating activity of acetic acid prompted us to consider its use as solvent for the reaction.[14]

3.2.2 Aim and summary of the research

The main aim of this work is the improvement of the degree of control on the selectivity of the reaction between glycerol and isopropenyl acetate in order to tune product distribution. Acetic acid was selected as reaction solvent and Amberlyst 15 as heterogeneous Brønsted catalyst: the optimization of the reaction conditions allowed to achieve complete glycerol conversion and to control producs distribution (i.e., equimolar production of Solketal acetate and triacetin). Hence, we decided to delve into the mechanisms governing the simultaneous reactions involved: the use of deuterated acetic acid allowed to determine the key role of acetic anhydride formed in situ during the reaction. Through these new insights, it was possible to tune the parameters of the reaction in order to have a quantitative conversion of glycerol and a yield in Solketal acetate >90%.

3.2.3 Results and discussion

3.2.3.1 The tandem synthesis of Solketal acetate and triacetin

As reported in the introduction, the identification of the solvent and the catalyst was the first step in the design of experimental conditions for the reaction of Glyc (**1**) with iPAc (**2**). After screening several solvents, including CPME and 2-methoxyethyl ether (Diglyme) that worked well for this reaction, we opted for acetic acid (AcOH) in large excess, both for its solvent properties as well as for its non-toxicity and its acetylating reactivity that could be complementary to that of iPAc. The commercial resin Amb15 was chosen as a model catalyst and used to prove the feasibility of Brønsted acid catalysts for this reaction.

First, reactions were carried out using a solution of Glyc (**1**, 1 mmol) in AcOH (10 mL; 0.1 M), a variable amount of iPAc (**2**; the molar ratio Q= **2**:**1** = 1–10) and Amb15 (15 mg; 15 wt%) as the catalyst. Control experiments were performed over a range of temperatures 30–70 °C, and times varying between 4–24 h. In all cases, the observed products were that reported in Scheme 3.5 and table 3.3: Solketal (**3**) and Solketal acetate (**4**) (along with trace amounts of the corresponding 6-membered ring isomers **3'**: 2,2-dimethyl-dioxane-5-ol; **4'**: 2,2dimethyl-1,3-dioxan-5-yl acetate, not reported in figure)[15]; two regioisomers of both glycerol monoacetate (monoacetins: **5/5'**) and glycerol diacetate (diacetins, **6/6'**); and glycerol triacetate (triacetin, **7**). The structures of derivatives **3–7** were assigned by GC/MS and NMR analyses and by comparison, when possible, with authentic commercial samples. Under the above described conditions, blank tests were also carried out either without a catalyst or without iPAc. Results are summarized in table 3.3.

The reaction of an equimolar mixture of **1** and **2** (Q = 1) showed that a quantitative conversion could be reached after 4 h even at the lowest investigated temperature (30 °C, entry 1): the overall selectivity towards GAs (3 + 4) was 71% while at higher temperatures the amounts of GAs decreased in favor of glyceryl esters: mono-acetins became the major products (5 + 5′ = 41–56%) along with diacetins (6 + 6′ = 7–8%) and triacetin (7: 6–13%) (entries 2 and 3). It was clear that the increase of the temperature modified the product distribution and these results were consistent with the previous studies that demonstrated

the higher kinetics of acetalization compared to acetylation in catalytic reactions, though the latter became predominant by increasing the temperature.[4,5] The tandem acetylation–acetalization selectivity could however not be controlled, as confirmed by prolonging the reaction for 24 h at 30 °C: under such conditions, both the transesterification and acetalization reached equilibrium with an amount of diglyceryl esters and triacetin (**6**+**6**'+**7**=80%) significantly exceeding that of acetal products (**3** + **4**= 20%) (entry 4). The product distribution was not altered by doubling the reaction time to 48 h.

Blank experiments carried out in the absence of iPAc (entries 5 and 6) proved that AcOH acted not only as a solvent but also contributed to the formation of glyceryl esters. However, notwithstanding the large molar excess of AcOH with respect to glycerol (AcOH:Glyc=175:1), only mixtures of mono- and diacetins were obtained with moderate Glyc conversions (31% and 71% at 30 °C and 50 °C, respectively). Longer 24 h tests at 30–70 °C further proved that the reaction of glycerol with AcOH was in no way a selective process (see figure A.3.27 in the appendix). Acetic acid was undeniably a far less active acetylating agent than iPAc and these results were in accordance with the ones already reported in literature.[12b]

The blank experiment in the absence of Amberlyst-15 demonstrated the need for an acidic catalyst since negligible conversion (1%) was observed after 24 h at 30 °C (entry 7) hence proving the importance of the added catalyst at such low temperature.

Significantly better selectivity of the tandem sequence was finally achieved at 30 °C, by simultaneously increasing the molar ratio (Q=3-10) and the reaction time (4 to 24 h). Indeed, this increase brought about a progressive and concurrent increase of Solketal acetate (**4**) and triacetin (**7**) at the expense of diacetins (**6/6'**) whose amount dropped (entries 4, 8–10) by improving the molar ratio Q. Thereafter, at Q = 10, a further control test prolonged for 32 h showed that compounds **4** and **7** could be obtained as sole products with a comparable selectivity of 51 and 49% i.e. in a 1:1 ratio (entry 11). These results proved our concept demonstrating for the first time that through a cooperative effect between the electrophilic reactivity of isopropenyl acetate, the solvent/acetylating properties of AcOH, and the use of an acid catalyst, conditions could be tuned to control the product distribution of the tandem sequence: glycerol was successfully upgraded into two derivatives by transesterification and acetalization reactions. An additional optimization study proved that the same (1:1) selectivity profile for compounds **4** and **7** was obtained at 30 °C by reducing the iPAc excess from 10 to 7.5 equivalents with respect to Glyc, and the AcOH volume of up to 20 times, from 10 to 0.5 mL.

Table 3.3: The reaction of Glyc with iPAc in presence of acetic acid as solvent and Amb15 as catalyst

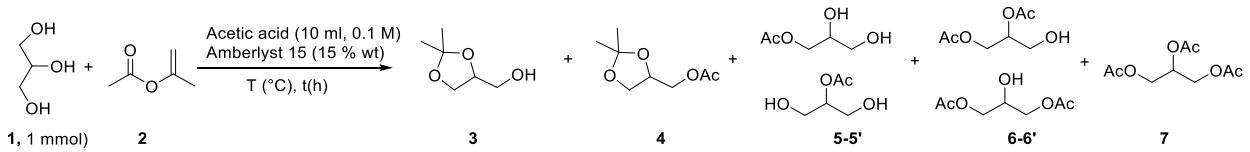

Entry	iPAc:Glyc Q	T (°C)	t (h)	Conversion Glyc (%)[a]	Acetals[a]		Esters[a]		
					3	**4**	**5-5'**	**6-6'**	**7**
1	1	30	4	>99	20	51	25	1	3
2	1	50	4	>99	12	35	41	7	6
3	1	70	4	>99	2	21	56	8	13
4	1	30	24	>99	6	14		77	3
5	0	30	4	31			81	19	
6	0	50	4	71			69	30	2
7[c]	1	30	24	1	99				
8	3	30	24	>99	7	28		60	5
9	5	30	24	>99	9	31		42	18
10	10	30	24	>99	4	41		11	44
11	10	30	32	>99		51			49

All reactions were carried out using a solution of Glyc (1 mmol) in AcOH (10 ml, 0.1M) with Amb15 (15 mg, 15% wt) as catalyst except differently stated. [a] Conversion of Glycerol; [b] Selectivity towards the different products; [c] reaction conducted in absence of the catalyst Amb15.

The latter was the minimum volume to obtain a homogenous solution of reactants **1** and **2**. This process intensification was not only beneficial to improve the carbon footprint and the safety of the procedure, but also to increase its overall efficiency since the higher reactant concentrations enhanced the rates of all the involved reactions.

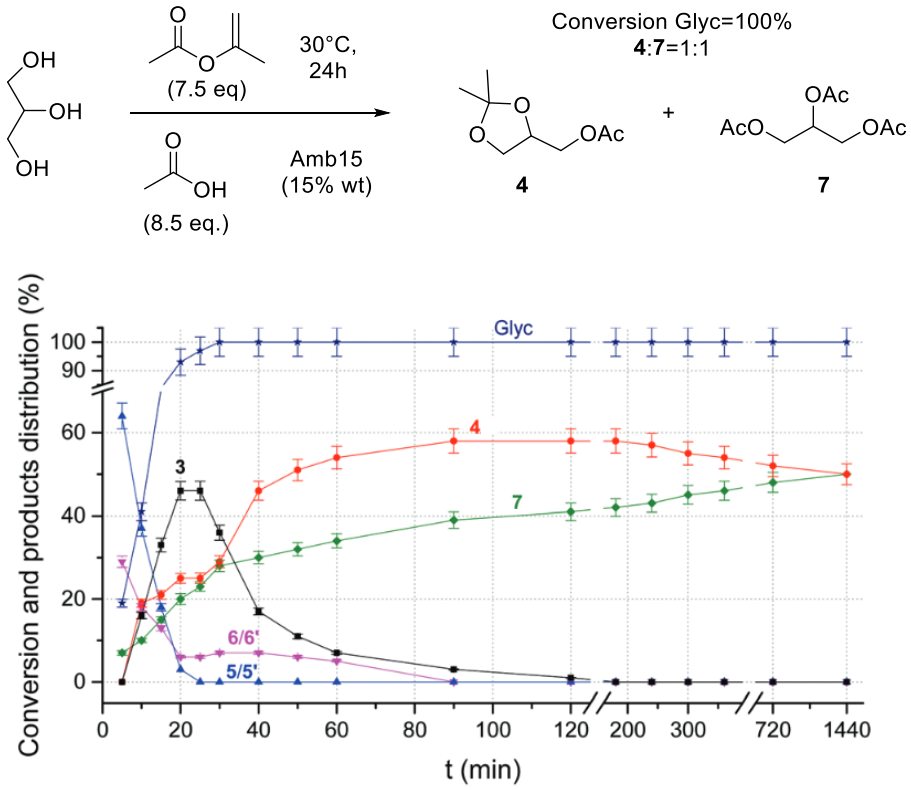

Figure 3.8: The product distribution over time of the reaction of Glyc (1.1 mmol) with iPAc (7.5 mmol), AcOH (8.7 mmol) and Amb15 (15.0 mg, 15% wt) at 30°C.

Figure 3.8 shows the variation over time of the products distribution in this optimized conditions: the reduction of the reaction volume compared to the conditions used in Table 3.3 highly impacted the kinetics. The conversion of glycerol was quantitative within the first 30 minutes. In the same time interval, the multiple transesterification of glycerol favored the formation of triacetin (**7**: 28%; green profile) and the onset of the acetalization reaction that gave rise to a steep increase of acetals. Solketal (**3**) reached a maximum (45%) after 25 min and then dropped with the orthogonal increase of Solketal acetate (**4**). **4** was plausibly obtained by the direct esterification of **3** and the acetalization of monoacetins (**5/5'**), thereby explaining the decline of the blue profile from 62% to zero in less than 20 min. Indeed, once formed, **5-5'** were consumed to feed both the transesterification process and the parallel acetalization reaction. In the next 90 minutes, competitive reactions proceeded with the gradual decrease of **3** and diacetins (**6/6'**, magenta curve) until their disappearance in favor of **4** and **7**. The final part of the sequence was a slow interconversion of **4** into **7** until the mixture reached the thermodynamic equilibrium distribution after 24 h with the final products present in equal quantities. The products distribution remained constant up to 48 hours of reaction.

Finally, the effect of catalyst amount was also explored and reported in Table 3.4: the catalyst:substrate ratio affects the kinetics of the multiple reactions involved but without altering the overall selective formation of **4** and **7**.

Table 3.4: Effect of the catalyst amount on the reaction of glycerol with a mixture of iPAc/AcOH

Entry	Amb-15 (wt%)	Conv. (%)[a]	Products distribution (%)[b]	
			4	7
1	15	≥99	49	51
2	10	≥99	61	39
3	5	≥99	67	33

Conditions: mixture of Glyc (1.00 mmol), iPAc (7.50 mmol), and AcOH (8.50 mmol, 0.5 mL) in the presence of variable amounts of Amberlyst-15 (5.00, 10.00, and 15.00 mg; 5, 10, and 15 wt%), t = 24h. [a] Conversion of glycerol. [b] Selectivity towards compounds **4** and **7.**

Decreasing the catalyst amount brought about a drop of the rate of all the reactions, albeit Solketal acetate **4** and triacetin **7** were the only observed products after 24 h in all cases. The corresponding amounts increased and decreased from 49 to 61 and 67% for **4**, and from 50 to 39 and 33% for **7** (entries 1-3). Results were consistent with profiles of Figure 3.8 in which the **4:7** ratio reached a maximum of ca 60:40 after 120 min, comparable to that achieved after 24 h with Amberlyst 15 at 10 wt%. No further investigations were carried out on this aspect.

The aforementioned optimized procedure involved a simple and safe experimental setup as well as an equally convenient work-up and purification of the products. Once the reaction was complete (24 h), the catalyst was filtered off and the mixture of **4** and **7** could be isolated by vacuum distillation (5 mBar, 50–80 °C) of the oily residue in nearly quantitative yields of 47% and 48%, respectively (based on Glyc as the limiting reagent). Moreover, the procedure could be scaled up by a factor of 10 without any appreciable variation in terms of product distribution, yields, and time.

3.2.3.2 Insights into the mechanism and the key role of acetic anhydride

Figure 3.8 highlighted that the amount of acetal acetates was higher than that of triacetin in the initial stages of the reaction (red and green profiles) although the acetylating mixture of iPAc/AcOH was in a very large excess compared to acetone released by acetylation mechanism. Since the direct acetalization of Glyc by iPAc was not plausible, the results led us to hypothesize that (excess) iPAc acted not only as a transesterification agent, but also as a source of acetone for acetalization through some kind of parallel reactions. The inspection of the literature indicated that at 100 °C, in the presence of H_2SO_4 as a catalyst, an equimolar mixture of AcOH and iPAc underwent an acyl nucleophilic substitution (acidolysis of iPAc) to provide acetone and acetic anhydride in almost quantitative yields (Scheme 3.7).[16]

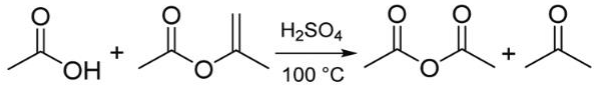

Scheme 3.7: reaction between iPAc and AcOH catalyzed by sulfuric acid

Presuming that the same reaction took place under the conditions of Table 3.3 and Figure 3.8 , the desired tandem sequence could be assisted by both acetone and acetic anhydride (Ac_2O) for the acetalization and acetylation reactions, respectively. Additional experiments were therefore carried out aiming at investigating the acidolysis of iPAc at 30 °C with Amberlyst 15 as a catalyst. The first test was performed by replicating the conditions of Figure 3.8. The complexity of the product mixture did not allow satisfactory GC/MS or NMR analyses to resolve signals of acetone and iPAc, but the presence of acetic anhydride was nonetheless verified through GC. A gradual increase of Ac_2O throughout the process (quantified in fig. A.3.28) offered convincing, albeit indirect, proof for the corresponding formation of an increasing amount of acetone which could in turn feed the acetalization of glycerol and monoacetins (Scheme 3.7). Additional evidence for the acetone formation was then gathered by the reaction of an equimolar mixture of isopropenyl acetate (5 mmol) and acetic acid in the presence of Amb15 as a catalyst (15 wt%). At 30 °C, after 24 h, acetic anhydride was observed in 80% yield (by GC). It was excluded that Ac_2O was obtained from the catalytic dehydration of AcOH since this reaction was reported only at much higher temperature or through the use of other auxiliaries.[17,18] The process also allowed to identify minor amounts of by-products (≤10% with respect to Ac_2O), the mass spectra of which was consistent with the formation of acetylacetone plausibly derived from an acid-promoted rearrangement of iPAc,[19] and the aldol condensation of acetone (see Fig. A3.29-33 for details). A not optimal resolution of acetone and iPAc prevented their quantification also in this case.

The in-situ formation of Ac_2O in the selected reaction conditions allowed us also to envisage another consequence: the involvement of the anhydride as an acetylating reagent in parallel with iPAc and AcOH. In this respect, a detailed study was carried out on the acetylation of Glyc with acetic anhydride under conditions as close as possible to those of Table 3.3, in which iPAc was replaced by Ac_2O. Experiments were performed at 30 °C, using a solution of Glyc (1 mmol) in AcOH (0.1 M, 10 mL), Amb15 (15% wt) and a Ac_2O:Glyc molar ratio in the range 1-5. The results reported in Table 3.5 suggested that the esterification of Glyc occurred much faster with Ac_2O than with AcOH alone (entry 1-2), and the presence of 5 equivalent of Ac_2O took to the selective formation of **7** (entry 3). This is in accordance with the classic industrial route for the production of triacetin (see Figure 3.1) and various papers that reported the use of a mixture of AcOH and Ac_2O for the synthesis of glycerol acetins.[14,20] The strong acetylation activity of the Ac_2O formed in situ was hence demonstrated.

Table 3.5: Acetylation of glycerol in presence of Ac_2O and acetic acid

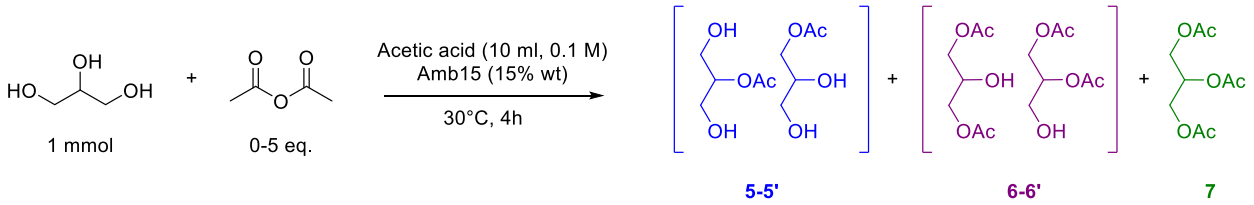

Entry	Ac_2O:Glyc (mol:mol)	Conversion Glyc (%)	Product distribution (%)		
			5-5'	6-6'	7
1	0	31	81	19	
2	1	100	55	40	5
3	5	100	0	0	100

The emerging picture confirmed the multiple role of iPAc and indicated that the investigated sequence was even more complicated than expected: in addition to the competitive (parallel or consecutive) acetylation due to iPAc and AcOH activity and the acetalization due to the acetone released by the transesterification process, the occurrence of the acidolysis of iPAc provided an extra supply of acetone and acetic anhydride, the latter serving as a co-acetylating agent. A limited hydrolysis of iPAc and glyceryl esters could also not be ruled out.[21,22] The complexity of a system in which different components (the enol ester, the acid and the anhydride) could simultaneously express the same reactivity as acetylating agents made it rather challenging to discriminate the contribution of each single partner. To shed light on this aspect, additional experiments were devised using D-isotope labelled acetic acid.

A control experiment was carried out under the conditions of Figure 3.8 by replacing AcOH with its perdeuterated analogue, CD_3COOD: (Glyc: 1 mmol, iPAc: 7.5 mmol; CD_3COOD: 0.5 mL, 8.5 mmol); Amb15: 15 wt%; 30 °C; 24 h). The GC/MS analysis of the reaction mixture allowed the identification of the expected products. Acetal acetates were detected as two species: the non- and the tri-deuterated compounds, 4 and 4*; Triacetin was detected in the form of four species, the non-, the tri-, the hexa-, and the nona-deuterated products, respectively (Scheme 3.8).

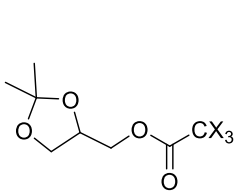

Solketal Acetate **4**: X=H
Solketal acetate-d_3 **4***: X=D

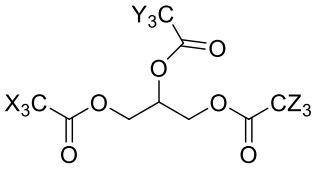

Triacetin
X=Y=Z=H
Triacetin-d_6
X=H; Y,Z=D

Triacetin-d3
X,Y=H; Z=D
Triacetin-d_9
X=Y=Z=D

Scheme 3.8: D-Isotope labelled products observed in the reaction of Glyc with iPAc/CD_3COOD.

A satisfactory GC resolution was achieved only for the acetal acetates while signals of the different triacetins were substantially superimposed. Comparison of the analytical data recorded in the full scan (TIC) and the SIM mode (set at the most abundant fragment ions, m/z = 159 and 162 for 4 and 4*, respectively) indicated that the relative amounts of 4* and 4 were 65% and 35%, meaning that the quantity of the tri-deuterated product was approximately twice that of the non-deuterated derivative (see appendix, Fig. A.3.34-38).

Relevant to this study was also the evidence of the formation of three differently deuterated acetic anhydrides, i.e., the non-, the tri-, and hexa-deuterated products which were present in a 1:3:2 ratio (by GC/MS) in the reaction mixture. These results were consistent with Scheme 3.9, in which CD_3COOD mediated the acidolysis not only of iPAc, but also of the produced (deuterated) anhydride.[23]

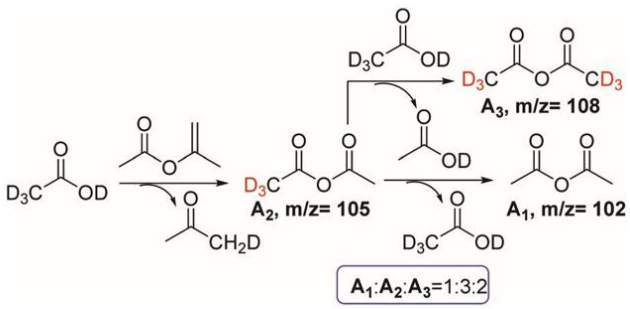

Scheme 3.9: Plausible pathways for the formation of the three observed species of acetic anhydride.

As a first approximation, excluding kinetic and equilibrium isotope effects,[24] the deuterated acid acted directly or indirectly (via the formation of A_2 and A_3) as acetylating agent to produce twice the amount of 4* with respect to 4. The latter instead was obtained from iPAc as such or its derivative A_1. From the stoichiometry of acidolysis and the 1 : 3 : 2 ratio of $A_1 : A_2 : A_3$ in Scheme 3.9 one could also estimate that about 58% of the total mixture of anhydrides was sourced from the deuterated acid.

3.2.3.3 The tandem synthesis of acetal acetates

The reaction of Glyc with the mixture iPAc/AcOH was further investigated with the aim to steer the overall process towards the selective formation of Solketal acetate **4**. To this end, several new experiments were carried out by changing the reactant molar ratio and by adding a large excess of acetone (20 molar equiv. with respect to Glyc) as a co-acetalizing agent. Although acetone (alike iPAc) was scantly soluble with glycerol [25] in the presence of AcOH a homogeneous solution of reactants was achieved. The salient aspects of this study are summarized in Figure 3.9, which shows the product distribution obtained during the reaction of a mixture of Glyc (1.0 mmol), AcOH (0.5 mL, 8.75 mmol), and acetone (0.9 mL, 20.0 mmol), in the presence of Amb15 (15 wt% with respect to glycerol) as a catalyst and variable amounts of iPAc (1–4 mmol), at 30 °C, after 24 h. Conversion of glycerol is not reported since it was quantitative in all tests.

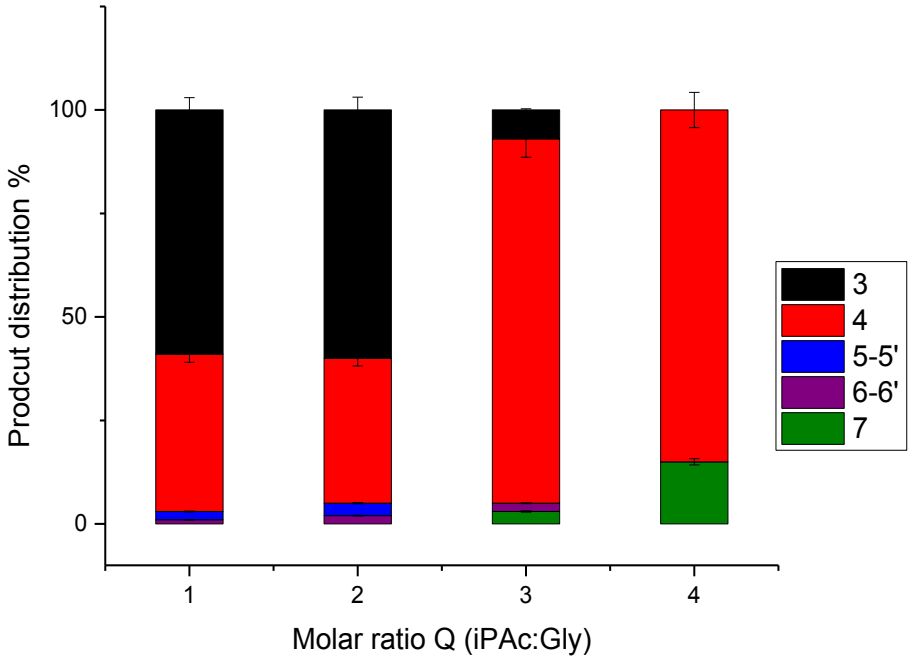

Figure 3.9: The reaction of glycerol with a mixture of iPAc/AcOH and acetone: the effect of increasing amounts of iPAc. Conditions: glycerol (1.0 mmol), isopropenyl acetate (1.0–4.0 mmol), acetic acid (8.75 mmol), acetone (20.0 mmol), Amberlyst-15 (15.0 mg; 15 wt%), 30 °C, 24 h.

The product distribution mirrored the intrinsic reactivity of acetone and iPAc. In the presence of equimolar amounts of glycerol and iPAc (Q=1), Solketal **3** was the predominant product (60%, black profile) followed by Solketal acetate **4** (37%, red profile) and traces of glyceryl esters implying that excess acetone favored acetalization versus acetylation. The result was comparable when the amount of iPAc was doubled (Q=2). Instead, for Q = 3 the formation of **3** dropped strikingly from 60% to 6% and **4** increased from 37% to 88%. The greater availability of iPAc and acetic anhydride (from the acidolysis of the enol ester) brought about a significant improvement of the transesterification reaction which, however, involved mainly the OH function of the acetals and not of glycerol. Indeed, the total amount of glyceryl esters remained low at ca. 6%. The results were consistent with the higher electrophilicity of acetone compared to esters and anhydrides that favored acetalization of glycerol to yield **3** which in turn underwent transesterification with iPAc/Ac_2O to the corresponding acetate **4.** A further increase of the iPAc:Glyc molar ratio (Q = 4) caused complete disappearance of **3** albeit with slightly lower selectivity towards **4** (85%) due to the formation of **7** (15%) by exhaustive acetylation of glycerol.

Additional tests demonstrated that the selectivity of the tandem sequence towards **4** could be further optimized by reducing the quantities of acetone and AcOH to 5 and 1.5 equivalents with respect to

glycerol, respectively. After 16 h under these conditions Solketal acetate was obtained in up to 91% yield (Scheme 3.10). Co-products were Solketal **3** (3%) and di- and triacetins (5/5': 2% and 7: 4%).

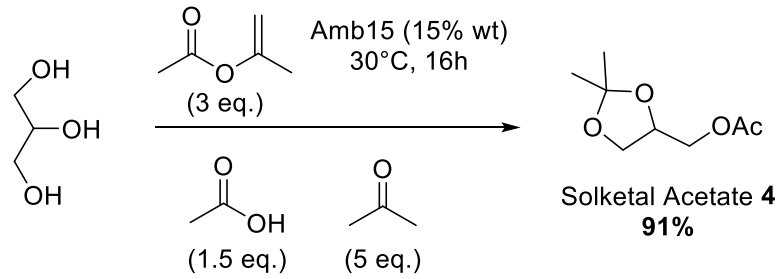

*Scheme 3.10: Optimized conditions for the selective synthesis of Solketal acetate (**4**)*

With respect to Figure 3.9, decreasing the reaction volume allowed to reduce the reaction time to 16 hours and, at the same time, under such conditions the reaction was scaled up by a factor of 10. Once the experiment was complete (16 h), the catalyst was filtered and vacuum distillation (5 mBar, 50–80 °C) of the oily residue allowed us to isolate **4** in an 87% yield (1.51 g, 8.7 mmol; based on glycerol as the limiting reagent), thereby further validating the mass balance and the synthetic efficiency of the process.

To the sake of completeness, it was our interest to explore the chances to achieve the same results by replacing iPAc with a mixture of Ac_2O and acetone, though earlier studies on the reaction of glycerol with mixtures of acetone and Ac_2O under reflux conditions yielded at best Solketal and Solketal acetate in a 9 : 1 ratio.[26] This reaction system was further examined by us through various attempts to optimize the reaction conditions (Table 3.6).

Experiments showed that reactants (Glyc, Ac_2O and acetone) were not mutually miscible, hence AcOH was used as a solvent. A 61% selectivity towards **4** is obtained by replacing iPAc with Ac_2O in the same conditions used in Scheme 3.10 (entry 1, table 3.6). Various other attempts to achieve the same selectivity obtained by the use of iPAc were unsuccessful (entry 2-7). At the best conditions founded, a complete conversion of glyc was achieved while Solketal acetate **4** was obtained in a 82% selectivity along with triacetin (18%) (entry 6). Compared to iPAc, not only the selectivity was lower, but acetone and Ac_2O had to be used in a significantly large excess of 20 and 5 equivalents respectively, with respect to Glyc. Finally, further experiments demonstrated that the tandem selectivity was elusive also by reacting Glyc with different mixtures of AcOH and acetone, in the presence of Amb15 as a catalyst: the amount of **4** did not exceed 32% (see table A.3.2). We can hence adfirm that iPAc play a key role in the tandem acetylation/acetalization process.

Table 3.6: The reaction of glycerol with acetone and acetic anhydride

Entry	Solvent	Glyc:Acetone:Ac_2O[a] (mol:mol:mol)	Conversion[b] (%)	Product distribution[c] (%)				
				3/3’	4/4’	5/5’	6/6’	7
1	AcOH (1.5 equivs.)	1:5:3	≥99		61		1	38
2		1:1:1	≥99	10	30	34	23	1
3		1:1:10	≥99		30		1	69
4		1:3:10	≥99		58		1	41
5		1:5:10	≥99		68		1	31
6		1:20:5	≥99		82			18
7		1:20:2.5	≥99	15	78		3	5

Conditions: glycerol (1.0 mmol), Ac_2O (1.0–10.0 eq), acetic acid (1.5 eq), acetone (1-20 mmol), Amberlyst-15 (15.0 mg; 15 wt%), 30 °C, 24 h [a] Molar ratio of the reactants. [b] Conversion of glycerol, by GC. [c] Products distribution, by GC.

With the aim to investigate the relative role of iPAc and acetone as acetalization agents, the rection reported in Scheme 3.10 was explored by replacing acetone with its d_6-isotope labelled analogue, CD_3COCD_3. The GC/MS analysis of the reaction mixture allowed us to identify the expected **4** as two species, the non and the hexa-deuterated compounds, respectively **4** and $\mathbf{4_{d6}}$. The comparison of the analytical data recorded in the full scan (TIC) and the SIM mode (set at the most abundant fragment ions, m/z = 159 and 162 for **4** and $\mathbf{4_{d6}}$, respectively) indicated that their relative amounts were 35% and 65%, i.e. the hexa-deuterated species was approximately twice as much the non-deuterated one (further details in appendix Scheme A.3.3 and Fig. A.3.39-40). The correspondence between the ions analyzed in SIM mode both for the tests with labelled acetic acid and acetone is noteworthy. Although ions with m/z = 159 and 162 were selected for both the investigations, the comparison of mass spectra proved that different fragmentation pathways occurred: (i) using d_4-acetic acid the isotopic marking of the considered ion regarded the acetyl group; (ii) when d_6-acetone was used, the marking was set on the acetalized portion of acetal acetates.

Although the apparent contribution of CD_3COCD_3 to the acetalization reaction was almost double that of acetone released by iPAc, the acetalizing capability of the enol ester was still remarkable considering the excess d_6-acetone used. Even more so considering the inverse secondary deuterium isotope effect described for the formation of ketals from the reaction of methanol and acetone/d_6-acetone, the measured K_H/K_D (equilibrium constants for non-deuterated and deuterated ketals) ratio was ~0.7.[27]

3.2.4 Conclusions

This study reports for the first time a one-pot tandem catalytic acetalization–acetylation sequence of glycerol where the presence of multiple reagents allows to control the product distribution. Crucial to this result is the cooperative reactivity of isopropenyl acetate and acetic acid in the presence of Amberlyst-15. The major role is played by the enol ester that acts as the acetylating agent of glycerol and at the same time, it undergoes acidolysis with acetic acid. Both these processes release acetone which in turn triggers the acetalization of glycerol. Moreover, acetic anhydride co-generated during the acidolysis of isopropenyl acetate further contributes to the acetylation of glycerol. Notwithstanding the complex network of reactions, this investigation demonstrates that the experimental conditions can be tuned to obtain the selective conversion of glycerol to either a 1:1 mixture of Solketal acetate **4** and triacetin **7**, or solely **4** in up to 89% isolated yield. The latter result is achieved simply by supplying extra acetone to the iPAc/AcOH mixture. Experiments using d_4-acetic acid and d_6-acetone suggest that acetic acid, mostly through the formation of acetic anhydride, is the major contributor (for about 65%) to the acetylation of the final products, while acetone released by iPAc provides ca. 35% of Solketal acetate formed even when excess acetone is sourced externally. Acetic acid, along with acidolysis, also serves as a solvent to overcome the issue of poor mutual solubility of iPAc and acetone with glycerol.

The approach used is original and genuinely green. The synthetic potential of the tandem sequence for the upgrading of glycerol involves a pool of innocuous reactants (glycerol, isopropenyl acetate, acetic acid and acetone) and mild/simple reaction conditions (30 °C and atmospheric pressure) which make the scale-up of the protocol safe and easy. This study has also proved that intensification of the process can be achieved by controlling (reducing) the reactant molar ratio.

3.2.5 Experimental Section

3.2.5.1 General

Reagents and solvents were commercially available compounds and were used as received unless otherwise stated. Glycerol, acetic acid, acetic anhydride, acetone, isopropenyl acetate, Amberlyst-15, d_4-acetic acid, and d_6-acetone, were sourced from Sigma Aldrich.

GC/MS (EI, 70 eV) analyses were performed on a HP5-MS capillary column (L = 30 m, Ø = 0.32 mm, film = 0.25 mm), and GC analyses (CG/FID) were performed on an Elite-624 capillary column (L = 30 m, Ø = 0.32 mm, film = 1.8 mm). ^{1}H and ^{13}C NMR spectra were recorded at 400 and 100 MHz, respectively. The chemical shifts were reported downfield from tetramethylsilane (TMS), and $CDCl_3$ was used as the solvent.

The conversion of glycerol and the product distribution were measured by GC/FID analysis upon calibration with standard solutions. Given the interest in the tandem sequence, the selectivity (product distribution) for **3, 4, 5 + 5', 6 + 6'** and **7** was defined according to the following expression:

$$S_i = [\text{mol } i/\text{conv. Glyc.}] \times 100$$

where S_i is the selectivity (%) for compound *i* (*i* = **3**, **4** , **5** + **5'**, **6** + **6'** and **7**), mol *i* stands for the total moles of compound *i* (by GC calibration) and conv. glyc. is the total conversion of glycerol for the combined transesterification and acetalization processes.

3.2.5.2 Catalytic tests

General procedure for the tandem synthesis of Solketal acetate and triacetin. Experiments were carried out under different conditions (Table 3.3 and Figure 3.8) which can be summarized as follows: in a 25- or 50-mL round-bottomed flask equipped with a condenser and a magnetic stir bar, a mixture of glycerol (1 mmol), isopropenyl acetate (1–10 mmol), acetic acid (0.5–10 mL) and Amberlyst-15 (5–15 mg) as a catalyst (5–15 wt%) was set to react at the temperature of choice (30–70 °C) and atmospheric pressure, for 24–32 h. Conversion of glycerol and products selectivity were determined by GC/FID analysis upon calibration.

Compound **4** ((2,2-dimethyl-1,3-dioxolan-4-yl)methyl acetate) and **7** (propane-1,2,3-triyl triacetate) were isolated from a reaction scaled up by a factor of 10, using 10 mmol of glycerol (other conditions: T = 30 °C; p = 1 atm; molar ratio Glyc : iPAc : AcOH = 1 : 7.5 : 8.75; Amberlyst 15 = 15 wt%; t = 24 h). Once the experiment was complete, the solid catalyst was filtered off, and the liquid solution was distilled under vacuum (5 mBar, 50–80 °C). Isolated yields were 47% and 48% for **4** and **7**, respectively. Products were characterized by both ^{1}H and ^{13}C NMR and GC/MS analyses. Data agreed with those reported in the literature.[28,29]

General procedure for the selective tandem synthesis of acetal acetates. Experiments were carried out under different conditions (Figure 3.9 and Scheme 3.9) which can be summarized as follows: in a 25- or 50-mL round-bottomed flask equipped with a condenser and a magnetic stir bar, a mixture of glycerol (1 mmol), isopropenyl acetate (1–4 mmol), acetic acid (0.5 mL), acetone (1–20 mmol) and Amberlyst-15 as a catalyst (15 wt%) was set to react at the temperature of choice (30–70 °C) and atmospheric pressure, for 16–24 h. Conversion of glycerol and product selectivity were determined by GC/FID analysis, upon calibration.

Solketal acetate **4** was isolated from a reaction scaled up by a factor of 10, using 10 mmol of glycerol (other conditions: T = 30 °C; p = 1 atm; molar ratio Glyc : iPAc : AcOH : Acetone = 1 : 3 : 1.5 : 5; Amberlyst 15 = 15 wt%; t = 16 h). Once the experiment was complete, the solid catalyst was filtered off, and the liquid solution was distilled under vacuum (5 mBar, 50–80 °C). The isolated yield of **4** was 87%. Product appeared as a yellowish liquid and it was characterized by both ^{1}H and ^{13}C NMR and GC/MS analyses; data agreed with those reported in the literature.[28,29]

The reactions with D-labelled compounds. Experiments with labelled reagents were carried out by replacing AcOH or acetone with the same quantity of the perdeuterated analogues, CD_3COOD or CD_3COCD_3. In the case of d_4-acetic acid, a mixture of glycerol (1 mmol), iPAc (7.5 mmol), CD_3COOD (0.5 mL, 8.75 mmol), and Amberlyst-15 (15 mg, 15 wt%) was set to react in a 25 mL round-bottomed flask at T = 30 °C and atmospheric pressure, under stirring for 24 h. In the case of d_6-acetone, a mixture of glycerol (1 mmol), isopropenyl acetate (3 mmol), d_6-acetone (5 mmol), acetic acid (1.5 mmol), and Amberlyst-15 (15 mg; 15 wt%) was set to react in a 25 mL round bottomed flask, at T = 30 °C and atmospheric pressure, under stirring for 16 h. The mixtures of labelled products were analyzed by GC/MS both in the full scan

mode (TIC, 70 eV) and in the SIM mode on the characteristic fragment ions m/z = 159 and 162 (other details are in the appendix).

3.2.6 References

[1] R. Miller, C. Abaecherli, A. Said and B. Jackson, in *Ullmann's Encyclopedia of Industrial Chemistry,* Wiley and sons eds., 2012, pp. 171-185.

[2] H. Wooster, C. Lushbaugh and C. Redeman, *Journal of the American Chemical Society*, 1946, **68**, 2743.

[3] https://echa.europa.eu/registration-dossier/-/registered-dossier/17298/7/3/2 accessed on 10/03/2021

[4] D. Mukherjee, B. Ali Shah, P. Gupta and S. C. Taneja, *The Journal of organic chemistry*, 2007, **72**, 8965-8968.

[5] D. Rigo, G. Fiorani, A. Perosa and M. Selva, *ACS Sustainable Chemistry & Engineering*, 2019, **7**, 18810-18818.

[6] V. R. Ruiz, A. Velty, L. L. Santos, A. Leyva-Pérez, M. J. Sabater, S. Iborra and A. Corma, *Journal of Catalysis*, 2010, **271**, 351-357;

[7] (a) F. M. Winnik, J. P. Carver and J. J. Krepinsky, *The Journal of Organic Chemistry*, 1982, **47**, 2701-2707; (b) K. Freudenberg and R. M. Hixon, *Berichte der deutschen chemischen Gesellschaft (A and B Series)*, 1923, **56**, 2119-2127.

[8] S. Guidi, M. Noè, P. Riello, A. Perosa and M. Selva, *Molecules*, 2016, **21**, 657.

[9] (a) A. R. Trifoi, P. Ş. Agachi and T. Pap, *Renewable and Sustainable Energy Reviews*, 2016, **62**, 804-814; (b) M. R. Nanda, Z. Yuan, W. Qin, H. S. Ghaziaskar, M.-A. Poirier and C. C. Xu, *Fuel*, 2014, **117**, 470-477.

[10] (a) J. Otera, *Chemical reviews*, 1993, **93**, 1449-1470.

[11] (a) B. A. Meireles and V. L. P. Pereira, *Journal of the Brazilian Chemical Society*, 2013, **24**, 17-57; (b) M. Khayoon and B. Hameed, *Applied Catalysis A: general*, 2013, **460**, 61-69.

[12] (a) U. I. Nda-Umar, I. Ramli, Y. H. Taufiq-Yap and E. N. Muhamad, *Catalysts*, 2019, **9**, 15; (b) P. H. Silva, V. L. Gonçalves and C. J. Mota, *Bioresource technology*, 2010, **101**, 6225-6229; (c) M. Rezayat and H. S. Ghaziaskar, *Green Chemistry*, 2009, **11**, 710-715.

[13] (a) P. San Kong, M. K. Aroua, W. M. A. W. Daud, H. V. Lee, P. Cognet and Y. Pérès, *RSC advances*, 2016, **6**, 68885-68905; (b) L. Zhou, T.-H. Nguyen and A. A. Adesina, *Fuel processing technology*, 2012, **104**, 310-318.

[14] (a) H. Cheung, R. S. Tanke and T. G.P., in *Ullmann's Encyclopedia of Industrial Chemistry*, Wiley & Sons

eds., 2011, pp. 1-26; (b) P. Anbukarasu, D. Sauvageau and A. Elias, *Scientific Reports*, 2015, **5**, 17884.

[15] The acetalization of glycerol (**1)** and glycerol monoacetin (**6a**) took to the selective formation of the corresponding 5-membered ring isomer, Solketal (**3**) and Solketal acetate (**4**) in a purity >97%, even if traces of the 6-membered rings (≈3%) can be found. Also commercial Solketal is sold as a mixture 97:3 of 5-membered ring:6-membered ring isomers. In all the reactions reported in this work, Solketal and Solketal acetate were formed with a 97:3 ratio between 5- and 6-membered ring products.

[16] H. J. Hagemeyer and D. C. Hull, *Industrial & Engineering Chemistry*, 1949, **41**, 2920-2924.

[17] N.-Y. He, C.-S. Woo, H.-G. Kim and H.-I. Lee, *Applied Catalysis A: General*, 2005, **281**, 167-178.

[18] M. Jean-Pierre, C. Marcel and B. Ahmed, *Chemistry Letters*, 1981, **10**, 523-526

[19] E. S. Rothman, *The Journal of Organic Chemistry*, 1966, **31**, 628-629.

[20] (a) X. Liao, Y. Zhu, S.-G. Wang and Y. Li, *Fuel Processing Technology*, 2009, **90**, 988-993; (b) X. Liao, Y. Zhu, S.-G. Wang, H. Chen and Y. Li, *Applied Catalysis B: Environmental*, 2010, **94**, 64-70.

[21] J. A. Landgrebe, *The Journal of Organic Chemistry*, 1965, **30**, 2997-3000.

[22] J. R. Dodson, T. d. C. Leite, N. S. Pontes, B. Peres Pinto and C. J. Mota, *ChemSusChem*, 2014, **7**, 2728-2734

[23] J. Huanc, J.-P. Leblanc and H. K. Hall, *Journal of Polymer Science, Part A:Polymer Chemistry*, 1992, **30**, 345–354.

[24] J. F. Marlier, *Accounts of Chemical Research*, 2001, **34**, 283-290.

[25] S. Guidi, M. Noè, P. Riello, A. Perosa and M. Selva, *Molecules*, 2016, **21**, 657.

[26] V. B. Vol'eva, I. S. Belostotskaya, A. V. Malkova, N. L. Komissarova, L. N. Kurkovskaya, S. V. Usachev and G. G. Makarov, *Russian Journal of Organic Chemistry*, 2012, **48**, 638-641.

[27] V. A. Stoute and M. A. Winnik, *Canadian Journal of Chemistry*, 1975, **53**, 3503-3512.

[28] K. Sugahara, N. Satake, K. Kamata, T. Nakajima and N. Mizuno, *Angewandte Chemie*, 2014, **126**, 13464-13468.

[29] R. Calmanti, M. Galvan, E. Amadio, A. Perosa and M. Selva, *ACS Sustainable Chemistry & Engineering*, 2018, **6**, 3964-3973.

3.3 Reaction of Glycerol with Trimethyl Orthoformate: Towards the Synthesis of New Glycerol Derivatives

3.3.1 Introduction

Glycerol is a renewable feedstock that can be transformed in a plethora of useful derivatives as already illustrated in the introduction (paragraph 1.4.1.2, figure 1.9) In this field, our research group has explored different thermal and catalytic synthetic approaches by reacting Glyc with dimethyl carbonate, formaldehyde, acetone, enol esters, ketals, and other sustainable derivatives. [1,2,3] In search to further expand this chemistry and to identify new bio-building blocks, we considered orthoesters (OEs) as another family of electrophilic partners for the upgrading of Glyc.

OEs are an importand class of organic compounds characterized by three alkoxy groups attached to the same carbon. Just like acetals, orthoesters undergo transetherification, allowing to prepare complex organic molecules bearing orthoester functionality starting from simpler homologs.

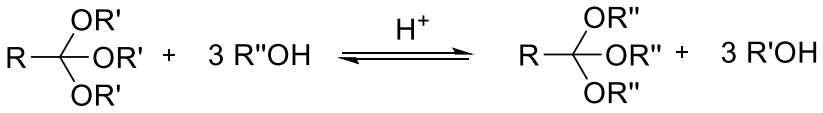

Scheme 3.11: Transetherification of orthoesters

Their synthesis routes are reviewed elsewhere,[4] and the most relevant examples provide for: i) the reaction of trihalogenated derivatives with alkoxides;[5] ii) addition of alcohols to ketene acetals;[6] iii) electrochemical oxidation of aldehyde acetals and toluene derivatives;[7] iv) reaction of orthocarbonates with Grignard reagents;[8] v) the Pinner synthesis consisting on the reaction of nitriles with alcohols under acidic conditions.[9] This last category was upgraded in a green fashion that avoid the use of light chlorinated solvents in recent years by our research group.[10]

The impressive reactivity of OEs (up to 20000 times higher than of the above cited ketones and aldehydes used for the functionalization of Glyc)[8] and their high stability towards nucleophile and bases, drew our attention towards its use. The main application of OEs is as protective groups for carboxylic acids, hydroxyl groups, esters and α-ketoacids. [11,] Nonetheless, naturally-occuring OEs are indispensable for the pharmacological activity of some antibiotic compounds[12] while they are also successfully exploited as alkylating agents,[13] dehydrating agents,[14] copolymers for the synthesis of polyorthoesters, [15] reactant for the synthesis of heterocyclic compounds[16] and a fascinating novel application in the synthesis of dynamic cryptands employed for the controlled release of metal ion guests. [17] Their wide scope in organic synthesis was recently reviewed.[18]

For what concerns the reaction between Glyc and OEs, some pioneering research dating back to the '60s and '80s highlighted the potential of these reactions. In 1964, Crank and Eastwood were the first to investigate the reaction between triols and triethylorthoformate to obtain bicyclic orthoesters (BOEs)[19a], demonstrating the formation of several BOEs from 1,2,4- 1,2,5- and 1,3,5-triols. By using Glyc as reagent,

they observed the formation of a mixture of the pentacyclic *cis*-/t*rans*-2-ethoxy-4-hydroxymethyl-1,3-dioxolane (**1'**) and its hexacyclic isomer *cis*-/t*rans*-2-ethoxy-5-hydroxy-1,3-dioxane (**4'**) (Figure 3.10a) in a 9:1 ratio with 67% of yield, which could thermally decomposed to ethanol, CO_2 and allyl alcohol [19b]. The bicyclic compound 2,6,7-trioxabyciclo[2.2.1]heptane (**2**) was not observed. A few years ago, Thshibalonza and Monbaliu revisited the reaction by focusing on the formic acid-catalyzed synthesis of allyl alcohol under continuous-flow conditions (Figure 3.10b).[20]

In the late '70s, Hall *et al.* successfully accomplished the synthesis of **2** (Figure 3.10c, Yield≈70%) and its further polymerization to 5-membered rings polyorthoesters.[21,22] Since then, the ring-opening polymerizations of BOEs (including **2**) has been extensively investigated and reviewed elsewhere.[23]

Furthermore, diglycerol-OEs were used also to develop acid-labile polymers for drug-delivery applications.[15,24]

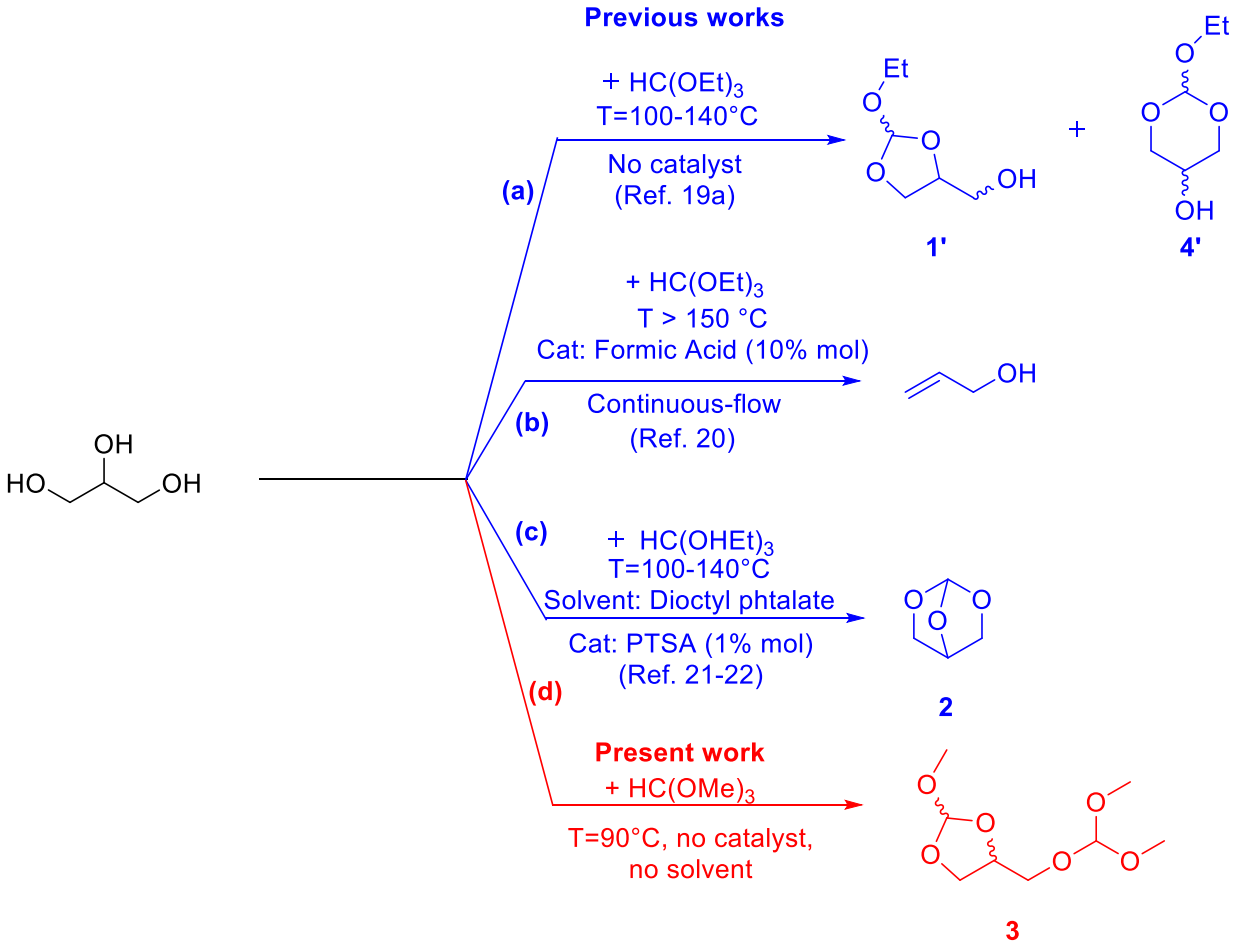

Figure 3.10: Reactions between Gly and OEs reported in literature and present work.

3.3.2 Aim and summary of the work

In this work the thermal and catalytic reaction between Gly and $HC(OMe)_3$ is studied with the aim to develop new reliable synthetic protocols for glycerol exploitation. The selective formation (up to 95% of yield) of a new glycerol-based 5-membered ring di-orthoester (the *cis*-/*trans*-4-(dimethoxymethoxy)methyl)-2-methoxy-1,3-dioxolane; **3**, Figure 3.10d) was accomplished by using $HC(OMe)_3$ as model OE *via* a dynamic and thermodynamically-controlled synthetic strategy. A variety of homogeneous and heterogeneous acids (PPTS, DBUHBr, sulfuric acid, Amberlyst-15, amberlyst-36, $FeCl_3$ and AlF_3) and ionic liquids ($BSMImHSO_4$, BSMImBr) were used as Brønsted/Lewis-acidic catalysts. In this context, the ionic liquids (ILs) were tested as they are known to give better yields, turnover numbers and frequencies, and improved catalysts recyclability.[25] The effect of basic catalysts (such as K_2CO_3 and trioctylmethylphosphonium methylcarbonate: $[P_{1888}]CH_3OCO_2^-$) was also investigated for comparison.

3.3.3 Results and discussion

The reactivity between Glyc and $HC(OMe)_3$ was first tested in the absence of any catalyst, in analogy to the reaction conditions previously reported in literature.[19a,21,22] The reaction was carried out in the absence of added solvents at 90 °C with a reagent molar ratio Q=1 (Q = $HC(OMe)_3$:Glyc) for 1 hour. The products were isolated and fully characterized by GC-MS, ^1H, ^{13}C and 2D-NMR analyses (see Material and Methods ant the appendix for further details) revealing the formation of the 5-membered ring OE **1**, the bicyclic compound 2,6,7-trioxabyciclo[2.2.1]heptane **2**, and the di-orthoester **3** (**1** and **3** as mixtures of diastereomers) in 82/11/7 selectivity respectively. Figure 3.11 shows the gaschromatogram of the crude reaction mixture.

The 6-membered ring isomers of **1** and **3** were not observed. This was unexpected since previous results for the reaction between Glyc and triethyl orthoformate reported a 5- and 6-membered ring isomeric ratio of 3:1[13] or 9:1 [19a] for compounds **1':4'** (see Figure 3.10a). A reasonable explanation is that, under our conditions, the reaction between glycerol and $HC(OMe)_3$ is kinetically rather than thermodynamically controlled. Indeed, the ring strain energy of 5-membered ring 1,3-dioxolane (7.3 kcal/mol) is higher than the 6-membered ring 1,3-dioxane analogs (2.9 kcal/mol)[26], while the stabilization energy due to their formation was 4.4 and 13.2 respectively.[27] These trends of energies show that 1,3-dioxane are more stable than 1,3-dioxolane. This explanation is also in agreement with the results reported by Yokohama et al. for the ring-opening polymerization of **2** that under kinetical control, leads to the almost exclusive formation of the 5-membered ring product.[22]

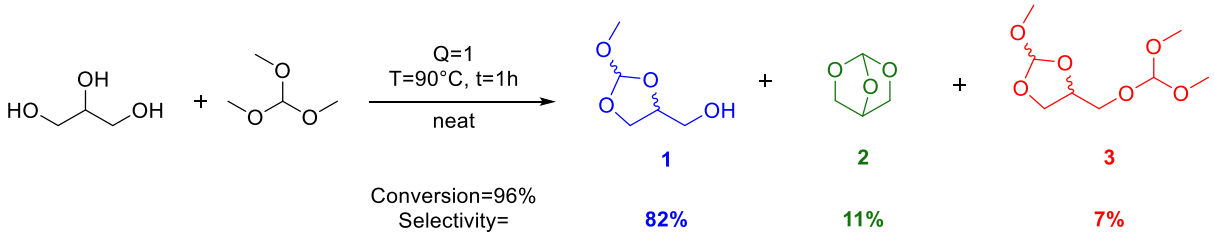

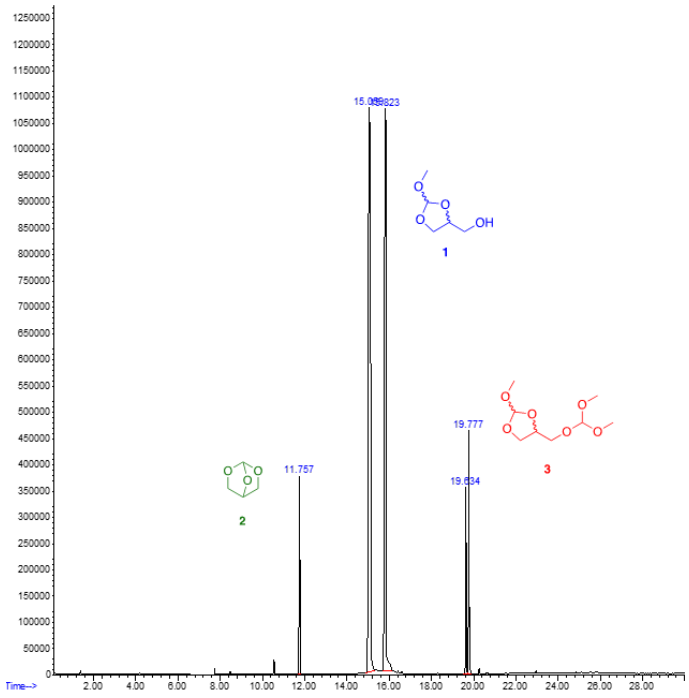

Figure 3.11: Gaschromatogram of the reaction between $HC(OMe)_3$ and Gly with Q = 1, 90 °C, 1h.

Since the characterization of the reaction products (especially **3**, isolated as a couple of diastereoisomers, **3a** and **3b** through the procedure reported in the experimental section) was not trivial, here it is interesting to discuss analytical evidence obtained by NMR that allowed to support the unambiguous identification of the product:

1) The ^{1}H NMR spectra (fig. A.3.56) highlights double signals in 1:1 ratio particularly for the protons 2, 4, 8 and 14.

2) The $^{13}C\{^{1}H\}$, DEPT-135, DEPT-90, APT NMR spectra (Figure A.3.57-60) show all the peaks relative to 3a,b as couple of signals in 1:1 ratio clearly separated.

3) COSY (Figure A.3.61) shows the presence of two series of identical coupling patterns for the two isomers **3a** and **3b**. Moreover, any couple of signals in 1:1 ratio do not reveal any crossing interactions. i.e. **6a** at 4.4 ppm does not match with the homologous **6b** at 4.2 ppm.

4) HMBC (Figure A.3.62) shows the correlation spots between H and C in position 6 and 8, while no correlation is present between 2 and 8 thus proving the presence of the 5-membered ring rather than the 6-membered ones.

Having established the structure of the compounds obtained during the reaction, further experiments were then carried out at different temperatures and Glyc:$HC(OMe)_3$ molar ratios by following the product distribution over time. At 90 °C, under reactive distillation conditions to remove methanol continuously during the reaction, the kinetic profile of the reaction was studied for 24 h at two different molar ratios Q = 1 and Q = 10 (Figure 3.11). In both cases within the first minutes of reaction the initial biphasic mixture turned homogeneous and vigorous distillation of methanol was observed. For both ratios Q = 1 and Q = 10, the Glyc conversion was almost quantitative after 0.5 h (based on GC analysis) towards formation of **1** and **3** respectively, thus proving that the formation of the glycerol-OEs is basically instantaneous yielding a statistical products distribution. After 24h, a relatively slow dynamic covalent exchange reaction yielded a thermodynamically controlled products distribution which is influenced by the reaction conditions. For example, with Q = 1, after 1 h the selectivity was shifted towards **1**, but prolonging the reaction time, **1** and **3** slowly decreased in favor of the formation of **2** (39% after 24h) via an intramolecular reaction favored by the continuous removal of methanol. When using an excess of $HC(OMe)_3$ (Q = 10) the initial selectivity was shifted towards the formation of **3** (80%, 1h), as expected; after 24h the reaction slowly proceeded further favoring conversion of **1** into **3** (97%, 24 h). It is worth to notice that under these conditions **3** could be isolated by simply evaporating the excess of $HC(OMe)_3$ without any further purification step (95% isolated yield with 98% purity by GC).

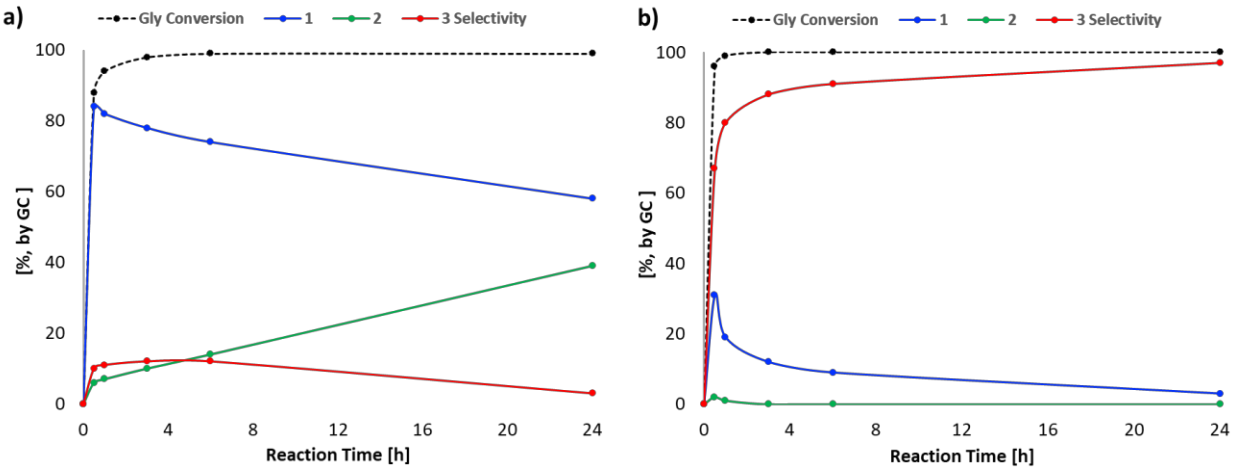

Figure 3.12: Conversion of Glyc and products selectivity for the catalyst-free reaction between Glyc and $HC(OMe)_3$. Reaction conditions: Glyc [5.43 mmol] and $HC(OMe)_3$ with Q = 1 (a) or Q = 10 (b) at 90 °C.

The experimental results indicated that – likewise to the known glycerol-orthoformate reactivity[19,20,22] and the alkoxy-exchange reactivity of OEs [28] – the initial fast reaction of $HC(OMe)_3$ with Glyc gives **1** which is in equilibrium with **2** and **3**, the latter formed by reaction with another molecule of orthoformate.

Interconversion of **2** and **3** goes through a dynamic covalent reaction involving **1** as the intermediate. Scheme 3.12 shows the hypothesized reaction pathways.

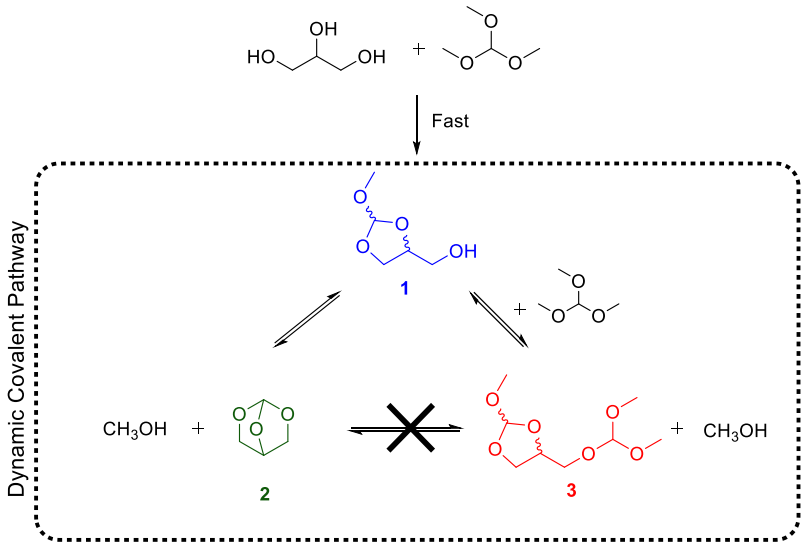

Scheme 3.12: Pathways for the formation of products in the reaction between Glyc and $HC(OMe)_3$

The reaction was further investigated by varying Q between 1 and 10, at T = 90 °C and 25 °C, for 24h. As shown in Table 3.7, **3** was formed selectively at 90 °C only with a large excess of $HC(OMe)_3$ (Q=10) (entry 5). At lower Q values instead (entry 1-4), the selectivity-determining dynamic equilibrium resulted in a statistical products distribution.

A less pronounced exchange equilibrium between the products was observed for the reactions conducted at 25 °C respect to the ones conducted at 90 °C. In fact, at 25 °C and Q = 1 the reaction was very slow and after 24h, conversion reached only 63% (90% conversion after 48h), with 79% selectivity towards formation of **1** (entry 6, and Figure A.3.72 for the reaction profile). At higher Q = 10, the reaction rate increased reaching almost quantitative conversion, but the product distribution was not shifted towards the formation of **3**, as was the case for the reaction conducted at 90 °C. Instead, a high (88%) selectivity towards **1** was observed after 1h, while after 24h the dynamic equilibrium promoted a 74/5/21 selectivity towards **1/2/3** respectively (entry 7 and Figure A.3.73 for the reaction profile).

Overall, the catalyst-free reaction between Glyc and $HC(OMe)_3$ lead to the selective synthesis of the thermodynamically-favored product **3** – a new orthoester derivative of glycerol – after 24h and in the presence of an excess of trimethyl orthoformate.

Table 3.7: Q and T effect on products distribution for the catalyst-free reaction of Gly with $HC(OMe)_3$.

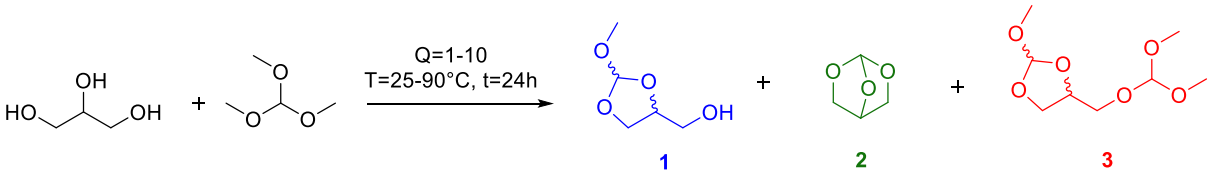

Entry	Q	T (°C)	Conversion Glyc (%)[a]	Selectivity (%) [a]		
				1	2	3
1	1	90	96	58	39	3
2	1.5	90	96	56	9	35
3	2	90	96	51	3	46
4	5	90	99	24	2	74
5	10	90	100	3	0	97
6	1	25	63	79	8	13
7	10	25	95	74	5	21

Reaction conditions: Glyc [5.43 mmol] and $HC(OMe)_3$ with Q = 1-10, T= 90 °C, t= 24 h. [a)] Conversion of Glyc and products selectivity determined by GC.

With the aim to accelerate attainment of the dynamic equilibrium among **1**, **2** and **3,** and to direct selectivity, different acid catalysts were then tested at Q = 10 and T = 90 °C. The results are listed in Table 3.8. In the presence of PPTS (10%w/w Glyc), known to catalyze the reaction of diglycerol with triethyl orthoformate[24], the reaction reached quantitative conversion and 97% selectivity towards **3** in 1h (entry 3 and 4). No further products were observed even after 24h, indicating that **3** is stable under the reaction conditions (Figure A.3.74 for the reaction profile). As shown in Table 3.8, all the other acid catalysts favored the formation of **3** already after **1** hour. Only for diazabicyclo-undecenium bromide (DBUHBr, entry 5-6) a slower dynamic equilibrium – in line with the uncatalyzed reaction – was observed (75% and 93% selectivity after 1 and 24h, respectively) likely due to the lower acidity.[29] Brønsted and Lewis acidic catalysts such as H_2SO_4, amberlyst-15, amberlyst-36, iron chloride and aluminium fluoride promoted moderate-to-good selectivity (84, 79, 87, 91, 87%, respectively; entries 7, 9, 11, 13, 15, Table 3.8) towards 3 after 1h along with small amount of ill-defined products (e.g. aldehydes, ethers or oligomers). The latter were probably formed by catalytic decomposition of **3** as already described in the literature for OEs.[20] The formation of reaction by-products became evident after 24h. In particular, the use of sulfuric acid caused formation of a large quantity (≈ 41%) of four major undefined products (see Figures A.3.75-79 for the gas-chromatography trace and MS spectra) after 24h at 90 °C. Instead, when using the ionic liquids butylsulfonylmethylimidazolium bromide (BSMImBr) and hydrogensulfate (BSMImHSO$_4$) as catalyst (entries 17-20) the fast reaction rates were always accompanied by the quantitative and selective formation of **3** (98%) and by the absence of side reactions (99% also after 24h). The same acidic ionic liquids allowed to perform the reaction at 25 °C, still with appreciable selectivity towards **3** (81-87 %;

entries 21-22). Finally, no conversion of Glyc was observed when using basic catalysts, such as K_2CO_3 or $[P_{8881}]CH_3OCO_2^-$,[30] owing to the stability of OEs towards bases.

To rationalize the catalytic behavior, the Hammett acidity functions (H_0) for the different catalysts were compared (see Table 3.8). H_0 was chosen since it is one of the most effective ways to express the Brønsted acidity in an organic medium.[31] It is readily apparent that stronger acidity (H_0<0, entry 7-12) prompts faster reactions but also higher formation of side products. On the other hand, when using weaker acids (H_0=1-3, entries 17-22) the reactions are more selective towards the formation of the desired product **3**.

Table 3.8: Catalyzed reaction between $HC(OMe)_3$ and Glyc

Entry	Catalyst	Time (h)	Conversion Glyc (%)[a]	Selectivity (%)[a]				H_0[b]
				1	**2**	**3**	others	
1	---	1	96	19	1	80	-	
2	---	24	>99	3	0	97	-	
3	PPTS	1	>99	0	3	97	-	
4	PPTS	24	>99	0	3	97	-	
5	DBUHBr	1	96	25	0	75	-	
6	DBUHBr	24	>99	7	0	93	-	
7	H_2SO_4	1	>99	9	2	84	5	-12.3 [32]
8	H_2SO_4	24	>99	42	1	16	41	
9	A-15	1	>99	12	3	79	6	-2.2 [33]
10	A-15	24	>99	17	1	70	12	
11	A-36	1	>99	7	1	87	5	-2.65 [33]
12	A-36	24	>99	13	1	75	11	
13	$FeCl_3$	1	>99	2	0	91	7	
14	$FeCl_3$	24	>99	10	1	78	11	
15	AlF_3	1	>99	9	1	87	3	
16	AlF_3	24	>99	3	1	92	4	
17	$BSMImHSO_4$	1	>99	0	2	98	-	1.02 [34]
18	$BSMImHSO_4$	24	>99	0	1	99	-	

19	BSMImBr	1	>99	0	2	98	-	2.91 [c,35]
20	BSMImBr	24	>99	0	1	99	-	
21	$BSMImHSO_4$ [d]	1	>99	17	2	81	-	
22	BSMImBr [d]	1	>99	11	2	87	-	
23	K_2CO_3	1	0	0	0	0	-	
24	$[P_{1888}]CH_3OCO_2^-$	1	0	0	0	0	-	

Reaction conditions: Glyc [5.43 mmol] and $HC(OMe)_3$ with Q = 10, catalyst (10%w/w_{Glyc}), 90 °C, 1-24h. [a)] Conversion of Glyc and products selectivity determined by GC. [b)] Hammett acidity function according to literature data. [c)] the value reported was calculated for butylsulfonylmethylimidazolium chloride. [d)] the reaction was carried out at T = 25 °C.

3.3.4 Conclusions

The thermal and catalytic reactivity of glycerol with trimethyl orthoformate was here fully explored for the first time. Under catalyst-free conditions, with an equimolar mixture of Glycerol and $HC(OMe)_3$ (Q = 1), the reaction leads to the unselective formation of a dynamic equilibrium mixture of products **1**, **2** and **3** (Scheme 3.12 and Table 3.7). The products were isolated and fully characterized by GC-MS, ^1H, ^{13}C and 2D-NMR spectroscopy revealing the formation exclusively of the 5-membered ring isomers of **1** and **3**, obtained as mixtures of two diastereoisomers. The equilibrium of this reaction is remarkably shifted towards the formation of **3** as evinced for longer reaction times, higher temperature and/or using a large excess of orthoformate (Q = 10). **3** could thus be obtained selectively in high yields at 90 °C with 10 equivalents of trimethyl orthoformate after 24 h.

Both the reaction time and temperature can be reduced by using Brønsted- and Lewis-acid catalysts. The strongest acidic catalysts (H_2SO_4, Amberlyst 15, Amberlyst 36, iron chloride and aluminium fluoride) accelerate attainment of the dynamic equilibrium of the reaction to yield preferentially **3**, but also promote ill-defined degradation products. Less acidic catalysts such as the ionic liquids $BSMImHSO_4$ and BSMImBr also accelerate attainment of the thermodynamically favored product **3** (98-99%) without however further degradations as indicated by the stability of **3** over time.

Overall, the present results shed light on the reaction pathway and on the equilibria that govern conversion of glycerol into its orthoesters **1** and **3** and it allows to selectively synthesize **3** as the couple of diastereoisomers by a proper choice of reaction conditions. The glycerol-based orthoesters represent new building blocks en route to the development of more complex glycerol-OEs architectures.

3.3.5 Experimental Section

3.3.5.1 General Information

All the chemicals were purchased from Aldrich and used as received. Trioctylmethylphosphonium methylcarbonate ($[P_{8881}]CH3OCO_2^-$) was synthesized according to a literature procedure.[30]

GC analyses were run using a Perkin Elmer Elite-624 capillary column (L=30 m, Ø=0.32 mm, film thickness=1.8 µm). The following conditions were used. Carrier gas: N_2; flow rate: 3.5 mL min^{-1}; split ratio: 1:1; initial T: 50 °C (4 min), ramp rate: 10 °C min^{-1}; final T: 180 °C; ramp rate: 20°C min, final T: 240 °C (10 min). GC-MS (EI, 70 eV) analyses were run using a Grace AT-624 capillary column (L=30 m, Ø=0.32 mm, film thickness=1.8 µm). The following conditions were used. Carrier gas: He; flow rate: 1.2 mL min^{-1}; split ratio: 10:1; initial T: 50 °C (4 min), ramp rate: 10 °C min^{-1} to 180 °C; ramp rate: 20°C min, final T: 240 °C (10 min). ^1H, $^{13}C\{1H\}$, DEPT-135, DEPT-90, APT, NOESY, HSQC, HMBC, COSY NMR spectra were recorded on a Bruker 400 MHz (^1H: 400 MHz; ^{13}C: 100 MHz) spectrometer. For ^1H and $^{13}C\{1H\}$ NMR the chemical shifts (δ) have been reported in parts per million (ppm) relative to the residual undeuterated solvent as an internal reference.

3.3.5.2 Synthesis/Isolation of reaction products

*Synthesis of (2-methoxy-1,3-dioxolan-4-yl)methanol (**1**)*

Glycerol (5.12g, 55.6 mmol) was added in a two-neck round bottom flask equipped with a dripping funnel and a heating condenser held at 70°C. The flask was heated at 90°C and $HC(OMe)_3$ (6.1 ml, 55.6 mmol) was added dropwise under stirring and kept for 1h. In Figure 3.11, the gaschromatographic trace of the reaction crude is reported highlighting the presence of diastereomers. The reaction mixture was then distilled over potassium carbonate three times to isolate one pure diastereoisomer of 1 in 10% yield, hereafter identified as **1a** (the peaks with retention time 15.0 min in Figure 3.11). The characterization of the other diastereoisomer 1b (retention time 15.8 min) is inferred from the spectra of the mixture.

^1H NMR (400 MHz, Acetone)**1a**: δ = 5.72 (s, 1H), 4.23 – 4.18 (m, 1H), 4.11 – 4.04 (m, 1H), 3.84 – 3.78 (m, 1H), 3.66 (ddd, J=6.0, 5.2, 2.7, 2H), 3.26 (s, 3H). 13C NMR (101 MHz, Acetone) δ = 115.93, 77.03, 65.47, 62.86, 50.22. GC-MS: 134 (M+,0);133 (1); 103 (100); 61 (31); 57 (46); 47 (15); 45(32); 44 (31); 43 (65). 1b: 5.73 (s, 1H), 4.32 (ddt, J=6.9, 5.6, 5.0, 1H), 4.11 – 4.04 (m, 1H), 3.84 – 3.78 (m, 1H), 3.57 (dd, J=6.0, 5.0, 2H), 3.23 (s, 3H). 13C NMR (101 MHz, Acetone) δ = 115.82, 76.09, 65.42, 62.22, 50.00. GC-MS: 134 (M+,0);133 (1); 103 (100); 74 (8); 61 (18); 57 (47); 47 (15); 45(28); 44 (14); 43 (46). All the ^1H, ^{13}C, COSY, HMBC, HSQC, COSY NMR and the GC-MS spectra are reported in Figure A.3.41-52.

*Synthesis of 2,6,7- trioxabyciclo[2.2.1]heptane (**2**).*

Any attempt to isolate 2 from the crude reaction mixture proved unsuccessful and it was identified only by GC-MS (Figure A.3.53). GC-MS: 102 (M+,8);101 (4); 45 (15); 44 (100); 43 (62); 42 (6).

*3.2.3 Synthesis of 4-(dimethoxymethoxy)methyl)-2-methoxy-1,3-dioxolane (**3**)*

Glycerol (0.526 g, 5.71 mmol) and $HC(OMe)_3$ (6.3 ml, 57.2 mmol) were added in a round-bottomed flask and the mixture was stirred at 90°C. During the reaction the methanol was distilled out the mixture by heating the condenser at 70°C. After 24h the mixture was cooled down and then concentrated under vacuum (60°C, 35 mbar). **3** was obtained a mixture of two diastereomers in 95% yield without any further purification (purity 98% by GC). The diastereoisomeric ratio of **3** was 1:1 according to GC and ^{1}H NMR analyses (Figure A.3.56). Any attempts to separate the two isomers (hereafter called **3a** or **3b**) failed. ^{1}H NMR (400 MHz, Acetone) **3a**+**3b** : δ = 5.76 (s, 1H), 5.73 (s, 1H), 5.11 (s, 1H), 5.10 (s, 1H), 4.44 (dq, J=6.9, 5.3, 1H), 4.34 – 4.27 (m, 1H), 4.11 (ddd, J=7.9, 6.8, 5.6, 2H), 3.81 – 3.77 (m, 2H), 3.71 (dd, J=10.6, 6.1, 1H), 3.65 – 3.61 (m, 1H), 3.57 (dd, J=6.2, 5.3, 2H), 3.31 – 3.29 (m, 12H), 3.26 (s, 3H), 3.25 (s, 3H). 13C NMR (101 MHz, Acetone) δ = 116.13, 115.86, 113.99, 113.95, 74.80, 74.11, 66.00, 65.68, 64.82, 63.80 (d, J=2.1), 50.72, 50.71, 50.21, 50.04. GC-MS: **3a**: 208 (M+,0);131 (1); 117 (8); 103 (12); 75 (100); 61 (13); 57 (25); 47 (11); 43(9). **3b**: 208 (M+,0);131 (2); 117 (8); 103 (12); 75 (100); 61 (13); 57 (25); 47 (11); 45(6); 43 (9). Further discussion on the structural characterization and the ^{1}H, ^{13}C{1H}, DEPT-135, DEPT-90, APT, NOESY, HSQC, HMBC and COSY NMR and GC-MS spectra (Figure A.3.54-64) are reported in supporting info.

3.3.5.3 Synthesis of the acidic catalysts

Synthesis of pyridinium para-toluensulfonate (PPTS).

The synthesis was carried out following a literature procedure.[36] ^{1}H NMR (400 MHz, MeOD) δ = 8.89 (dt, J=5.2, 1.6, 2H), 8.68 (tt, J=7.9, 1.6, 1H), 8.16 – 8.09 (m, 2H), 7.75 – 7.69 (m, 2H), 7.27 – 7.22 (m, 2H), 2.38 (s, 3H). The spectrum is in agreement with the literature (Figure A.3.65).

Synthesis of diazobicycloundecenium bromide (DBUHBr).

An aqueous solution of hydrobromic acid (40% v/v, 13.2 mmol) was dripped into a vessel containing an equimolar amount of DBU under continuous stirring. After 24 h, the aqueous solution was concentrated by rotary evaporation (60°C, 40 mbar) and any trace of water was removed under reduced pressure (60°C, 1 mbar) until a white solid was obtained (yield = 99%). ^{1}H NMR (400 MHz, D2O) δ = 3.50 (dt, J=18.0, 5.6, 4H), 3.28 (t, J=5.9, 2H), 2.62 – 2.55 (m, 2H), 1.97 (tt, J=7.2, 5.2, 2H), 1.74 – 1.60 (m, 6H). ^{13}C NMR (101 MHz, D_2O) δ = 165.95, 54.19, 48.26, 38.01, 32.87, 28.47, 25.90, 23.34, 18.96. (Figure A.3.66-67)

Synthesis of butylsulfonylmethylimidazolium hydrogensulfate ($BSMImHSO_4$).

1-methylimidazole and 1,4-butane-sultone were charged into a 100 mol round-bottom flask in an equimolar amount (0.1 mol) and stirred at 80°C for 16h. The white solid zwitterionic product was washed with ethyl ether (10x5ml) to remove any unreacted starting materials and the solid was dried in vacuum. Then, a stoichiometric amount of sulfuric acid (95% v/v H_2O) was added and the mixture stirred at 60°C for 10 h, to obtain the ionic liquid $BSMImHSO_4$. The IL was washed again with dichloromethane and ether and dried under vacuum. $BSMImHSO_4$ was obtained in 95% of yield and it was used without any further purification. ^{1}H NMR (400 MHz, D2O) δ = 8.61 (s, 1H), 7.38 (s, 1H), 7.31 (s, 1H), 4.11 (s, 2H), 3.77 (s, 3H), 2.82 (s, 2H), 1.88 (s, 2H), 1.62 (s, 2H). ^{13}C NMR (101 MHz, D_2O) δ = 135.90, 123.60, 122.11, 50.01, 48.86, 35.61, 28.04, 20.87. All spectra (Figure A.3.68-69) are in agreement with those reported in literature.[37]

Synthesis of Butylsulfonylmethylimidazolium bromide (BSMImBr)

1-methylimidazole and 1,4-butane-sultone were charged into a 100 mol round-bottom flask in an equimolar amount (0.1 mol) and stirred at 80°C for 16h. The white solid zwitterionic product was washed with ethyl ether (10x5ml) and dried in vacuum (yield=90%). Then a stoichiometric amount of hydrobromic acid (40% v/v H_2O) was added and the mixture stirred at 60°C for 10 h to yield to the ionic liquid BSMImBr. The ionic liquid (IL) was washed again with dichloromethane and ether to remove non-ionic residues and dried under vacuum. The IL was obtained with a 90% yield and used without any further purification. ^{1}H NMR (400 MHz, D_2O) δ = 8.66 – 8.61 (m, 1H), 7.40 (t, J=1.8, 1H), 7.34 (t, J=1.8, 1H), 4.15 (t, J=7.0, 2H), 3.79 (d, J=0.6, 3H), 2.87 – 2.81 (m, 2H), 1.97 – 1.87 (m, 2H), 1.68 – 1.58 (m, 2H). ^{13}C NMR (101 MHz, D_2O) δ = 135.92, 123.63, 122.14, 50.04, 48.90, 35.68, 28.08, 20.90. (Figure A.3.70-71).

3.3.5.4 General procedures for the Gly-HC(OMe)$_3$ reactions

Catalyst-free conditions.

Glycerol (0.5 g, 5.43 mmol) and cyclopentyl methyl ether (100 µl) as an internal standard were added in a two-neck round-bottomed flask equipped with a dripping funnel and a condenser. The mixture was stirred at the selected temperature (T = 25 or 90°C) and $HC(OMe)_3$ was added dropwise by varying the molar ratio Q from 1 to 10. The reaction was allowed to proceed for 24 h under stirring and samples were collected and analyzed by GC at regular intervals. For reactions run at 90 °C, the condenser was heated at 70°C in order to continuously distill methanol.

Catalyzed reaction.

The above reported procedure was followed with the exception that the selected catalyst (10% w/w Glyc) was added with glycerol and cyclopentyl methyl ether, before the addition of $HC(OMe)_3$.

*Catalytic procedure for the synthesis of **3**.*

Glycerol (0.5 g, 5.43 mmol), $HC(OMe)_3$ (5.9 ml, 54.3 mmol) and a catalytic amount of the selected catalyst ($BSMImHSO_4$, BSMImBr, 3% mol/mol glyc) were added in a round-bottomed flask and the mixture was stirred at 90°C. During the reaction the methanol was distilled out the mixture by heating the condenser at 70°C. After 1h, the mixture was cooled down and the solution was passed through a short plug of alumina. The filtered solution was concentrated under vacuum (60°C, 35 mbar). **3** was obtained as a mixture of two diastereomers in 96% yield without any further purification (purity 98% by GC).

3.3.6 Reference

[1] S. Guidi, R. Calmanti, M. Noè, A. Perosa and M. Selva, *ACS Sustainable Chemistry & Engineering*, 2016, **4**, 6144-6151; (b) L. Cattelan, A. Perosa, P. Riello, T. Maschmeyer and M. Selva, *ChemSusChem*, 2017, **10**, 1571-1583; (c) M. Selva, S. Guidi and M. Noè, *Green Chemistry*, 2015, **17**, 1008-1023.

[2] S. Guidi, M. Noè, P. Riello, A. Perosa and M. Selva, *Molecules*, 2016, **21**, 657.

[3] (a) A. Perosa, A. Moraschini, M. Selva and M. Noè, *Molecules*, 2016, **21**, 170; (b) R. Calmanti, M. Galvan, E. Amadio, A. Perosa and M. Selva, *ACS Sustainable Chemistry & Engineering*, 2018, **6**, 3964-3973 ; (c) D. Rigo, R. Calmanti, A. Perosa and M. Selva, *Green Chemistry*, 2020, **22**, 5487-5496.

[4] (a) R. H. DeWolfe, *Synthesis*, 1974, 153–172; (b) U. Pindur, Acid Derivatives, John Wiley & Sons, 1992.

[5] P. P. Sah, *Journal of the American Chemical Society*, 1928, **50**, 516-518.

[6] S. M. McElvain and D. Kundiger, *Journal of the American Chemical Society*, 1942, **64**, 254-259.

[7] K.-H. G. Brinkhaus, E. Steckhan and D. Degner, *Tetrahedron*, 1986, **42**, 553-560.

[8] Cordes, E.; Bull, H. Mechanism and catalysis for hydrolysis of acetals, ketals, and ortho esters. *Chemical Reviews* **1974**, *74*, 581-603.

[9] J. G. Erickson, *The Journal of Organic Chemistry*, 1955, **20**, 1573-1576.

[10] M. Noè, A. Perosa and M. Selva, *Green chemistry*, 2013, **15**, 2252-2260.

[11] (a) T. W.Greene, P. G. M.Wuts in *Protective Groups in Organic Synthesis*, JohnWiley & Sons, 1999, pp.369–453; (b) P. J. Kocienski in *Protecting Groups*, Thieme, 2005, pp.100–106.

[12] S.-G. Liao, H.-D. Chen and J.-M. Yue, *Chemical reviews*, 2009, **109**, 1092-1140.

[13] D. R. Chaffey, T. E. Davies, S. H. Taylor and A. E. Graham, *ACS Sustainable Chemistry & Engineering*, 2018, **6**, 4996-5002.

[14] Gabriele, B.; Mancuso, R.; Salerno, G.; Veltri, L.; Costa, M.; Dibenedetto, A., *ChemSusChem*, 2011, **4**, 1778-1786.

[15] (a) Zhou, X.; Luo, S.; Tang, R.; Wang, R.; Wang, J*., Macromolecular Bioscience,* 2015, **15**, 385-394; (b) J. Heller, J. Barr*, Biomacromolecules*, 2004, **5**, 1625-1632.

[16] R. A. Bunce, *Organic Chemistry*, 2020, **1**, 400-436.

[17] (a) Brachvogel, R.-C.; Hampel, F.; Von Delius, M., *Nature communications,* 2015, *6*, 7129: (b) Löw, H.; Mena-Osteritz, E.; von Delius, M., *Chemical science,* 2018, **9**, 4785-4793.

[18] Z. Nazarian and M. Dabiri, *ChemistrySelect*, 2020, **5**, 4394-4412.

[19] (a) G. Crank and F. Eastwod, *Australian Journal of Chemistry*, 1964, **17**, 1385-1391; (b) G. Crank and F. Eastwood, *Australian Journal of Chemistry*, 1964, **17**, 1392-1398.

[20] N. N. Tshibalonza and J.-C. M. Monbaliu, *Green Chemistry*, 2017, **19**, 3006-3013.

[21] H. Hall Jr, F. DeBlauwe and T. Pyriadi, *Journal of the American Chemical Society*, 1975, **97**, 3854-3854.

[22] Y. Yokoyama, A. B. Padias, F. De Blauwe and H. Hall Jr, *Macromolecules*, 1980, **13**, 252-261.

[23] (a) J. Heller, J. Barr, S. Y. Ng, K. S. Abdellauoi and R. Gurny, *Advanced drug delivery reviews*, 2002, **54**, 1015-1039; (b) A. B. Padias, R. Szymanski and H. K. Hall, in *Ring-Opening Polymerization*, American

Chemical Society, 1985, vol. 286, ch. 23, pp. 313-333; (c) Y. Yokoyama and H. Hall, in *New Polymerization Reactions*, Springer, 1982, pp. 107-138.

[24] L. Zhang, M. Yu, J. Wang, R. Tang, G. Yan, W. Yao and X. Wang, *Macromolecular bioscience*, 2016, **16**, 1175-1187.

[25] A. S. Amarasekara, *Chemical reviews*, 2016, **116**, 6133-6183.

[26] J. Cox, *Tetrahedron*, 1963, **19**, 1175-1184.

[27] S. E. Fletcher, C. T. Mortimer and H. D. Springall, *Journal of the Chemical Society (Resumed)*, 1959, **12**, 580-584.

[28] R.-C. Brachvogel and M. von Delius, *Chemical science*, 2015, **6**, 1399-1403.

[29] K. Kaupmees, A. Trummal and I. Leito, *Croatica Chemica Acta*, 2014, **87**, 385-395.

[30] M. Fabris, V. Lucchini, M. Noè, A. Perosa and M. Selva, *Chemistry–A European Journal*, 2009, **15**, 12273-12282.

[31] (a) C. Thomazeau, H. Olivier-Bourbigou, L. Magna, S. Luts and B. Gilbert, *Journal of the American Chemical Society*, 2003, **125**, 5264-5265; (b) D.-J. Tao, J. Wu, Z.-Z. Wang, Z.-H. Lu, Z. Yang and X.-S. Chen, *RSC Advances*, 2014, **4**, 1-7.

[32] G.A. Olah, G.K.S. Prakash, J. Sommer, Superacids, Wiley, Chichester, 1985.

[33] R. Bringué, M. Iborra, J. Tejero, J. F. Izquierdo, F. Cunill, C. Fité and V. J. Cruz, *Journal of Catalysis*, 2006, **244**, 33-42.

[34] L. Ni, J. Xin, K. Jiang, L. Chen, D. Yan, X. Lu and S. Zhang, *ACS Sustainable Chemistry & Engineering*, 2018, **6**, 2541-2551.

[35] Yao, L.; Liu, S.; Li, L.; Yu, S.; Liu, F.;Song, Z.; *Bullettin of Ethiopian Chemical Society,* **2016**, *30*, 283–6.

[36] M. Miyashita, A. Yoshikoshi and P. A. Grieco, *The Journal of Organic Chemistry*, 1977, **42**, 3772-3774.

[37] D.-J. Tao, J. Wu, Z.-Z. Wang, Z.-H. Lu, Z. Yang and X.-S. Chen, *RSC Advances*, 2014, **4**, 1-7.

4 Conclusions

This Ph.D. thesis concerned with the development of greener, more efficient processes for the synthesis of bio-based chemicals from low-value feedstocks. The uptake of a "green" toolbox guides the research path whatever the application field.

Exploit waste renewable feedstocks; synthesize benign-by-design chemicals; avoid the use of extra-solvents, especially toxic or environmentally concerning ones; avoid the use of auxiliaries (including catalysts) when chemical reactions achieve unrivalled performance in their absence; employ strategies designed to avoid the handling of toxic and harmful substances whenever possible; tend to an overall process intensification that yield a maximized productivity while prevent accident through an inherently safer chemistry; the easy recover of reaction products through smart procedures that replace costlier and environmentally-burden procedures such as chromatography and the use of large amounts of solvents for purification; the recycle of catalysts (when used). A continuous effort to keep in mind these principles was applied throughout this thesis: irrespective of whether the results are satisfactory or not, this approach is desirable to reach the scope of "not-feigned" sustainable processes. First, we attempted to apply these concepts in the synthesis of cyclic organic carbonates.

In the primary research, the synthesis of tungstate -based catalysts was explored and the synthesis of tungstate ionic liquids (TILs) was designed through a greener route compared to those found in literature. TILs were studied as catalysts for the CO_2 fixation into epoxides and they resulted suitable to this use. Epoxides, however, are not-benign chemicals which poses concerns for their toxicity and potential mutagenicity: they should not be handled. For this reason, TILs were exploited also to explore the direct oxidative carboxylation of olefins. The optimized protocol led to the direct synthesis of cyclic organic carbonates staring from terminal olefins of different chain lengths (C_6 – C_{16}) while a simplified procedure was extended to the direct oxidative carboxylation of internal olefins which are contained in renewable feedstocks (i.e. methyl oleate): this is the first time that a tandem oxidative carboxylation process was applied to oleochemicals. The greenness of the process relies on the conceiving of an assisted tandem catalysis approach where TILS acted as oxidation catalyst, phase transfer catalysts and CO_2 insertion catalysts. Their use prompted also the simultaneous retention of the stereospecificity when pure cis olefins were used. Other green features were: the use of hydrogen peroxide as oxidant (only water as by-product); the employment of CO_2 at atmospheric pressure as C_1 source; the use of simple alkali halide salts such as KBr and KI as halide source that favour the ring-opening of the epoxide; the easy recover of the reaction products from the biphasic reaction mixtures.

The application of TILs has apparently terrific proficiencies in the direct oxidative carboxylation of olefins. However the use of tungsten-based catalyst cannot be considered sustainable at all, since the limited availability related to the wide use of this metal (figure 1.1), the social unacceptance of tungsten mining, the uncertainty on environmental and toxic effects of this metal, the introduction of tungsten between the "conflict minerals" (along with tin, tantalum and gold) which "finance armed groups, fuel forced labour and other human right abuses, support corruption and money laundering" by the European commission. The use of a more sustainable and abundant metal (e.g. Iron-based catalyst) or the use of organic metal-free catalysts should be deepened in future researches.

In our second work, we explored the chances to carry out the CO_2 fixation into epoxides in continuous-flow system through the use of simple catalytic system based on diethylene glycol and NaBr, which are economic and commercially viable compounds. The CO_2 insertion in continuous-flow reactors is

challenging as demonstrated by the scarce literature on the argument and the difficult uniform mixing of a gas/liquid mixture in continuous-flow conditions. Despite harsh conditions were employed, our protocol allowed to reach high yields in cyclic organic carbonates and higher productivity respect to the reaction performed in batch conditions. Moreover, a simple method to recover and reuse the catalytic system was developed.

A second part of the Ph. D. thesis focused on the use of glycerol as feedstock for the synthesis of high value-added compounds.

In the first work, the continuous-flow esterification of glycerol and glycerol derivatives was developed in catalyst-free conditions with different esters. Isopropenyl acetate (iPAc) led to outstanding performance when compared to other esters: a quantitative yield in triacetin and solketal acetate was obtained through the use of iPAc in just 20 minutes of residence time at 220°C.

This work suggested us to explore a successive catalytic tandem process. The impressive catalytic activity of iPAc is due to the acetone released during the reaction that promote an irreversible esterification in presence of a nucleophile: we hence developed a catalytic tandem method to promote the monoesterification of glycerol and the concurrent reuse of the acetone released from iPAc through the acetalization of the vicinal hydroxyl group contained in glycerol. In this way, Solketal acetate or a 1:1 mixture of Solketal acetate and Triacetin was attained through the use of a heterogeneous acid commercial catalyst (Amberlyst-15).

Finally, the reactivity of glycerol with orthoesters was investigated: a regioselective synthesis of diastereoisomeric derivatives of glycerol orthoesters was carried out through a catalyst-free procedure.

Therefore, this Ph.D. thesis represents a step forward in the synthesis of cyclic organic carbonates and glycerol derivatives through green and sustainable processes.

4.1 Papers originated from this thesis

Overall topics investigated during this Ph.D. thesis led to the drafting of 7 scientific papers and a review article. A list follows:

- Calmanti, R.; Galvan, M.; Amadio, E.; Perosa, A.; Selva, M., High-Temperature Batch and Continuous-Flow Transesterification of Alkyl and Enol Esters with Glycerol and Its Acetal Derivatives. *ACS Sustainable Chemistry & Engineering* **2018,** *6* (3), 3964-3973.
- Calmanti, R.; Amadio, E.; Perosa, A.; Selva, M., Reaction of Glycerol with Trimethyl Orthoformate: Towards the Synthesis of New Glycerol Derivatives. *Catalysts* **2019,** *9* (6), 534.
- Calmanti, R.; Selva, M.; Perosa, A., Tungstate ionic liquids as catalysts for CO_2 fixation into epoxides. *Molecular Catalysis* **2020,** *486*, 110854.
- Rigo, D.; Calmanti, R.; Perosa, A.; Selva, M., A transesterification–acetalization catalytic tandem process for the functionalization of glycerol: the pivotal role of isopropenyl acetate. *Green Chemistry* **2020,** *22* (16), 5487-5496.
- Selva, M.; Perosa, A.; Fiorani, G.; Rigo, D.; Calmanti, R., Diethylene glycol/NaBr catalyzed CO_2 insertion into terminal epoxides: from batch to continuous flow. *ChemCatChem* **2021**, in press.

- R. Calmanti, M. Selva and A. Perosa; One-pot tandem oxidative carboxylation for the direct synthesis of cyclic organic carbonates from olefins and carbon dioxide. *Green Chemistry*, **2021**, *23*, 1921-1941.
- Calmanti, R.; Selva, M.; Perosa, A., Assisted tandem tungsten-based catalysis for the direct oxidative carboxylation of olefins into cyclic carbonates, *paper in draft.*
- Calmanti, M; Sargentoni, N.; Selva, M.; Perosa, A., One-pot tandem synthesis of cyclic organic carbonates from oleochemicals, *paper in draft*.

5 Appendix

Appendix A.1

Appendix A.2 Chapter 2

Appendix A.2.1.

Tungstate ionic liquids as catalysts for CO_2 fixation into epoxides

FT-IR spectra

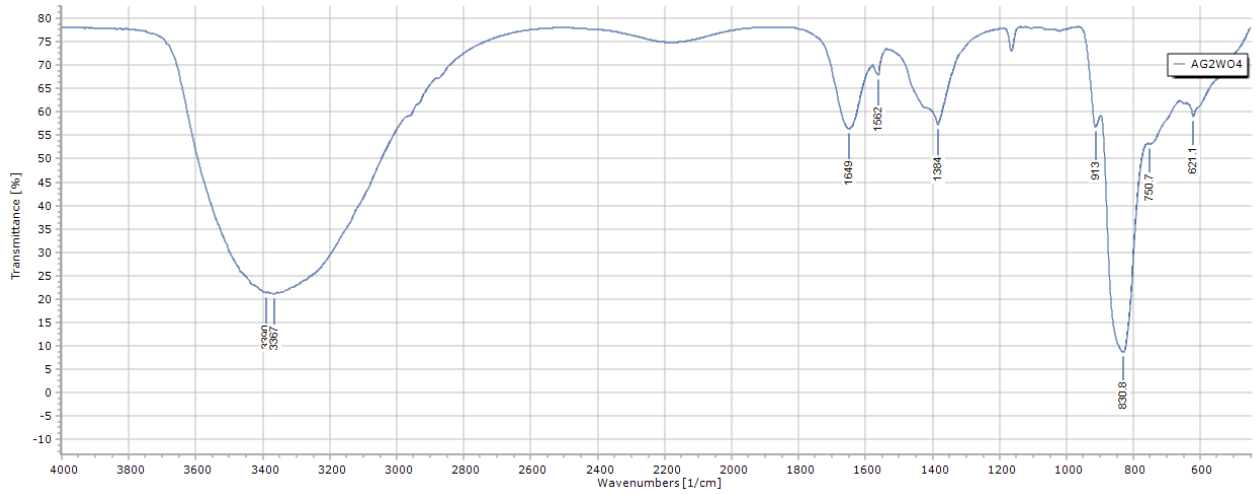

Figure A 2.1: FT-IR spectra of Ag_2WO_4

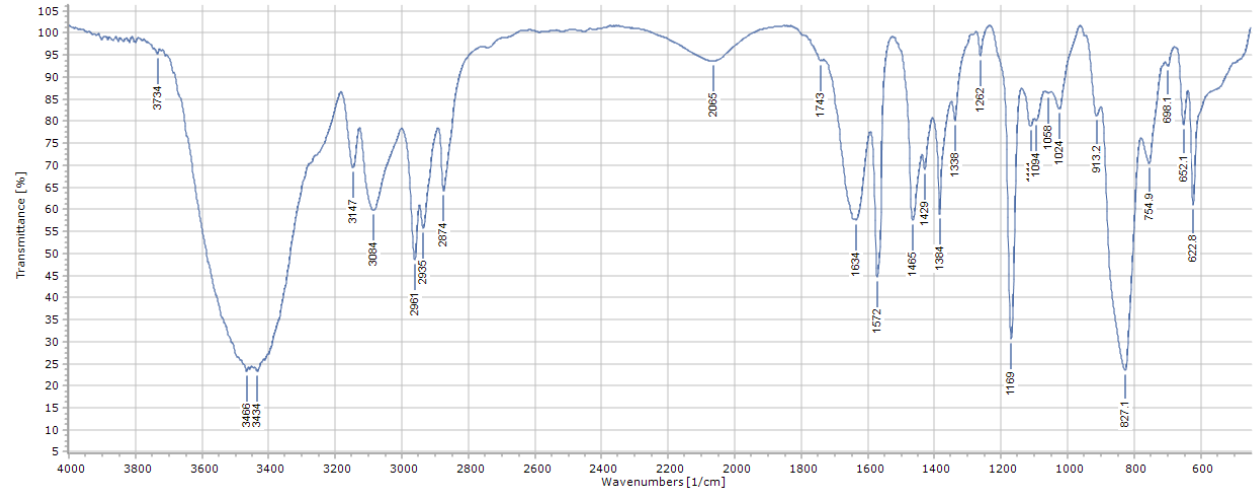

Figure A 2.2: FT-IR spectra of $BMIM_2WO_4$

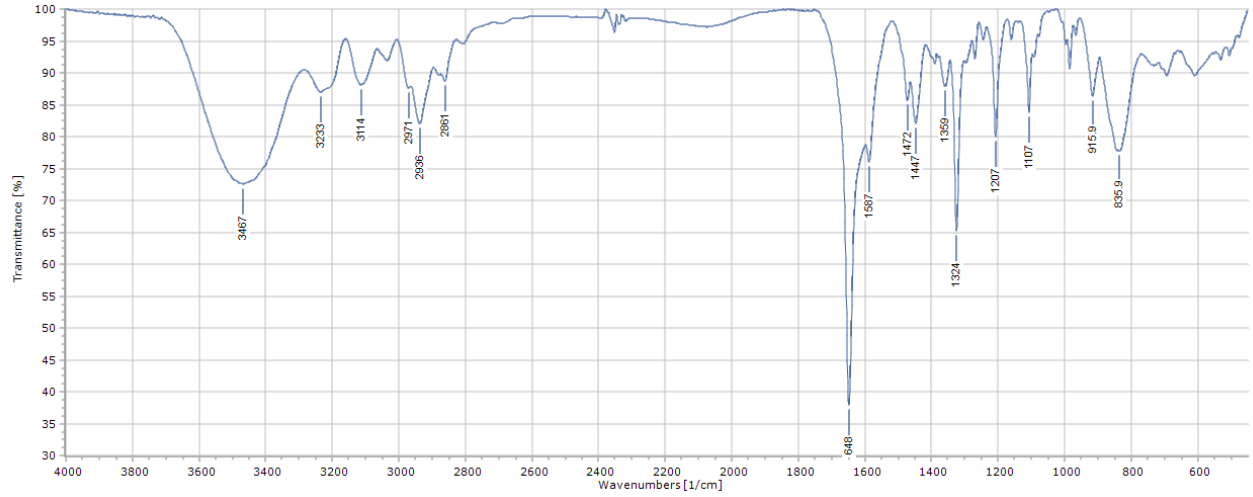

Figure A 2.3: FT-IR spectra of $(DBUH)_2WO_4$

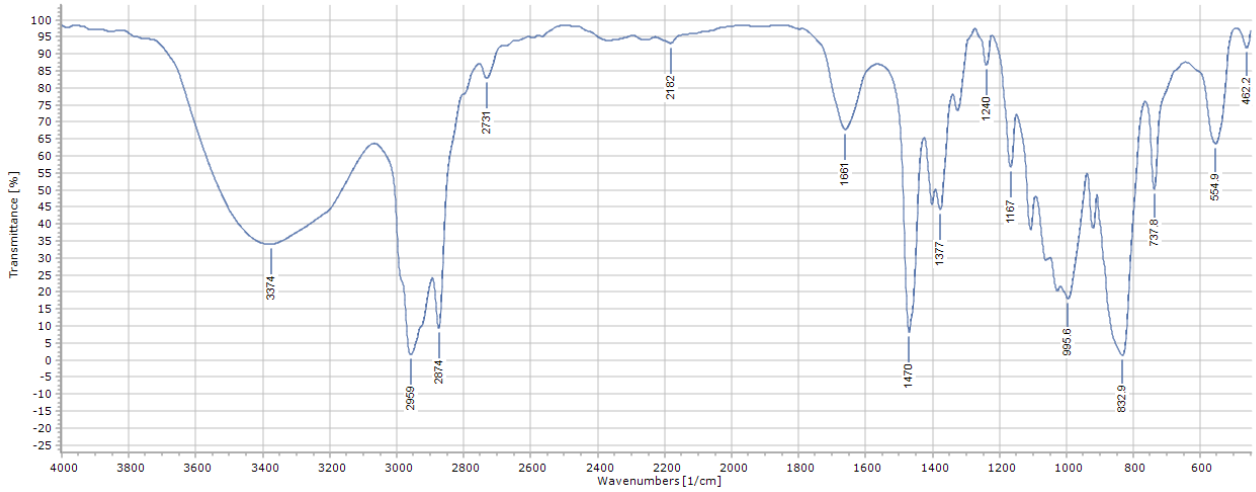

Figure A 2.4: FT-IR spectra of $[N_{4,4,4,4}]_2WO_4$

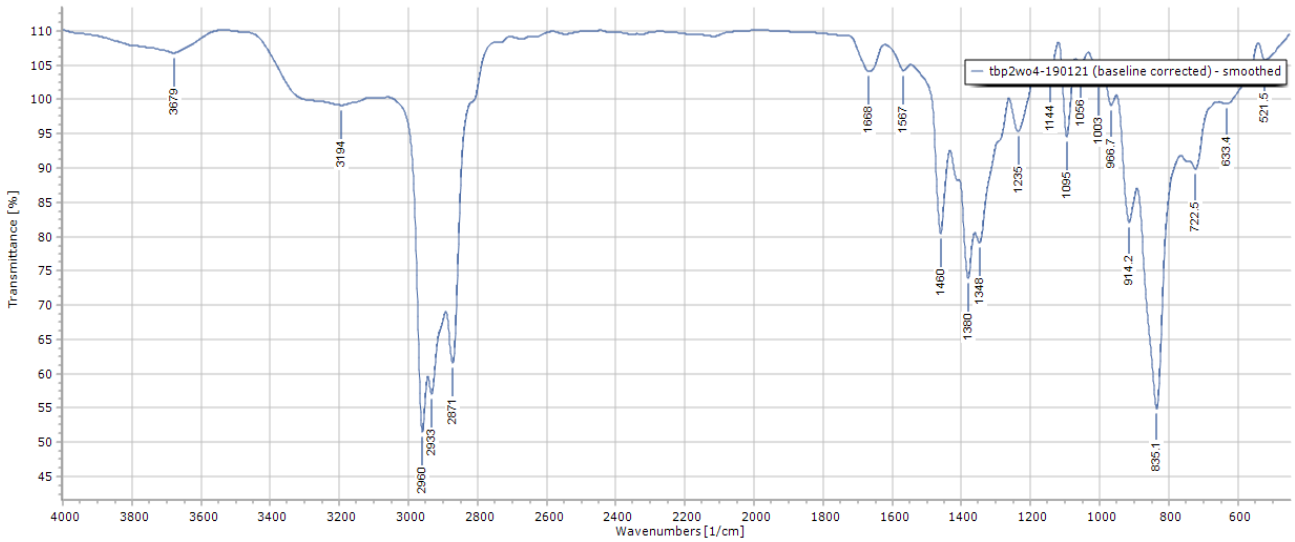

Figure A 2.5: FT-IR spectra of $[P_{4,4,4,4}]_2WO_4$

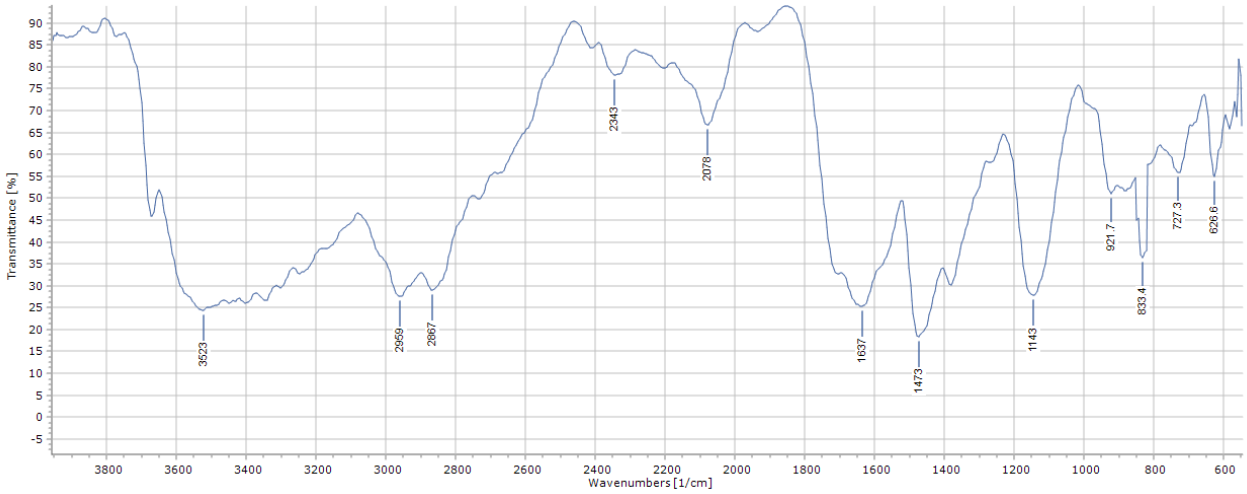

Figure A 2.6: FT-IR spectra of $(N_{8,8,8,1})_2WO_4$

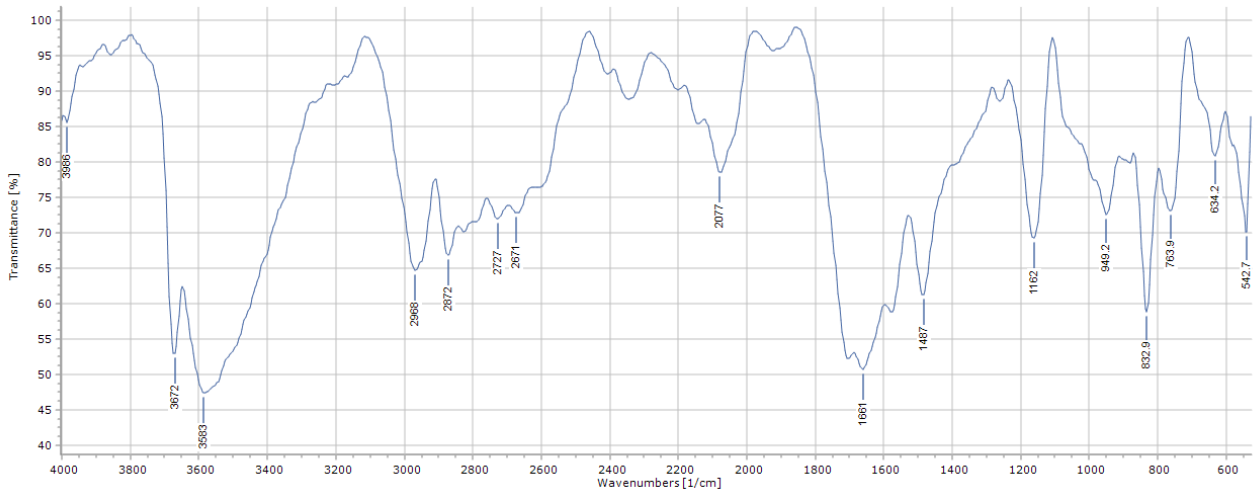

Figure A 2.7: FT-IR spectra of $(N_{8,8,8,1})_2W_2O_3(O_2)_4$

^{1}H NMR and ^{13}C NMR spectra

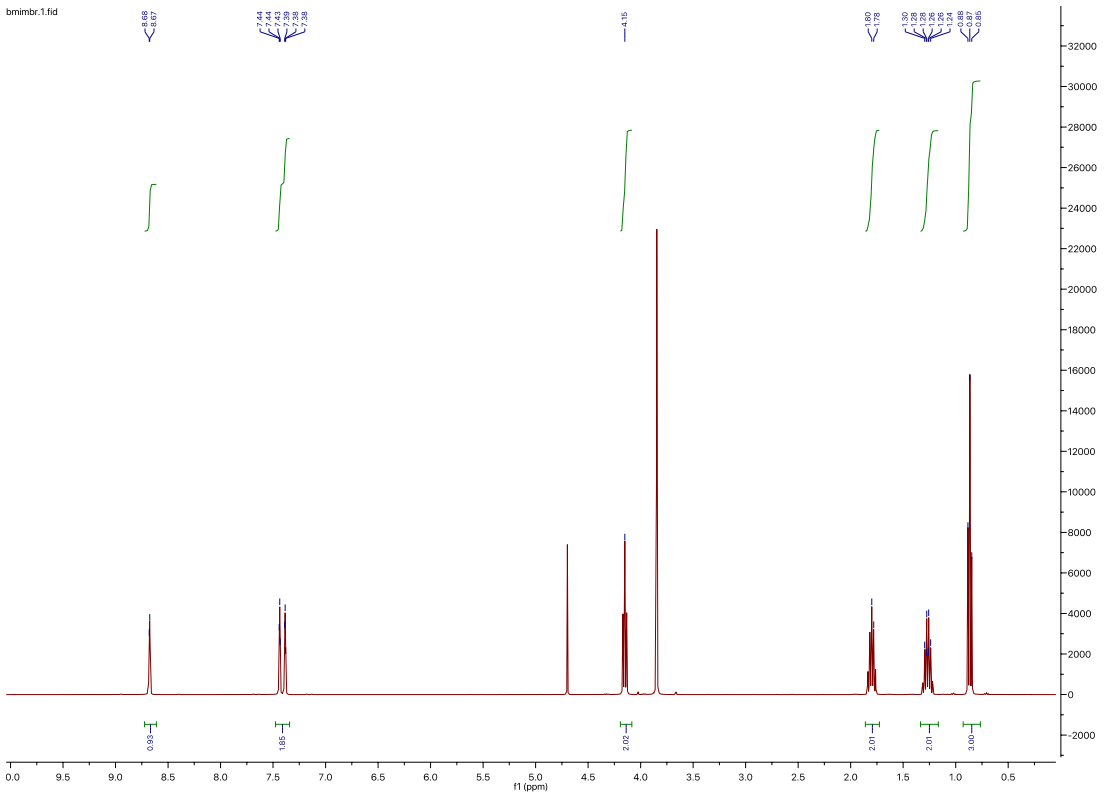

Figure A 2.8: ^{1}H NMR (400 MHz, D_2O) BMImBr: δ = 8.65 (d, 1H), 7.43 (t, 1H), 7.38 (t, 1H), 4.15 (s, 2H), 1.79 (d, 2H), 1.38 – 1.10 (m, 2H), 0.85 (t, 3H).

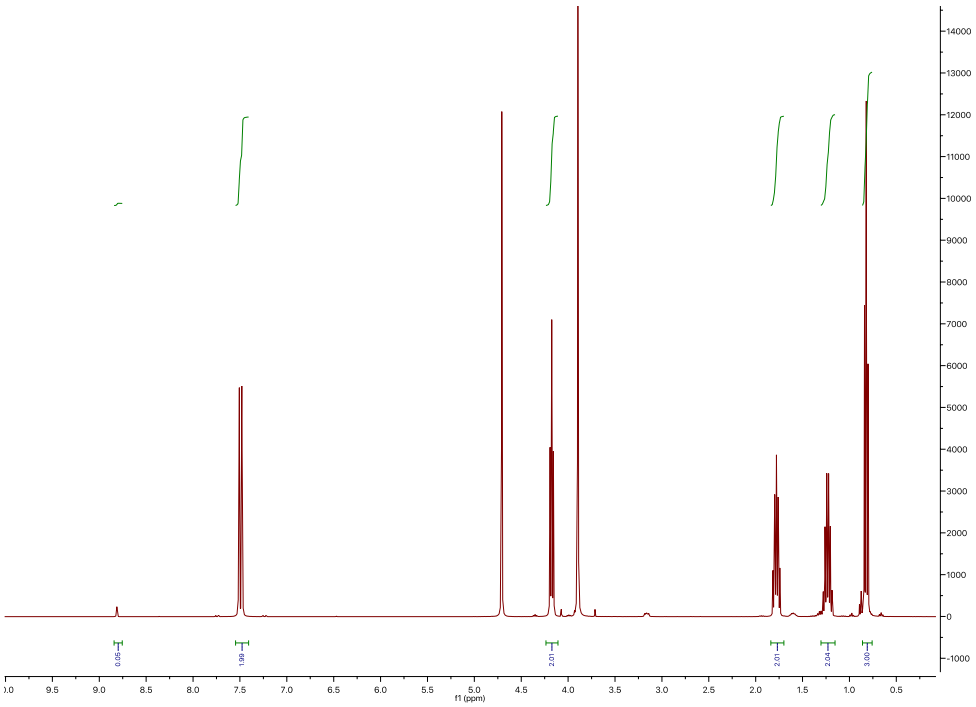

Figure A 2.9: ^{1}H NMR (400 MHz, D_2O) $BMIM_2WO_4$: δ = 8.84 (s, 1H), 7.51 (d, 1h), 7.48 (d, 1h), 4.17 (t, 2H), 1.78 (m, 2H), 1.23 (m, 2H), 0.82 (t, 3H).

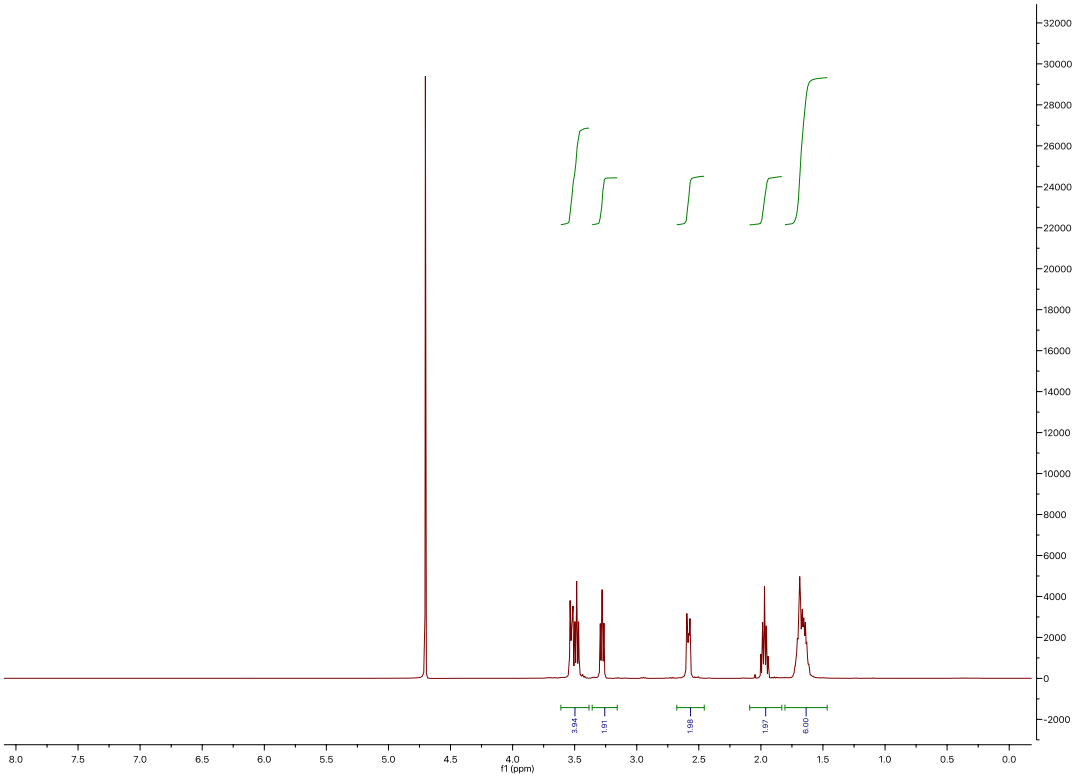

Figure A 2.10: ^{1}H NMR (400 MHz, D_2O) DBUHBr: δ = 3.60 – 3.40 (m, 4H), 3.38 – 3.19 (m, 2H), 2.64 – 2.49 (m, 2H), 2.05 – 1.89 (m, 2H), 1.77 – 1.52 (m, 6H).

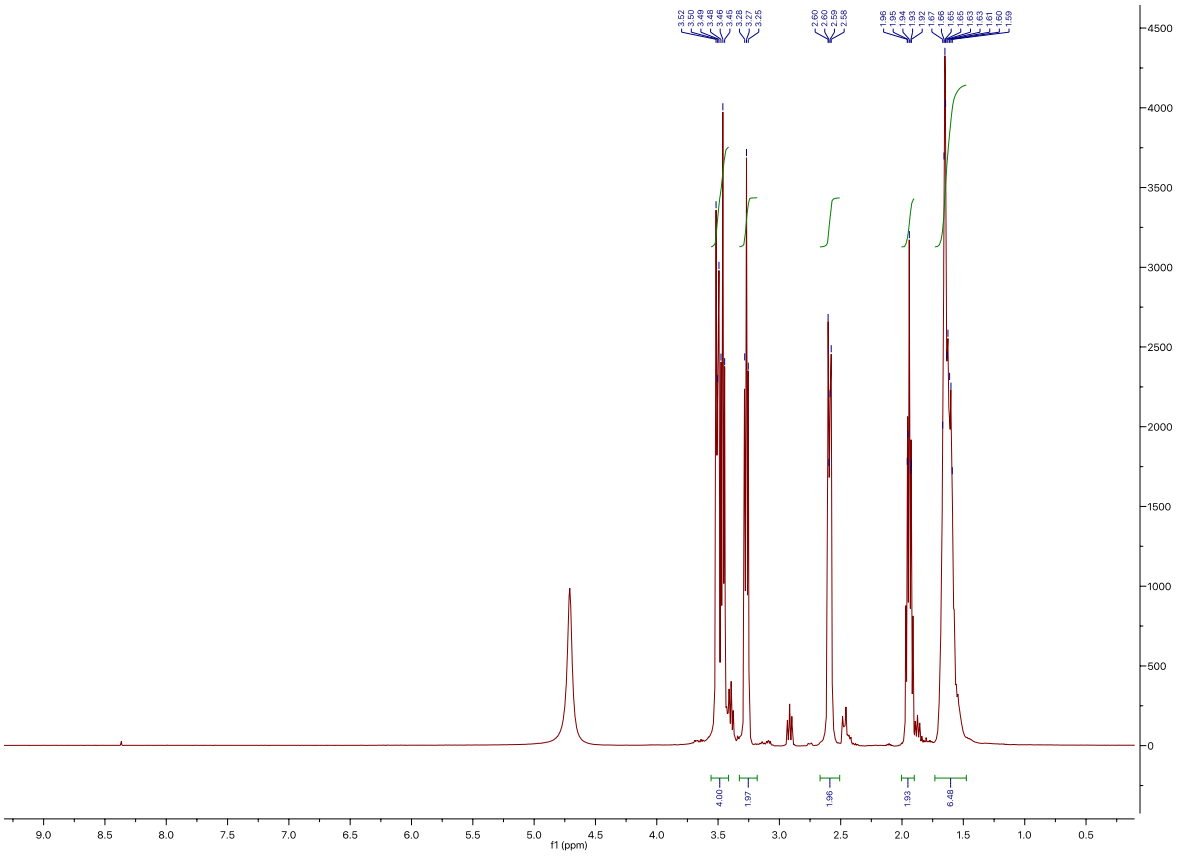

Figure A 2.11: ^{1}H NMR (400 MHz, D_2O) $[DBUH]_2WO_4$: δ = 3.59 – 3.39 (m, 4H), 3.27 (t,2H), 2.65 – 2.54 (m, 2H), 2.00 – 1.88 (m, 2H), 1.63 (ddt, 6H).

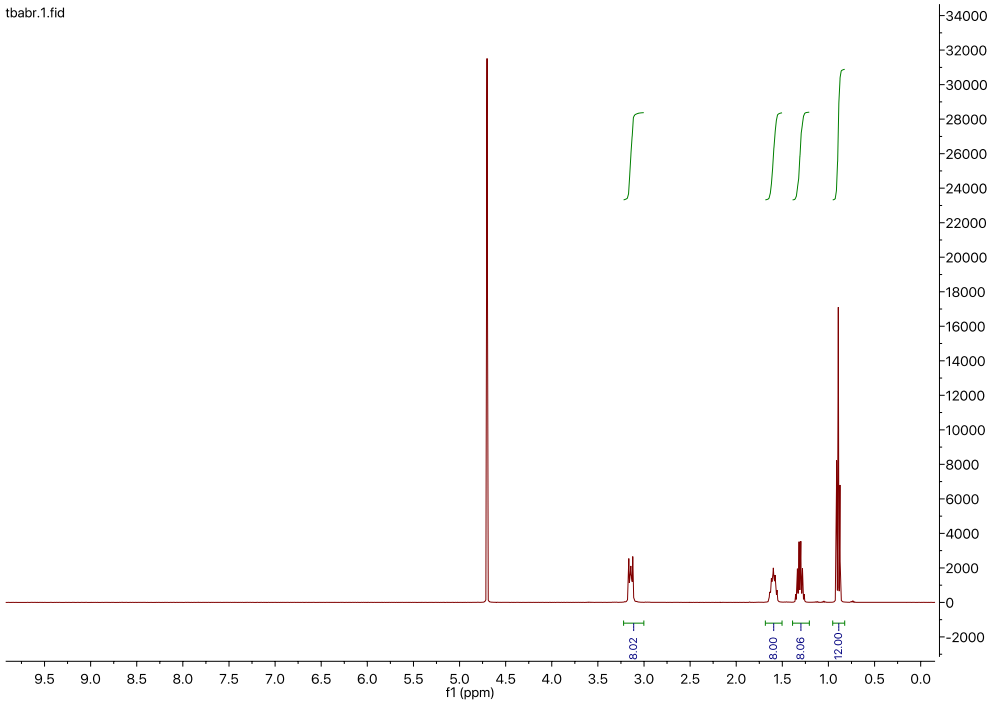

Figure A 2.12: ^{1}H NMR (400 MHz, D_2O) $[N_{4,4,4,4}]Br$: δ = 3.20 – 3.11 (t, 8H), 1.60 (m, 8H), 1.32 (m, 8H), 0.91 (t, 12H)

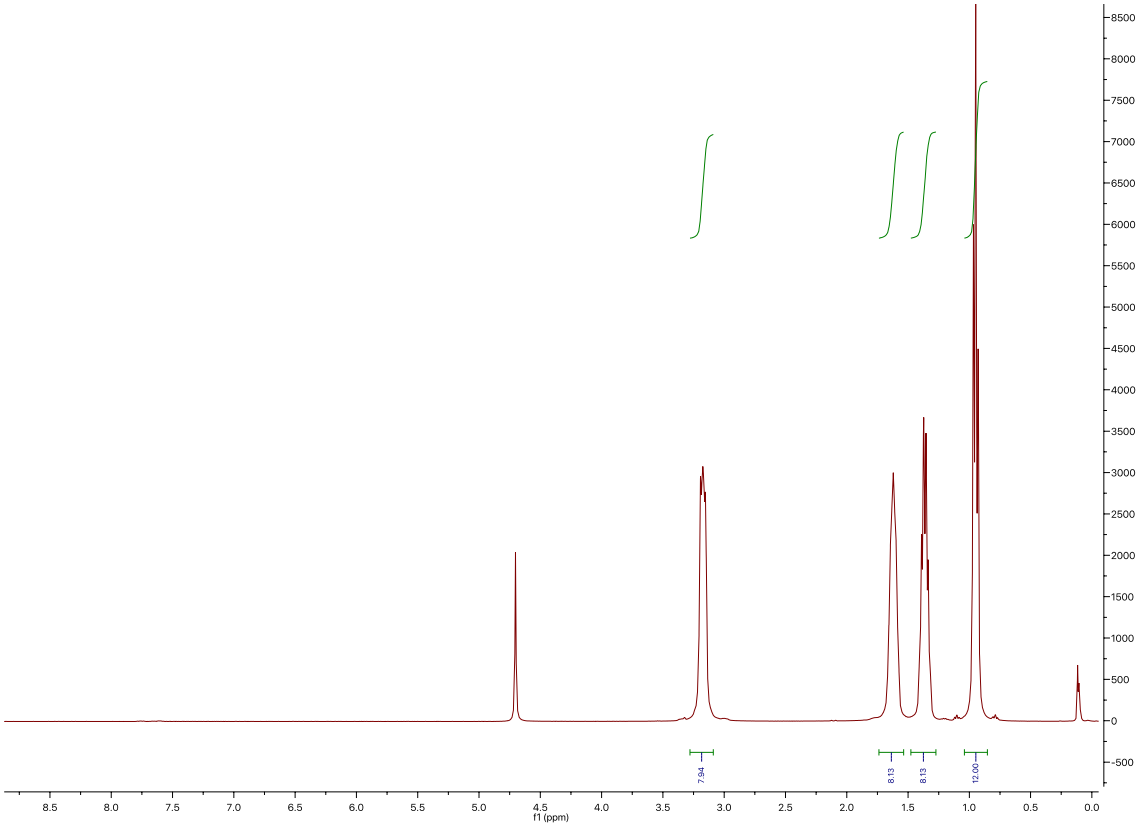

Figure A 2.13: ^{1}H NMR (400 MHz, D_2O) $[N_{4,4,4,4}]_2WO_4$: δ = 3.23 – 3.13 (t, 8H), 1.62 (m, 8H), 1.36 (m, 8H), 0.95 (t, 12H).

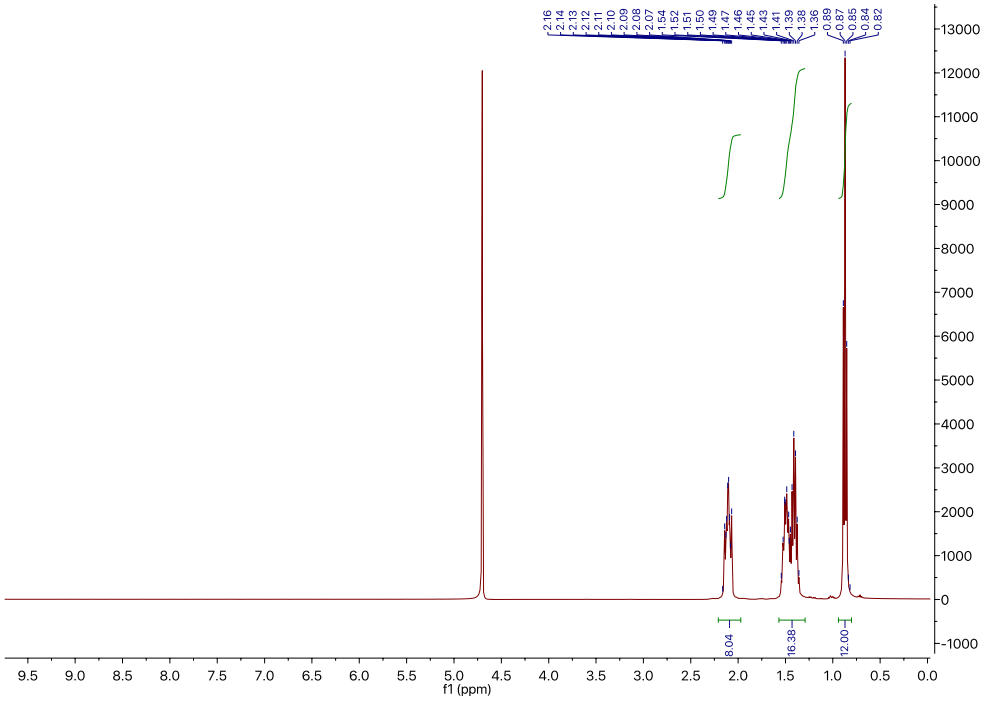

Figure A 2.14: : ^{1}H NMR (400 MHz, D_2O) $[P_{4,4,4,4}]Br$ δ = 2.21 – 1.96 (m, 8H), 1.55-1.30 (d, 16H), 0.93-0.79 (t, 12H).

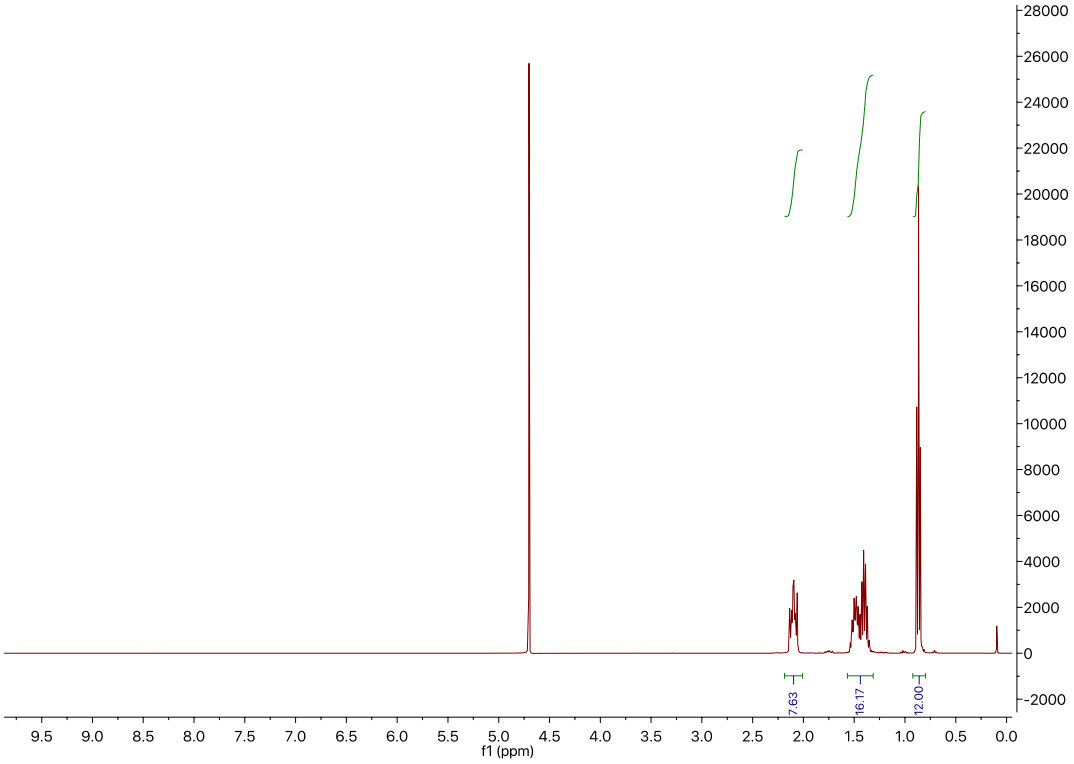

Figure A 2.15: ^{1}H NMR (400 MHz, D_2O) $[P_{4,4,4,4}]_2WO_4$: δ = 2.21 – 1.96 (m, 8H), 1.56 – 1.31 (m, 16H), 0.93 – 0.79 (t, 12H).

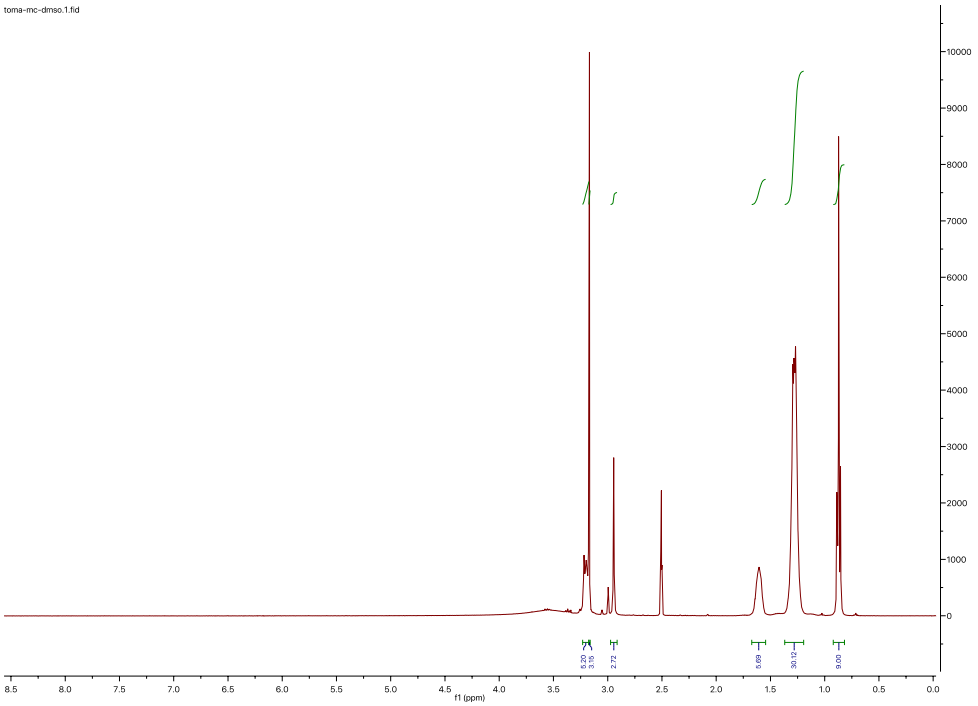

Figure A 2.16: ^{1}H NMR (400 MHz, DMSO) $(N_{8,8,8,1})CH_3OCOO$: δ = 3.23 – 3.17 (m, 6H), 3.17 (s, 3H), 2.92 (s, 3H), 1.62 (m, 6H), 1.37 – 1.19 (m, 30H), 0.92 – 0.82 (t, 9H).

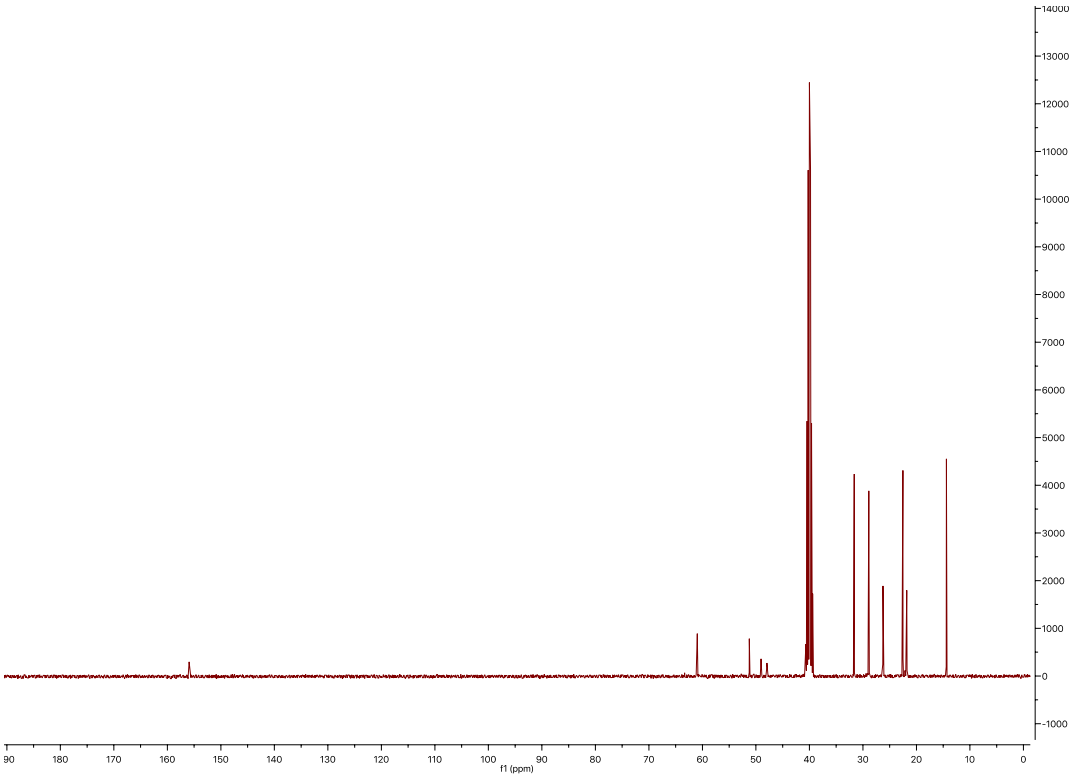

Figure A 2.17: ^{13}C NMR (101 MHz, DMSO) $(N_{8,8,8,1})CH_3OCOO$: δ = 155.94, 60.96, 51.23, 49.03, 47.95, 31.63, 28.91, 26.25, 22.52, 21.80, 14.40.

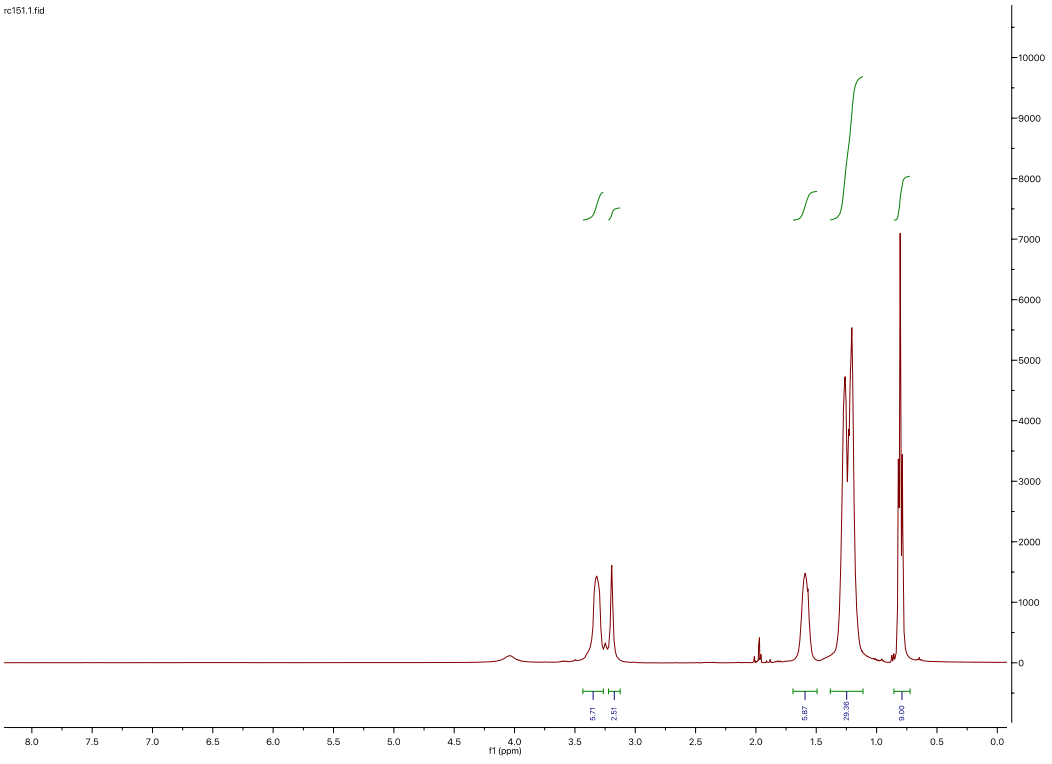

Figure A 2.18: ^{1}H NMR (400 MHz, CD_3CN) $(N_{8,8,8,1})_2WO_4$: δ = 3.43 – 3.26 (t, 6H), 3.19 (s, 3H), 1.64-1.57 (dt, 6H), 1.38 – 1.11 (m, 30H), 0.80 (t, 9H).

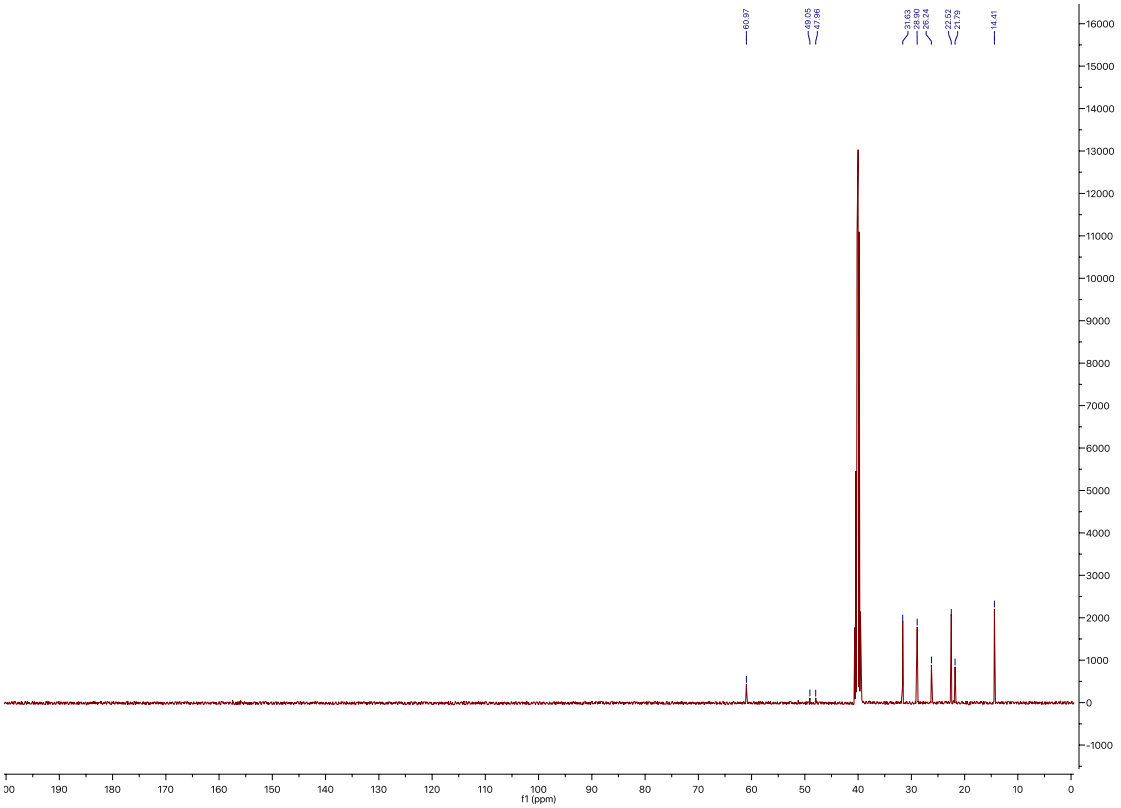

Figure A 2.19: ^{13}C NMR (101 MHz, DMSO) $(N_{8,8,8,1})_2WO_4$: δ = 60.97, 49.05, 47.96, 31.63, 28.90, 26.24, 22.52, 21.79, 14.41.

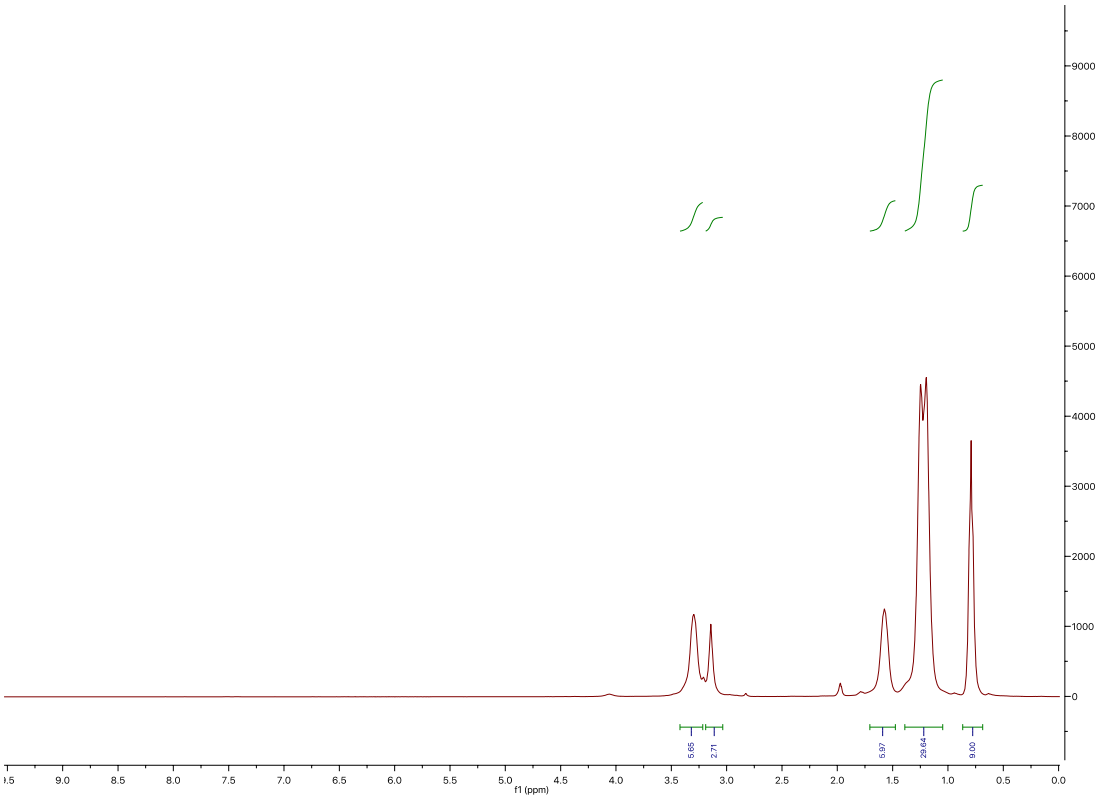

Figure A 2.20: ^{1}H NMR (400 MHz, CD_3CN) $(N_{8,8,8,1})_2W_2O_3(O_2)_4$: δ = 3.43 - 3.29 (t, 6H), 3.14 (s, 3H), 1.67 - 1.60 (dt, 6 h), 1.39 – 1.05 (m, 30H), 0.79 (t, 9H).

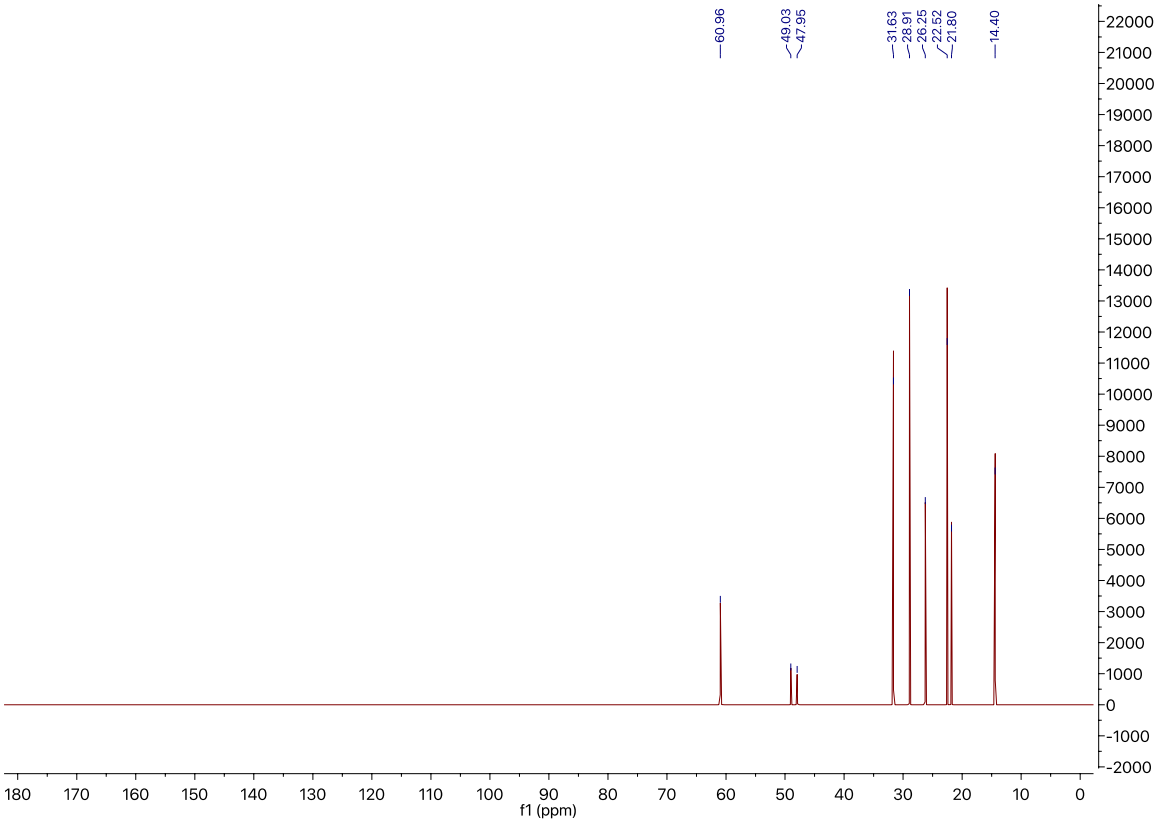

Figure A 2.21: ^{13}C NMR (101 MHz) $(N_{8,8,8,1})_2W_2O_3(O_2)_4$: δ 60.96, 49.03, 47.95, 31.63, 28.91, 26.25, 22.52, 21.80, 14.40.

^{183}W NMR Spectra

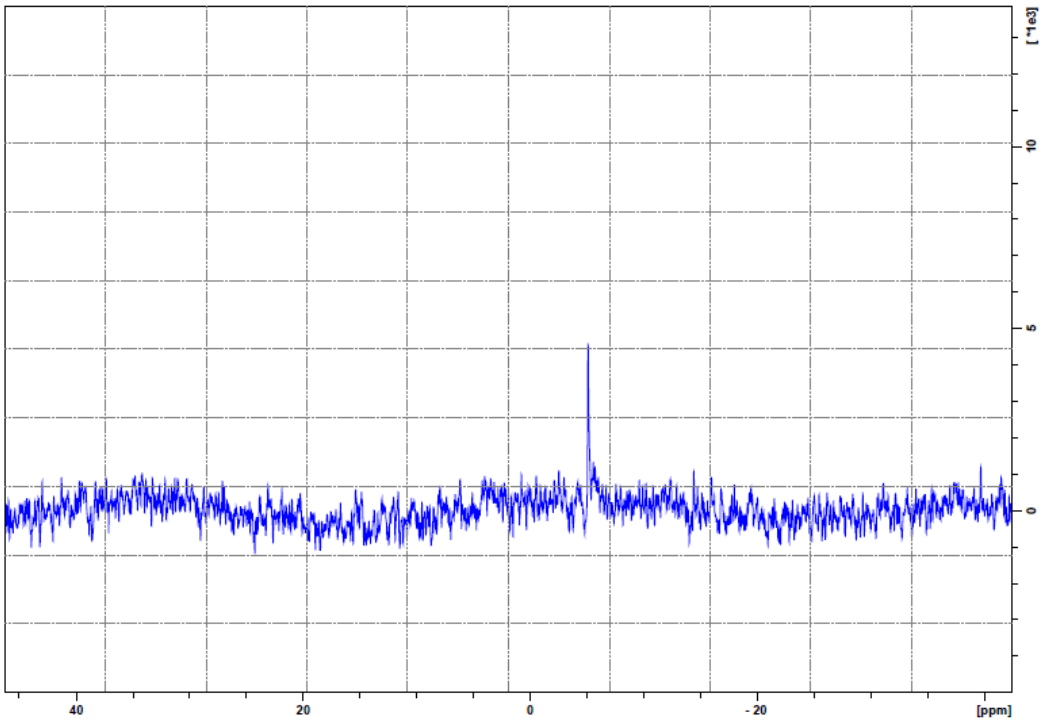

Figure A 2.22: ^{183}W NMR spectra of $BMIM_2WO_4$

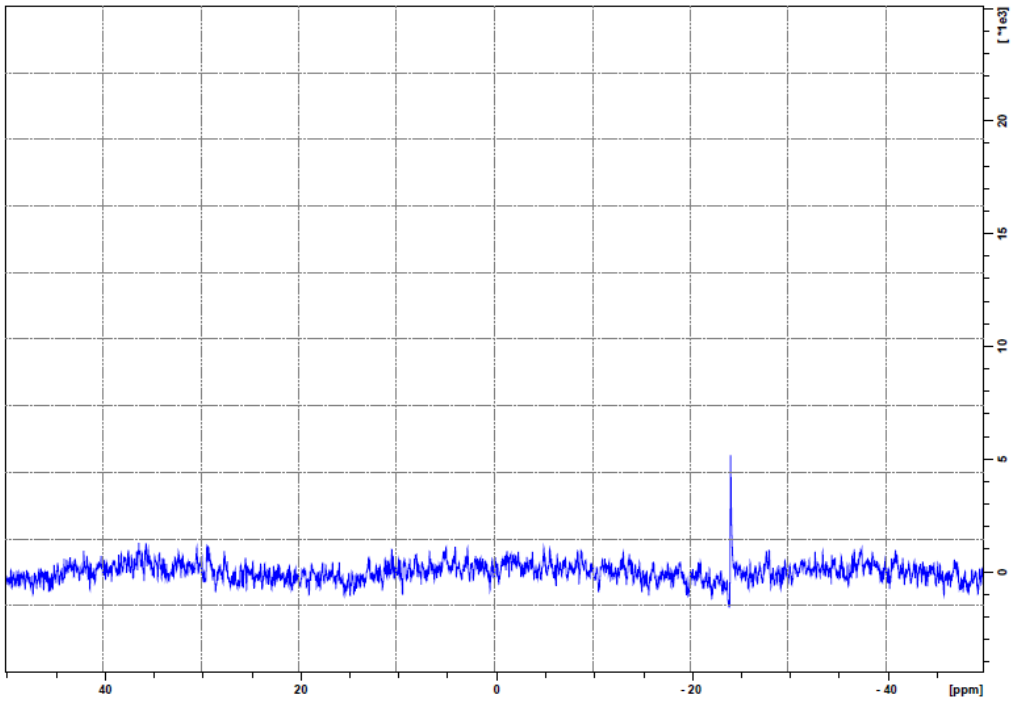

Figure A 2.23: ^{183}W NMR spectra of $(DBUH)_2WO_4$

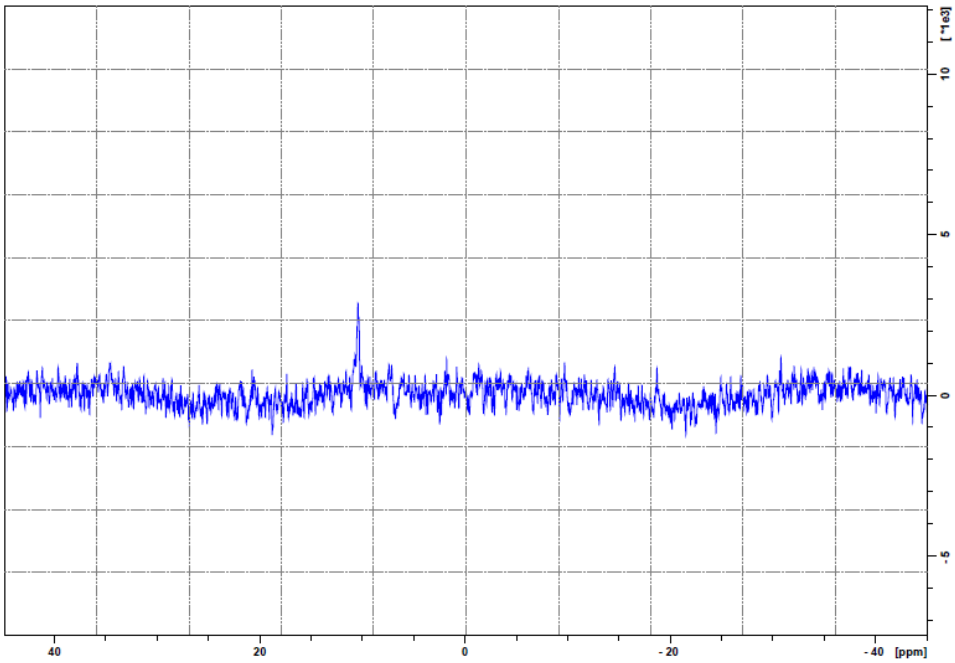

Figure A 2.24: ^{183}W NMR spectra of $[N_{4,4,4,4}]_2WO_4$

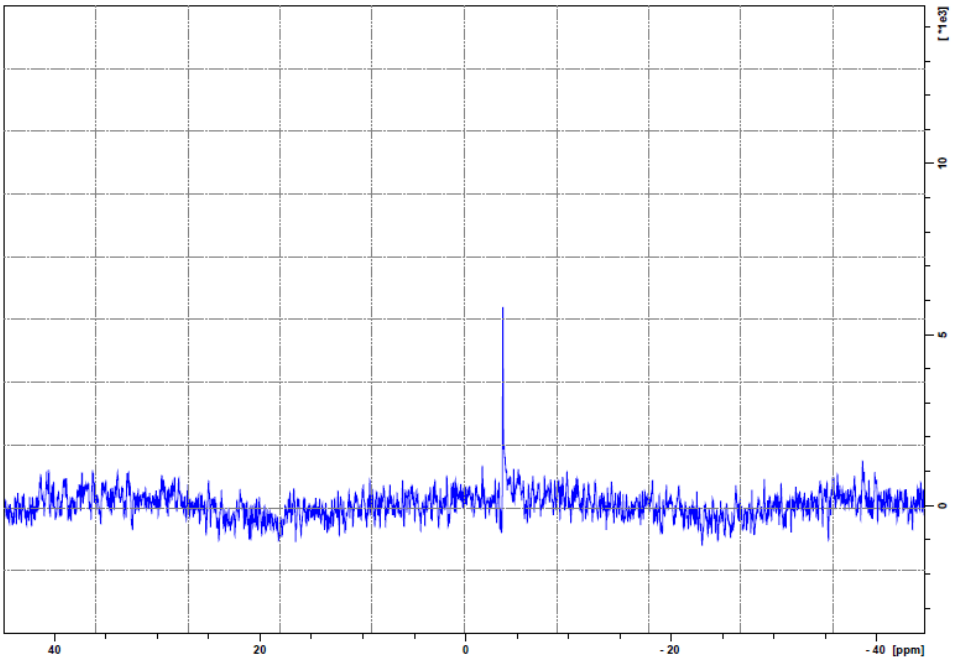

Figure A 2.25: ^{183}W NMR spectra of $[P_{4,4,4,4}]_2WO_4$

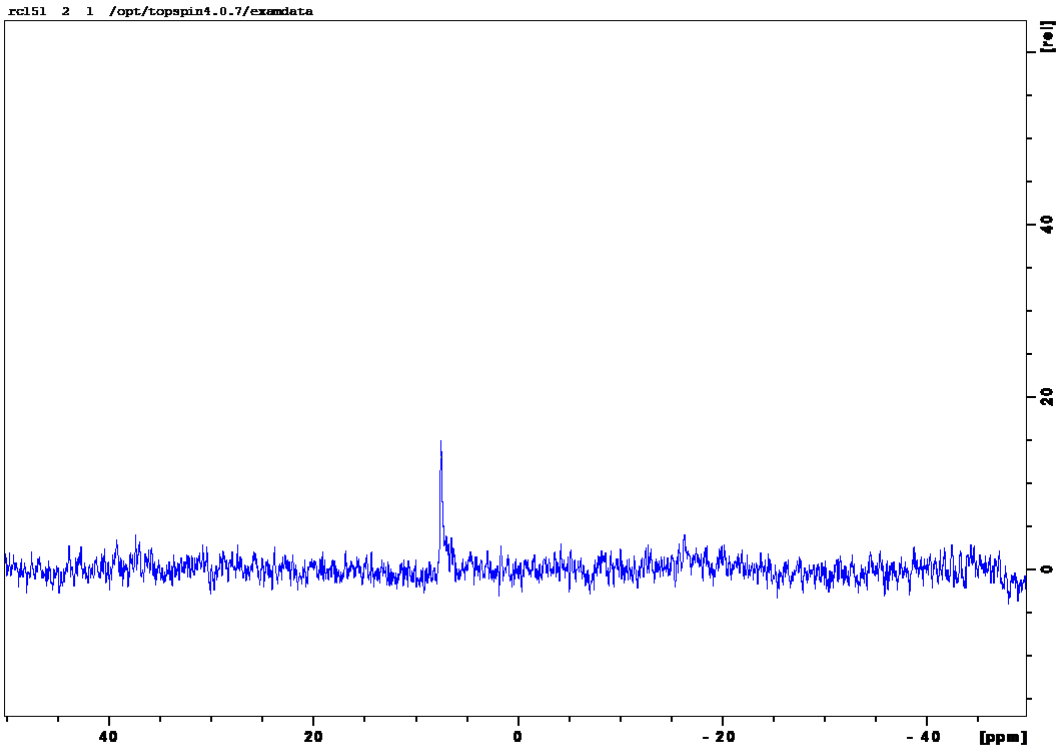

Figure A 2.26: ^{183}W NMR spectra of $N_{8,8,8,1}WO_4$

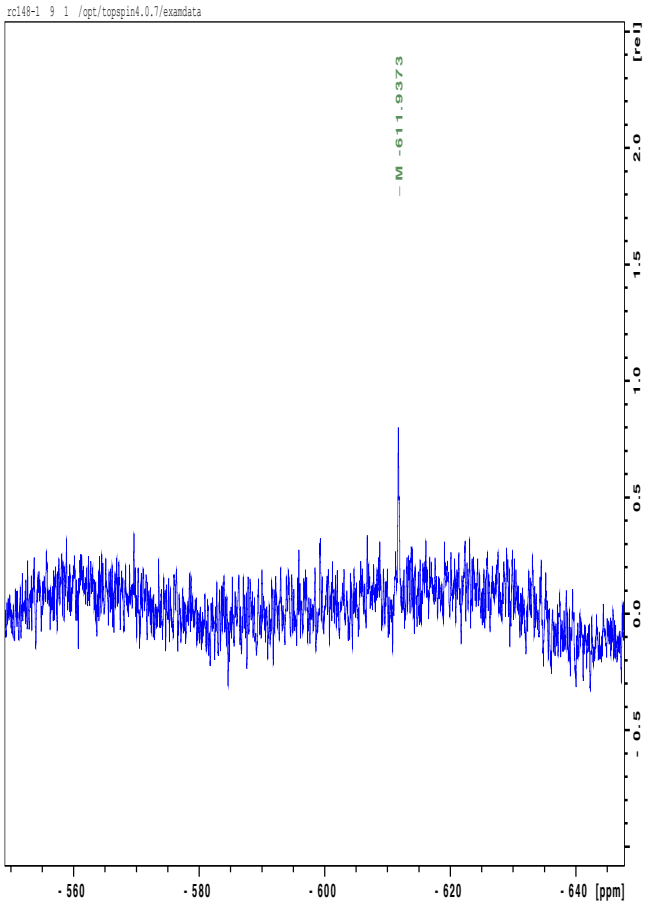

Figure A 2.27: ^{183}W NMR spectra of $(N_{8,8,8,1})_2W_2O_3(O_2)_4$

Styrene carbonate (8)

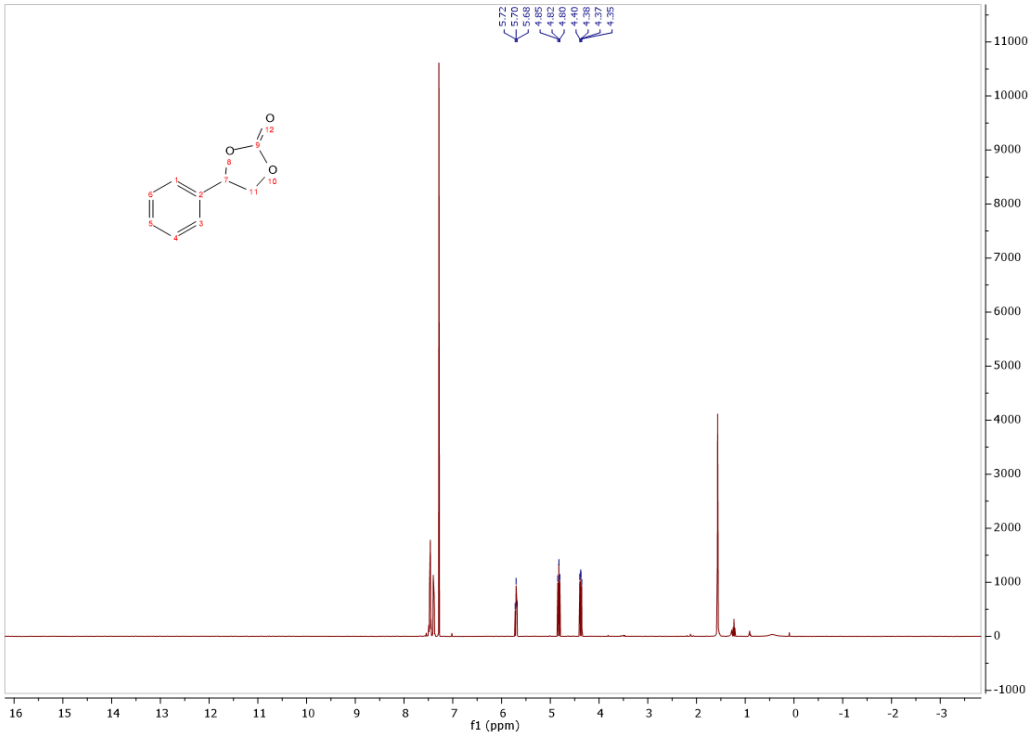

Figure A 2.28: ^{1}H NMR of Styrene Carbonate (400 MHz, 298 K, $CDCl_3$). δ (ppm): 7.51-7.35 (m, 5H), 5.70 (t, 1H), 4.82 (t, 1H), 4.37 (dd, 1H).

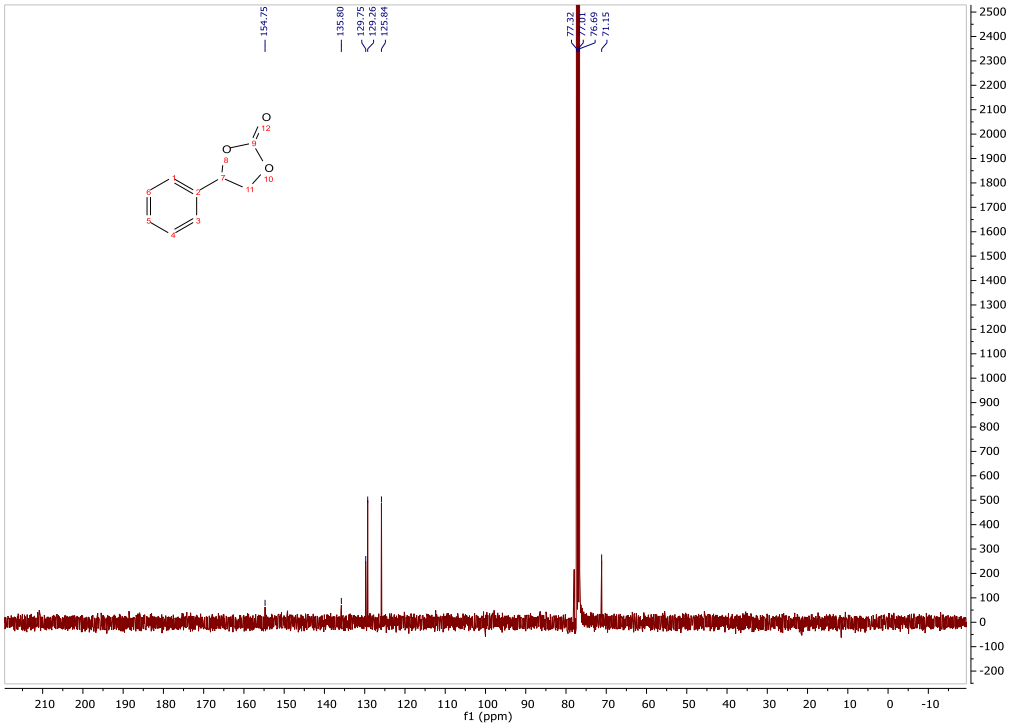

Figure A 2.29: ^{13}C NMR of Styrene Carbonate (100 MHz, 298 K, $CDCl_3$). δ (ppm): 155.08, 77.06, 69.40, 33.89, 31.77, 29.30, 29.14, 29.10, 24.36, 22.61, 14.06.

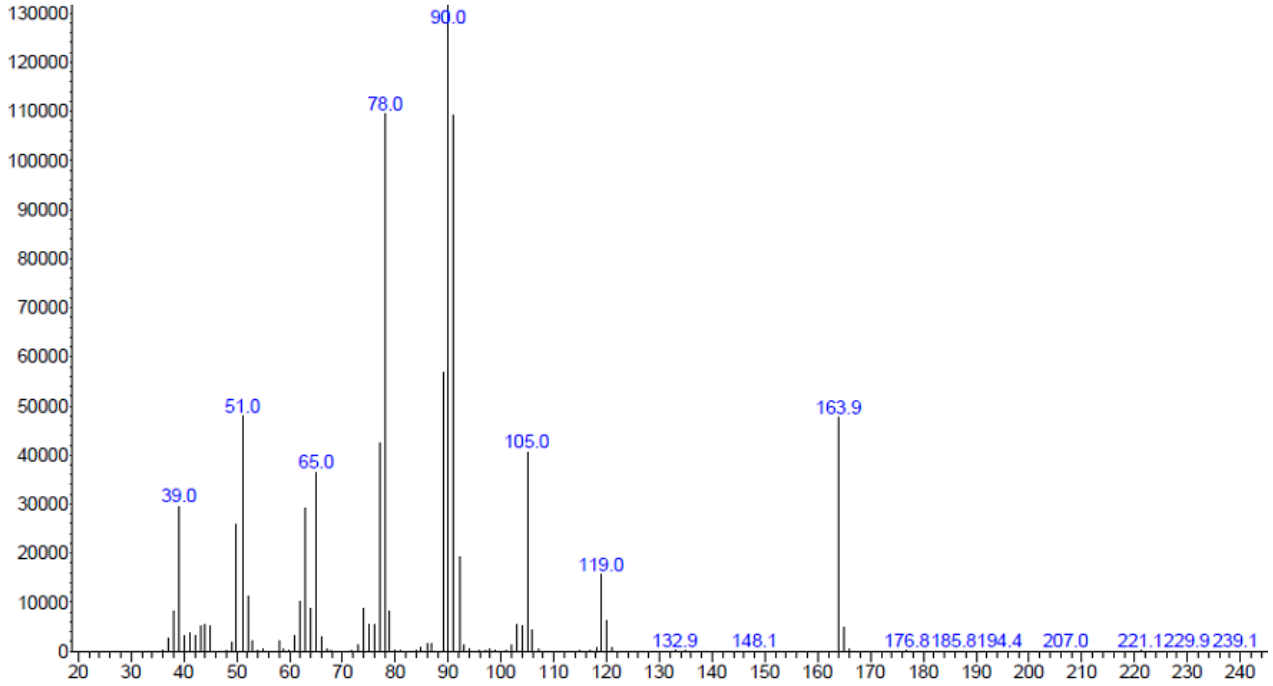

*Figure A 2.30: Mass spectra (EI, 70 eV) of styrene carbonate (**8**). m/z: 165.0 (4) [M⁺], 163.9 (43) [M⁺], 119.0 (13), 105.0 (32), 91.0 (84), 90.0 (100), 78.1 (84), 77.0 (33), 65.0 (29), 51.0 (37), 39.0 (22).*

Appendix A.2.2.
Assisted tandem tungsten-based catalysis for the direct oxidative carboxylation of olefins into cyclic carbonates

The epoxidation of 1-decene with 2-6 equivalents of H_2O_2 in presence of $[N_{8,8,8,1}]_2[WO]_4$ as catalyst.

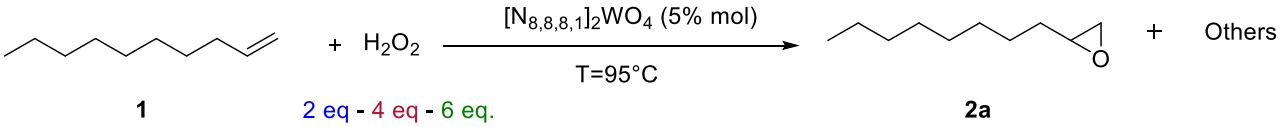

1 2 eq - 4 eq - 6 eq. **2a**

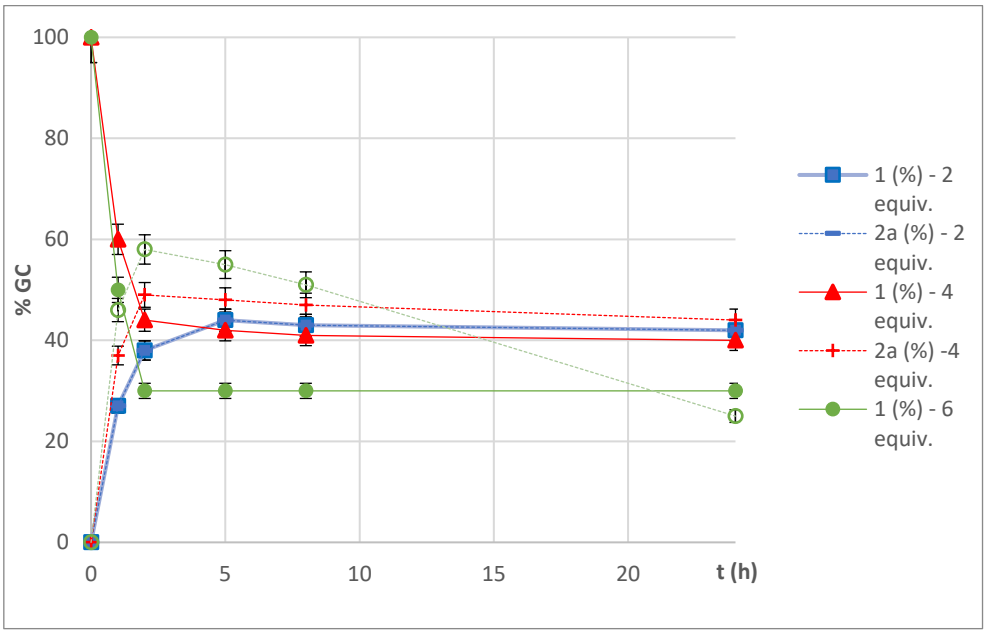

Figure A 2.31. Reaction conditions: 1-decene (4 mmol), H_2O_2 (30% w/w, 2-6 equivalents), $[N_{8,8,8,1}]_2[WO_4]$ (5% mol) coducted at 95°c for 24 hours.

Indication of the pH of hydrogen peroxide solutions (30% w/w) with various phosporous-based

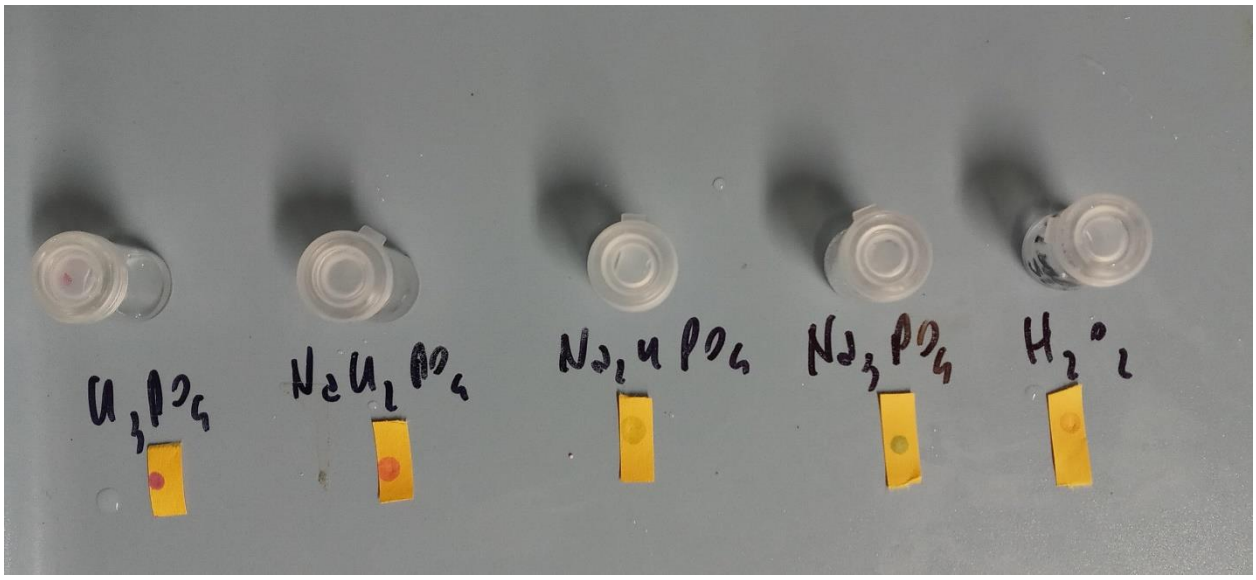

Figure A 2.32. Aqueous solution (identical to that used in fig. 2.13) constituted by H_2O_2 (30% wt, 0.73 ml) and the selected P-based auxiliary (0.6% mol respect to H_2O_2). From left to right: H_3PO_4, NaH_2PO_4, Na_2HPO_4, Na_3PO_4, in absence of co-catalyst. The litmus test allows to have a raw indication of the pH of the aqueous solutions employed: we suggested that the acidity of the solution has not a strong effect on the performance of epoxidation. What matters is the formation of different phosphoperoxotungstate species at different pH and with different P-based auxiliaries.

Assisted tandem direct oxidative carboxylation of 1-decene to 1-decene carbonate

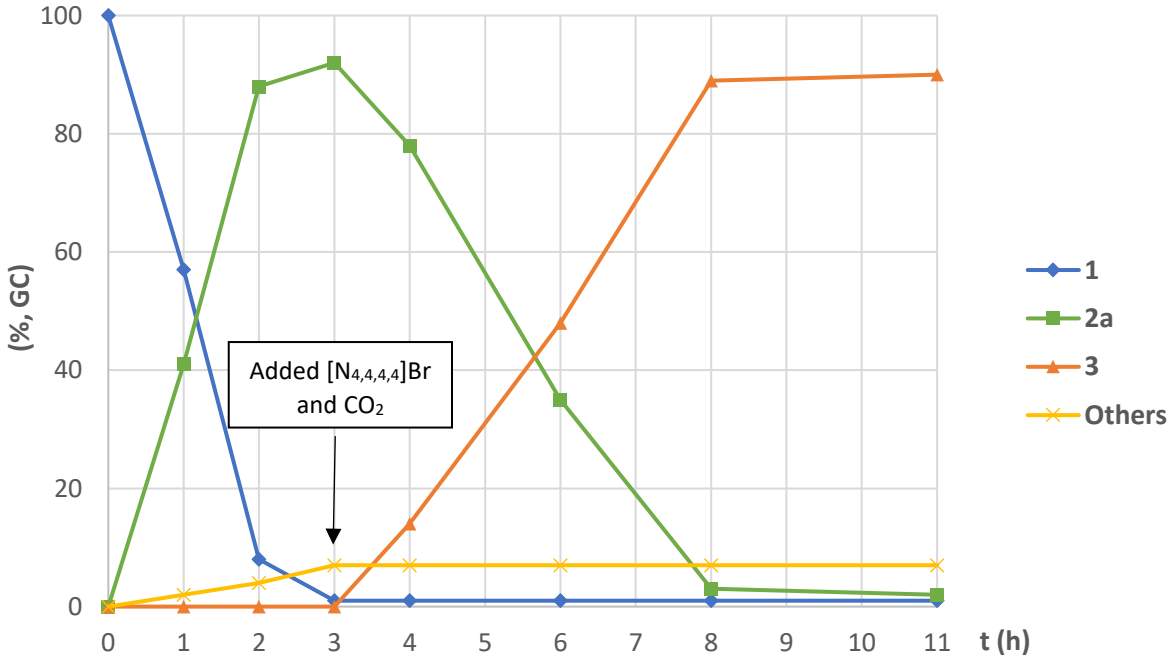

Figure A 2.33: One-pot assisted tandem reaction. Reaction conditions: 1-decene (4 mmol), H_2O_2 (30% w/w, 2 equivalents), $[N_{8,8,8,1}]_2[WO_4]$ (2.5% mol), H_3PO_4 (1.25% mol) performed at 85°C for 3 hours, followed by the raw addition of $[N_{4,4,4,4}]Br$ (2.5% mol) and CO_2 (50 bar) without any intermediate work-

up. The reaction was further performed for 8 h at T=85°C in an autoclave; Product distribution according to GC analysis using mesytilene as internal standard

^{31}P NMR tests on the formation of phosphoperoxotungstate species

Experiments were performed to demonstrate the formation of phosphoperoxotungstate species in situ by a mixture of H_3PO_4, H_2O_2 and $[N_{8,8,8,1}]_2WO_4$. A solution containing H_3PO_4 (4.4 mg, 0.045 mmol) in D_2O (0.3 ml) was analyzed through ^{31}P NMR (red spectra, **a**). Then, H_2O_2 (30% w/w, 0.73 ml, 7.15 mmol) was added to the solution and the mixture was heated at 50°C for 30 minutes and then analyzed by ^{31}P NMR spectra (green spectra, **b**). Finally $[N_{8,8,8,1}]_2WO_4$ (94.0 mg, 0.09 mmol) was added to the reaction mixture and the mixture heated at 50°C for 30 minutes. A last ^{31}P NMR spectra was conducted (blue spectra, **c**) demonstrating the complete shift of the H_3PO_4 peak due to the formation of a phosphoperoxotungstate species ($[HPW_2O_{14}]^{2-}$) already reported in literature.[1]

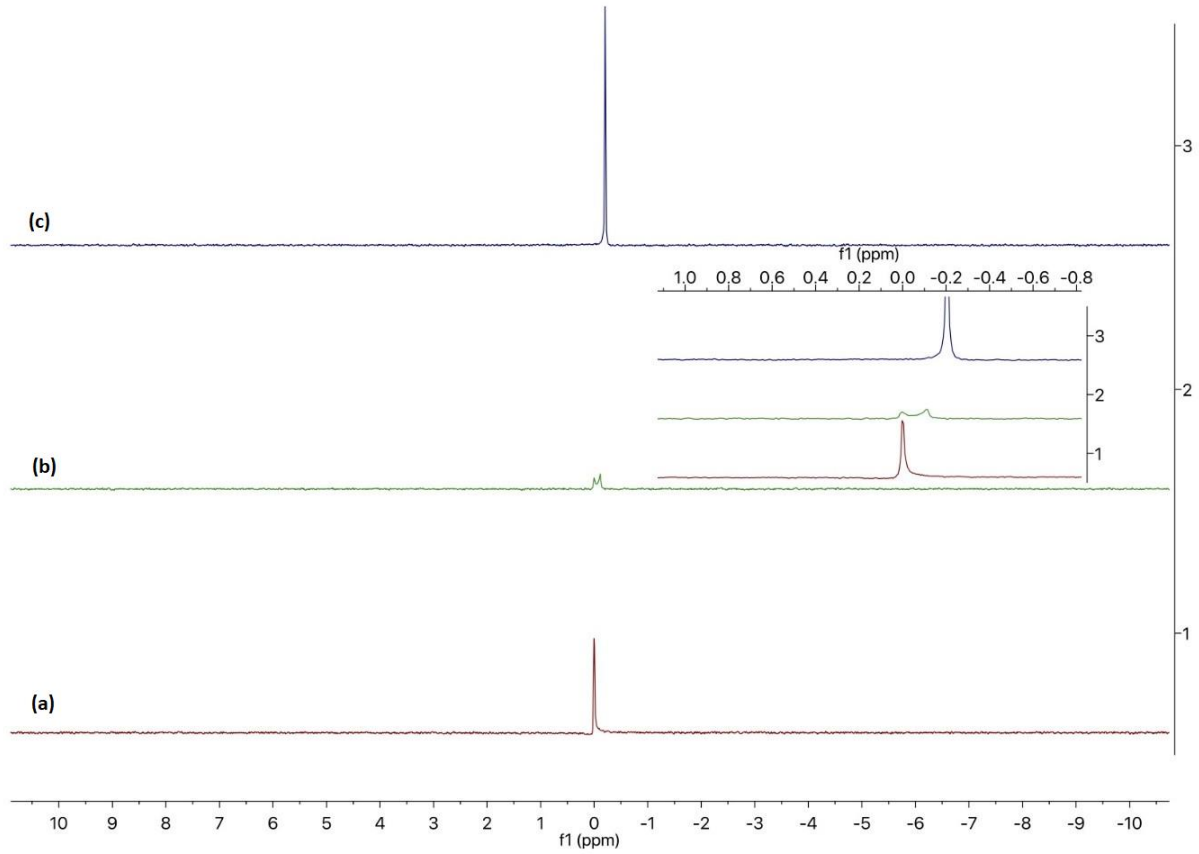

*Figure A 2.34: ^{31}P NMR spectra of: H_3PO_4 solution in D_2O (red spectra, **a**); H_3PO_4 + H_2O_2 solution in D_2O (green spectra, **b**); H_3PO_4 + H_2O_2 + $[N_{8,8,8,1}]_2WO_4$ in D_2O (blue spectra, **c**).*

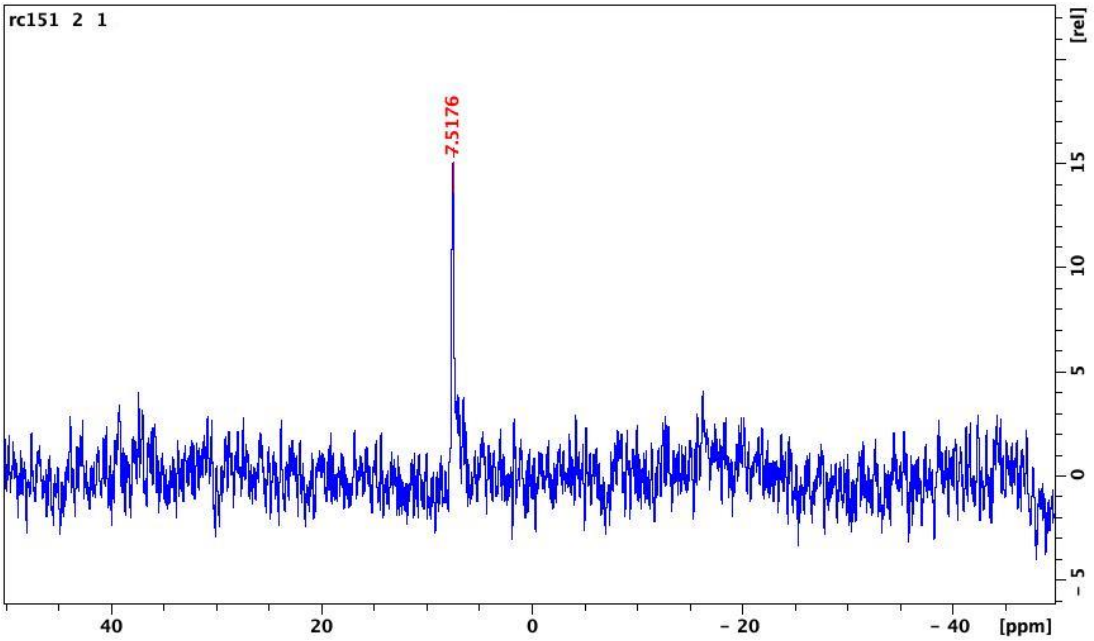

Figure A 2.35: ^{183}W NMR spectra of $[N_{8,8,8,1}]_2WO_4$ in D_2O

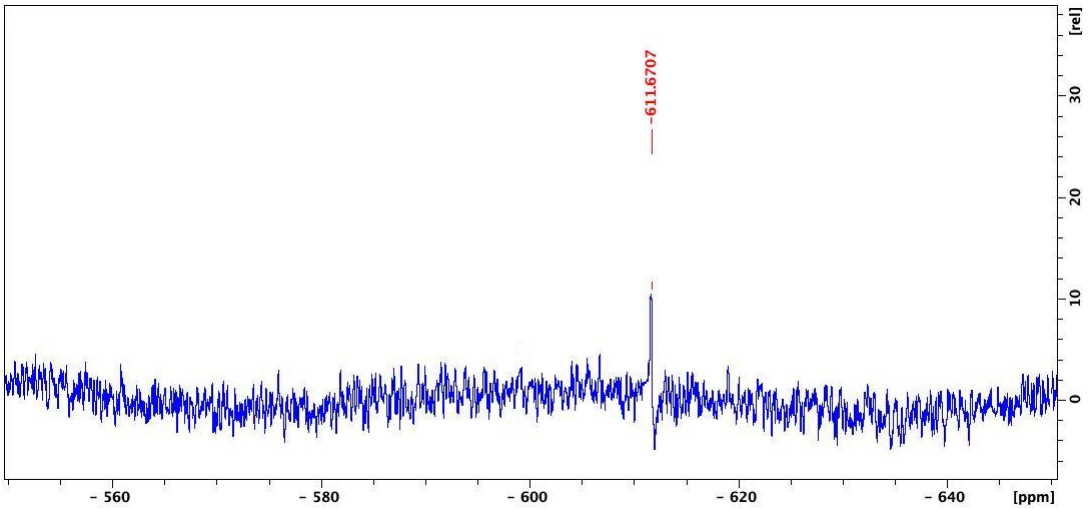

Figure A 2.36: ^{183}W NMR spectra of the peroxotungstate species formed in situ by $[N_{8,8,8,1}]_2WO_4$ and hydrogen peroxide. Spectra recorded by using D_2O as solvent.

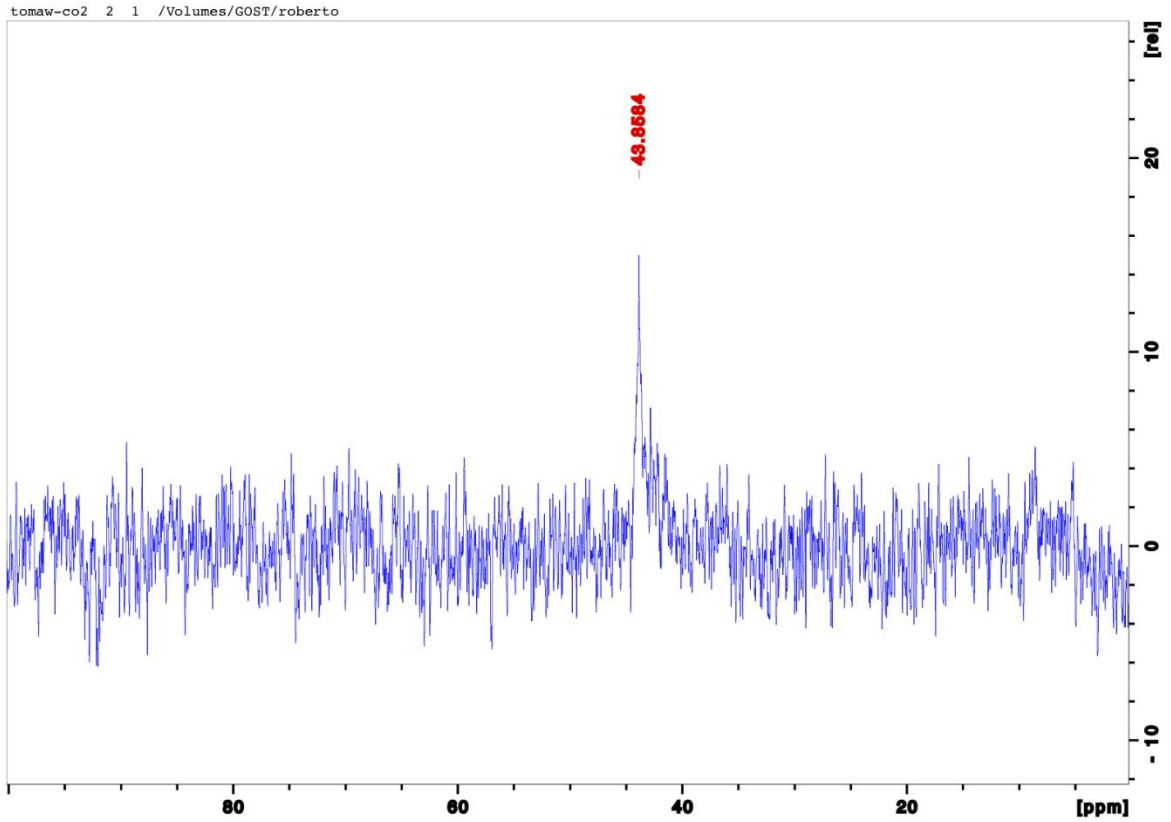

Figure A 2.37: ^{183}W NMR spectra of the adduct $WO_4 \cdot CO_2$. A NMR tube was charged with $[N_{8,8,8,1}]_2WO_4$ (0.2 g), D_2O (0.4 ml) and placed in an autoclave that was sealed, degassed via two vacuum-CO_2 cycles and pressurized with 10 bar of CO_2. The mixture was placed at 85°C for 5 hours, then the autoclave was slowly vented and the NMR spectra was recorded.

NMR spectra of Cyclic organic Carbonates

2a - (1,2-Decylene Oxide)

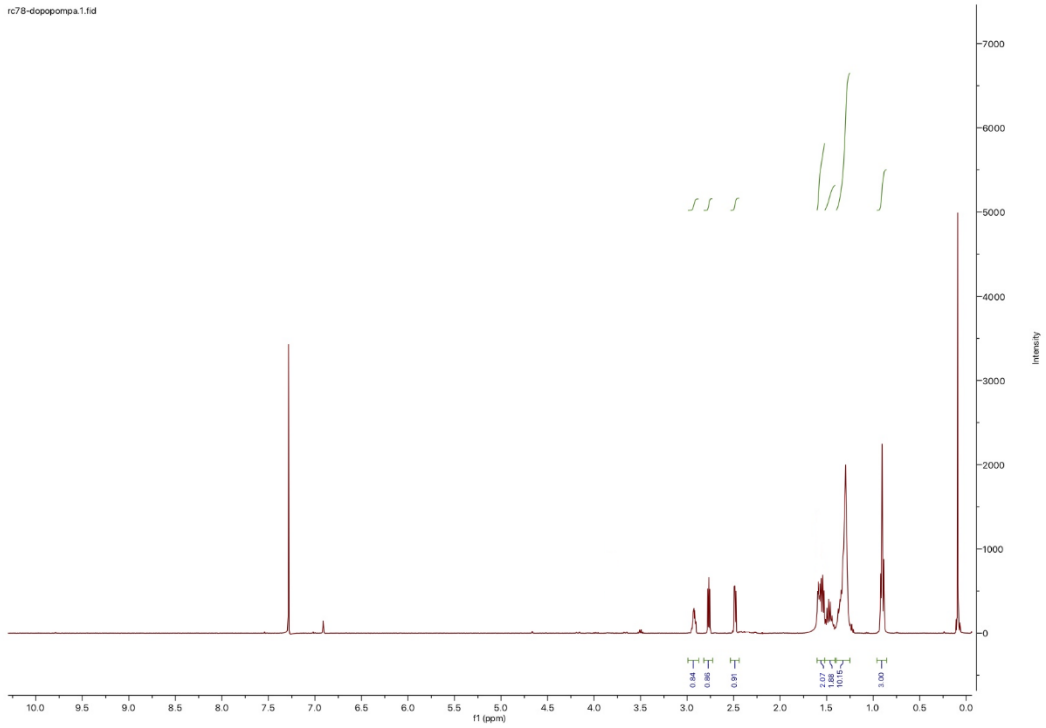

*Figure A 2.38: ^{1}H NMR of product **2a** (400 MHz, 298 K, $CDCl_3$). δ (ppm): 2.98-2,87 (m, 1H), 2.85-2.74 (dd, 1H), 2.59-2.42 (dd, 1H), 1.59-1.51 (m, 2H), 1.51-1.16 (m, 12H), 1.02-0.74 (m, 3H).*

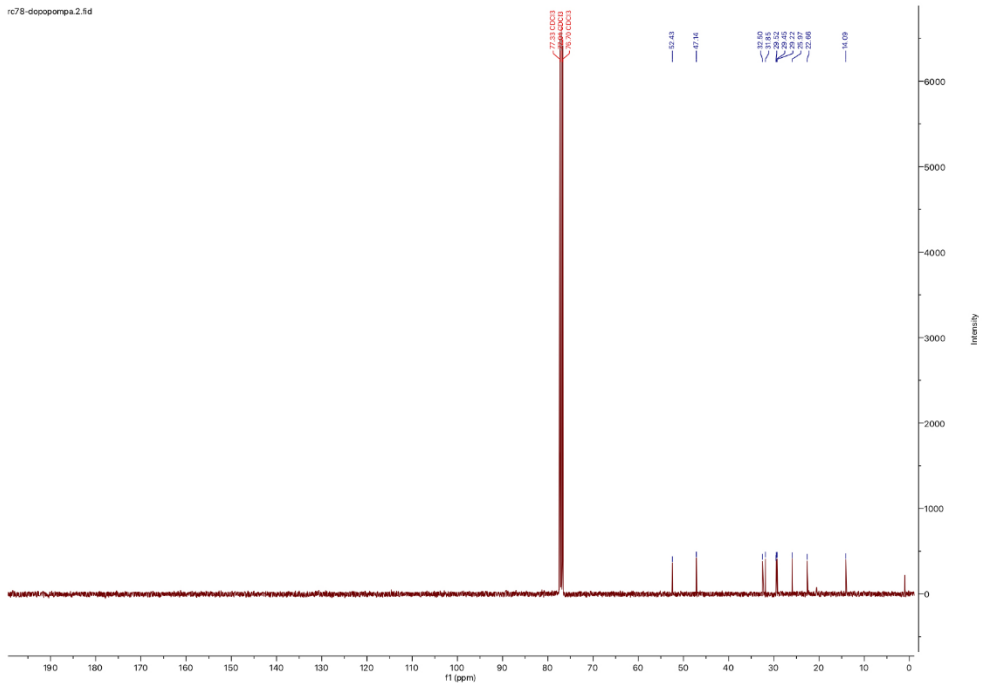

*Figure A 2.39: ^{13}C NMR of product **2a** (100 MHz, 298 K, $CDCl_3$). δ (ppm): 52.43, 47.14, 32.50, 31.85, 29.52, 29.45, 29.22, 25.97, 22.66, 14.09*

```
File       :C:\msdchem\1\DATA\Rob\RC67-A-3H.D
Operator   : NICOLA
Acquired   :  1 Dec 2020  15:26     using AcqMethod 100(2)-240(10)@20_D2.M
Instrument :   US61623096
Sample Name:
Misc Info  :
Vial Number: 1
```

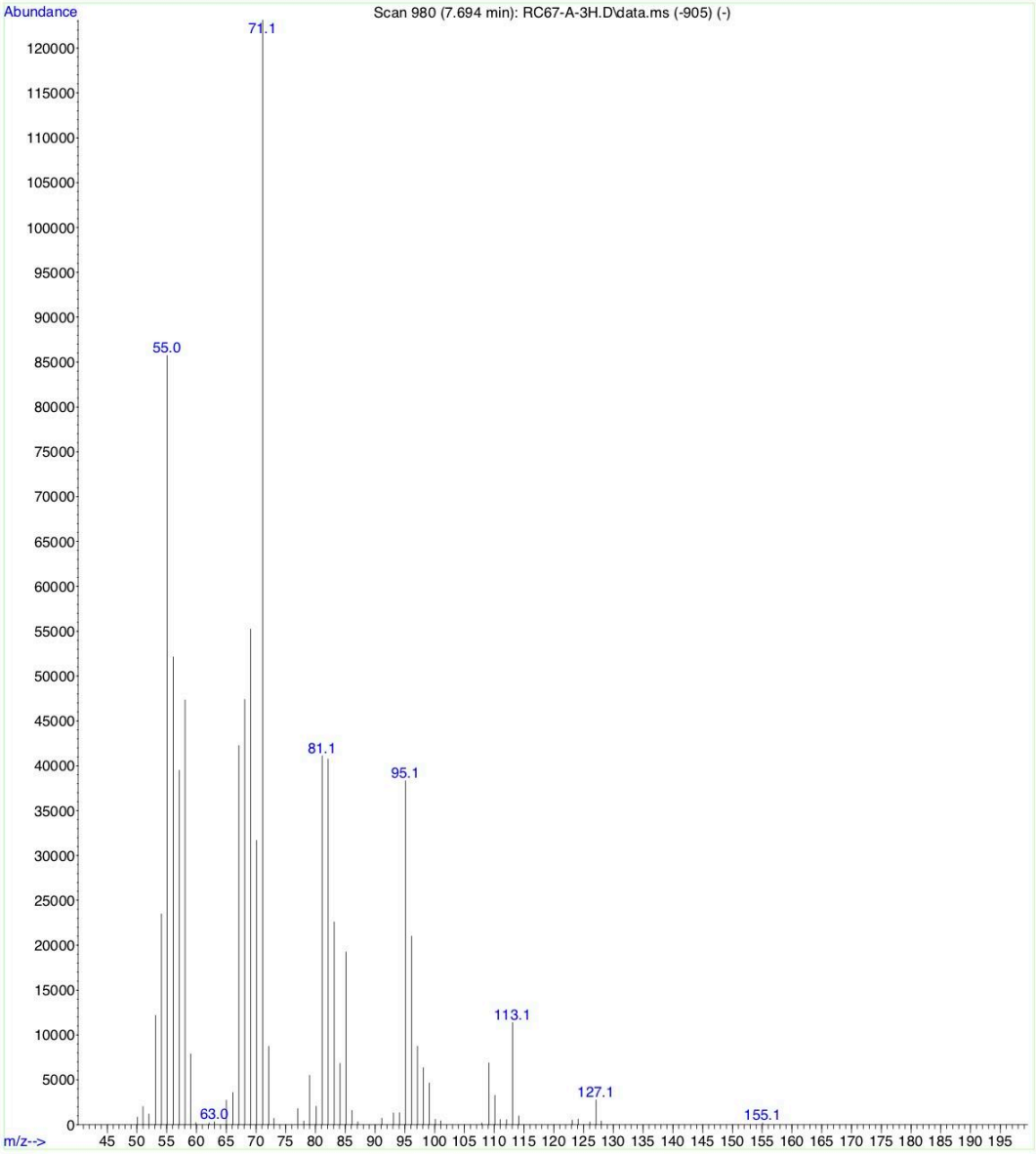

*Figure A 2.40: MS spectrum of 1-decene oxide (**2a**) (EI, 70 eV). m/z (70 eV): 156 (M^+, 0), 113 (9), 96 (17), 95 (31), 85 (16), 83 (18), 82 (33), 81 (33), 71 (100), 70 (26), 69 (45=, 68 (38), 67 (34), 58 (38), 57 (32), 56 (42), 55 (70), 54 (19), 53 (10)*

3a: 4-octyl-1,3-dioxolan-2-one (1-decene carbonate)

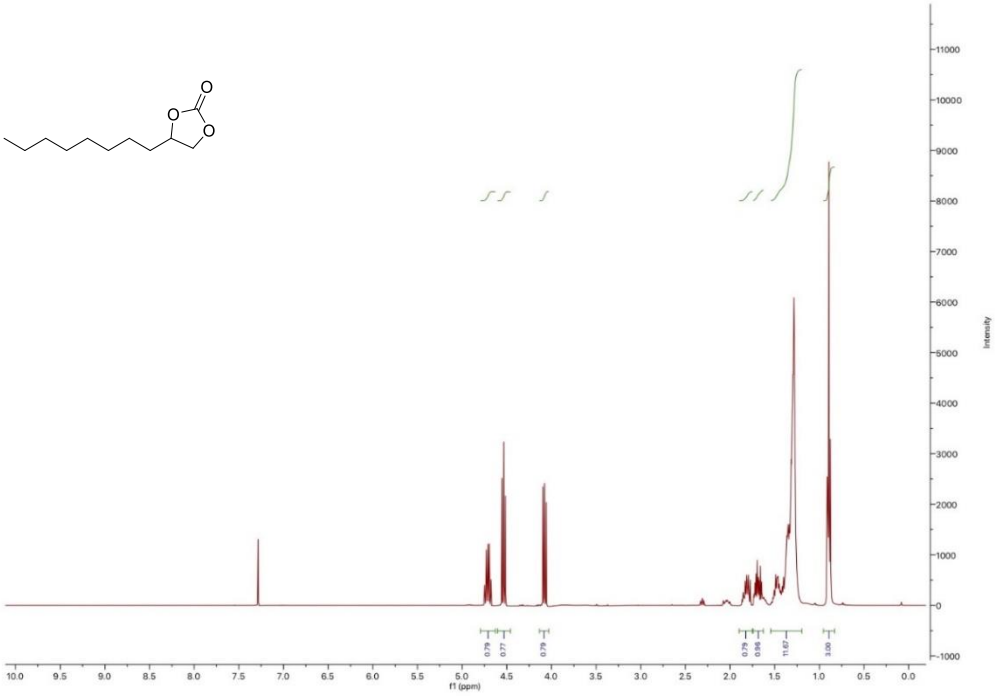

*Figure A 2.41: ^{1}H NMR of product **2d** (400 MHz, 298 K, $CDCl_3$). δ (ppm): 4.81-4.64 (m, 1H), 4.59-4.46 (dd, 1H), 4.16-3.97 (dd, 1H), 1.90-1.75 (m, 1H), 1.75-1.60 (m, 1H), 1.55-1.16 (m, 12H), 1.02-0.74 (m, 3H).*

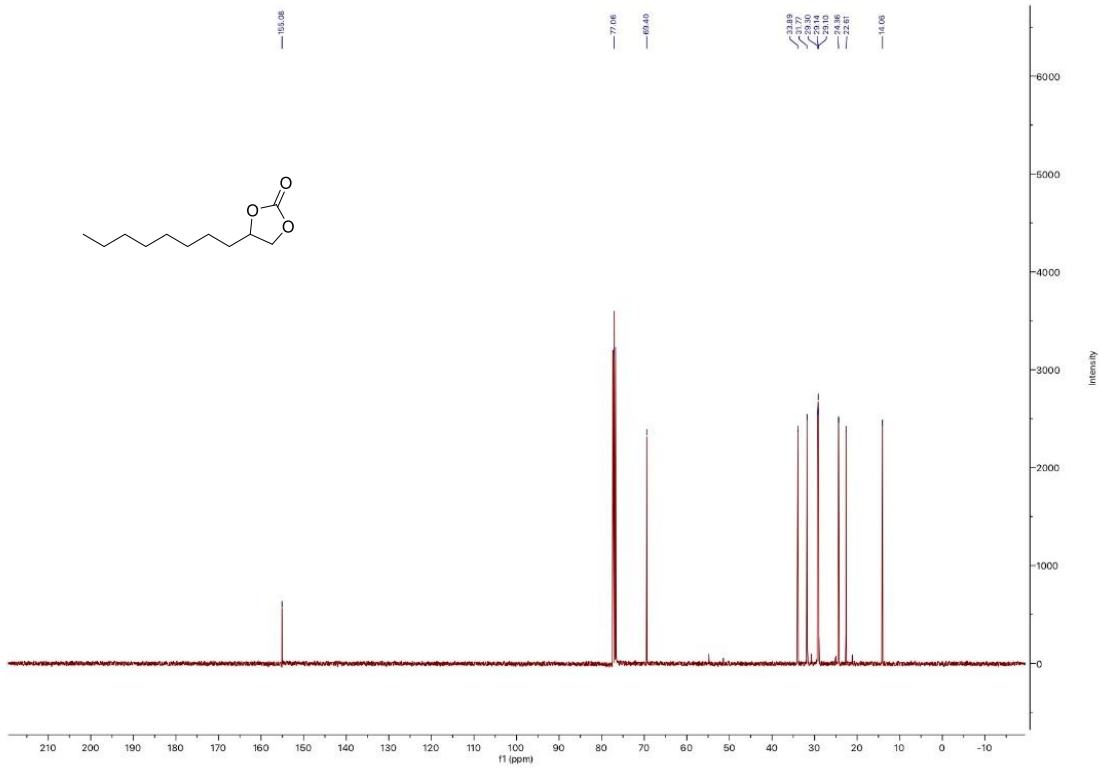

*Figure A 2.42. ^{13}C NMR of product **2d** (100 MHz, 298 K, $CDCl_3$). δ (ppm): 155.08, 77.06, 69.40, 33.89, 31.77, 29.30, 29.14, 29.10, 24.36, 22.61, 14.06.*

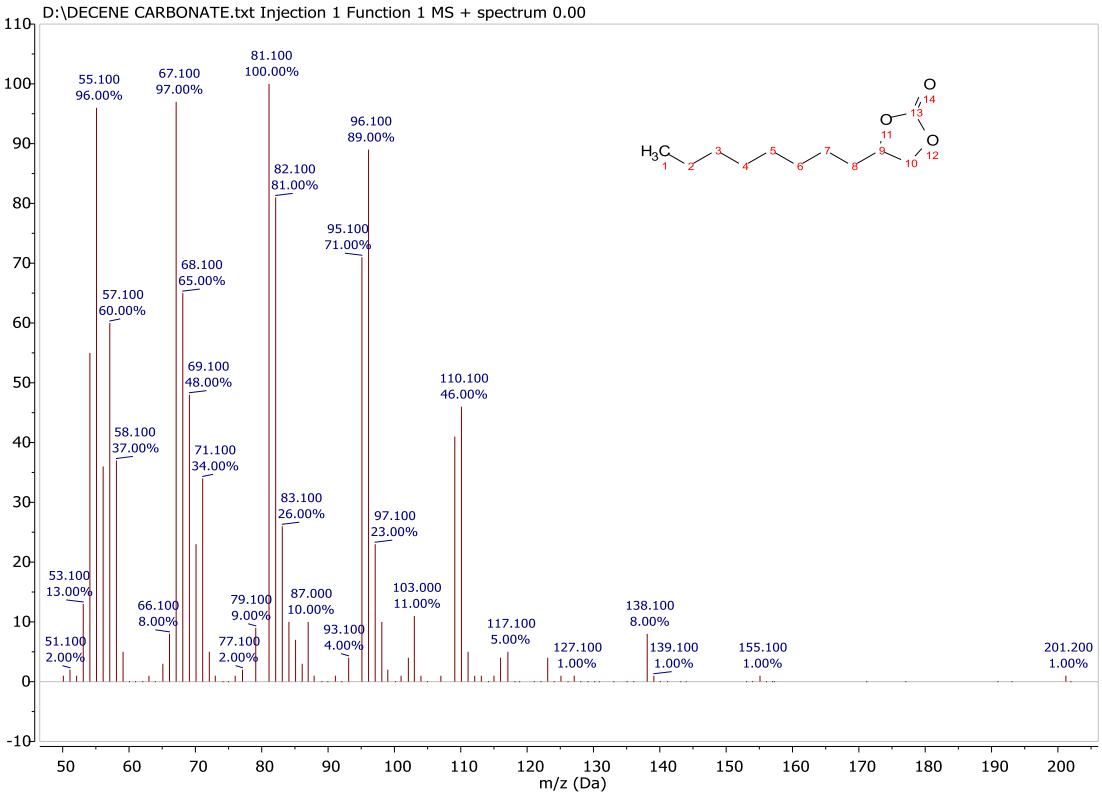

*Figure A 2.43: MS spectrum of product **2d** (EI, 70 V). m/z (70 eV): 201 (MH^+, 1), 110 (46), 96 (89), 81 (100), 67 (97), 55 (96).*

3a: 4-butyl-1,3-dioxolan-2-one (1-hexene carbonate)

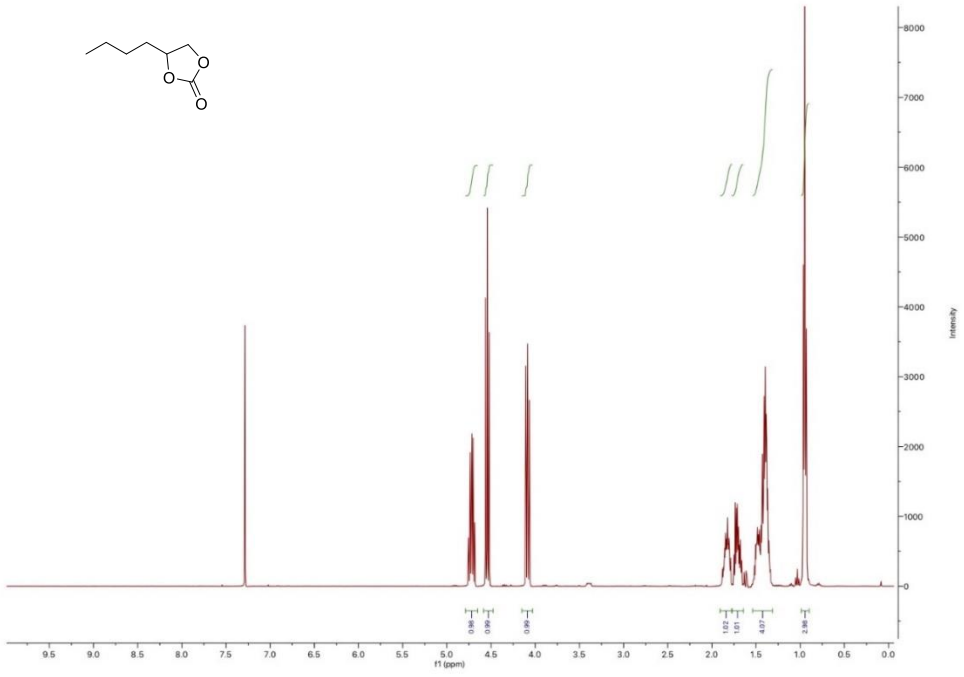

*Figure A 2.44: ^1H NMR of product **2c** (400 MHz, 298 K, $CDCl_3$). δ (ppm): 4.80-4.65 (m, 1H), 4.61-4.48 (dd, 1H), 4.13-4.03 (dd, 1H), 1.92-1.76 (m, 1H), 1.77-1.64 (m, 1H), 1.55-1.30 (m, 4H), 1.00-0.89 (t, 3H).*

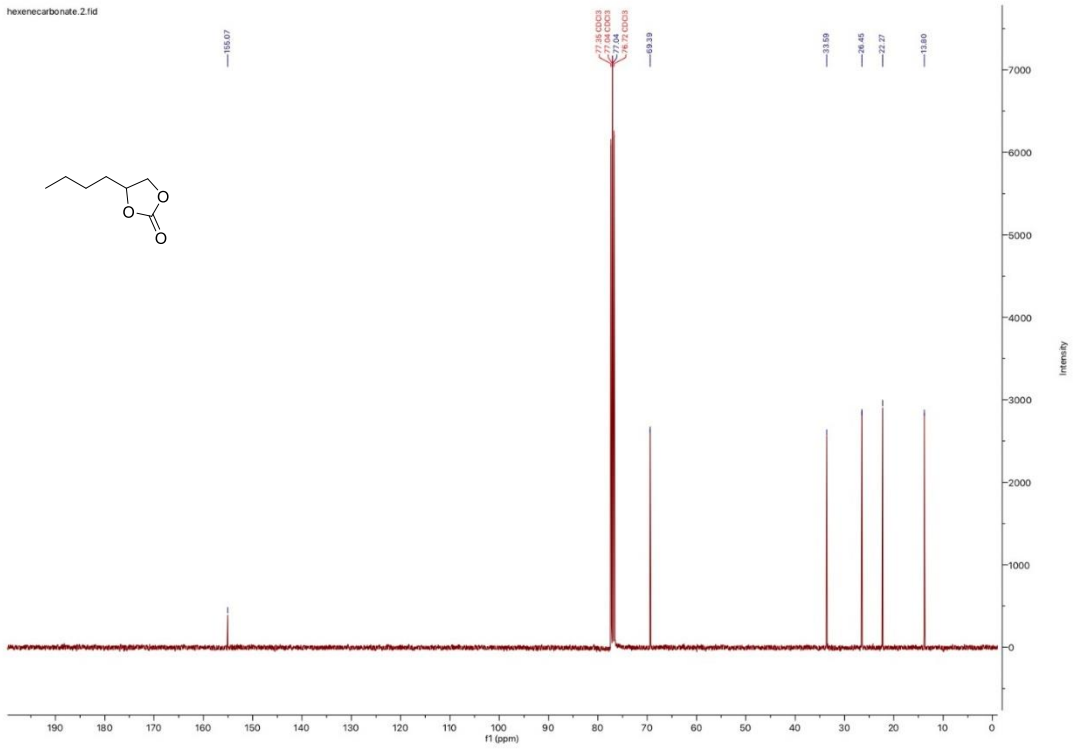

*Figure A 2.45: ^{13}C NMR of product **2c** (100 MHz, 298 K, $CDCl_3$). δ (ppm): 155.07, 77.04, 69.39, 33.59, 26.45, 22.27, 13.80.*

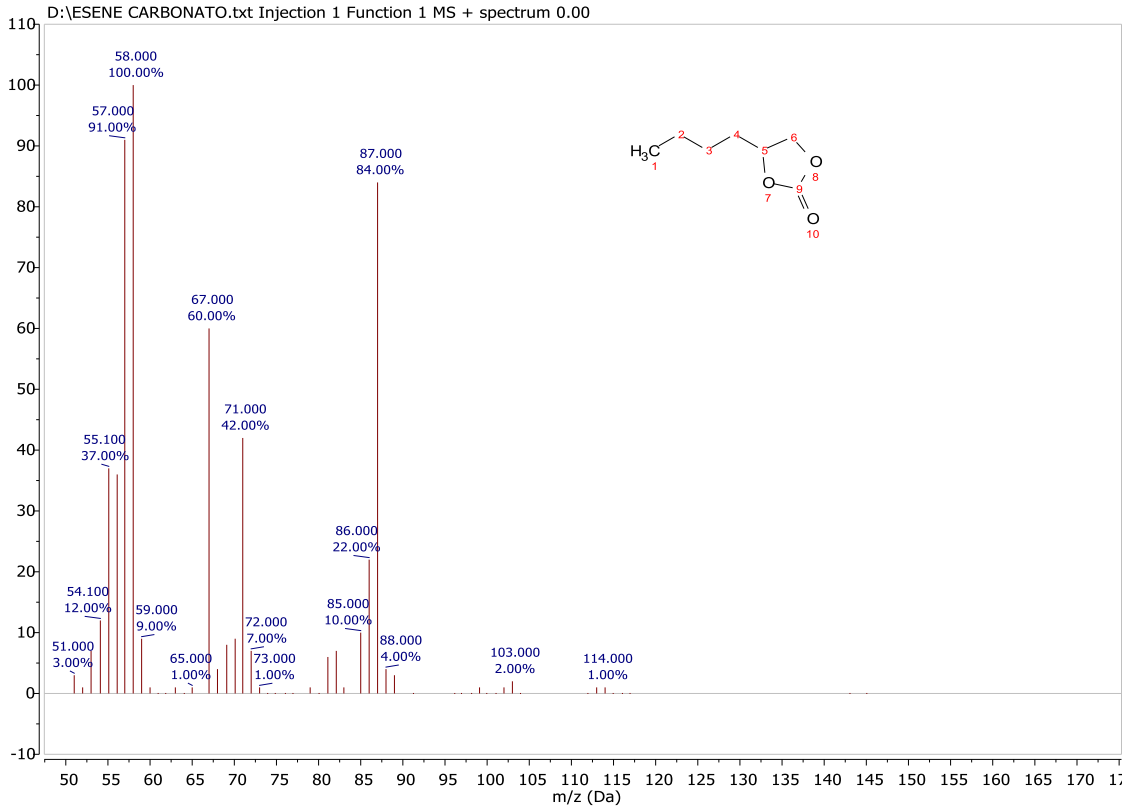

*Figure A 2.46: MS spectrum of product **2c** (EI, 70 V). m/z (70 eV): 114 (1), 87 (84), 71 (42), 67 (70), 58 (100), 57 (91), 55 (37).*

1g: *Methyl cis-9-octadecanoate (Methyl Oleate)*

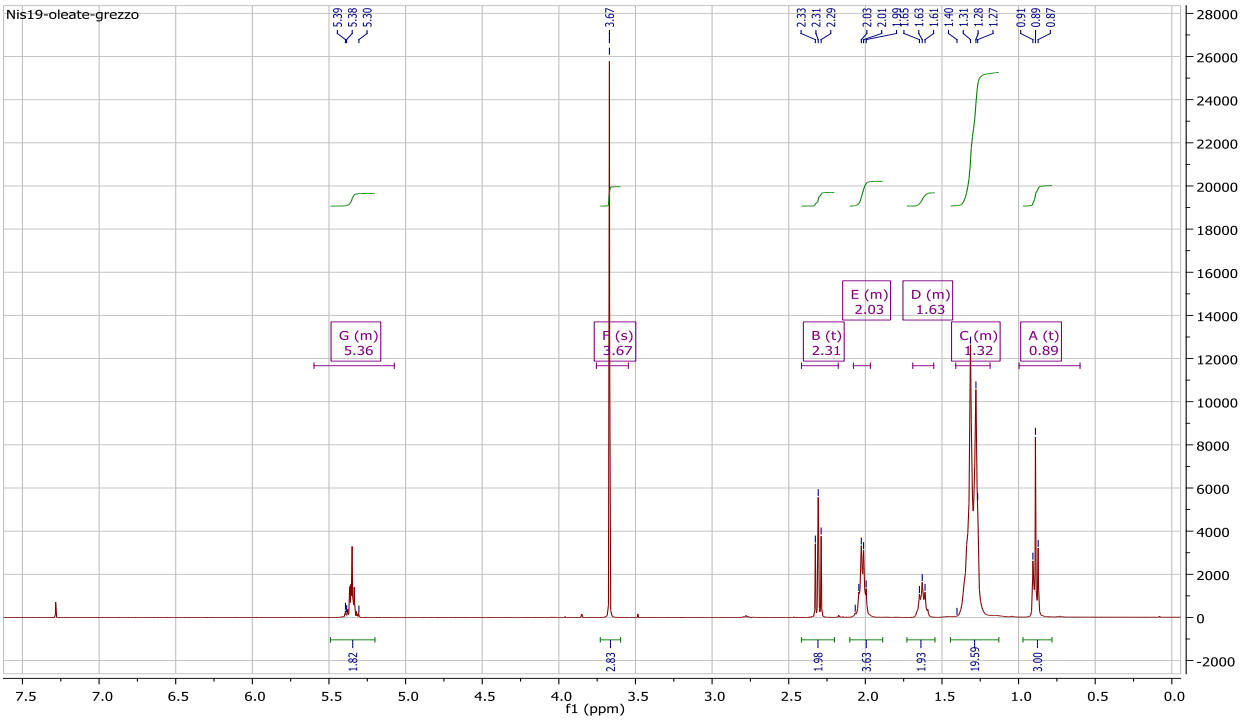

*Figure A 2.47: ^{1}H NMR of product **1g** (400 MHz, 298 K, $CDCl_3$). δ = 0.89 (t, J=6.9Hz, 3H), 1.25-1.40 (m, 20H), 1.63 (m, 2H), 2.03 (m, 4H), 2.31 (t, J=7.6Hz, 4H), 3.67 (s, 3H), 5.30-5.39 (m, 2H).*

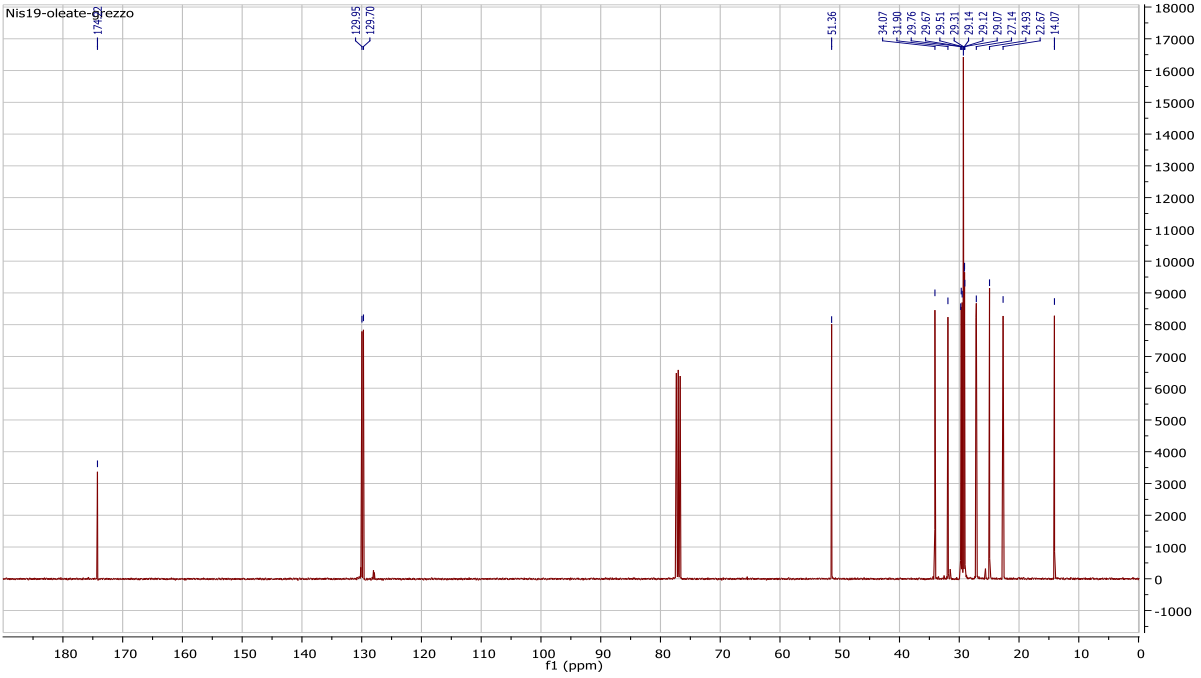

*Figure A 2.48: ^{13}C NMR of product **1g** (400 MHz, 298 K, $CDCl_3$). δ = 14.07, 22.67, 24.93, 27.14, 27.20, 29.07, 29.12, 29.14, 29.31, 29.51, 29.67, 29.76, 31.90, 34.07, 51.36, 129.70, 129.95, 174.42.*

```
File       :C:\msdchem\1\DATA\NicolaS\METIL OLEATO4.D
Operator   :
Acquired   : 21 Jan 2021  16:59     using AcqMethod 100(2)-300(30)@20_D3.M
Instrument :   US10081001
Sample Name:
Misc Info  :
Vial Number: 1
```

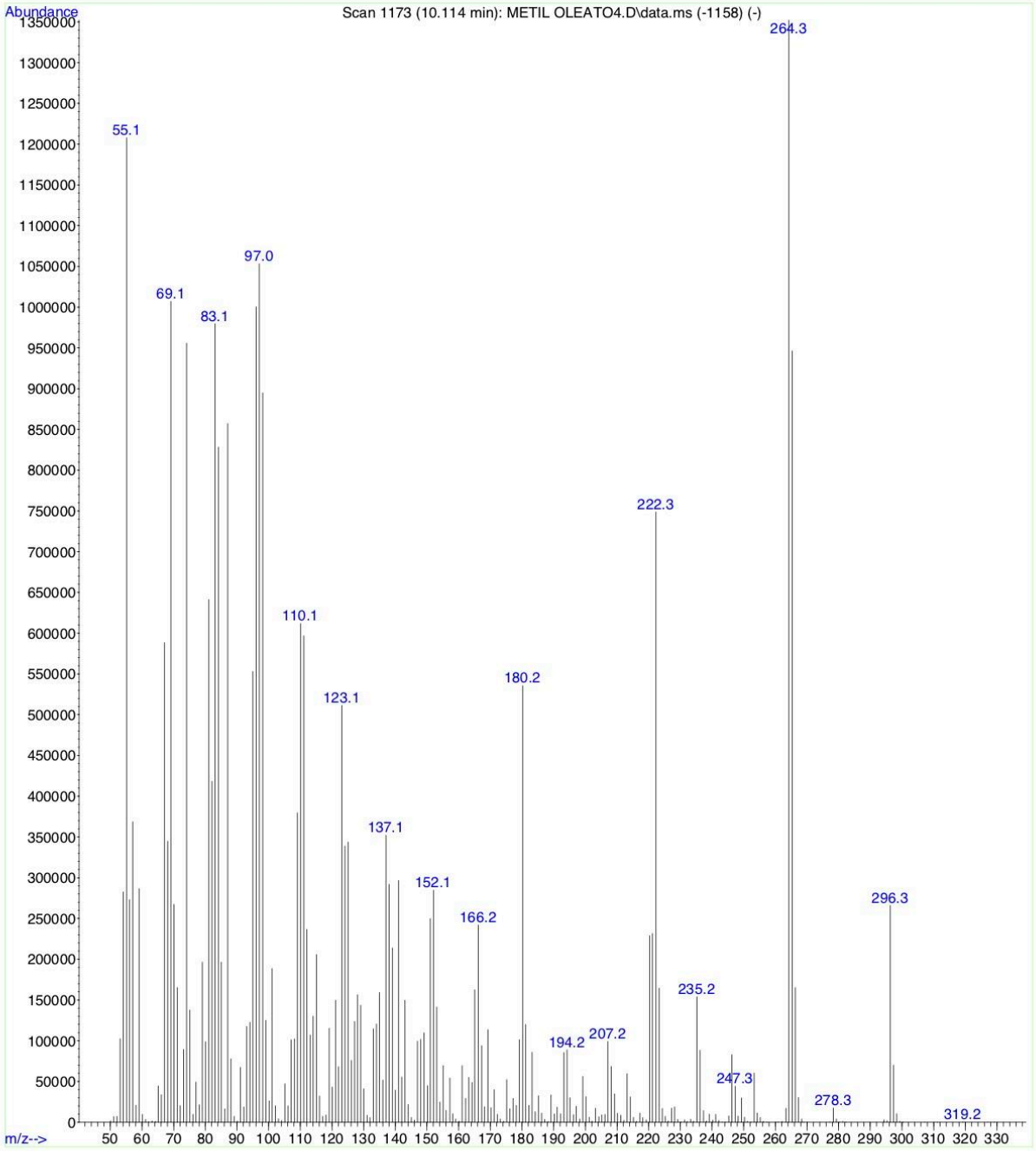

*Figure A 2.49: MS spectrum **1g** (EI, 70 V). m/z (70 eV): 297 (M^{+1}, 5), 296 (M, 20), 265 (71), 264 (100), 235 (11), 222 (56), 180 (41), 166 (18), 152 (22), 151 (19), 141 (22), 138 (22), 137 (27), 125 (26), 124 (26), 123 (39), 98 (68), 97 (79), 96 (76), 95 (42), 87 (64), 84 (63), 83 (74), 82 (32), 81 (49), 74 (72), 69 (76), 68 (26), 67 (44), 57 (28), 55 (91), 54 (21)*

2g: *Methyl 8-((2R,3S)-3-octyloxiran-2-yl) octanoate (epoxidized methyl oleate)*

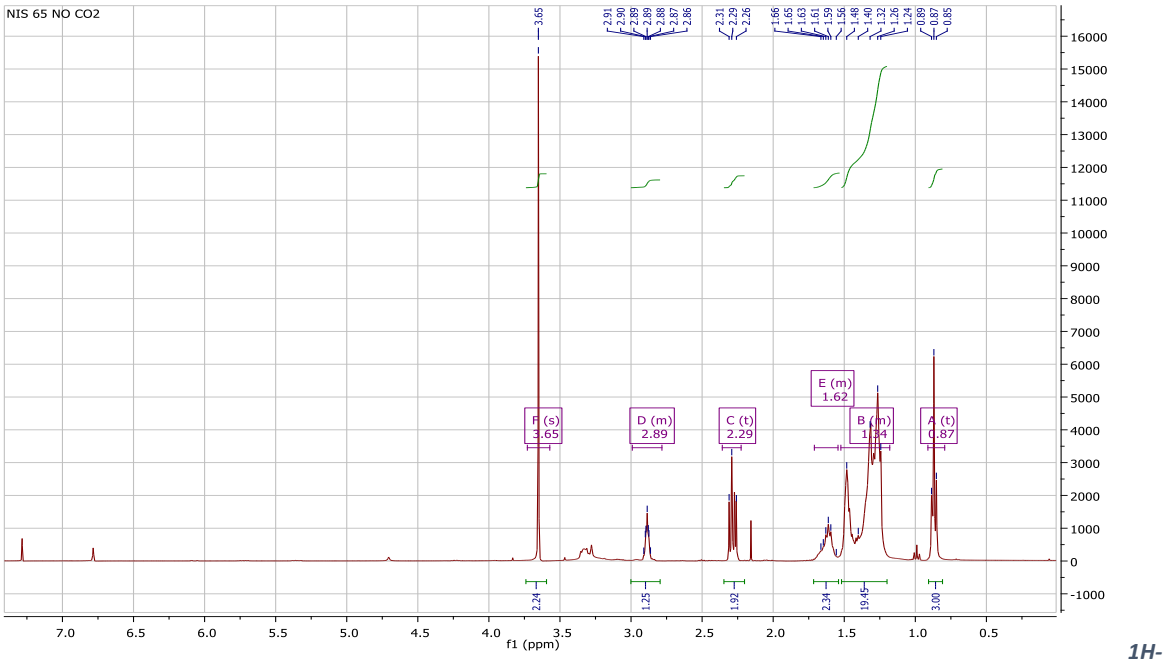

1H-

*Figure A 2.50: ^{1}H NMR of product **2g** (400 MHz, 298 K, $CDCl_3$). δ = 0.87 (t, J=6.9Hz, 3H), 1.20-1.55 (m, 20H), 1.55-1.70 (m, 2H), 2.25-2.32 (t, J=10.32Hz, 2H), 2.89 (m, 2H), 3.65 (s, 3H).*

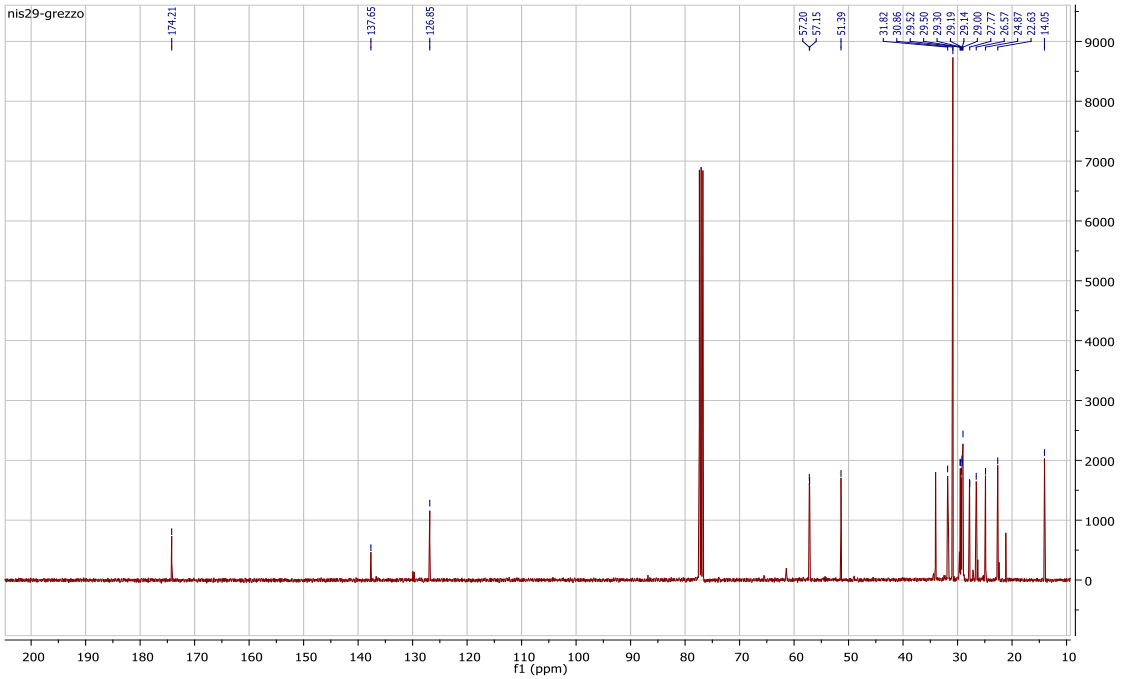

*Figure A 2.51: ^{13}C NMR of product **2g** (100 MHz, 298 K, $CDCl_3$). δ = 14.05, 22.63, 24.87, 26.57, 27.77, 29.00, 29.14, 29.19, 29.30, 29.50, 29.52, 30.86, 31.82, 51.39, 57.15, 57.20, 174.21.*

```
File       :C:\msdchem\1\DATA\NicolaS\NIS 104.D
Operator   :
Acquired   :  2 Dec 2020  11:18     using AcqMethod 50(2)-300(15)@20_D3.M
Instrument :   US10081001
Sample Name: 1 h
Misc Info  :
Vial Number: 1
```

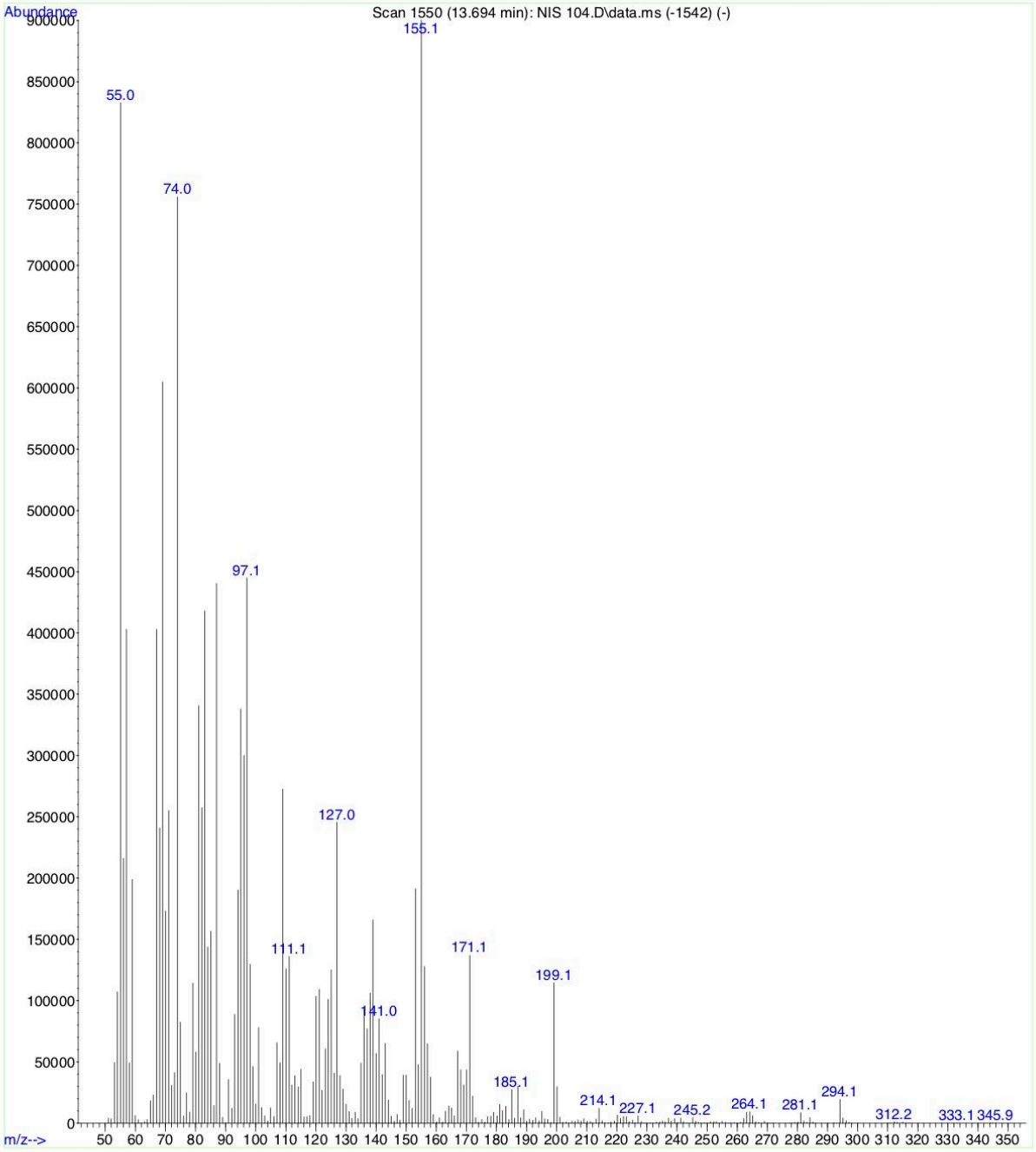

*Figure A 2.52: MS spectrum **2g** (EI, 70 V). m/z (70 eV):312 (M^+, 1), 199 (13), 171 (15), 156 (14), 155 (100), 154, (5), 153 (21), 139 (18), 138 (12), 137 (9),136 (10), 127 (27), 125 (14), 124 (11), 121 (12), 120 (12), 111 (15), 110 (14), 109 (30), 98 (14), 97 (49), 96 (33), 95 (38), 94 (21), 93 (10), 87(49), 85*

(17), 84 (16), 83 (46), 82 (29), 81 (38), 79 (13), 74 (84), 71 (28), 70(19), 69 (67), 68 (27), 67 (45), 59 (22), 57 (45), 56 (24), 55 (93), 54 (12).

3g - *Methyl 8-((4R,5S)-5-octyl-2-oxo-1,3-dioxolan-4-yl)octanoate (Carbonated methyl oleate)*

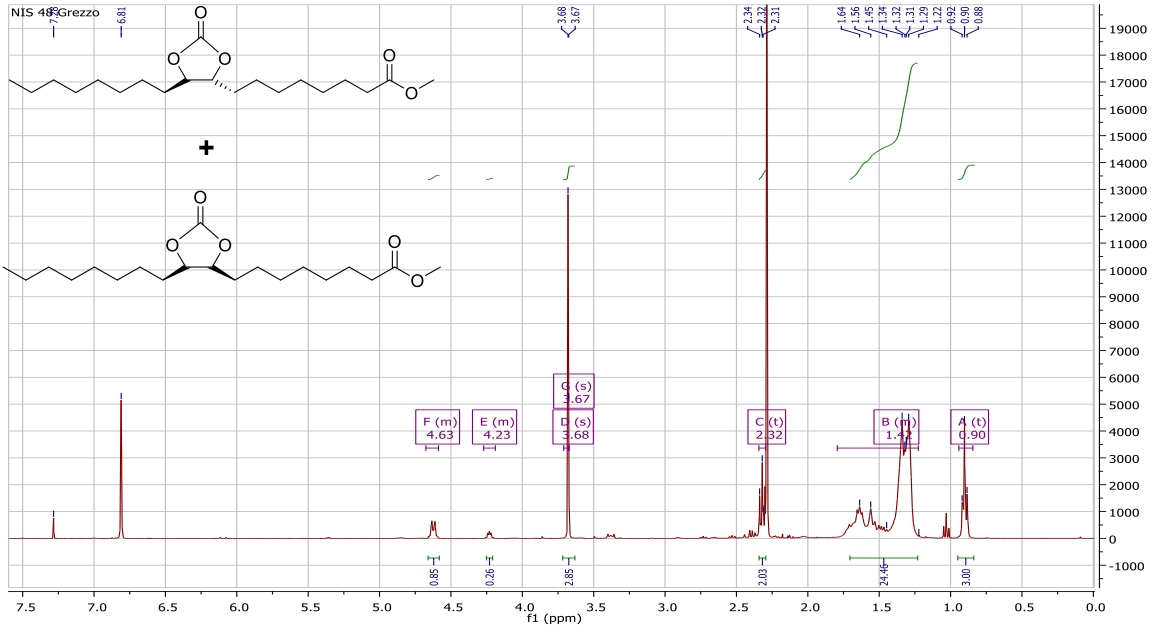

*Figure A 2.53: [1]H NMR of product **2g**. δ = 0.90 (t, J=6.9Hz, 3H), 1,25-1,75 (m, 24H), 2.37 (t, J=4.9Hz, 2H), 3.67 (s, 3H), 3.68 (s, 3H), 4.23 (m, 2H), 4.63 (m, 2H).*

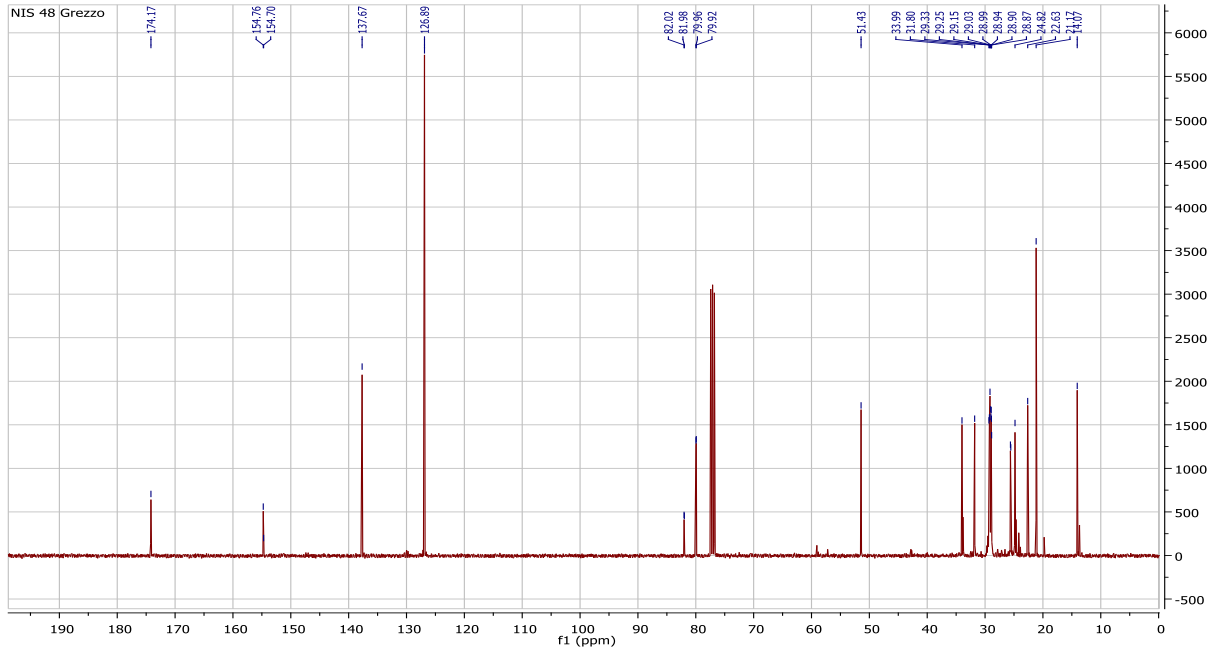

*Figure A 2.54: [13]C NMR of product **2g** (100 MHz, 298 K, $CDCl_3$): δ = 13.68, 14.07, 21.17, 22.63, 24.82, 25.55, 25.61, 28.87, 28.90, 28.94, 29.03, 29.12, 29.15, 29.18, 29.25, 29.33, 31.80, 33.90, 51.40, 51.43, 79.92, 79.96, 137.67, 154.70, 154.76, 174.17*

```
File       :C:\msdchem\1\DATA\NicolaS\NIS 76 CARBONATO.D
Operator   :
Acquired   : 20 Nov 2020  12:32     using AcqMethod 50(2)-300(30)@20_D6.M
Instrument :   US10081001
Sample Name:
Misc Info  :
Vial Number: 1
```

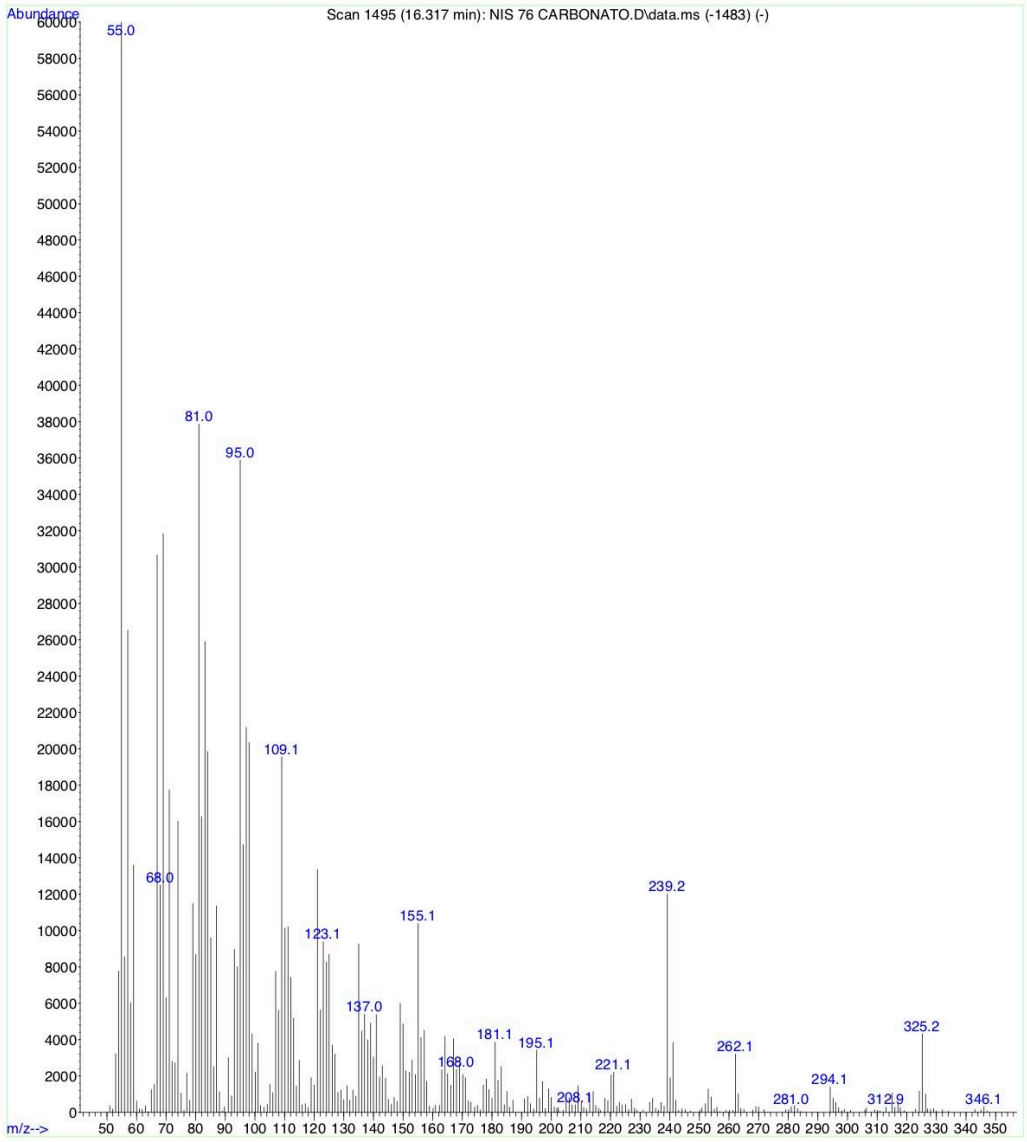

*Figure A 2.55: MS spectrum **3g** (EI, 70 V). m/z (70 eV):312 (M^+, 1), 199 (13), 171 (15), 156 (14), 155 (100), 154, (5), 153 (21), 139 (18), 138 (12), 137 (9),136 (10), 127 (27), 125 (14), 124 (11), 121 (12), 120 (12), 111 (15), 110 (14), 109 (30), 98 (14), 97 (49), 96 (33), 95 (38), 94 (21), 93 (10), 87(49), 85 (17), 84 (16), 83 (46), 82 (29), 81 (38), 79 (13), 74 (84), 71 (28), 70(19), 69 (67), 68 (27), 67 (45), 59 (22), 57 (45), 56 (24), 55 (93), 54 (12).*

Appendix A.2.3.
Diethylene glycol/NaBr catalyzed CO2 insertion into terminal epoxides: from batch to continuous flow

***Collecting the reaction mixture at the CF reactor outlet*: comparison of different solvents and mass recovery**

Initial CF experiments proved that the recovery of the reaction products and the unreacted starting material was problematic because volatile species, particularly the starting epoxide, were stripped from the flow of CO_2. This was an issue for the quantitative evaluation of conversion and products' distribution (and therefore, for the reproducibility and the mass balance of the protocol). After testing several procedures, an efficient method was designed by conveying the mixture from the reactor outlet into a collection flask filled with a liquid biphasic system comprising of water and an immiscible organic solvent.

Different organic solvents including diethyl ether, diethyl carbonate (DEC), cyclopentyl methyl either (CPME), *n*-hexane and ethyl acetate were compared to this purpose (Table A 2.1).

Table A 2.1: Comparative experiments for the recovery/analysis of CF-reactions

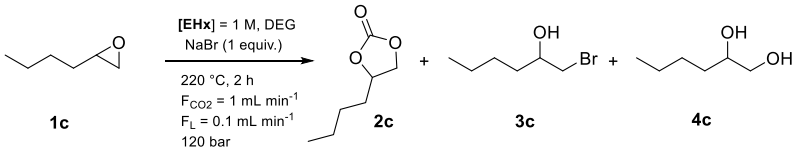

Entry	Solvent[a]	Conv.[b] (%)	Products selectivity (%) [c]			Mass recovery (%)[d]
			2c	3c	4c	
1	diethyl ether	88	81	15	4	98
2	DEC	86	82	13	5	98
3	CPME	85	80	16	4	97
4	*n*-hexane	89	78	17	5	97
5	ethyl acetate	87	81	15	4	n.d.

The CF insertion of CO2 into hexene oxide (**1c**) was carried out under the following conditions: [**1c**] = 1M in DEG, NaBr 1 equiv., T = 220°C, *p* = 120 bar, FCO2= 1 mL·min-1, and FL=0.1 mL·min-1. From GC and GC-MS analyses, the products detected in the organic phase were hexylene carbonate (**2c**), 1-bromohexan-2-ol (**3c**: BHO), and hexane-1,2-diol (**4c**) [a] A liquid biphasic system comprising of water (10 mL) and an immiscible organic solvent (10 mL) was used to recover the reaction mixture out of the CF-reactor. [b] Conversion of 1,2-hepoxyhexane. [c] Selectivity (%) towards hexene carbonate, bromohexan-2-ol, and hexane-1,2-diol. [d] Mass recovery of reactant and products in the organic phase. n.d. = not determined.

The extraction efficiency in each solvent was defined by the % mass recovery, defined as:

Mass Recovery (%) = [total molar amount of unconverted epoxide and reaction products extracted in the organic phase (mmol) / molar amount of the starting epoxide (mmol)] x 100.

The molar amount of unconverted epoxide and reaction products in the organic phase were evaluated after collecting the reaction mixture for 2 hours. Once the experiment was complete, the two phases were separated. The aqueous phase was dried under vacuum, and the DEG + NaBr mixture was quantitively recovered. The organic phase was dried with Na_2SO_4, filtered, and then the excess of solvent was removed and recovered in vacuo. Quantitative isolation of the products mixture (**2c+3c+4c**) was easily achieved.

In diethyl ether, DEC, CPME and n-hexane (entry 1-4), it was noticed that DEG was absent in the organic phase. This result was beneficial not only for the isolation of the reaction products, but also for the catalyst and co-catalyst (NaBr and DEG) recycling. Ethyl acetate proved instead, unsuitable for the recovery of the reaction mixture due to the partition of DEG between the organic and the aqueous phases, and the corresponding mass recovery (%) was not determined. The choice of the extraction solvent finally fell on DEC which was not only safer and greener than other tested solvents, but also the most suited to dissolve carbonate products.

Validation of the mass balance during recycle experiments.

The mass balance (mass recovery) was validated during recycle experiments with respect to the catalyst/co-catalyst system (DEG/NaBr) and the reaction products (**2c**-**4c**) . Under the conditions of Scheme 2.4 and Figure 2.24, the mixture at the reactor outlet was recovered into a H_2O/DEC biphase, during four subsequent recycle tests. The separation of DEG/NaBr and reaction products occurred in the aqueous and organic phases, respectively, in each case. The water solution was dried *in vacuo*, while the organic phase was dried over Na_2SO_4, filtered, and rotary-evaporated (T = 30°C, p = 50 mbar) for the removal of the solvent. Both mixtures of DEG/NaBr and products **2c**, **3c**, and **4c** were recovered in >97% and >96% yield, respectively, after all recycles. Results are reported in Table A 2.2. The mass recovery of the DEG/NaBr was reported considering the loss of Br^- ions due to the formation of bromohydrin **3c**.

In addition, the carbonate **2c** was isolated by FCC (stationary phase: Silica gel, eluent: hexane/ethyl acetate 3:1 v/v) after each of the four recycle test. The corresponding (isolated) yields were 66%, 71%, 65 %, and 68%.

*Table A 2.2: Mass recovery of the DEG/NaBr and mixtures of products **2c**, **3c**, and **4c** during the recycles.*

Entry	Mixture	First reaction (g)[a]	Recycle (g) [b]				Mass recovery (%)[c]
			1	2	3	4	
1	DEG/NaBr	14.32	14.24	14.20	14.09	13.92	97
2	products **2c**, **3c**, and **4c**	1.20	1.19	1.18	1.17	1.15	96

Flow reaction conditions: [**1c**] = 1 M in DEG, NaBr:**1c** = 1.0 mol/mol; FL = 0.1 mL·min-1, FCO2 = 1 mL·min-1, p = 120 bar, T = 220 °C [a] Amounts (g) of DEG/NaBr and products **2c**, **3c**, and **4c** used in the first reaction. [b] Amounts (g) of DEG/NaBr and products **2c**, **3c**, and **4c** recovered after each recycle. [c] Mass Recovery (%) = [total molar amount of the mixture (extracted in acqueous phase or organic phase)/ molar amount of the starting mixture (extracted in acqueous phase or organic phase)] x 100.

Isolation of 1-bromohexan-2-ol (3c: BHO).

In a 10 mL-round bottomed flask equipped with a condenser and a magnetic stir bar, a 1 M solution of epoxide **1c** (1 mmol) in DEG was set to react in the presence of NaBr (1 equiv. with respect to **1c**), at T = 60 °C for t = 1 h. Once the experiment was concluded, the mixture was extracted using a liquid biphasic system comprised of water (10 mL) and Et_2O (10 mL). The organic solution was separated, dried over Na_2SO_4, filtered, and rotary-evaporated (T = 30°C, *p* = 50 mbar) to remove the excess of the solvent. Crude BHO was isolated in a 93% yield and characterized by ^{1}H and ^{13}C NMR.

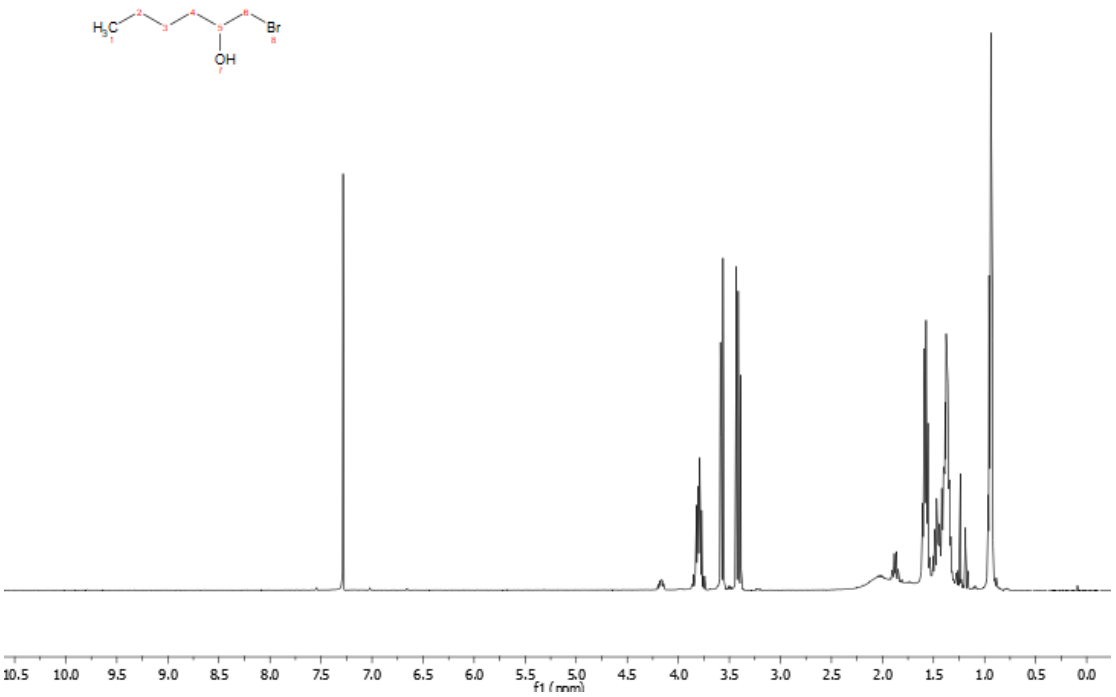

Figure A 2.56; ^{1}H NMR spectrum of 1-bromo-2-hexanol (400 MHz, 298 K, $CDCl_3$). δ (ppm): 3.77 (m, 1H), 3.55 (m, 1H), 3.39 (m, 1H), 2.16 (1H, br s), 1.26-1.49 (m, 4H), 0.89 (m, 3H).

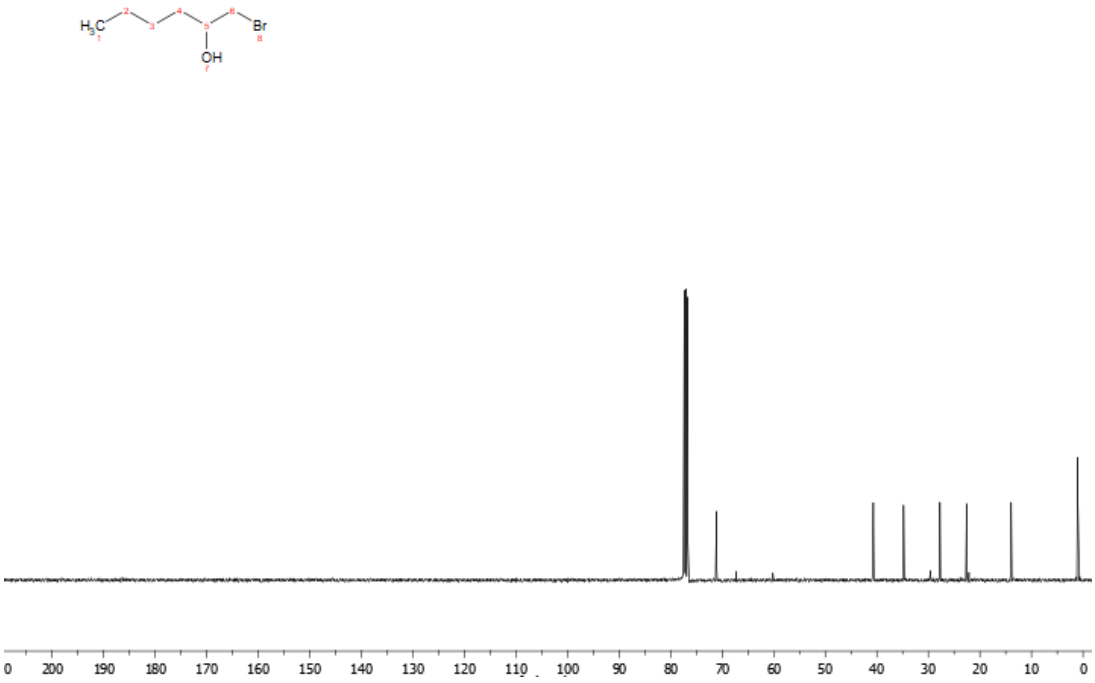

Figure A 2.57: ^{13}C NMR spectrum of 1-bromo-2-hexanol (100 MHz, 298 K, $CDCl_3$). δ (ppm): 71.1; 40.7; 34.8; 27.8; 22.6; 13.9.

***1,2-Hexandiol*.**

This compound was observed product as a by-product in the CO_2 insertion to 1,2-epoxyhexane carried out in the CF-mode. The structure was assigned by GC/MS and by comparison to an authentic sample and literature data.[2]

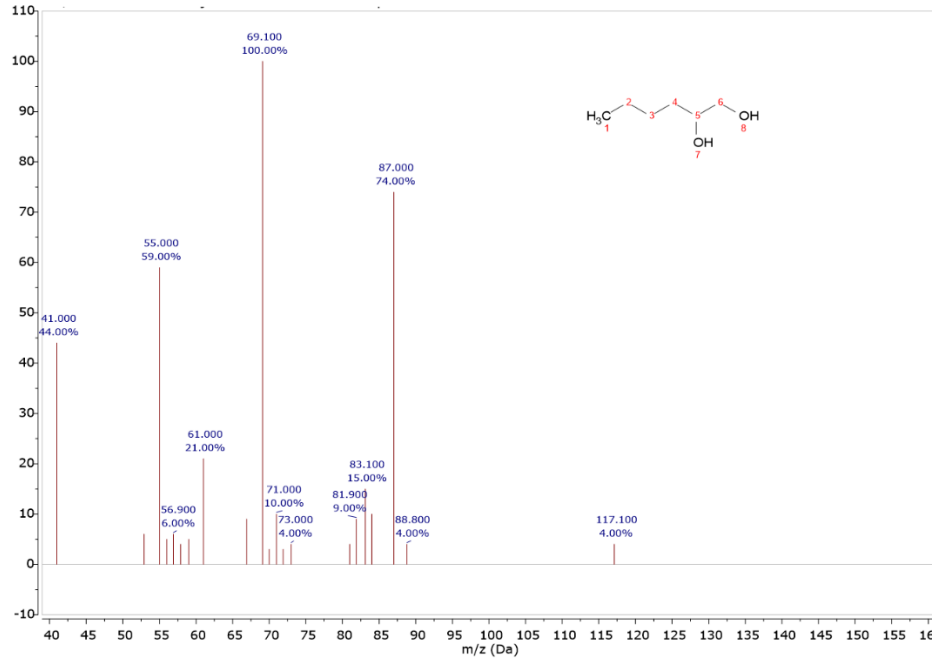

Figure A 2.58: MS spectrum of 1,2-hexandiol (EI, 70 eV). m/z (70 eV): 117 (4), 87 (74), 83 (15), 69 (100), 55 (59), 41 (44).

Characterization of Cyclic organic carbonates.

2a: 4-phenyl-1,3-dioxolan-2-one (styrene carbonate)

Spectra were in agreement with those reported in the literature.[3]

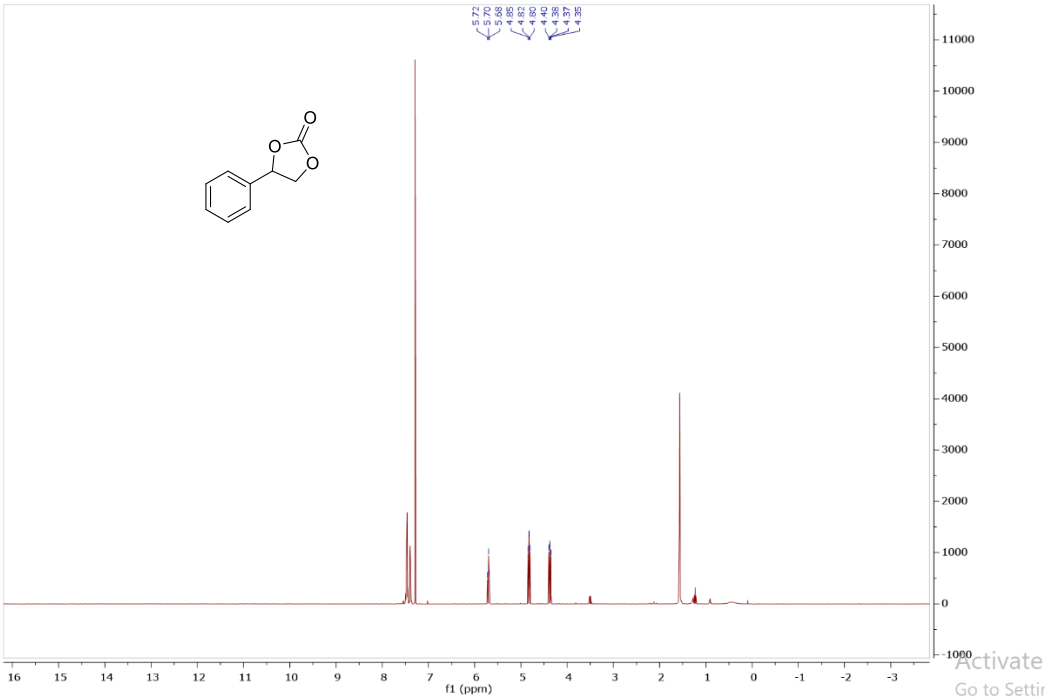

*Figure A 2.59: [1]H NMR of product **2a** (400 MHz, 298 K, $CDCl_3$). δ (ppm): 7.51-7.35 (m, 5H), 5.70 (t, 1H), 4.82 (dd, 1H), 4.37 (dd, 1H).*

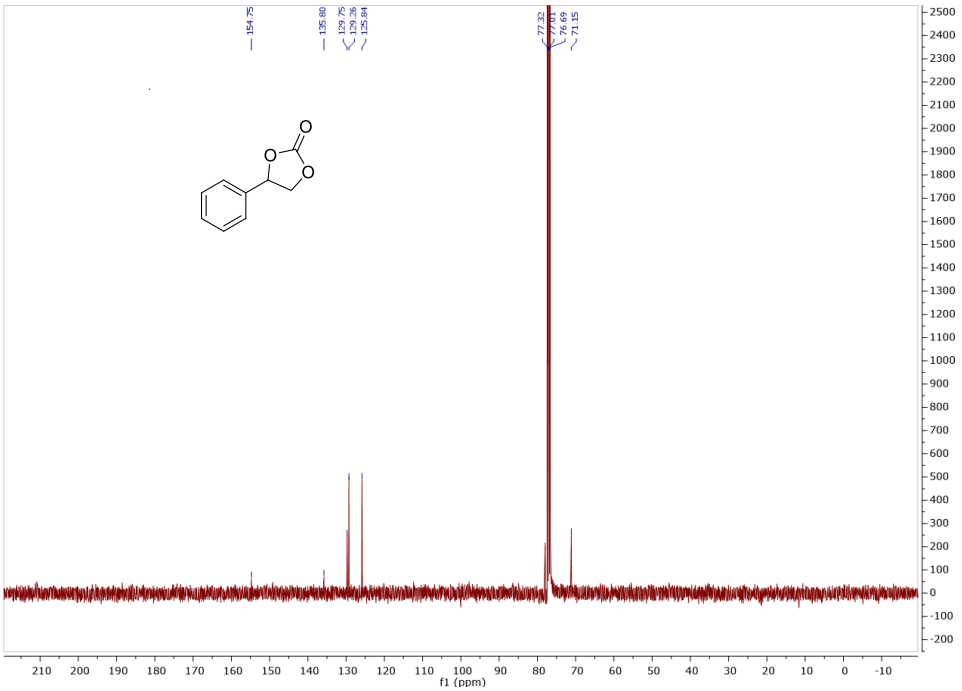

*Figure A 2.60: [13]C NMR of product **2a** (100 MHz, 298 K, $CDCl_3$). δ (ppm): 154.7, 135.8, 129.7, 129.2, 125.8, 77.3, 77.0, 76.6, 71.1.*

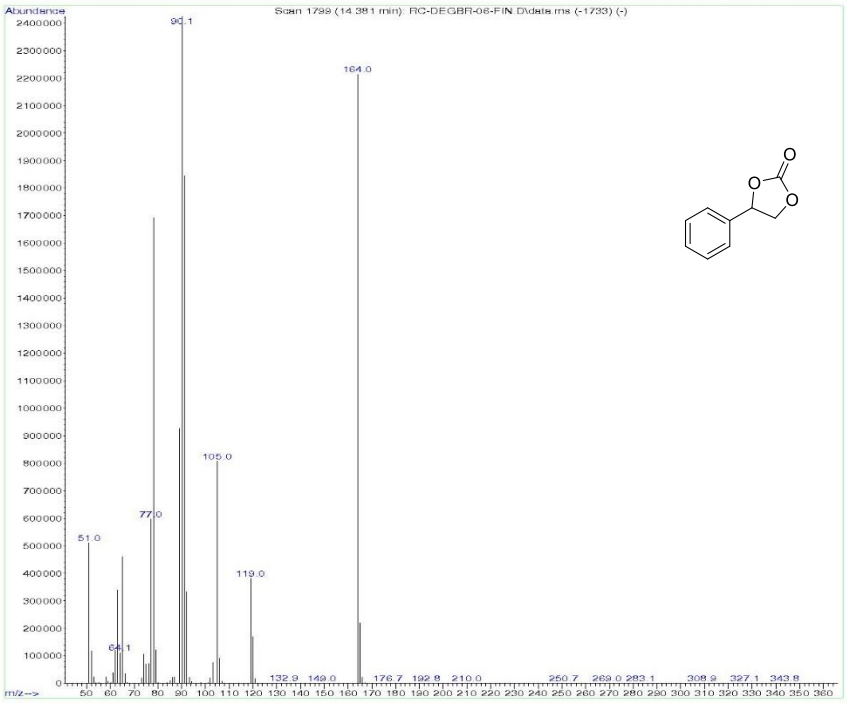

*Figure A 2.61: MS spectrum of product **2a** (EI, 70 eV). m/z (70 eV): 166 (M^{+2},1); 164 (M^{+},91); 119(16); 92 (14); 91 (76); 90 (100); 89 (38); 78 (70); 77 (25); 65 (19); 63 (14); 51 (21).*

2e: 4-(butoxymethyl)-1,3-dioxolan-2-one (butyl glycidyl carbonate)

Spectra were in agreement with those reported in the literature.[3]

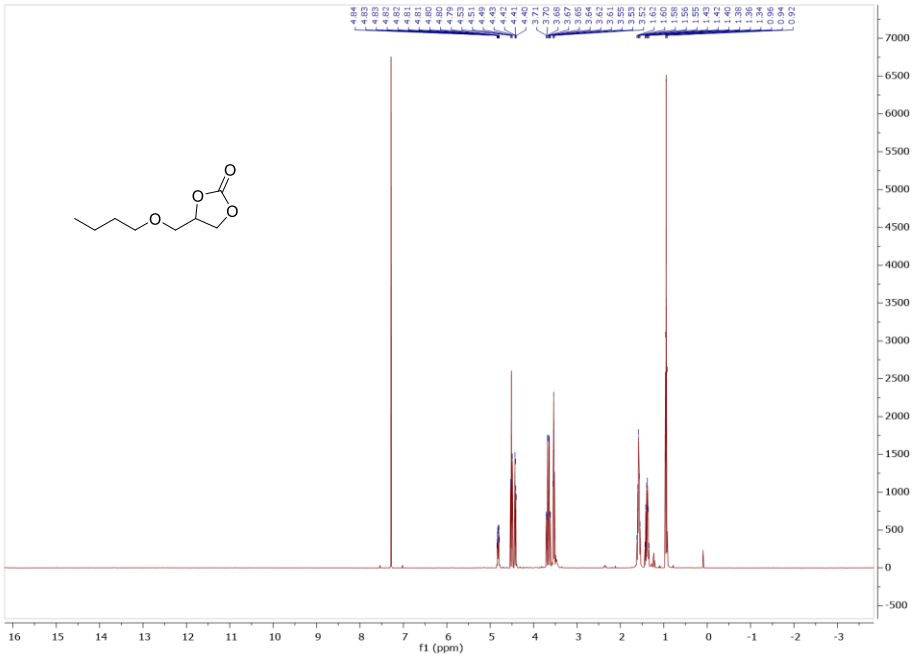

*Figure A 2.62: ^{1}H NMR of product **2e** (400 MHz, 289 K, $CDCl_3$). δ (ppm): 4.84-4.79 (m, 1H), 4.51 (dd, 1H), 4.41 (dd, 1H), 3.69 (dd, 1H), 3.63 (dd, 1H), 3.54 (t, 2H), 1.65-1.52 (m, 2H), 1.46-1.31 (m, 2H), 0.94 (t, 3H).*

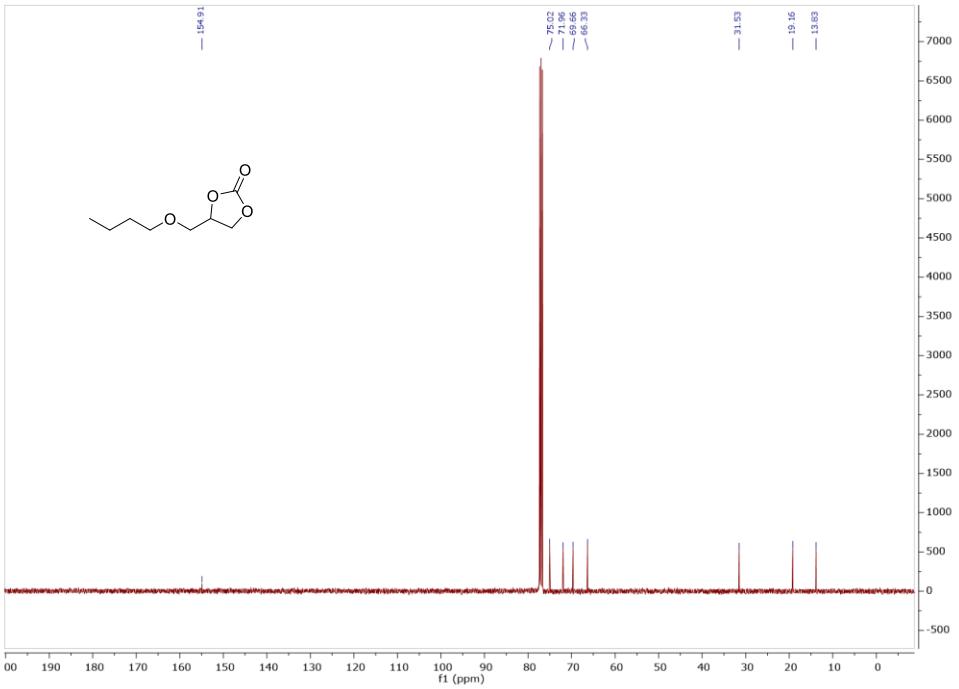

*Figure A 2.63: ^{13}C NMR of product **2e** (100 MHz, 289 K, $CDCl_3$). δ (ppm): 154.9, 75.0, 71.9, 69.6, 66.3, 31.5, 19.1, 13.8.*

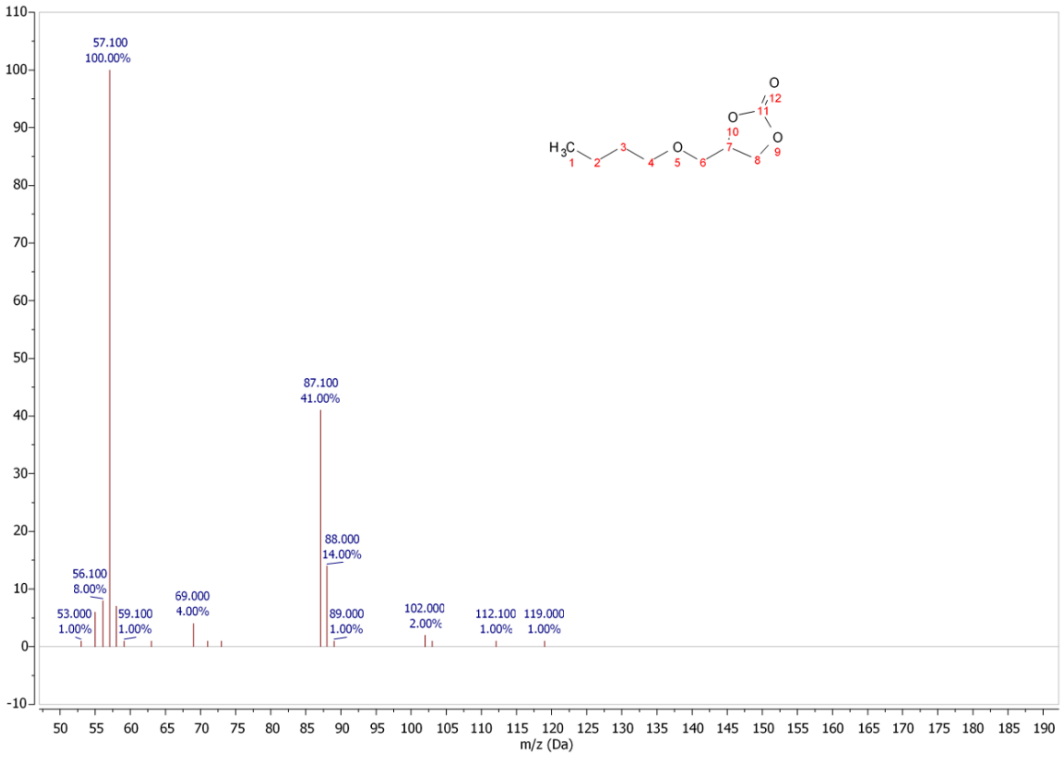

*Figure A 2.64: MS spectrum of product **2e** (EI, 70 eV). m/z (70 eV): 119 (1), 87 (41), 69 (4), 57 (100).*

2f: 4-(phenoxymethyl)-1,3-dioxolan-2-one (phenyl glycidyl carbonate)

Spectra were in agreement with those reported in the literature.[3]

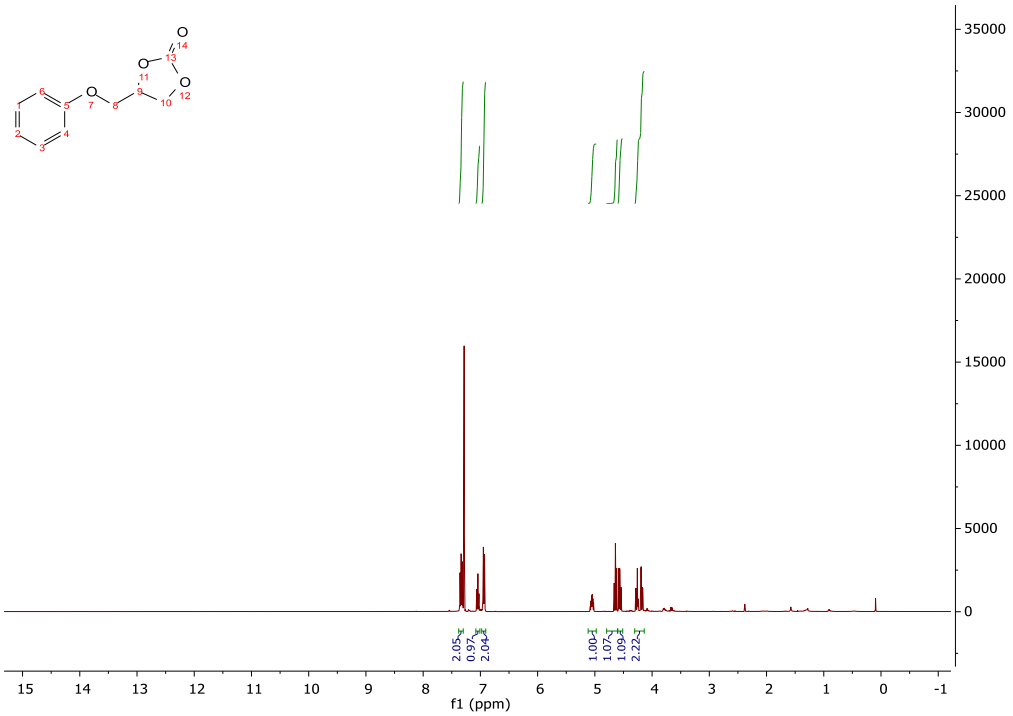

*Figure A 2.65: [1]H NMR spectrum of product **2e** (400 MHz, 298 K, $CDCl_3$). δ (ppm): 7.34 (m, 2H), 7.04 (m, 1H), 6.94 (m, 2H), 5.09-5.01 (m, 1H), 4.68-4.52 (m, 2H), 4.30-4.16 (m, 2H).*

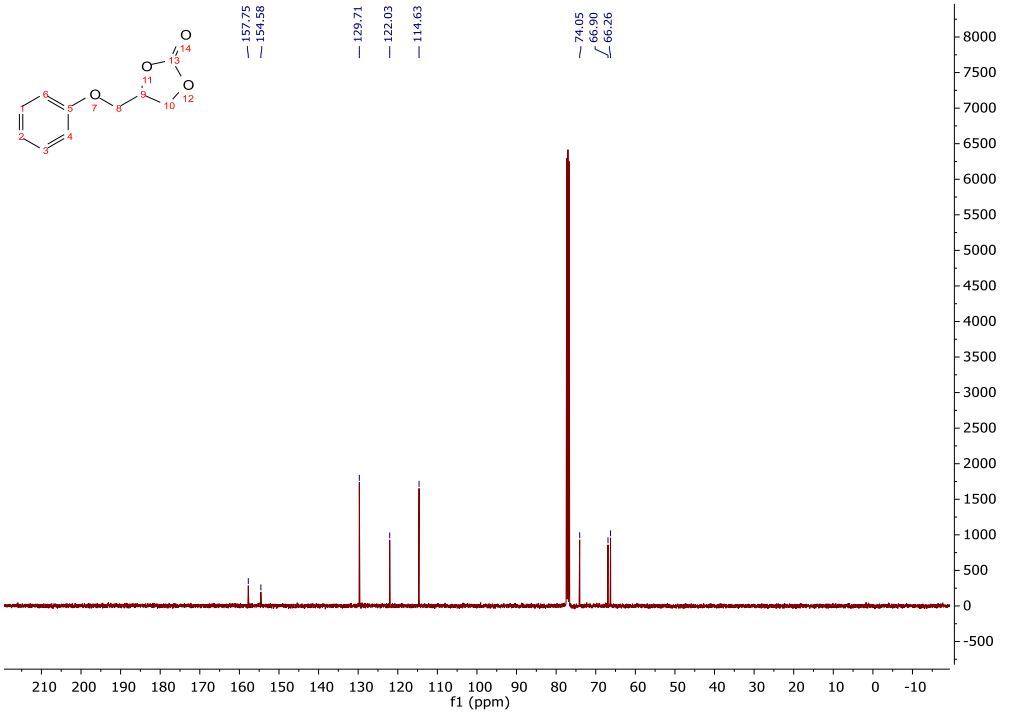

*Figure A 2.66: [13]C NMR spectrum of product **2e** (100 MHz, 298 K, $CDCl_3$). δ (ppm): 157.75, 154.58, 129.71, 122.03, 114.63, 74.05, 66.90, 66.26.*

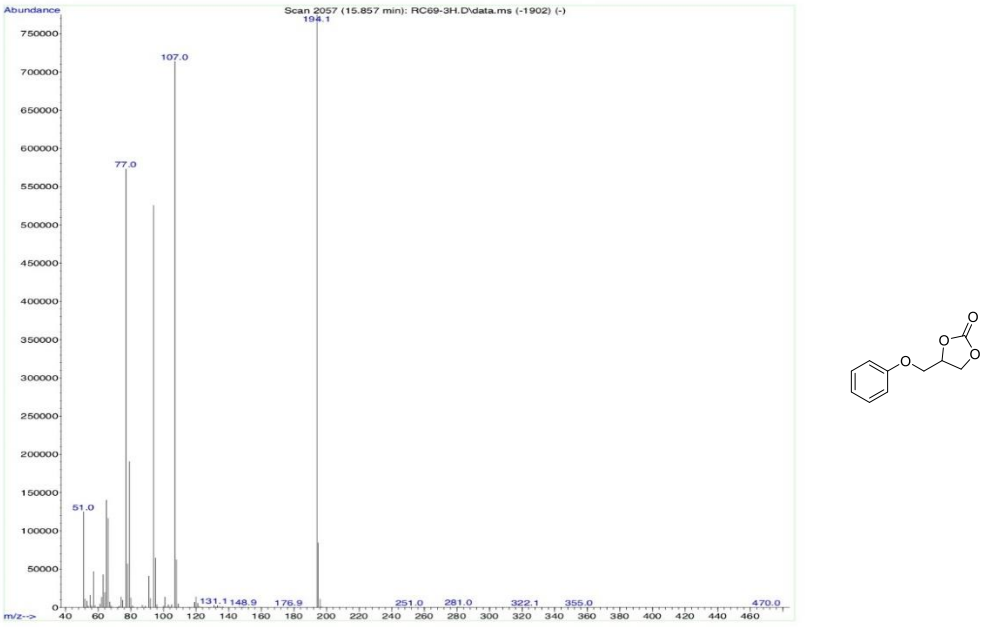

*Figure A 2.67: MS spectrum of product **2e** (EI, 70 V). m/z (70 eV): 196 (MH_2^+,1); 195(M^{+1},11); 194 (M^+,100);107 (92); 95 (8); 94 (68); 79 (25); 77 (74); 66 (15); 65 (18); 63 (6); 51 (16).*

2c: 4-butyl-1,3-dioxolan-2-one (hexylene carbonate)

Spectra were in agreement with those reported in the literature.[3]

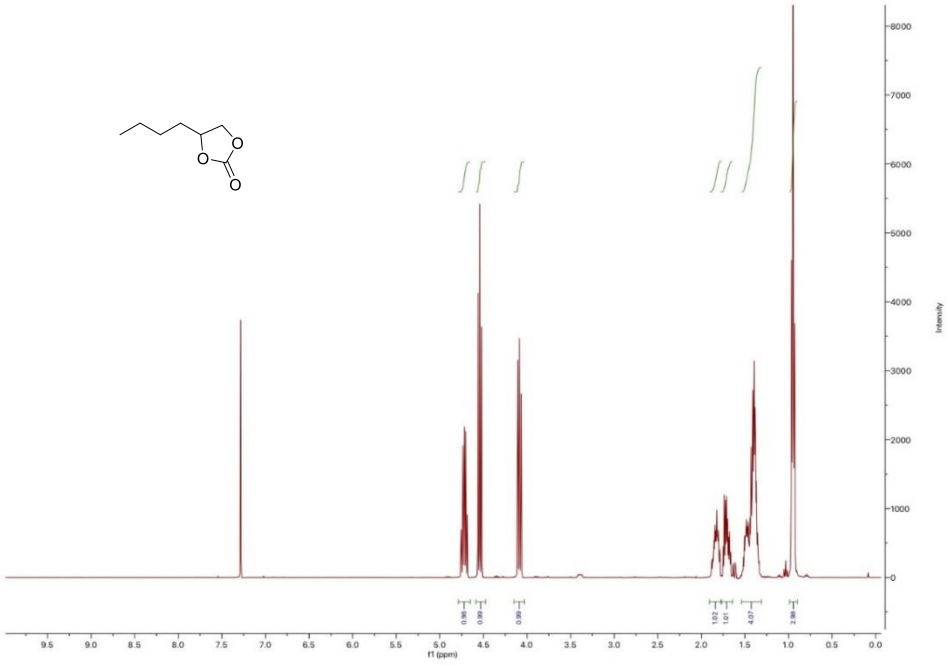

*Figure A 2.68: ^1H NMR of product **2c** (400 MHz, 298 K, $CDCl_3$). δ (ppm): 4.80-4.65 (m, 1H), 4.61-4.48 (dd, 1H), 4.13-4.03 (dd, 1H), 1.92-1.76 (m, 1H), 1.77-1.64 (m, 1H), 1.55-1.30 (m, 4H), 1.00-0.89 (t, 3H).*

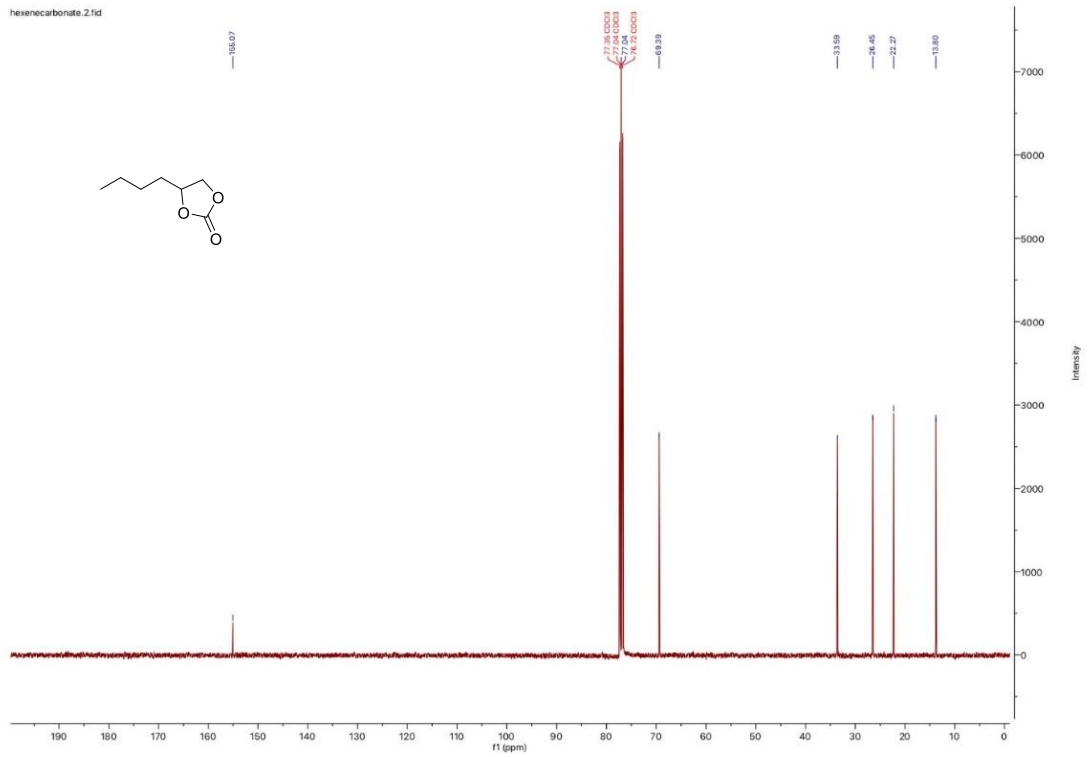

*Figure A 2.69: ^{13}C NMR of product **2c** (100 MHz, 298 K, $CDCl_3$). δ (ppm): 155.07, 77.04, 69.39, 33.59, 26.45, 22.27, 13.80.*

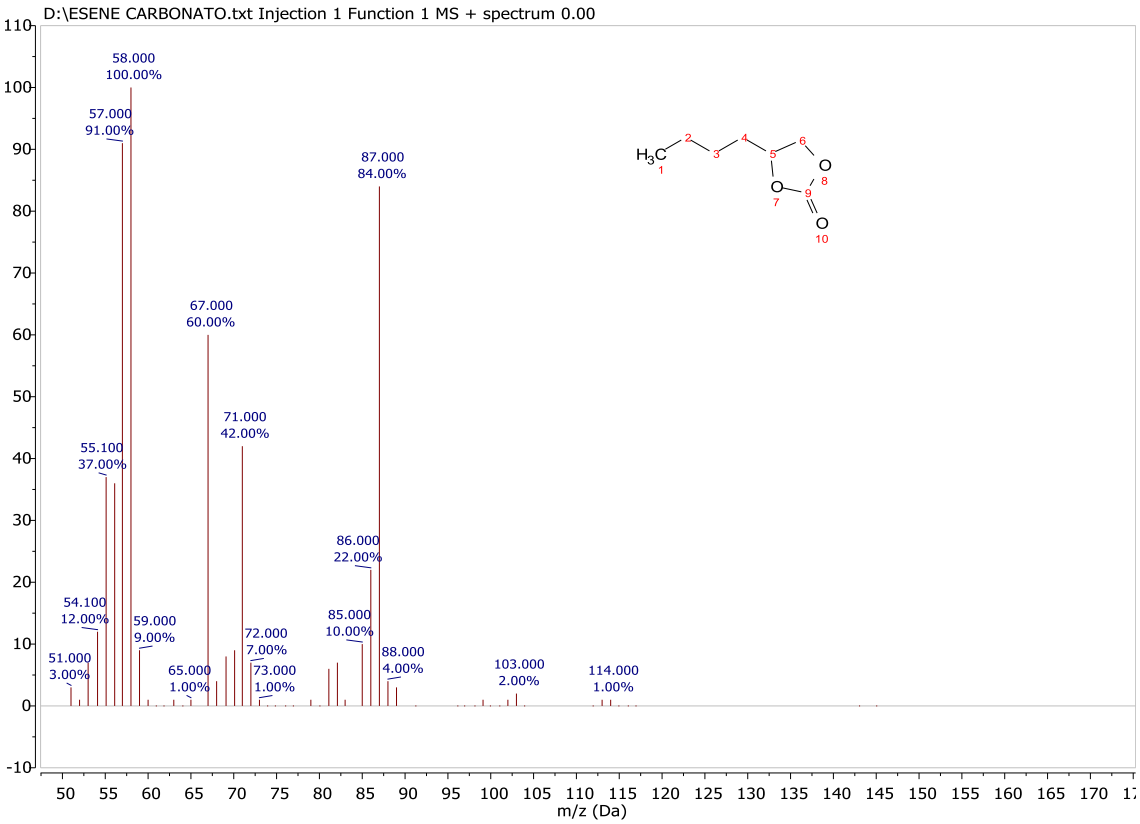

*Figure A 2.70: MS spectrum of product **2c** (EI, 70 V). m/z (70 eV): 114 (1), 87 (84), 71 (42), 67 (70), 58 (100), 57 (91), 55 (37).*

2b: 4-ethyl-1,3-dioxolan-2-one (butylene carbonate)

Spectra were in agreement with those reported in the literature.[3]

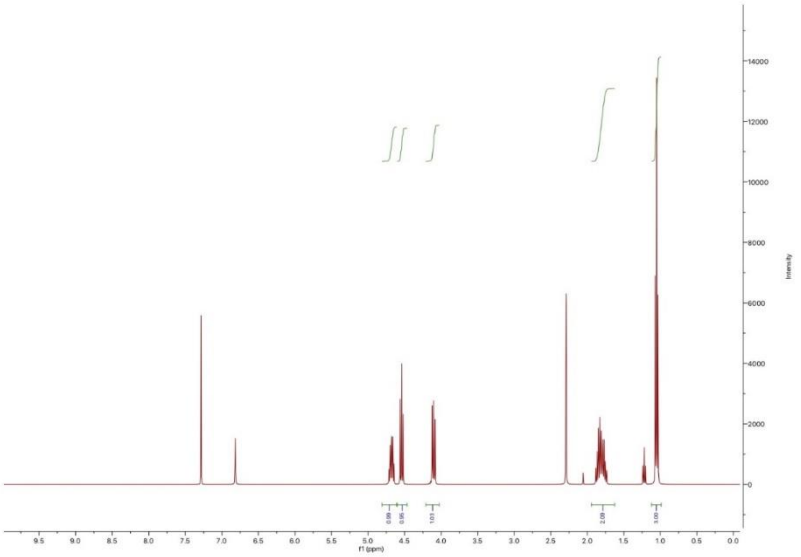

*Figure A 2.71: ^{1}H NMR of product **2b** (400 MHz, 298 K, $CDCl_3$). δ (ppm): 4.86-4.58 (dd, 1H), 4.60-4.39 (t, 1H), 4.23-4.00 (dd, 1H), 1.93-1.70 (m, 2H), 1.18-0.84 (t, 3H). The peaks at 6.82 ppm and 2.30 ppm are relative to mesitylene used as internal standard.*

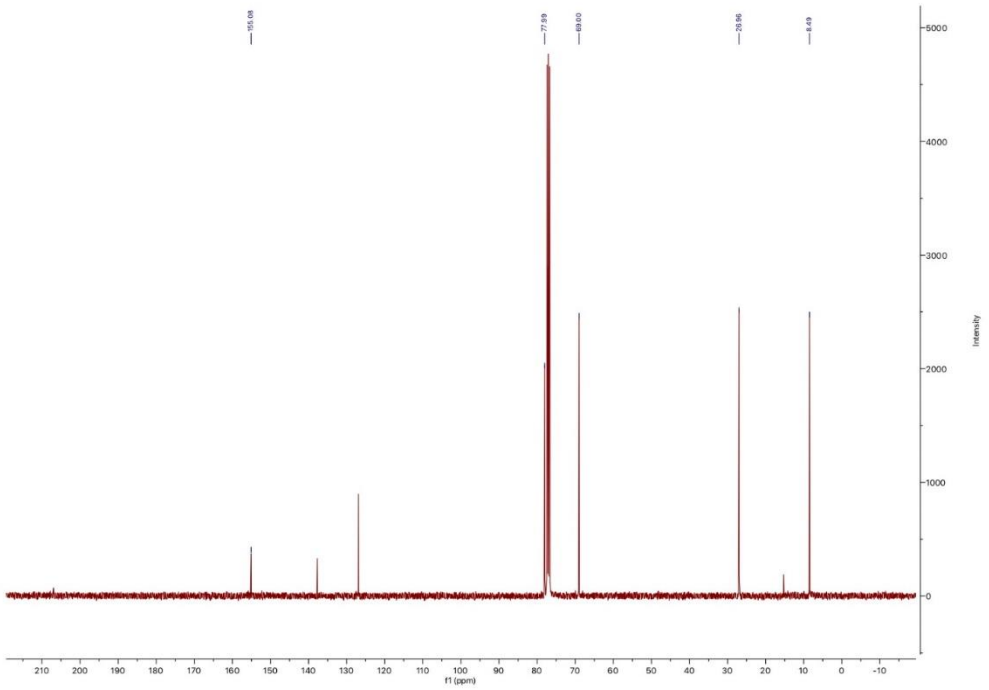

*Figure A 2.72: ^{13}C NMR of product **2b** (100 MHz, 298 K, $CDCl_3$). δ (ppm): 155.08, 77.99, 69.00, 26.96, 8.49.*

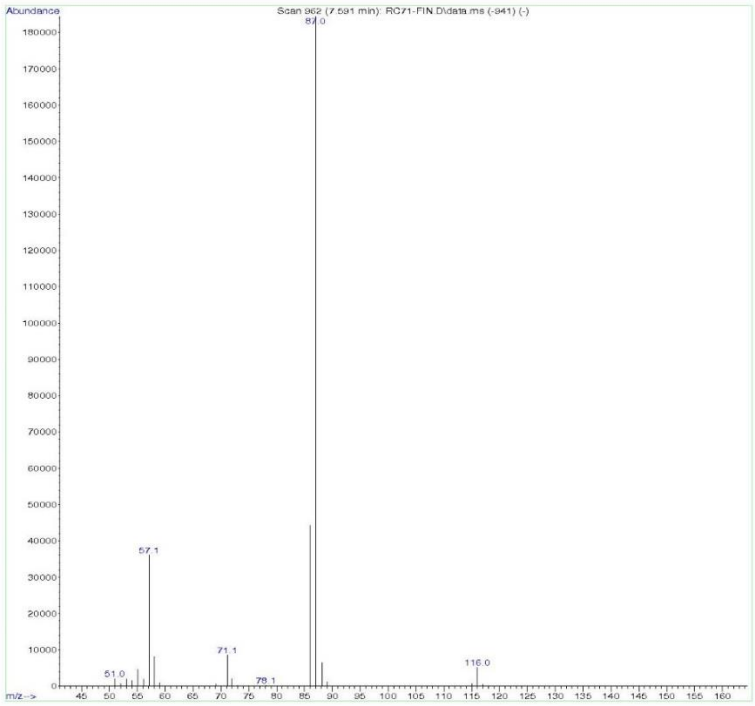

*Figure A 2.73: MS spectrum of product **2b** (EI, 70 V). m/z (70 eV): 116 (M^+,3); 87 (100); 86 (24); 57 (20).*

2d: 4-octyl-1,3-dioxolan-2-one (decene carbonate)

Spectra were in agreement with those reported in the literature.[3]

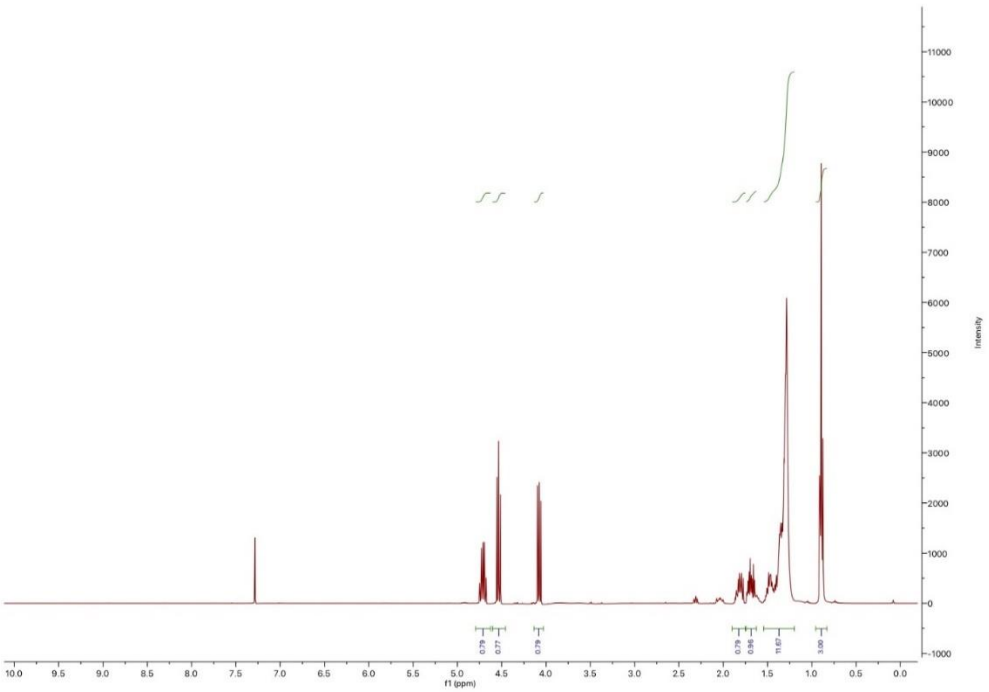

*Figure A 2.74: ^{1}H NMR of product **2d** (400 MHz, 298 K, $CDCl_3$). δ (ppm): 4.81-4.64 (m, 1H), 4.59-4.46 (dd, 1H), 4.16-3.97 (dd, 1H), 1.90-1.75 (m, 1H), 1.75-1.60 (m, 1H), 1.55-1.16 (m, 12H), 1.02-0.74 (m, 3H).*

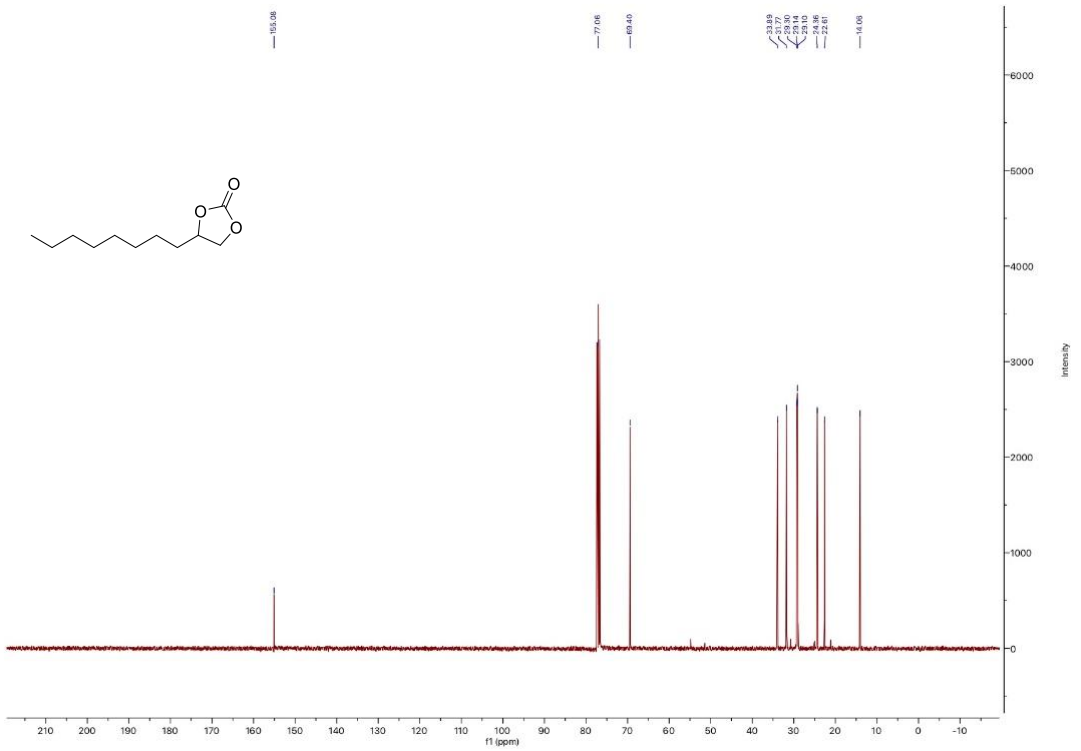

*Figure A 2.75. ^{13}C NMR of product **2d** (100 MHz, 298 K, $CDCl_3$). δ (ppm): 155.08, 77.06, 69.40, 33.89, 31.77, 29.30, 29.14, 29.10, 24.36, 22.61, 14.06.*

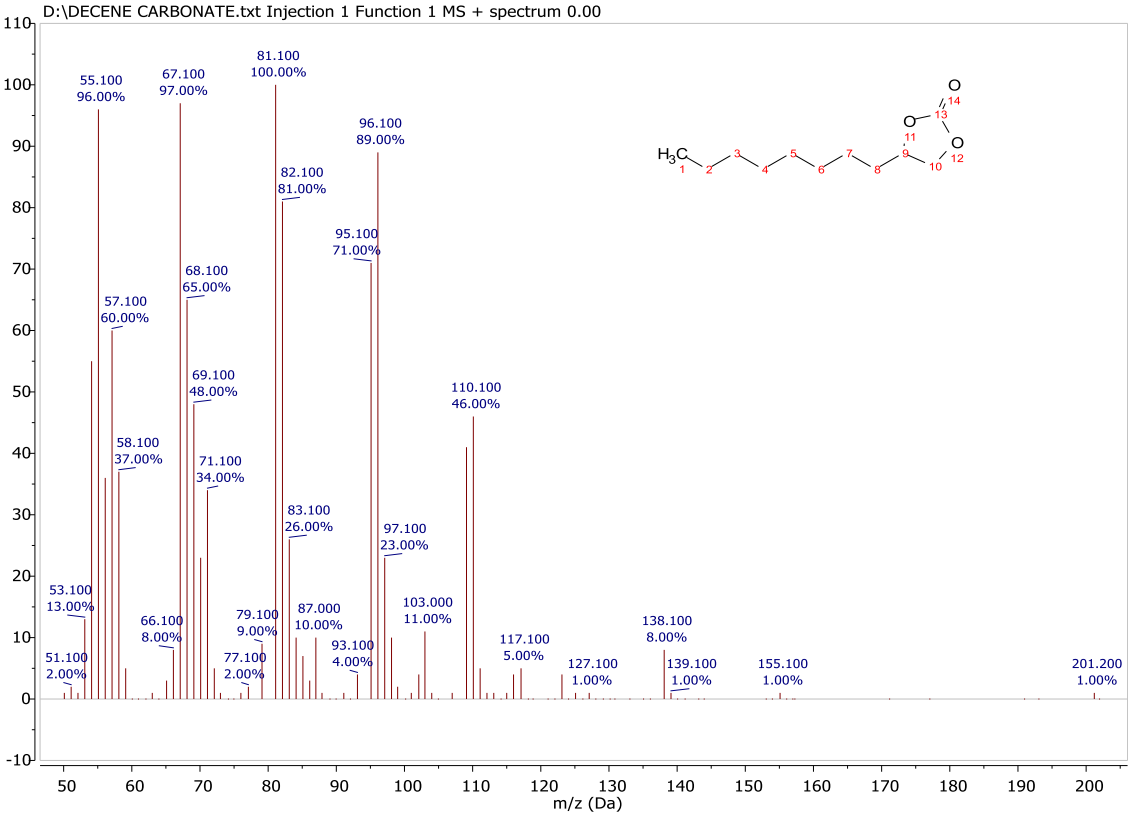

*Figure A 2.76: MS spectrum of product **2d** (EI, 70 V). m/z (70 eV): 201 (MH^+, 1), 110 (46), 96 (89), 81 (100), 67 (97), 55 (96).*

2g: 4,4'-((butane-1,4-diylbis(oxy))bis(methylene))bis(1,3-dioxolan-2-one)

Spectra were in agreement with those reported in the literature.[4,5]

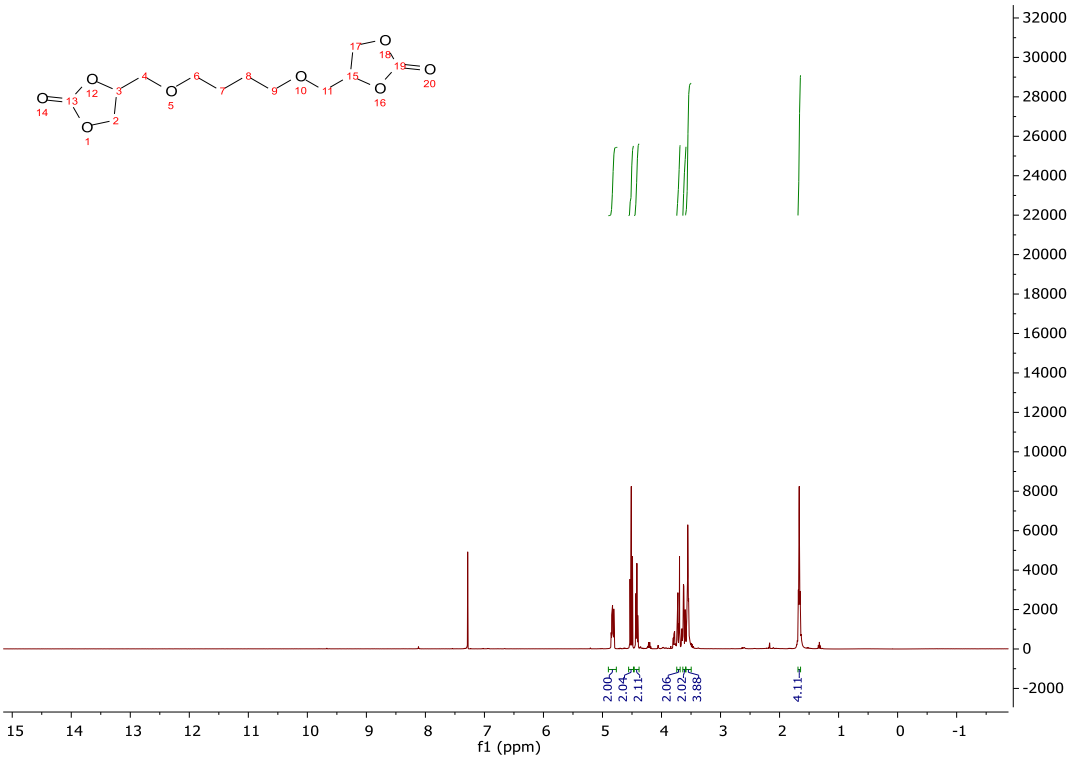

*Figure A 2.77: ^{1}H NMR of product **2g** (400 MHz, 298 K, $CDCl_3$). δ (ppm): 4.85-4.80 (m, 2H), 4.50 (t, 2H), 4.40 (m, 2H), 3.70 (m, 2H), 3.60 (m, 2H), 3.55 (m, 4H), 1.65 (m, 4H).*

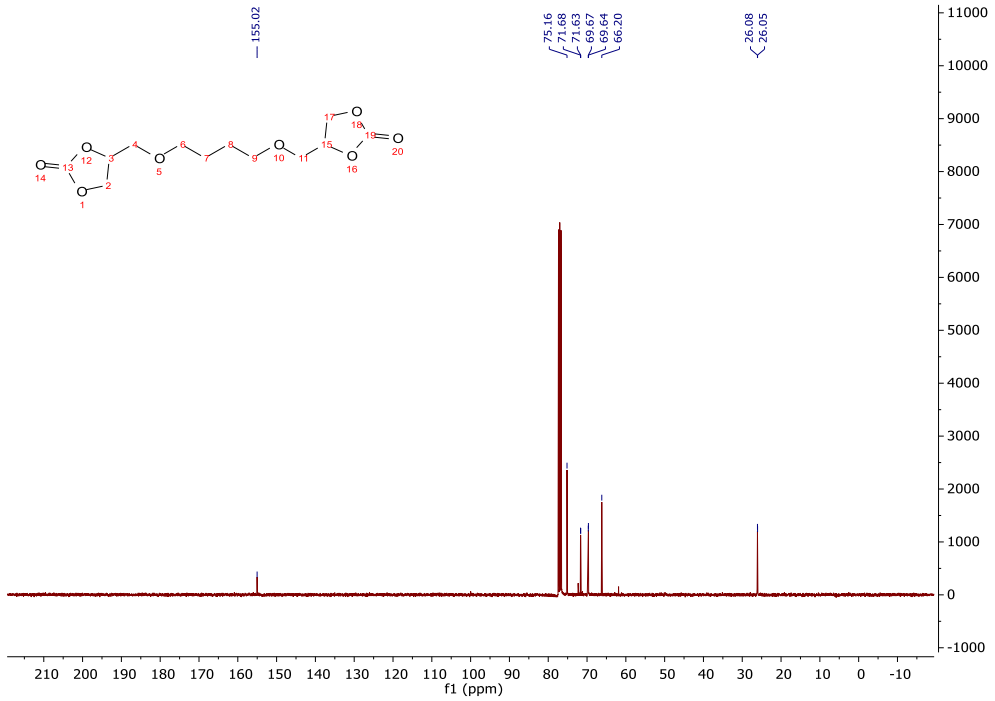

*Figure A 2.78: ^{13}C NMR of product **2g** (100 MHz, 298 K, $CDCl_3$). δ (ppm): 155.02, 75.16, 71.68, 71.63, 69.67, 69.64, 66.20, 26.08, 26.05.*

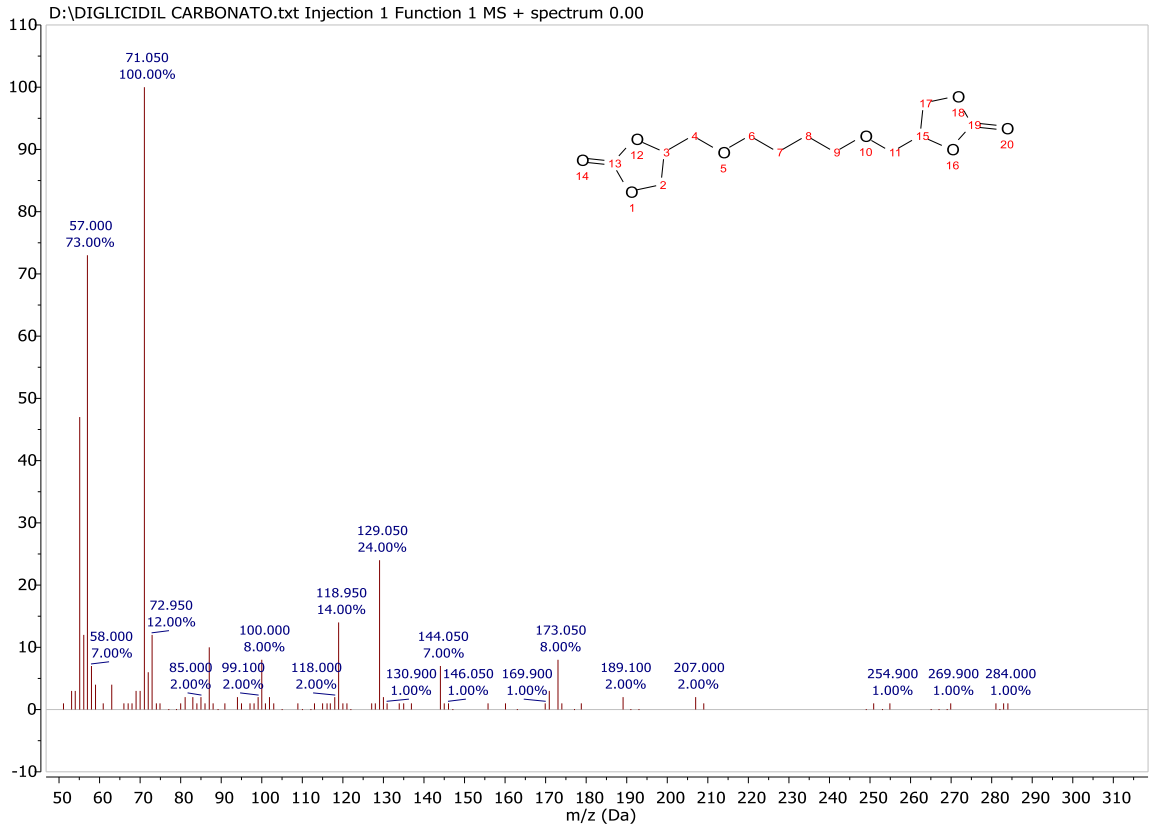

*Figure A 2.79: MS spectra of product **2g** (EI, 70 V). m/z (70 eV): 173 (8), 129 (24), 119 (14), 71 (100), 57 (73).*

References

[1] L. Salles, C. Aubry, R. Thouvenot, F. Robert, C. Doremieux-Morin, G. Chottard, H. Ledon, Y. Jeannin, J.M. Bregeault, Inorganic Chemistry, 1994, **33**, 871-878;

[2] Jr. C. Garry, N. Kenneth, *Chem. Commun.*, **2013**, *49*, 8199 – 8201.

[3] J. A. Castro-Osma, A. Lara-Sánchez, M. North, A. Otero, P. Villuendas, *Catal. Sci. Technol.*, **2012**, *2*, 1021-1026.

[4] G. Ting-Ting, S. Xiao-Fang, X. Xianxiu, Y. Jin, Y. Li-Kai, M. Jian-Fang, *Inorg. Chem.*, **2019**, *58*, 16518-16523.

[5] X. Meng, Z. Ju, S. Zhang, X. Liang, N. Von Solms, X. Zhang, X. Zhang, *Green Chem.*, **2019**, *21*, 3456-3463.

Appendix A.3 – Chapter 3

Appendix A.3.1
BATCH AND CONTINUOS-FLOW TRANSESTERIFICATION OF ALKYL AND ENOL ESTERS WITH GLYCEROL AND ITS ACETAL DERIVATIVES UNDER THERMAL (CATALYST-FREE) CONDITIONS

Liquid-vapor pressure profile of isopropenyl acetate

A modification of the Wagner equation, the extended Antoine equation, was used to predict the liquid-vapor profile of pure isopropenyl acetate. Wagner used an elaborate statistical method to develop an equation for representing the vapor pressure behavior of N_2 and Ar. The extended Antoine equation can represent the vapor pressure behavior of most substances over the entire liquid range.[1]

$$\ln p_i\,(Pa) = a + \frac{b}{T_i + c} + T_i \cdot d + e \cdot \ln T_i + f \cdot T_i^{\,g}$$

where p_i (Pascal) is the saturated vapour pressure at the temperature T_i (kelvin). The values a, b, c, d, e, f, g, for isopropenyl acetate are 76.599, -7049.1, 0, 0, -7.792, $2.151 \cdot 10^{-17}$, $2.151 \cdot E^{-17}$, 6, respectively.[2]

The liquid-vapor prediction is reported in figure A.3.1.

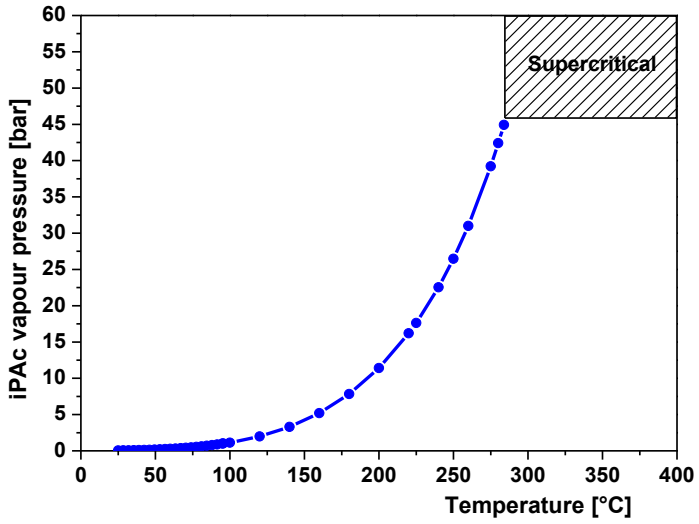

Figure A 3.1: Predictive phase diagram of pure iPAc calculated by the extended Antoine equation.

Karl-Fisher titrations

Titrations of solketal (**1a**), isopropenyl acetate (**2f**) and glycerol were carried out by using HYDRANAL®-composite one from Sigma-Aldrich. The titration procedure is described in detail elsewhere. [3] Every titration was repeated three times.

The water content of each compound is calculated from the volume consumed and the water equivalent (WE) of the HYDRANAL®-reagent (**HR**):

$$mg\ (H_2O) = a \cdot WE$$

$$\%(H_2O) = \frac{a \cdot WE}{10 \cdot e}$$

Where:

a= consumption of reagent **HR** in mL

WE= water equivalent of the reagent **HR** in mg H_2O/mL = 0.8-1.2 mg/mL

e= weight of the sample in g

Table A 3.1: Amount of water calculated in solketal, iPAc and Glyc

Substrate	Amount (g)	Volume HR (mL)	H_2O	
			mg[a]	%, mol
Solketal (**1a**)	2.13 g	3.1	3.1 ± 0.6	1.07 ± 0.2
Isopropenyl acetate (**2f**)	3.64	0.7	0.7 ± 0.1	0.11 ± 0.02
Glycerol	1.009	3.9	3.9 ± 0.7	1.99 ± 0.35 %

[a] mg of water per mL of substrate

The Reaction of solketal (1a) with iPAc and added AcOH

At 180 °C, three experiments were carried in which a mixture of solketal (4.0 mmol) and iPAc (80 mmol) in a 1:20 molar ratio, respectively, was set to react in the presence of increasing amounts of AcOH corresponding to 1, 5, and 20 mol% (0.04-0.8 mmol) with respect to solketal. Reactions were duplicated to check for reproducibility. Tests afforded values of conversion (determined by GC/MS) which differed by less than 5% from one experiment to another. Selectivity towards solketal acetate (**3a**) was always >98%.

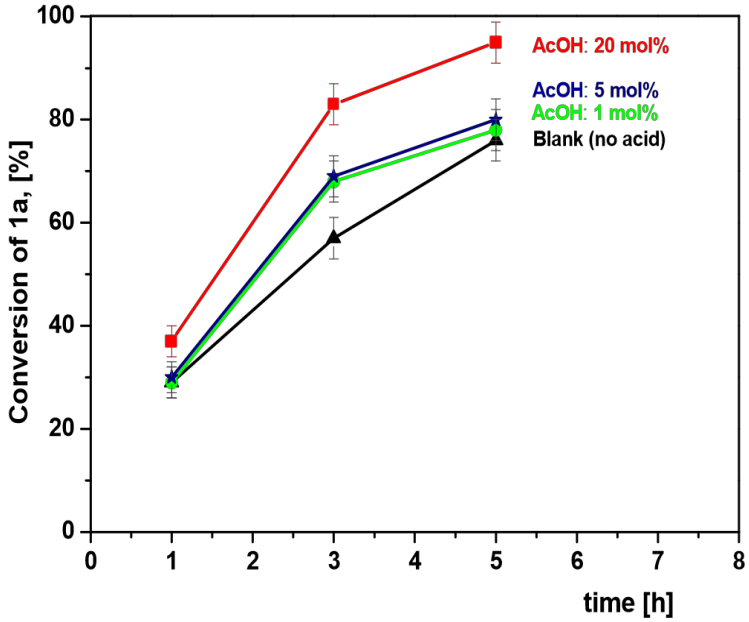

*Figure A 3.2: reaction of solketal (**1a**) with isopropenylacetate in the presence of increasing amounts of AcOH (1, 5, and 20 mol% with respect to solketal). Conditions: Solketal and iPAc in a 1:20 molar ratio; 180 °C.*

Reaction of glycerol with isopropenyl acetate with molar ratio Glyc:iPAc=Q=1

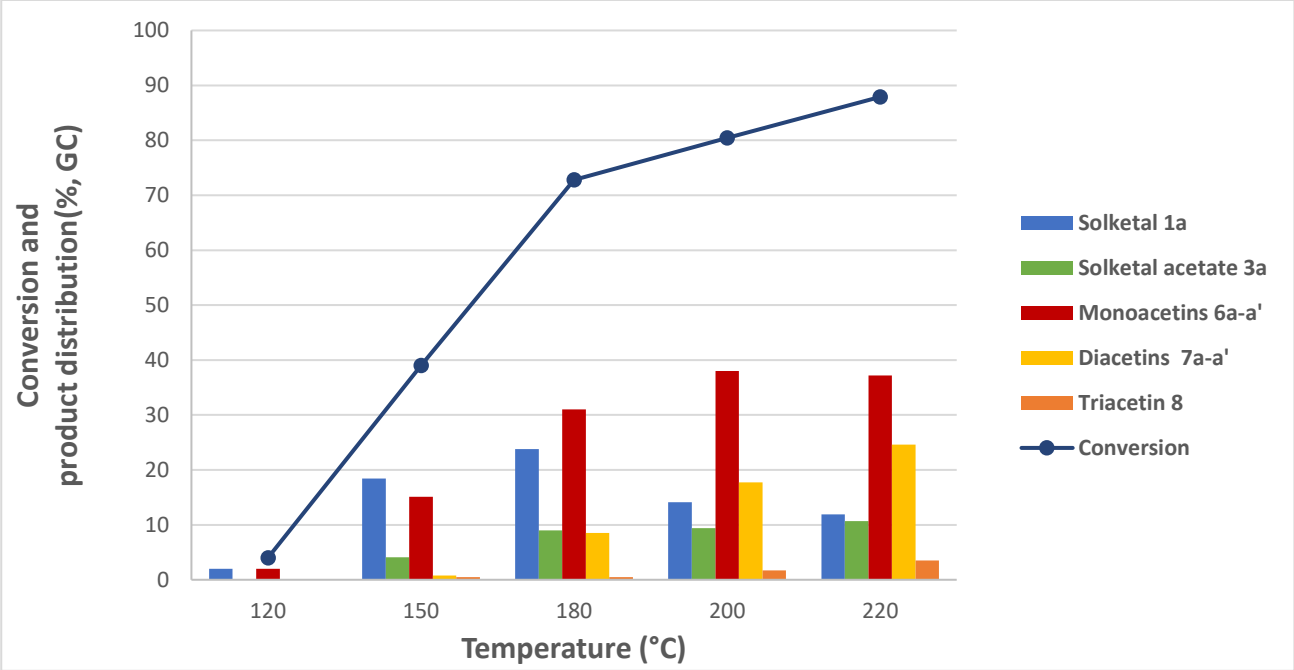

Figure A 3.3 Reaction of glycerol with isopropenyl acetate at equimolar ratio (iPAc:Glyc=Q=1), t=5h, T=120-220°C

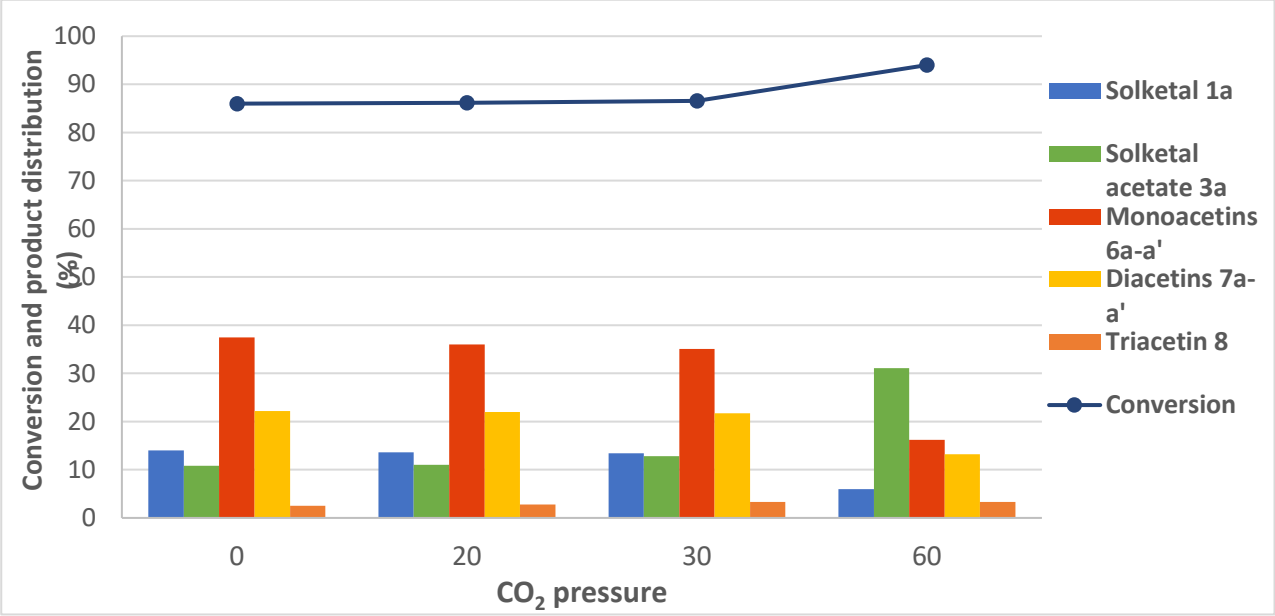

Figure A 3.4 : Effect of additional pressure of CO_2 (0-60 bar) to conversion and products distribution of the reaction between Glyc and iPAc at equimolar ratio (Q=1), T=180°C, t=15h.

Isolation and characterization

Solketal Methyl acetate (**3a**):

With reference to the experiment in fig. 3.2 (**2f)**, the reaction mixture was concentrated by rotary evaporation (60°C, 40 mbar). The liquid residue was purified by FCC with Petroleum ether:Ethyl acetate= 9:1 v/v Title product was obtained in 96 % yield (615 mg, 99% purity by GC-MS). The product appeared as a yellowish liquid and was characterized by ^{1}H NMR, ^{13}C NMR and GC/MS.

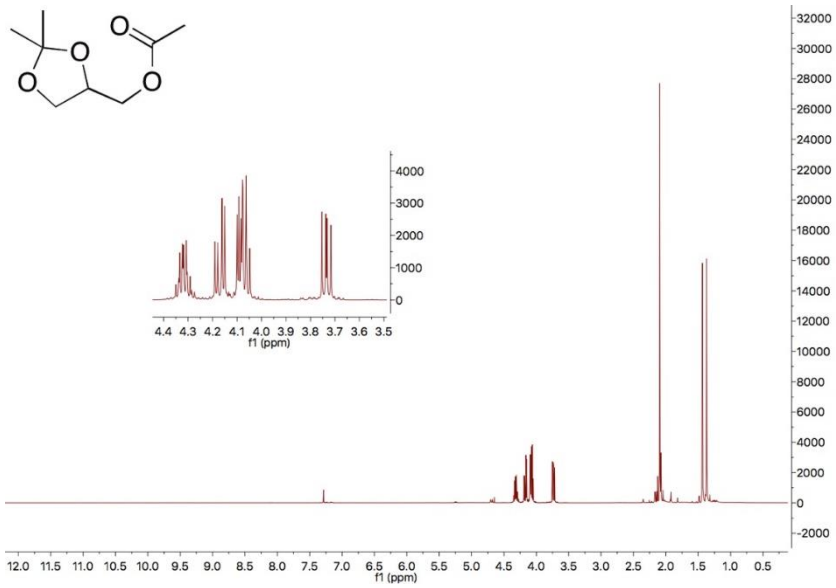

Figure A 3.5: ^{1}H NMR (400 MHz, Chloroform-d) δ: 4.32 (m, J = 6.2, 4.6 Hz, 1H), 4.17 (dd, J = 11.5, 4.6 Hz, 1H), 4.11 – 4.03 (m, 2H), 3.73 (dd, J = 8.5, 6.2 Hz, 1H), 2.09 (s, 3H), 1.43 (s, J = 0.8 Hz, 3H), 1.37 (s, J = 0.8 Hz, 3H).

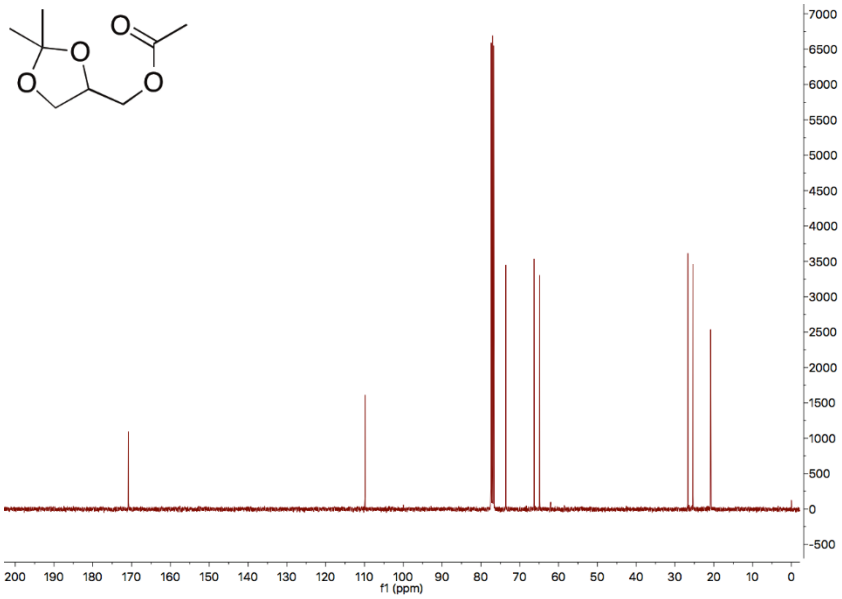

Figure A 3.6: ^{13}C NMR (100 MHz, Chloroform-d) δ: 170.81, 109.88, 73.61, 66.30, 64.85, 26.68, 25.38, 20.83.

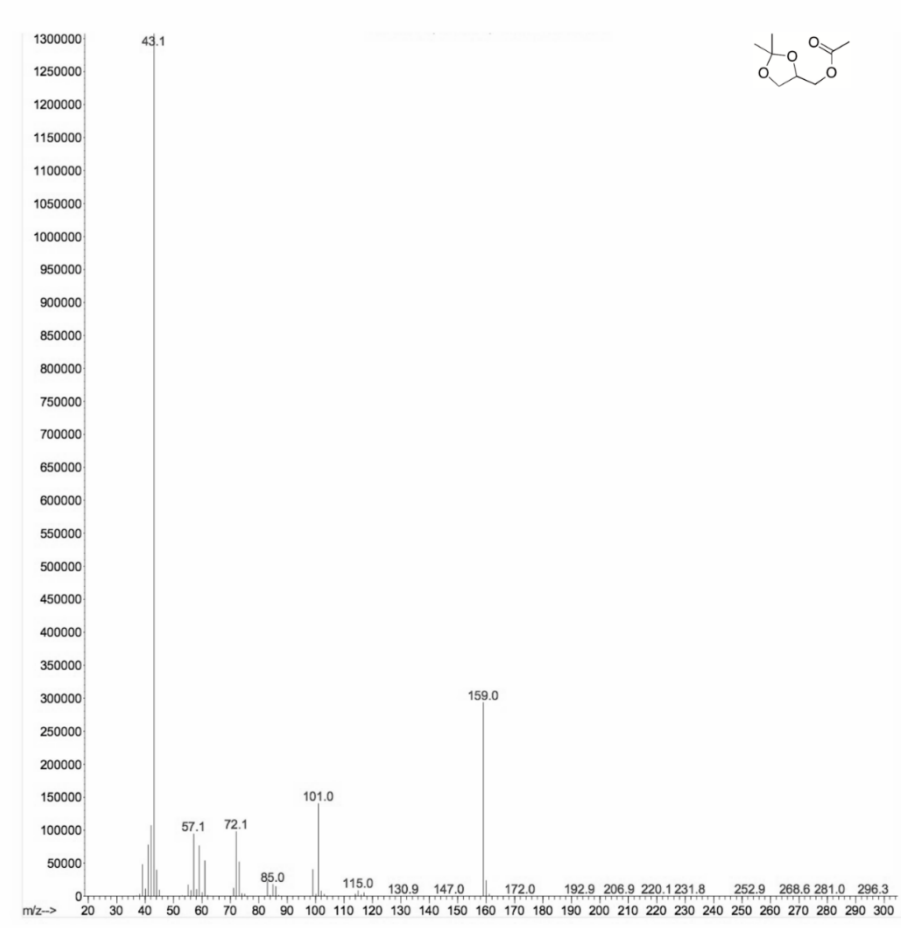

*Figure A 3.7: Mass spectra of **3a** (relative intensity, 70 eV) m/z: 160.00 (1); 159.00 (17); 101.00 (8); 73.00 (3); 72.00 (6); 57.00 (6); 43.00 (100); 42.00 (8); 41.00 (6)*

Solketal formate (**3b**):

With reference to the experiment in fig. 3.2 (**2d)**, the reaction mixture was concentrated by rotary evaporation (60°C, 40 mbar). The liquid residue was purified by FCC with Petroleum ether:Ethyl acetate= 8:2 v/v. Title product was obtained in 60 % yield (360 mg, 98% purity by GC-MS). The product appeared as a colorless liquid and was characterized by ^{1}H NMR, ^{13}C NMR and GC/MS.

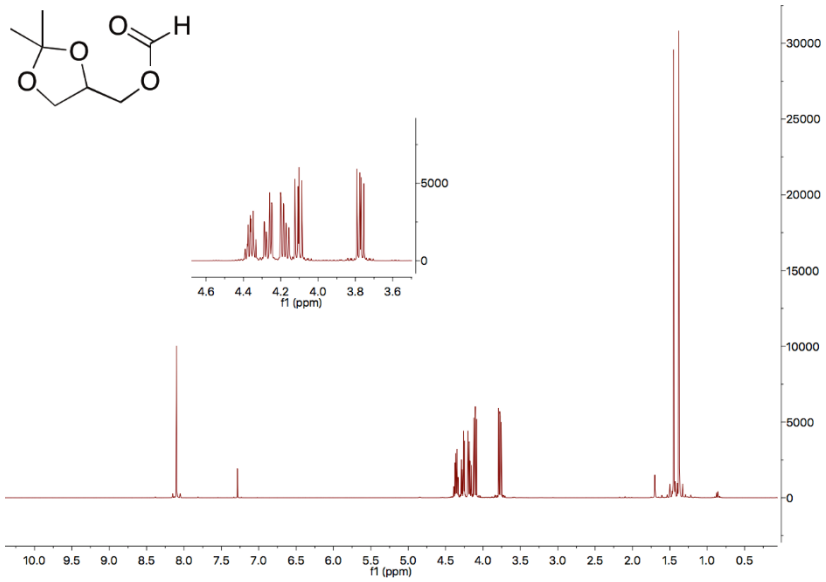

Figure A 3.8: ^{1}H NMR (400 MHz, Chloroform-d) δ: 8.10 (s, 1H), 4.36 (m, J = 6.1, 4.5 Hz, 1H), 4.27 (m, J = 11.4, 4.6, 0.9 Hz, 1H), 4.18 (m, J = 11.4, 6.2, 0.8 Hz, 1H), 4.10 (m, J = 8.5, 6.5 Hz, 1H), 3.77 (dd, J = 8.5, 6.0 Hz, 1H), 1.45 (s, J = 0.8 Hz, 3H), 1.38 (s, J = 0.8 Hz, 3H).

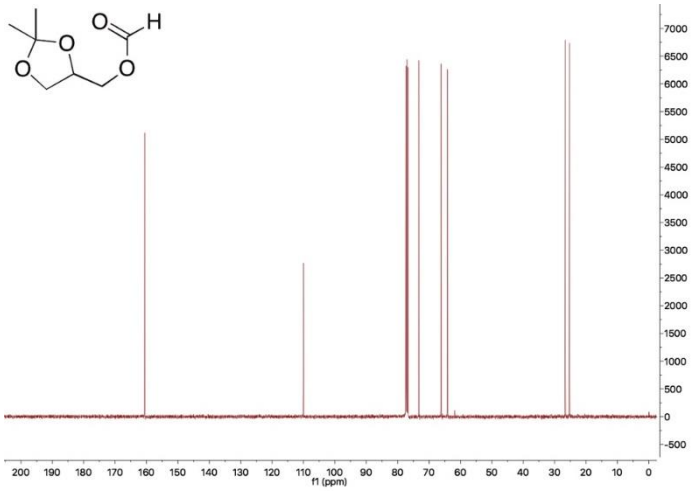

Figure A 3.9: ^{13}C NMR (101 MHz, Chloroform-d) δ 160.54, 109.98, 73.27, 66.20, 64.12, 26.66, 25.28.

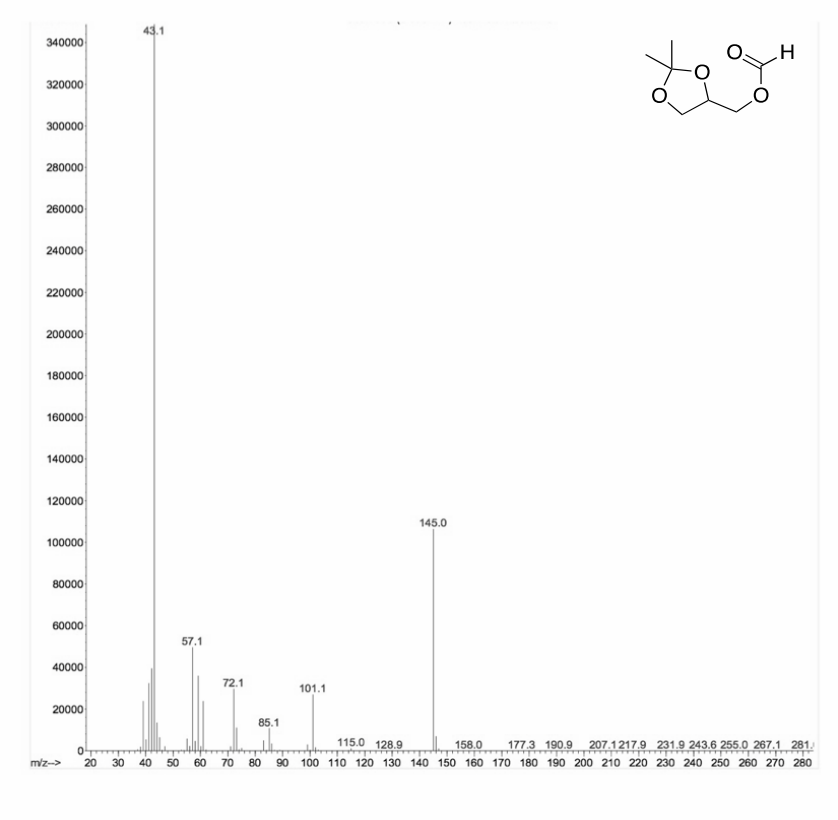

Figure A 3.10: ^{13}C NMR (101 MHz, Chloroform-d) δ 160.54, 109.98, 73.27, 66.20, 64.12, 26.66, 25.28.

Solketal lactate (**3c**):

With reference to the experiment in fig. 3.2 (**2e)**, the reaction mixture was concentrated by rotary evaporation (60°C, 40 mbar). The liquid residue was purified by FCC with Petroleum ether:Ethyl acetate= 1:9 v/v. Title product was obtained in a small amount as a colorless liquid and was characterized by ^{1}H NMR, ^{13}C NMR and GC/MS.

^{1}H NMR and ^{13}C NMR highlighted the formation of the two diastereoisomers, ((*R*)-2,2-dimethyl-1,3-dioxolan-4-yl)methyl (*S*)-2-hydroxypropanoate and ((*R*)-2,2-dimethyl-1,3-dioxolan-4-yl)methyl (*S*)-2-hydroxypropanoate.

Furthermore, the spectra of the two unidentified by-products are reported. Though it was not possible to separate them from the reaction mixture since they were in low amounts, GC-MS spectra highlighted the presence of typical fragments (m/z: 43.00, 57.00, 85.00, 101.00) of solketal-derived compounds.

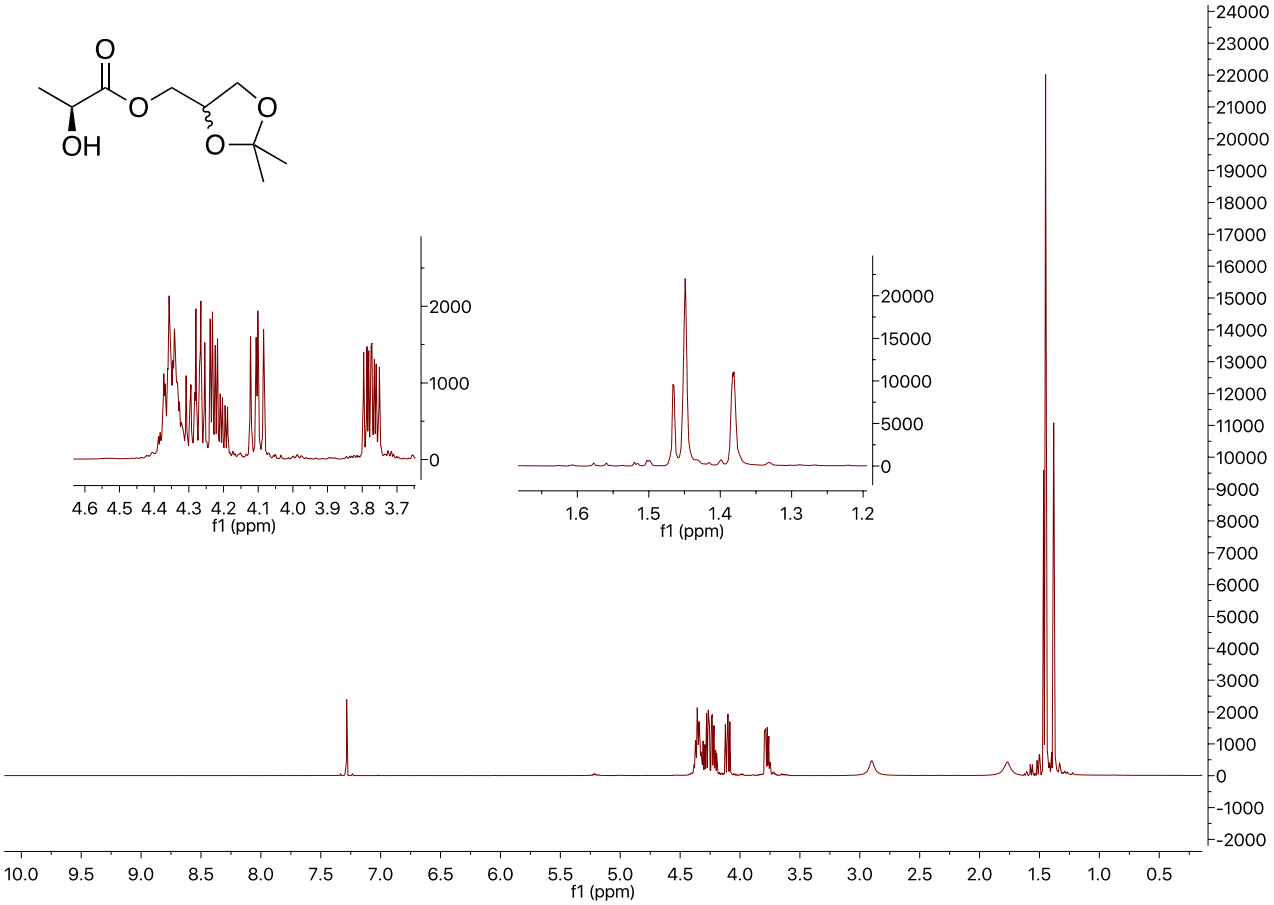

Figure A 3.11: [1]H NMR (400 MHz, Chloroform-d) δ 4.39 – 4.32 (m, 4H), 4.28 (m, J = 11.5, 5.6, 4.5 Hz, 2H), 4.21 (m, J = 11.5, 5.8, 2.7 Hz, 2H), 4.10 (m, J = 8.6, 6.5, 0.7 Hz, 2H), 3.77 (m, J = 8.5, 5.8, 3.7 Hz, 2H), 1.47 (d, J = 0.7 Hz, 3H), 1.45 (m, J = 0.9 Hz, 9H), 1.38 (m, J = 1.5, 0.7 Hz, 6H

The other signals correspond to traces of ethyl acetate

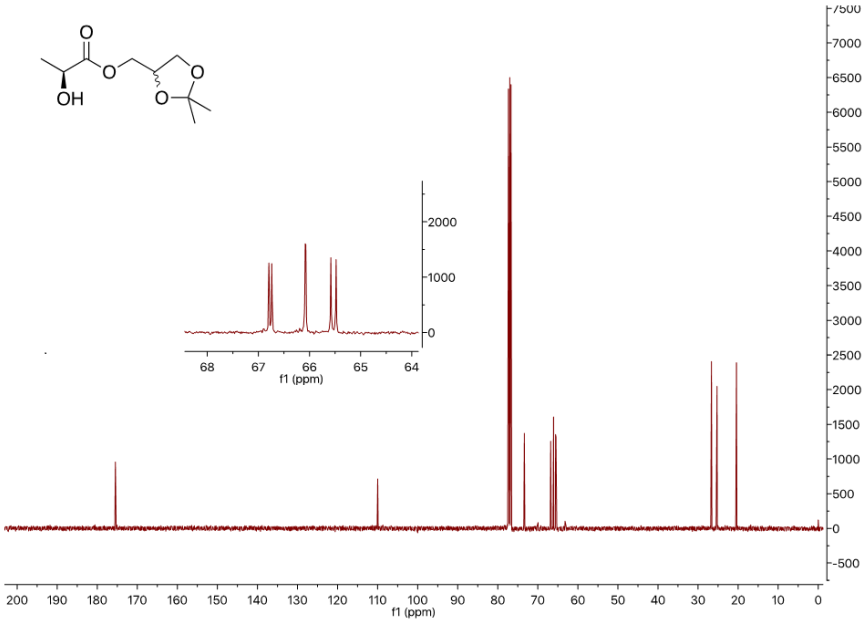

Figure A 3.12: Figure A 3.27: 13C NMR (101 MHz, Chloroform-d) δ 175.48, 109.98 (d, J = 2.4 Hz), 73.36 (d, J = 4.4 Hz), 66.77 (d, J = 5.8 Hz), 66.08 (d, J = 1.4 Hz), 65.53 (d, J = 10.2 Hz), 26.66, 25.27, 20.42.

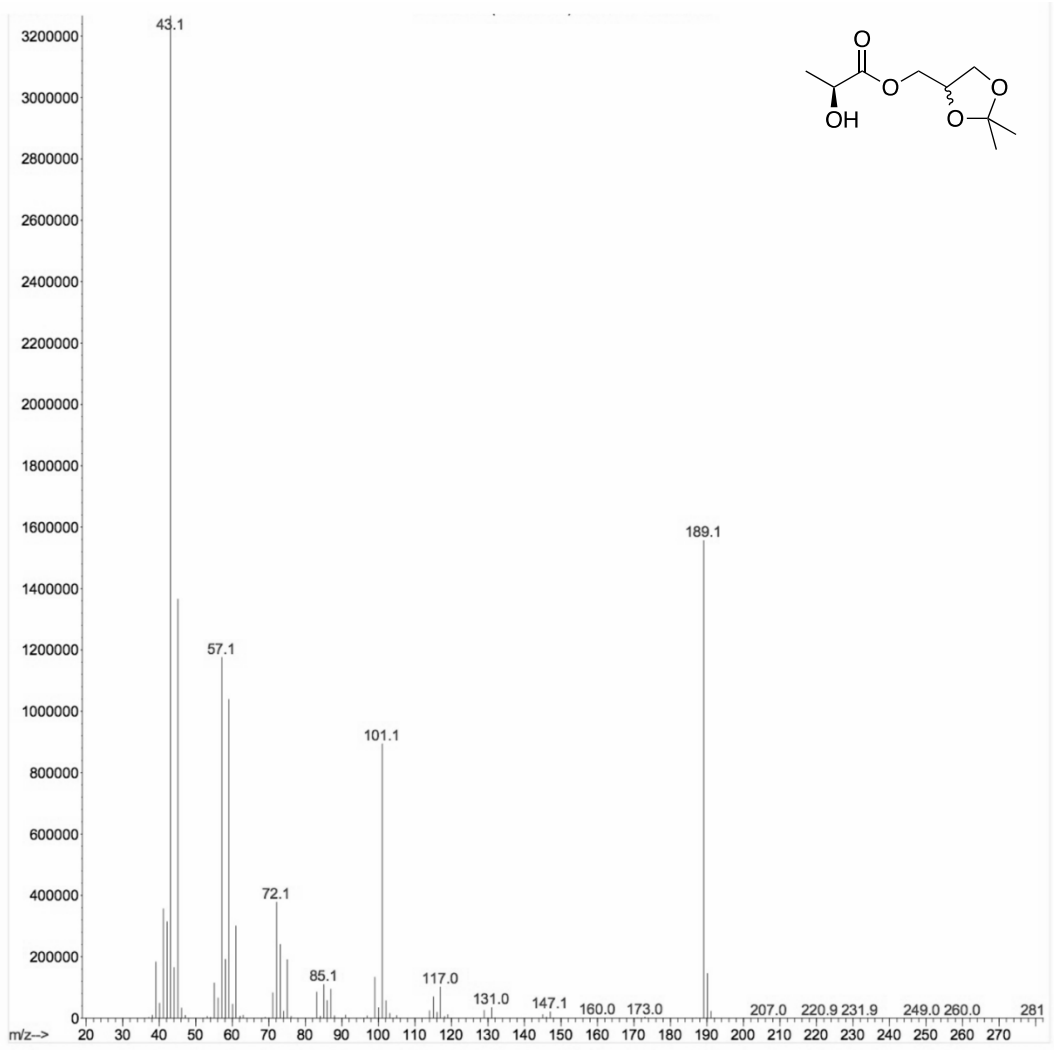

Figure A 3.13: Mass spectra of 3c (relative intensity, 70 eV) m/z: 189.00 (48); 117.00 (3); 101.00 (26); 85.00 (3); 72.00 (11); 57.00 (35); 45.00 (41); 43.00 (100)

As mentioned in the main text, the reaction of solketal with ethyl lactate produced also two by-products (B1 and B2; respectively). Although the structure of these compounds was not resolved, their GC/MS spectra clearly indicated the presence of typical fragments coming from the parent solketal (m/z: 43, 57, 85, 101). These (fragments) are highlighted within the red dashed rectangles of Figure A.3.14 and A.3.15 which report the mass spectra of B1 and B2.

By-product B1 observed in the reaction between solketal and ethyl lactate

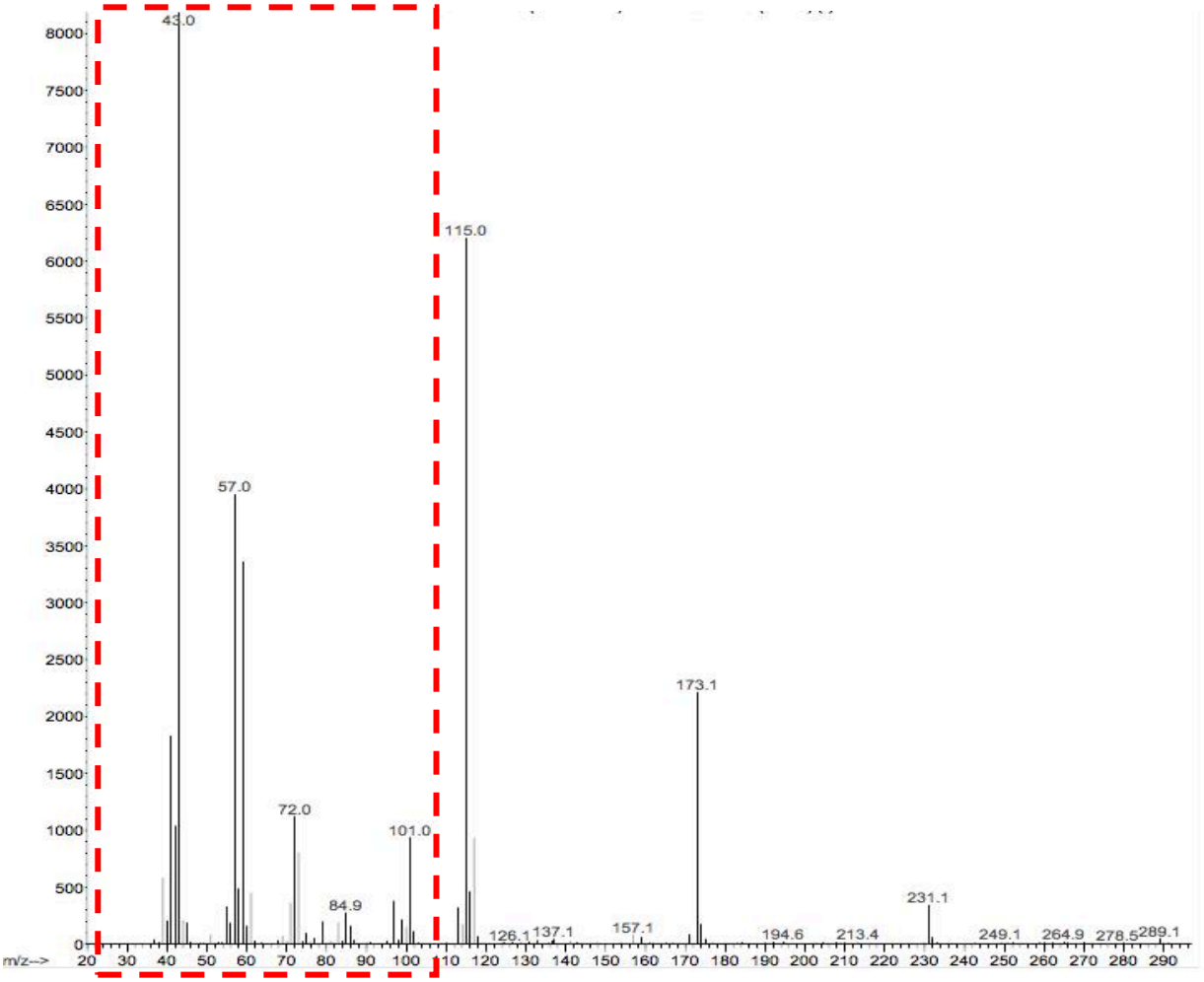

Figure A 3.14: Mass spectrum of by-product B1 (relative intensity, 70 eV): 231.00 (4); 173.00 (25); 115.00 (74); 101.00 (13); 85.00 (4); 73.00 (12); 72.00 (12); 59.00 (41); 57.00 (47); 43.00 (100); 41.00 (24). The part of the spectra highlighted in red is the typical fragmentation of solketal.

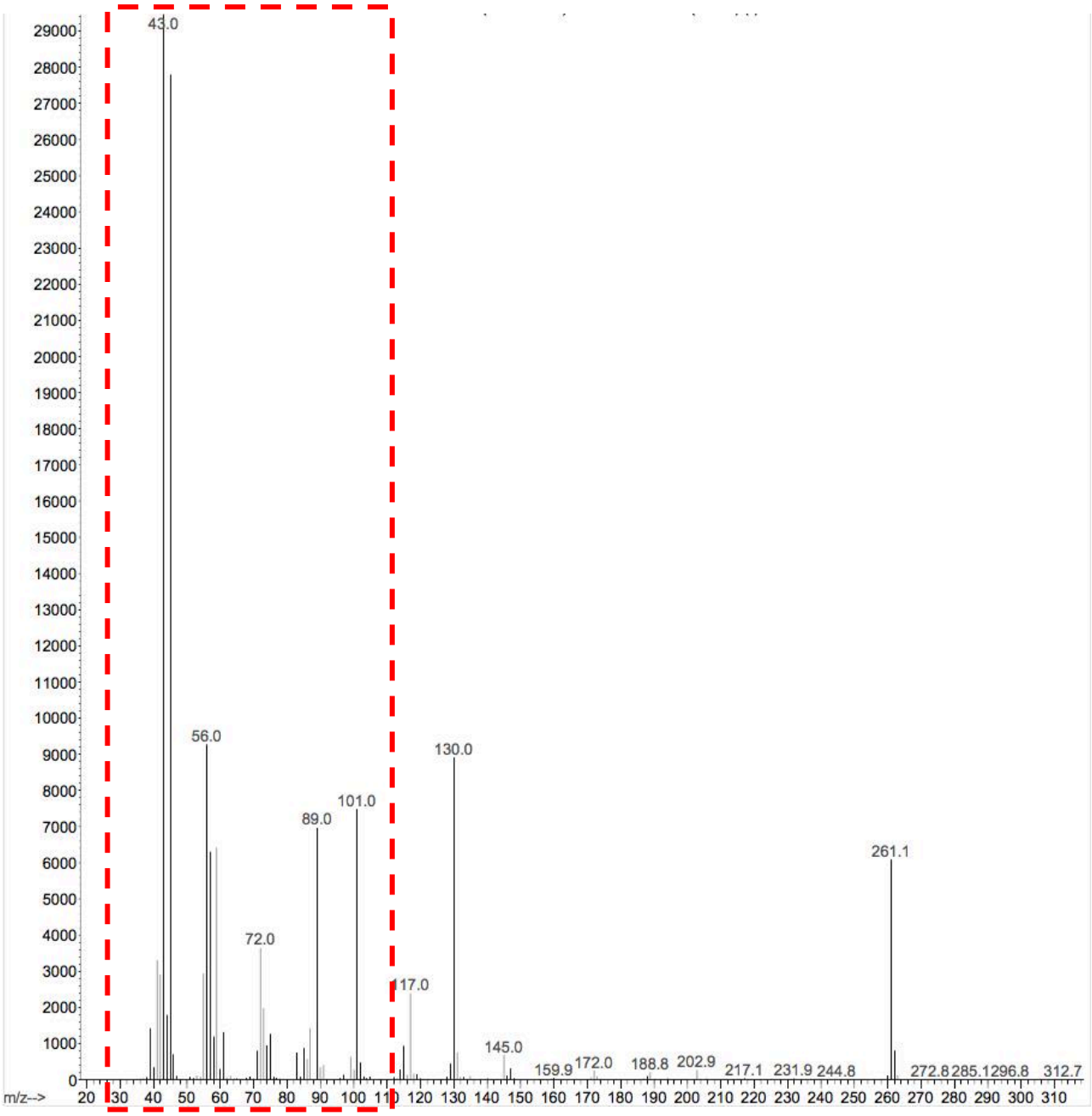

Figure A 3.15: Mass spectrum of unidentified by-product B2 (relative intensity, 70 eV): 261.00 (21); 145.00 (2); 117.00 (8); 101.00 (26); 89.00 (23); 72.00 (12); 59.00 (23); 57.00 (2); 56.00 (30); 45.00 (92); 43.00 (100); 41.00 (11). The part of the spectra highlighted in red is the typical fragmentation of solketal.

Glycerol formal acetate (**5a-a'**):

With reference to the experiment in fig. 3.5 (**220°C**), the reaction mixture was concentrated by rotary evaporation (60°C, 40 mbar). The liquid residue was purified by FCC with Petroleum ether:Ethyl acetate= 6:4 v/v. Title products were obtained in a 92% yield (530 mg, 98% purity by GC-MS) as a colorless liquid and were characterized by ^{1}H NMR, ^{13}C NMR and GC/MS.

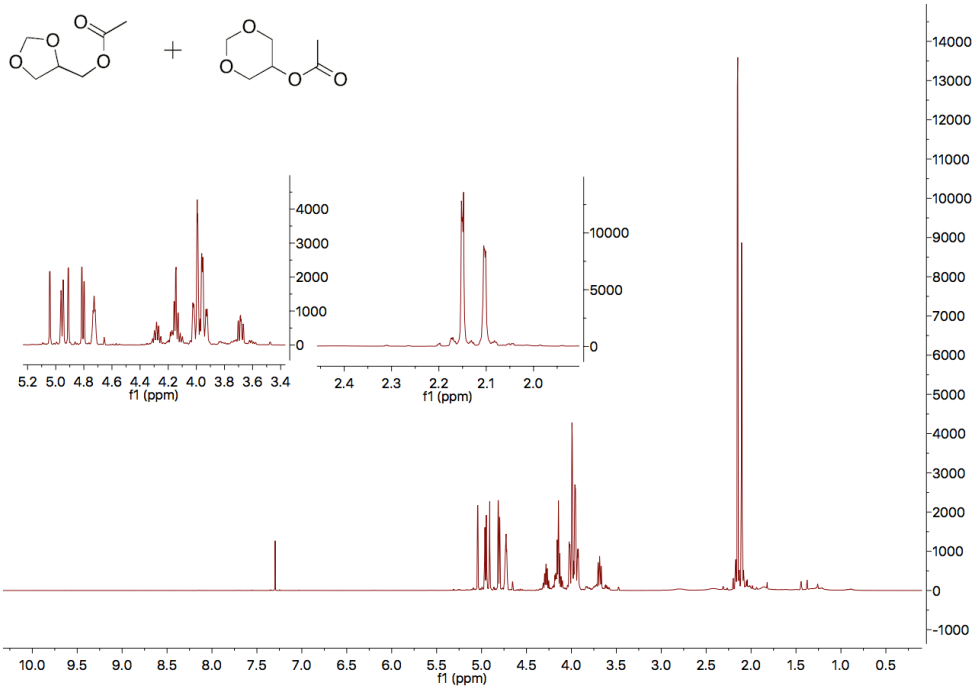

Figure A 3.16: ^{1}H NMR (400 MHz, Chloroform-d) δ 5.04 (d, J = 1.4 Hz, 1H), 4.95 (m, J = 6.2, 1.3 Hz, 1H), 4.91 (d, J = 1.3 Hz, 1H), 4.81 (m, J = 6.2, 1.3 Hz, 1H), 4.73 (m, J = 5.4, 3.5, 2.3, 1.7, 0.9 Hz, 1H), 4.34 – 4.23 (m, 1H), 4.23 – 4.04 (m, 2H), 4.04 – 3.88 (m, 5H), 3.73 – 3.61 (m, 1H), 2.17 – 2.14 (m, 3H), 2.14 – 2.07 (m, 3H).

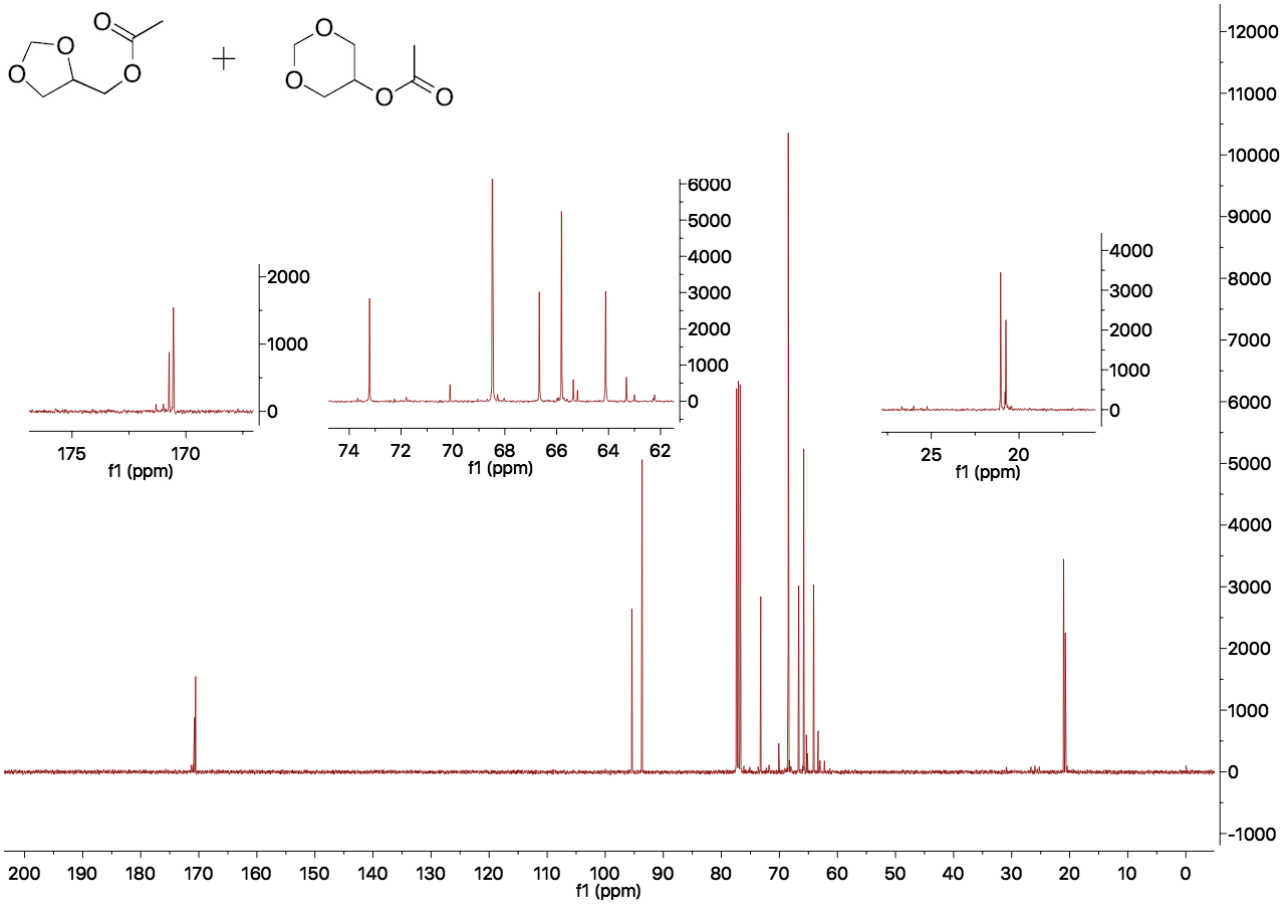

Figure A 3.17: ^{13}C NMR (101 MHz, Chloroform-d) δ 170.73, 170.55, 95.41, 93.64, 73.22, 68.48, 66.67, 65.81, 64.11, 21.05, 20.75.

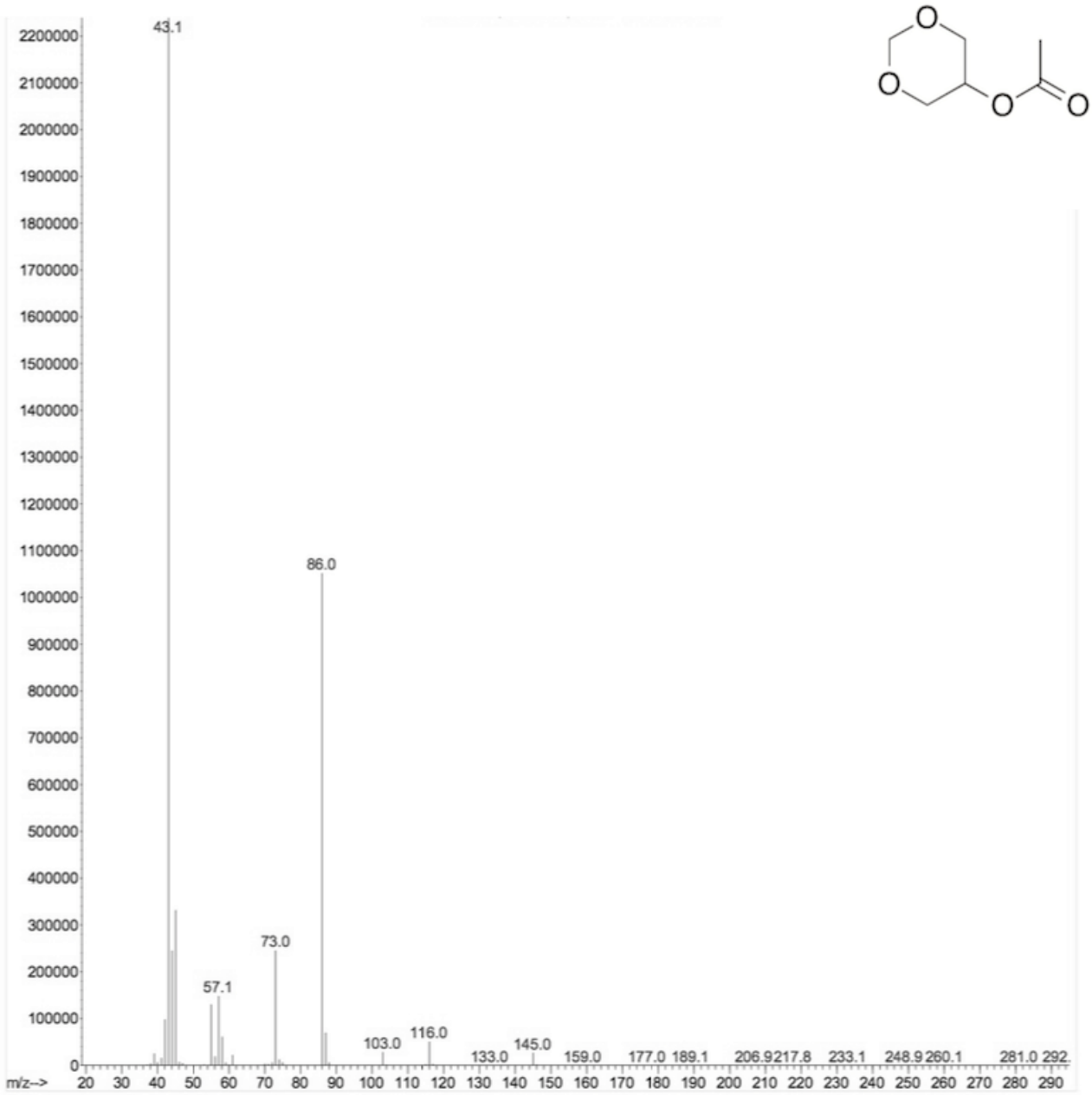

*Figure A 3.18: Mass spectra of **5a** (relative intensity, 70 eV) m/z: 145.00 ($M^{+\cdot}$,1); 116.00 (1); 86.00 (20); 73.00 (28); 57.00 (10); 55.00 (3); 45.00 (32); 43.00 (100)*

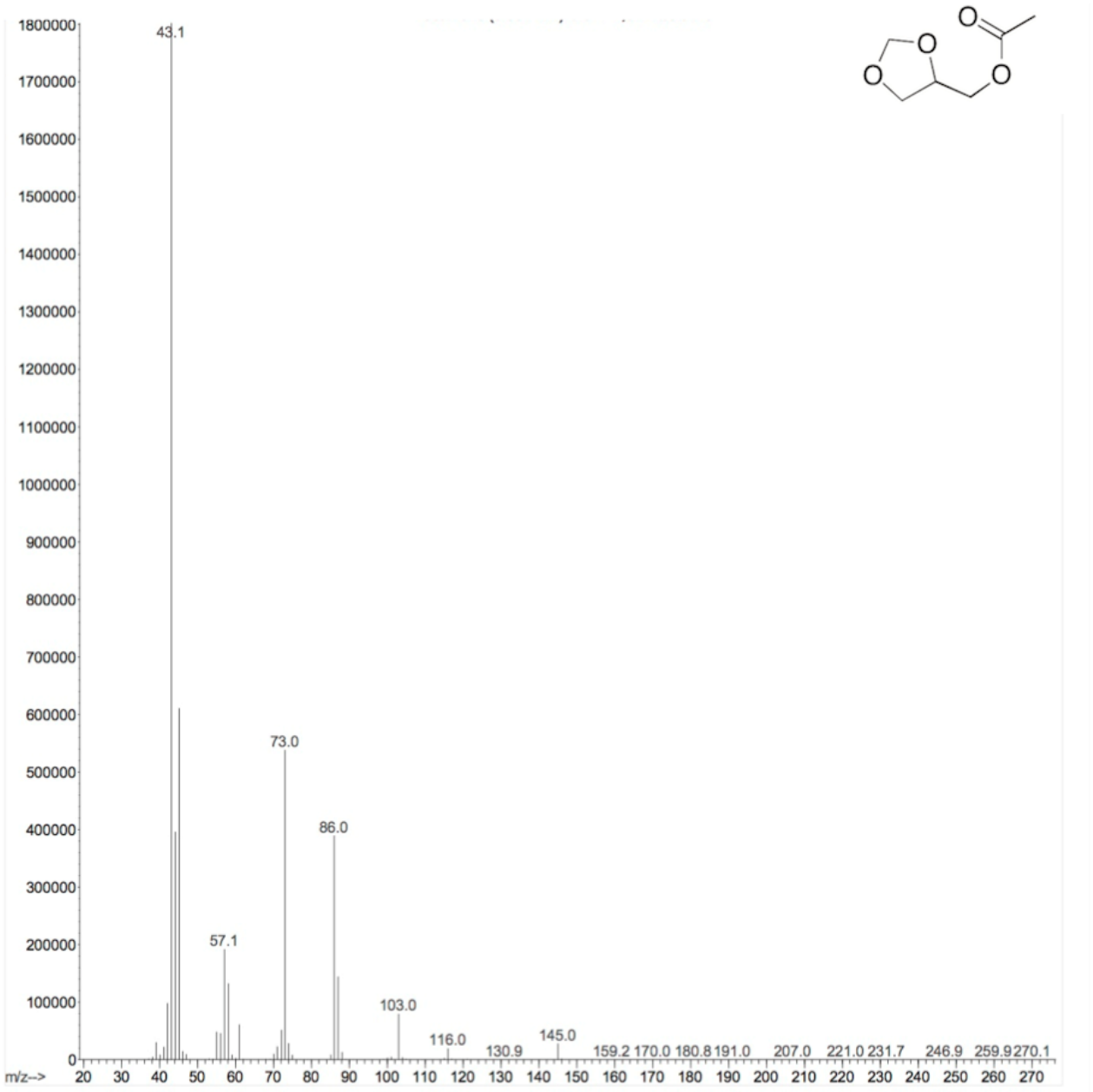

*Figure A 3.19: Mass spectra of **5a** (relative intensity, 70 eV) m/z: 145.00 (M^+,1); 116.00 (2); 86.00 (41); 73.00 (9); 57.00 (6); 45.00 (14); 43.00 (100)*

Glycerol formal formate (**6a**-**6a'**):

With reference to the experiment in scheme 3.3 (**2d**), the reaction mixture was concentrated by rotary evaporation (60°C, 40 mbar). The liquid residue was purified by FCC with Petroleum ether:Ethyl acetate= 1:1 v/v. Title products were obtained in a 45% yield (230 mg, 98% purity by GC-MS). The products appeared as a colorless liquid and were characterized by ^{1}H NMR, ^{13}C NMR and GC/MS.

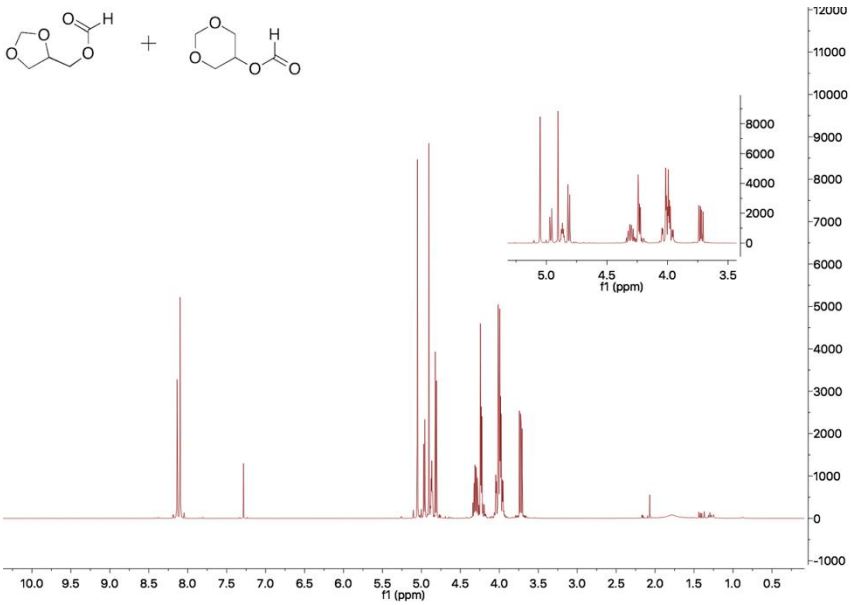

Figure A 3.20: ^{1}H NMR (400 MHz, Chloroform-d) δ 8.14 (s, J = 0.9 Hz, 1H), 8.10 (s, J = 0.9 Hz, 1H), 5.09 – 4.78 (m, 5H), 4.37 – 4.17 (m, 4H), 4.03 – 3.97 (m, 4H), 3.72 (dd, J = 8.5, 5.5 Hz, 1H).

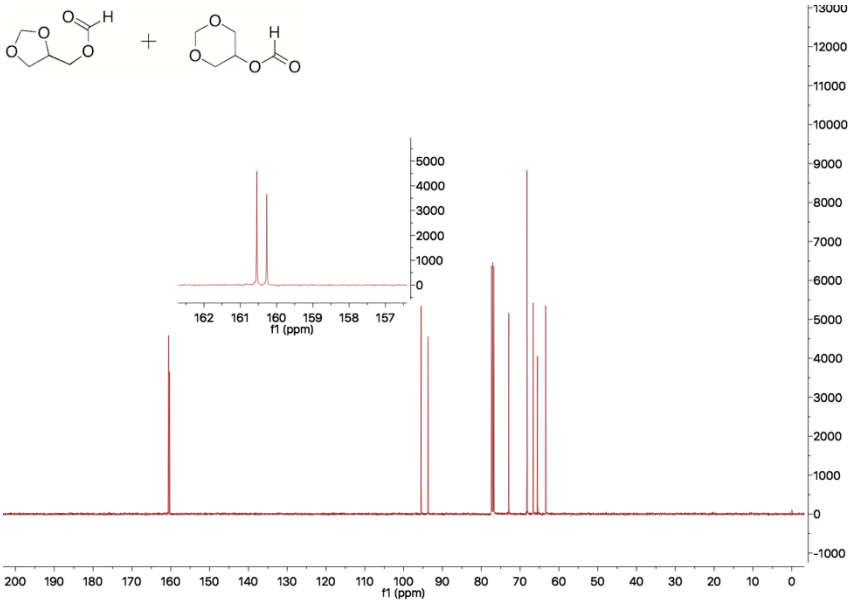

Figure A 3.21: ^{13}C NMR (101 MHz, Chloroform-d) δ 160.54, 160.27, 95.49, 93.69, 72.91, 68.24, 66.62, 65.53, 63.41.

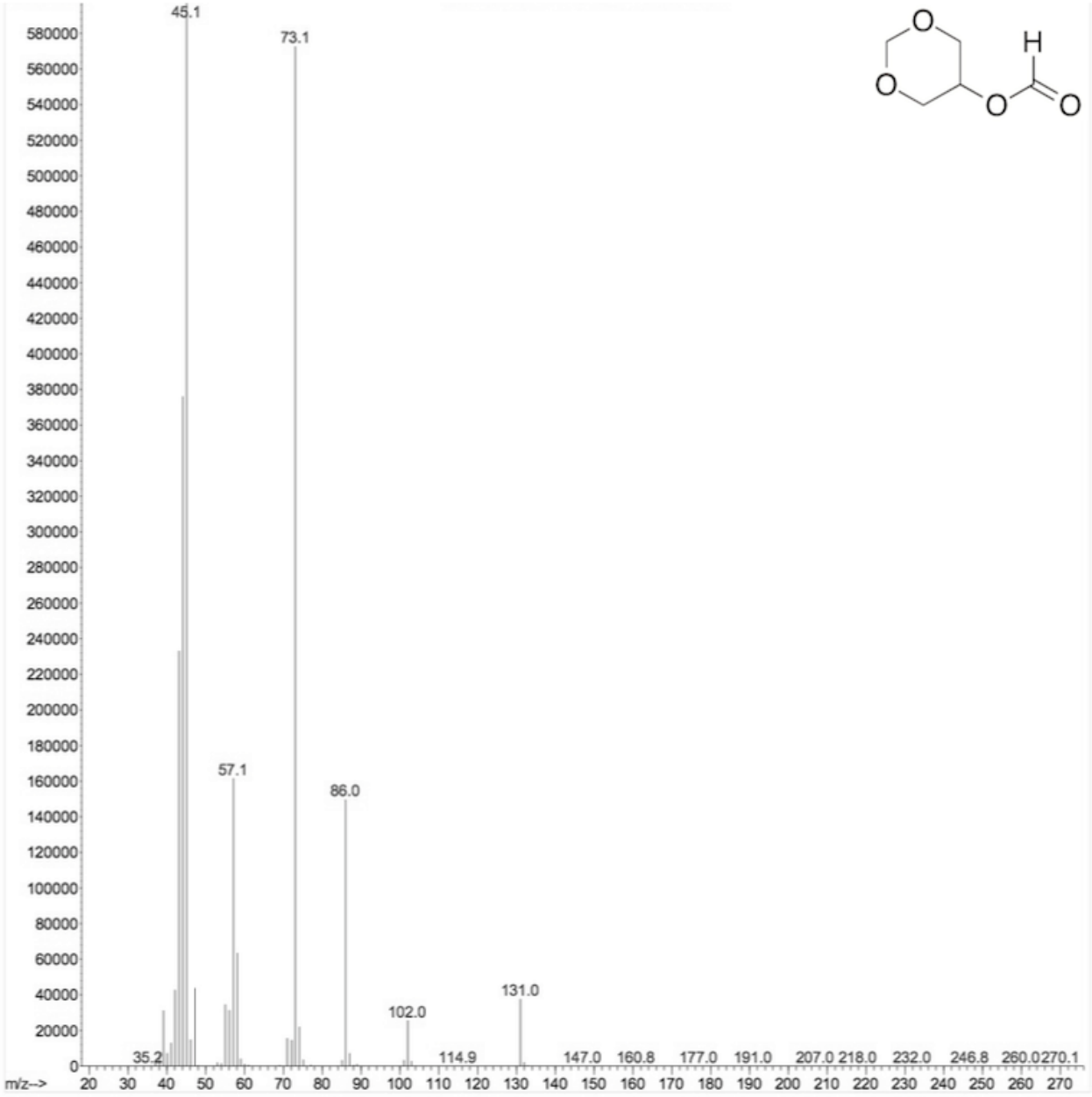

*Figure A 3.22: Mass spectra of **5a** (relative intensity, 70 eV) m/z: 131.00 (M,6); 102.00 (4); 86.00 (25); 73.00 (95); 57.00 (27); 55.00 (6); 45.00 (100); 44.00 (62); 43.00 (39)*

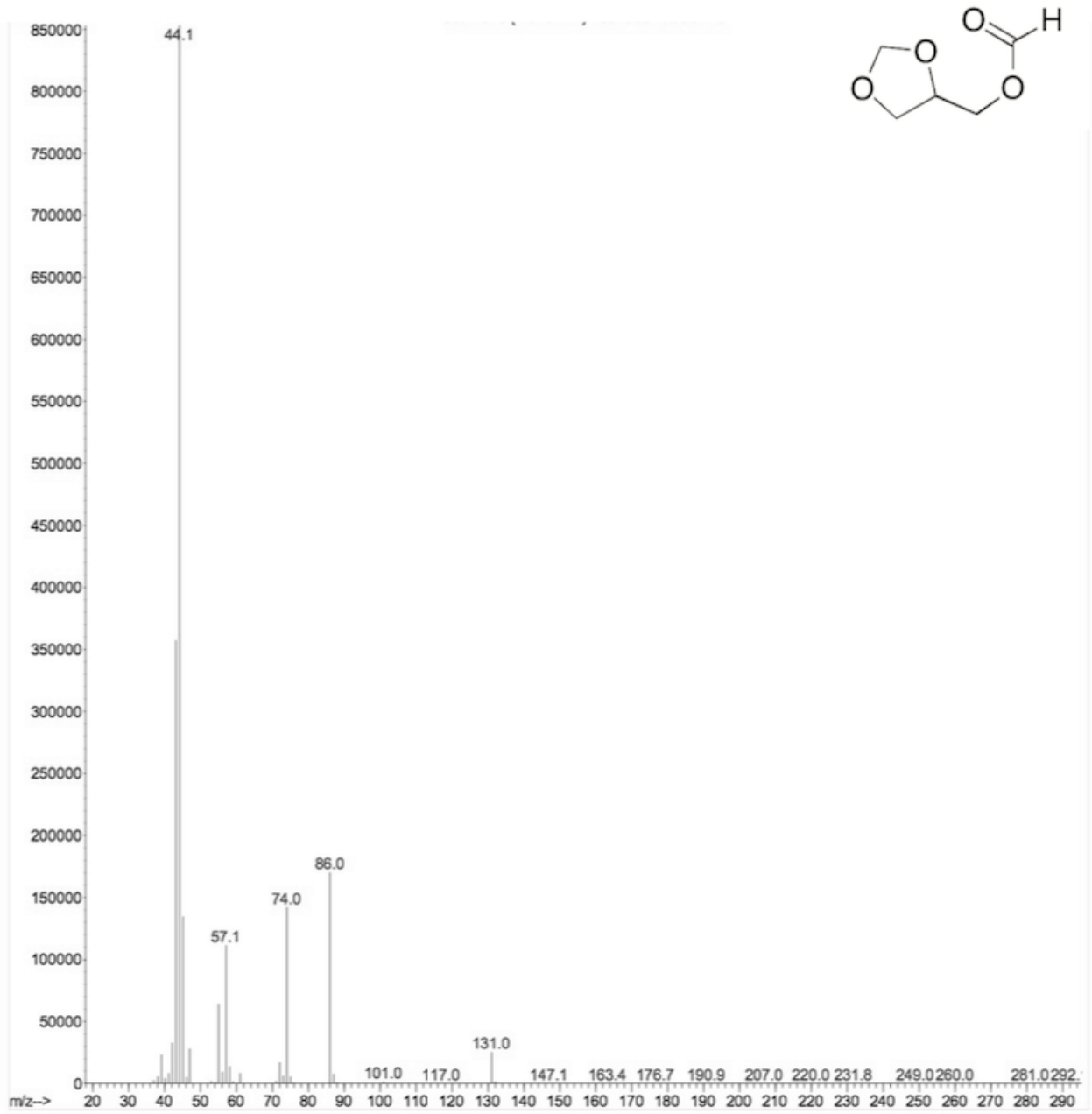

*Figure A 3.23: Mass spectra of **5a** (relative intensity, 70 eV) m/z: 131.00 (M^+,3); 86.00 (20); 74.00 (16); 57.00 (13); 44.00 (100); 43.00 (41)*

Triacetin (**8**):

With reference to the experiment in table 3.2 (entry 8), the reaction mixture was concentrated by rotary evaporation (60°C, 40 mbar). Title product was obtained in 99 % yield (1.30 g, 99% purity by GC-MS). The product appeared as a yellowish liquid and was characterized by ^{1}H NMR, ^{13}C NMR and GC/MS.

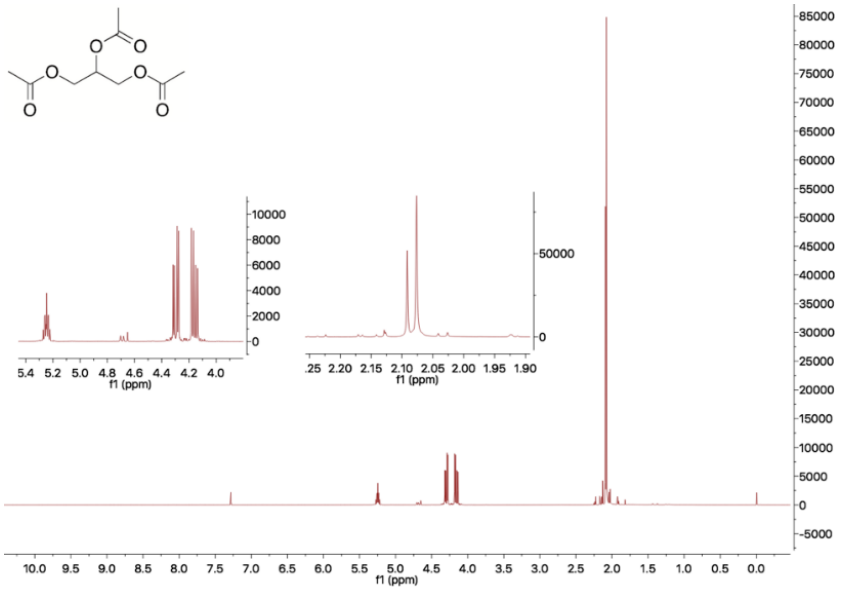

Figure A 3.24: ^{1}H NMR (400 MHz, Chloroform-d) δ 5.25 (tt, J = 5.8, 4.3 Hz, 1H), 4.30 (dd, J = 12.0, 4.3 Hz, 2H), 4.16 (dd, J = 12.0, 5.9 Hz, 2H), 2.09 (s, 3H), 2.08 (s, 6H).

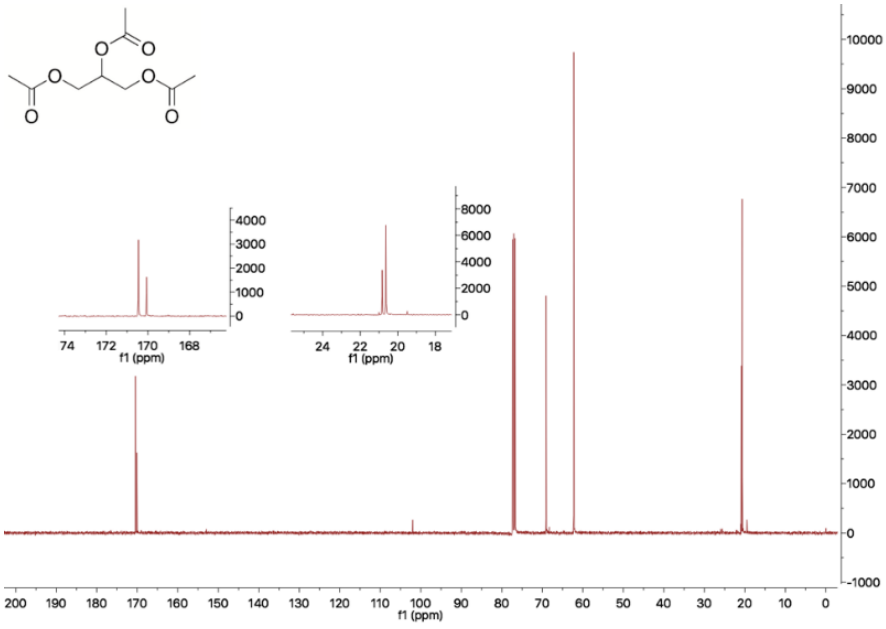

Figure A 3.25: ^{13}C NMR (101 MHz, Chloroform-d) δ 170.46, 170.07, 69.06, 62.23, 20.83, 20.63.

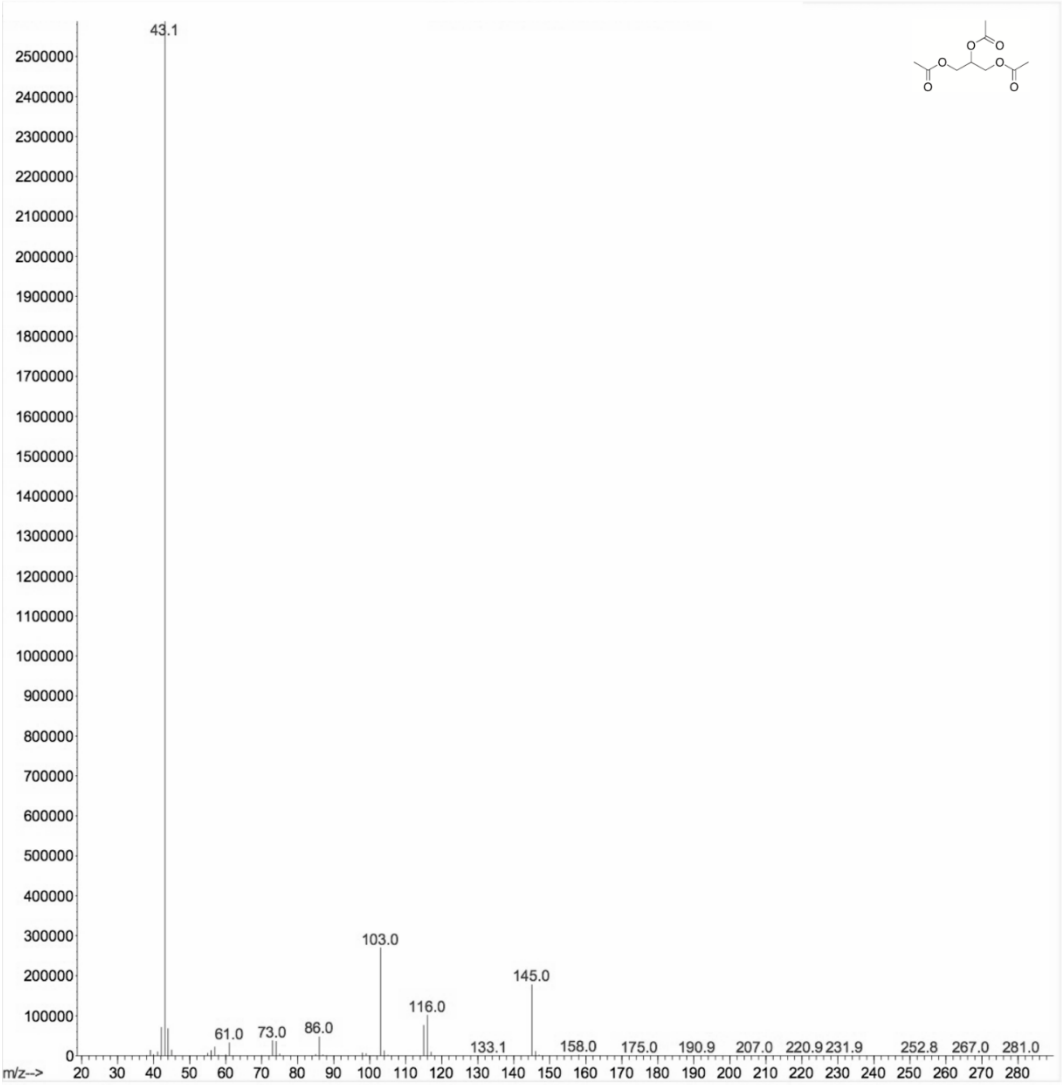

Figure A 3.26: Mass spectra of triacetin(relative intensity, 70 eV) m/z: 145.00 (18); 116.00 (10); 103.00 (24); 43.00 (100).

References

[1] Poling, E.; Prausnitz, J. M.; O'Connell, J. P. Vapor pressures and enthalpies of vaporization of pure fluids. In The Properties of Gases and Liquids, Fifth Edition, McGraw-Hill, 2004.
[2] Z. Wang, B. Wu, J. Zhu, K. Chen, W. Wang, *Fluid Phase Equilibria* **2012**, *314*, 152-155.
[3] Scholz, E.; HYDRANAL®-manual, 2012, Sigma-Aldrich Laborchemikalien GmbH, Seelze, Germany

Appendix A.3.2
Development of a catalytic tandem process for the concurrent acetylation/acetalization of glycerol

The acetylation of glycerol with AcOH in presence of Amberlyst 15 as catalyst

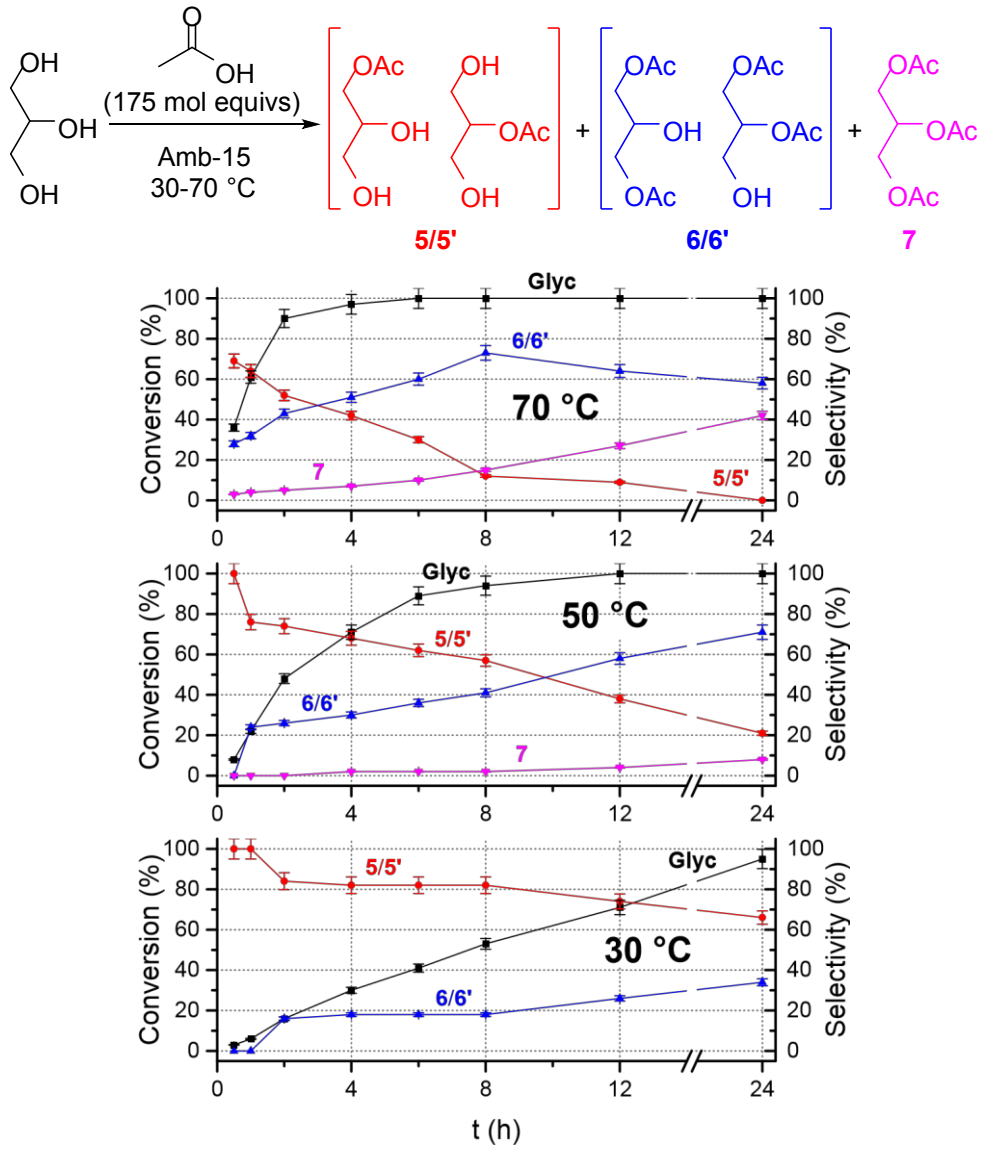

*Figure A 3.27: The reaction between glycerol and acetic acid at different temperatures of 30, 50 and 70 °C (bottom, mid, and top, respectively). Conditions: solution of glycerol (1.0 mmol) in acetic acid (10 mL, 0.1 M), Amberlyst-15 (15.0 mg; 15 wt%) as a catalyst. (-■-) Glycerol conversion; (-•-) selectivity towards monoacetin (**5/5'**); (-▲-) selectivity towards diacetin (**6/6'**); (-▼-) selectivity towards triacetin (**7**)*

Quantification of Acetic anhydride formed in situ by the reaction between Glyc, iPAc and AcOH

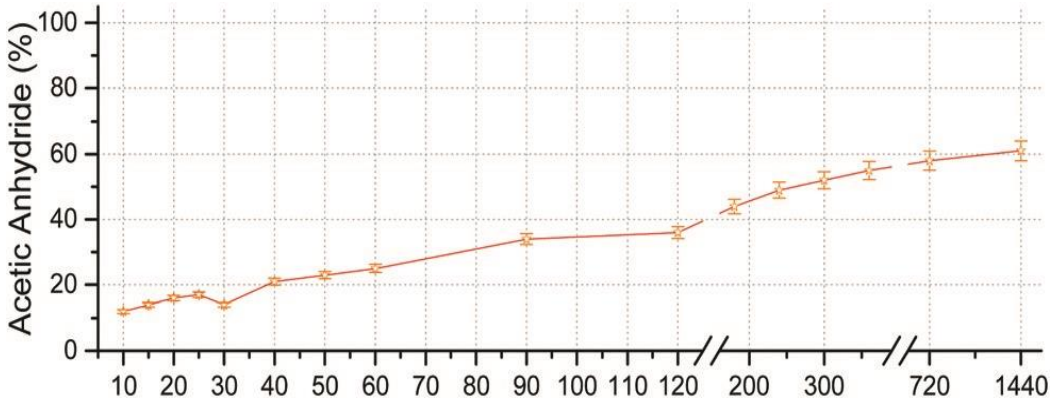

Figure A 3.28: The formation of Ac_2O during the reaction of a mixture of glycerol (1 mmol), iPAc (7.5 mmol), acetic acid (0.5 mL; 8.5 mmol), and Amberlyst-15 (15.0 mg; 15 wt%), at = 30 °C. Amount calculated as the % of acetic anhydride with respect to the moles of the other products (3, 4, 5/5', 6/6' and 7) observed during the reaction and calculate through GC analysis.

By-products formed during the reaction between iPAc and acetic acid

The mass spectra of compounds **B1-B5** are reported in Figure A.3.29-33 and were consistent with the formation of acetylacetone, and of products of the aldol condensation of acetone, both the aldol, 4-hydroxy-4-methylpentan-2-one, and the two isomers of the α,β-unsaturated carbonyl derivative, 4-methylpent-3-en-2-one and 4methylpent-4-en-2-one. In addition, the formation of 4-oxopentan-2-yl acetate was observed. Comparison with spectra of authentic compounds available from the NIST library of the GC/MS ChemStation afforded a match quality >60% in all cases.

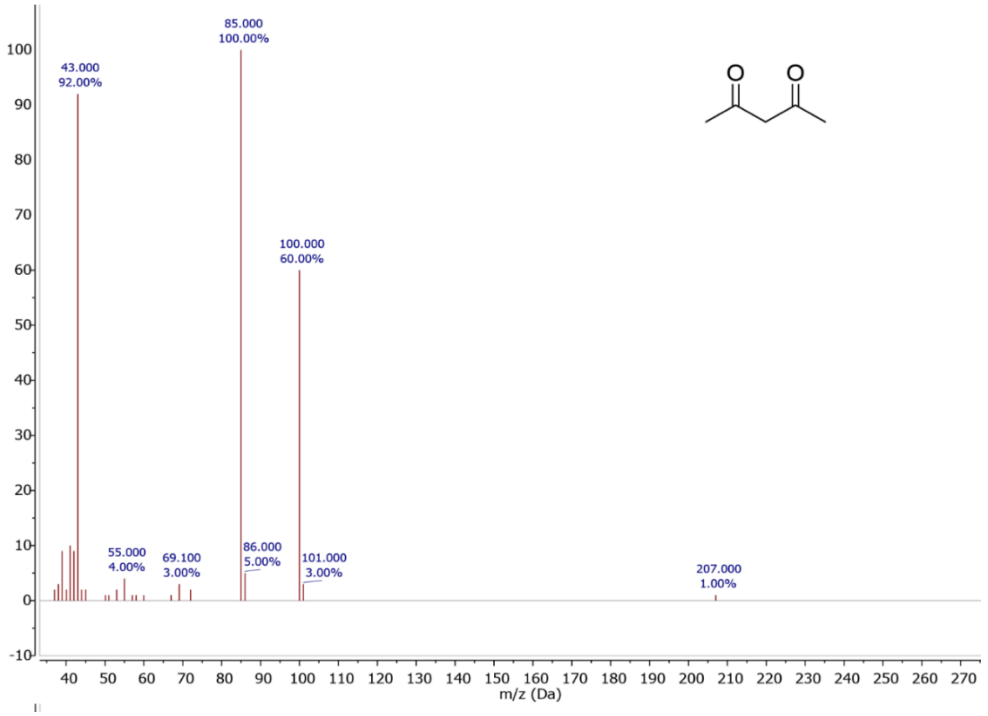

Figure A 3.29: GC-MS spectra of acetylacetone

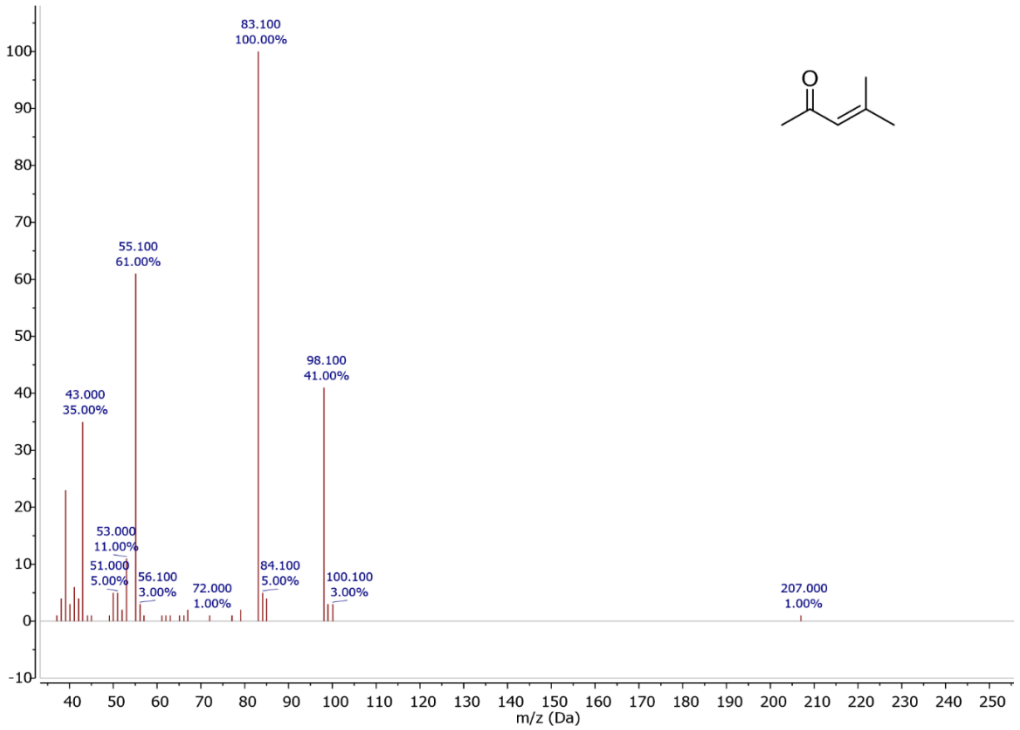

Figure A 3.30: GC-MS spectra of 4-methylpent-3-en-2-one

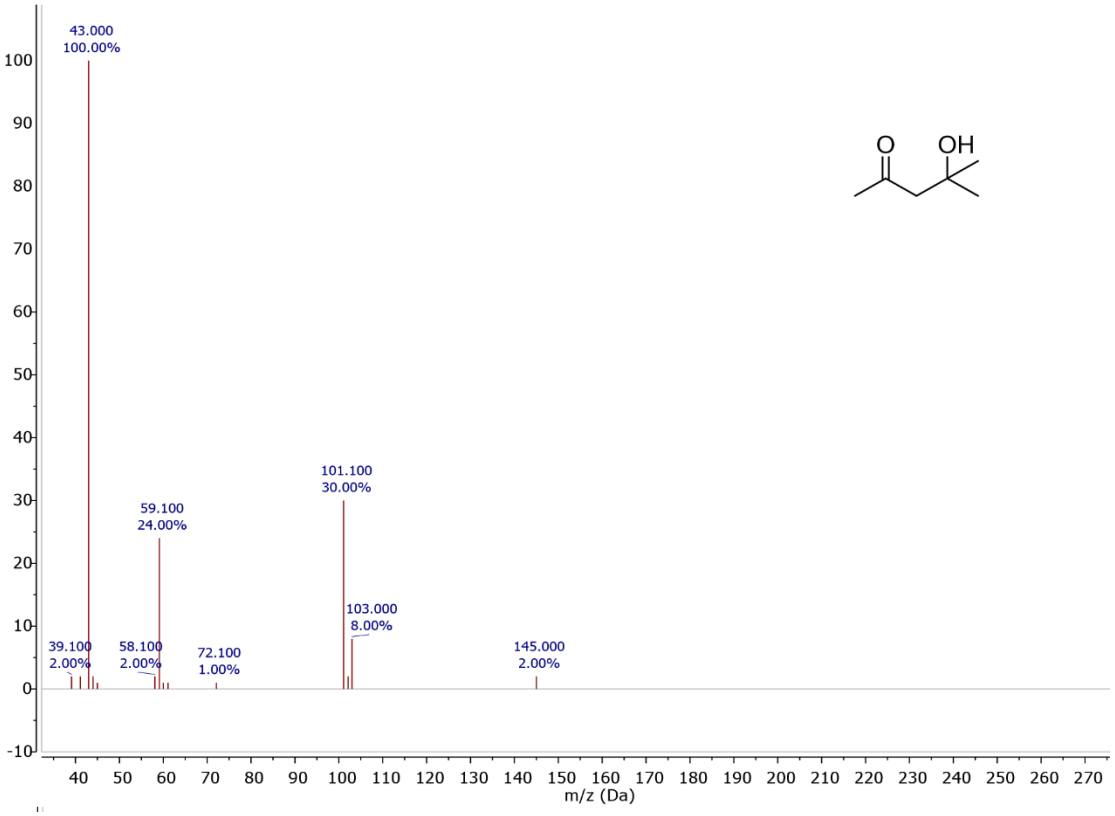

Figure A 3.31: GC-MS spectra of 4-hydroxy-4-methylpentan-2-one

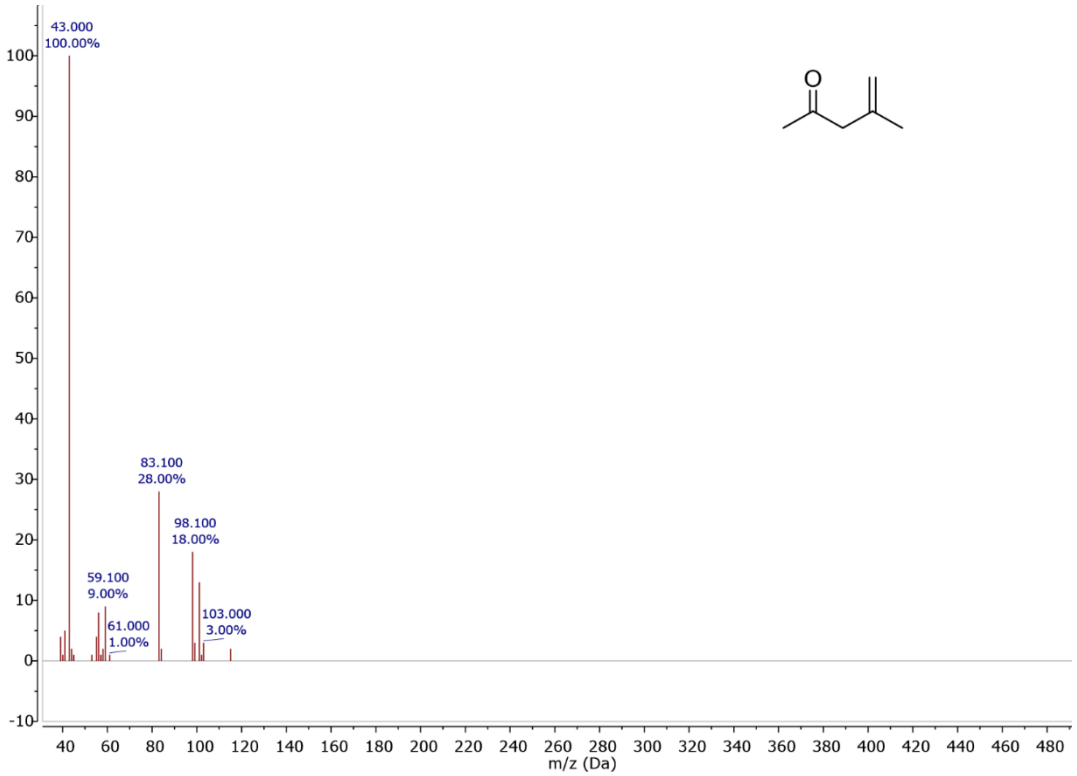

Figure A 3.32: GC-MS spectra of 4-methylpent-4-en-2-one.

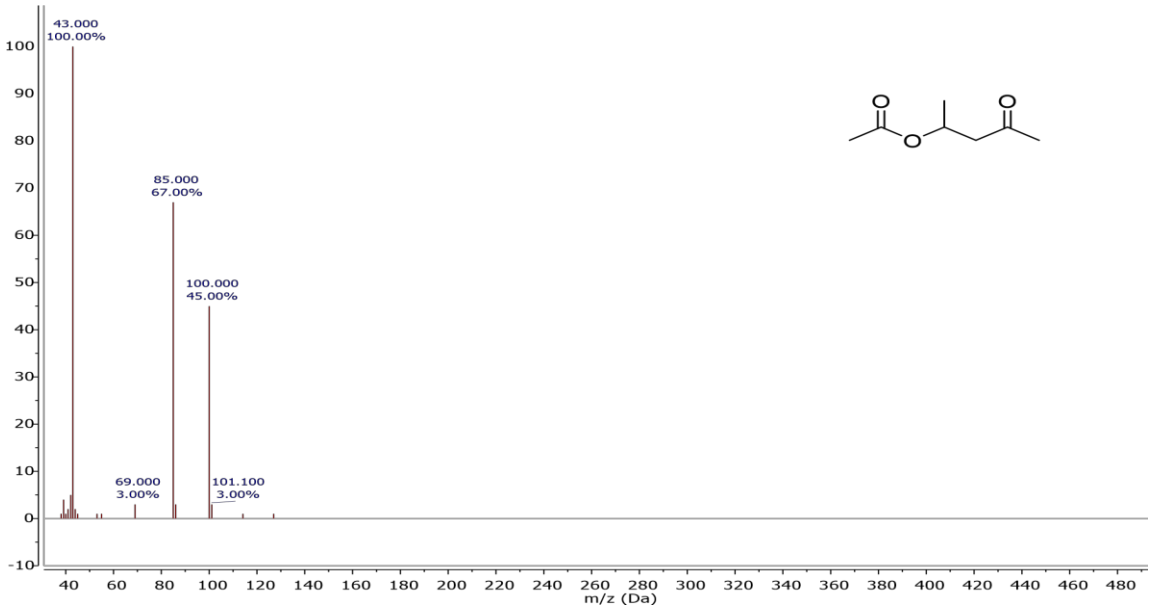

Figure A 3.33: GC-MS spectra of of 4-oxopentan-2-yl acetate.

Experiments with d_4-isotope labelled acetic acid.

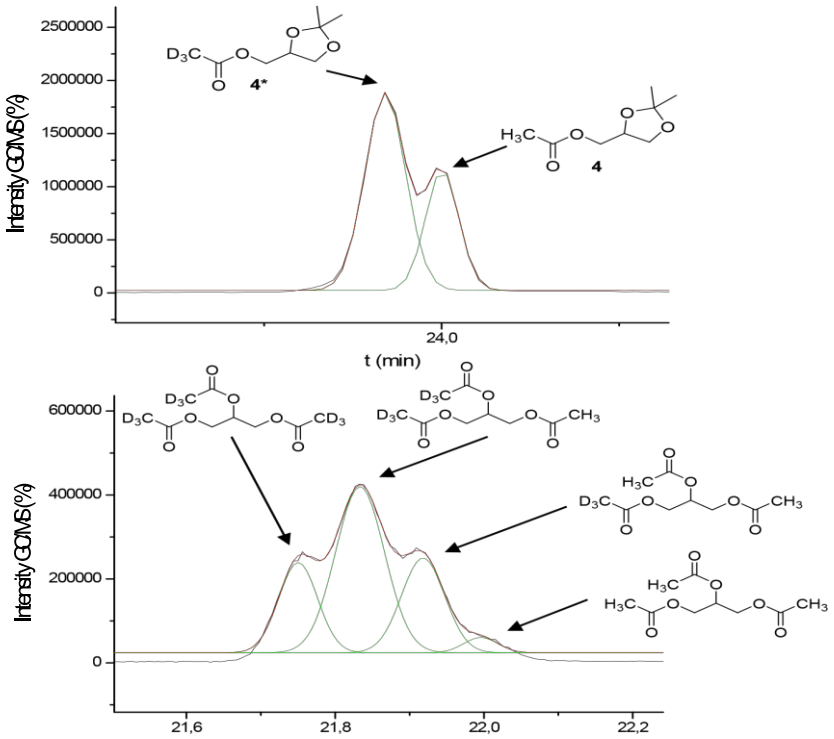

Figure A 3.34: Top: the red profile shows the GC/MS signals for solketal acetate; the corresponding d_3- and non-deuterated derivatives are indicated from left to right, respectively. Bottom: the red profile shows the GC/MS signals for triacetin; the corresponding d_9-, d_6-, d_3- and non-deuterated derivatives are indicated from left to right, respectively.

In the figure, red profiles were the authentic GC/MS analyses, while green profiles were obtained by the deconvolution of the red ones, carried out by the "Gaussian polynomial fitting" available in the OriginPro Software (ver. 9.1, Origin Lab. Corp.). Thanks to a more satisfactory resolution, signals of solketal acetate (compounds **4** and **4***, top) allowed not only a more reliable integration of the area under the corresponding peaks, but also a better reading/interpretation of GC/MS spectra, than those of different triacetins.

The investigation was then continued considering only products **4** and **4***. From deconvolution, the relative amounts of **4*** and **4** were 67% and 33%, meaning that the quantity of the tri-deuterated solketal acetate was twice as much the non-deuterated derivative. From the mass spectra recorded in the full scan (TIC, 70 eV), fragment ions at m/z = 159 and 162 were recognized as the most abundant and easily distinguishable ions for **4** and **4***, respectively (Figure A.3.35 and A.3.36).

The characteristic absence of the molecular ion peak (M^+=174 and 177 for **4** and **4***, respectively) was already noticed in a previous paper reported by us.[1] The fragment ions 159 and 162 were consistent with the loss of a methyl radical from the acetal ring (Scheme 3.1)

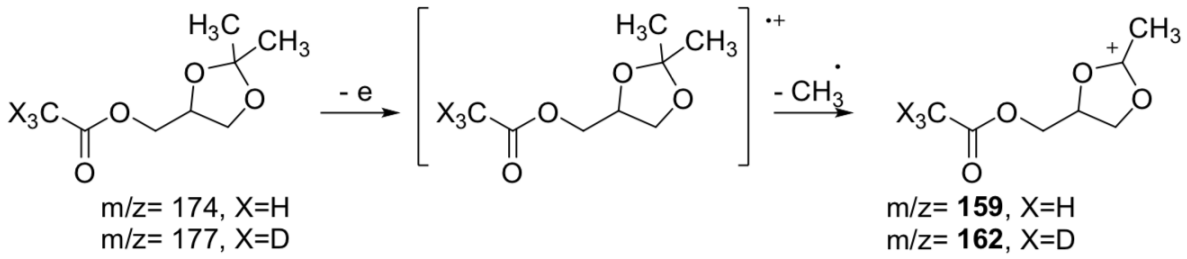

*Scheme A 3.1: Plausible fragmentation pathway for the formation of ions 159 and 162 from compounds **4** and **4***

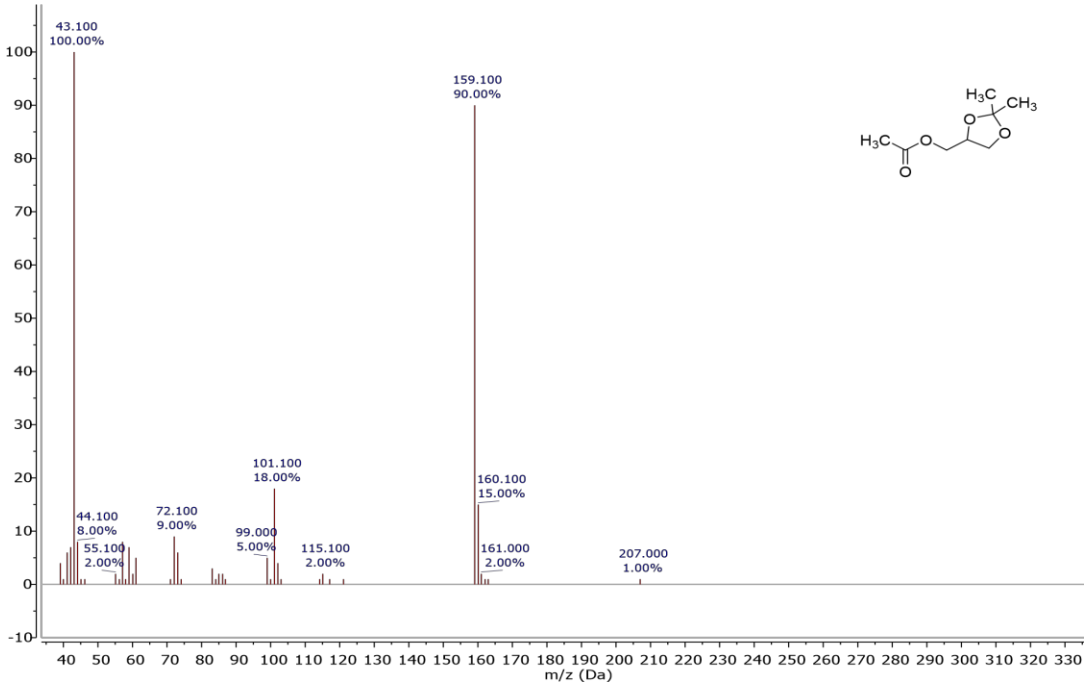

Figure A 3.35: GC-MS spectra of solketal acetate

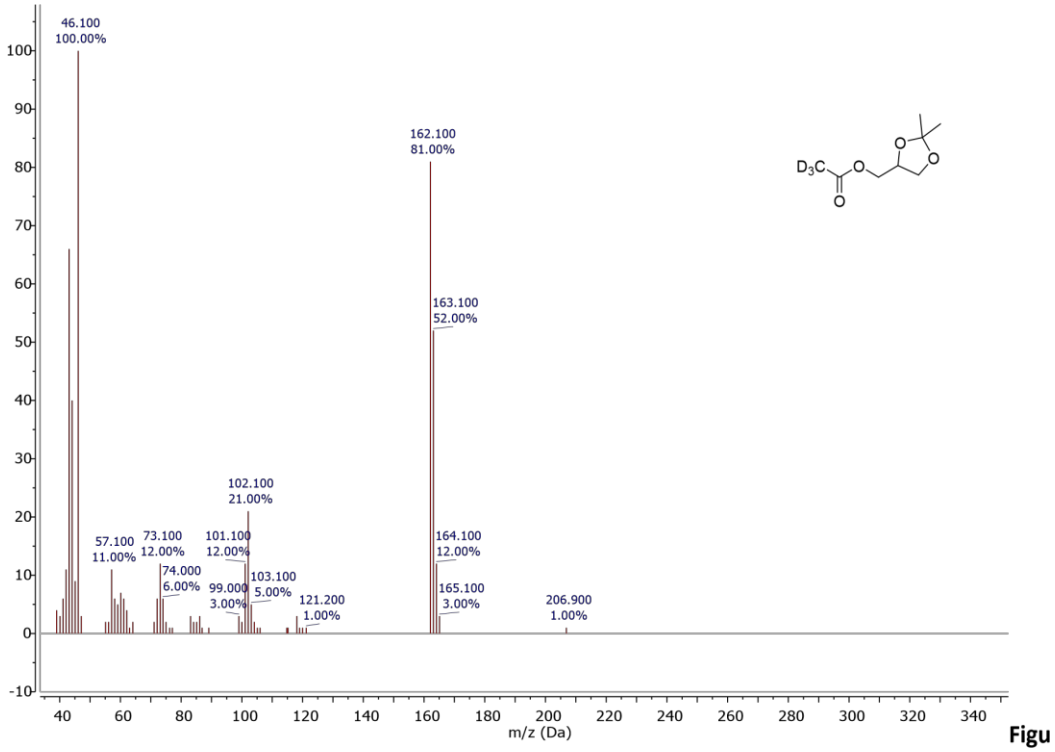

Figure A 3.36: GC-MS spectra of solketal acetate-d_3

To improve sensitivity, mass spectra were then acquired in the SIM mode on the characteristic fragment ions m/z = 159 and 162 (70 eV) (Figure A.3.37).

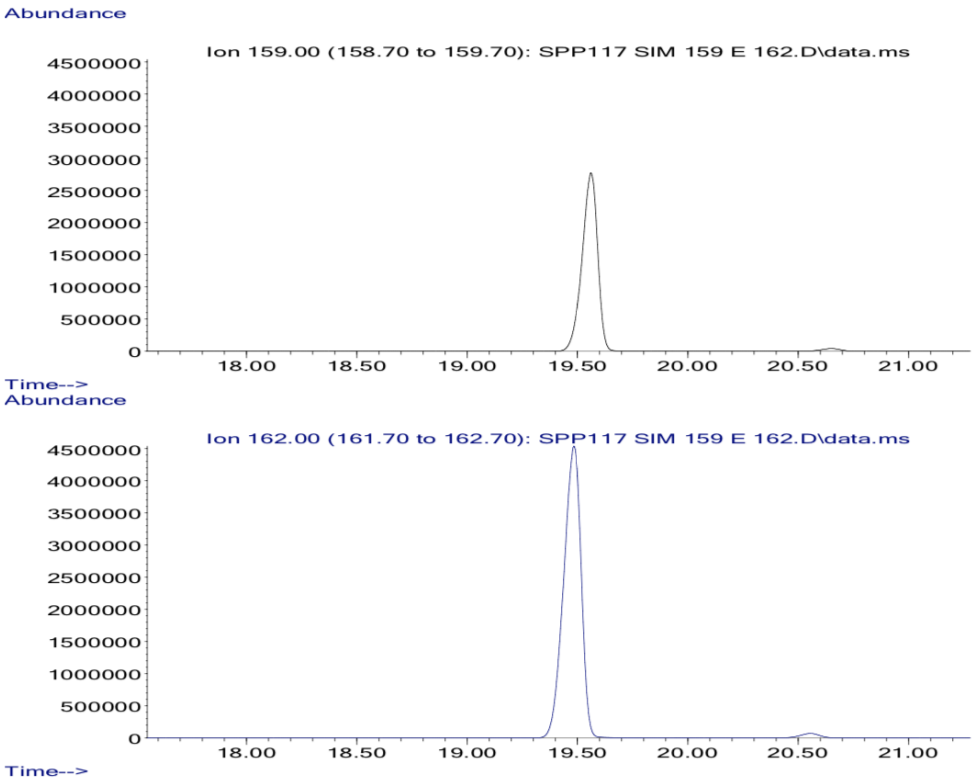

*Figure A 3.37: SIM chromatograms of selected fragment ions m/z = 159 and 162 for products **4** (top) and **4*** (bottom), respectively.*

The GC/MS analysis of the same reaction mixture also indicated the formation of three species of acetic anhydride, i.e. the non-, the tri-, and hexa-deuterated products (Figure A.3.38).

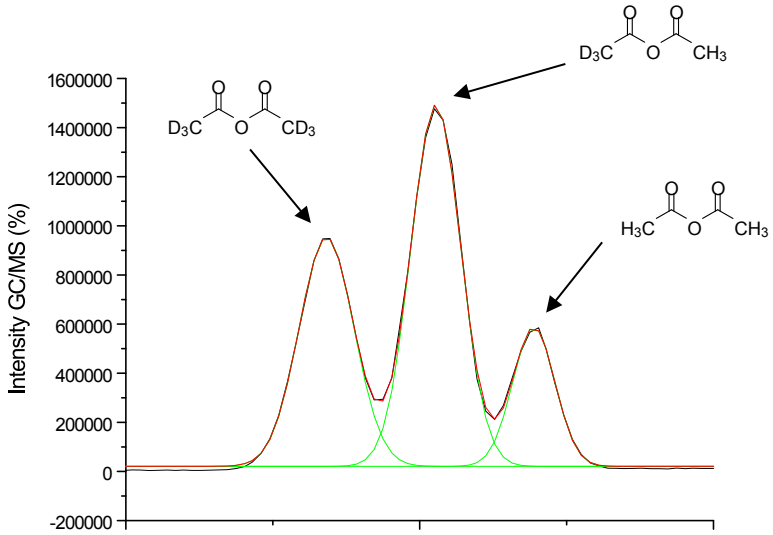

Figure A 3.38: The red profile shows the GC/MS signals for acetic anhydride: the corresponding d_6-, d_3-, and non-deuterated derivatives are indicated from left to right, respectively. The green profile represents the deconvolution of the red profiles carried out by the "Gaussian polynomial fitting" available in the OriginPro Software (ver. 9.1).

From deconvolution (green profile), the integration of the area under the corresponding peaks allowed to estimate that non-deuterated, d_3- and d_6- species of acetic anhydride were present in a 1:3:2 ratio, respectively.

The reaction of glycerol with AcOH and acetone.

Table A 3.2: The reaction of glycerol with acetone and acetic acid

Entry	Glyc:Acetone:AcOH[a] (mol:mol:mol)	Conversion[b] (%)	Selectivity[c] (%)				
			3/3'	4/4'	5/5'	6/6'	7
1	1:1:1	70	56	12	30	2	-
2	1:1:10	95	8	15	51	25	1
3	1:3:10	96	33	26	33	7	-
4	1:5:10	≥99	48	32	15	5	-
5	1:20:5	≥99	95	5	-	-	-
6	1:20:2.5	≥99	97	3	-	-	-

Conditions: glycerol (1.0 mmol), Acetic acid (1.0–10.0 eq), acetone (1-20 eq.), Amberlyst-15 (15.0 mg; 15 wt%), 30 °C, 24 h. [a] Molar ratio of the reactants. [b] Conversion of glycerol, by GC. [c] Products selectivity (by GC) calculated as described in the main text

The reaction with d_6-acetone.

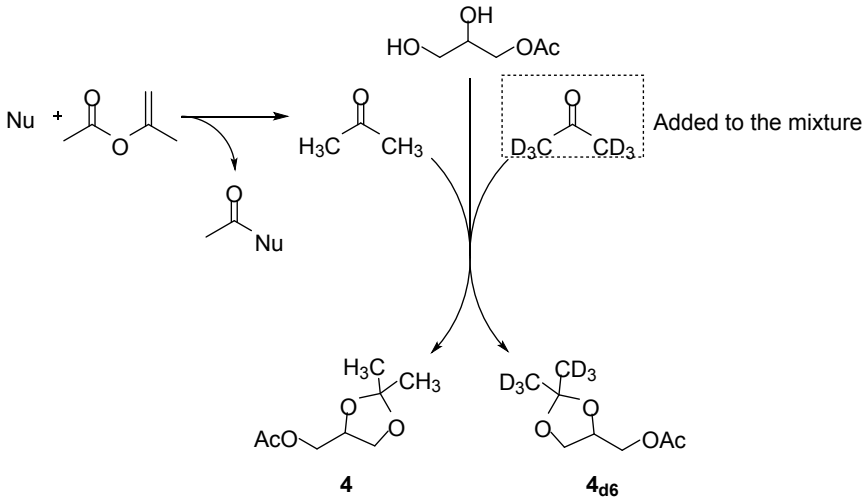

Scheme A 3.2: Pathways for the formation the non-deuterated and the d_6- solketal acetate (4 and 4_{d6}, respectively)

The acetylation of any nucleophilic species available in the reaction environment (Nu: glycerol, mono- or di-acetins) by iPAc, releases acetone (CH_3COCH_3) which competitively reacts with d_6-acetone (CD_3COCD_3, added to the mixture) for the acetalization of glycerol, affording the nondeuterated 4 and the d_6- solketal acetate 4_{d6}, respectively).

GC/MS analyses recorded in the full scan (TIC, 70 eV) allowed to identify fragment ions at m/z = 159 and 162 as the most abundant and easily distinguishable ions for 4 and 4_{d6}, respectively.

In analogy to Scheme A.3.1, the fragment ions 159 and 162 were consistent with the loss of a methyl radical from the acetal ring (Scheme A.3.3).

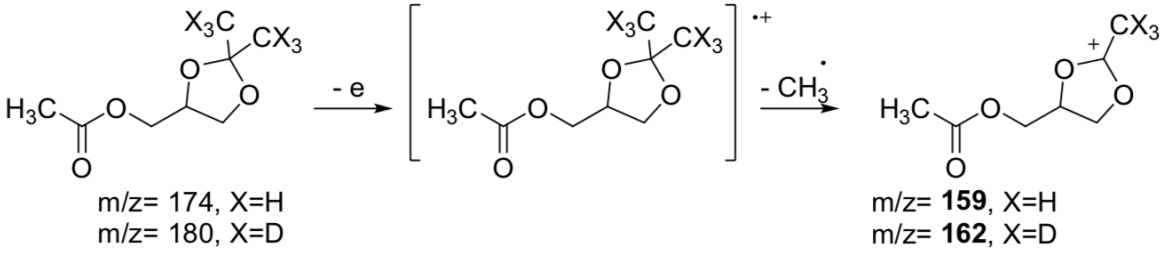

Scheme A 3.3: Plausible fragmentation pathway for the formation of ions 159 and 162 from compounds 4 and 4_{d6}

Although ions with m/z = 159 and 162 were the same selected when labelled acetic acid was used, the analysis of mass spectra proved that compound 4* bearing the isotopic marking on the acetyl group underwent a different fragmentation pathway with respect to compound 4_{d6} where the marking was on the methyl group of the acetal ring. The comparison of Figure A.3.36 and Figure A.3.39 highlights this difference. The characteristic fragment ions for 4* were 162 (81), 102 (21), 73 (12), 57 (11), 46 (100), 43 (66), while those for 4_{d6} were 162 (100), 107 (30), 76 (18), 65 (12), 46 (88), 43 (86).

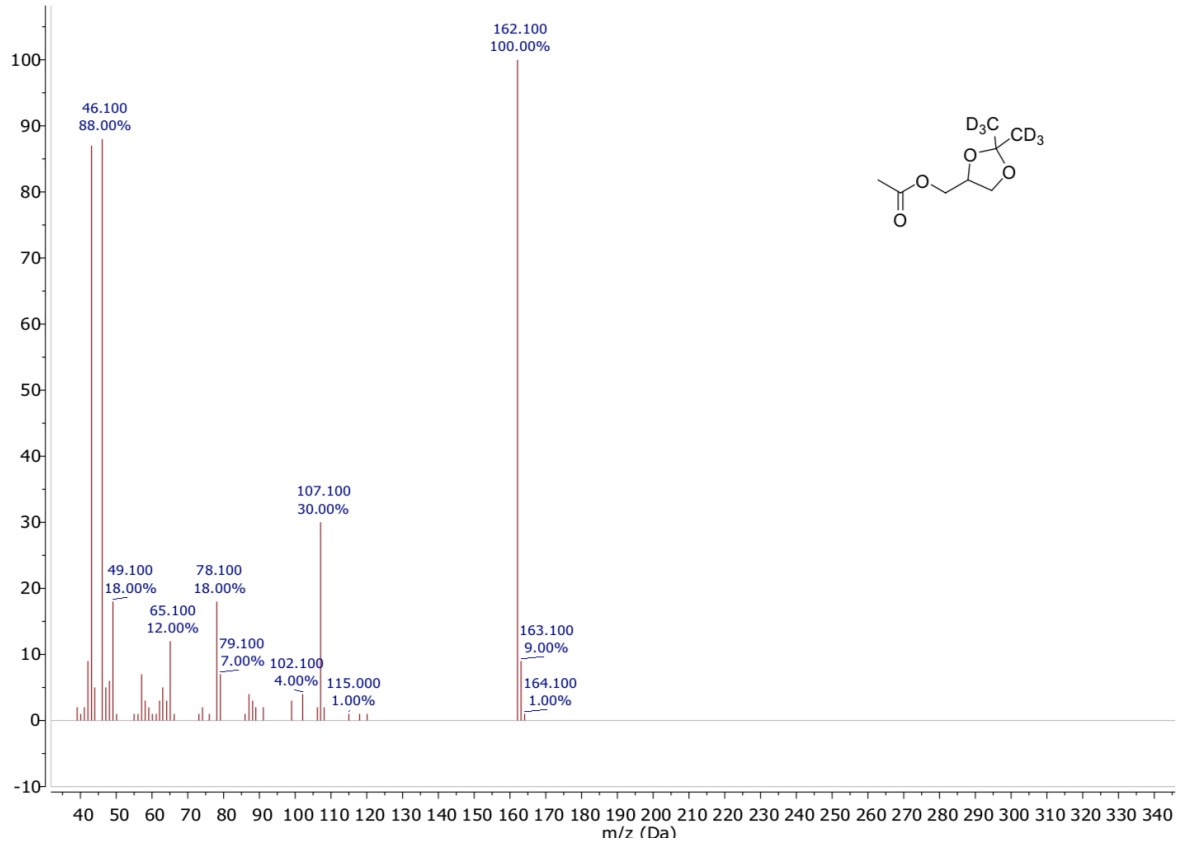

*Figure A 3.39: Mass spectra of product **4**$_{d6}$. For the comparison with mass spectra of product **4** see Figure A 3.35*

Mass spectra were then acquired in the SIM mode on the fragment ions m/z = 159 and 162 for compounds **4** and **4**$_{d6}$, respectively. Integration of signals in the SIM chromatograms proved that relative areas under the peaks of target ions 159 and 162 were 65% and 35%, respectively, thereby confirming that the parent compounds **4**$_{d6}$ and **4** were formed in a ratio of about 2:1.

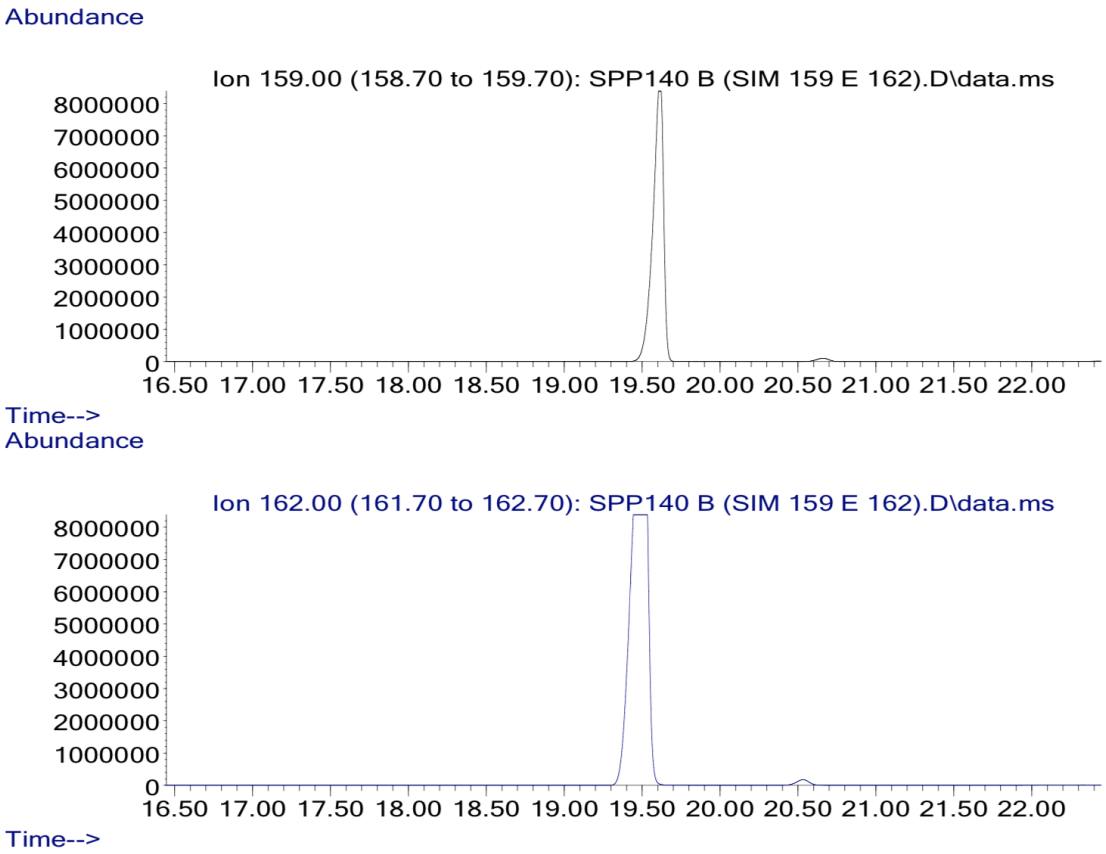

*Figure A 3.40: SIM chromatograms of fragment ions m/z = 159 and 162 from products **4** and **4**$_{d6}$, respectively.*

Appendix A.3.3
Reaction of Glycerol with Trimethylorthoester: Towards the Synthesis of New Glycerol Derivatives

Synthesis/Isolation of reaction products

(2-methoxy-1,3-dioxolan-4-yl)methanol (1).

The isomer identified as **1a** was isolated by distillation over potassium carbonate, as reported in Materials and Methods. The characterization of the isomer **1b** were derived by both GC-MS and by NMR by subtracting the known peaks of **1a** to the spectra ofthe mixture **1a-1b**. Hereafter, the GC/MS spectra of **1a** (Figure A.3.41) or **1b** (Figure A.3.47) and the ^{1}H, ^{13}C, HSQC, HMBC and COSY NMR of both **1a** (Figure A.3.42-46) and the mixture **1a-1b** (Figure A.3.48-52) are reported.

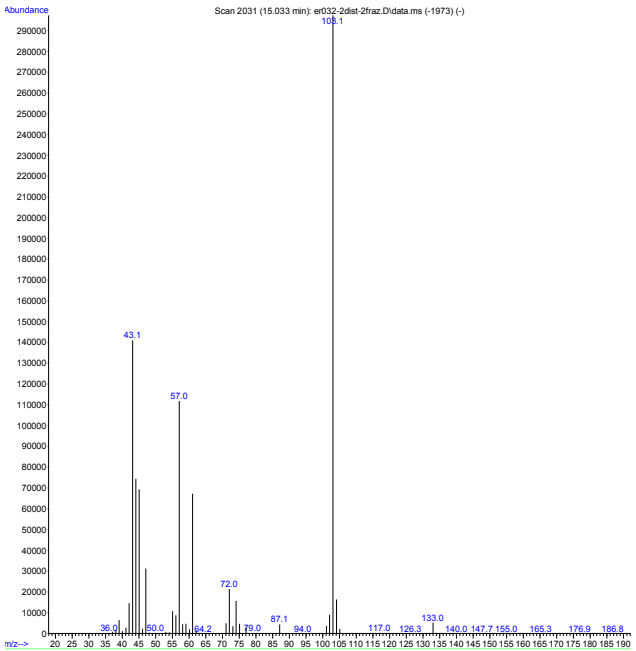

*Figure A 3.41: MS spectra of **1a:** 134 (M^{+},0);133 (1); 103 (100); 61 (31); 57 (46); 47 (15); 45(32); 44 (31); 43 (65).*

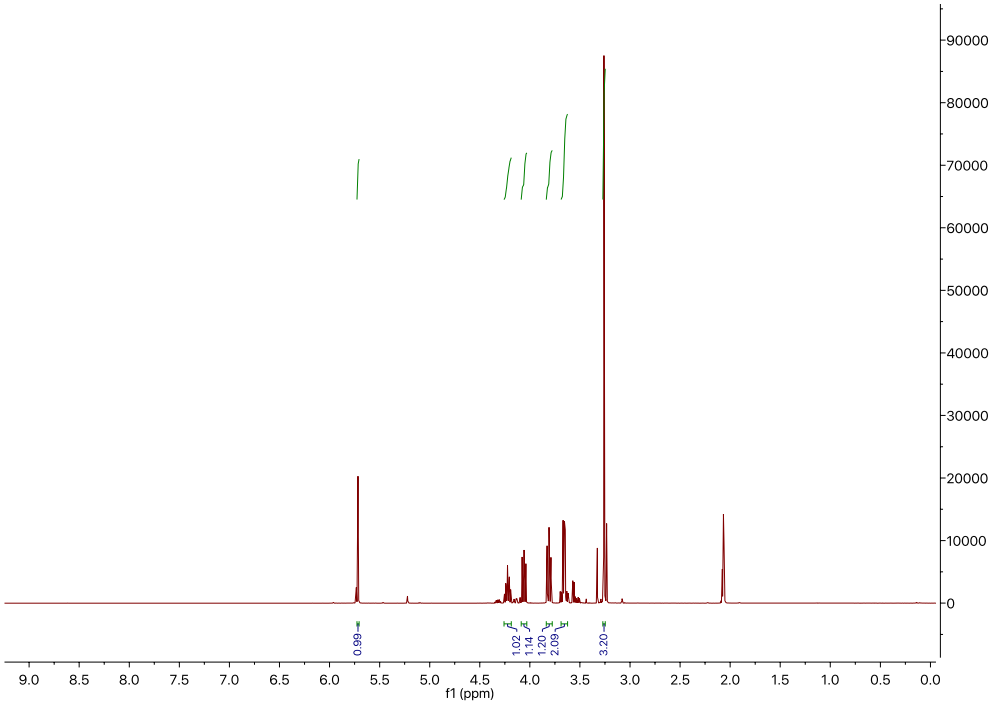

*Figure A 3.42: ^{1}H NMR of **1a** (400 MHz, Acetone-d_6): δ = 5.72 (s, 1H), 4.22 (tt, J=7.2, 5.2, 1H), 4.09 – 4.03 (m, 1H), 3.84 – 3.78 (m, 1H), 3.69 – 3.62 (m, 2H), 3.26 (s, 3H).*

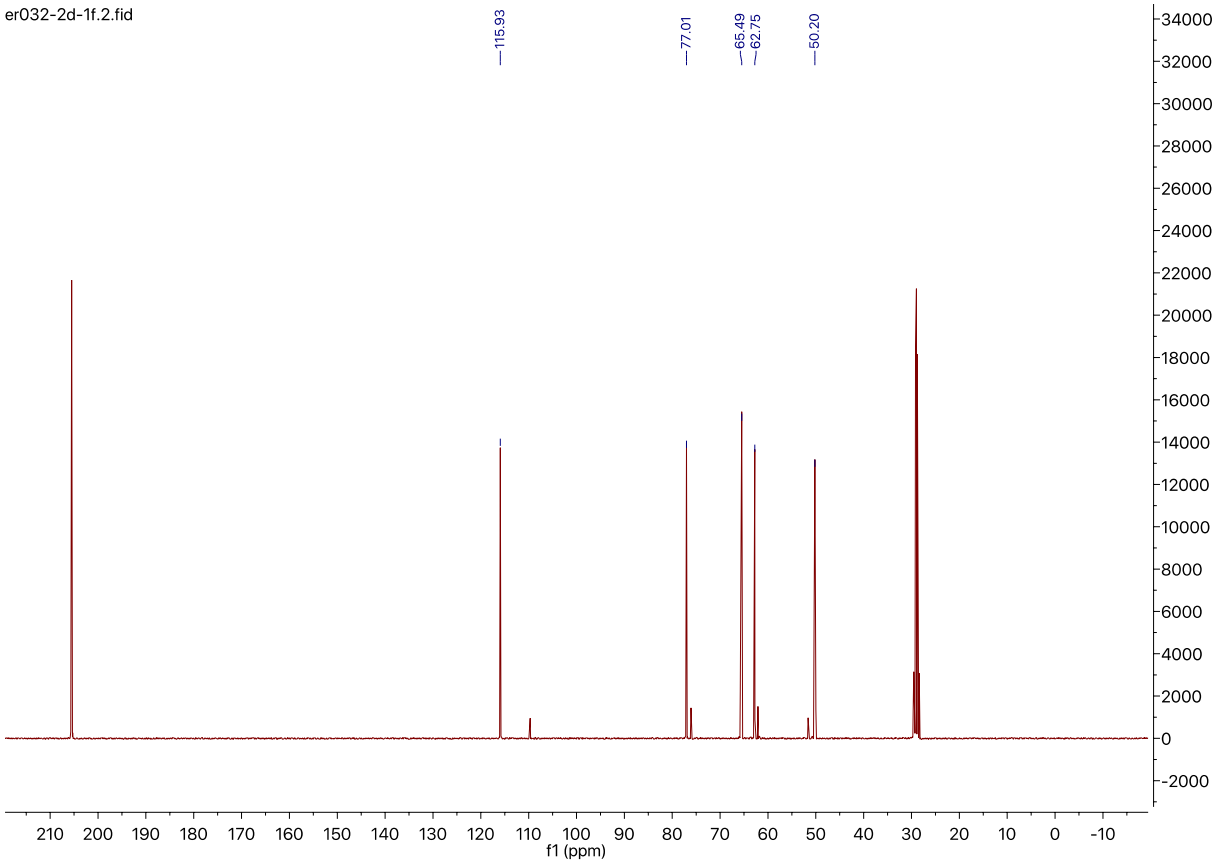

*Figure A 3.43: ^{13}C {^{1}H} NMR of **1a** (101 MHz, Acetone-d_6) δ = 115.93, 77.01, 65.49, 62.75, 50.20.*

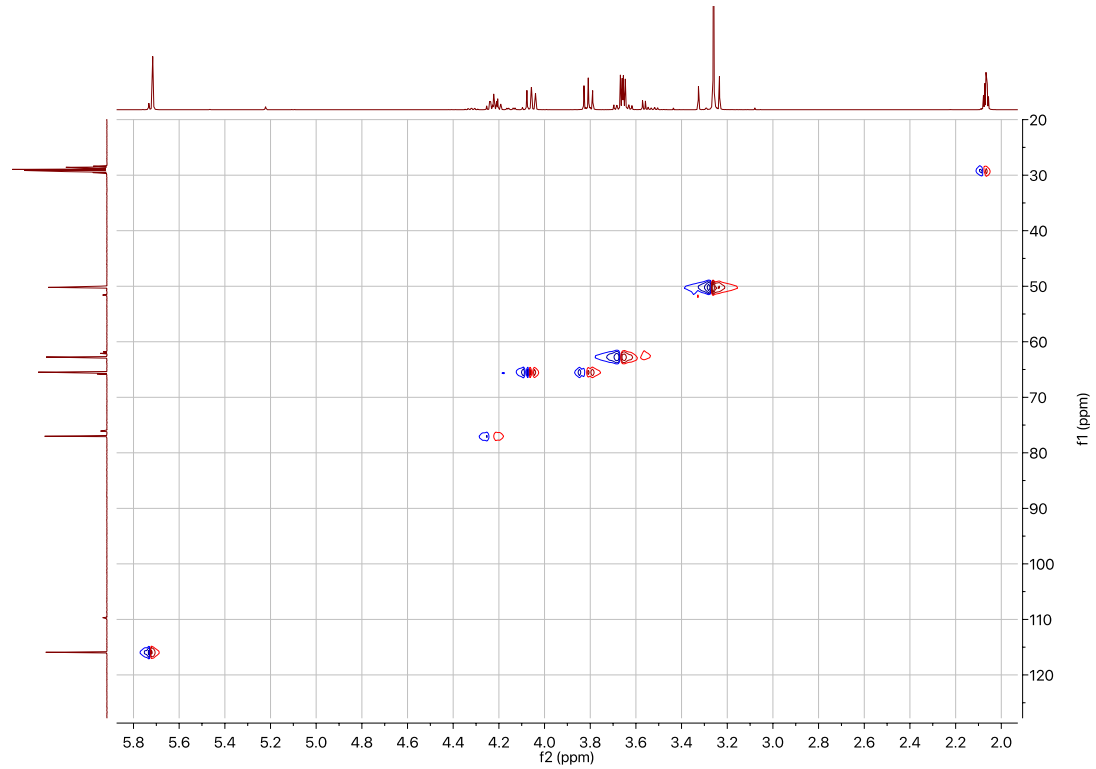

Figure A.3.3.44: HSQC of 1a (Acetone-d_6).

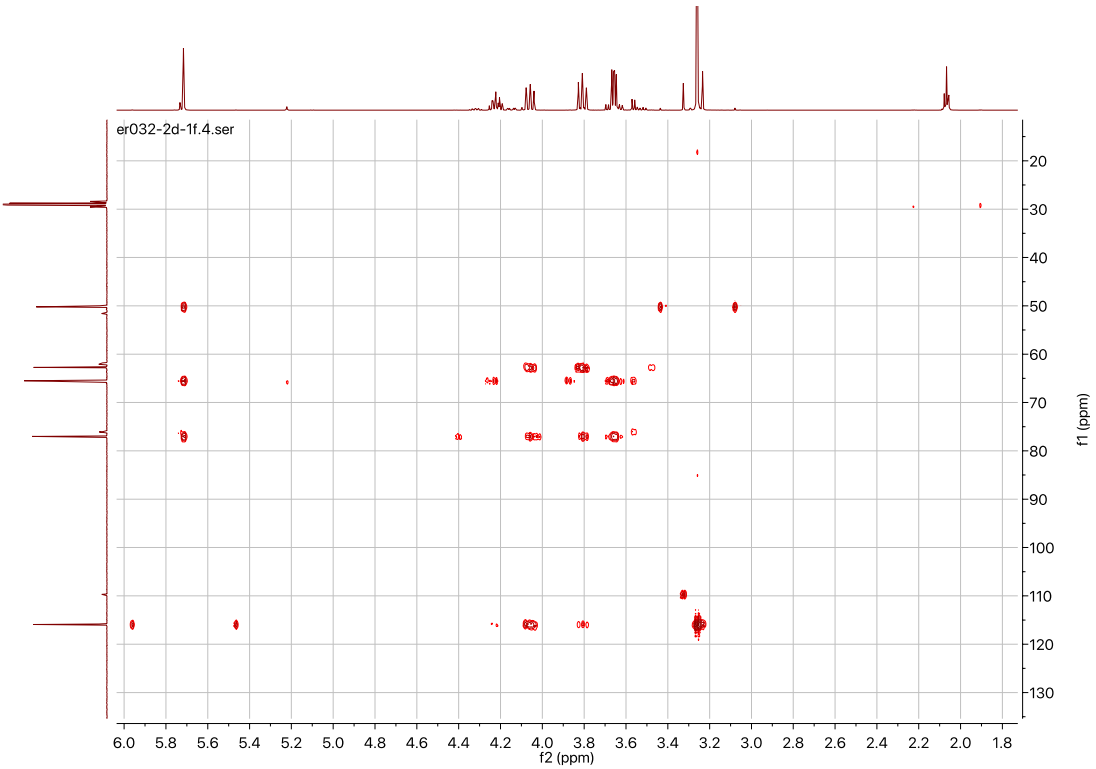

*Figure A 3.45: HMBC of **1a** (Acetone-d_6).*

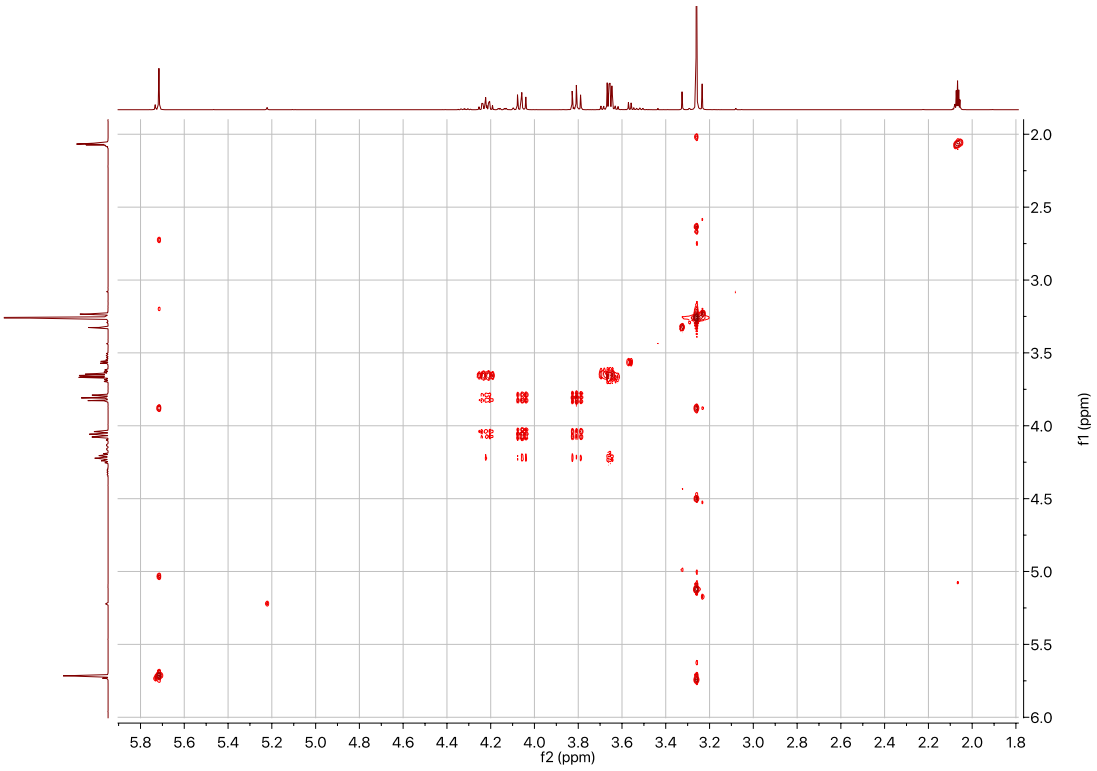

*Figure A 3.46: COSY of **1a** (Acetone-d6).*

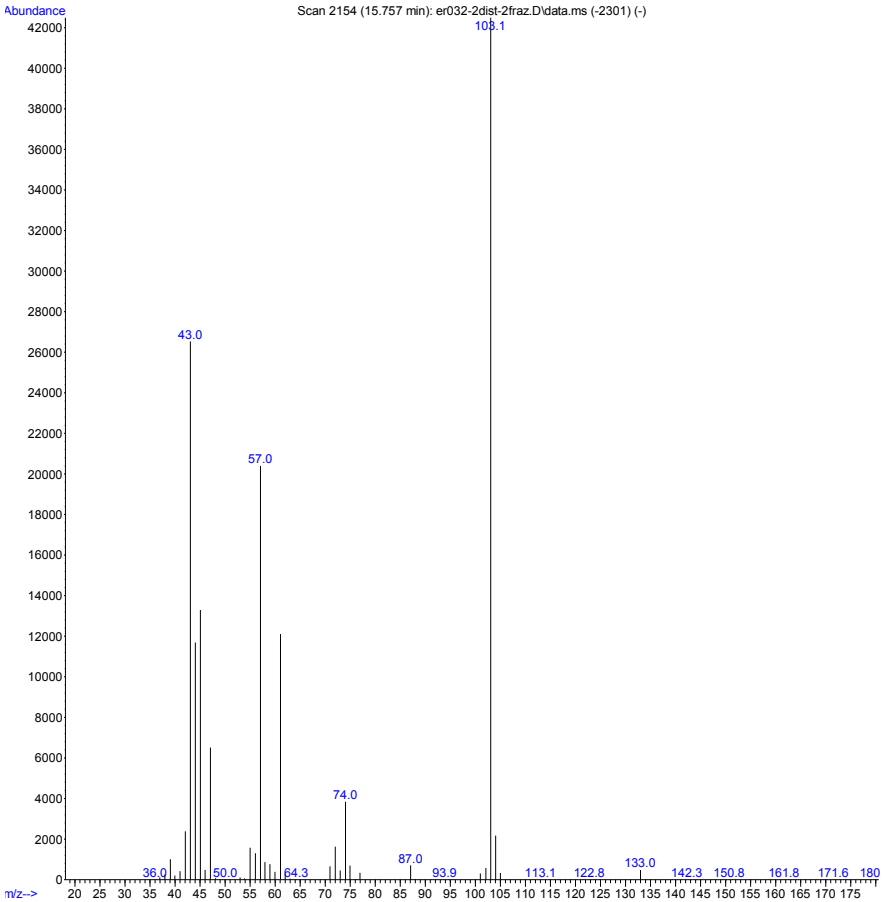

*Figure A 3.47: MS spectra **1b:** 134 (M^+,0);133 (1); 103 (100); 74 (8); 61 (18); 57 (47); 47 (15); 45(28); 44 (14); 43 (46).*

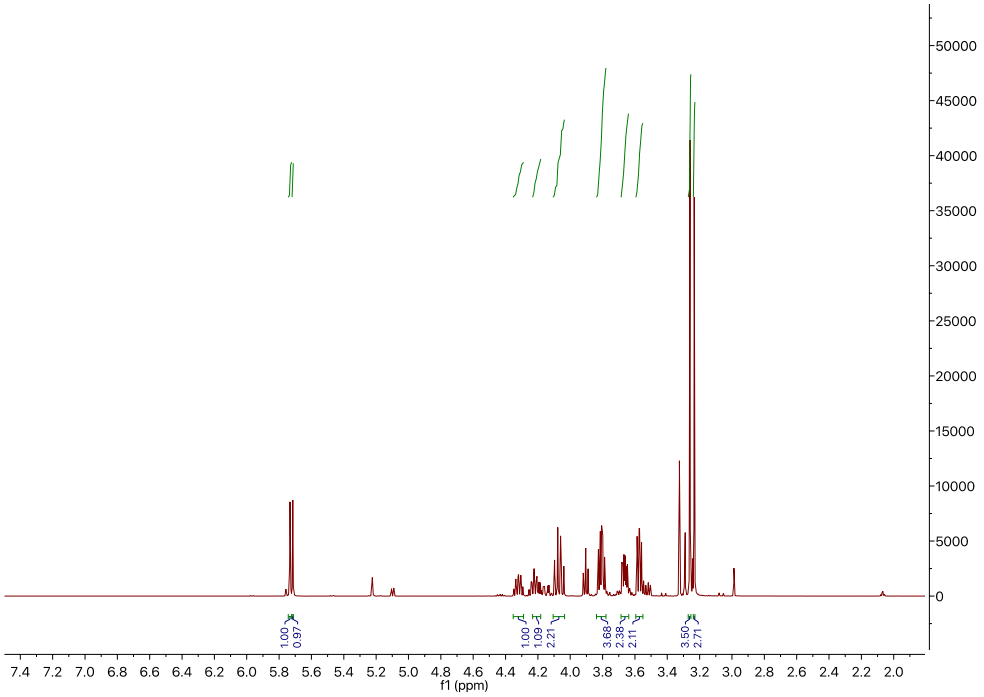

Figure A 3.48: 1H NMR of 1a,b (400 MHz, Acetone-d6): 1a δ = 5.72 (s, 1H), 4.23 – 4.18 (m, 1H), 4.11 – 4.04 (m, 1H), 3.84 – 3.78 (m, 1H), 3.66 (ddd, J=6.0, 5.2, 2.7, 2H), 3.26 (s, 3H). 1b: 5.73 (s, 1H), 4.32 (ddt, J=6.9, 5.6, 5.0, 1H), 4.11 – 4.04 (m, 1H), 3.84 – 3.78 (m, 1H), 3.57 (dd, J=6.0, 5.0, 2H), 3.23 (s, 3H).

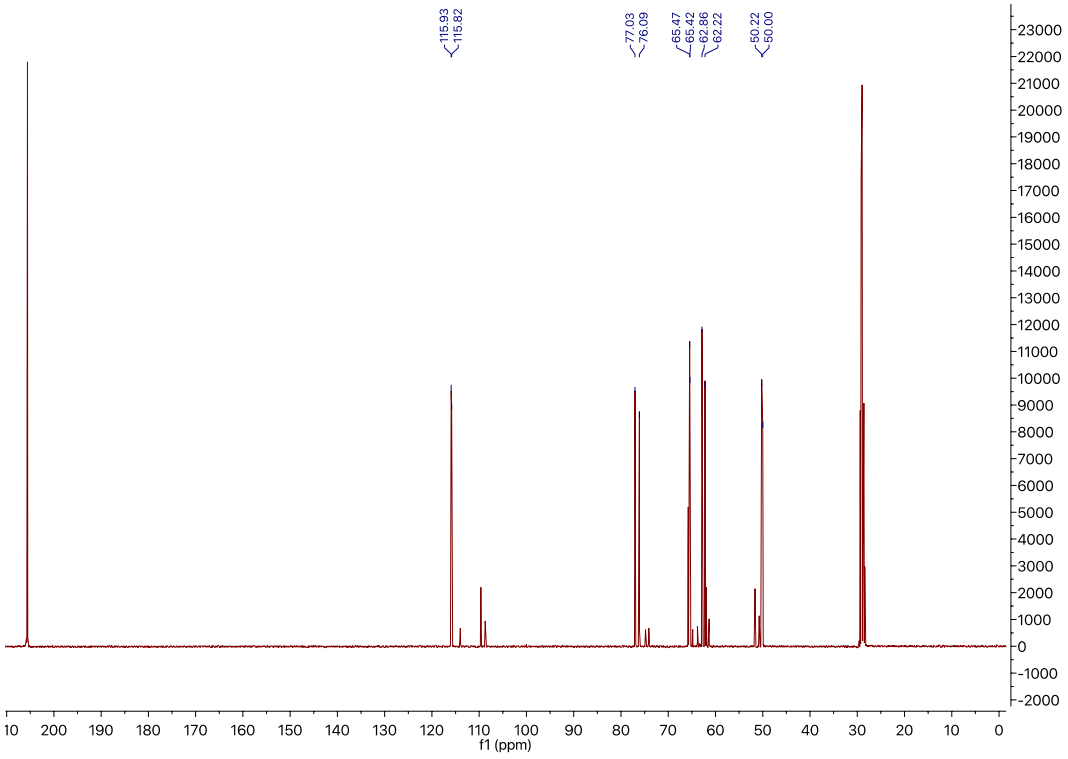

*Figure A 3.49: ^{13}C {^{1}H} NMR of **1a,b** (101 MHz, Acetone-d6): **1a** δ = 115.93, 77.03, 65.47, 62.86, 50.22, **1b:** δ = 115.82, 76.09, 65.42, 62.22, 50.00.*

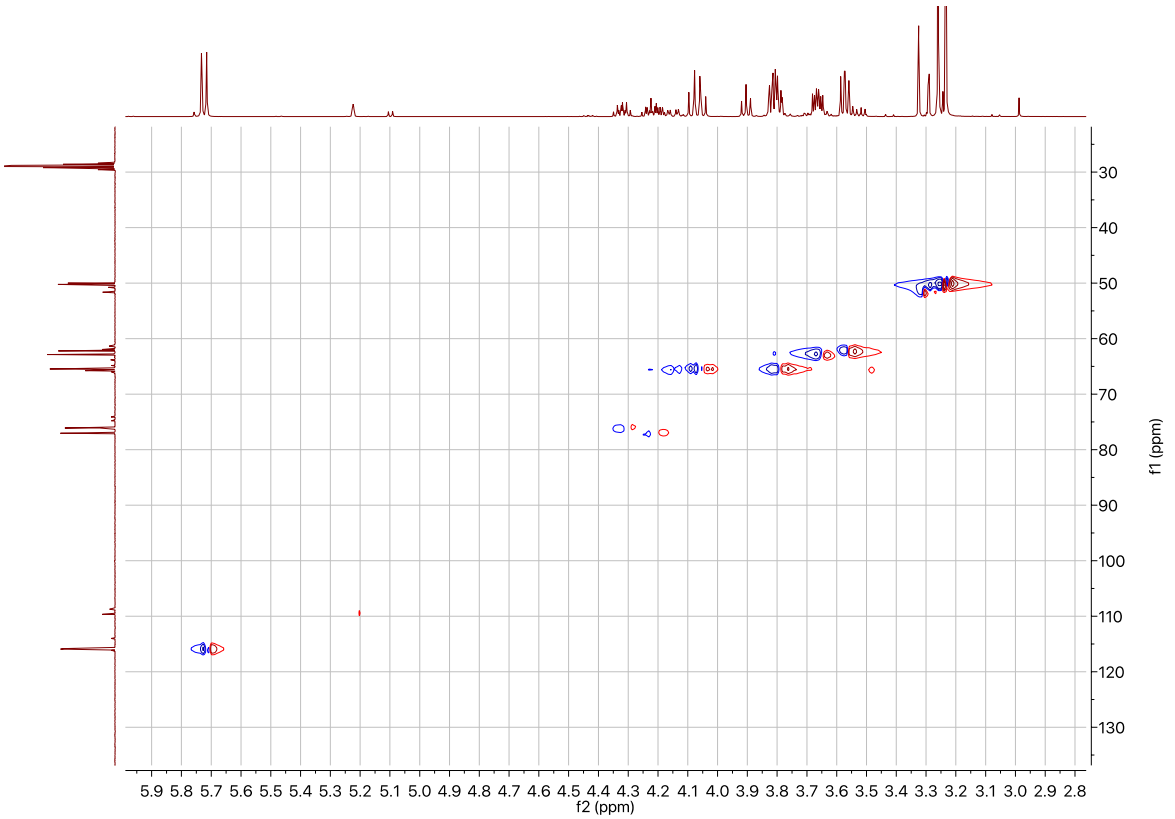

*Figure A 3.50: HSQC of **1a,b** (Acetone-d6).*

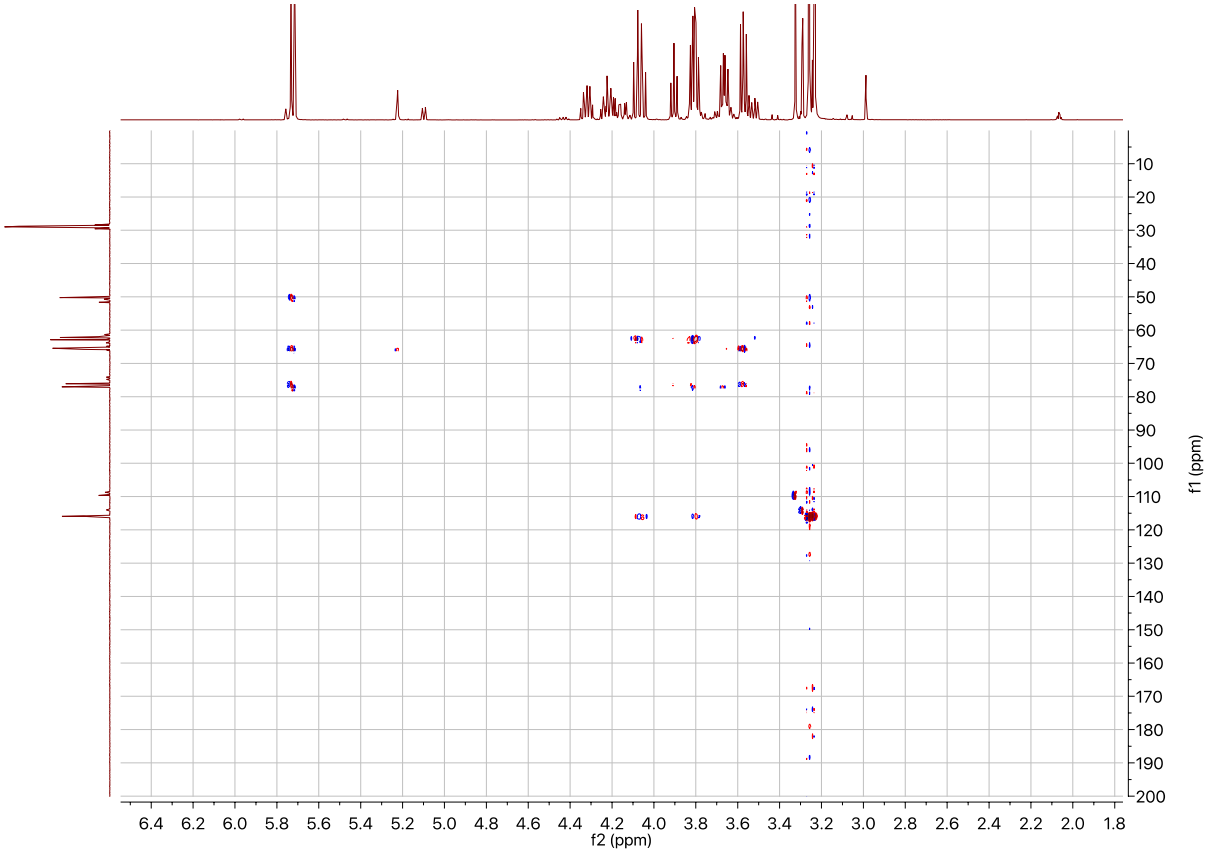

*Figure A 3.51: HMQC of **1a,b** (Acetone-d6).*

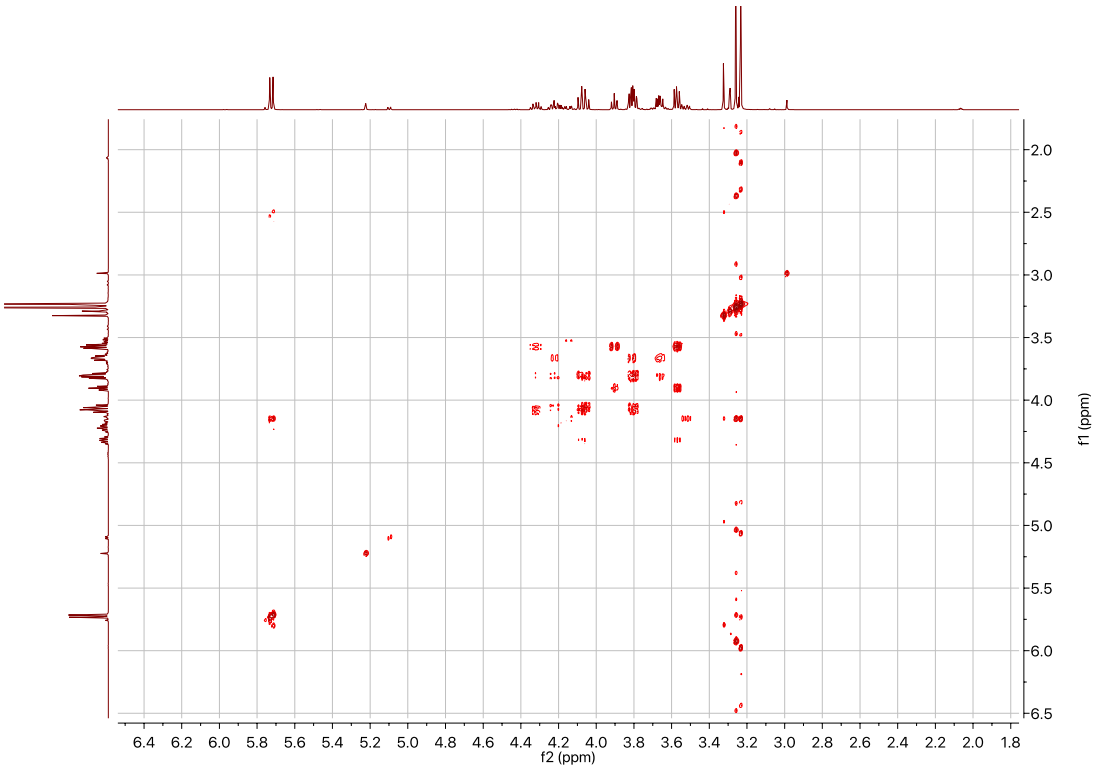

*Figure A 3.52: COSY of **1a,b** (Acetone-d6).*

2,6,7- trioxabyciclo[2.2.1]heptane (2).

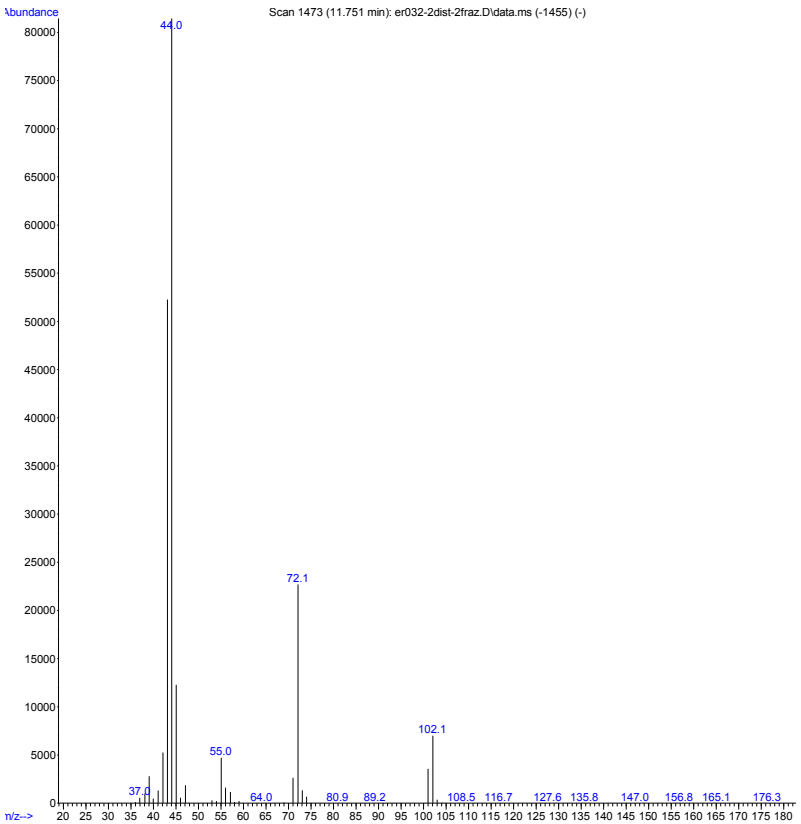

*Figure A 3.53: GC-MS spectra of **2:** 102 (M^+,8);101 (4); 45 (15); 44 (100); 43 (62); 42 (6).*

4-(dimethoxymethoxy)methyl)-2-methoxy-1,3-dioxolane (3).

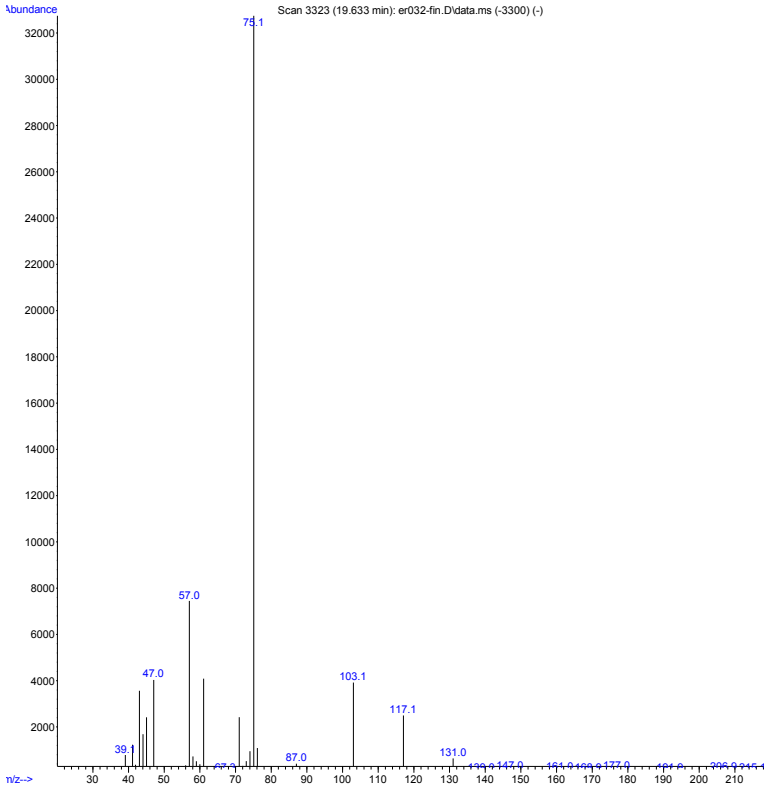

*Figure A 3.54: MS spectra of **3a:** 208 (M^+,0);131 (1); 117 (8); 103 (12); 75 (100); 61 (13); 57 (25); 47 (11); 43(9).*

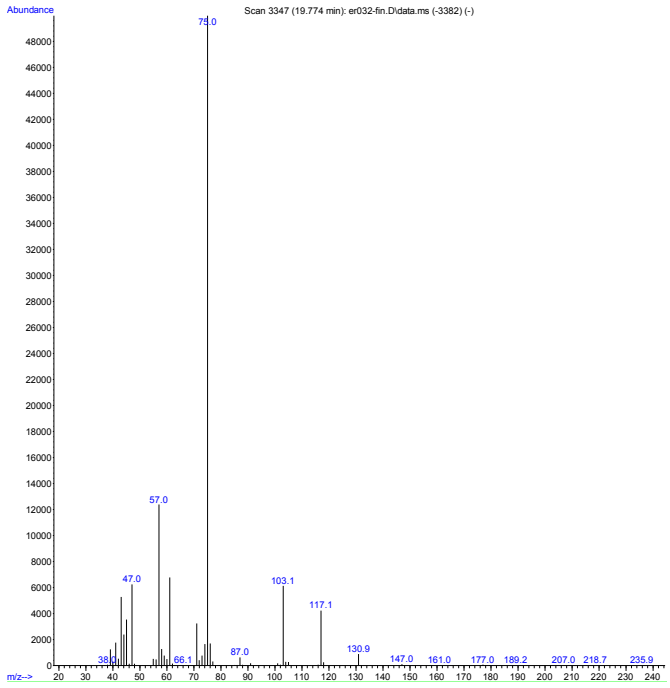

*Figure A 3.55: MS spectra of **3b:** 208 (M^+,0);131 (2); 117 (8); 103 (12); 75 (100); 61 (13); 57 (25); 47 (11); 45(6); 43 (9).*

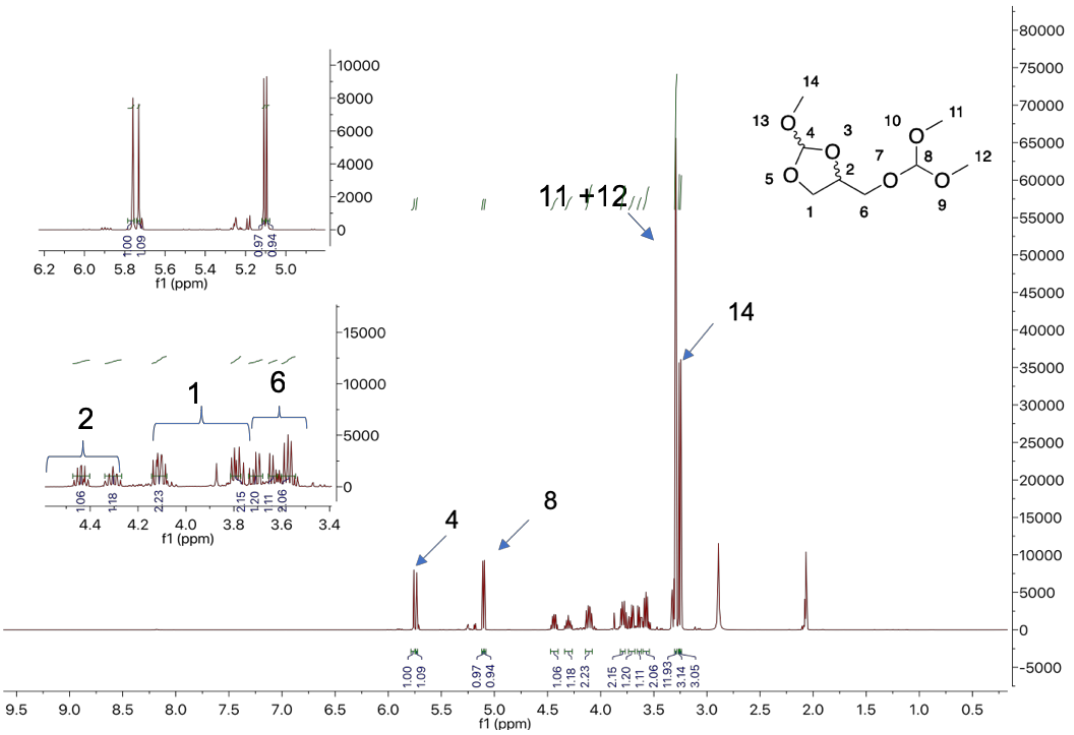

*Figure A 3.56: ^{1}H NMR of **3a,b** (400 MHz, Acetone) δ = 5.76 (s, 1H), 5.73 (s, 1H), 5.11 (s, 1H), 5.10 (s, 1H), 4.44 (dq, J=6.9, 5.3, 1H), 4.34 – 4.27 (m, 1H), 4.11 (ddd, J=7.9, 6.8, 5.6, 2H), 3.81 – 3.77 (m, 2H), 3.71 (dd, J=10.6, 6.1, 1H), 3.65 – 3.61 (m, 1H), 3.57 (dd, J=6.2, 5.3, 2H), 3.31 – 3.29 (m, 12H), 3.26 (s, 3H), 3.25 (s, 3H).*

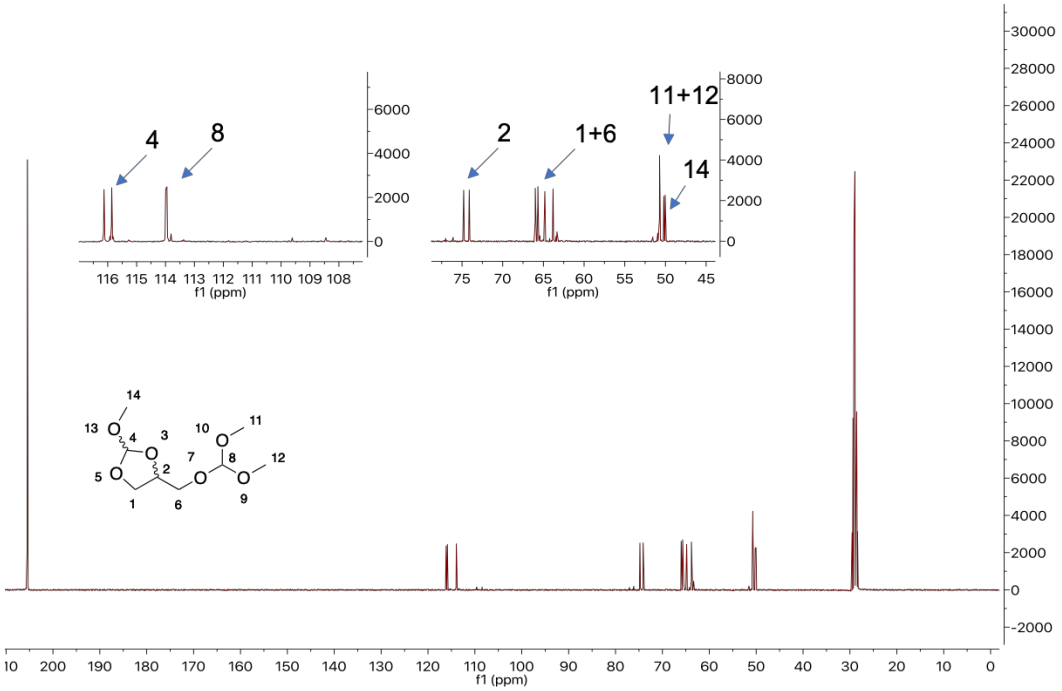

*Figure A 3.57: ^{13}C {^{1}H} NMR of **3a,b** (101 MHz, Acetone-d6) δ = 116.13, 115.86, 113.99, 113.95, 74.80, 74.11, 66.00, 65.68, 64.82, 63.80 (d, J=2.1), 50.72, 50.71, 50.21, 50.04.*

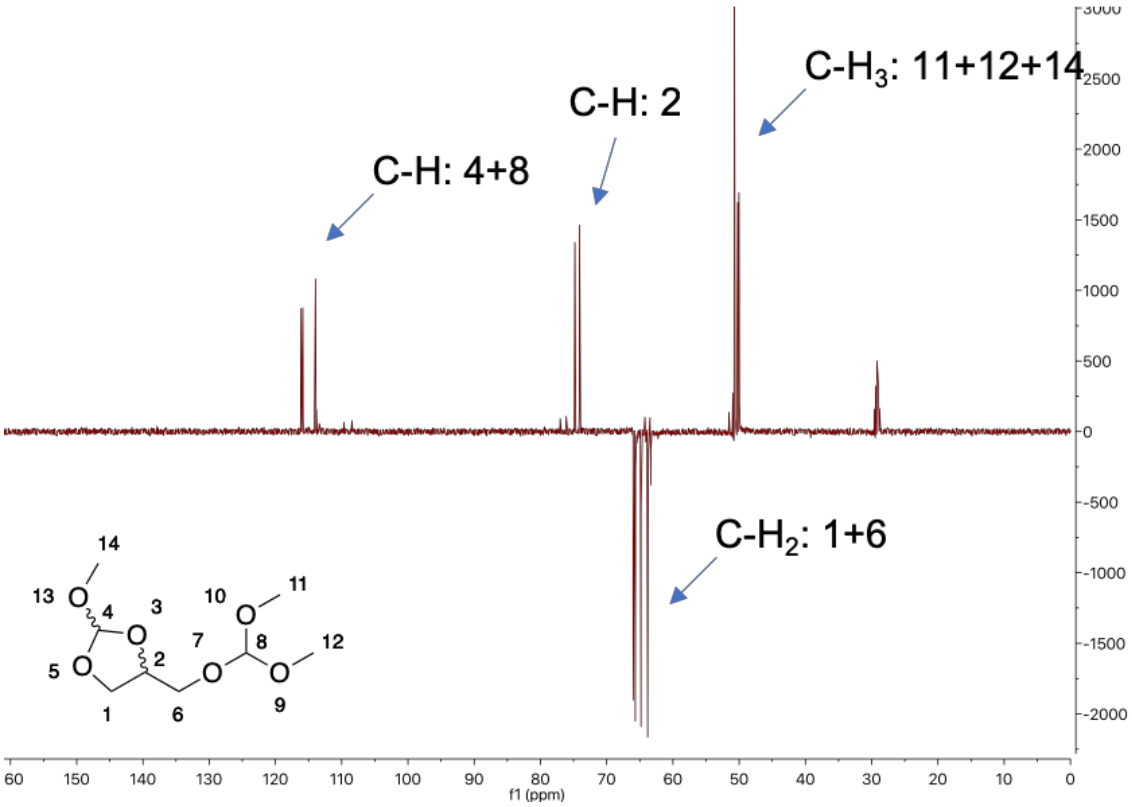

*Figure A 3.58: DEPT135 of **3a,b** (Acetone-d6).*

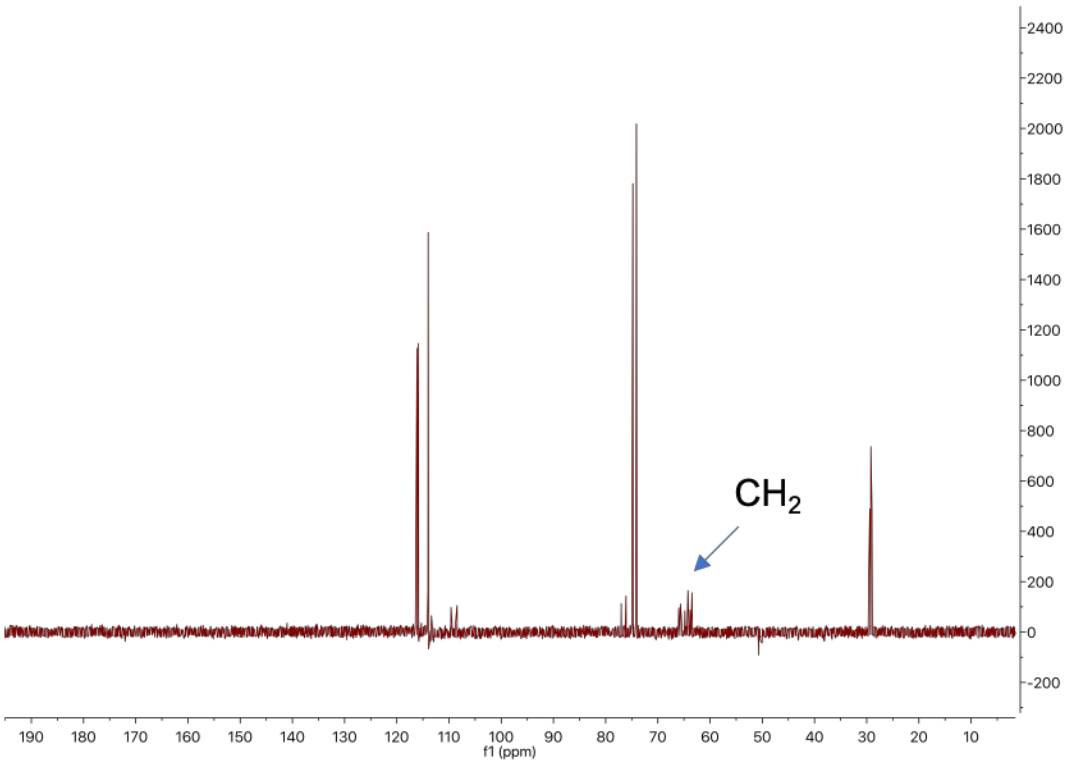

*Figure A 3.59: DEPT-90 of **3a,b** (Acetone-d6).*

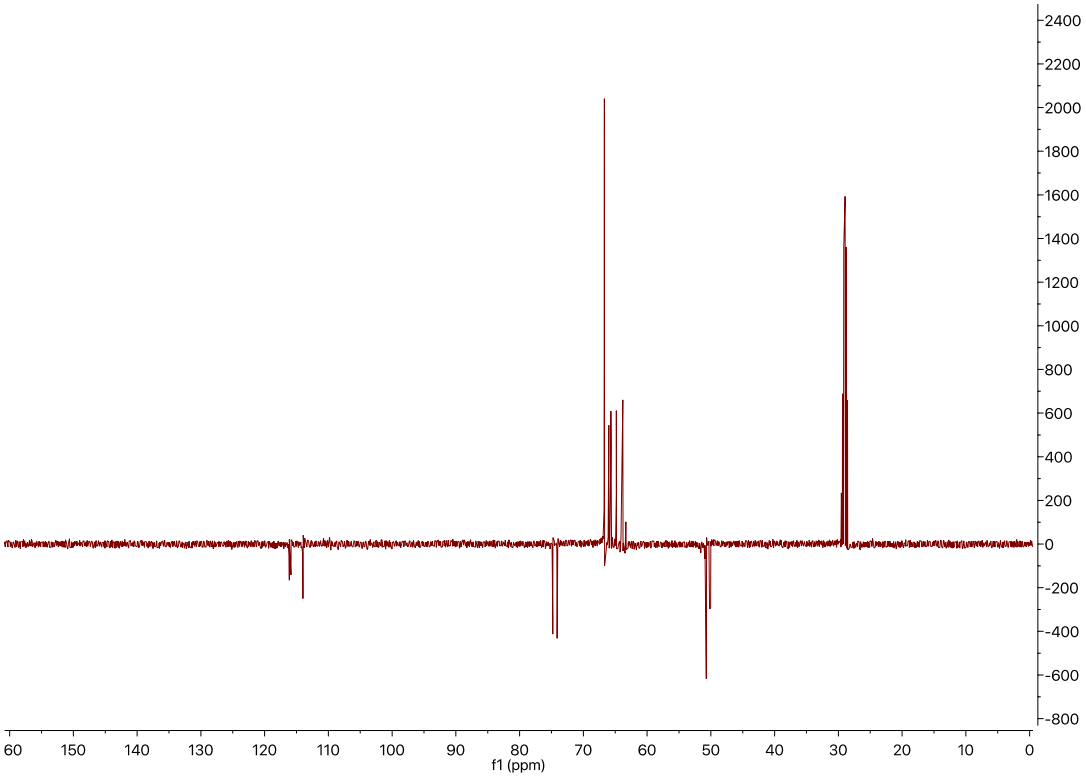

*Figure A 3.60: ATP of **3a,b** (Acetone-d6).*

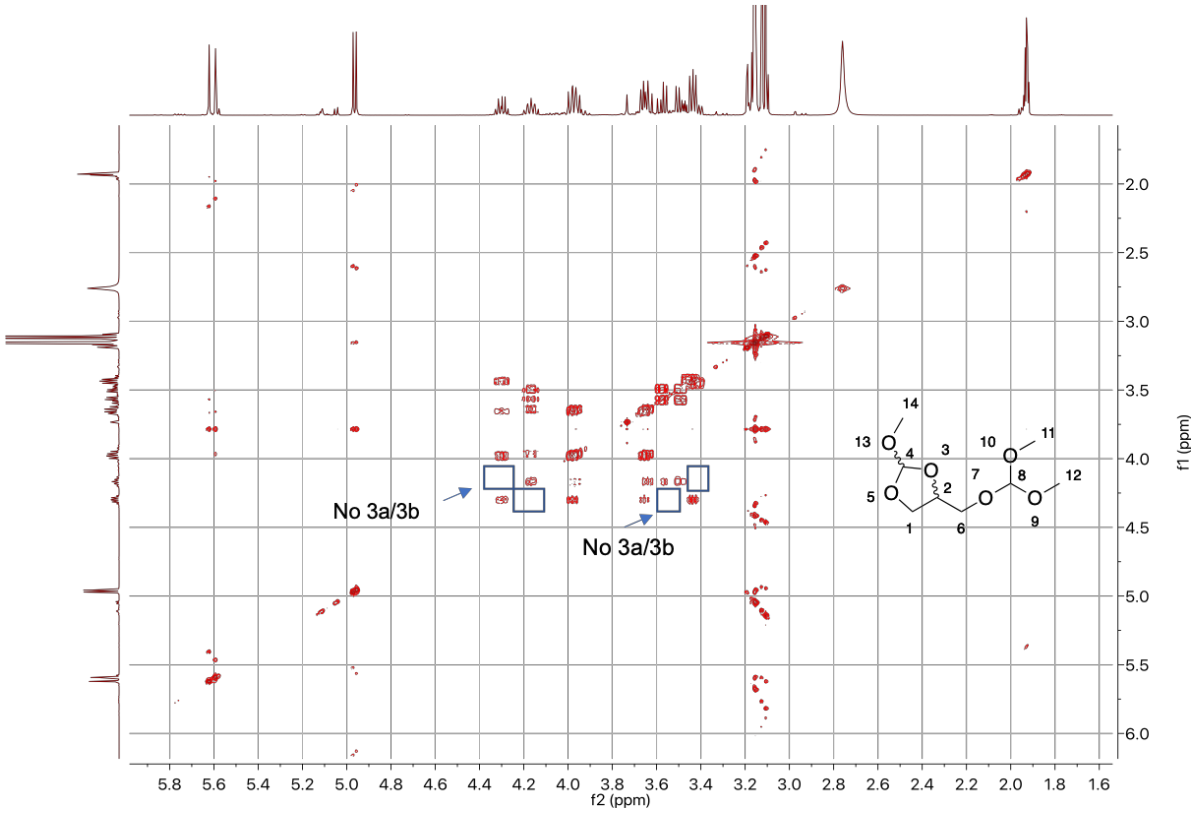

*Figure A 3.61: COSY of **3a,b** (Acetone-d6).*

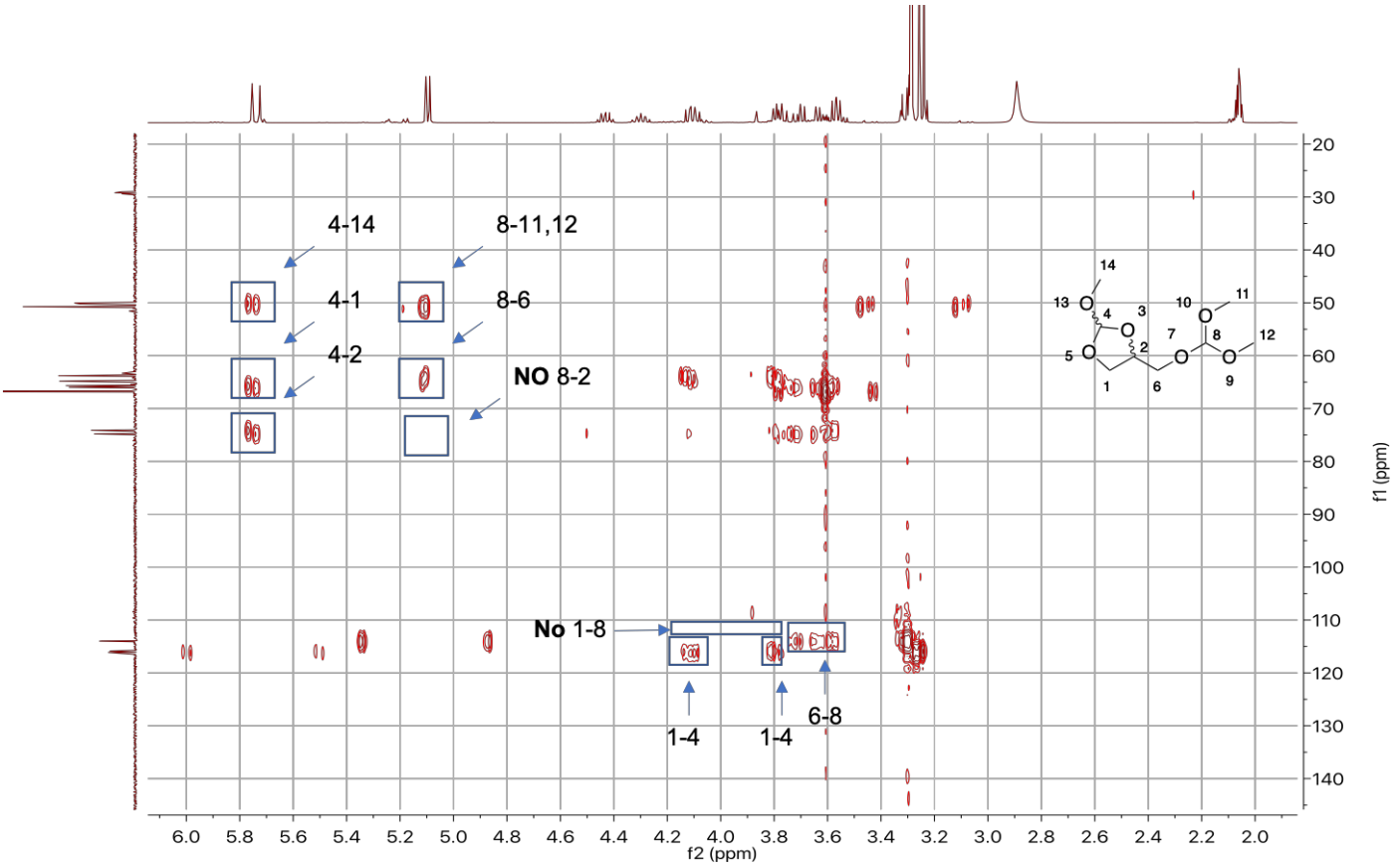

*Figure A 3.62: HMBC of **3a,b** (Acetone-d6).*

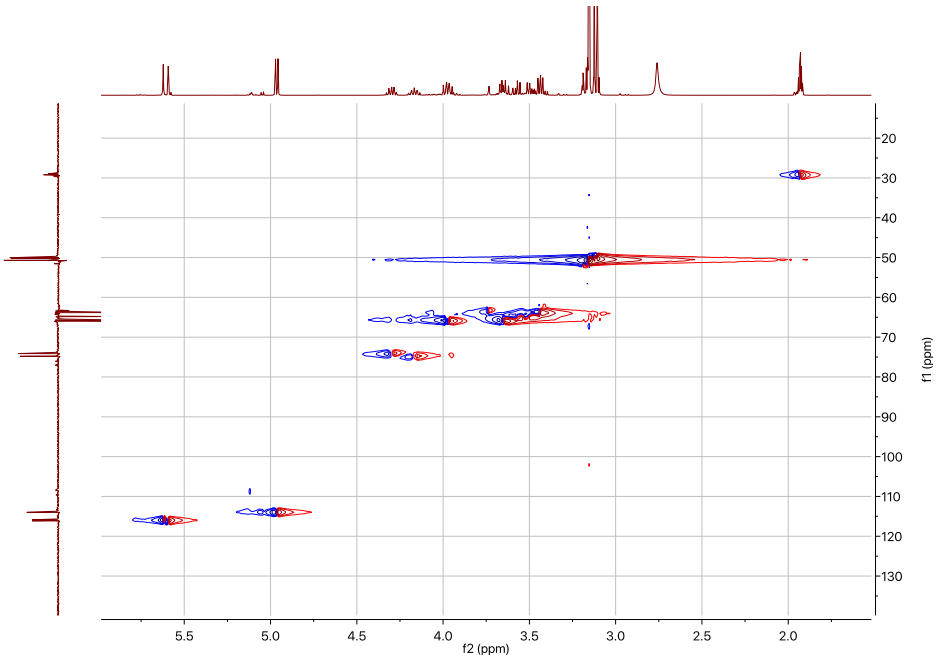

*Figure A 3.63 : HSQC of **3a,b** (Acetone-d6).*

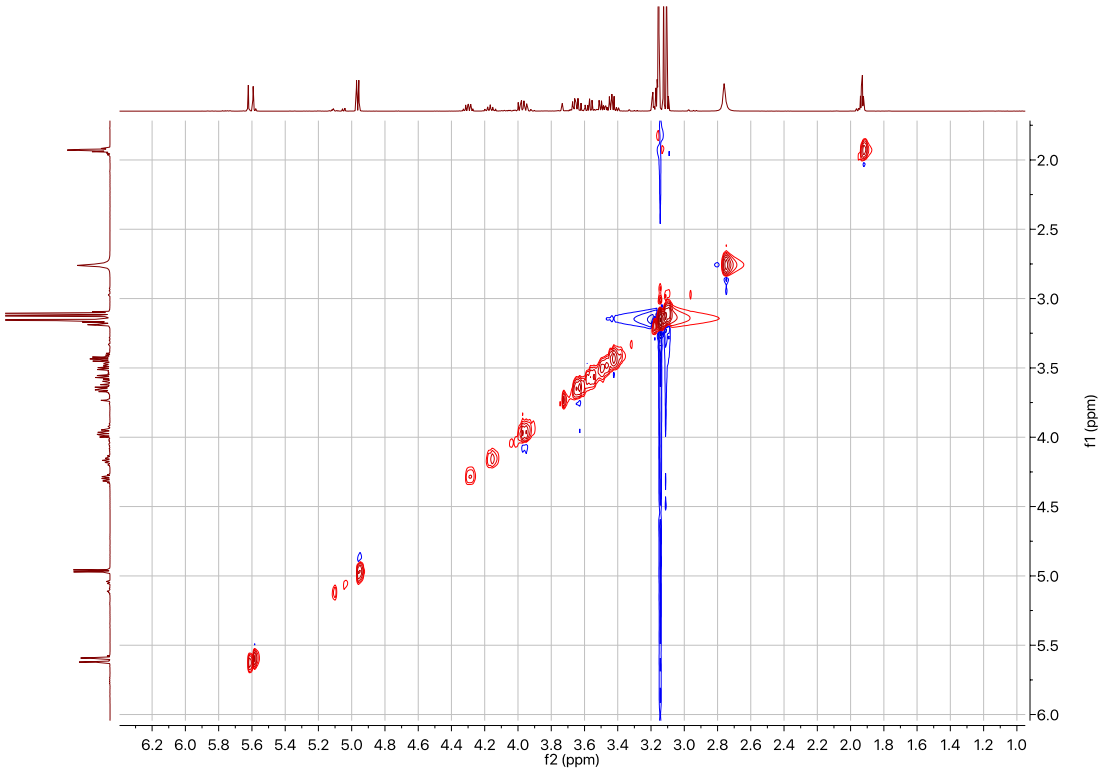

*Figure A 3.64: NOESY of **3a,b** (Acetone-d6).*

Characterization of Bronsted acidic ionic liquids (BAILs)

Pirydinium paratoluensolfonate (PPTS)

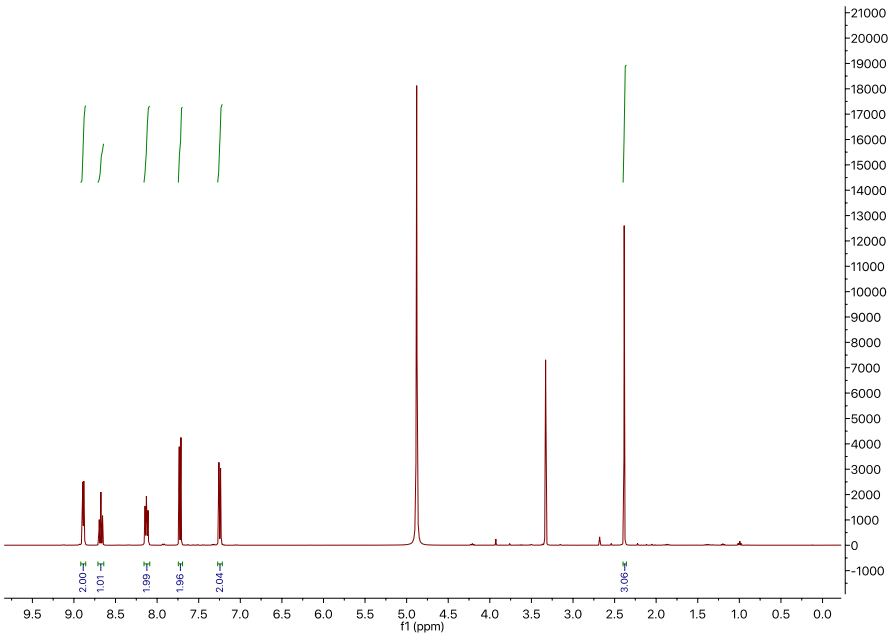

Figure A 3.65: ^{1}H NMR of PPTS (400 MHz, MeOD) δ = 8.89 (dt, J=5.2, 1.6, 2H), 8.68 (tt, J=7.9, 1.6, 1H), 8.16 – 8.09 (m, 2H), 7.75 – 7.69 (m, 2H), 7.27 – 7.22 (m, 2H), 2.38 (s, 3H).

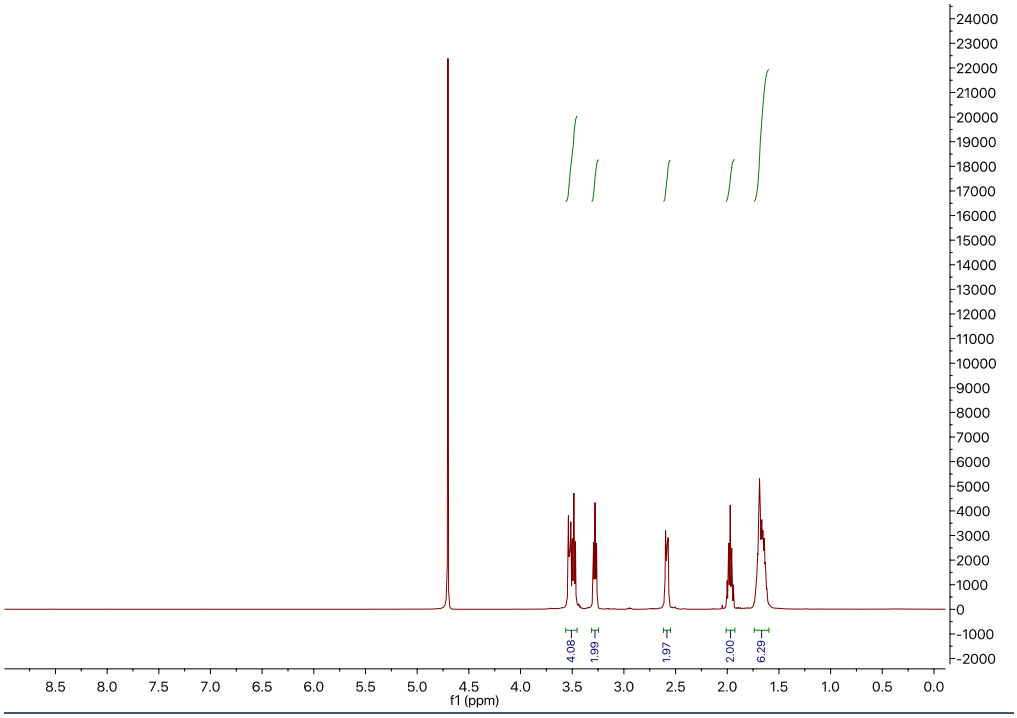

Figure A 3.66: ^{1}H NMR of DBUHBr (400 MHz, D_2O) δ = 3.50 (dt, J=18.0, 5.6, 4H), 3.28 (t, J=5.9, 2H), 2.62 – 2.55 (m, 2H), 1.97 (tt, J=7.2, 5.2, 2H), 1.74 – 1.60 (m, 6H).

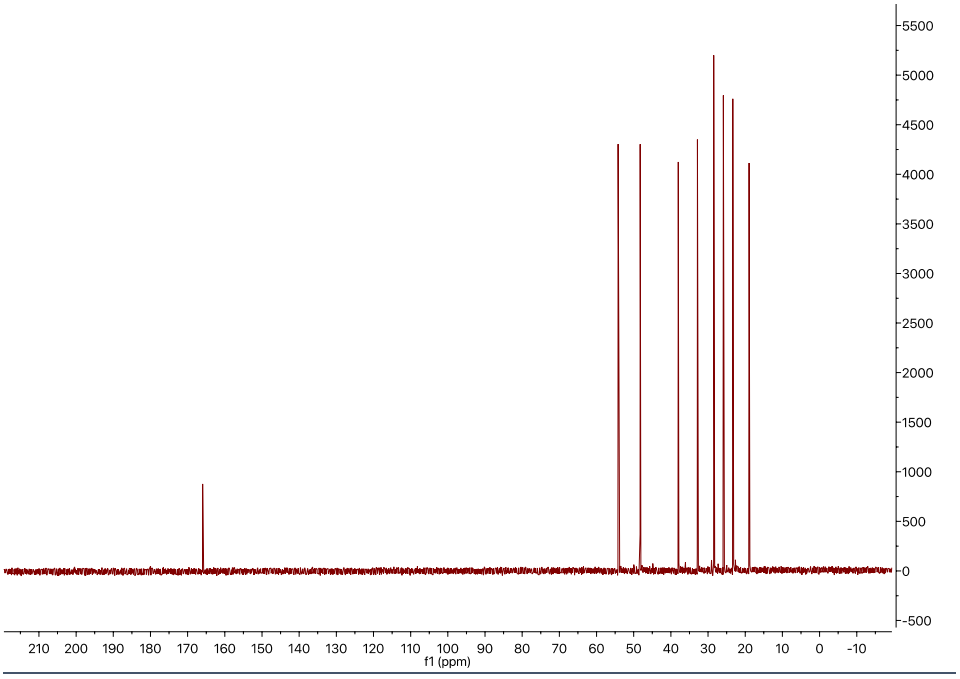

Figure A 3.67: ^{13}C {^{1}H} NMR of DBUHBr (101 MHz, D_2O) δ = 165.95, 54.19, 48.26, 38.01, 32.87, 28.47, 25.90, 23.34, 18.96.

Butylsolfonylmethylimidazolium hydrogen sulfate ($BSMImHSO_4$)

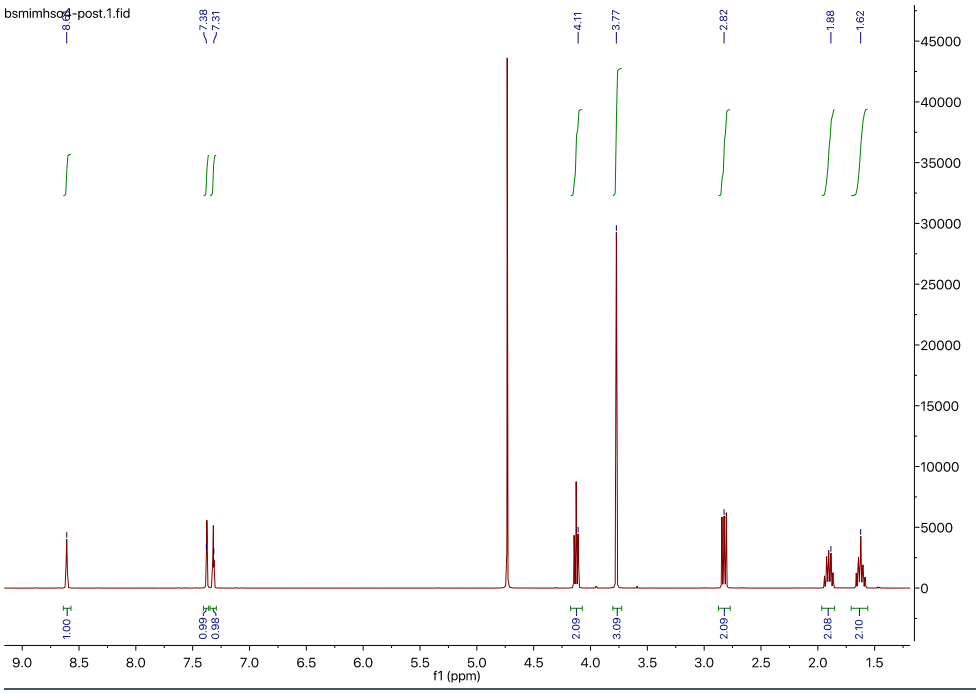

Figure A 3.68: ^{1}H NMR of $BSMImHSO_4$ (400 MHz, D_2O) δ = 8.61 (s, 1H), 7.38 (s, 1H), 7.31 (s, 1H), 4.11 (s, 2H), 3.77 (s, 3H), 2.82 (s, 2H), 1.88 (s, 2H), 1.62 (s, 2H).

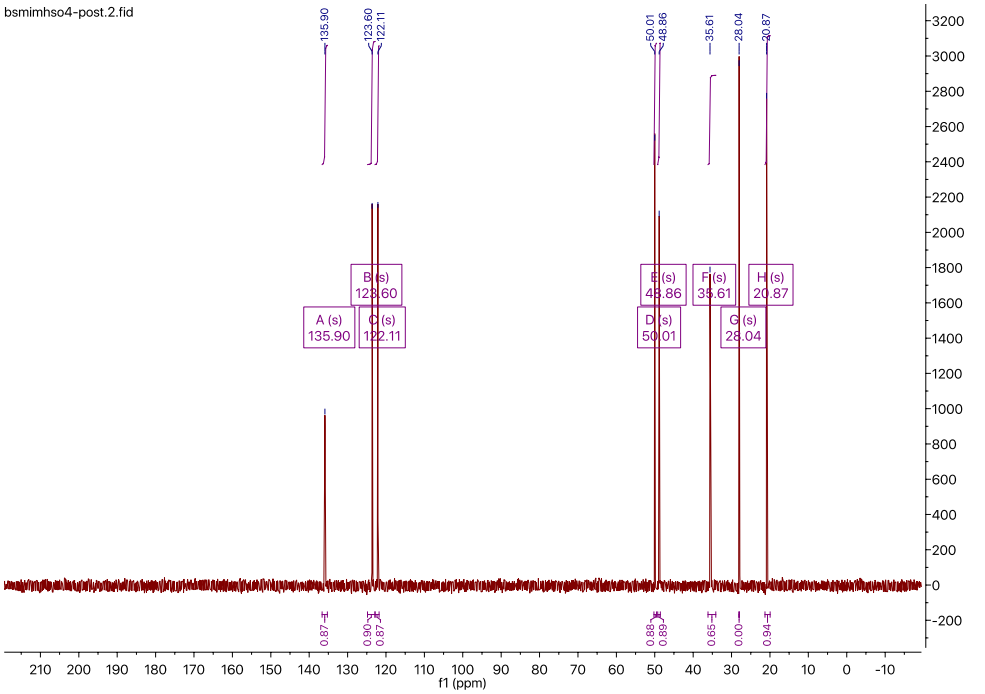

Figure A 3.69: $^{13}C\{^{1}H\}$ NMR of $BSMImHSO_4$ (101 MHz, D_2O) δ = 135.90, 123.60, 122.11, 50.01, 48.86, 35.61, 28.04, 20.87.

Butylsolfonylmethylimidazolium bromide (BSMImBr)

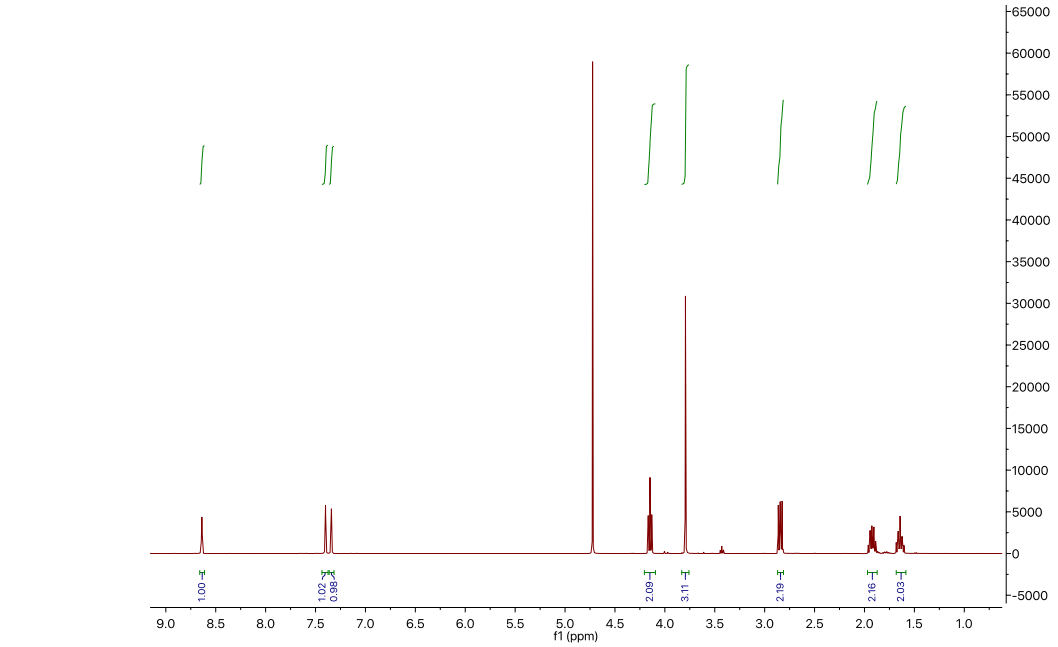

Figure A 3.70: ^{1}H NMR of BSMImBr (400 MHz, D_2O) δ = 8.66 – 8.61 (m, 1H), 7.40 (t, J=1.8, 1H), 7.34 (t, J=1.8, 1H), 4.15 (t, J=7.0, 2H), 3.79 (d, J=0.6, 3H), 2.87 – 2.81 (m, 2H), 1.97 – 1.87 (m, 2H), 1.68 – 1.58 (m, 2H).

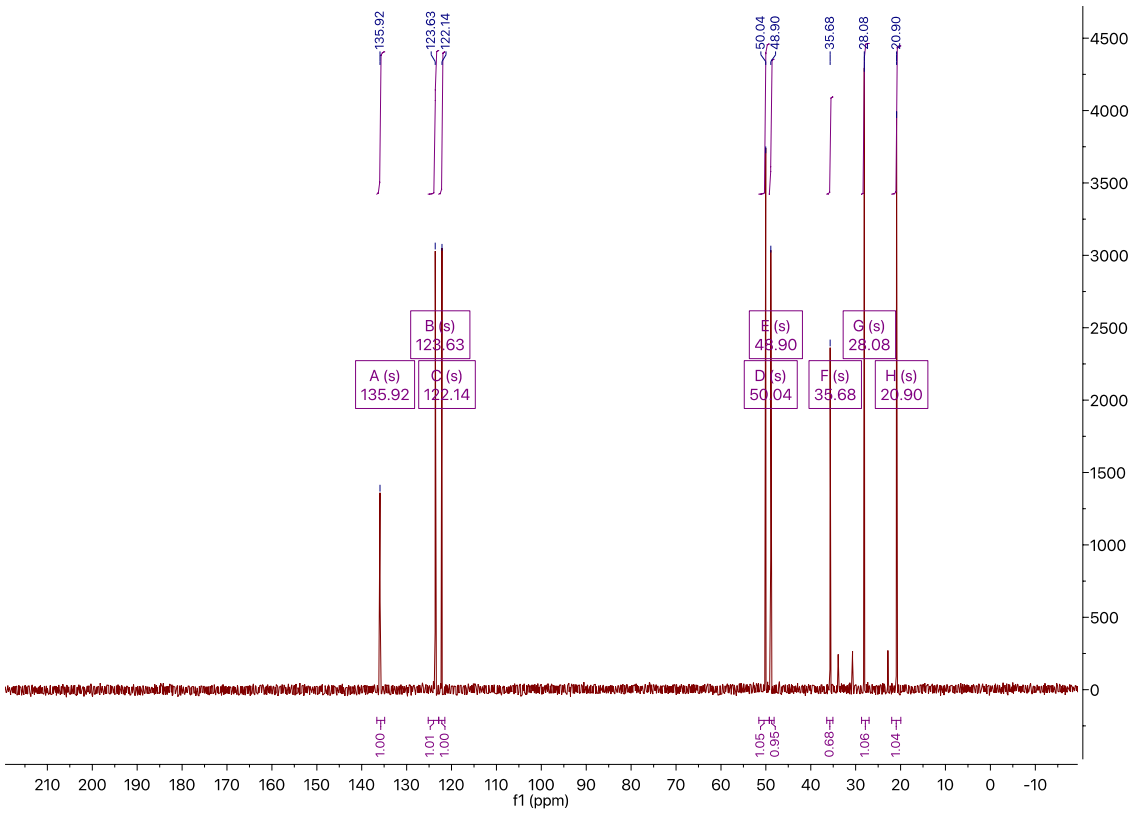

Figure A 3.71: $^{13}C\{^{1}H\}$ NMR of BSMImBr (101 MHz, D_2O) δ = 135.92, 123.63, 122.14, 50.04, 48.90, 35.68, 28.08, 20.90

Reaction profiles

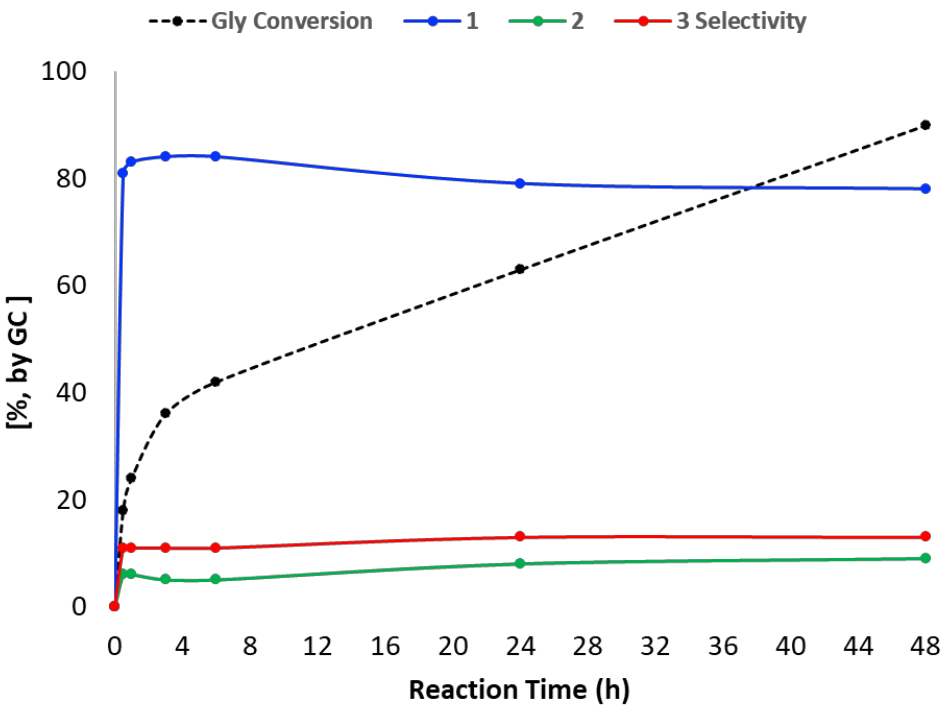

Figure A 3.72: Conversion of Gly and products selectivity for the catalyst-free reaction between Gly and $HC(OCH_3)_3$ in function of the reaction time at room temperature and Q=1.

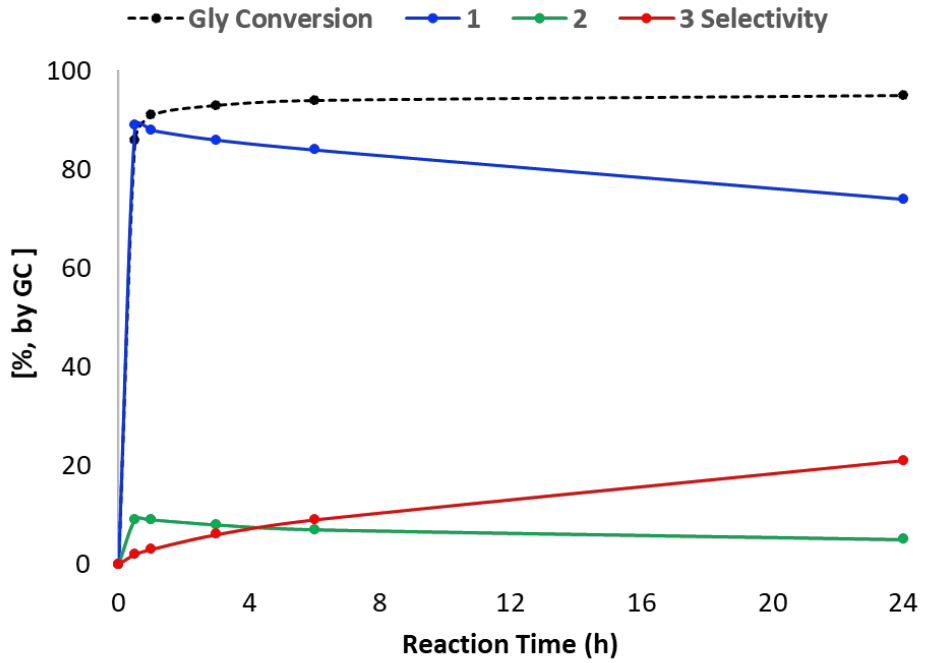

Figure A 3.73: Conversion of Gly and products selectivity for the catalyst-free reaction between Gly and $HC(OCH_3)_3$ in function of the reaction time at room temperature and Q=10.

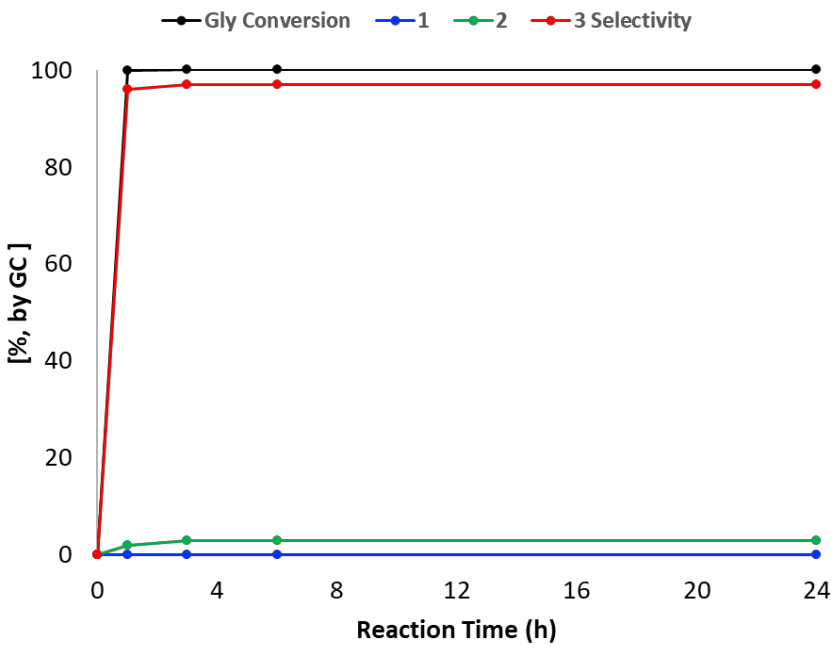

Figure A 3.74: Conversion of Gly and and products selectivity for the reaction between $HC(OMe)_3$ and Gly in presence of Pyr-PTSA (10% w/w_{Gly}) in function of the reaction time at room temperature and Q=10.

Reaction of glycerol with $HC(OMe)_3$ in presence of sulfuric acid as catalyst

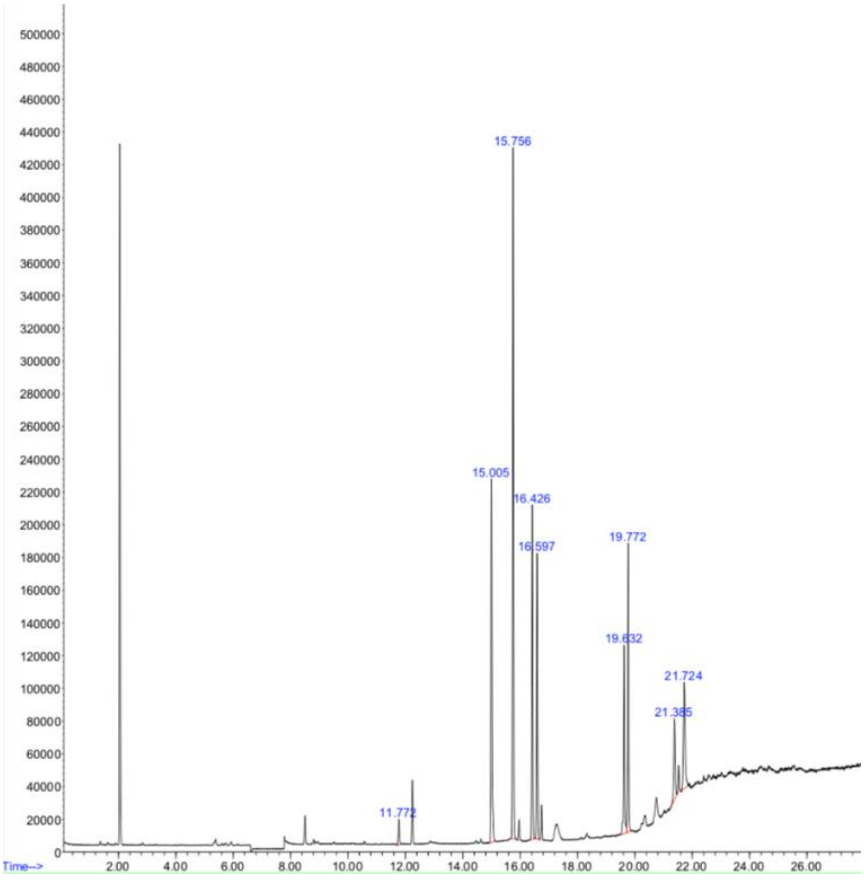

Figure A 3.75: GC-MS chromatograph of the reaction between $HC(OMe)_3$ and Gly (Q=10, 90°C, 24h) in presence of sulfuric acid.

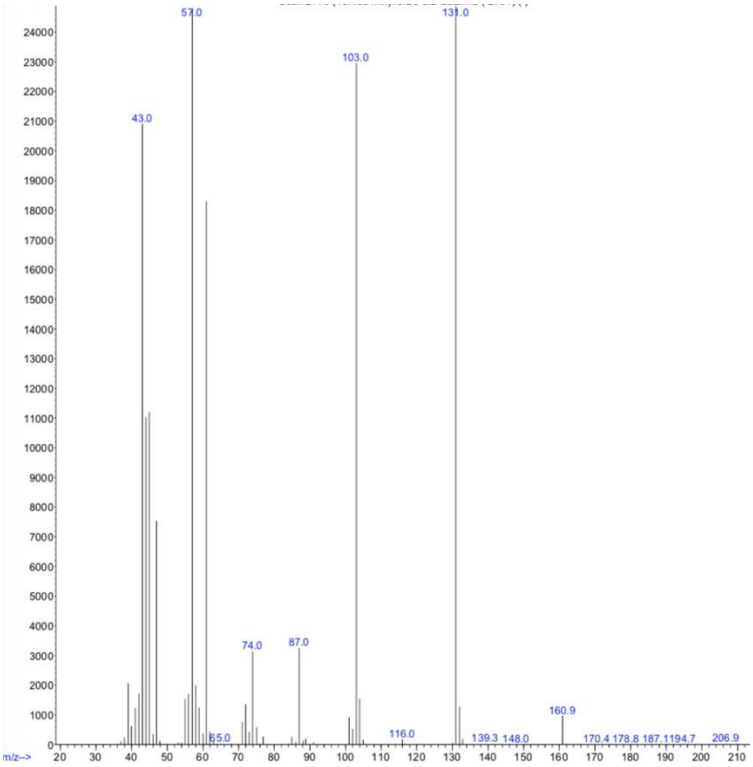

Figure A 3.76: MS spectra of the undefined compounds with retention time: 16.43 min. 161 (4);131 (95); 103 (84); 87 (13); 74 (12); 61 (84); 57 (100); 47 (32); 45(44); 44 (49); 43 (85).

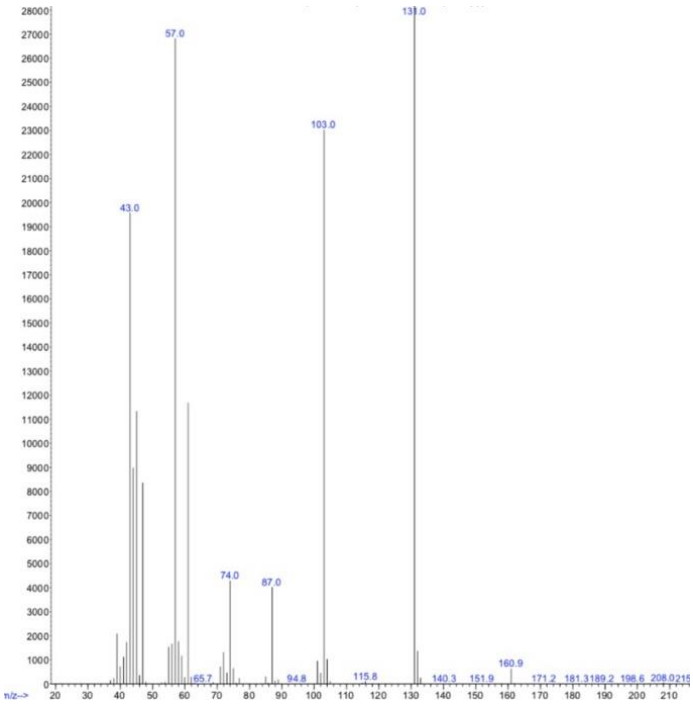

Figure A 3.77: MS spectra of the undefined compounds with retention time: 16.59 min. 161 (2);131 (100); 103 (82); 87 (13); 74 (15); 61 (41); 57 (95); 47 (30); 45(40); 44 (32); 43 (69).

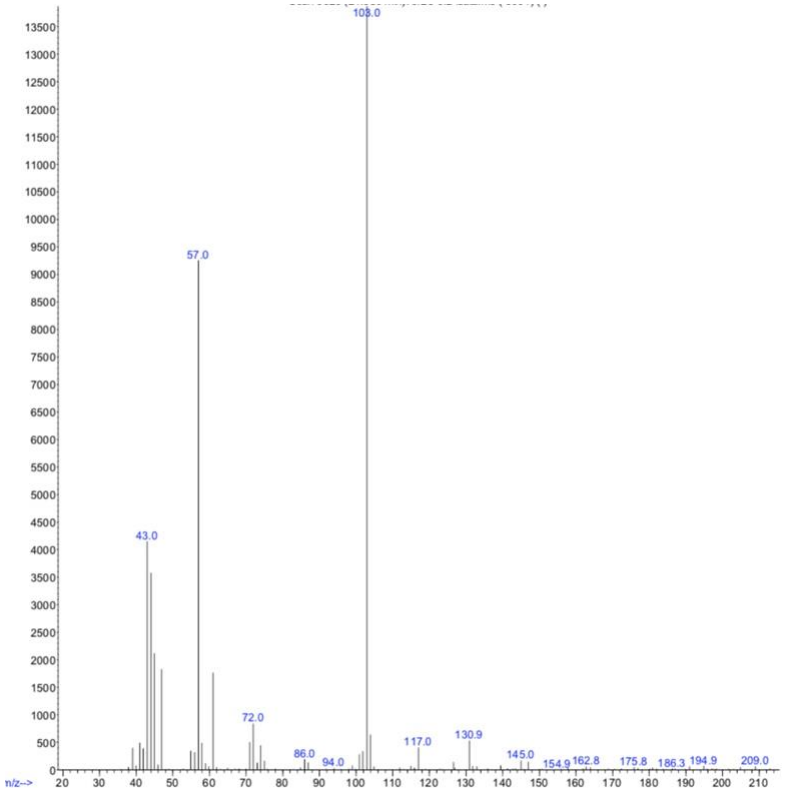

Figure A 3.78: MS spectra of the undefined compounds with retention time: 16.43 min. 209 (1); 195 (1); 163 (1); 145 (1); 103 (100); 61 (12); 57 (67); 47 (13); 45(15); 44 (26); 43 (30).

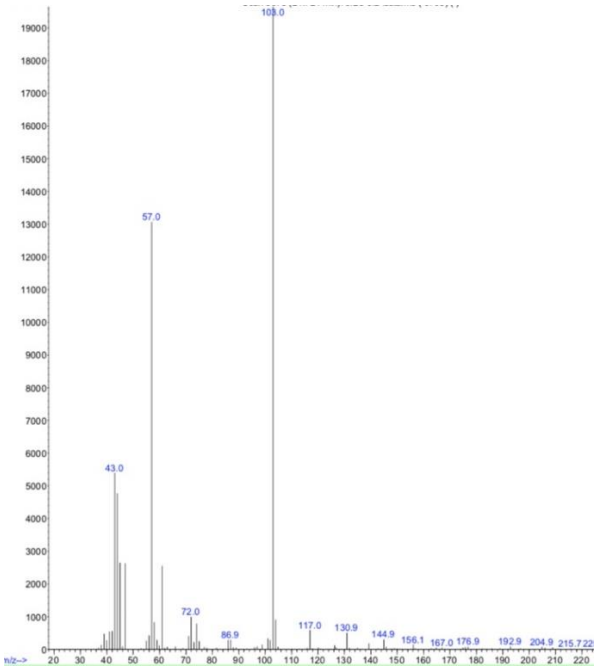

Figure A 3.79: MS spectra of the undefined compounds with retention time:21.72 min. 205 (1); 193 (1); 177 (1); 145 (2); 103 (100); 61 (12); 57 (67); 47 (12); 45(14); 44 (24); 43 (28).

References

[1] R. Calmanti, M. Galvan, E. Amadio, A. Perosa, M. Selva, *ACS Sustainable Chem. Eng.* 2018, **6(3)**, 3964-3973.